



Northern Illinois
University



Brookhaven
National Laboratory

U.S. Particle Accelerator School

Education in Beam Physics and Accelerator Technology

Colliders

for High Energy and Nuclear Physics

*by Vladimir Shiltsev (NIU), Vadim Ptitsyn
and Chuyu Liu (both - BNL)*

US Particle Accelerator School, Jan 26 – Jan 31, 2025

Purpose and Audience

Since the middle of the 20th century, charged particle colliders have been at the forefront of scientific discoveries in high-energy and nuclear physics. Collider accelerator technology and beam physics have progressed immensely and modern facilities now operate at energies and luminosities many orders of magnitude greater than the pioneering colliders of the early 1960s. In addition, the field of colliders remains extremely dynamic and continues to develop many innovative approaches. A number of novel concepts are currently being considered for designing and constructing even more powerful colliders. This course will review colliding-beam method and the history of colliders, survey the fundamental accelerator physics phenomena, present the major achievements of operational machines and the key features of near-term collider projects that are currently under development in both high-energy and nuclear physics. We will also briefly overview future project directions in High Energy Physics (HEP) and Nuclear Physics (NP). This course is designed for graduate students and researchers in physics or engineering who want to learn in more detail about the basic concepts and beam physics of particle colliders.

Prerequisites, Objectives, Credit Requirements

- Courses in classical mechanics, electrodynamics, special relativity and physical or engineering mathematics, all at entrance graduate level; and the USPAS course *Fundamentals of Accelerator Physics and Technology with Simulations and Measurements Lab* or equivalent familiarity with accelerators at undergraduate or graduate level are required. It is recommended that students have general familiarity with the following topics: spin dynamics, RF focusing, impedances, instabilities for mono-energetic continuous beam and point-like bunches, Landau damping for a continuous beam, and particle passage through a medium (energy loss, multiple scattering, nuclear scattering).
It is the responsibility of the student to ensure that they meet the course prerequisites or have equivalent experience.

- **Objectives**

On completion of this course, the students are expected to understand the physical principles that make high energy particle colliders function, become familiar with: leading operational and near-future colliders (LHC, SuperKEKB, EIC, etc); the limits of present colliding beam technologies and the promise of future ones, and the issues presented by forefront applications.

- **Credit Requirements**

Students will be evaluated based on the following performances: Homework assignments (60% course grade), Final exam (40% course grade)

Useful Readings and Materials

(Supposed to be provided by the USPAS) *Particle Accelerator Physics* (Fourth Edition) by Helmut Wiedemann, Springer, 2015. A pdf of this book is available for free at <https://www.springer.com/gp/book/9783319183169>.

Perspective students can prepare for the course in advance and/or evaluate the fit of the course to their goals, by studying the following comprehensive review of high energy physics colliders:

V. Shiltsev, F. Zimmermann, “Modern and Future Colliders,” *Rev. Mod. Phys.* 93, 015006 (2021)
<https://journals.aps.org/rmp/abstract/10.1103/RevModPhys.93.015006>

and/or the following freely distributed books:

“Accelerator Physics at the Tevatron Collider,” V. Lebedev and V. Shiltsev, editors, Springer (2014)
<https://link.springer.com/book/10.1007/978-1-4939-0885-1>

“Elementary Particles · Accelerators and Colliders”, S. Myers, H. Schopper, editors Springer (2013)
<https://materials.springer.com/bp/docs/978-3-642-23053-0>

CERN Accelerator Schools, including the latest on Colliders (2018)
<https://cas.web.cern.ch/schools/zurich-2018>

Lecturers and Assistants



Vladimir
Shiltsev



Vadim Ptitsyn
(BNL)



Chuyu Liu
(BNL)

	Mon 01/27	Tue 01/28	Wed 01/29	Thur 01/30	Fri 01/31
09:00-10:00	Intro Lect VS1 Energy & Lumi	Homework reports	Homework reports	Homework reports	Exams
10:00-11:00	Lect VS2 Technology, Hist	Lect VS4 Beam-beam 2	Lect VS6 Circular ee/HFs	Lect VS8 Muon Colliders	Exams
11:00-12:00	Lect VS3 Beam-beam 1	Lect VS5 Other effects	Lect VS7 Tevatron, LHC	Lect VS9 Advanced Colliders	Exams
12:00-13:30	lunch	lunch	lunch	Lunch	Lunch
13:30-14:30	Lect CL1 Linear Optics, x&s coupling	Lect VP1 Motion in RF well, action-phase var	Lect VP3 Lum.evol. Model	Lect VP5 Beam polarization	
14:30-15:30	Lect CL2 chromaticity of FF and its compens.	Lect VP2 Emittance growth IBS, noise, etc	Lect VP4 EIC	Lect VP6 Beam cooling	
15:30-18:00	Recit VS/CL home work assign	Recit VS/VP home work assign	Recit VS/VP home work assign	Recit VS/VP exam probl assign	
19:00-21:00+	self-work w.TA	self-work w.TA	self-work w.TA	prepare for exams	

Main PoC (point of contact)

Chuyu Liu (BNL)
chuyu.liu@gmail.com



U.S. Particle Accelerator School
Education in Beam Physics and Accelerator Technology



Colliders – Lectures VS1-3: Introduction Technologies and History Beam-Beam Effects (1)

Vladimir Shiltsev, Northern Illinois University

part of the “Colliders” class by V.Shiltsev, V.Ptitsyn and C. Liu

US Particle Accelerator School, Jan 27 – Jan 31, 2025

Kinematics of collisions

Two particles $(E_{1,2}, m_{1,2})$ collide at angle θ_c

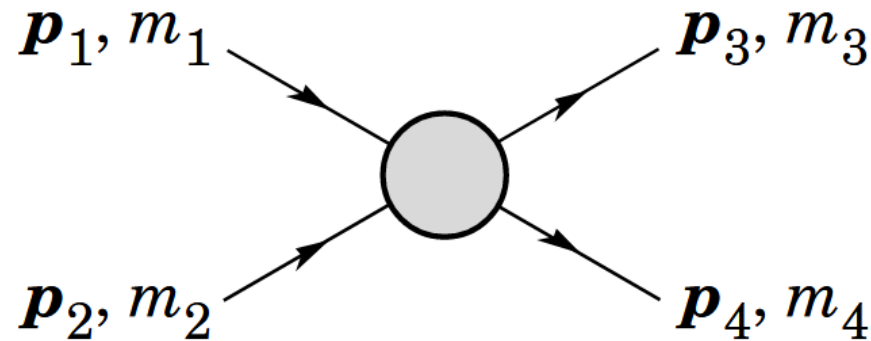
$$E_{cme} = \left(2E_1 E_2 + (m_1^2 + m_2^2)c^4 + 2 \cos \theta_c \sqrt{E_1^2 - m_1^2 c^4} \sqrt{E_2^2 - m_2^2 c^4} \right)^{1/2}$$

One particle stationary ($E_2 = m_2 c^2$) $E_{cme} \approx \sqrt{2Emc^2}$

Both particles move ($E_{1,2} \gg m_{1,2} c^2$) $E_{cme} \approx 2\sqrt{E_1 E_2}$

Gain for ($E = 6500 \text{ GeV}$, $m = 0.936 \text{ GeV}$) is ~ 120 times (0.11 vs 13 TeV)

Lorentz-Invariant Mandelstam Variables



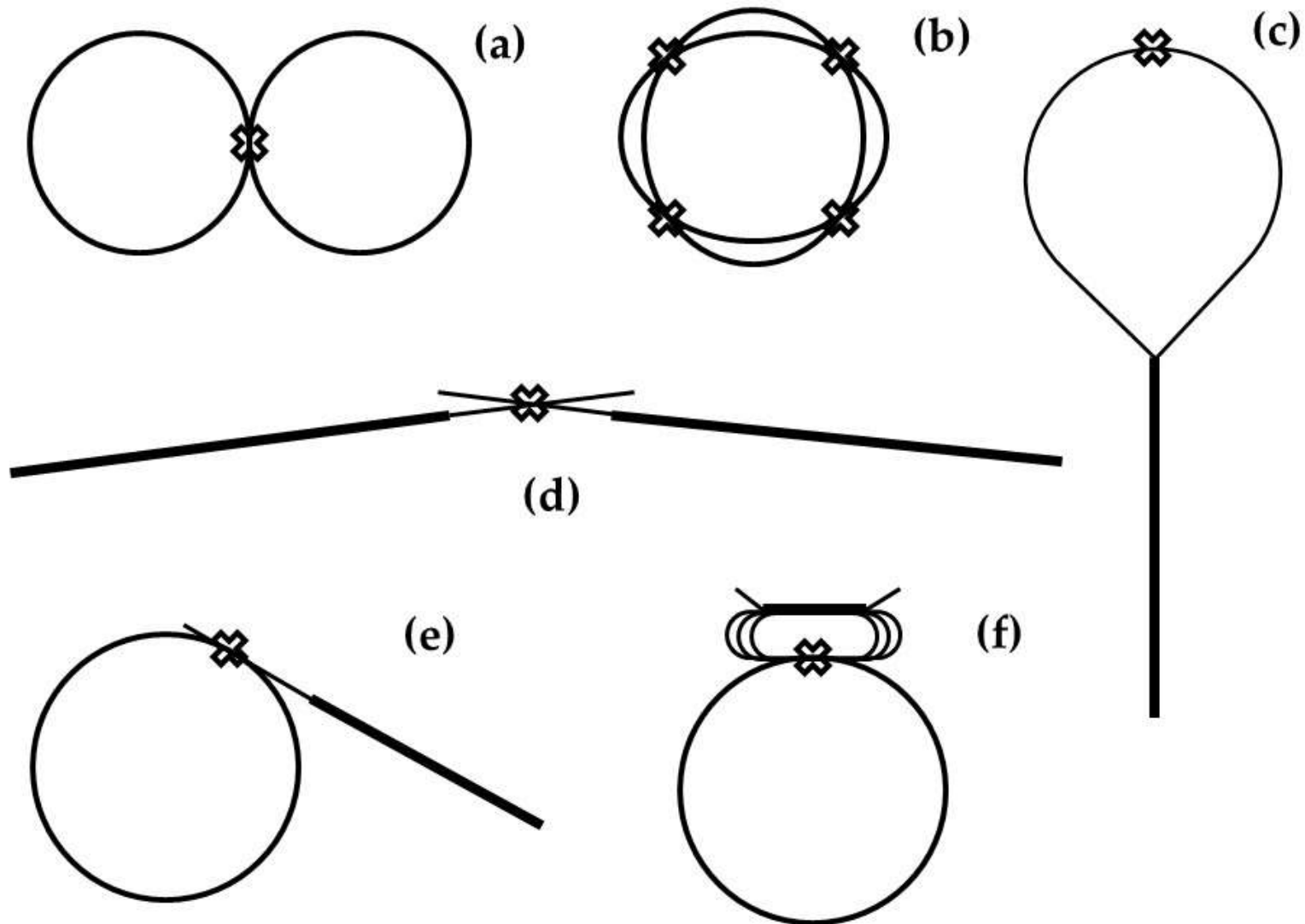
$$s = (p_1 + p_2)^2 = (p_3 + p_4)^2$$
$$= m_1^2 + 2E_1 E_2 - 2\mathbf{p}_1 \cdot \mathbf{p}_2 + m_2^2$$

} $s = E_{cme}^2$

$$t = (p_1 - p_3)^2 = (p_2 - p_4)^2$$
$$= m_1^2 - 2E_1 E_3 + 2\mathbf{p}_1 \cdot \mathbf{p}_3 + m_3^2$$

$$u = (p_1 - p_4)^2 = (p_2 - p_3)^2$$
$$= m_1^2 - 2E_1 E_4 + 2\mathbf{p}_1 \cdot \mathbf{p}_4 + m_4^2$$

Types of colliding beam facilities



Colliders Landscape

58 years since 1st collisions

- Spring 1964 AdA and VEP-1

31 operated since

- (see RMP review)

7 in operation now

- see next slides

2 under construction

- NICA (2025) and EIC (2032)

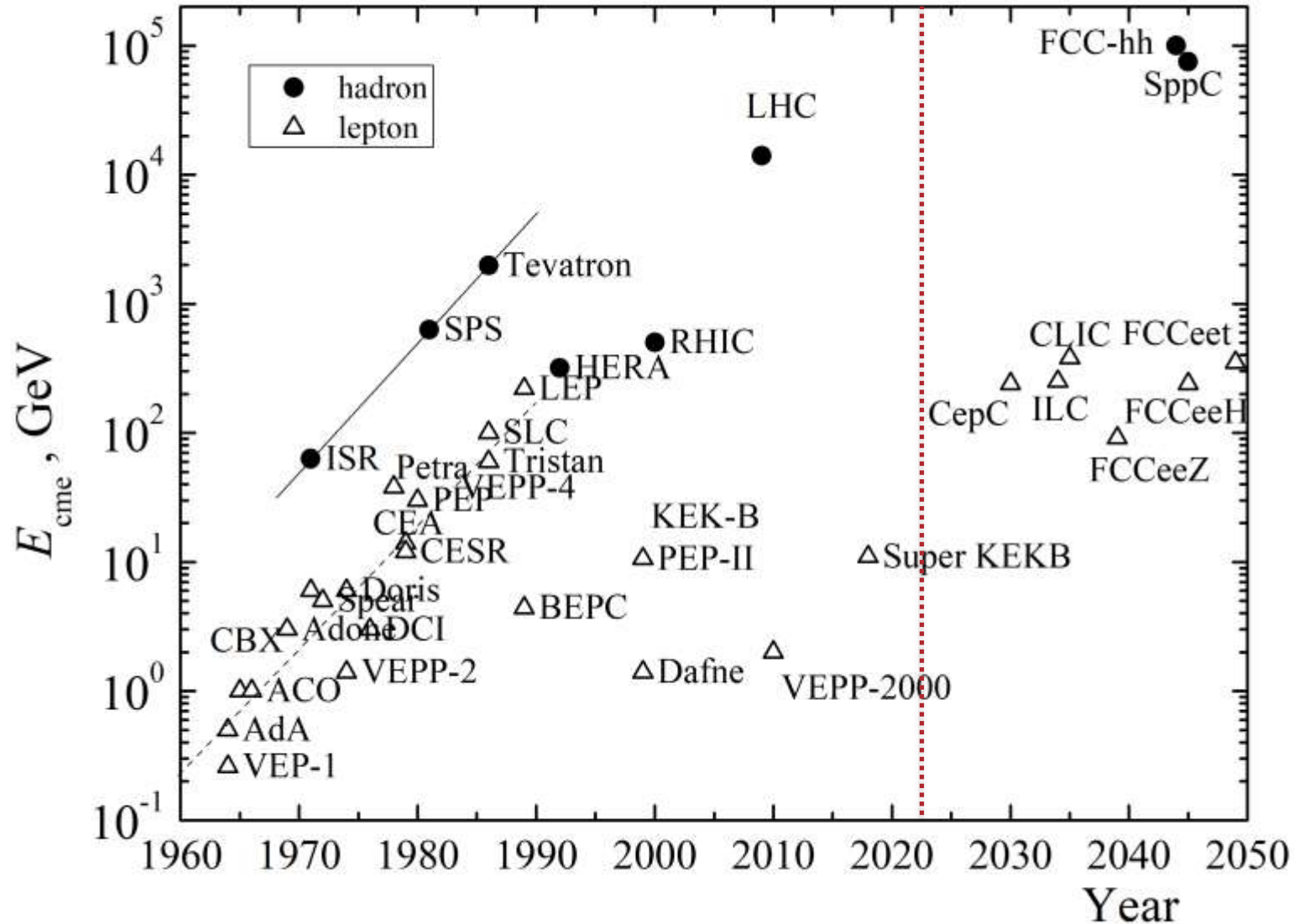
At least 2 more types needed

- Higgs/Electroweak factories
- Frontier $E \gg$ LHC

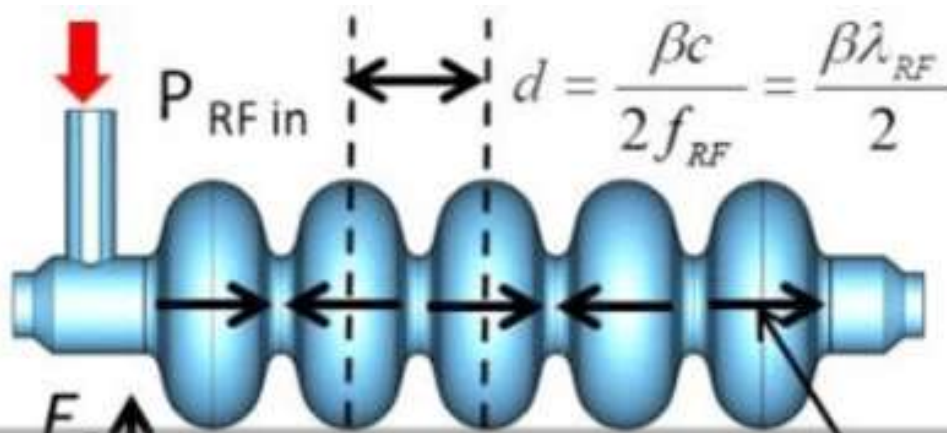
	Species	E_b , GeV	C , m	\mathcal{L}_{peak}^{max}	Years
AdA	e^+e^-	0.25	4.1	10^{25}	1964
VEP-1	e^-e^-	0.16	2.7	5×10^{27}	1964-68
CBX	e^-e^-	0.5	11.8	2×10^{28}	1965-68
VEPP-2	e^+e^-	0.67	11.5	4×10^{28}	1966-70
ACO	e^+e^-	0.54	22	10^{29}	1967-72
ADONE	e^+e^-	1.5	105	6×10^{29}	1969-93
CEA	e^+e^-	3.0	226	0.8×10^{28}	1971-73
ISR	pp	31.4	943	1.4×10^{32}	1971-80
SPEAR	e^+e^-	4.2	234	1.2×10^{31}	1972-90
DORIS	e^+e^-	5.6	289	3.3×10^{31}	1973-93
VEPP-2M	e^+e^-	0.7	18	5×10^{30}	1974-2000
VEPP-3	e^+e^-	1.55	74	2×10^{27}	1974-75
DCI	e^+e^-	1.8	94.6	2×10^{30}	1977-84
PETRA	e^+e^-	23.4	2304	2.4×10^{31}	1978-86
CESR	e^+e^-	6	768	1.3×10^{33}	1979-2008
PEP	e^+e^-	15	2200	6×10^{31}	1980-90
$SppS$	$p\bar{p}$	455	6911	6×10^{30}	1981-90
TRISTAN	e^+e^-	32	3018	4×10^{31}	1987-95
Tevatron	$p\bar{p}$	980	6283	4.3×10^{32}	1987-2011
SLC	e^+e^-	50	2920	2.5×10^{30}	1989-98
LEP	e^+e^-	104.6	26659	10^{32}	1989-2000
HERA	ep	30+920	6336	7.5×10^{31}	1992-2007
PEP-II	e^+e^-	3.1+9	2200	1.2×10^{34}	1999-2008
KEKB	e^+e^-	3.5+8.0	3016	2.1×10^{34}	1999-2010
VEPP-4M	e^+e^-	6	366	2×10^{31}	1979-
BEPC-I/II	e^+e^-	2.3	238	10^{33}	1989-
DAΦNE	e^+e^-	0.51	98	4.5×10^{32}	1997-
RHIC	p, i	255	3834	2.5×10^{32}	2000-
LHC	p, i	6500	26659	2.1×10^{34}	2009-
VEPP2000	e^+e^-	1.0	24	4×10^{31}	2010-
S-KEKB	e^+e^-	7+4	3016	8×10^{35} *	2018-

Colliders: Energy

FIG. 2. Center of mass energy reach of particle colliders vs their start of operation. Solid and dashed lines indicate a ten-fold increase per decade for hadron (circles) and lepton (triangles) colliders (adapted from [37]).

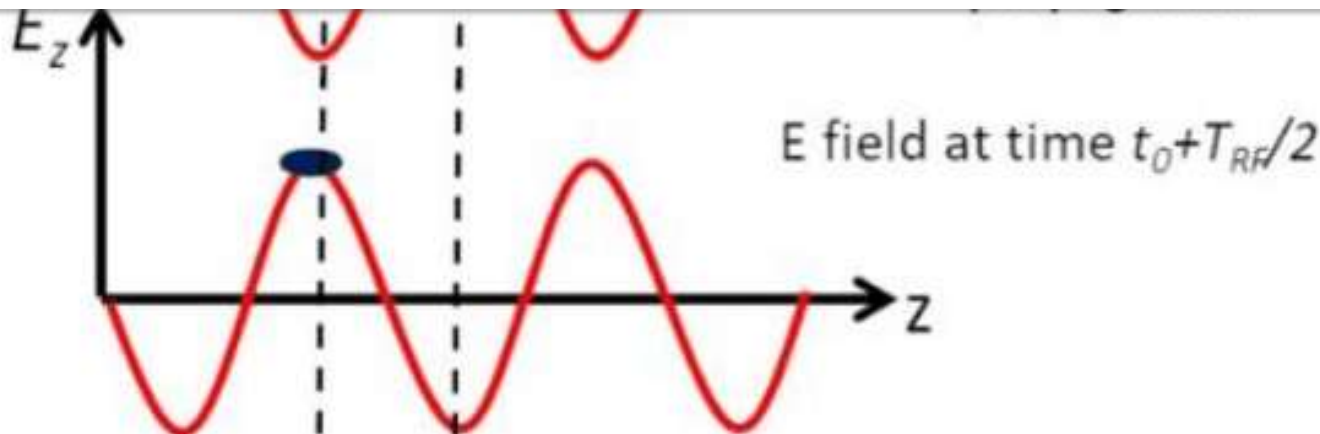


Only Electric Field Boosts Energy



$$\omega_{rf} = 2\pi f_{rf}$$

$$\Delta E_b = e \int E v dt = e V_{acc} \cos(\omega_{rf} t + \phi)$$



How much power is needed

$$P_{\text{rf}} = P_b + P_{\text{loss}} = I_b \Delta E_b + \frac{V_{\text{acc}}^2}{2R_s}$$

Where “*shunt impedance*”: $R_s = Q(R/Q)$

“Quality factor”

~10⁴ for Copper 300K

10⁽⁹⁻¹⁰⁾ for SC Nb cavities

“R/Q” cavity geometry factor

~100 for “open” elliptic cavities

196 Ohm for “pillbox” cavity

RF Cavities

LEP-I 352 MHz

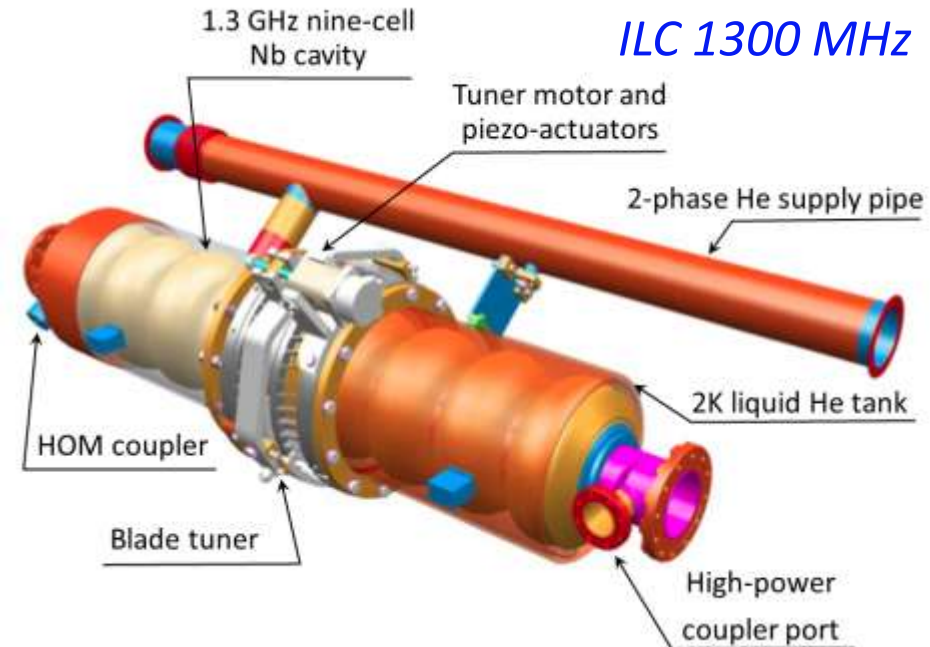
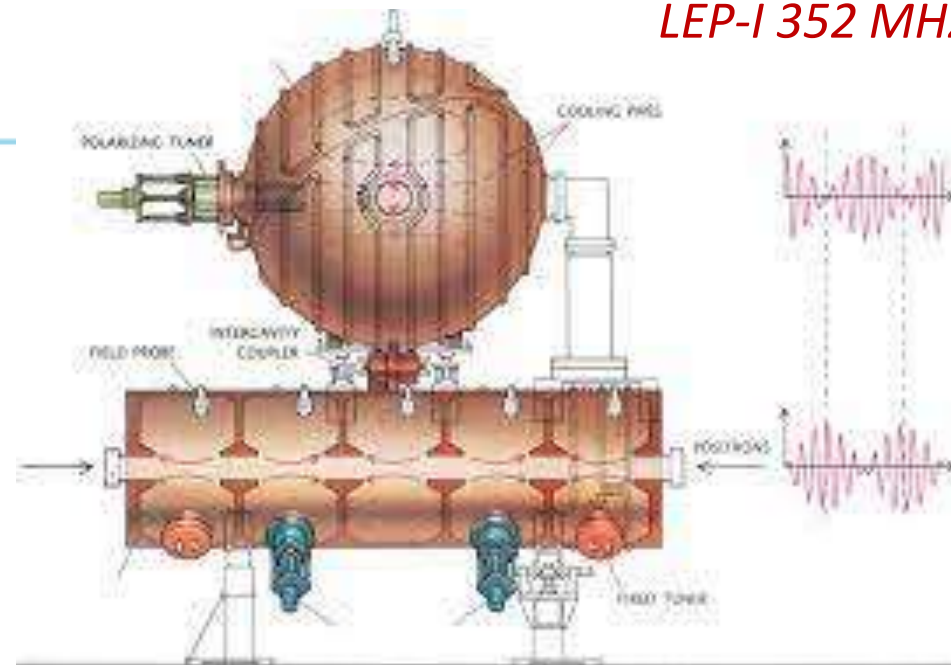
Resonant cavity, eg “pill-box”:

$$\omega_c = \frac{2.405 c}{R_c}$$

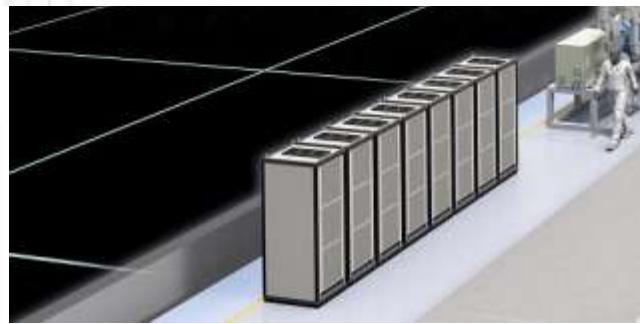
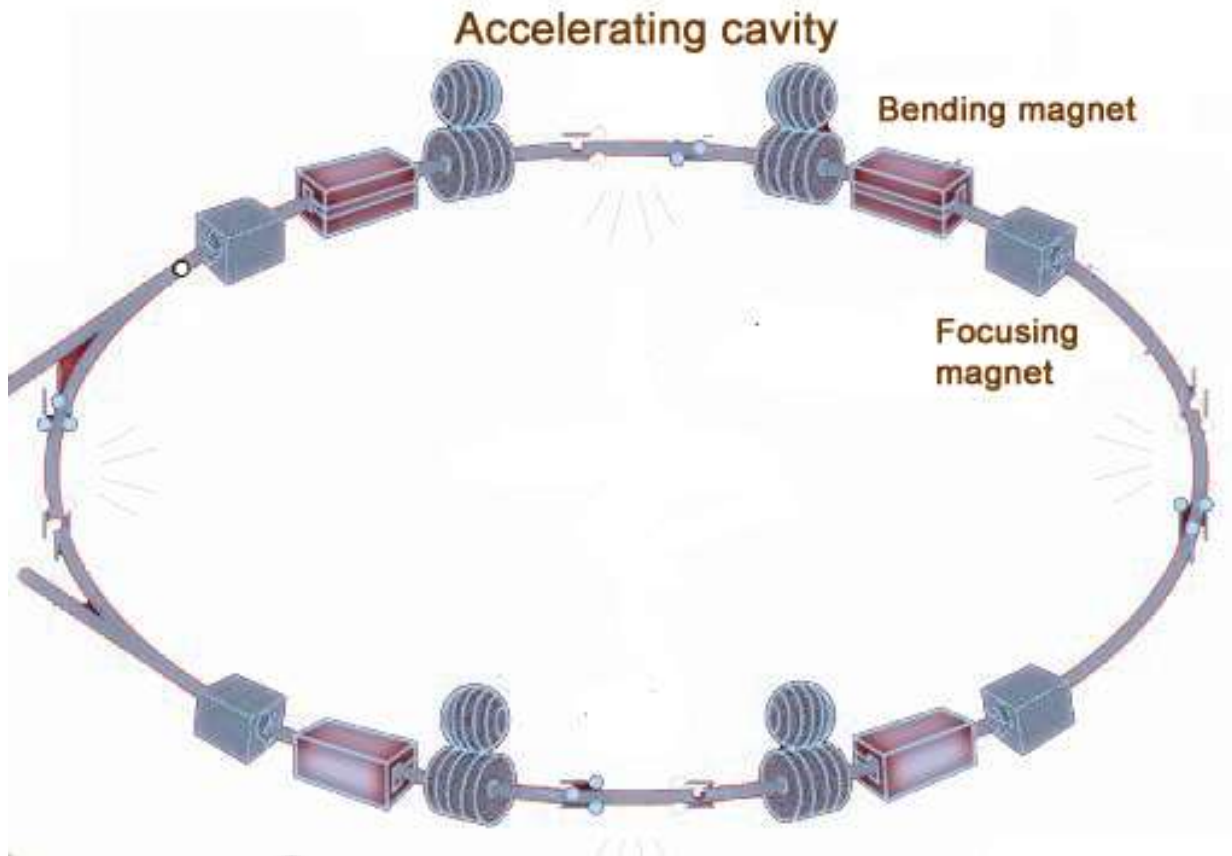
$R=10\text{cm}$ at $f_{RF}=1.14\text{ GHz}$

Max gradient/voltage per cavity:

- *Is determined by RF power and shunt impedance*
- *Is limited by breakdown or dark current radiation or loss of superconductivity*
 - depends on frequency, CW or pulse duration, geometry, material, temperature, etc
- *Max ~100 MV/m in normal-conducting cavities at 12 GHz*
- *Max ~31.5 MV/m SRF cavities 1.3GHz*

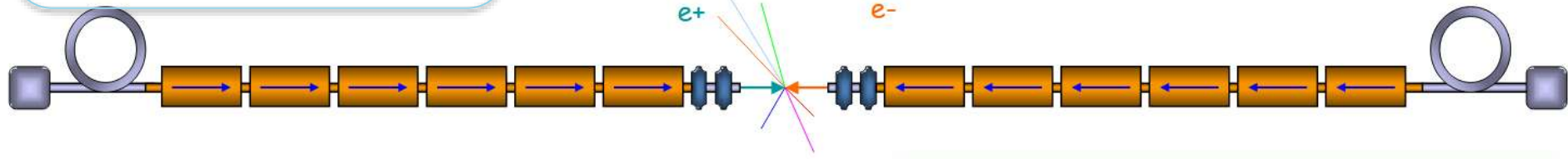


Rings vs Linacs



$$I_b \Delta E_b + \frac{V_{acc}^2}{2R_s}$$

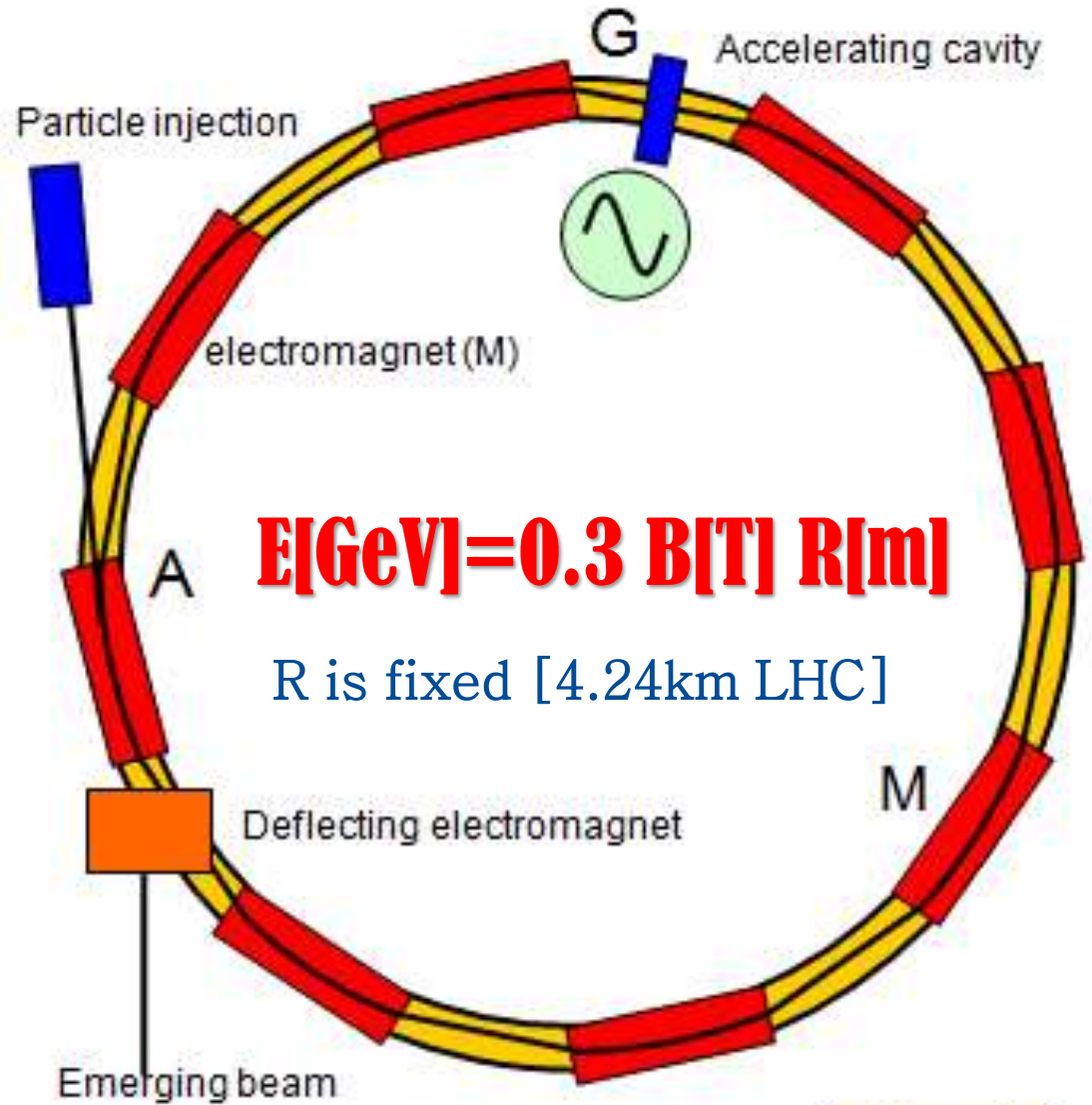
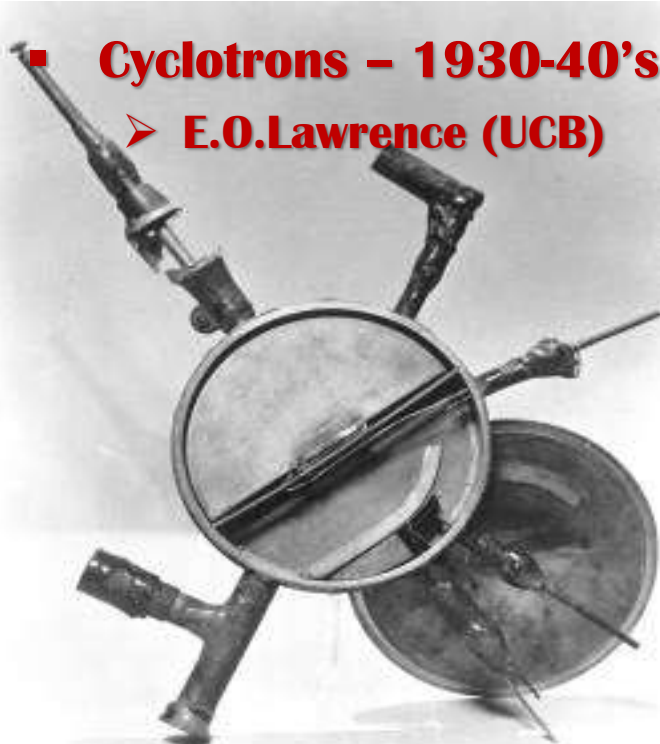
lower V_{acc} if you can



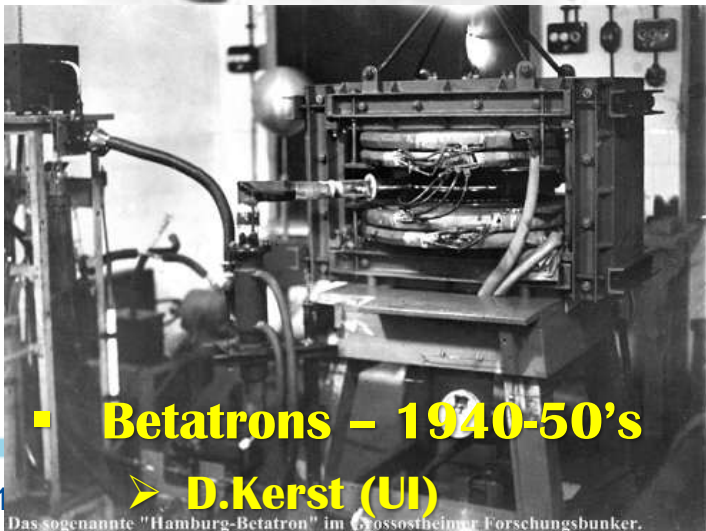
Types of Circular Accelerators

Synchrotrons (Tevatron, LHC)

- **Cyclotrons – 1930-40's**
 - **E.O.Lawrence (UCB)**



- **Betatrns – 1940-50's**
 - **D.Kerst (UI)**



Das sogenannte "Hamburg-Betatron" im Grossschneimer Forschungsbunker.

Figure 1

Highest Energy = Highest Field SC Magnets

4.5T

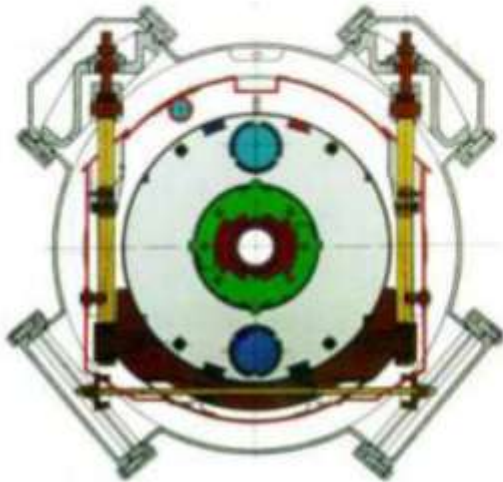
Tevatron,
6 m, 76 mm
774 dipoles



4.5 K He, NbTi
+ warm iron
small He-plant

5.3T

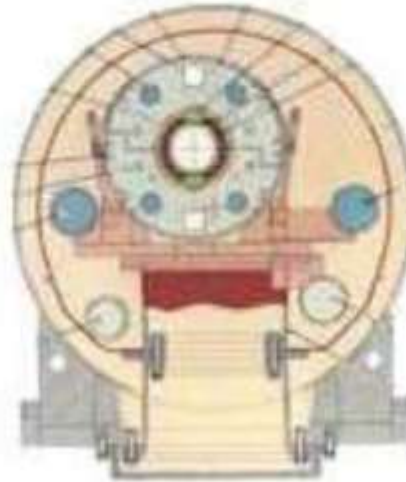
HERA,
9 m, 75 mm
416 dipoles



NbTi cable
cold iron
Al collar

3.5T

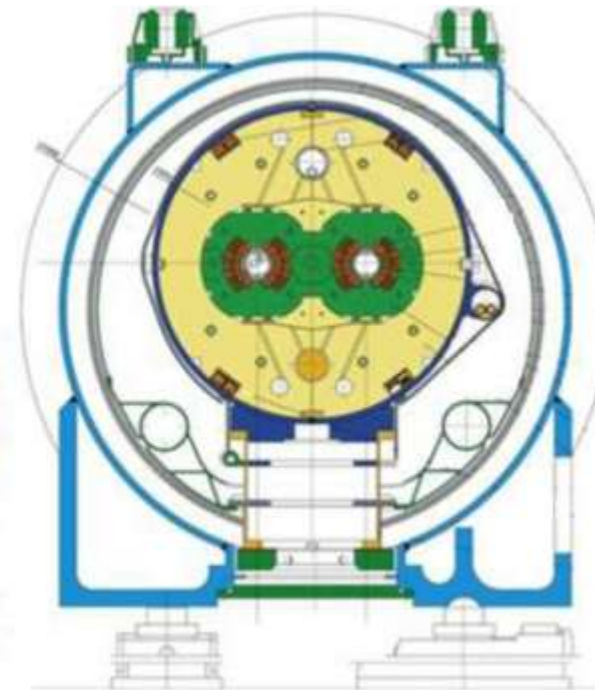
RHIC,
9 m, 80 mm
264 dipoles



NbTi cable
simple &
cheap

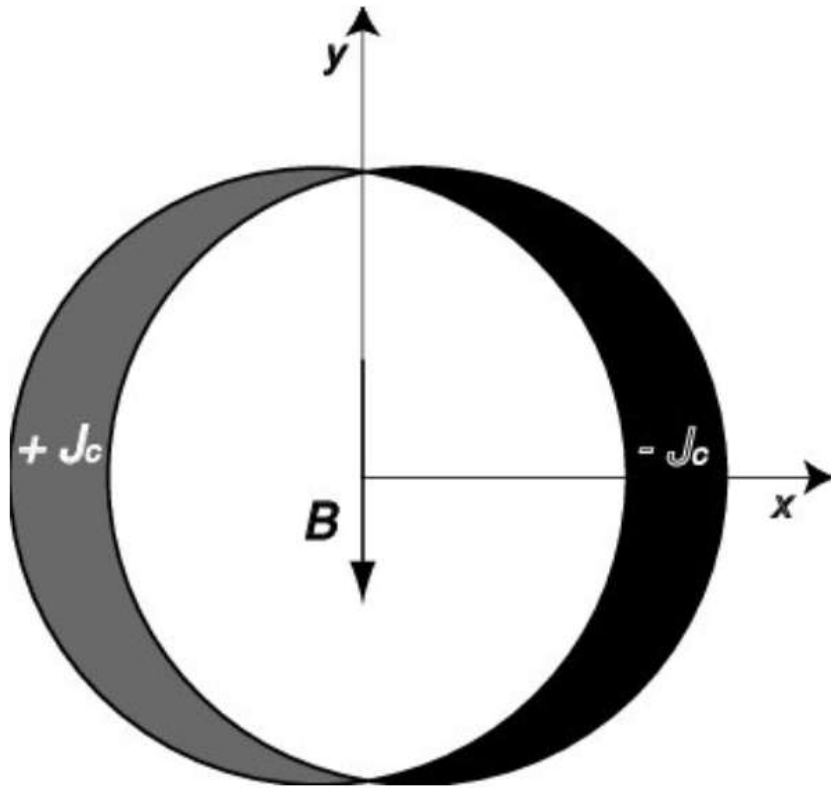
8.3T

LHC,
15 m, 56 mm
1276 dipoles



NbTi cable
2K He
two bores

Key for Magnets: Current Density



Generation of a pure dipole
by a $\cos \theta$ current distribution

Scaling: $B_{max} \sim J/A_{aperture}$
(assume all A is filled by conductor)

$J \sim j(\text{current density}) \times A^2$

$$B_{max} \sim j \times A$$

but Cost $\sim A^2$ (cost of needed
conductor) \times length $\sim A^2/B \sim$

$$\sim A/j$$

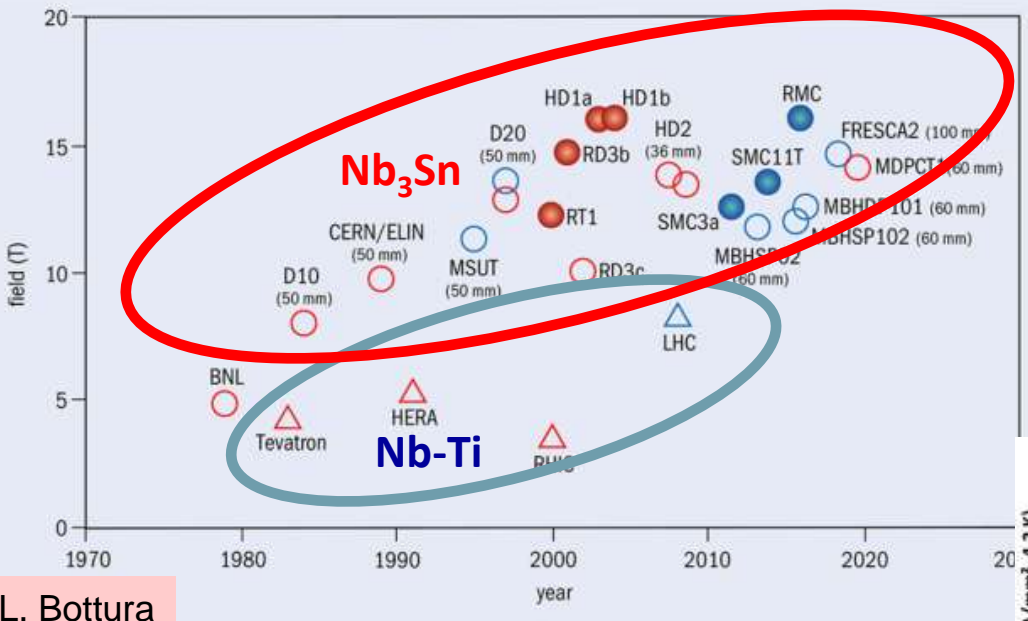
Therefore, high(est) current density
is needed to maximize B-field and
minimize Cost

- For room temperature copper
 $j \sim (1-10) \text{ A/mm}^2$
- For superconductors $\rightarrow \text{kA/mm}^2$

SC Magnets: Fields and Current Densities

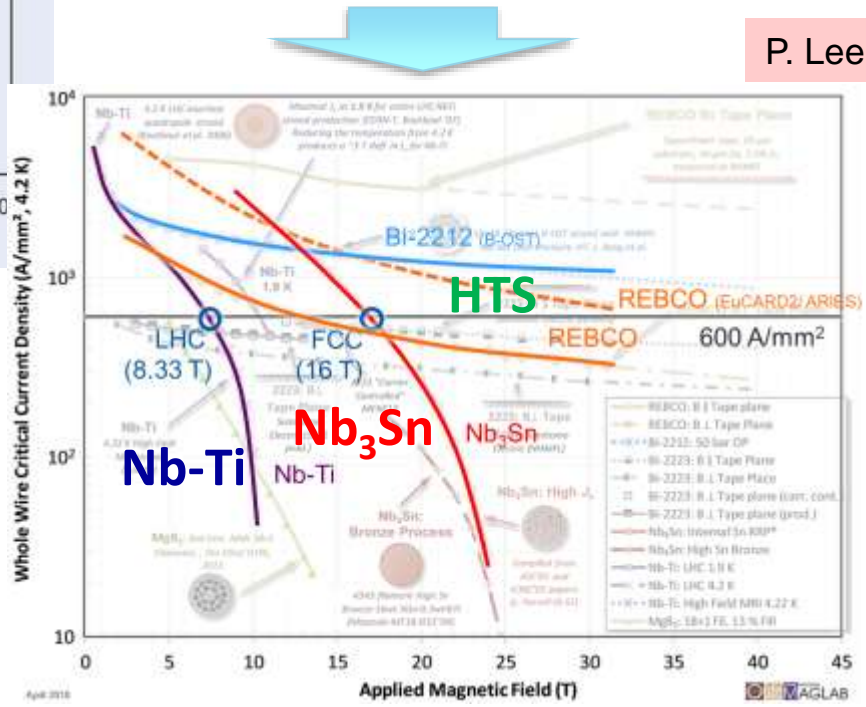
Superconducting wire critical current density versus magnetic field: three main materials **Nb-Ti**, **Nb₃Sn**, HTS

P. Lee



L. Bottura

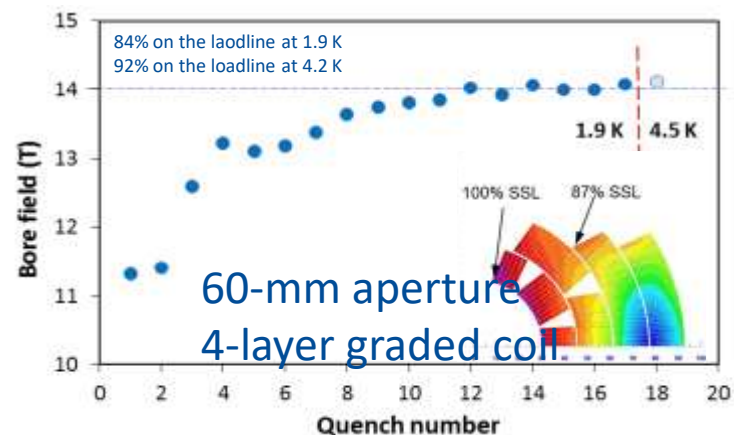
Record fields attained with dipole magnets of various configurations and dimensions, and either at liquid (4.2 K, red) or superfluid (1.9 K, blue) helium temperature.



SC Accelerator Magnets: Current Record 14.5T

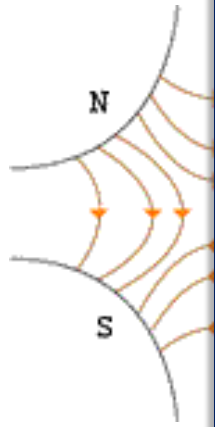


$\cos\theta$ dipole



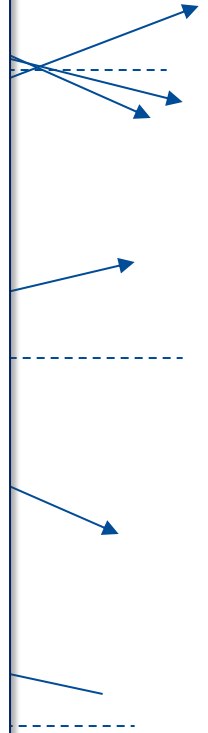
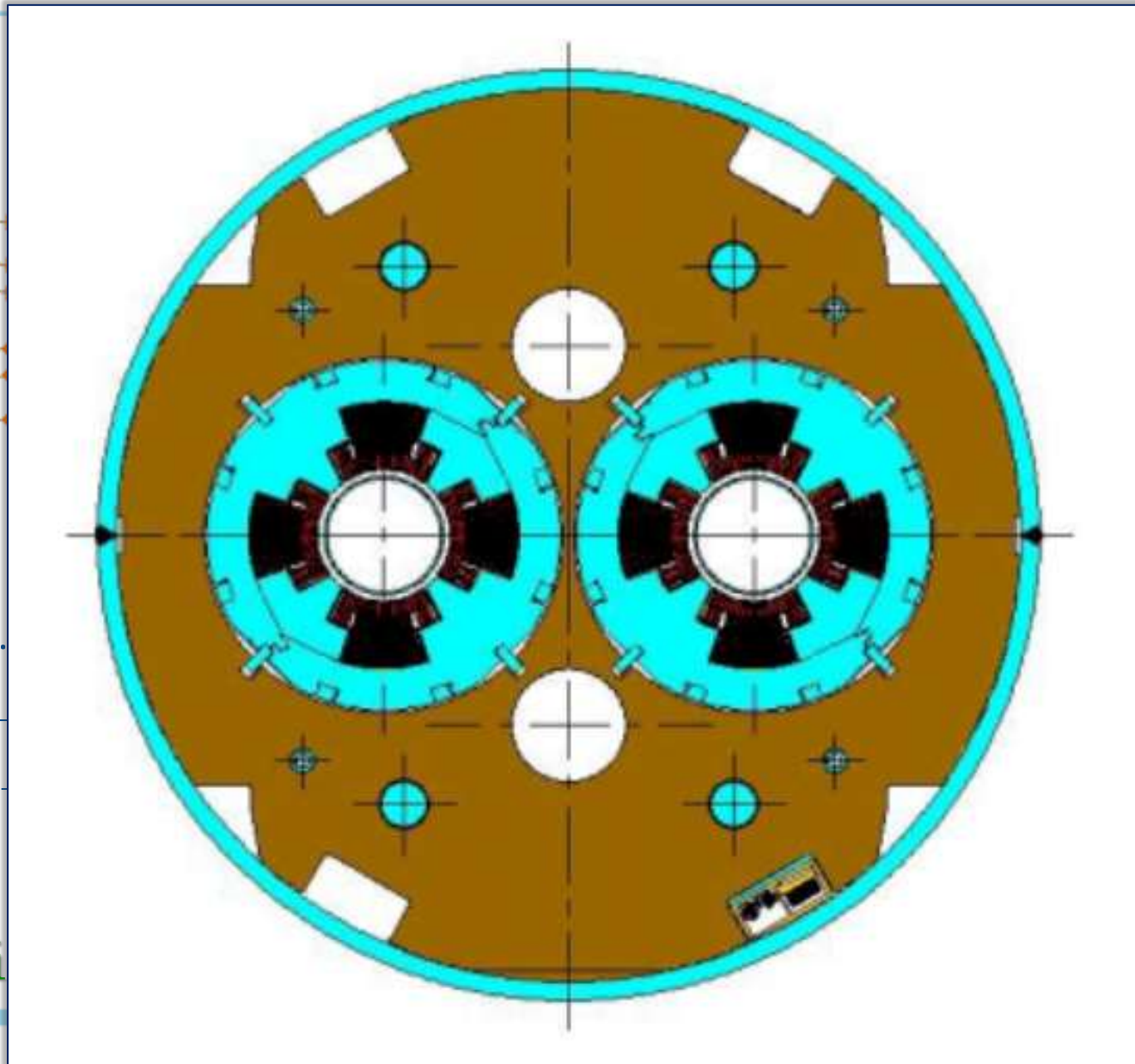
- 15 T dipole demonstrator
- Staged approach: In first step pre-stressed for 14 T
- Second test in June 2020 with additional pre-stress reached 14.5 T

Focusing Beams with Quadrupole Magnets



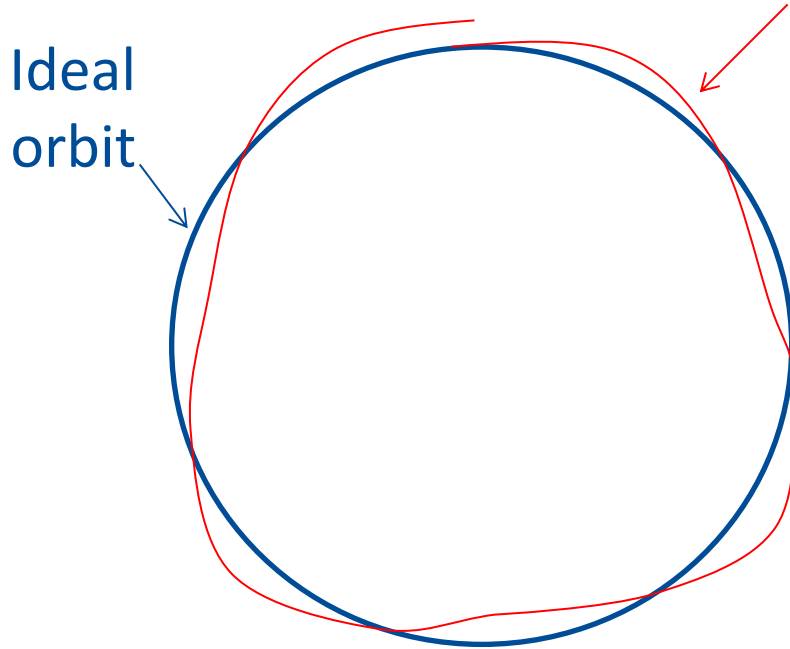
Luckily.

...pair



) cell"

Betatron Oscillations, Tune



Particle trajectory

- As particles go around a ring, they will undergo a number of betatron oscillations ν (sometimes Q) given by

$$\nu = \frac{1}{2\pi} \oint \frac{ds}{\beta(s)}$$

- This is referred to as the “tune”

- We can generally think of the tune in two parts:

Integer : magnet/aperture optimization \rightarrow **64.31** \leftarrow **Fraction:** Beam Stability

see lectures VL1-2

Particle Equations of Motion (1)

$$x'' + K_x x = 0, \quad \text{with} \quad K_x \equiv \frac{e}{p} \frac{\partial B_y}{\partial x} + \frac{1}{\rho^2},$$

$$y'' + K_y y = 0, \quad \text{with} \quad K_y \equiv -\frac{e}{p} \frac{\partial B_y}{\partial x},$$

$$z' = -x/\rho,$$

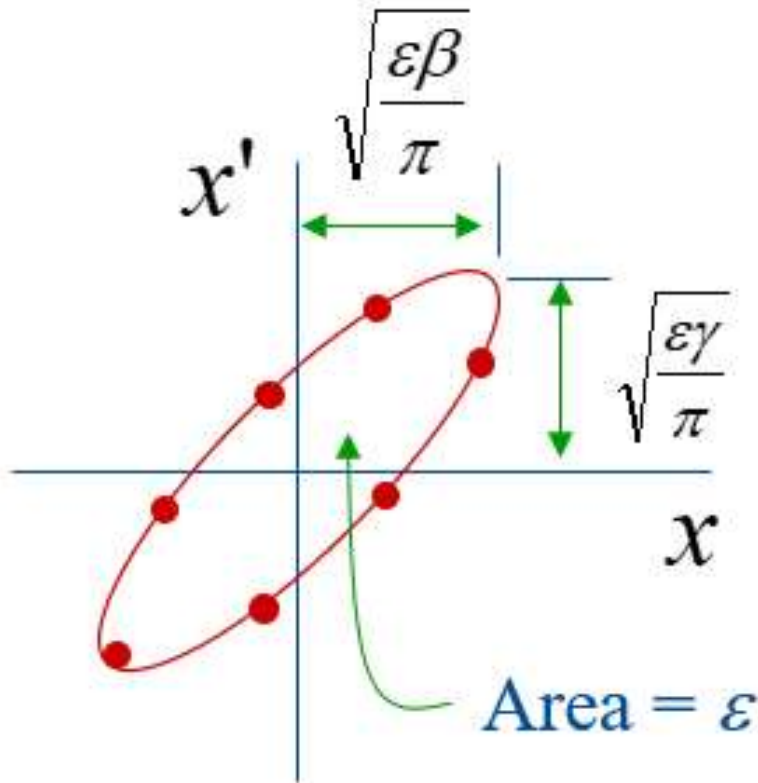
Solution:

$$x(s) = \sqrt{2J_x \beta_x} \cos \psi_x, \quad d\psi_x/ds = 1/\beta_x,$$

$$x'(s) = -\sqrt{\frac{2J_x}{\beta_x}} [\alpha \cos \psi_x + \sin \psi_x],$$

So, tune: $Q_x = \frac{1}{2\pi} \oint d\psi_x = \frac{1}{2\pi} \oint \frac{ds}{\beta_x(s)}$

Key beam parameter: Emittance



$$\gamma_T x^2 + 2\alpha_T x x' + \beta_T x'^2 = \frac{\epsilon}{\pi}$$

Twiss
Parameters

As a particle returns to the same point on subsequent revolutions, it will map out an ellipse in phase space – see **lectures VL1-2**

- Product size x angle $X_{rms} \times X'_{rms}$ is called **emittance**
- **Emittance** \times **gamma** is adiabatic invariant
- **Luminosity (tbd)** $\sim 1/\epsilon$

Most Important Equations

normalized emittance

$$\varepsilon_n(x,y) = \gamma \cdot \sigma_{x,y} \sigma'_{x,y}$$

$$\sigma_{x,y} = \sqrt{\frac{\varepsilon_n \cdot \beta_{x,y}}{\gamma}}$$

rms beam size

$$\sigma'_{x,y} = \sqrt{\frac{\varepsilon_n}{\gamma \cdot \beta_{x,y}}} = \frac{\sigma_{x,y}}{\beta_{x,y}}$$

rms beam
angular spread

Particle Equations of Motion (2)

Beta-functions are defined by

$$2\beta_x\beta_x'' - \beta_x'^2 + 4\beta_x^2K_x = 4$$

Eg symmetric solution in free space ($K=0$):

$$\beta_x(s) = \beta_x^* + \frac{s^2}{\beta_x^*}$$

Also, note that nonlinear fields on beam orbit add complexity:

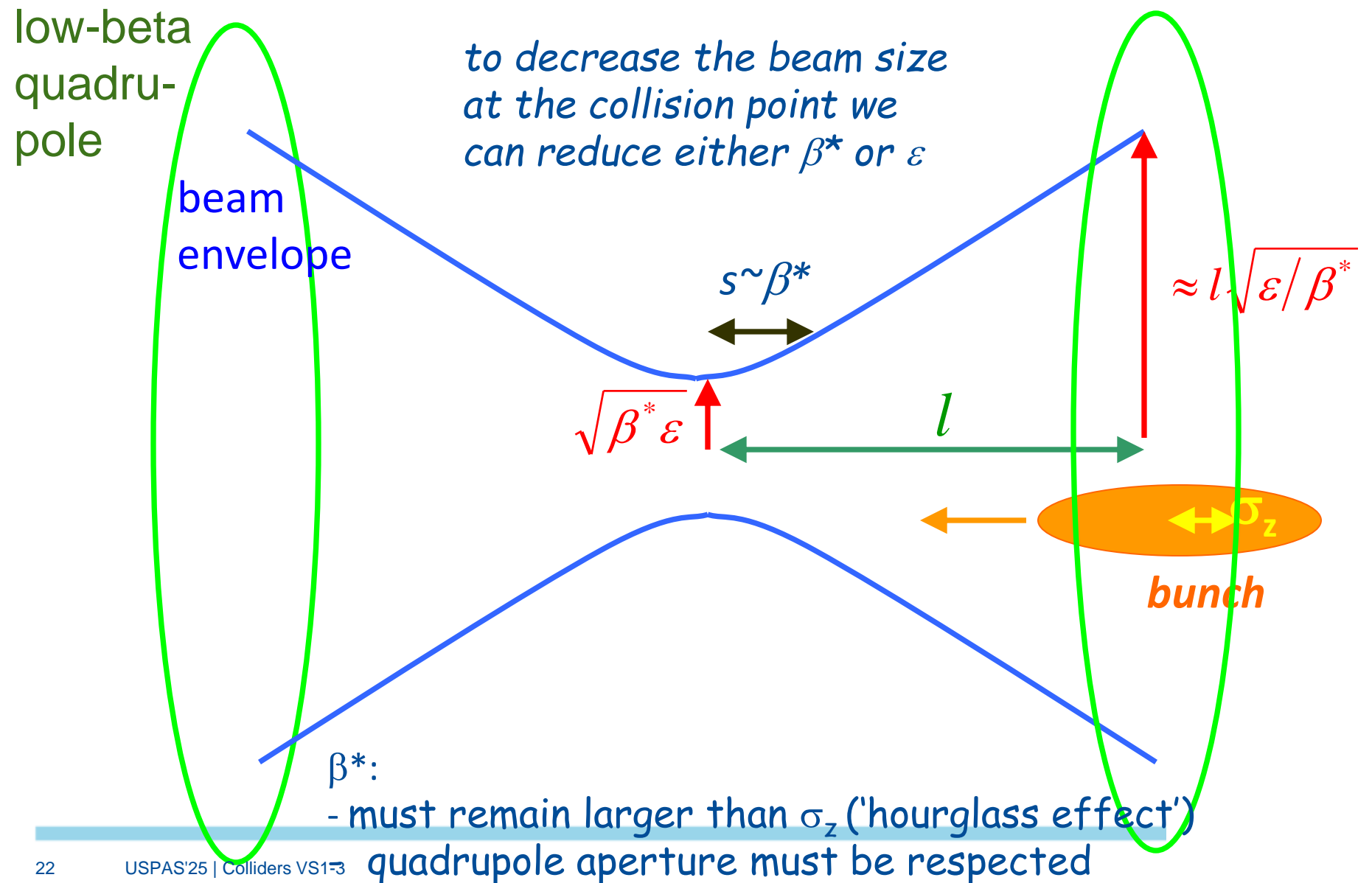
$$B_y + iB_x = \sum_{n=1}^{\infty} (B_n + iA_n)(x + iy)^{n-1}$$

$n=1$ dipole
 $n=2$ quadrupole
 $n=3$ octupole
 $n=4,5,6\dots$

especially at resonant frequencies

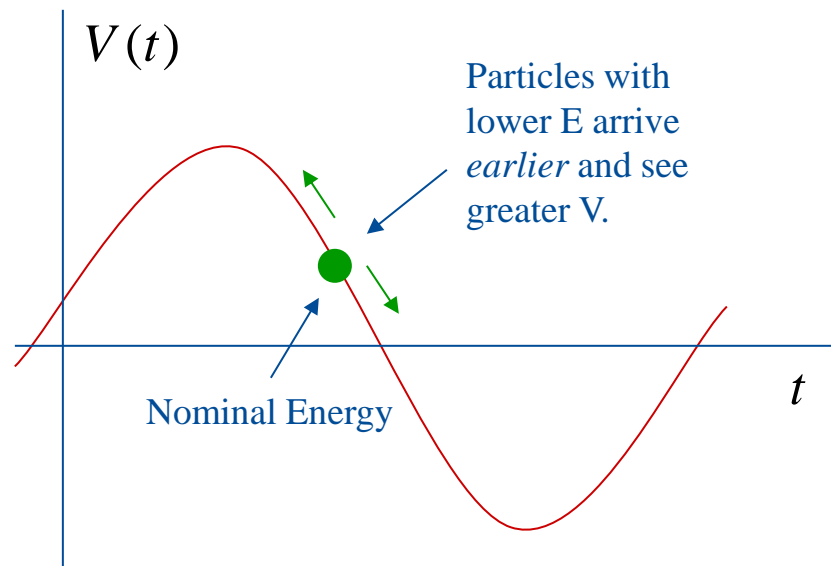
$$kQ_x + lQ_y = m, \text{ where } k, l, \text{ and } m \text{ are integers.}$$

Collider Spot Size



Longitudinal Motion: Phase Stability

Particles are typically accelerated by radiofrequency (“RF”) structures. Stability depends on particle arrival time relative to the RF phase. Note: the speed is **fixed** = speed of light, so time of arrival depends only on the energy (in the bunch – energy deviation wrt “reference central particle”)



see lecture VL6

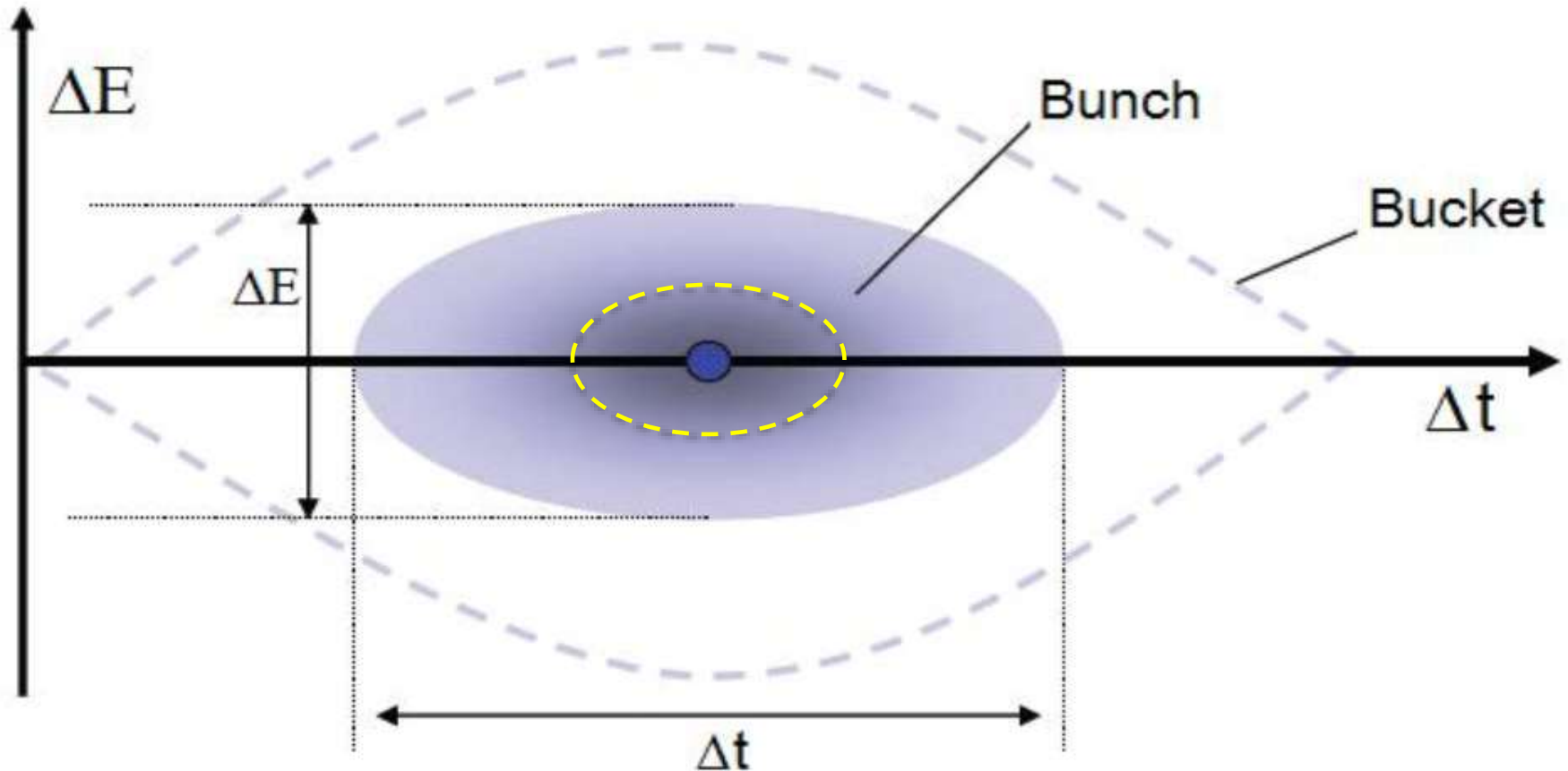
Example: LHC RF Frequency 400 MHz (35640 times revolution frequency)

• RF Voltage = 8 cavities x 2 MV = 16 MV / turn (max)

In collisions $dE/dn = 0$ V/turn (synchronous phase ~ 0)

Slow energy-position oscillations (23 Hz or ~ 500 turns)

rms energy spread $1.3e-4$ (1GeV) rms bunch length ~ 8 cm



Scales of Time-scales/Frequencies

Longitudinal oscillations are the slowest of all the periodic processes that take place in the accelerators. For example, in the LHC, the frequency of synchrotron oscillations at the top energy of 7 TeV is about $f_s = 23$ Hz, the revolution frequency is $f_{\text{rev}} = 11.3$ kHz, the frequency of betatron oscillations is about $Q_{x,y}f_{\text{rev}} = 680$ kHz, and the rf frequency is $f_{\text{rf}} = 400.8$ MHz ($h = 35\,640$).

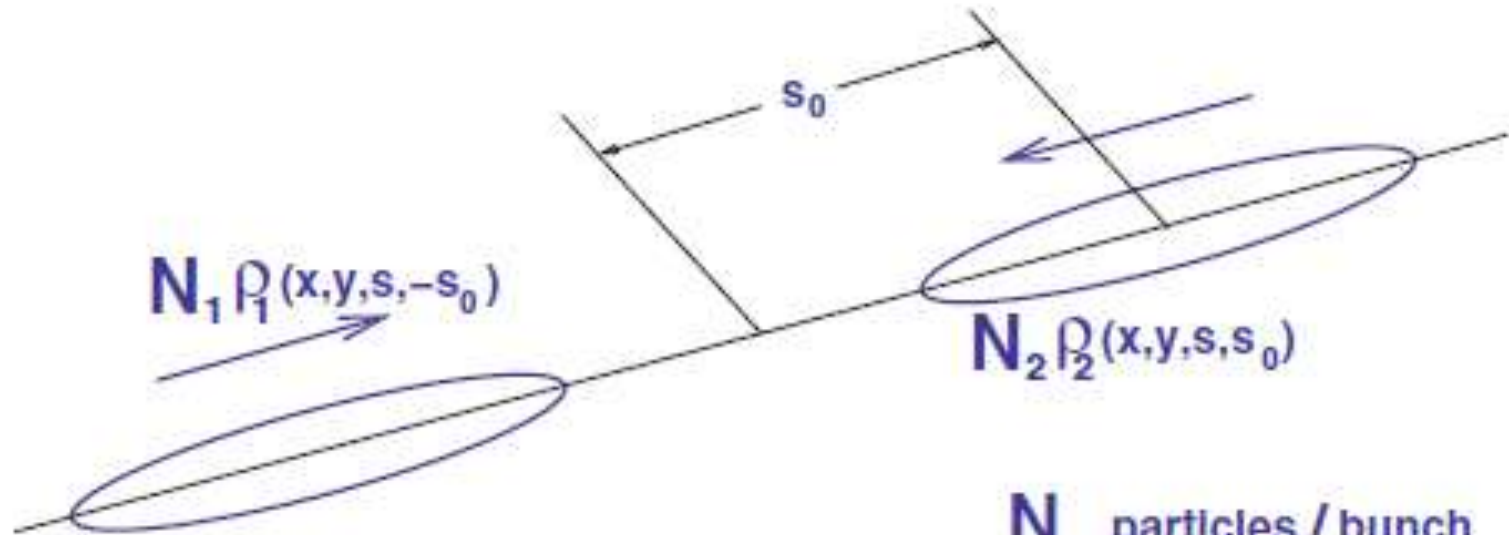
...even slower might be operational processes :

- injection/extraction (1/sec... 1/min... 1/hr ... 1/day)
- beam cooling (sometimes - hours)
- luminosity decay (min... days)

BREAK (!...?)

Luminosity

$$N_{\text{exp}} = \sigma_{\text{exp}} \cdot \int \mathcal{L}(t) dt.$$



N particles / bunch

ρ density \neq const.

For (same size) Gaussian bunches:

$$\mathcal{L} = f_{\text{coll}} \frac{N_1 N_2}{4\pi \sigma_x^* \sigma_y^*}$$

Luminosity: Unequal Bunches

$$\rho_{iz}(z) = \frac{1}{\sigma_z \sqrt{2\pi}} \exp\left(-\frac{z^2}{2\sigma_z^2}\right) \quad \text{where } i = 1, 2, \quad z = x, y$$

$$\rho_s(s \pm s_0) = \frac{1}{\sigma_s \sqrt{2\pi}} \exp\left(-\frac{(s \pm s_0)^2}{2\sigma_s^2}\right)$$

$$K = \sqrt{(\vec{v}_1 - \vec{v}_2)^2 - (\vec{v}_1 \times \vec{v}_2)^2/c^2}$$

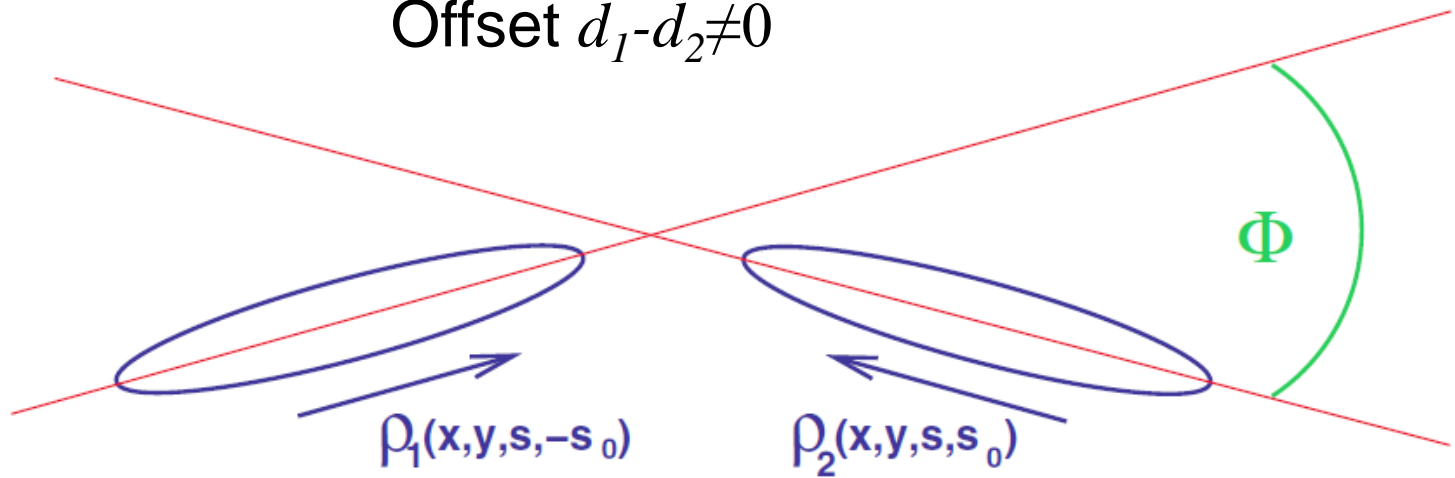
$$\mathcal{L} \propto K N_1 N_2 \cdot \int \int \int \int_{-\infty}^{+\infty} \rho_1(x, y, s, -s_0) \rho_2(x, y, s, s_0) dx dy ds ds_0$$

yields:

$$\mathcal{L} = \frac{N_1 N_2 f_c}{2\pi \sqrt{\sigma_{1x}^2 + \sigma_{2x}^2} \sqrt{\sigma_{2y}^2 + \sigma_{2y}^2}}$$

Correction for Crossing Angle and Offset

Offset $d_1 - d_2 \neq 0$



$$\mathcal{L} = \frac{N_1 N_2 f N_b}{4\pi \sigma_x \sigma_y} \cdot W \cdot e^{\frac{B^2}{A}} \cdot S$$

where:

$$A = \frac{\sin^2 \frac{\phi}{2}}{\sigma_x^2} + \frac{\cos^2 \frac{\phi}{2}}{\sigma_s^2}$$

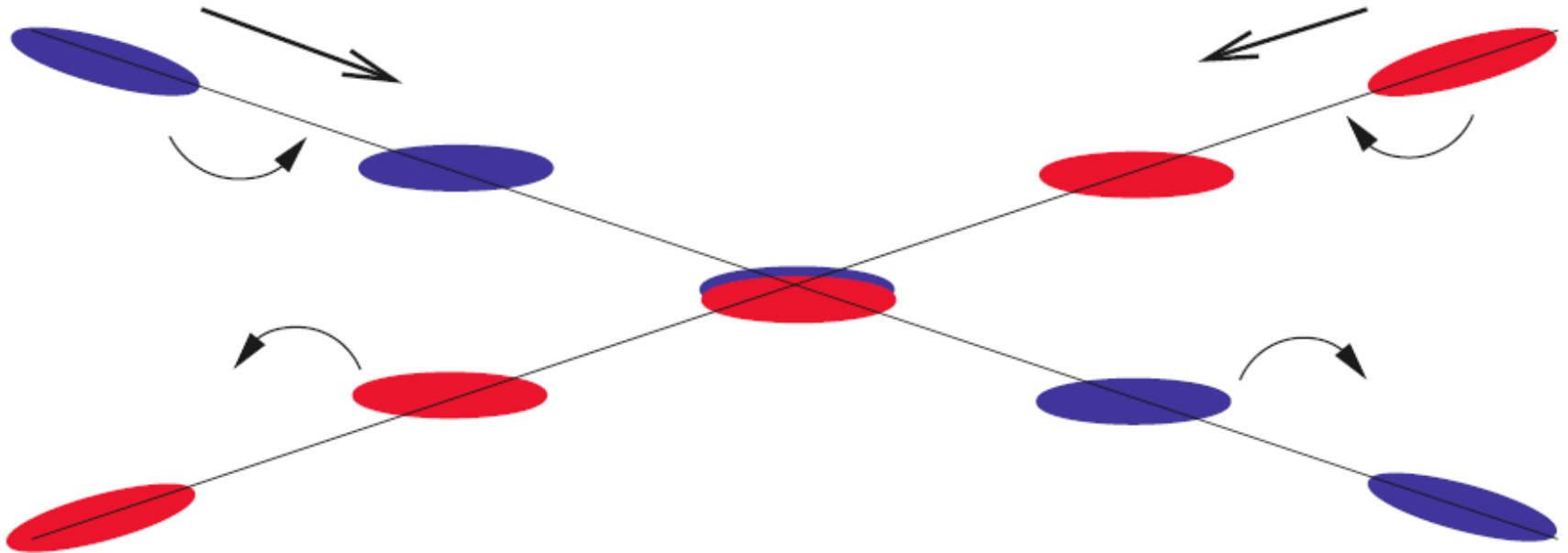
$$B = \frac{(d_2 - d_1) \sin(\phi/2)}{2\sigma_x^2}$$

$$W = e^{-\frac{1}{4\sigma_x^2} (d_2 - d_1)^2}$$

$$S = \frac{1}{\sqrt{1 + \left(\frac{\sigma_s}{\sigma_x} \tan \frac{\phi}{2}\right)^2}} \approx \frac{1}{\sqrt{1 + \left(\frac{\sigma_s}{\sigma_x} \frac{\phi}{2}\right)^2}}$$

“Crab Crossing” Collisions

Head-tail rotation by RF dipole deflectors



Note: either the crossing angle or amplitude of the crabbing affect instantaneous luminosity → can be used for “luminosity leveling”

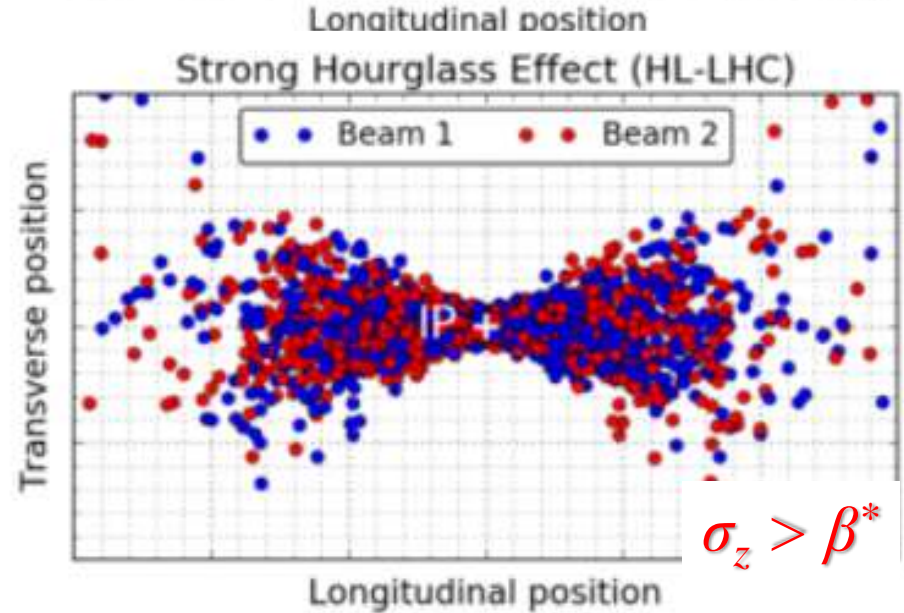
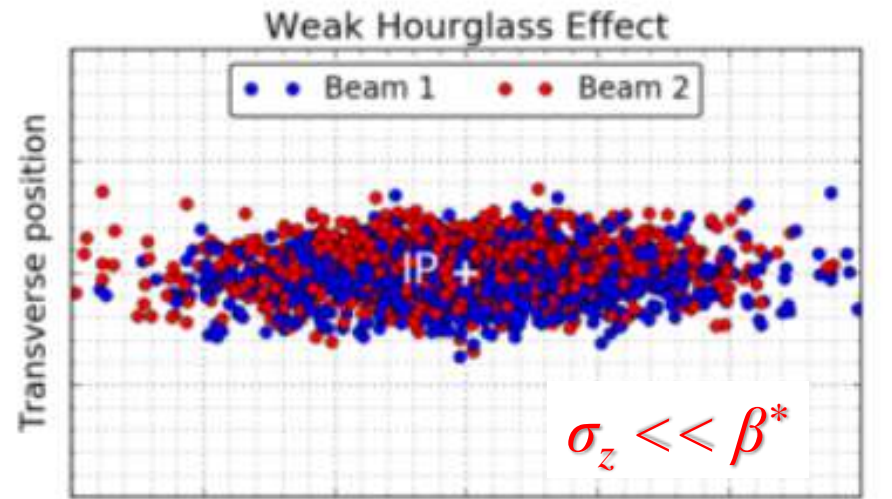
Hour-Glass Effect

$$\beta(s) = \beta^* \left(1 + \left(\frac{s}{\beta^*} \right)^2 \right)$$



Same for
beam size

$$\sqrt{\beta} \varepsilon$$



$$\frac{\mathcal{L}(\sigma_s)}{\mathcal{L}(0)} = \int_{-\infty}^{+\infty} \frac{1}{\sqrt{\pi}} \frac{e^{-u^2}}{\sqrt{\left[1 + \left(\frac{u}{u_x} \right)^2 \right] \cdot \left[1 + \left(\frac{u}{u_y} \right)^2 \right]}} du$$

$u_x = \beta_x^* / \sigma_s$

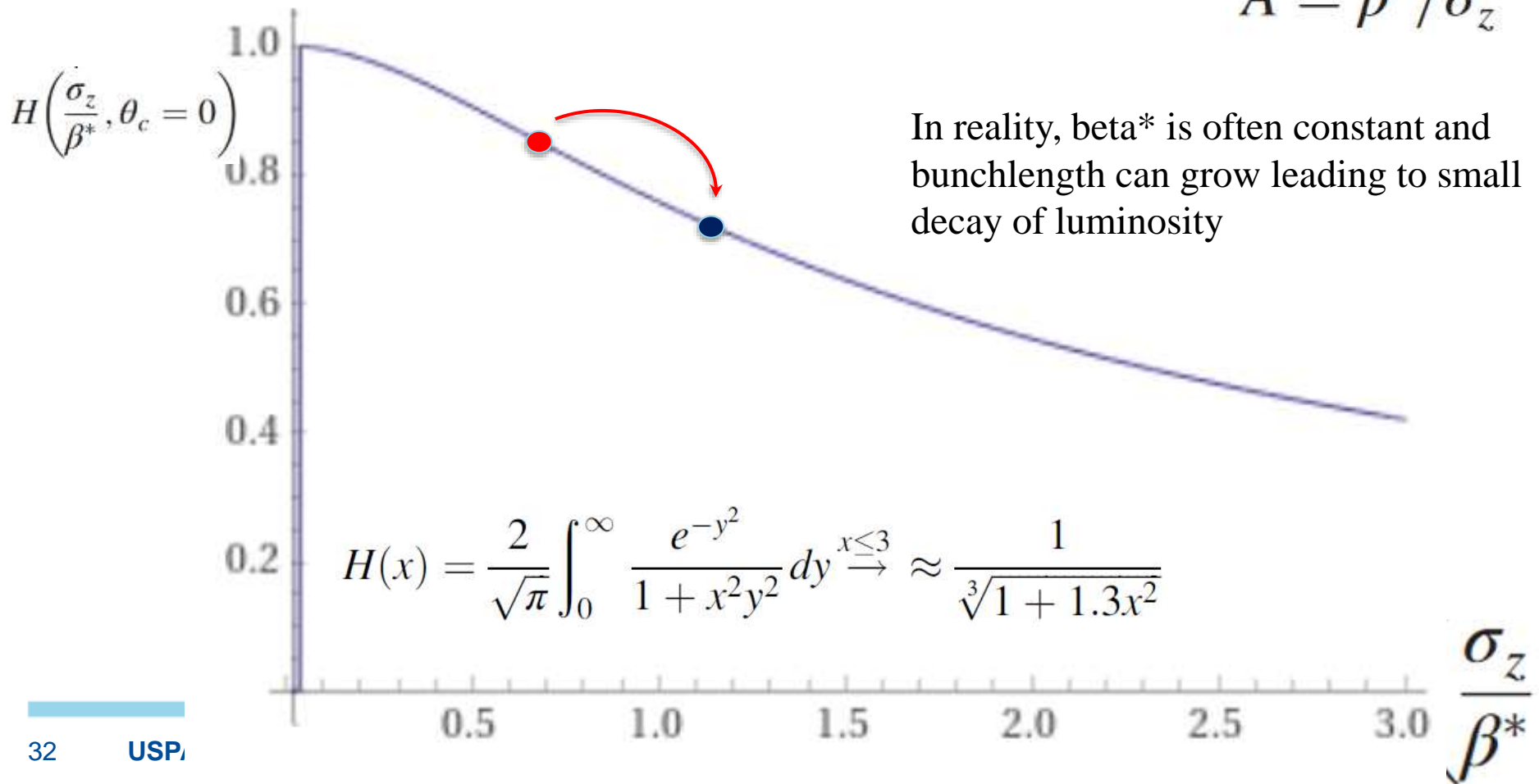
$u_y = \beta_y^* / \sigma_s$

Luminosity Reduction Due to Hourglass

For round beams, equal beta's and no crossing angle, H -factor

$$\frac{\mathcal{L}(\sigma_s)}{\mathcal{L}(0)} = H\left(\frac{\sigma_z}{\beta^*}, \theta_c = 0\right) = \sqrt{\pi} A \exp(A^2) \operatorname{erfc}(A)$$

$$A = \beta^* / \sigma_z$$



Luminosity Summary : Key Factors

Want it higher
*either smaller rings = higher B
or high rep linear collider (= power)*

High E helps
This factor comes from adiabatic reduction of the rms beam size for the same emittance

Higher intensity drives L *note that $N(\text{bunch})$ comes squared while # of bunches linear; sometimes N is limited by beam-beam, often $n_b N$ is limited \rightarrow try to put all charge in one bunch*

$$\mathcal{L} = f_0 \gamma n_b \frac{N^2}{4\pi \epsilon_n \beta^*} H \left(\frac{\sigma_z}{\beta^*}, \theta_c \right)$$

Smallest *emittance*
that's where most of beam physics goes to – cooling to stop heating, noises, dynamics in injectors, etc etc etc

Minimize *beta*
need stronger focusing = larger aperture and stronger LB quads

Keep H under control
keep bunch length and β^ more or less matched, be aware of the crossing angle (sometimes need it \rightarrow crabs)*

Colliders: Luminosity

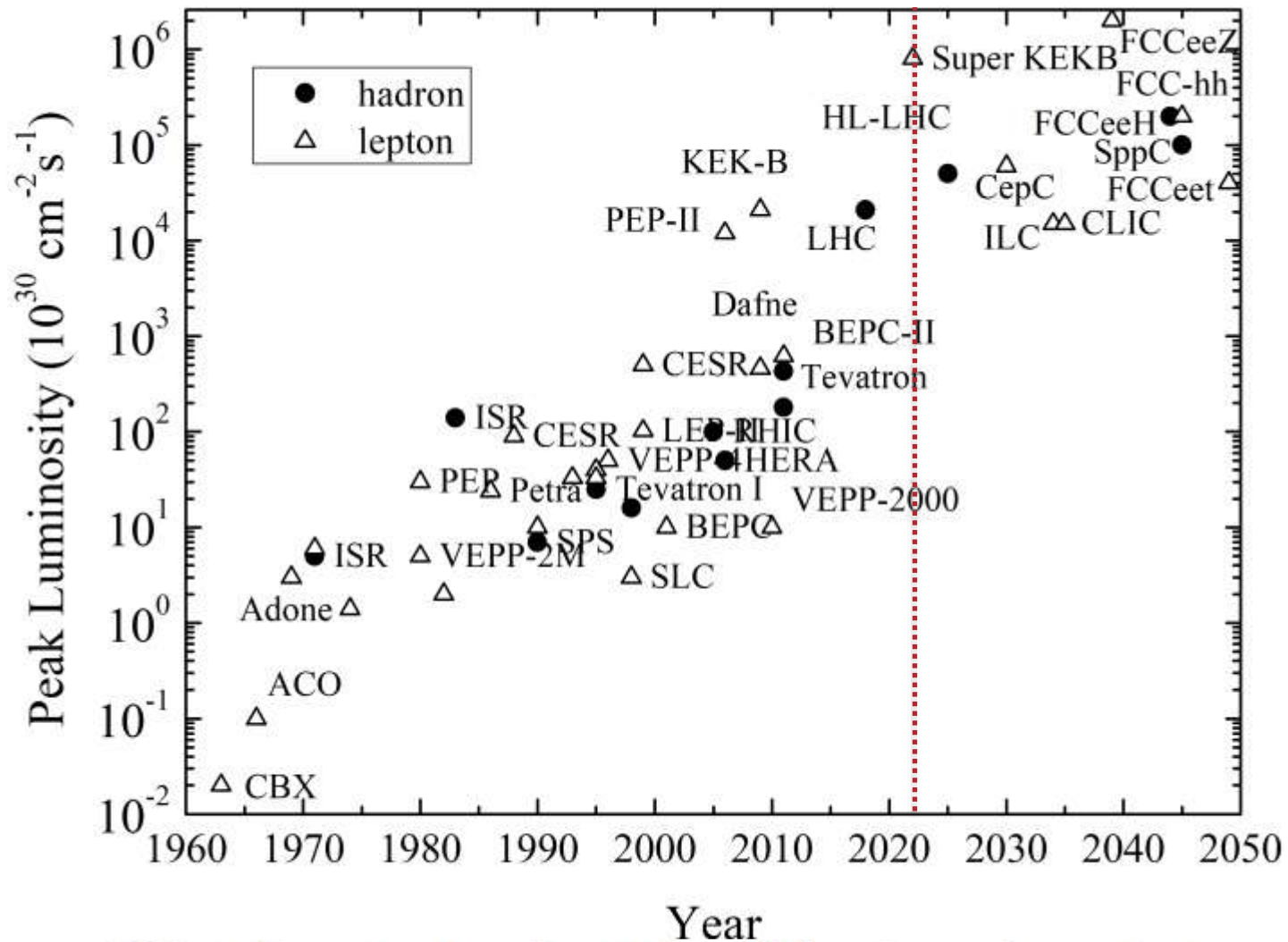
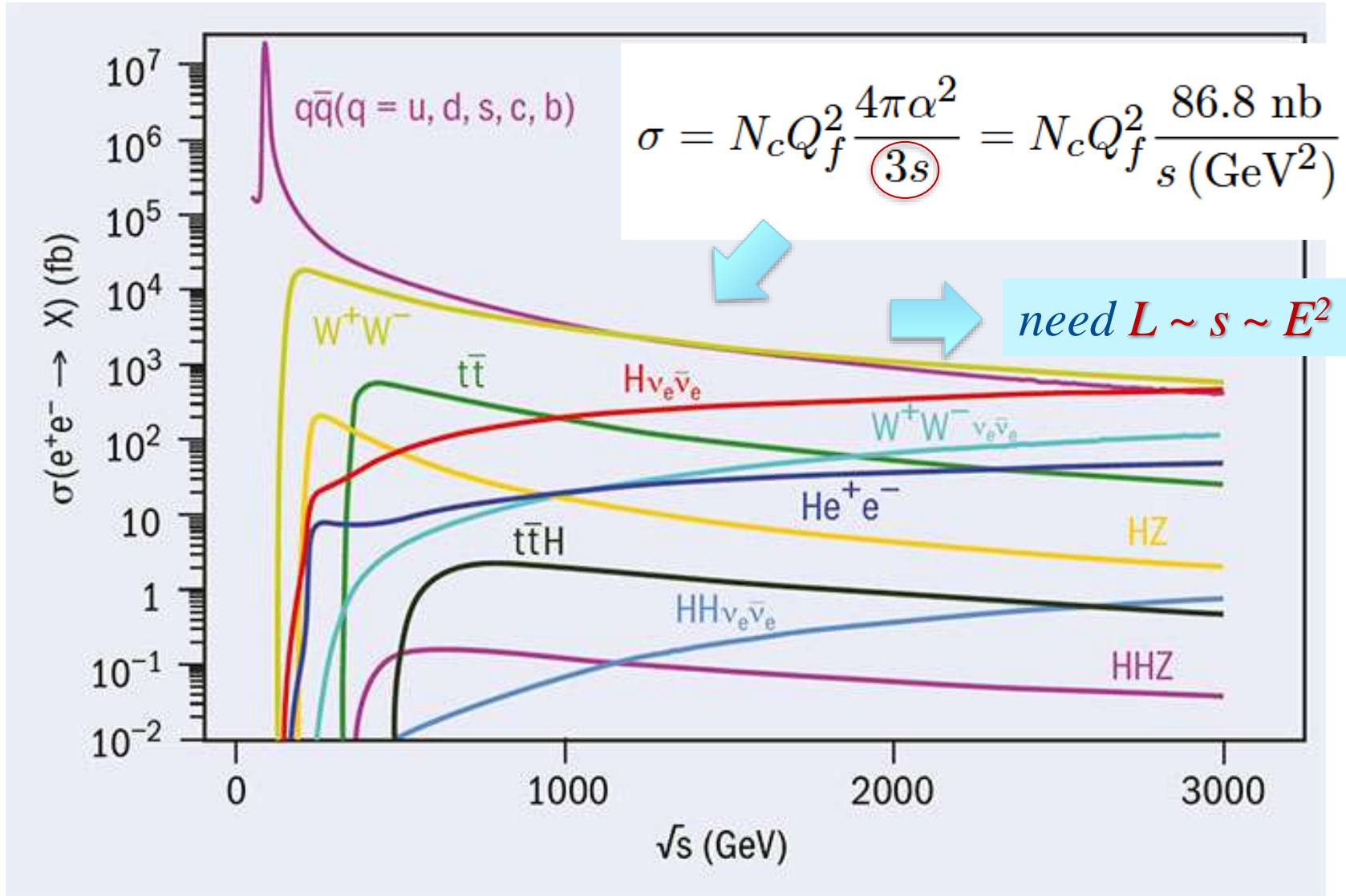
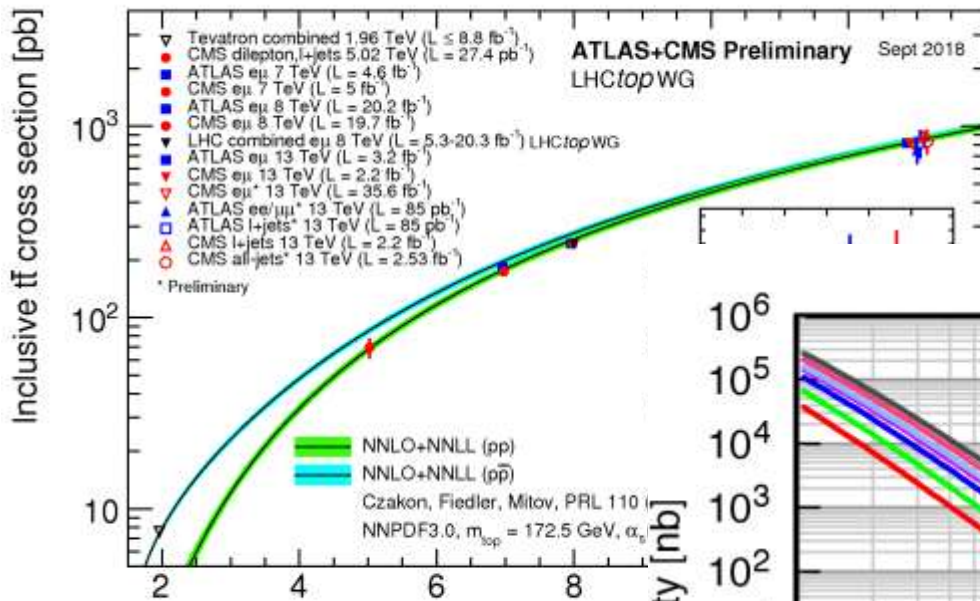


FIG. 3. Luminosities of particle colliders (triangles are lepton colliders and full circles are hadron colliders, adapted from [37]). Values are per collision point.

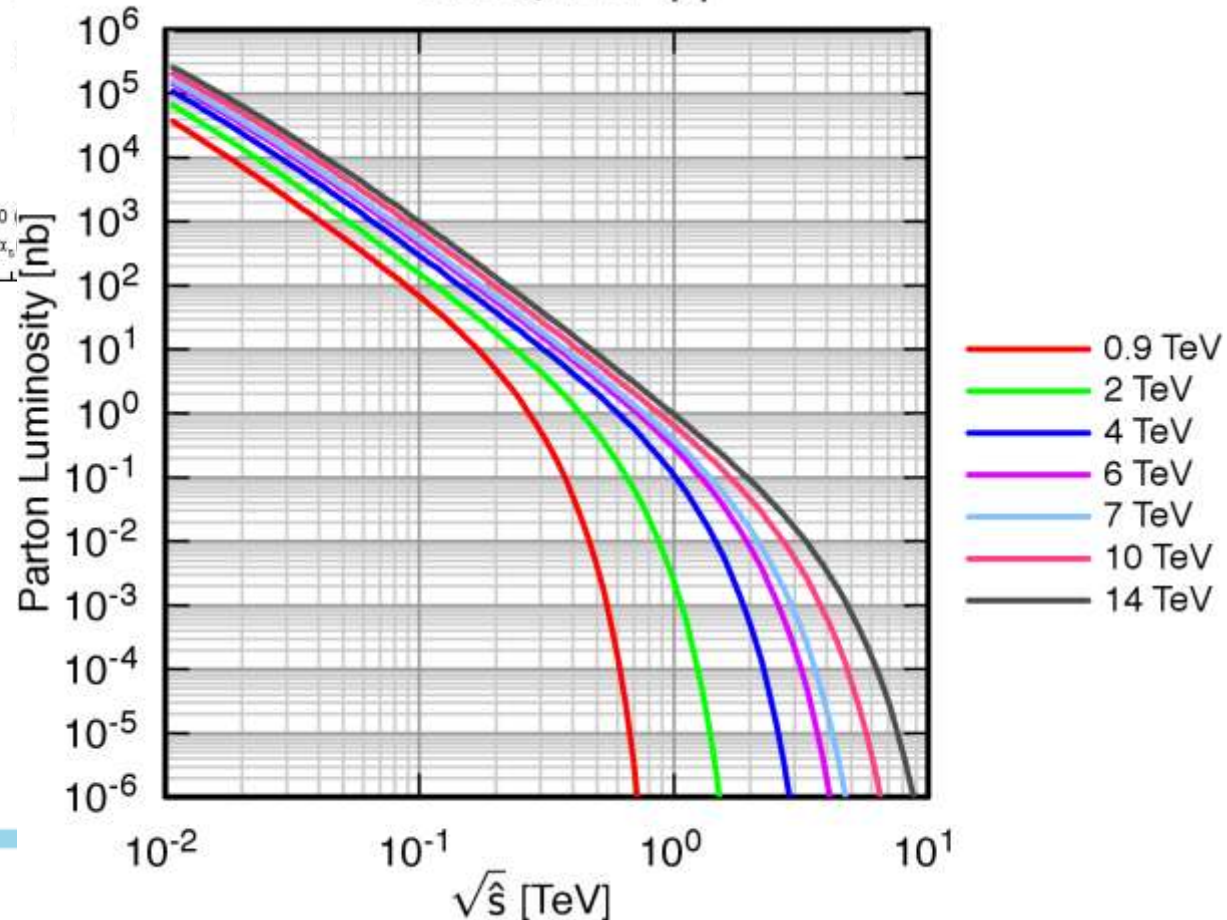
Luminosity Demand : Leptons



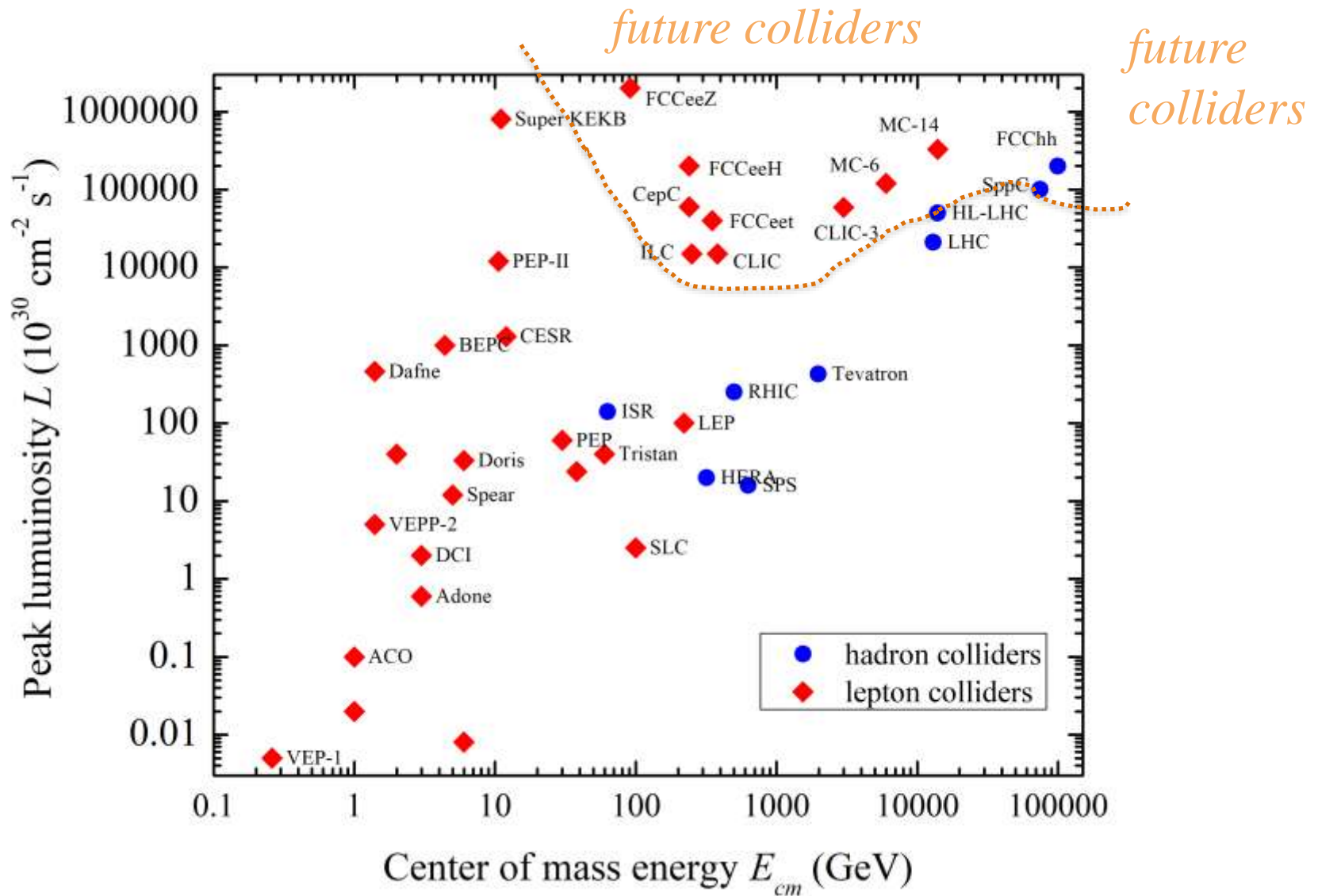
Hadron Cross Sections – Inclusive vs Parton



CTEQ6L1: qq



Colliders: Luminosity vs Energy



Luminosity evolution

$$L = \gamma f_B \frac{N_1 N_2}{4\pi\beta^* \varepsilon} H(\sigma_s / \beta^*)$$

- Factors change in time

$$L(t) = C \frac{N_1(t) N_2(t)}{\varepsilon(t)} H(t)$$

- Therefore, the lifetime

$$\tau_L^{-1} = \frac{dL(t)}{L(t)dt} = \tau_{N1}^{-1} + \tau_{N2}^{-1} - \tau_{\varepsilon}^{-1} + \tau_H^{-1}$$

LHC Lumi Lifetime (~7 hrs) and Integral

LHC Page1

Fill: 6629

E: 6499 GeV

t(SB): 08:30:56

01-05-18 20:38:29

PROTON PHYSICS: STABLE BEAMS

Energy:

6499 GeV

I(B1):

1.56e+14

I(B2):

1.72e+14

Inst. Lumi [(ub.s)⁻¹]

IP1: 8155.99

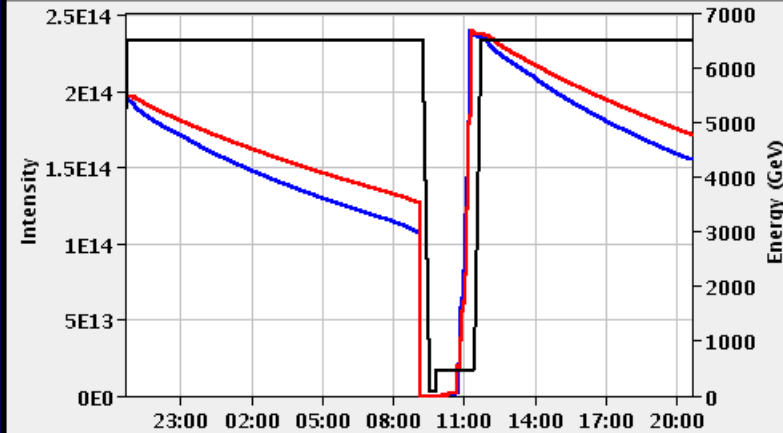
IP2: 1.76

IP5: 7827.12

IP8: 330.93

FBCT Intensity and Beam Energy

Updated: 20:38:28



Instantaneous Luminosity

Updated: 20:38:28



BIS status and SMP flags

B1

B2

Comments (01-May-2018 14:18:10)

Fill for physics (1887b)

XRPs IN

continous crossing angle leveling in IP1/5

Link Status of Beam Permits

true true

Global Beam Permit

true true

Setup Beam

false false

Beam Presence

true true

Moveable Devices Allowed In

true true

Stable Beams

true true

Colliders : Most Important Topics/Effects

- Engineering of magnets, RF, PSs, vacuum, sources, targets, diagnostics, collimators, etc
 - Exciting science: new acceleration techniques/plasma
- Beam physics
 - One particle: beam optics, long-term stability, resonances, losses, noises, diffusion/emittance growth, etc
 - One beam: instabilities, synchrotron radiation, beam-induced radiation deposition, intrabeam scattering, cooling, space-charge effects and compensation
 - Two-beams: beam-beam effects and compensation, beamstrahlung, machine-detector interface, etc
- Assuming particle physics interest → choice of accelerator scheme depends on
 - Readiness, cost and power consumption vs E , L reach

(Very) Brief History of Colliders

- Notable machines and most notable effects/discoveries/breakthroughs
- Note that we later will consider in detail:
 - LEP, KEK-B and Super-KEKB (lecture VS6)
 - Tevatron (lecture VS7)
 - LHC and HL-LHC (lecture VS8)
 - RHIC and EIC (lecture VS9)
 - SLC and linear colliders (lecture VS12)

Collider Patent R.Wideroe Sept. 8, 1943

Erteilt auf Grund des Ersten Überleitungsgesetzes vom 8. Juli 1949
(WZGL S. 173)

BUNDESREPUBLIK DEUTSCHLAND



DEUTSCHES PATENTAMT

PATENTSCHRIFT

Nr. 876 279

KLASSE 21g GRUPPE 36

W 687 VIII c 21g

AUSGEGEBEN AM
11. MAI 1953

Dr.-Ing. Rolf Wideröe, Oslo
ist als Erfinder genannt worden

Aktiengesellschaft Brown, Boveri & Cie, Baden (Schweiz)

Anordnung zur Herbeiführung von Kernreaktionen

Patentiert im Gebiet der Bundesrepublik Deutschland vom 8. September 1943 an
Patentanmeldung bekanntgemacht am 18. September 1952
Patenterteilung bekanntgemacht am 26. März 1953

Kernreaktionen können dadurch herbeigeführt werden, daß geladene Teilchen von hoher Geschwindigkeit und Energie, in Elektronenvolt gemessen, auf die zu untersuchenden Kerne geschossen werden. Wenn die geladenen Teilchen in einem gewissen Mindestabstand von den Kernen gelangen, werden die Kernreaktionen eingeleitet. Da aber neben den zu untersuchenden Kernen noch die gesamten Elektronen der Atomhülle vorhanden sind und auch der Wirkungsquerschnitt des Kernes sehr klein ist, wird der größte Teil der geladenen Teilchen von den Hüllenelektronen abgebremst, während nur ein sehr kleiner Teil die gewöhnlichen Kernreaktionen herbeiführt.

Erfindungsgemäß wird der Wirkungsgrad der Kernreaktionen dadurch wesentlich erhöht, daß die Reaktion in einem Vakuumgefäß (Reaktionsröhre) durchgeführt wird, in welchem die geladenen Teilchen hoher Geschwindigkeit gegen einen Strahl von den zu untersuchenden und sich entgegengesetzt bewegenden

Kernen auf einer sehr langen Strecke laufen müssen. Dies kann in der Weise durchgeführt werden, daß die geladenen Teilchen zum mehrmaligen Umlauf in einer Kreisröhre gezwungen werden, wobei die zu untersuchenden Kerne auf derselben Kreisbahn, aber in entgegengesetzter Richtung umlaufen. Da die geladenen Teilchen dabei nicht von bei der Reaktion unwirksamen Elektronen abgebremst werden und andererseits auf einer sehr langen Wegstrecke gegen die Kerne sich bewegen können, wird die Wahrscheinlichkeit für das Eintreten der Kernreaktionen wesentlich größer und der Wirkungsgrad der Reaktion sehr stark erhöht.

Um die bei der Kreisbewegung entstehenden Zentrifugalkräfte aufzuheben, müssen die umlaufenden Teilchen von nach innen gerichteten Ablenkkraften gesteuert werden, während eine Diffusion der Teilchen mittels stabilisierender, von allen Seiten auf den Teilchen gerichteter Kräfte verhindert wird. Falls die gegen-

Zu der Patentanmeldung

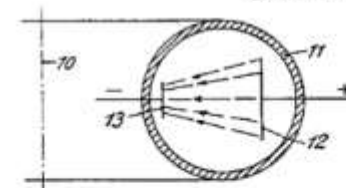


Abb. 1

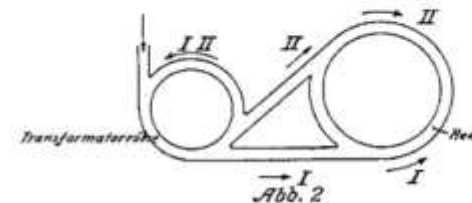


Abb. 2

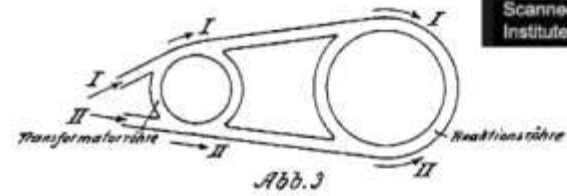


Abb. 3

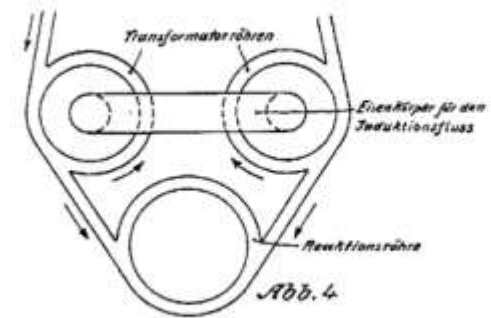
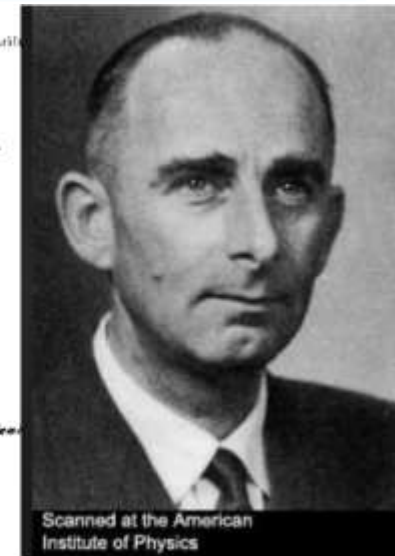


Abb. 4

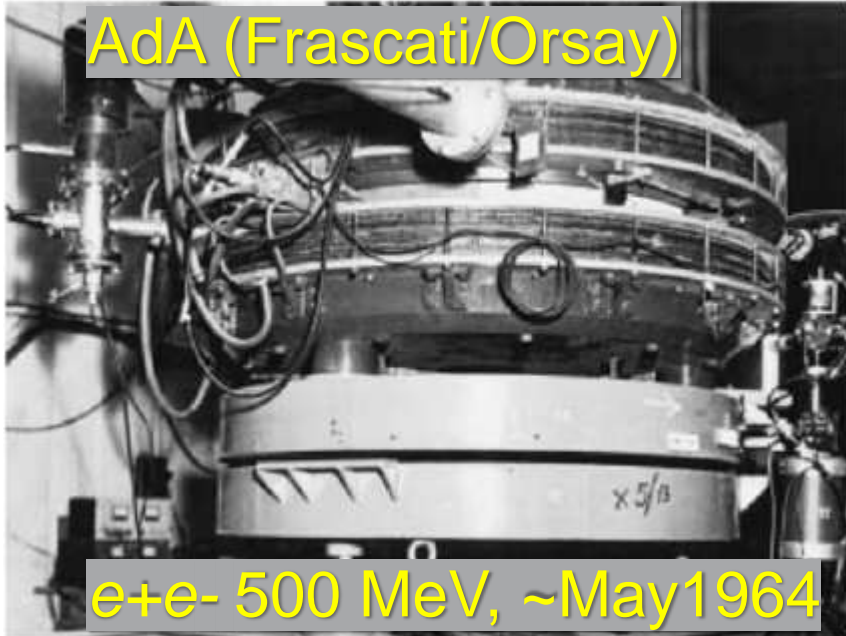


Scanned at the American Institute of Physics

During rough war times, a patent was the only way to communicate the notion!

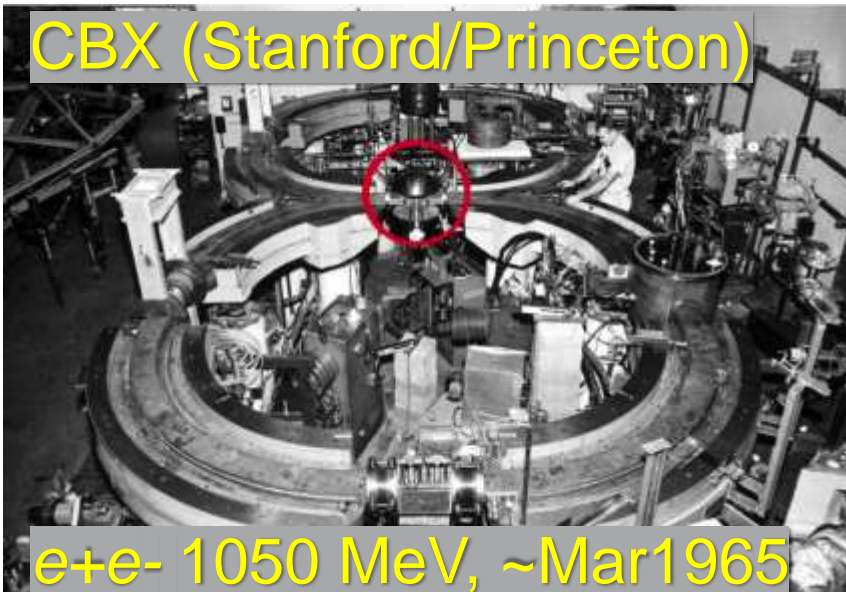
First Colliders

AdA (Frascati/Orsay)



e^+e^- 500 MeV, ~May 1964

CBX (Stanford/Princeton)



e^+e^- 1050 MeV, ~Mar 1965



VEP-1 (Novosibirsk)

e^-e^- 320 MeV, May 19, 1964

The First “Trio” of Colliders

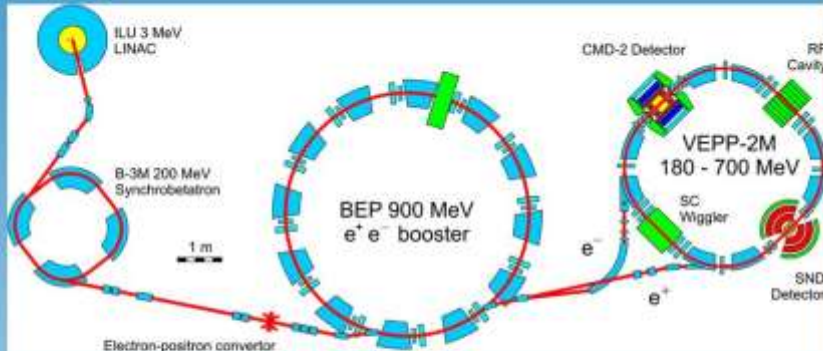
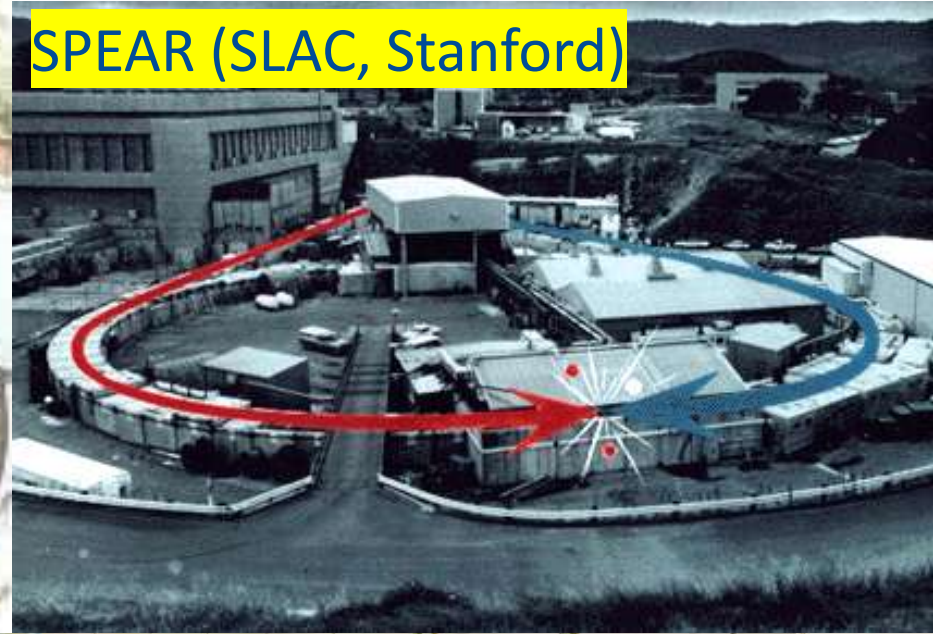
- Technological challenges addressed:
 - development of nano-second-fast injector kickers
 - attainment of an ultrahigh vacuum of about a micropascal or better
 - reliable luminosity monitoring and other beam diagnostics
- Beam physics advances:
 - Touschek effect (low energy beam losses due to particle scattering inside beam leading to e+e- getting out of RF buckets)
 - luminosity degradation due to beam-beam effects at $\xi_{x,y} \sim 0.02\text{--}0.04$
 - complex beam dynamics at non-linear high-order resonances
 - coherent instabilities due to resistive vacuum pipe walls

1970s-80s “small” e+e- (C=20...200 m)

ADONE (INFN, Frascati)



SPEAR (SLAC, Stanford)



• VEPP-2M collider: 0.36-1.4 GeV in c.m., $L \approx 10^{30}$ 1/cm²s at 1 GeV

• Detectors C

VEPP-2 (INP, Novosibirsk)



DORIS (DESY, Hamburg)

1970s-80s “small” e+e-

- Technological challenges addressed:
 - longitudinal phase feedback system developed and installed (ADONE)
 - 7.5 T SC wiggler to decrease the damping time (VEPP-2M)
- Beam physics advances:
 - Luminosity scaling in SR dominated beams $\mathcal{L} \propto \gamma^4$ (ADONE)
 - Sokolov-Ternov effect: the buildup of electron spin polarization through synchrotron radiation (VEPP-2 and ACO)
 - CEA: first time a low-beta insertion optics with a small $\beta_y \approx 2.5$ cm
 - SPEAR: Transverse horizontal and vertical head-tail instabilities were observed and suppressed a positive chromaticity $Q' > 0$
 - DCI: first four-beam compensation attempt (limited success)
 - $dE/E \sim 10^{-5}$ resolution via resonant depolarization method (VEPP-2M)
 - Multibunch, e.g. 480 bunches in each ring in DORIS

1980s-90s “large” e+e- ($C=2\dots 27$ km)

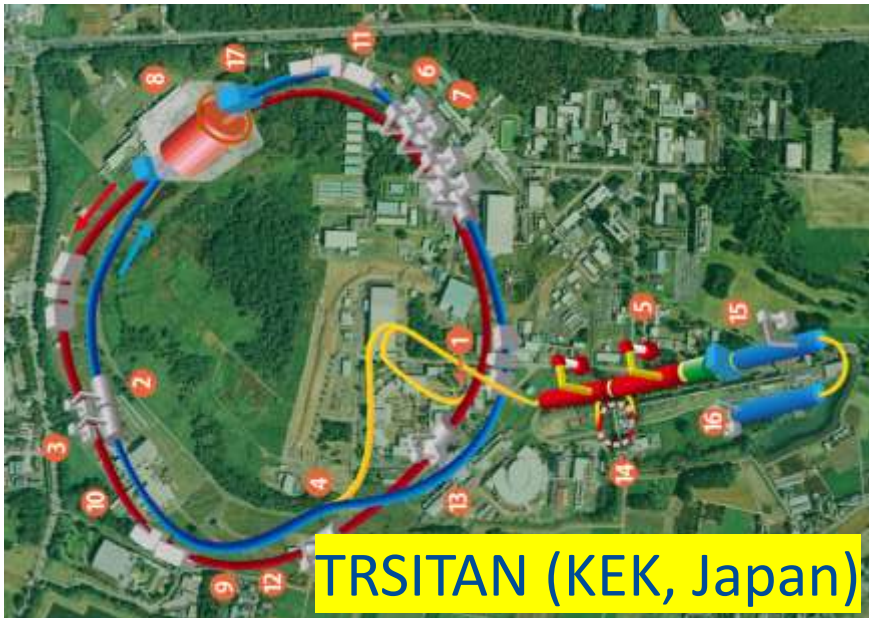
PETRA (DESY, Hamburg)



SLC (SLAC, Stanford)



TRISTAN (KEK, Japan)



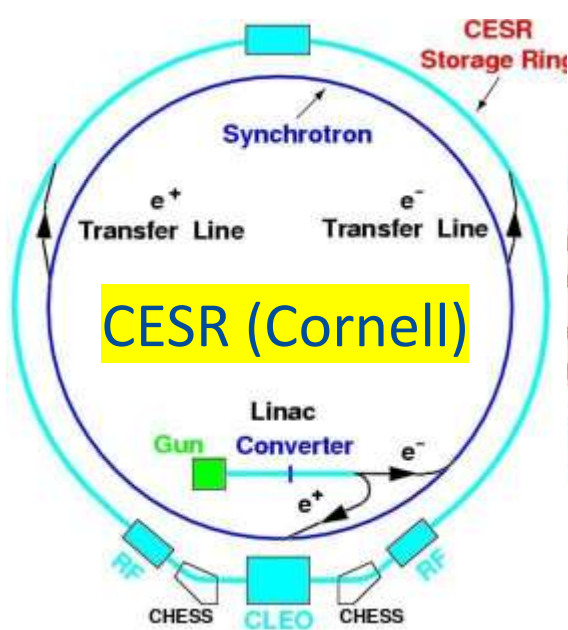
LEP (CERN)



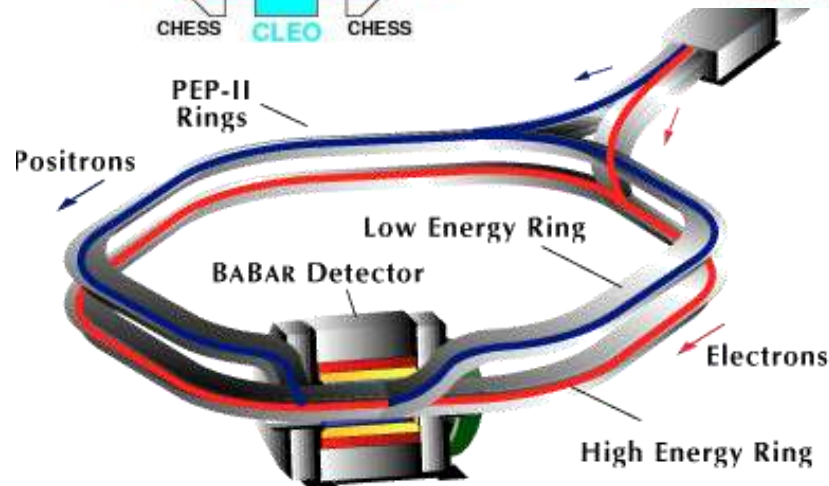
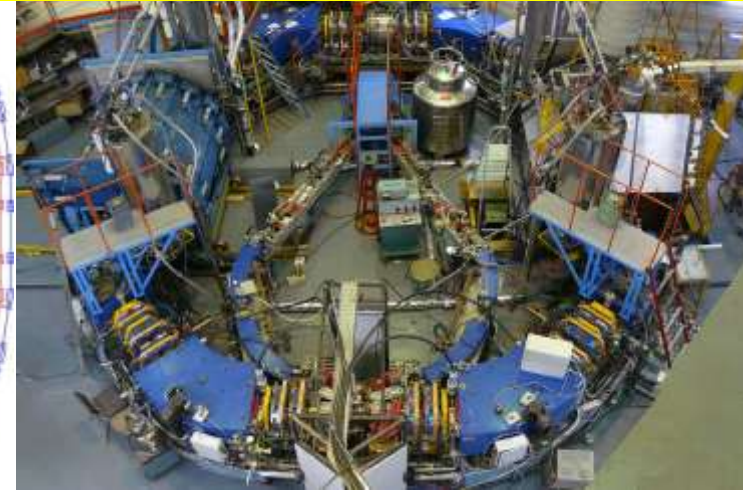
1980s-90s “large” e+e-

- Technological challenges addressed:
 - SLC: first ever (and only) linear collider – many subsystems
 - pioneer SRF technology - TRISTAN: 508 MHz 0.4 GV/turn; LEP 352 MHz SC niobium-on-copper cavities, 3.5 GV/turn
 - High current positron sources, incl. 80% polarized e- (SLC)
- Beam physics advances:
 - LEP: losses via e+/e- scattering off thermal photons in RT beampipe
 - LEP single-bunch current limited by TMCI at injection energy
 - LEP: beam-beam record tune shift $4x\xi y=0.33$
 - SLC : BNS (Balakin-Novokhatsky-Smirnov) damping of BBI
 - SLC: $\sim x2$ increase of luminosity due to disruption enhancement @IP

2000s-now “factories” e^+e^- (Φ^- , Charm-, B-meson)



VEPP-2000 (BINP, Novosibirsk)



KEK-B \rightarrow SuperKEKB (KEK, Japan)



DAΦNE (INFN, Frascati)

2000s-now “factories” e+e-

- Technological challenges addressed:
 - HV electrostatic orbit separation for e+e- (CESR)
 - Efficient SRF for *Ampere*-class currents, HOM damping
 - Asymmetric rings – KEK-B, PEP-II, Super-KEKB
 - Tight detector background control - vacuum and collimation
 - Since PEP-II/KEKB: top-up injection mode of operation
- Beam physics advances:
 - Advanced optics for tight vertical focusing with $\beta_y \sim 1\text{cm}$ – few mm
 - VEPP2000 : “round beams” concept $\xi \sim 0.25$
 - (less successful) CESR “Moebius ring” collider scheme (x-y flips)
 - DAΦNE : “crab waist” focusing optics, demo “wire b-b compensation”
 - KEK-B: crab crossing (limited success) \rightarrow nonobeams (Super-KEKB)

1970s-2010s Hadron Colliders (C=1...7 km)

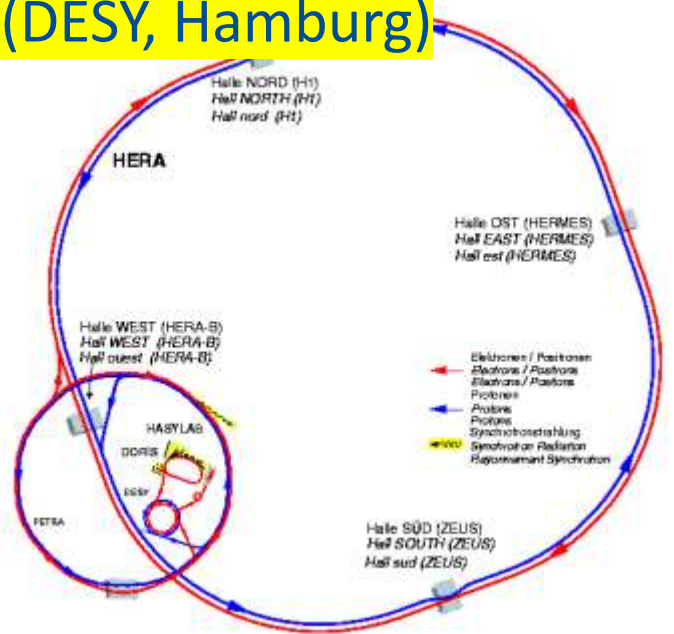
ISR (CERN)



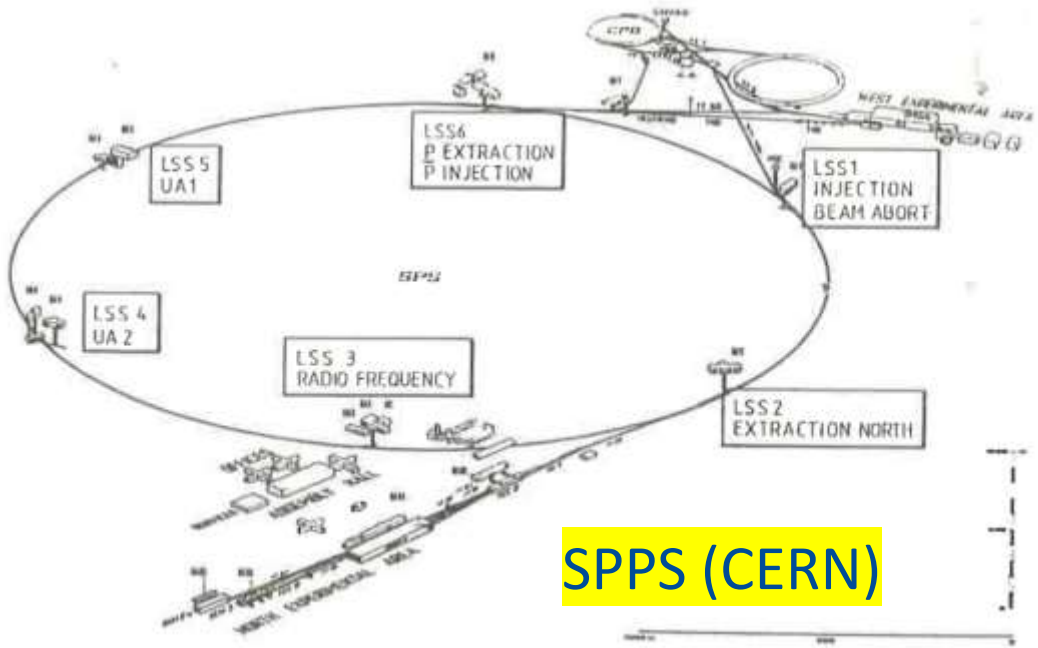
Tevatron (FNAL, Batavia)



HERA (DESY, Hamburg)



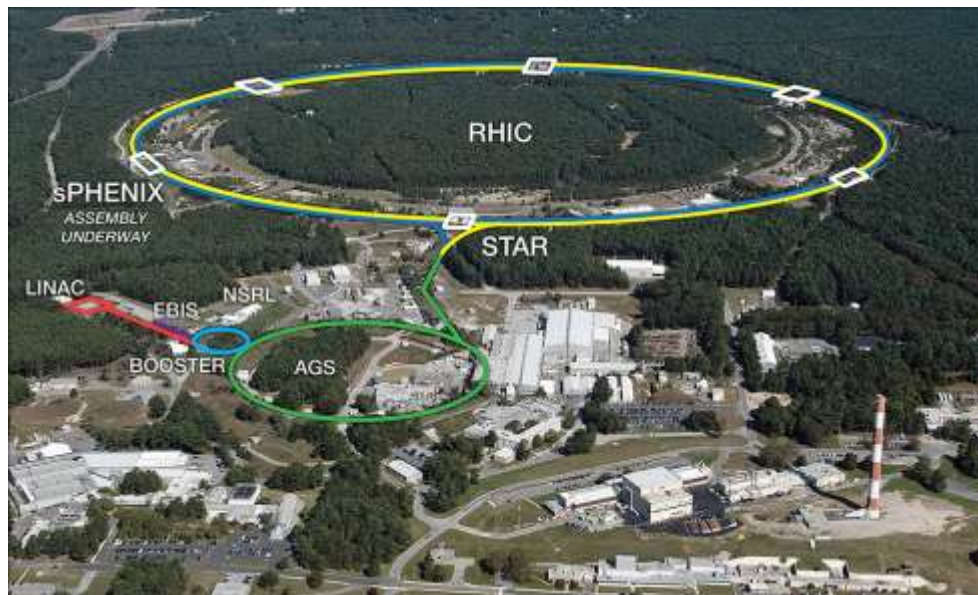
SPPS (CERN)



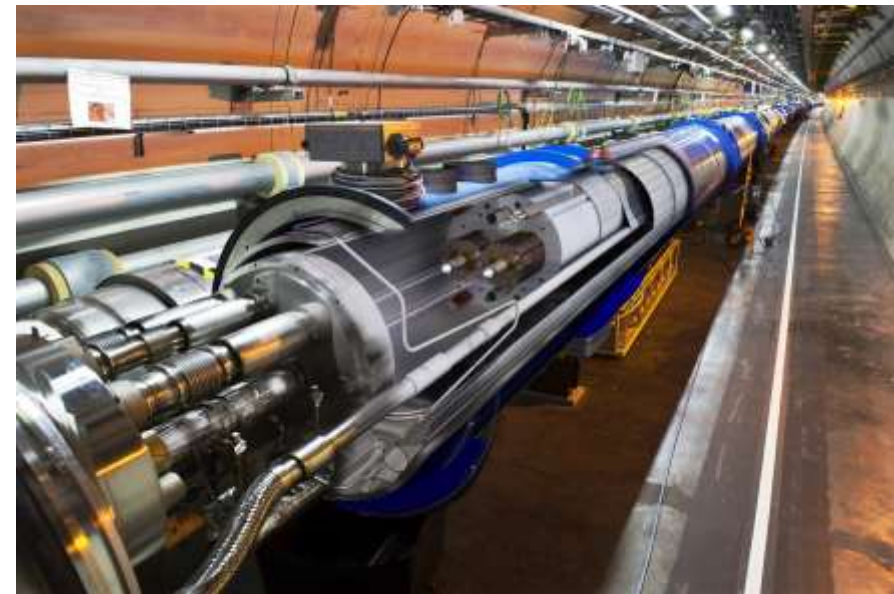
1970s-2000's Hadron Colliders (1)

- Technological challenges addressed:
 - ISR: world's first pp collider (and pp Lumi record holder for >20 yrs)
 - SC NbTi magnets 4-8 T (Tevatron → HERA → RHIC → LHC)
 - SPPS, & Tevatron: technology of antiproton production & scienc of stochastic (Nobel prize) and electron cooling (up to 4 MeV e-)
 - Tevatron: permanent magnets (3.3 km 8 GeV Recycler)
 - Two-stage collimation systems (HERA, Tevatron)
- Beam physics advances:
 - Longitudinal manipulations : momentum stacking (ISR), slip-stacking and momentum mining (Tevatron)
 - Tevatron: beam-beam record at $\xi_{x,y} \sim 0.025$, first successful demo b-b compensation by electron lenses, hollow e-lens collimation
 - HERA: first e-p collider, transversely polarized e- & spin rotators to 1

2000s-now Hadron Colliders ($C=4...27$ km)



RHIC (BNL, Brookhaven)



LHC (CERN)

2000s-now Hadron Colliders (2)

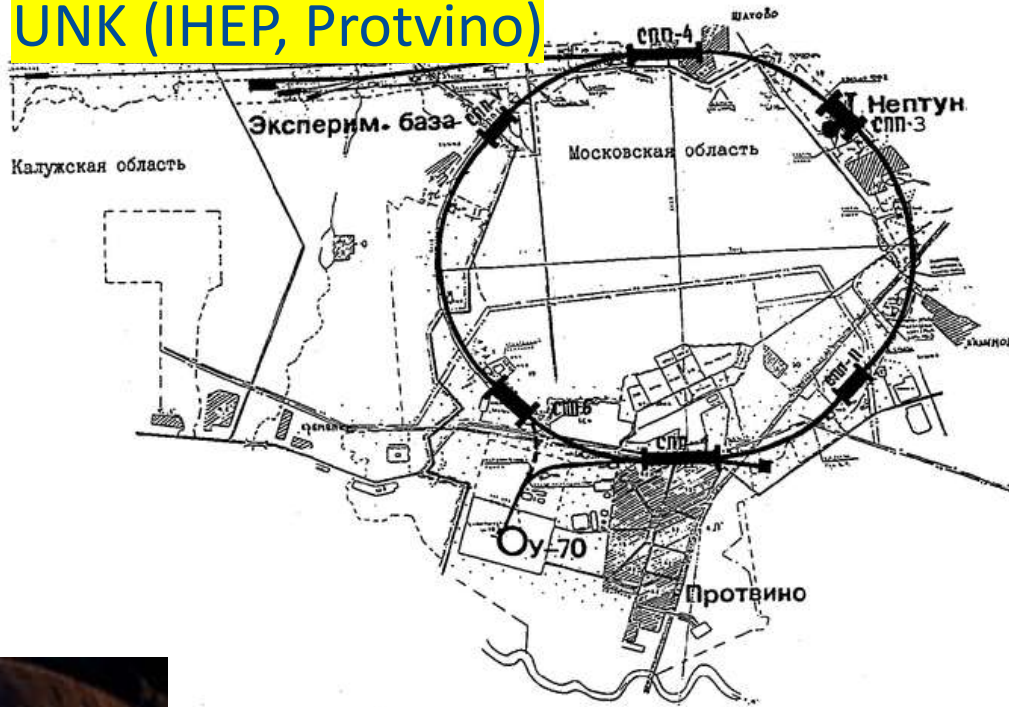
- Technological challenges addressed:
 - First use of Nb₃Sn SC magnets (HL-LHC)
 - Three (4) stage 99.99% efficient collimation system (LHC)
 - Ions sources and ion-ion, ion-p collisions (RHIC, LHC)
 - Sophisticated polarization control along the chain (55% in RHIC)
- Beam physics advances:
 - RHIC: bunched beam stochastic cooling, bunched beam electron cooling
 - RHIC: head-on beam-beam compensation with electron lenses
 - LHC: sophisticated control of electron-cloud and other instabilities
 - LHC: novel achromatic telescopic squeeze optics to lower beta*
 - LHC: demo wire compensation of long-range beam-beam effects

Super-Colliders That Were Not (1990's)

SSC (Waxahachie, TX)



UNK (IHEP, Protvino)

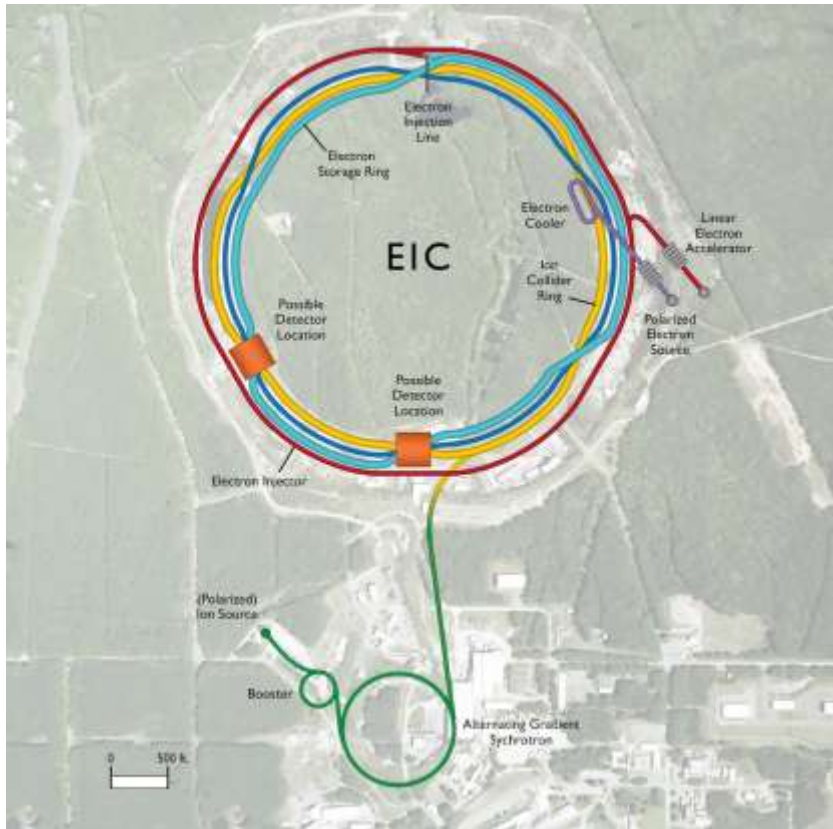


Colliders That Will Be

NICA (JINR, Dubna)



EIC (BNL, Brookhaven)



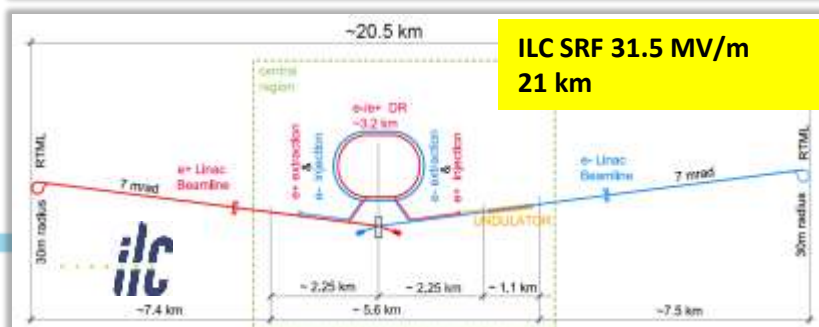
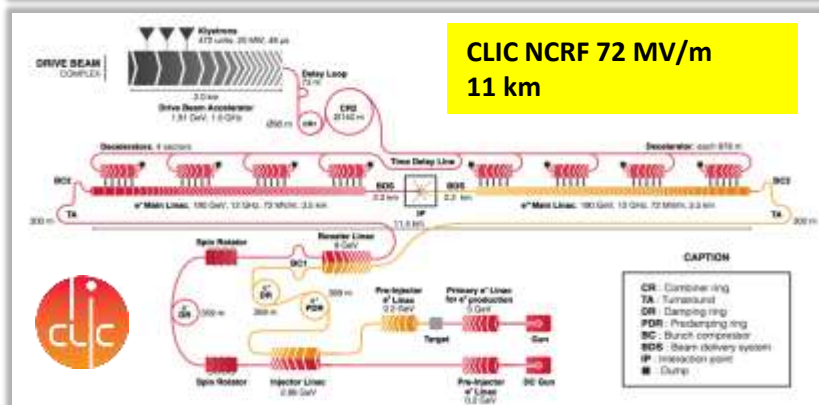
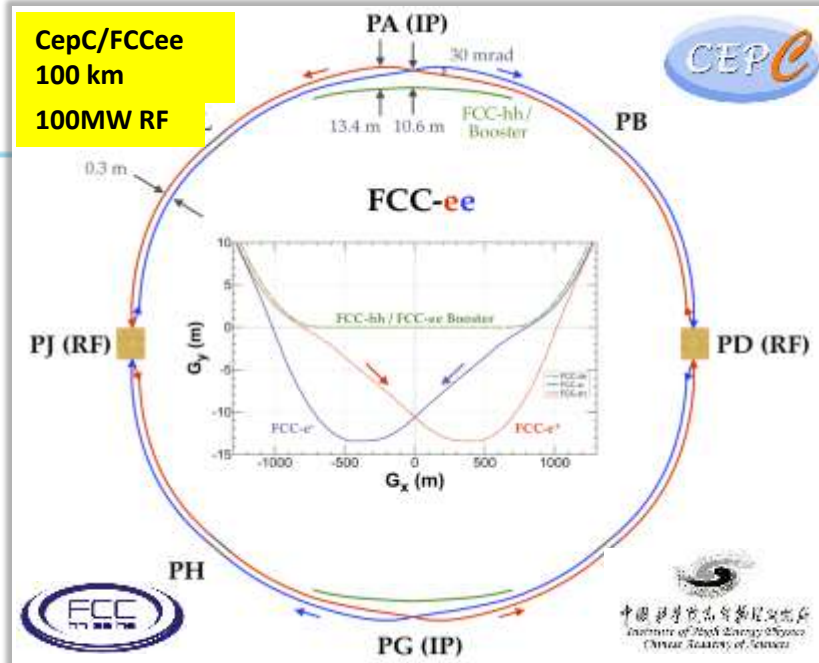
BINP C/Tau-Factory (Novosibirsk)



Colliders That Might Be :

Higgs factories proposals

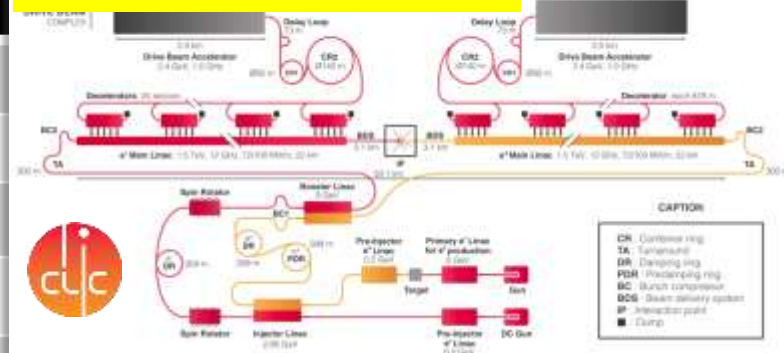
Name	Details
CepC	e^+e^- , $\sqrt{s} = 0.24$ TeV, $L = 3.0 \times 10^{34}$
CLIC (Higgs factory)	e^+e^- , $\sqrt{s} = 0.38$ TeV, $L = 1.5 \times 10^{34}$
ERL ee collider	e^+e^- , $\sqrt{s} = 0.24$ TeV, $L = 73 \times 10^{34}$
FCC-ee	e^+e^- , $\sqrt{s} = 0.24$ TeV, $L = 17 \times 10^{34}$
gamma gamma	X-ray FEL-based $\gamma\gamma$ collider
ILC (Higgs factory)	e^+e^- , $\sqrt{s} = 0.25$ TeV, $L = 1.4 \times 10^{34}$
LHeC	ep , $\sqrt{s} = 1.3$ TeV, $L = 0.1 \times 10^{34}$
MC (Higgs factory)	$\mu\mu$, $\sqrt{s} = 0.13$ TeV, $L = 0.01 \times 10^{34}$



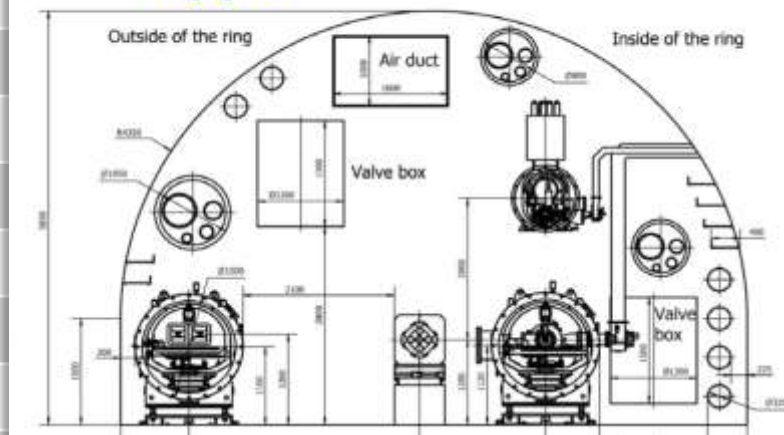
Far-Future High Energy Collider Concepts/Proposals

Name	Details
Cryo-Cooled Copper linac	e^+e^- , $\sqrt{s} = 2$ TeV, $L = 4.5 \times 10^{34}$
High Energy CLIC	e^+e^- , $\sqrt{s} = 1.5 - 3$ TeV, $L = 5.9 \times 10^{34}$
High Energy ILC	e^+e^- , $\sqrt{s} = 1 - 3$ TeV
FCC-hh	pp , $\sqrt{s} = 100$ TeV, $L = 30 \times 10^{34}$
SPPC	pp , $\sqrt{s} = 75/150$ TeV, $L = 10 \times 10^{34}$
Collider-in-Sea	pp , $\sqrt{s} = 500$ TeV, $L = 50 \times 10^{34}$
LHeC	ep , $\sqrt{s} = 1.3$ TeV, $L = 1 \times 10^{34}$
FCC-eh	ep , $\sqrt{s} = 3.5$ TeV, $L = 1 \times 10^{34}$
CEPC-SPPpC-eh	ep , $\sqrt{s} = 6$ TeV, $L = 4.5 \times 10^{33}$
VHE-ep	ep , $\sqrt{s} = 9$ TeV
MC – Proton Driver 1	$\mu\mu$, $\sqrt{s} = 1.5$ TeV, $L = 1 \times 10^{34}$
MC – Proton Driver 2	$\mu\mu$, $\sqrt{s} = 3$ TeV, $L = 2 \times 10^{34}$
MC – Proton Driver 3	$\mu\mu$, $\sqrt{s} = 10 - 14$ TeV, $L = 20 \times 10^{34}$
MC – Positron Driver	$\mu\mu$, $\sqrt{s} = 10 - 14$ TeV, $L = 20 \times 10^{34}$
LWFA-LC (e^+e^- and $\gamma\gamma$)	Laser driven; e^+e^- , $\sqrt{s} = 1 - 30$ TeV
PWFA-LC (e^+e^- and $\gamma\gamma$)	Beam driven; e^+e^- , $\sqrt{s} = 1 - 30$ TeV
SWFA-LC	Structure wakefields; e^+e^- , $\sqrt{s} = 1 - 30$ TeV

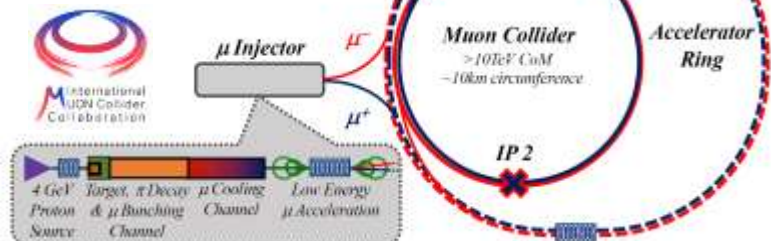
CLIC e^+e^- 3 TeV, 100 MV/m 50 km



pp 100 km : SPPC 75 TeV, 12 T magnets, FCChh 100/16 T



$\mu^+\mu^-$ 10-14 TeV cme
10-14 km, 16 T magnets



BREAK (!...?)

BEAM-BEAM (1)

Beams as moving charges

- Beam is a collection of charges
- Represent electromagnetic potential for other
- charges
- Forces on itself (**space-charge**) and opposing beam (**beam-beam effects**)
 - Main limit for present and future colliders
 - Important for high density beams, i.e. high intensity and/or small beams = for **high luminosity !**

Beam-Beam Effects

- Remember:

$$\Rightarrow \mathcal{L} = \frac{N_1 N_2 f B}{4\pi \sigma_x \sigma_y} = \frac{N_1 N_2 f B}{4\pi \cdot \sigma_x \sigma_y}$$

- Overview: which effects are important for
- present and future machines (LEP, PEP,
- Tevatron, RHIC, LHC, ...)
- Qualitative and physical picture of the effects
- Mathematical derivations in:
- **Proceedings, Zeuthen 2003**

Beam-Beam Effects

- A beam acts on particles like an electromagnetic lens, but:
 - Does not represent simple form, i.e. well-defined multipoles
 - Very non-linear form of the forces, depending on distribution
 - Can change distribution as result of interaction (time dependent forces ..)
- Results in many different effects and problems

Fields and Forces (1)

- Start with a point charge q and integrate over the particle distribution.
- In rest frame only electrostatic field: $\mathbf{E} \neq 0$ while $\mathbf{B} = 0$
- Transform into moving frame and calculate
- Lorentz force

$$E_{\parallel} = E'_{\parallel}, \quad E_{\perp} = \gamma \cdot E'_{\perp} \quad \text{with :} \quad \vec{B} = \vec{\beta} \times \vec{E} / c$$

$$\vec{F} = q(\vec{E} + \vec{\beta} \times \vec{B})$$

- Note that $F \approx 0$ if velocities are collinear

Fields and Forces (2)

- Derive potential $U(x, y, z)$ from Poisson equation:

$$\Delta U(x, y, z) = -\frac{1}{\epsilon_0} \rho(x, y, z)$$

- The fields become:

$$\vec{E} = -\nabla U(x, y, z)$$

- Example Gaussian distribution:

$$\rho(x, y, z) = \frac{Ne}{\sigma_x \sigma_y \sigma_z \sqrt{2\pi}^3} \exp\left(-\frac{x^2}{2\sigma_x^2} - \frac{y^2}{2\sigma_y^2} - \frac{z^2}{2\sigma_z^2}\right)$$

A Common Example: Gaussian

- For 2D case the potential becomes:

$$U(x, y, \sigma_x, \sigma_y) = \frac{ne}{4\pi\epsilon_0} \int_0^\infty \frac{\exp\left(-\frac{x^2}{2\sigma_x^2+q} - \frac{y^2}{2\sigma_y^2+q}\right)}{\sqrt{(2\sigma_x^2+q)(2\sigma_y^2+q)}} dq$$

- Can derive E and B fields and therefore forces
- Also easy for uniform distribution: E and B scale linear with r for $r < a$, and $1/r$ for $r > a$... easy for simple easily integrable axisymmetric distributions
- For arbitrary distribution (non-Gaussian):
 - difficult (or impossible, numerical solution required)

Further Simplification: Round Gaussian

- Round beams: $\sigma_x = \sigma_y = \sigma$
- Only components **E_r** and **B** are non-zero
- Force has only radial component, i.e. depends only on distance **r** from bunch center, i.e. $r^2 = x^2 + y^2$.

$$F_r(r) = -\frac{ne^2(1 + \beta^2)}{2\pi\epsilon_0 \cdot r} \left[1 - \exp\left(-\frac{r^2}{2\sigma^2}\right) \right]$$

Beam-Beam Kick

- Kick $\Delta r'$ - angle by which the particle is deflected during the passage
- Derived from force by integration over the collision
assume: $\mathbf{m}_1 = \mathbf{m}_2$ and $\beta_1 = \beta_2$

$$F_r(r, s, t) = -\frac{Ne^2(1 + \beta^2)}{\sqrt{(2\pi)^3 \epsilon_0 r \sigma_s}} \left[1 - \exp\left(-\frac{r^2}{2\sigma^2}\right) \right] \cdot \left[\exp\left(-\frac{(s + vt)^2}{2\sigma_s^2}\right) \right]$$

→ Newton's law $\Delta r' = \frac{1}{mc\beta\gamma} \int_{-\infty}^{\infty} F_r(r, s, t) dt$

Beam-Beam Kick

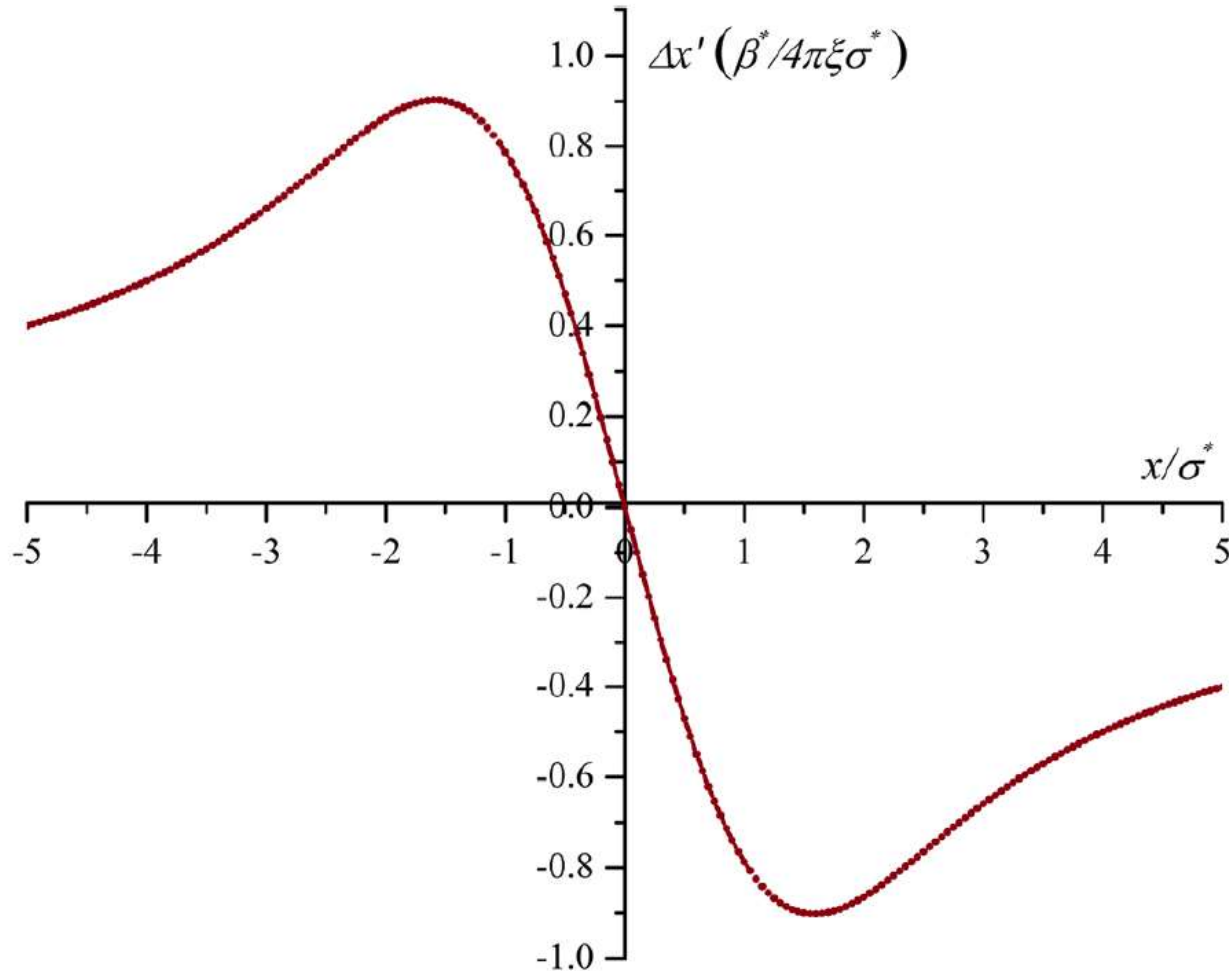
- Using the classical particle radius: $r_0 = e^2 / 4\pi\epsilon_0 mc^2$
- we get radial kick and in Cartesian coordinates:

$$\Delta r' = -\frac{2Nr_0}{\gamma} \cdot \frac{r}{r^2} \cdot \left[1 - \exp\left(-\frac{r^2}{2\sigma^2}\right) \right]$$

$$\Delta x' = -\frac{2Nr_0}{\gamma} \cdot \frac{x}{r^2} \cdot \left[1 - \exp\left(-\frac{r^2}{2\sigma^2}\right) \right]$$

$$\Delta y' = -\frac{2Nr_0}{\gamma} \cdot \frac{y}{r^2} \cdot \left[1 - \exp\left(-\frac{r^2}{2\sigma^2}\right) \right]$$

Beam-Beam Kick



Kick(force) varies strongly with amplitude:

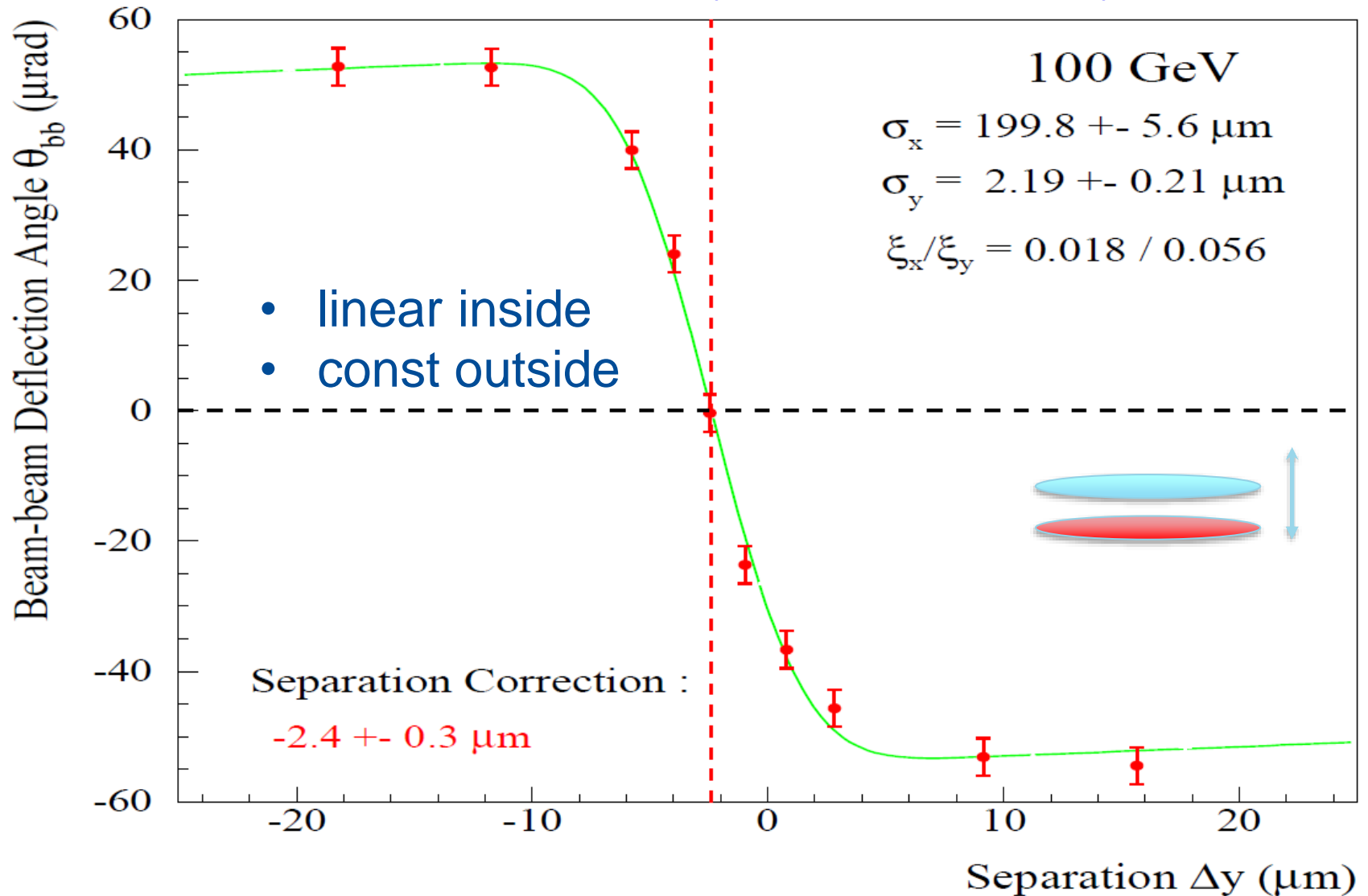
- linear inside \rightarrow like quadrupole \rightarrow tune shift amplitude independent at $\ll \sigma$
- $1/r$ outside the beam core \rightarrow amplitude dependent tune shift

Highly nonlinear btw 1 and 3 sigma:

- contains many high order multipoles

What if the beams are not round?

Deflection scan (LEP measurement)



Beam-beam strength parameter \rightarrow tunes shift

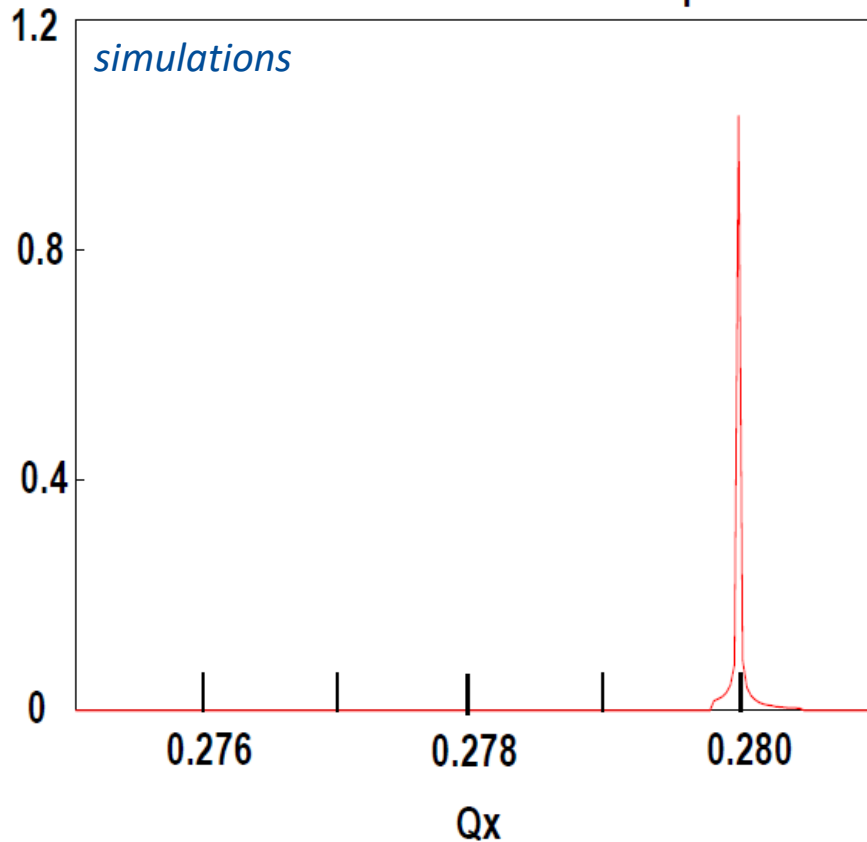
- Slope of force at zero amplitude \rightarrow proportional to (linear) tune shift ΔQ_{bb} from beam-beam interaction
- This defines: *beam-beam parameter* ξ
- For head-on interactions we get:

$$\xi_{x,y} = \frac{N \cdot r_o \cdot \beta_{x,y}}{2\pi \gamma \sigma_{x,y} (\sigma_x + \sigma_y)}$$

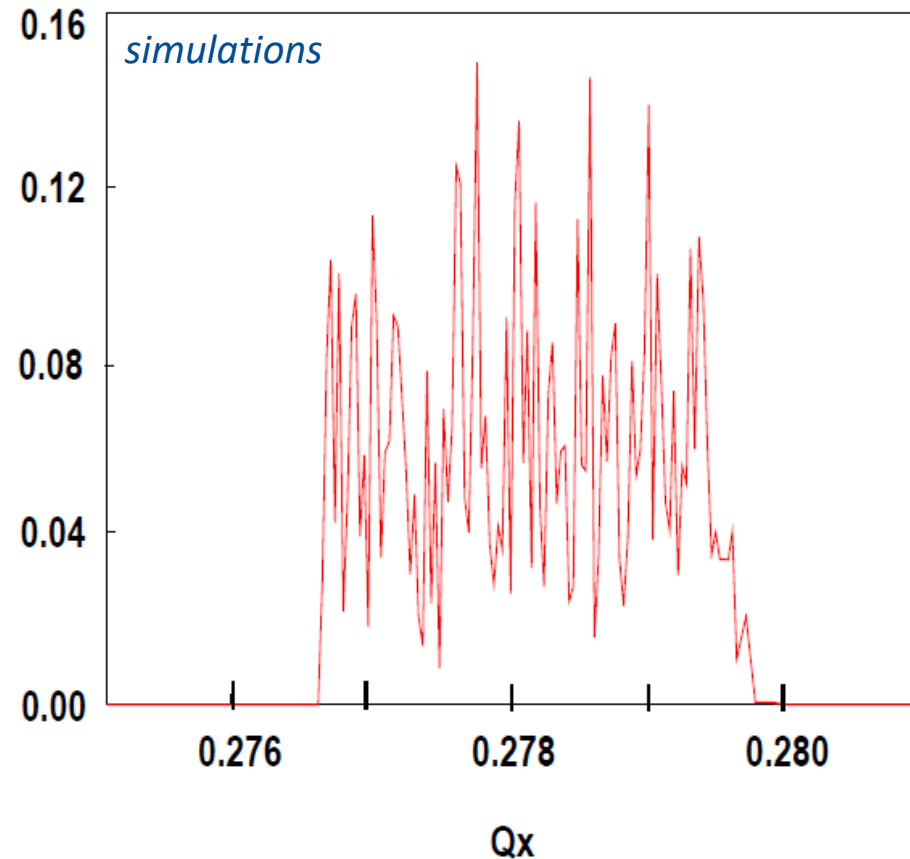
- so far: only an additional “quasi-quadrupole” BUT non-linear part of beam-beam force scales with ξ

Note that for flat beams $\sigma_x \gg \sigma_y$ $\xi_y \gg \xi_x$

Tune Spectra: with/w.o. Beam-Beam



Linear force →
all particles have same tune
→ **one line in the spectrum of transverse oscillations**



Non-linear force →
particles with different amplitudes have different frequencies (tunes)
We get frequency (tune) spectra
Width of the spectra: $\sim \xi$

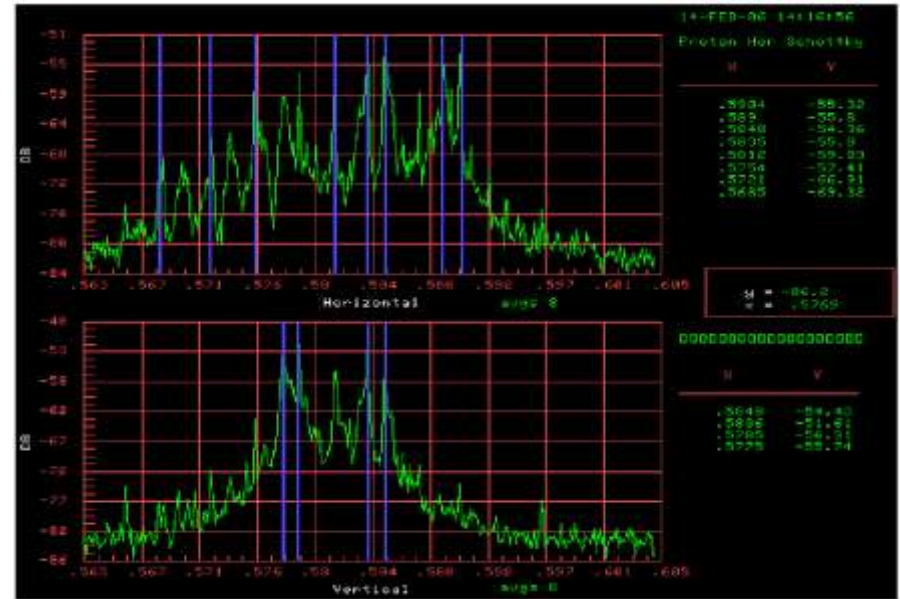
In Reality – Even More Complex

Tevatron 980 GeV p and
980 GeV antiprotons ($p\bar{b}$)

Colliding with $\xi \sim 0.028$

Force is focusing \rightarrow **tuneshift is positive**

Measured with 21MHz Schottky monitors

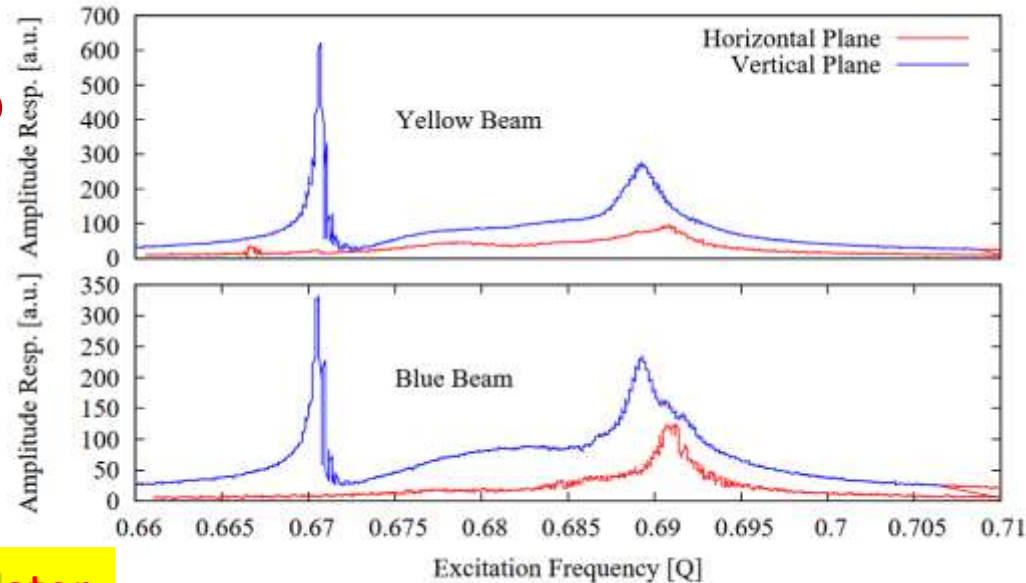


RHIC 100 GeV p + 100 GeV p

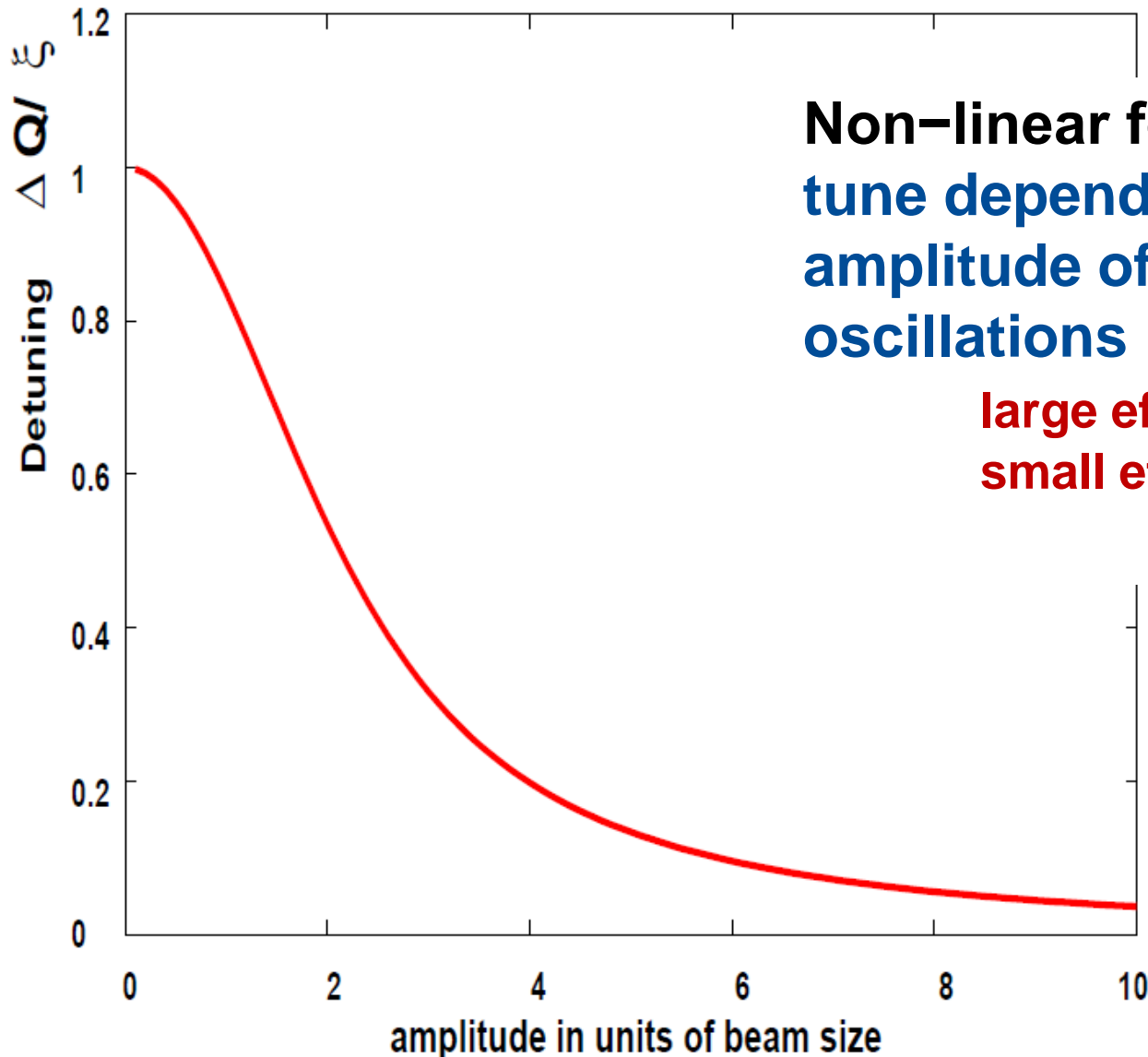
Colliding with $\xi \sim 0.020$

Force is de-focusing \rightarrow **tuneshift is negative**

Measured with BTF (beam transfer function) monitor



Beam-beam Detuning with Amplitude

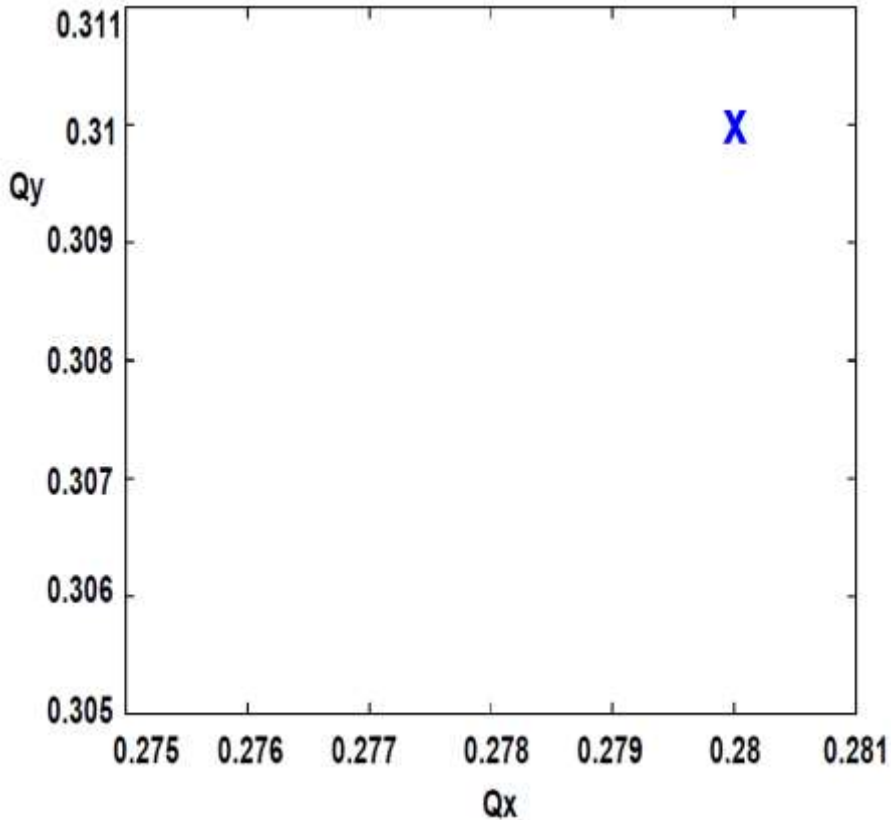


**Non-linear force →
tune depends on the
amplitude of betatron
oscillations**

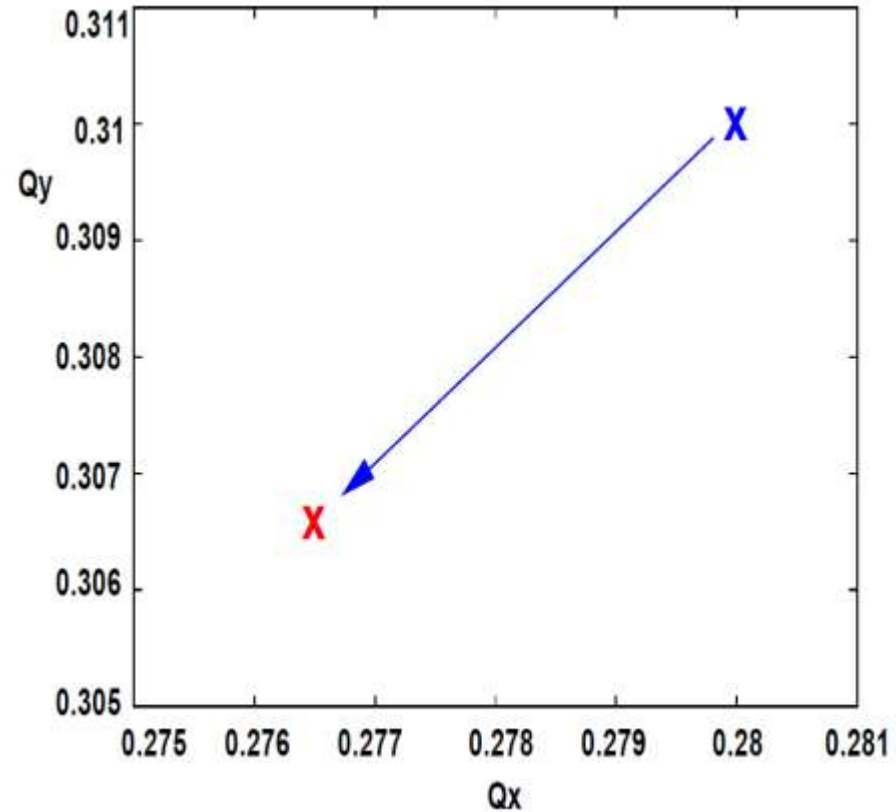
**large effect for $A < \sigma$
small effect for $A \gg \sigma$**

Linear tune shift - two dimensions

“bare lattice” tune

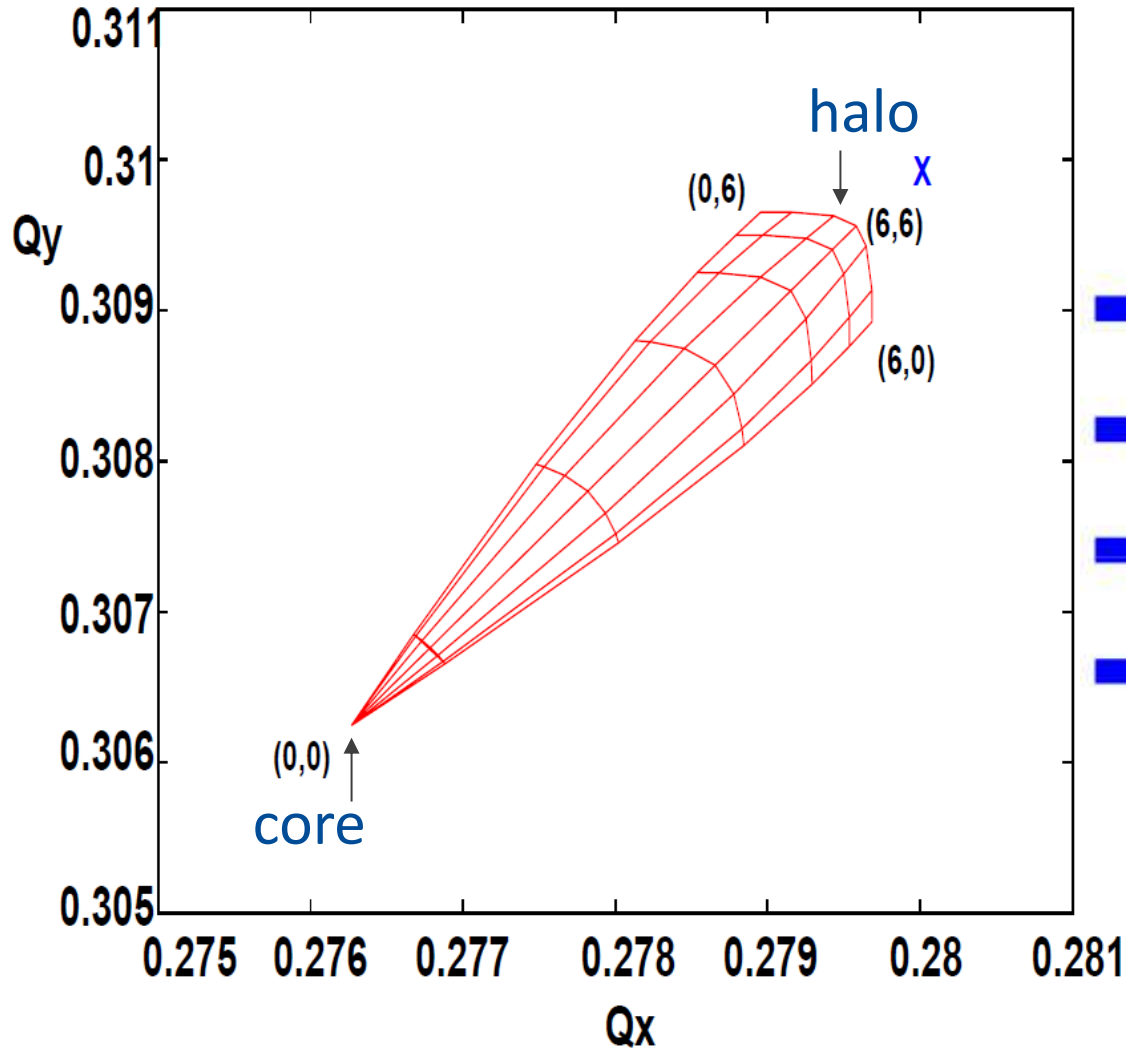


“bare lattice” tune + linear shift due to beam-beam (=core particles)



Non-linear tune shift in two dimensions

Tune footprint for head-on collision



- Tunes depend on x **and** y amplitudes
- No single tune in the beam
- Compute and plot for every amplitude (pair) the tunes in both planes
- In 2 dimensions:
plotted as **footprint**

e+e- LEP vs p-pbar collider Tevatron

	LEP	Tevatron
Beam sizes	160 - 200 μm · 2 - 4 μm	30 μm · 30 μm
Intensity N	4.0 · 10 ¹¹ /bunch	3 · 10 ¹¹ /bunch
Energy	100 GeV	980 GeV
β_x^* · β_y^*	1.25 m · 0.05 m	0.28 · 0.28 m
Beam-beam parameter(ξ)	0.0700	0.012 x2 IPs

Observations (Reality of Beam-Beam)

- Remember:

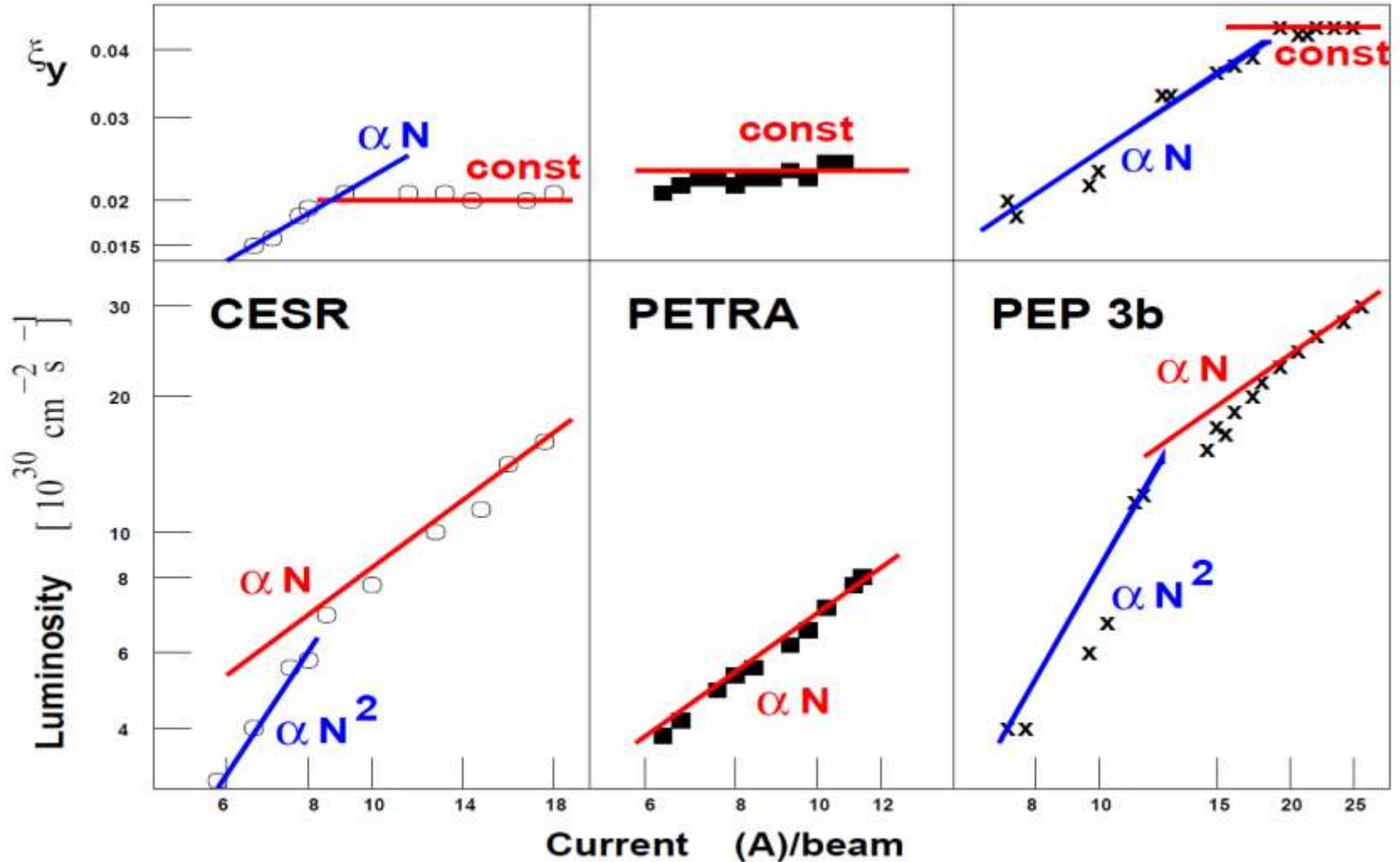
$$\mathcal{L} = \frac{N_1 N_2 f B}{4\pi\sigma_x\sigma_y}$$

- Luminosity should increase $\propto N_1 N_2$
for:

$$N_1 = N_2 = N \quad \rightarrow \quad \propto N^2$$

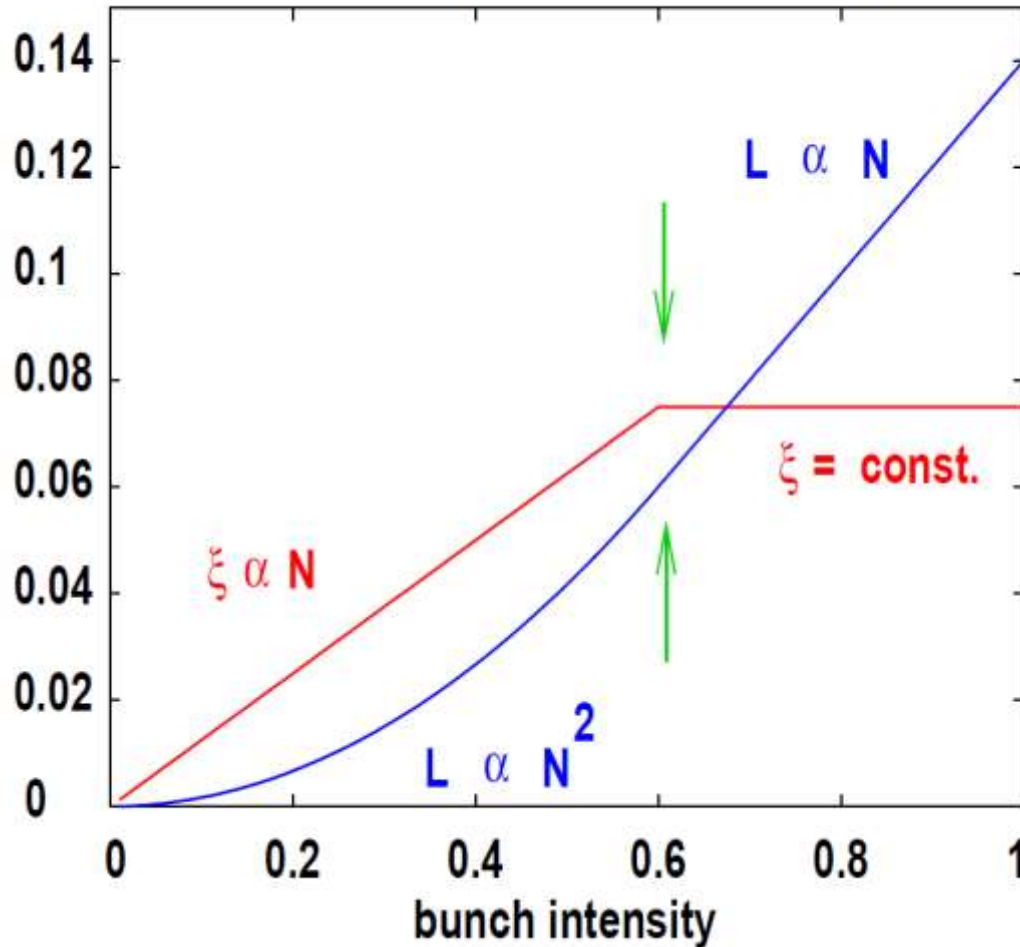
- Beam-beam parameter should increase $\propto N$
- But:

Beam-Beam Limits : e+e- Colliders



Beam-beam Limit on Luminosity

beam-beam parameter and luminosity



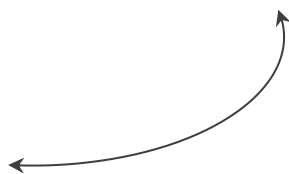
First - Beam-beam parameter increases linearly with intensity
Saturation above some intensity

Then - luminosity increases only linearly with N above the so-called **beam-beam limit**

What's happening?

$$\xi_y = \frac{N r_0 \beta_y}{2\pi \gamma \sigma_y (\sigma_x + \sigma_y)} \quad (\sigma_x \gg \sigma_y) \quad \approx \quad \frac{r_0 \beta_y}{2\pi \gamma (\sigma_x)} \cdot \frac{N}{\sigma_y}$$

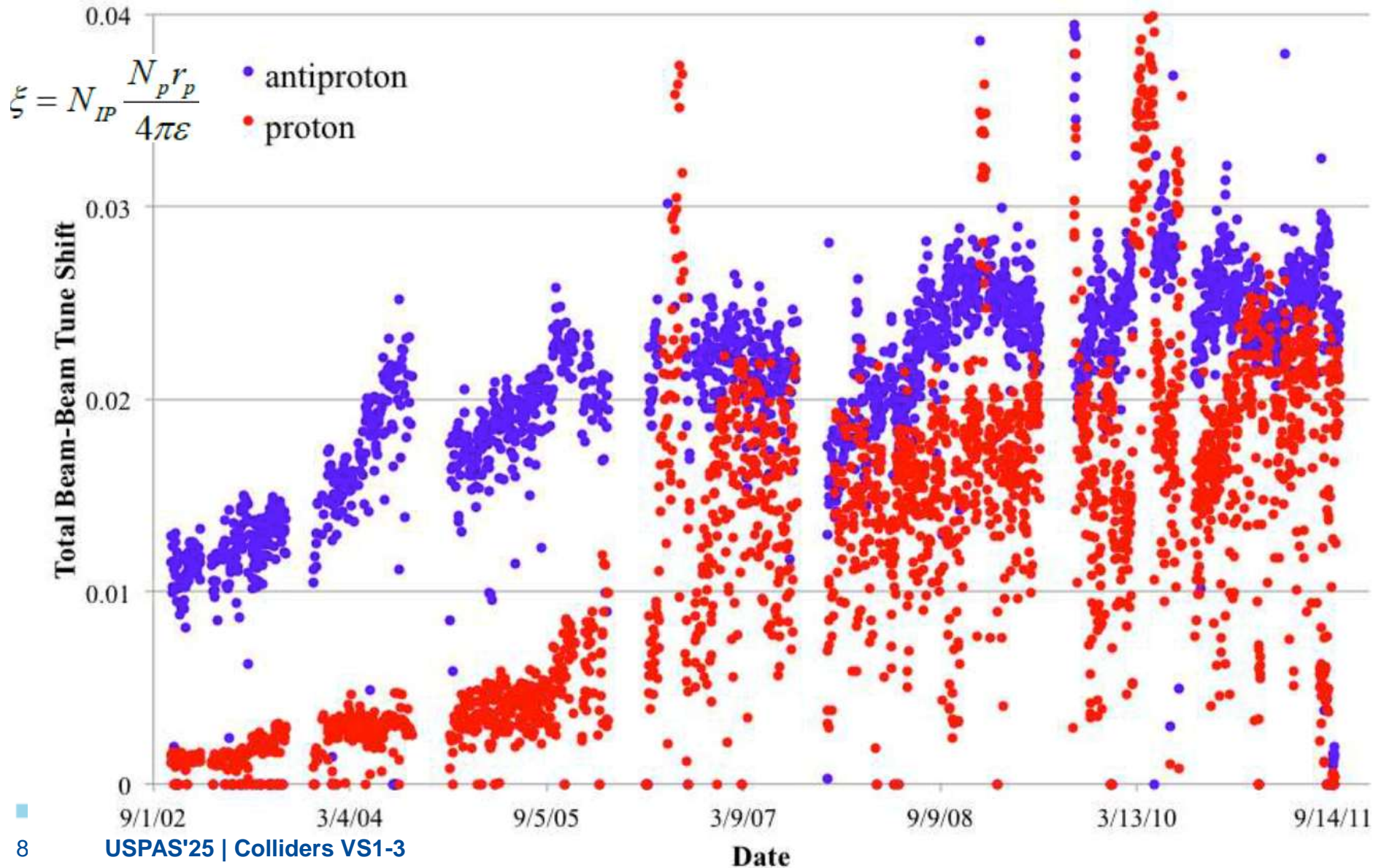
and

$$\mathcal{L} = \frac{N^2 f B}{4\pi \sigma_x \sigma_y} = \frac{N f B}{4\pi \sigma_x} \cdot \frac{N}{\sigma_y}$$


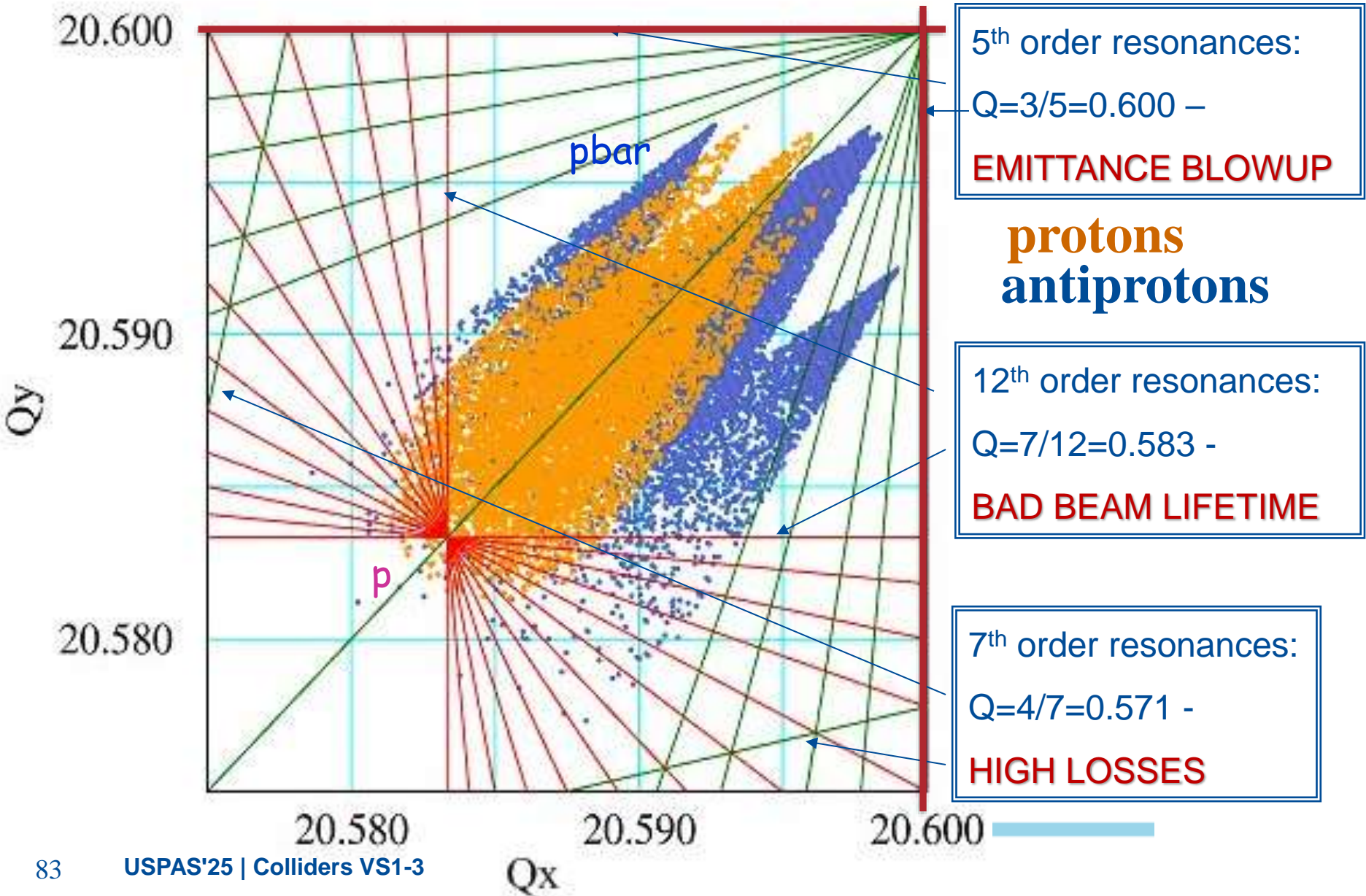
- Above beam-beam limit: σ_y increases when N increase
 - to keep \mathcal{L} constant \rightarrow **equilibrium emittance !**
- Therefore:
- \mathcal{L} is NOT a universal constant !
 - depends on tunes/WPs, damping rates, etc
 - difficult to predict exactly for hadron machines

Beam-Beam Limits: pp/pbar Colliders

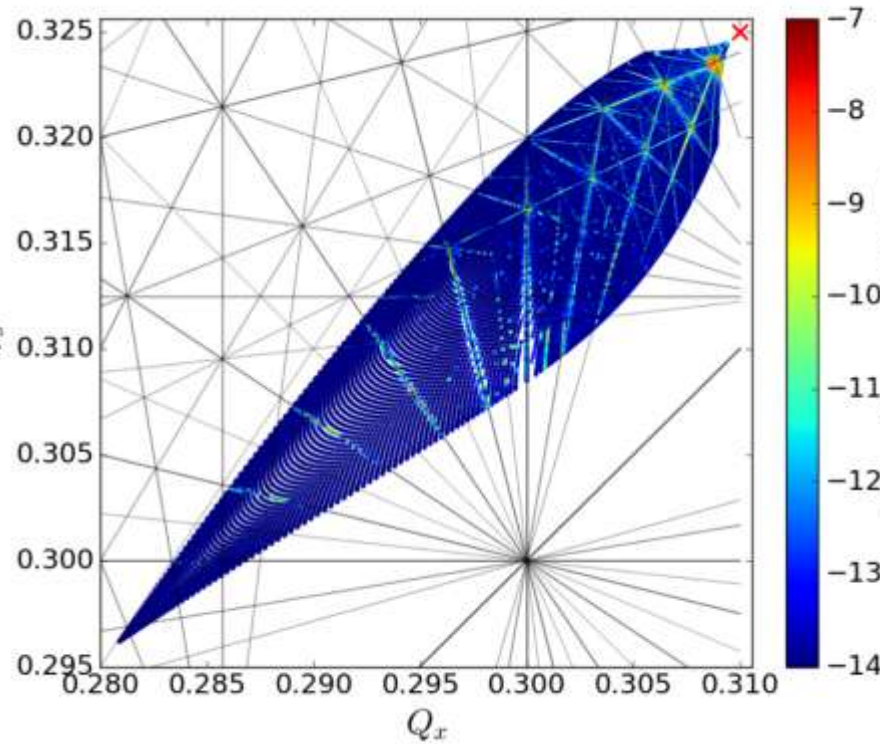
Tevatron Collider Run II



Tevatron Tune Footprint “Confinement”

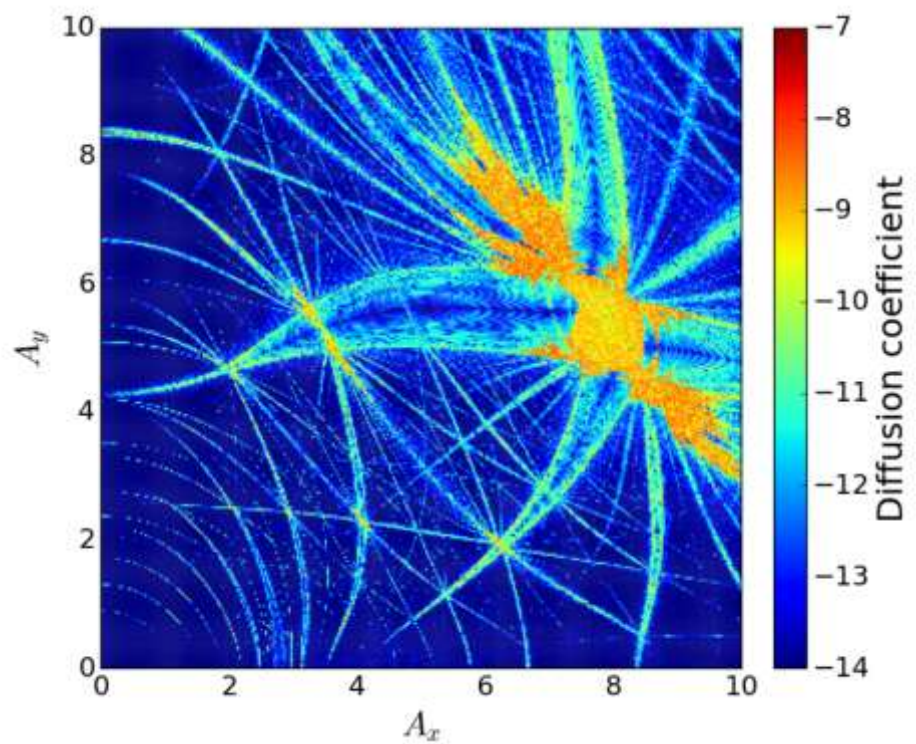


Resonances matter! ... Diffusion



Tune map: LHC (simul)
Shown resonances up to order 20

- $\xi_{tot} = 0.03$, $Q_x = 0.31$, $Q_y = 0.325$
 $N_{mp} = 1e5$, 4D BB, $Q' = 0$

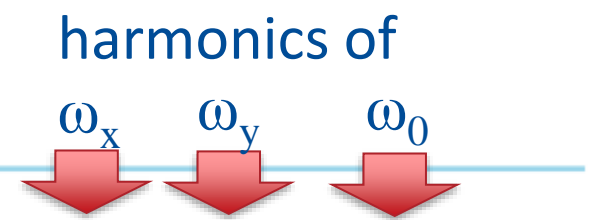


Amplitude map: LHC (simul)
Shown diffusion rates vs A_x/A_y

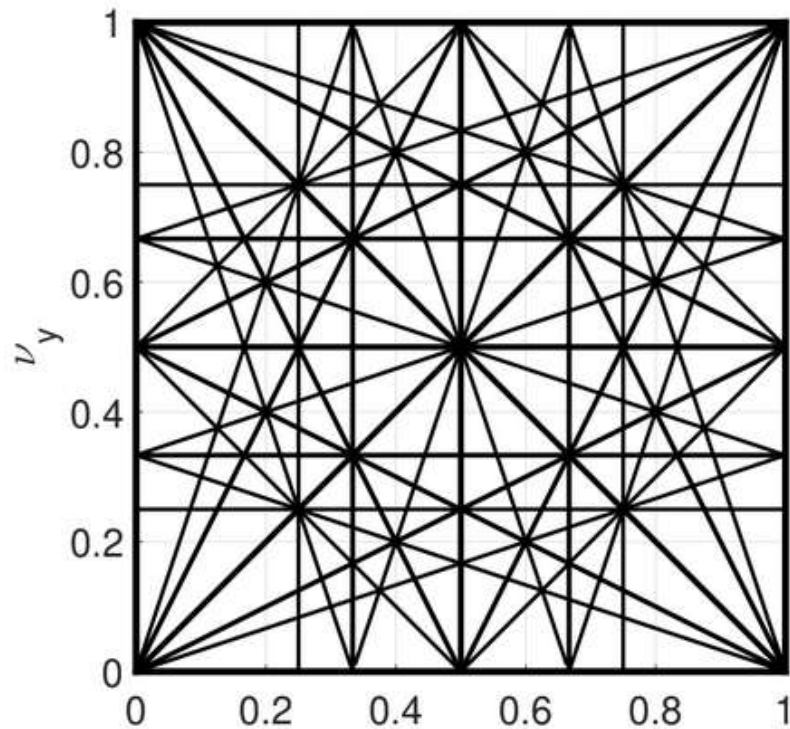
$$D_i = \log_{10} \sqrt{\frac{dQ_{x,i}^2}{dt_{turn}} + \frac{dQ_{y,i}^2}{dt_{turn}}}$$

Measure tune of a particle based on (here) 4096 turns - Calculate linear change over 10 measurements, separated by 10k turns

Non-linear Resonances



- Nonlinear terms in the force $F(x,y,t) \sim x^l y^p \delta(t-kT)$ lead to appearance of driving terms oscillating with frequencies $mQ_x + nQ_y$, and therefore open opportunities for nonlinear resonances if



$$mQ_x + nQ_y = p$$

$|m| + |n|$ is order of the resonance



i.e. resonance diagram up to fourth order; importance of the resonance depends on the force shape and order (low order = more serious; often longitudinal deviations matter if $mQ_x + nQ_y + lQ_s = p$)



Thanks for your Attention!

Questions !?



Literature

- V.Shiltsev, F.Zimmermann, Modern and Future Colliders (Rev.Mod.Phys., 2021)

<https://journals.aps.org/rmp/abstract/10.1103/RevModPhys.93.015006>

- V.Lebedev, V.Shiltsev, Tevatron Book

https://indico.cern.ch/event/774280/attachments/1758668/2915590/2014_Book_AcceleratorPhysicsAtTheTevatro.pdf

W.Herr, CAS school

<https://cds.cern.ch/record/941319/files/p379.pdf>

Proc. 2013 ICFA mini-workshop on "Beam-Beam Effects in Hadron Colliders"

<https://indico.cern.ch/event/189544/>

Comprehensive *JUAS-book* (2371 pages – all topics!)

<https://doi.org/10.23730/CYRSP-2024-003>.



U.S. Particle Accelerator School
Education in Beam Physics and Accelerator Technology



Colliders – Lectures VS4-5: Beam-Beam Effects (2) Other Effects

Vladimir Shiltsev, Northern Illinois University

part of the “Colliders” class by V.Shiltsev, V.Ptitsyn and C. Liu

US Particle Accelerator School, Jan 27 – Jan 31, 2025

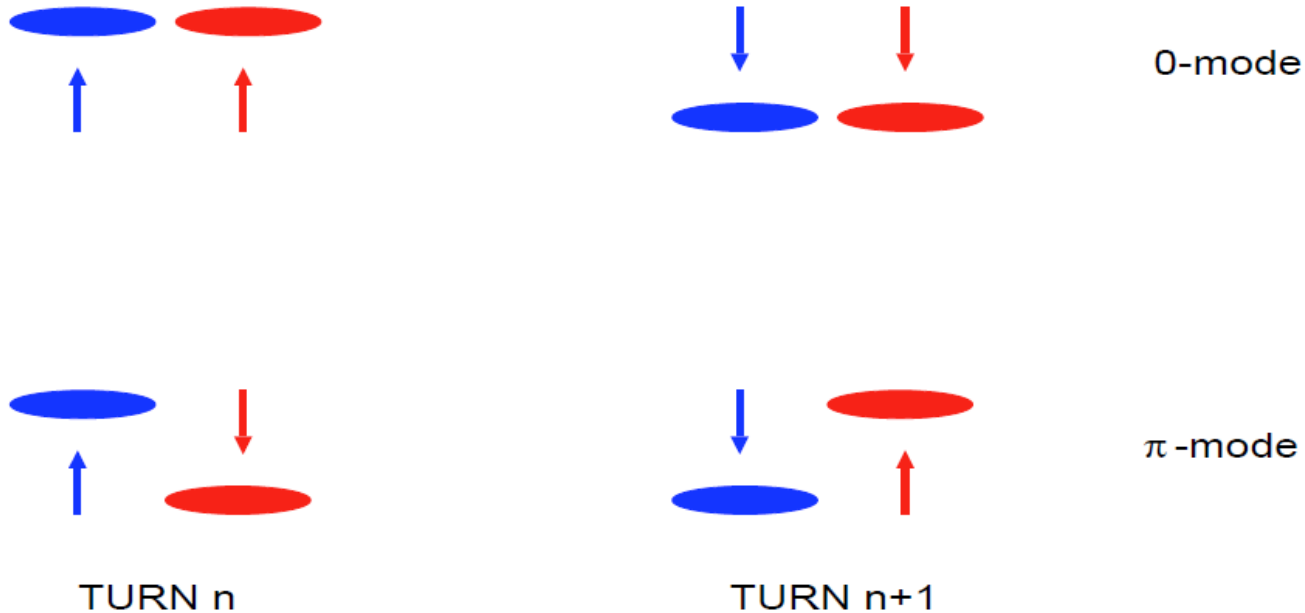
Complications : Strong-Strong vs Weak-Strong

- Both beams are very strong (**strong-strong**):
 - Both beams are affected and change due to beam-beam interaction
 - Examples: LHC, LEP, RHIC, ...
- One beam much stronger (**weak-strong**):
 - Only the weak beam is affected and changed due to beam-beam interaction
 - Examples: SPS collider, Tevatron (early in Run II) , ...

Incoherent vs Coherent Beam-Beam Effects

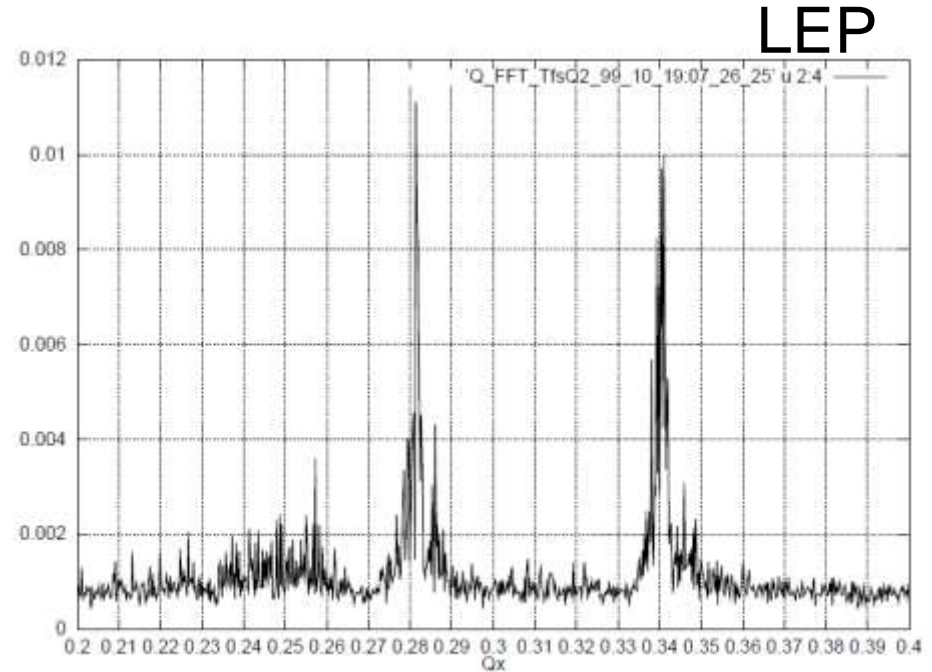
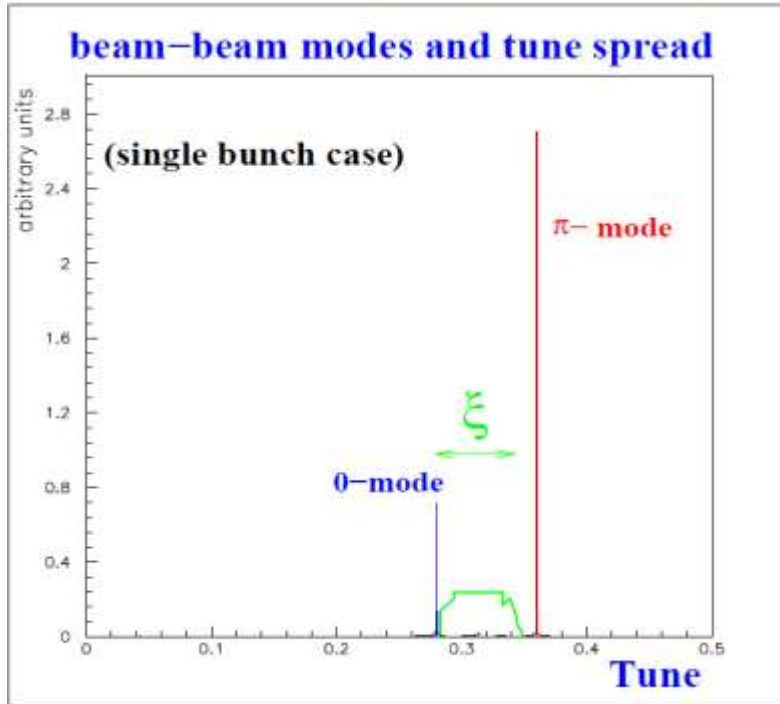
- Incoherent (single particle effects):
 - Single particle dynamics - treat as a particle passing through a static electromagnetic lens
 - Basically, non-linear dynamics effects:
 - unstable and/or irregular motion (“chaos”)
 - beam size blow up or bad lifetime
 - Very bad: unequal beam sizes (studied at SPS, HERA, Tevatron)
- Coherent (bunches affected as a whole):
 - Collective modes
 - Bunch-by-bunch differences in:
 - Orbits
 - Tunes
 - Chromaticities

Coherent Beam-Beam: Modes



- Coherent mode: two bunches are "locked" in a coherent oscillations
 - 0-mode is stable (Mode with **NO** tune shift)
 - π -mode can become unstable (Mode with **LARGEST** tune shift)

Coherent Beam-Beam: Modes



▶ 0-mode is at unperturbed tune

▶ π -mode is shifted by $1.1 - 1.3 \cdot \xi$

Two modes clearly visible
 Can be distinguished by phase relation, i.e.
 sum and difference signals

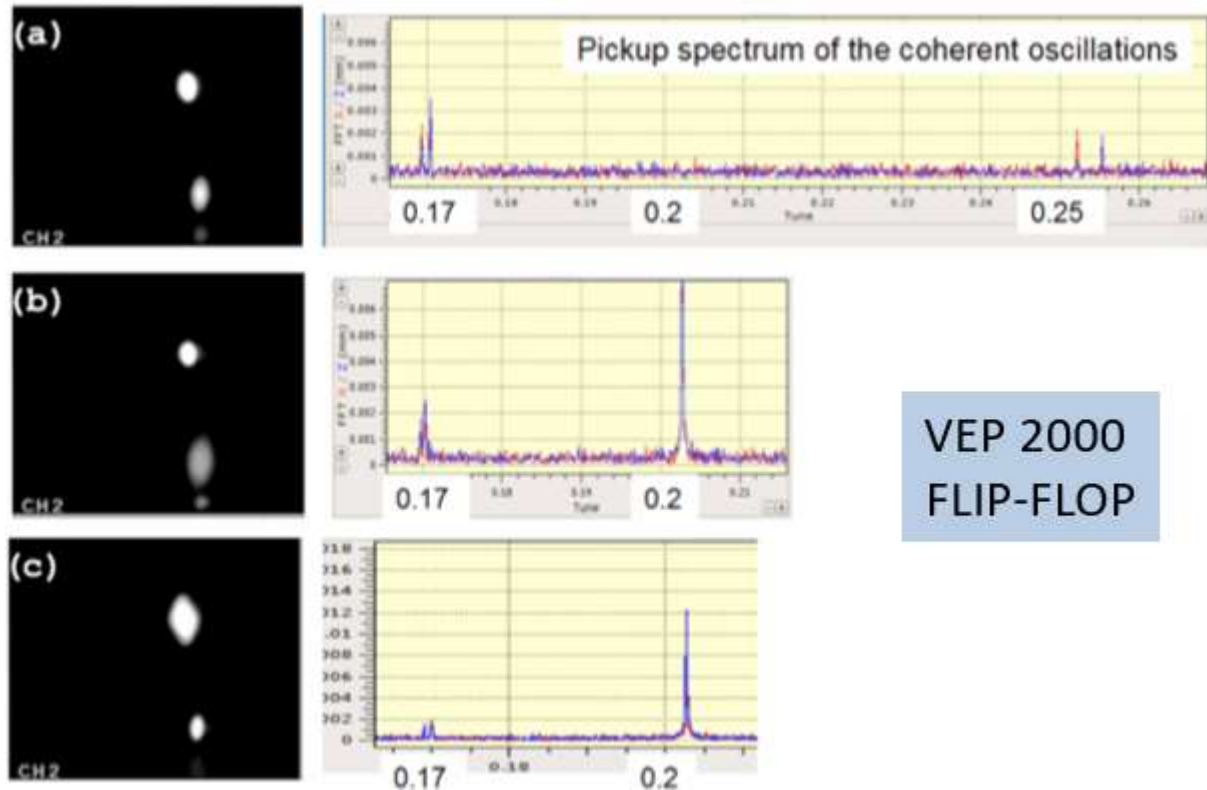
Coherent Beam-Beam: Flip-Flop

Bunch sizes get bigger or smaller out of phase

(PEP-II, VEPP-2000, etc)

The intensity threshold for the flip-flop depends on:

- asymmetry in beam intensities
- x-y coupling



3D Flip-Flop effects triggered by non-linearities of lattice. π -mode on 1/5 resonance. The effect have shown a strong sensitivity to X-Y coupling, beta unbalance and bunch length \rightarrow main limitation in VEPP 2000.

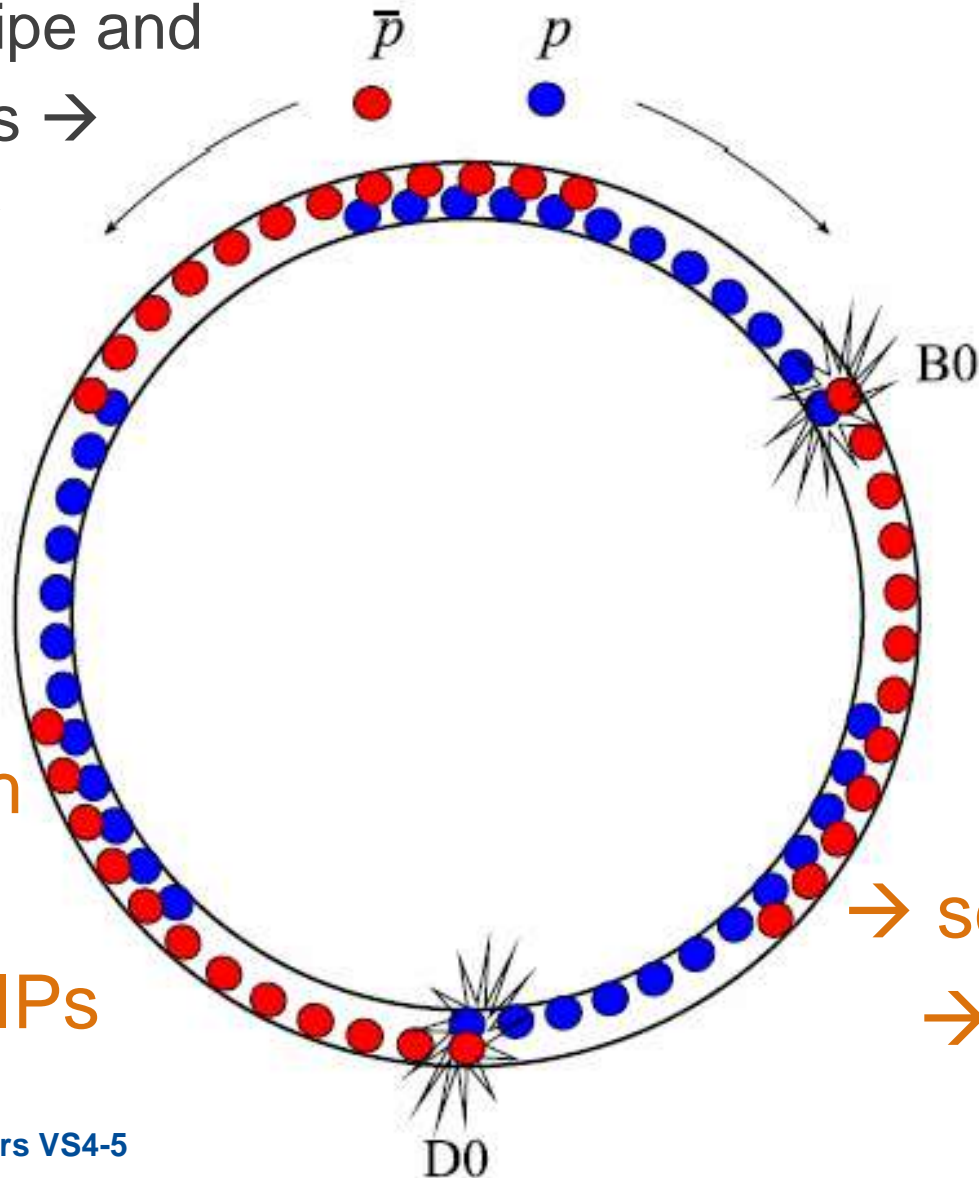
Multi-Bunch Operation: Need and Issues

$$\mathcal{L} = \frac{N_1 N_2 f \cdot B}{4\pi\sigma_x\sigma_y}$$

- How to collide many bunches (for high L) ??
- Must avoid unwanted collisions !! Otherwise $\xi \rightarrow 2B\xi$
- Separation of the beams:
 - Pretzel/helix scheme (SPS, LEP, Tevatron)
 - Bunch trains (LEP, PEP)
 - Crossing angle (LHC)

Tevatron: 36 proton x 36 antiproton

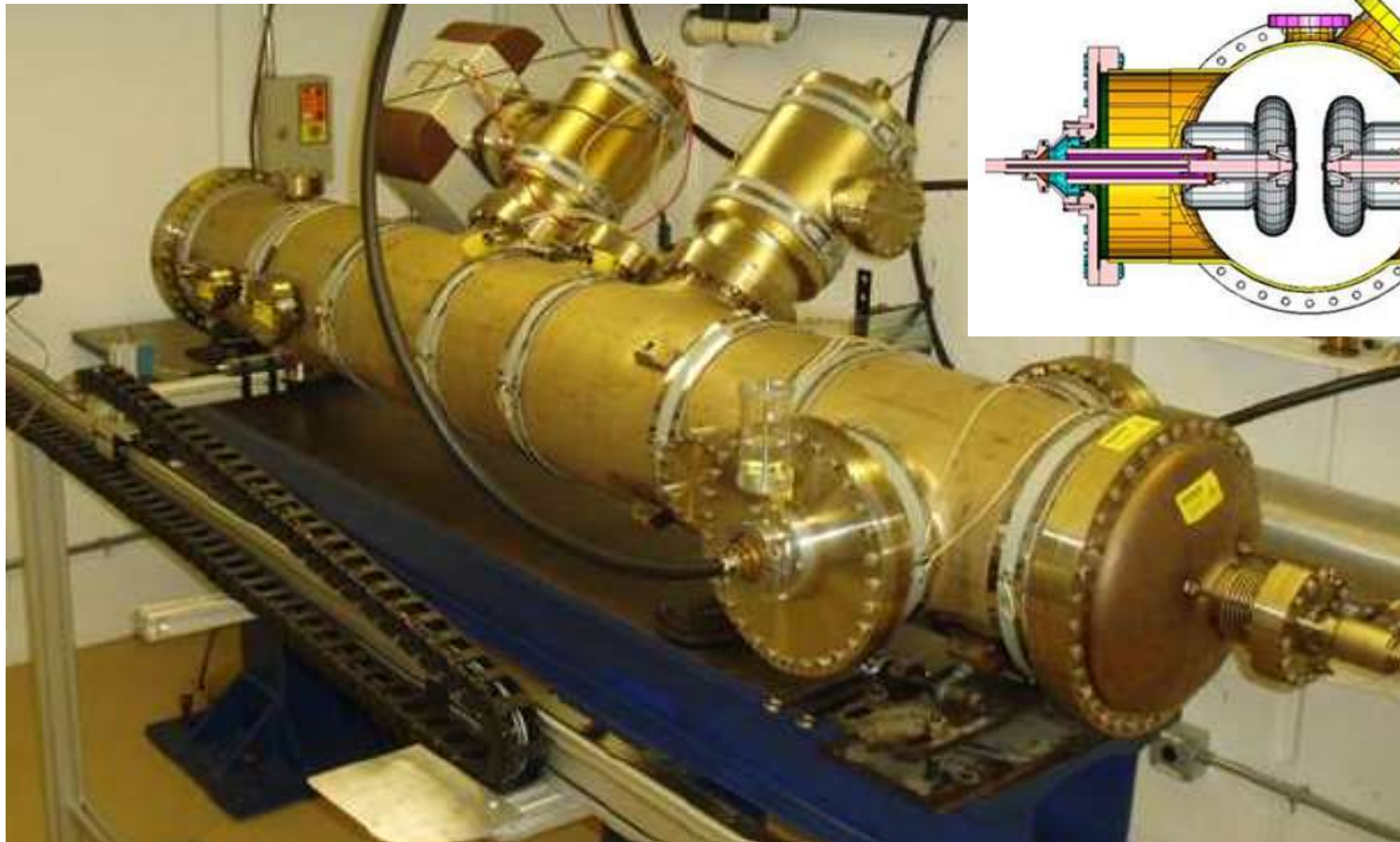
Same beam pipe and
magnetic fields →
same orbits →
72 IPs



396 ns bunch
separation
→ 59 m btw IPs

Need only 2
→ separate at 70
→ Electric field

Tevatron High Voltage Electrostatic Separators



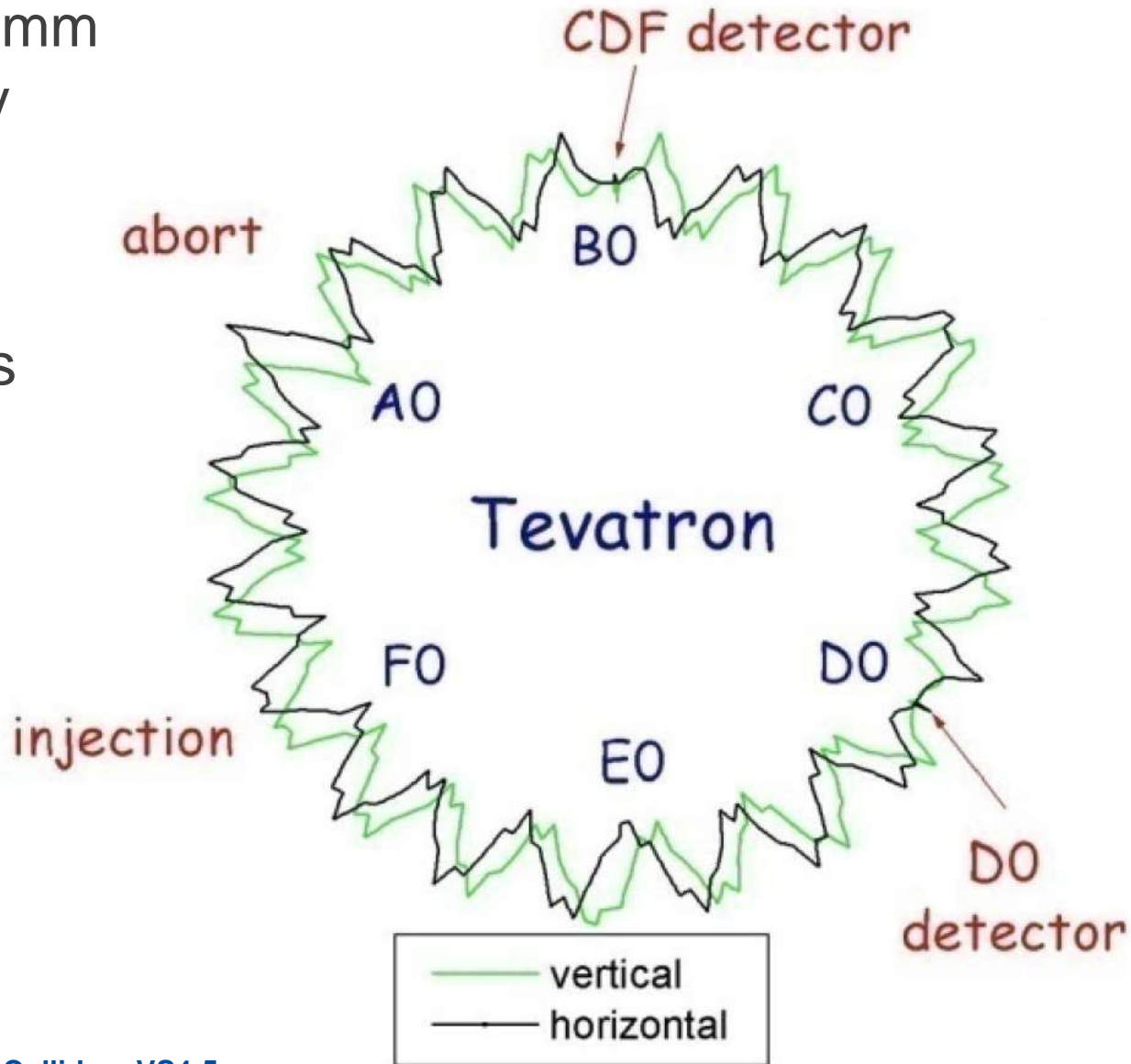
300 kV over 50 mm gap; 3 m ; 24 of them (H/V)

Tevatron Helix

24 electrostatic separators are used

size 12-15 mm
at 150 GeV

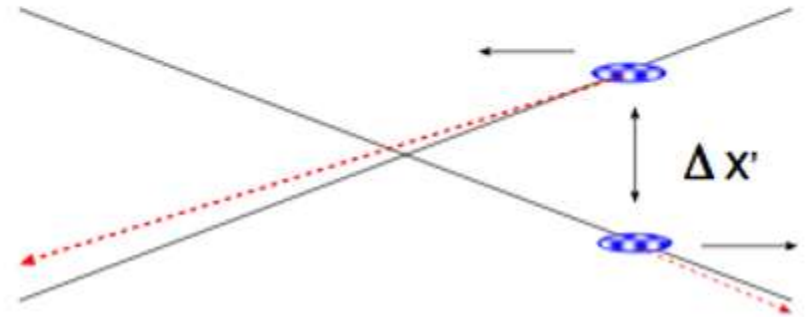
6-8 mm
at collisions



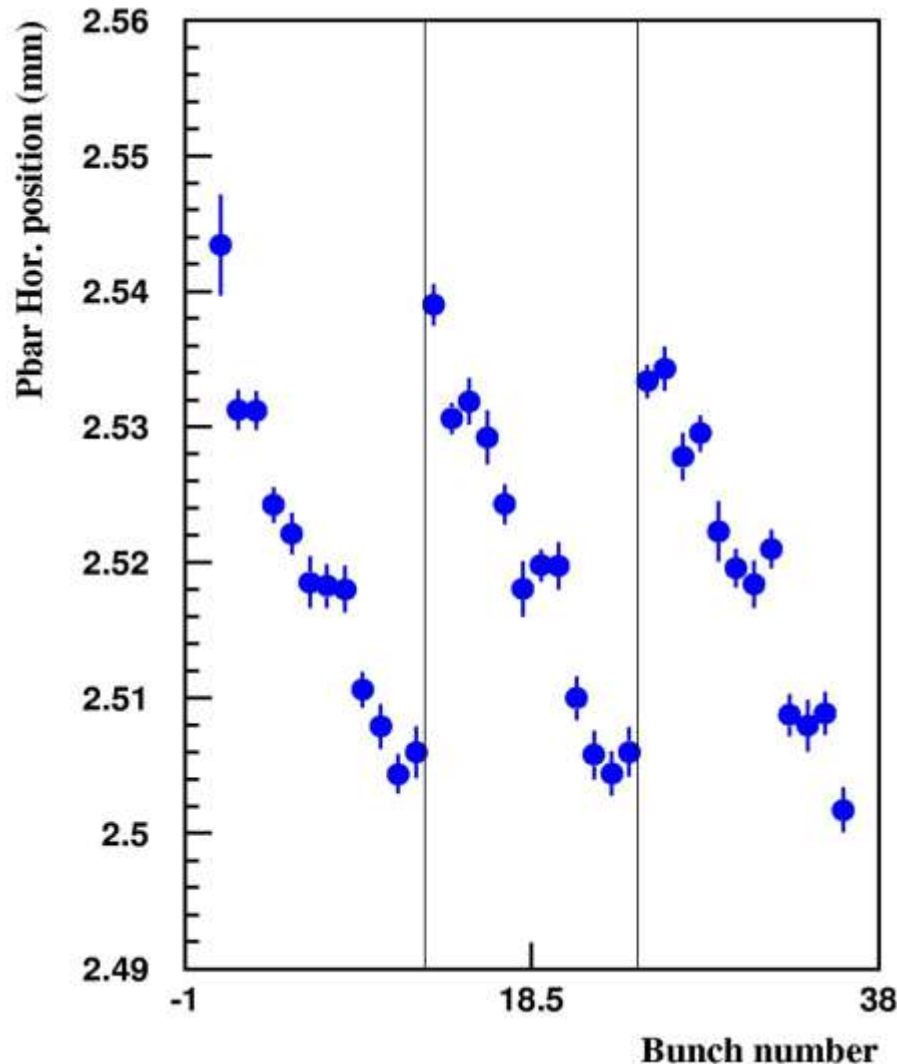
All beam indicators become bunch dependent due to long-range beam-beam effects

- Orbits
- Tunes, couplings
- Chromaticities
- In both – protons and pbars
- Have 3-fold symmetry (trains of 12)

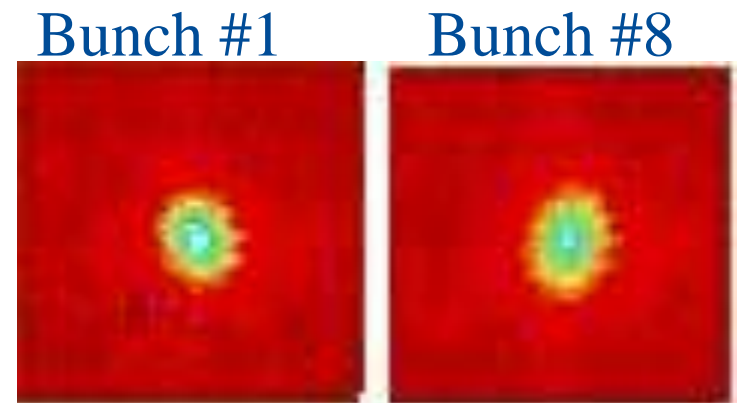
$$\Delta x' = \frac{\text{const}}{d} \left[1 - \frac{x}{d} + O\left(\frac{x^2}{d^2}\right) + \dots \right]$$



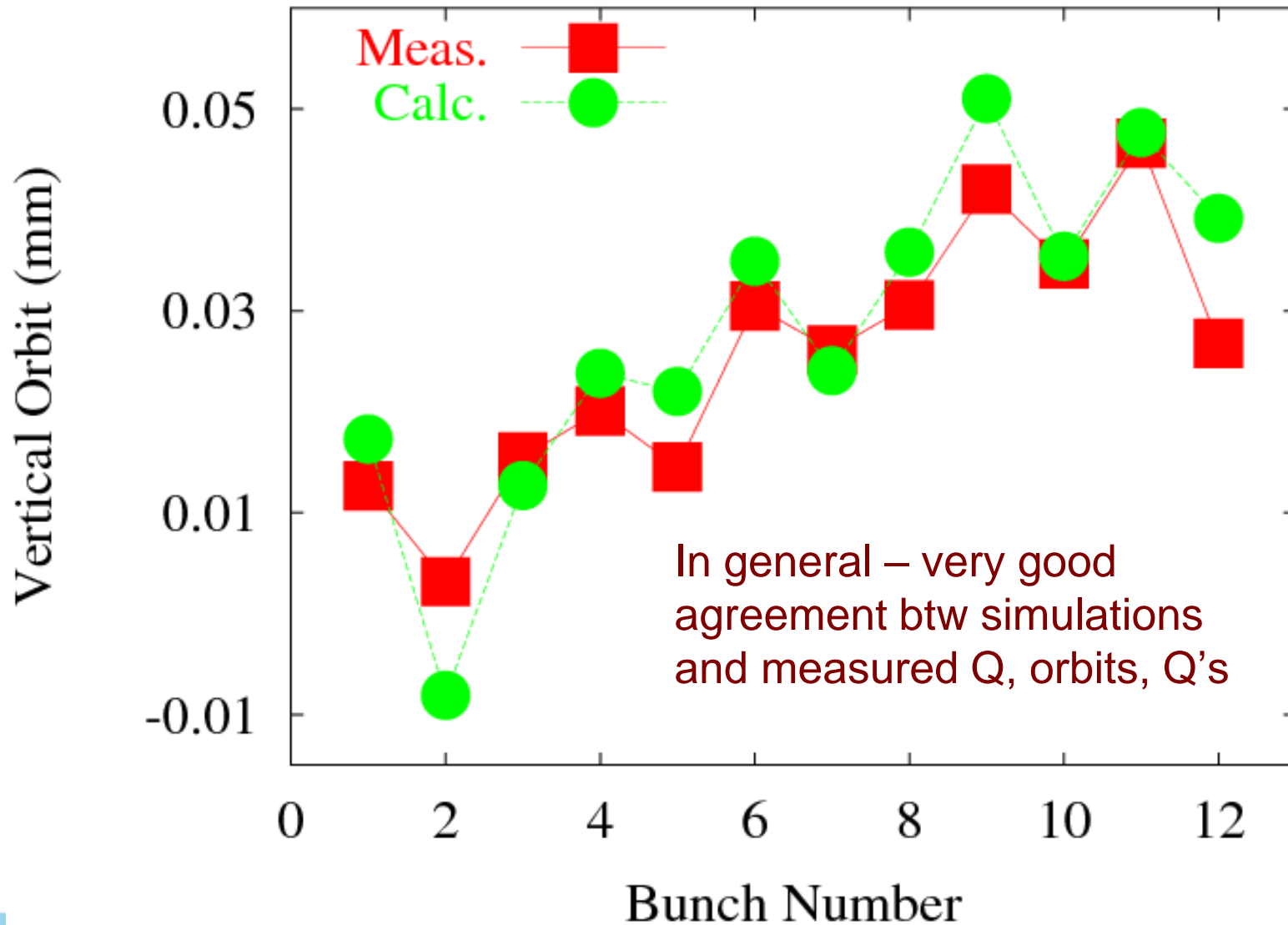
Long-range B-B Seen at Low-Beta (980 GeV)



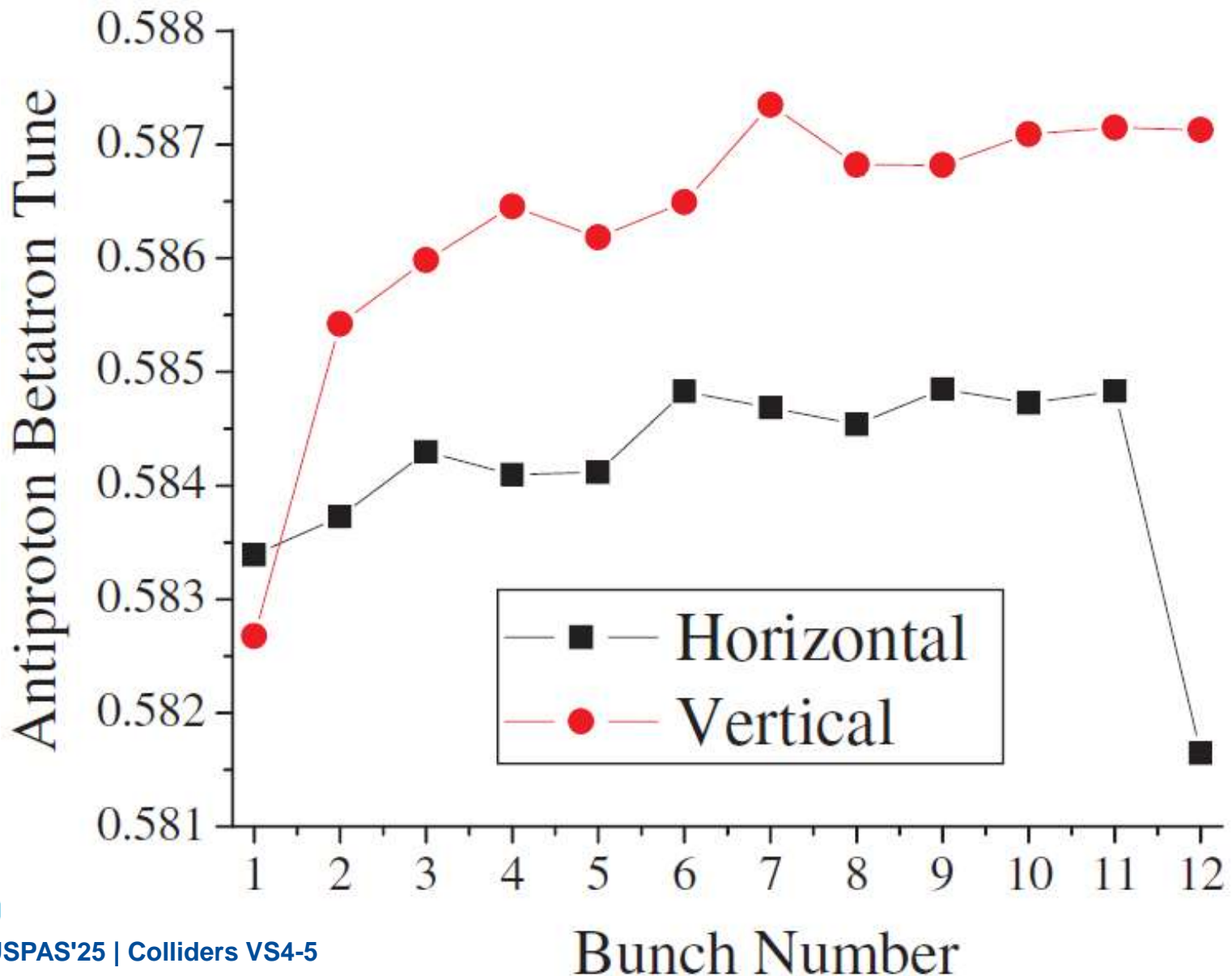
- Synchrotron light monitors show 40 micron b-by-bunch horizontal orbit variation along the bunch train with 3-train symmetry (4 microns for protons)
- Also indicate coupling differences →



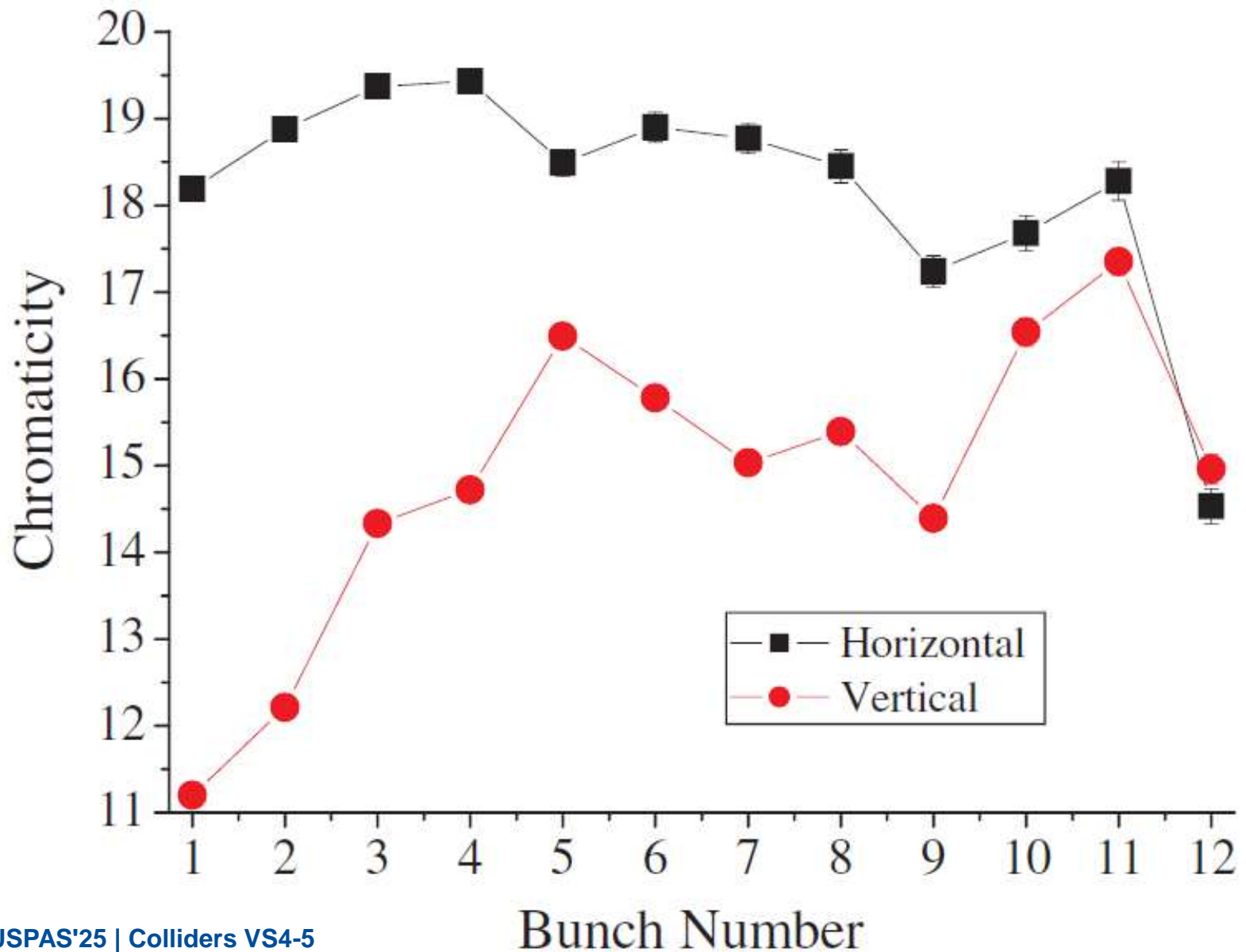
Antiproton Vertical Orbit



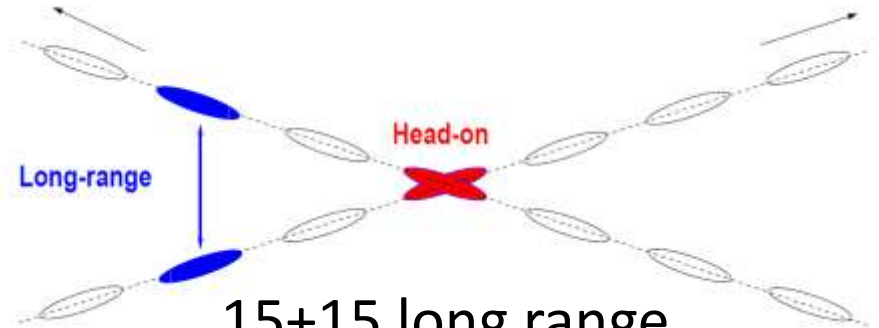
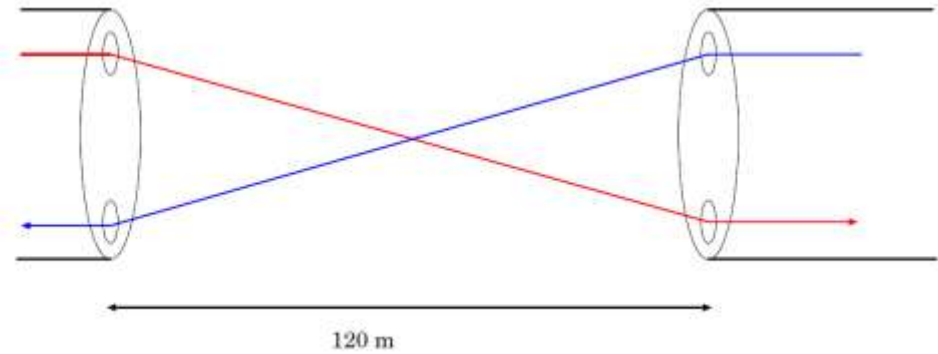
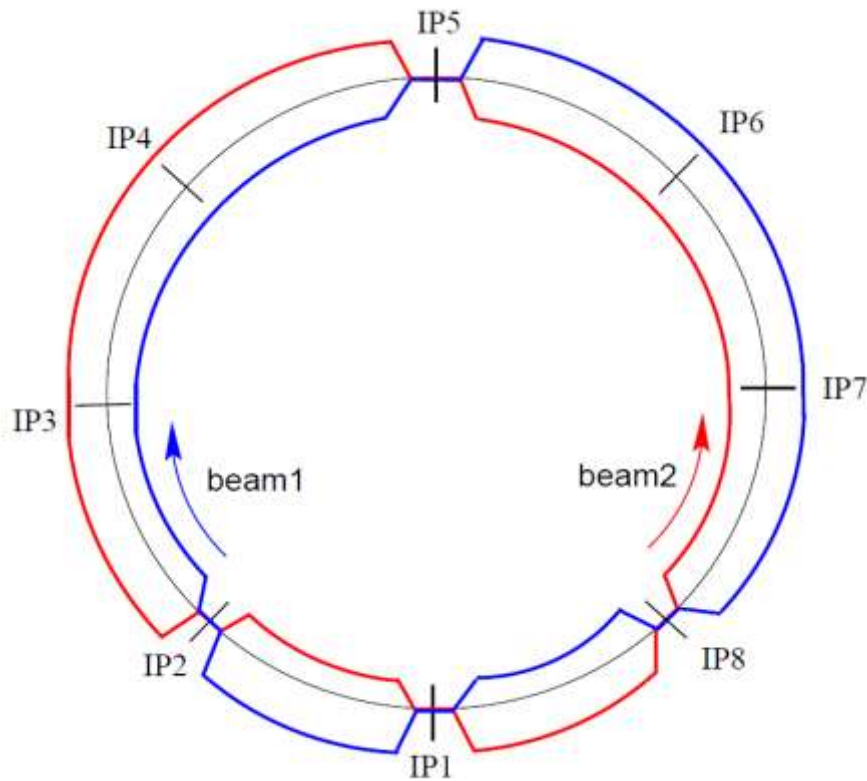
Pbar Bunch Tunes in Collisions



Pbar Bunch Chromaticity in Collisions



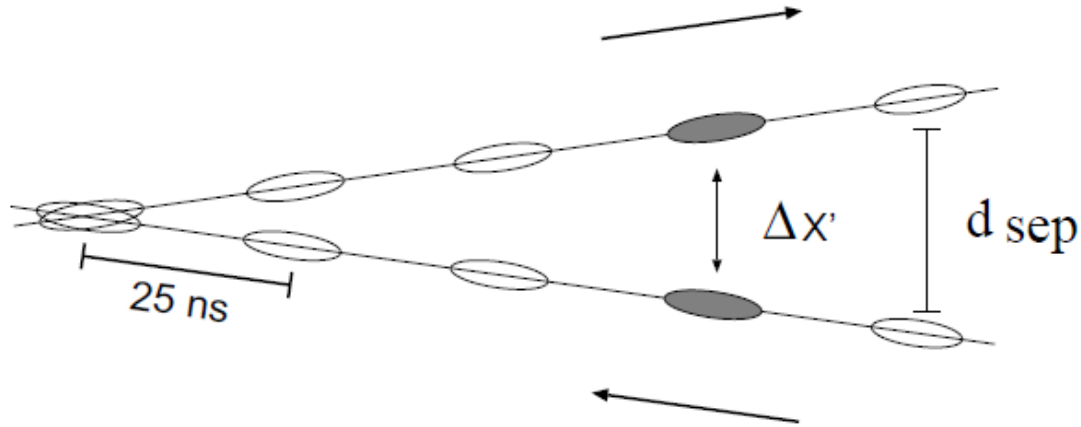
In the LHC



15+15 long range
interactions ($6-12 \sigma$)

- 2808 p bunches in each beam, every 25 ns
- Two beams in separate beam pipes except in common chamber around 4 experiments
- **Local** separation via two horizontal and two vertical crossing angles

Parasitic Beam-beam Kicks



For horizontal separation d :

$$\Delta x'(x + d, y, r) = -\frac{2Nr_0}{\gamma} \cdot \frac{(x + d)}{r^2} \left[1 - \exp\left(-\frac{r^2}{2\sigma^2}\right) \right]$$

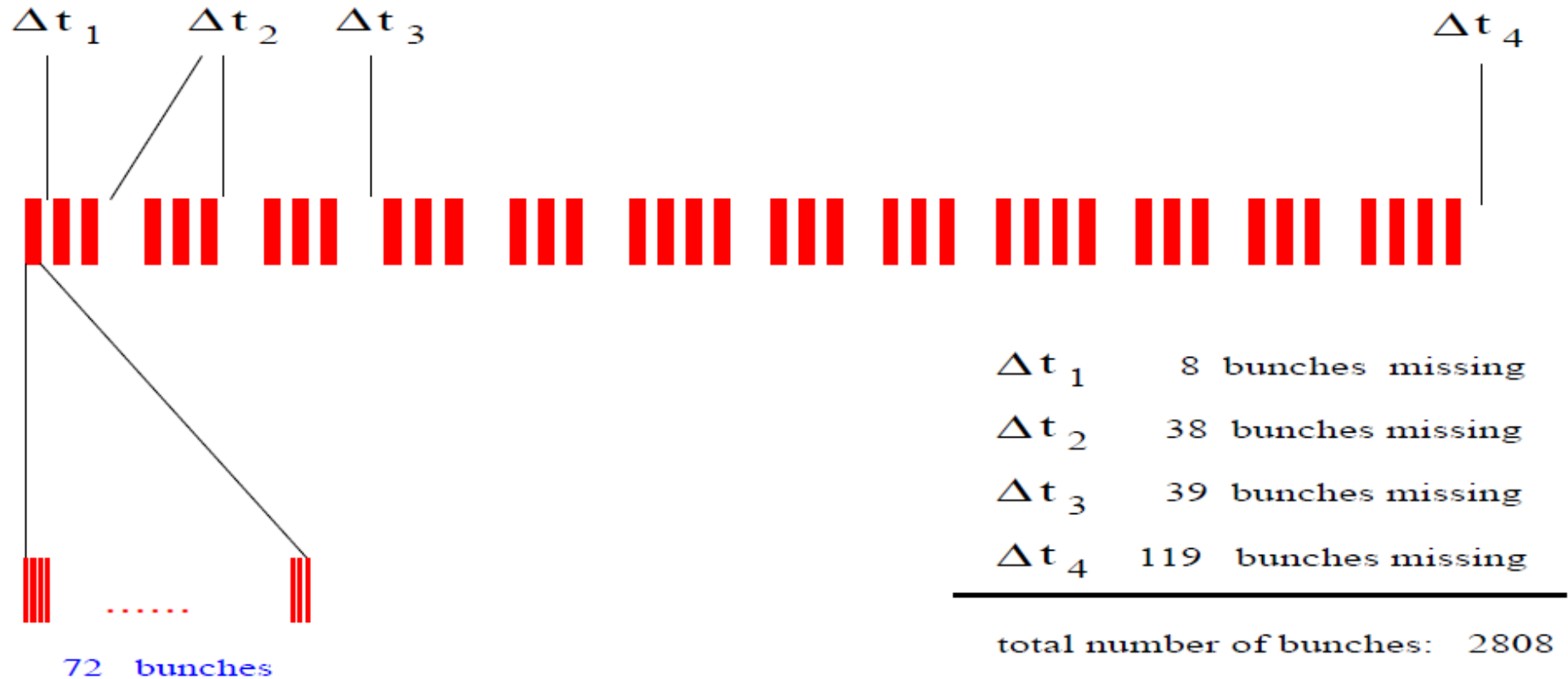
(with: $r^2 = (x + d)^2 + y^2$)

In LHC 15 collisions on each side, 120 in total!
Effects depend on separation, eg tunes shift

$$\Delta Q \propto -\frac{N}{d^2}$$

PAMCMAN bunches due to gaps

- Average orbit and tune variations can be corrected, **but:**



LHC bunch filling not continuous: holes for injection, extraction, dump ..

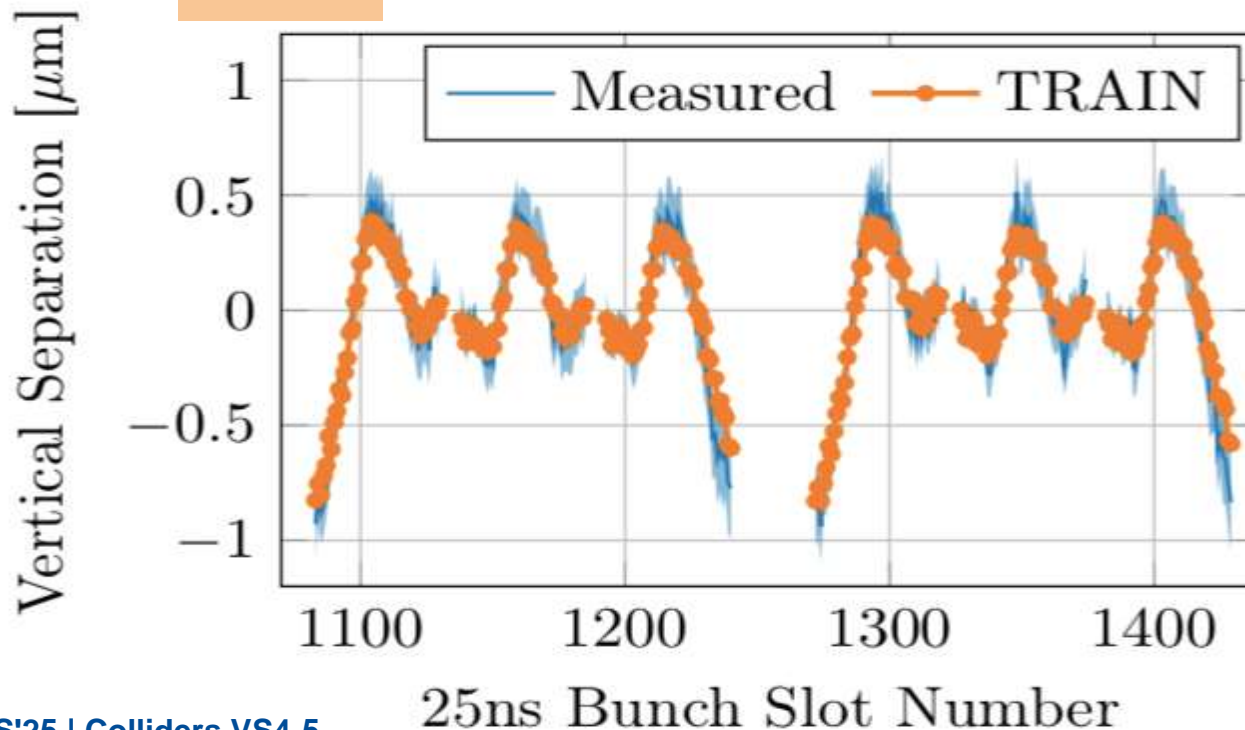
"Only" 2808 of 3564 possible bunches circulate ! 1756 "holes"

"Holes" meet "holes" at the interaction point - But not always ...

Effect of PACMAN bunches (end of train)

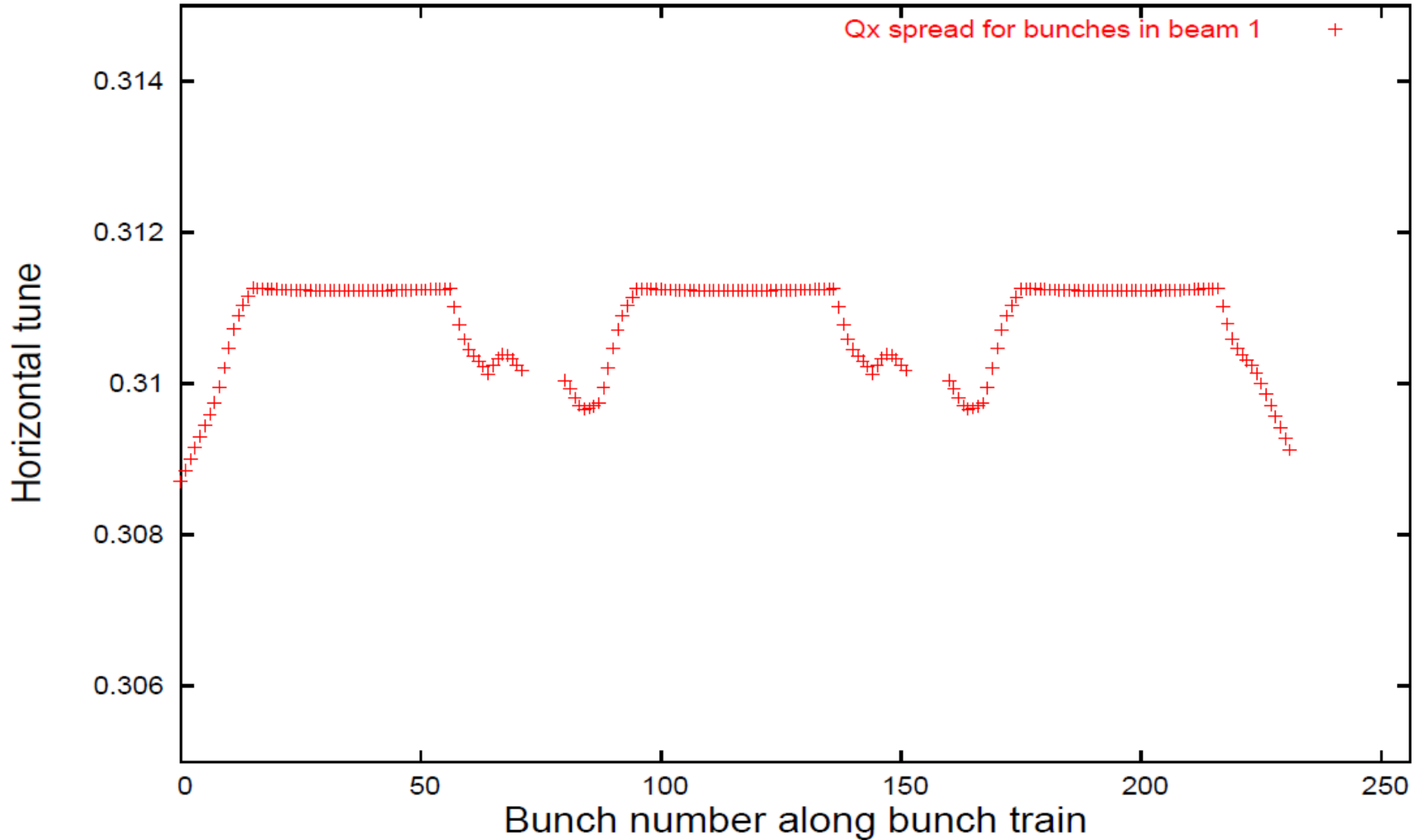
- Some bunches can meet a hole/holes (at beginning and end of bunch train) →
- They see fewer unwanted interactions in total: between 120 (max) and 40 (min) long range collisions → Different integrated beam-beam effect for different bunches

LHC



Tune Spread - too large for safe operation

Tune along bunches



How to control beam-beam effects?

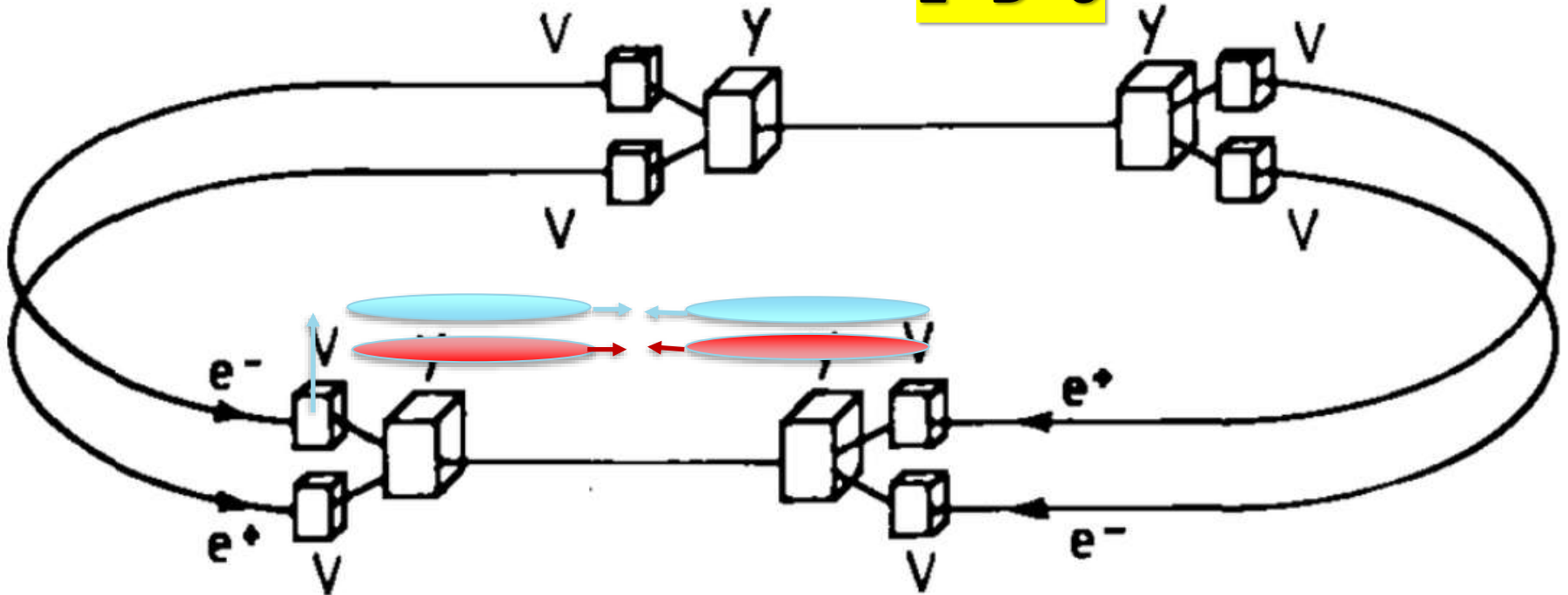
- Find 'lenses' to correct beam-beam effects
- Head on effects:
 - Linear "electron lens" to shift tunes
 - Non-linear "electron lens" to reduce spread
 - Successful e-lenses at FNAL and RHIC
- Long range effects:
 - At very large distance: force is $1/r$
 - Same force as a wire !
- Overall - success with **active** compensation

Attempt #1: Four beams e-e+ e-e+

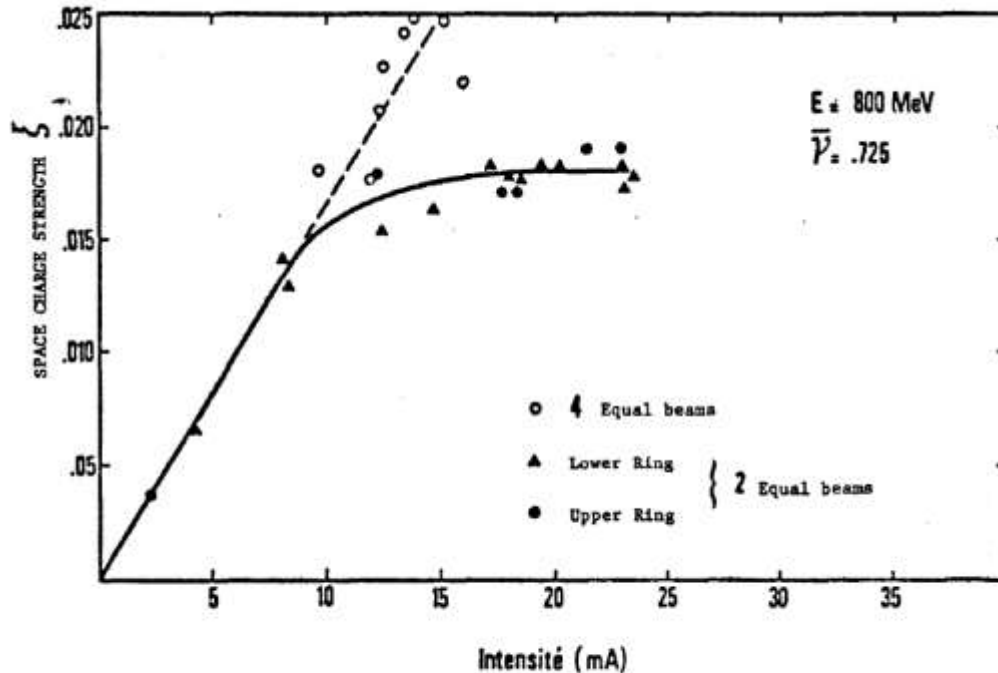
four-beam collider *Dispositif de Collisions dans l'Igloo* (DCI, 1970s) at Orsay with two 0.8 GeV electron beams and two positron beams of the same energy, all meeting at the same interaction point (*J.LeDuff et al*)

$$Q1+Q2+Q3+Q4=0 \quad J1+J2+J3+J4=0$$

$$E=B=0$$



Attempt #1: Four beams compensation



No improvement of performance was obtained in the four-beam configuration compared to collisions of just two beams of electrons and positrons.

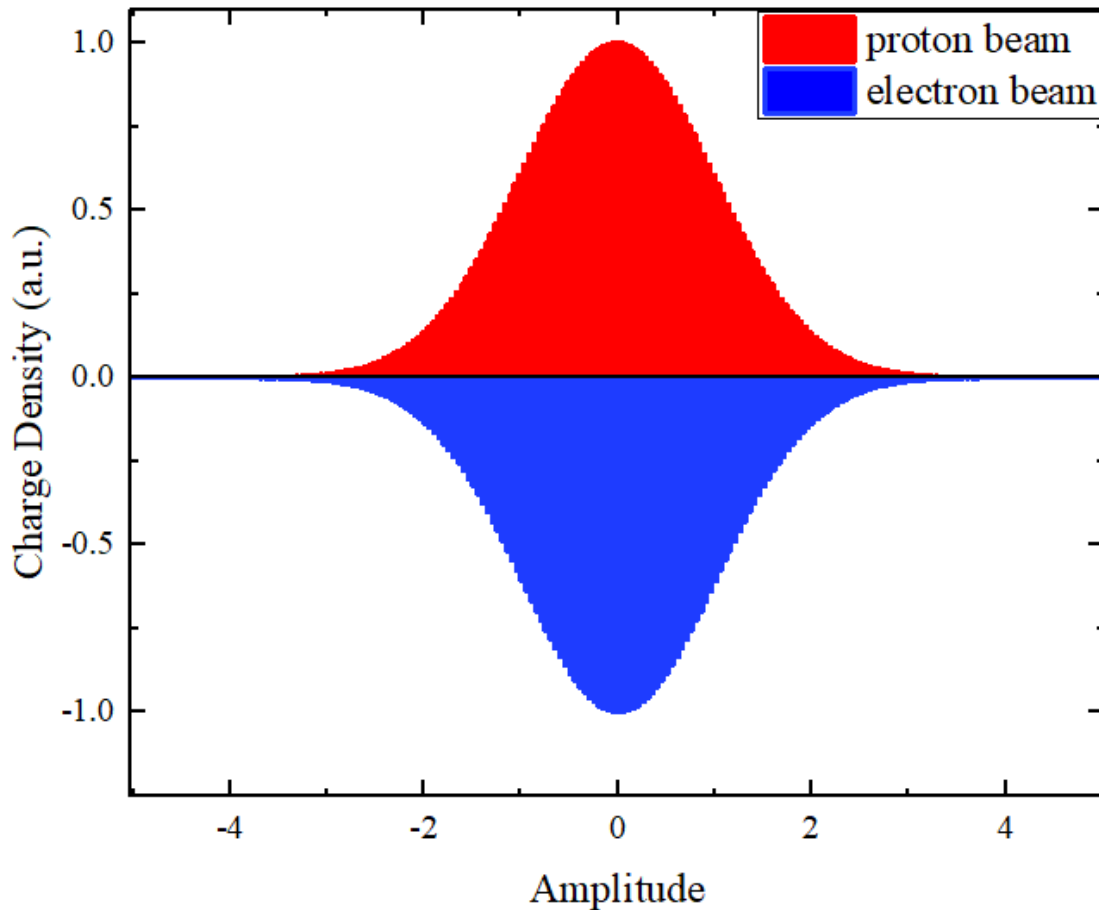
A transverse dipole feedback as well as a detuning of the two rings did not help.

The compensation is believed to be unsuccessful due to the loss of beam stability, both for dipole and higher order modes of coherent motion.

Fig. 12. Comparison between four beams and two beams: ξ versus current at $E = 800 \text{ MeV}$ and $\bar{\nu} = .725$

Approach #2: Electron lens

e- profile same as p^+ $N_e = N_{IP}N_p/(1 + \beta_e)$.



Protons focus pbars +
Electrons defocus

Net effect = zero

Footprint compressed

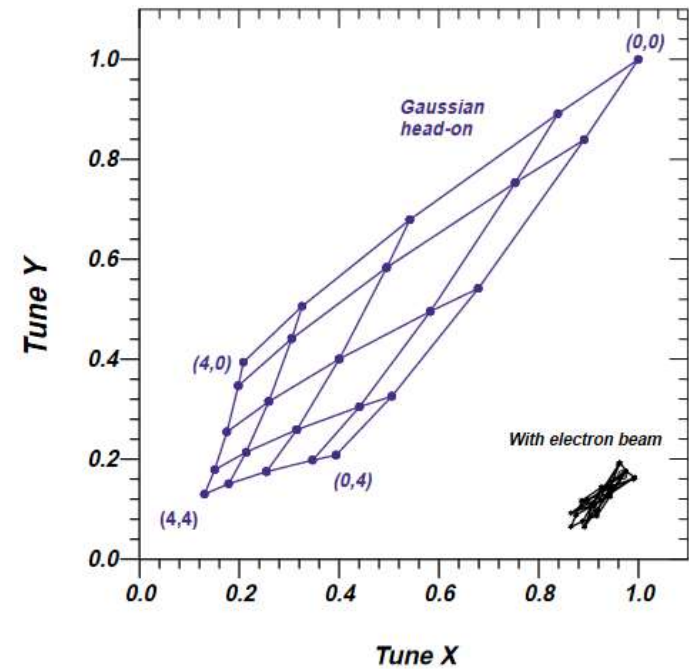
PHYSICAL REVIEW SPECIAL TOPICS - ACCELERATORS AND BEAMS, VOLUME 2, 071001 (1999)

Considerations on compensation of beam-beam effects in the Tevatron with electron beams

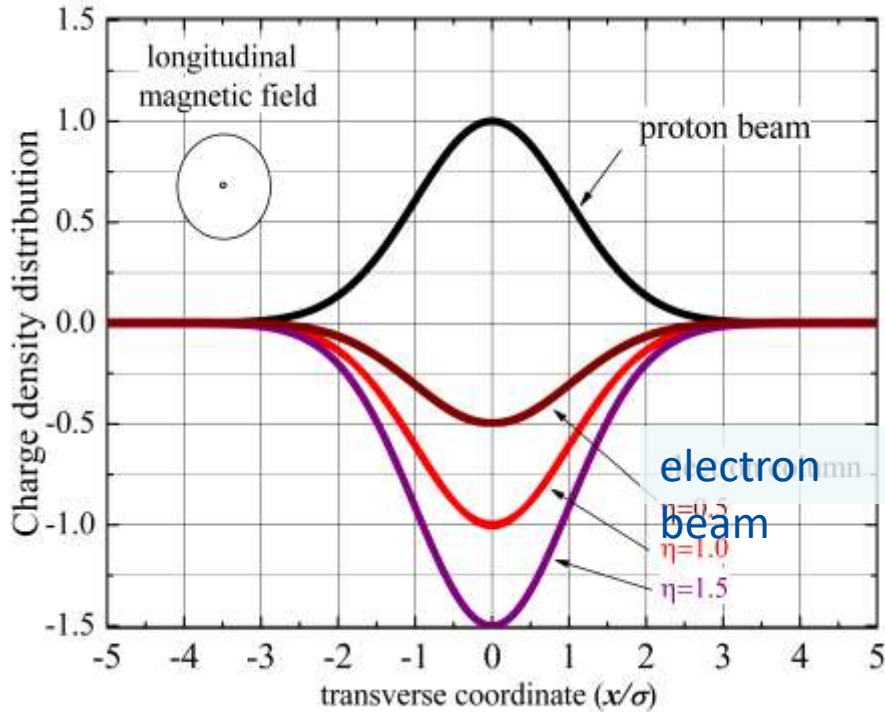
V. Shiltsev, V. Danilov,* D. Finley, and A. Sey†
Fermi National Accelerator Laboratory, Batavia, Illinois 60510
(Received 5 October 1998; published 28 July 1999)

The beam-beam interaction in the Tevatron collider sets limits on bunch intensity and bunch-to-bunch spacing. These limits are caused by a trans spread in each bunch which is mostly due to head-on collisions, but there is also a bunch-to-bunch trans spread due to parasitic collisions in multibunch operation. We propose to compensate these effects with the use of a countertraveling electron beam, and we present general considerations and physics limitations of this technique.

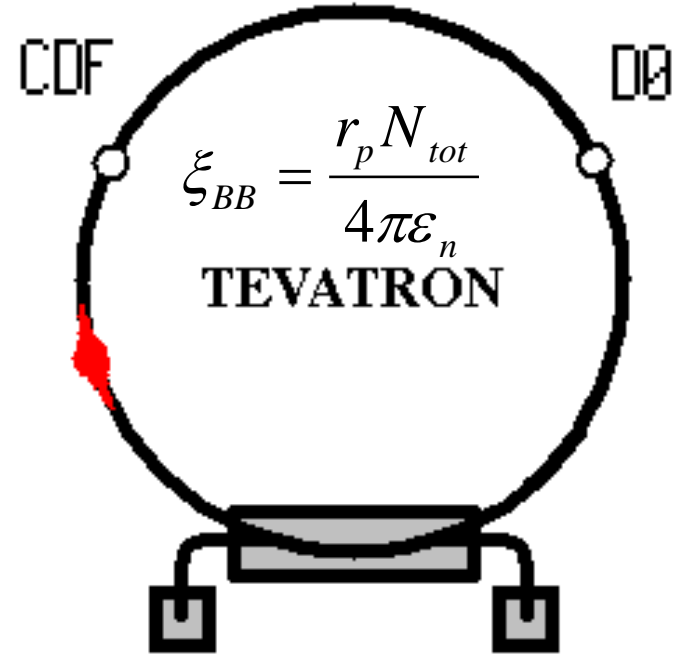
DOI: 10.1103/PhysRevSTAB.2.071001



Electron Lens Compensation



Antiproton bunch Electron beam

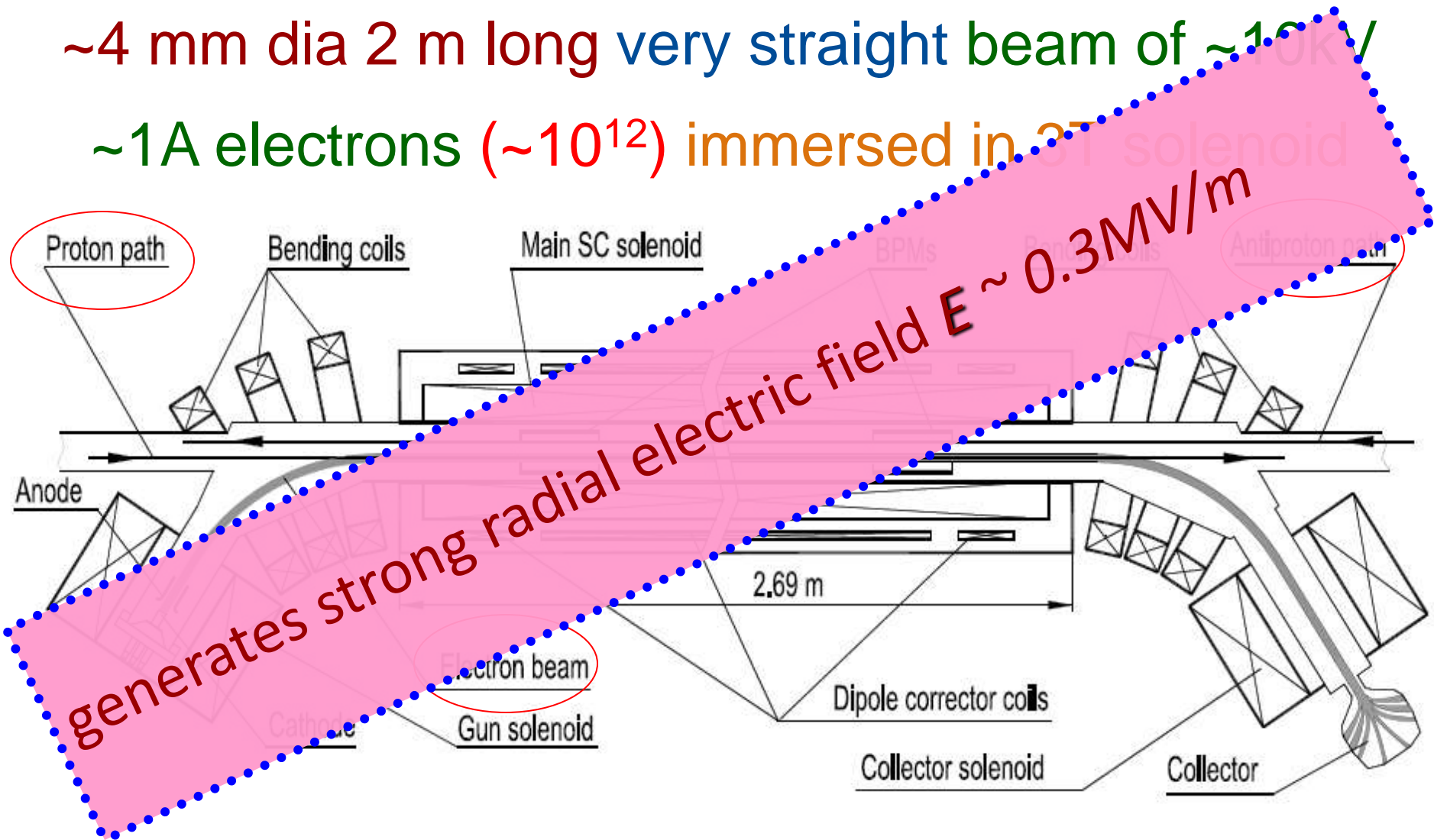


$$dQ_{x,y} = \mp \frac{\beta_{x,y}}{2\pi} \cdot \frac{1 \pm \beta_e}{\beta_e} \cdot \frac{J_e \cdot L_e \cdot r_p}{e \cdot c \cdot a_e^2 \cdot \gamma_p}$$

“...to compensate (in average) space charge forces of positively charged protons acting on antiprotons in the Tevatron by interaction with a negative charge of a low energy high-current electron beam “

Some Facts on Electron Lenses

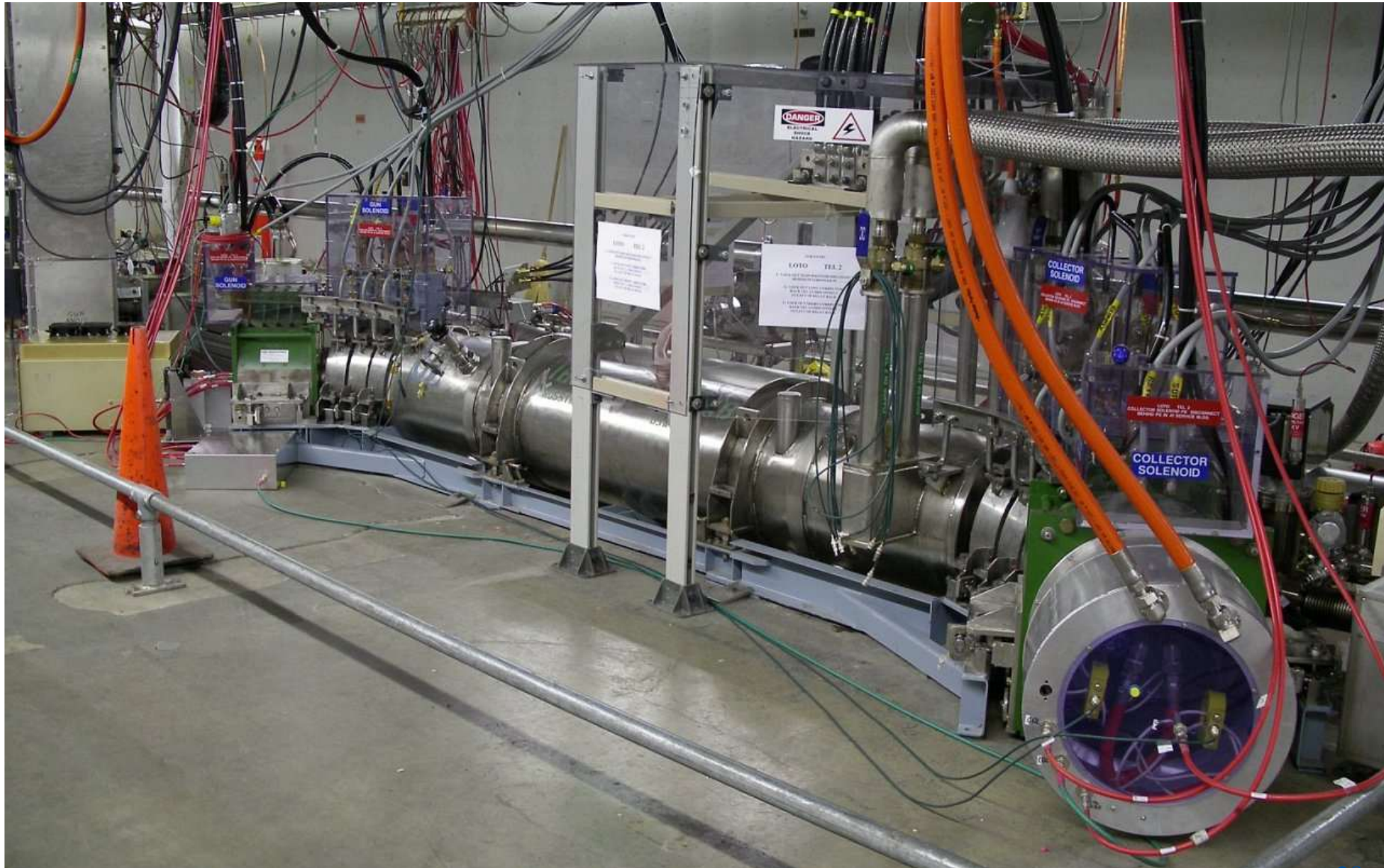
~4 mm dia 2 m long very straight beam of ~ 100 keV
~1A electrons ($\sim 10^{12}$) immersed in 3T solenoid



Tevatron Electron Lens #1 (F48)

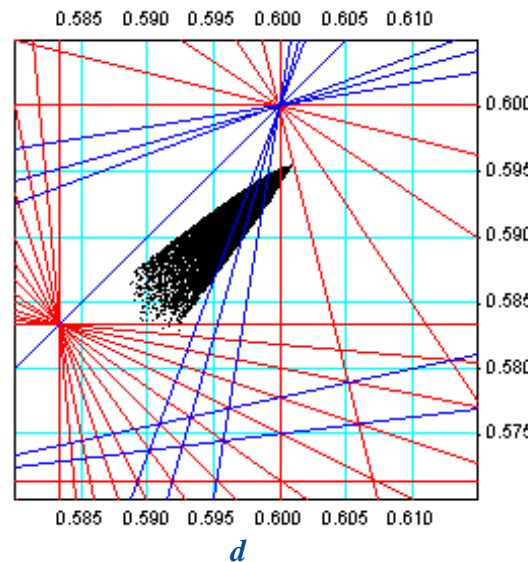
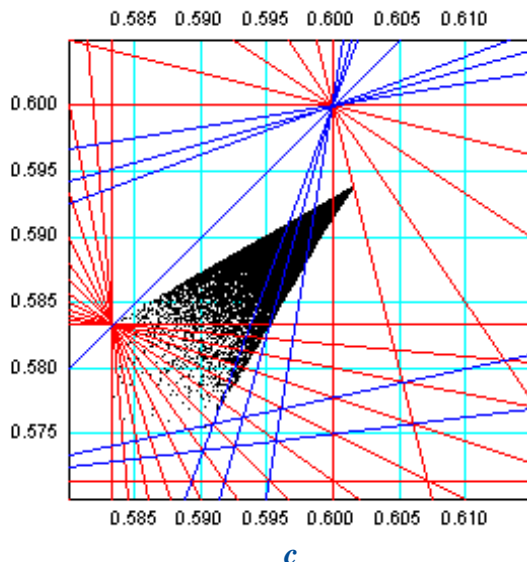
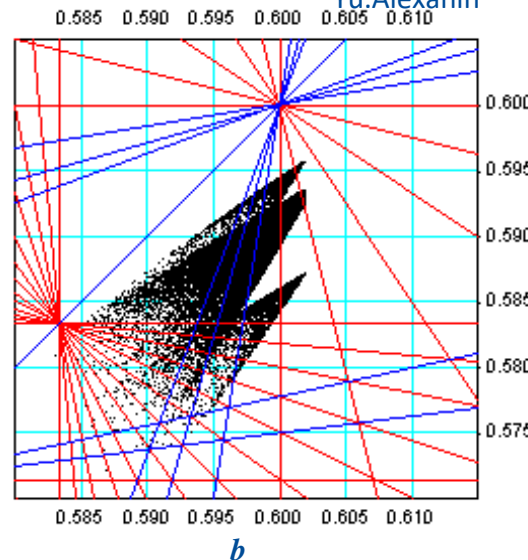
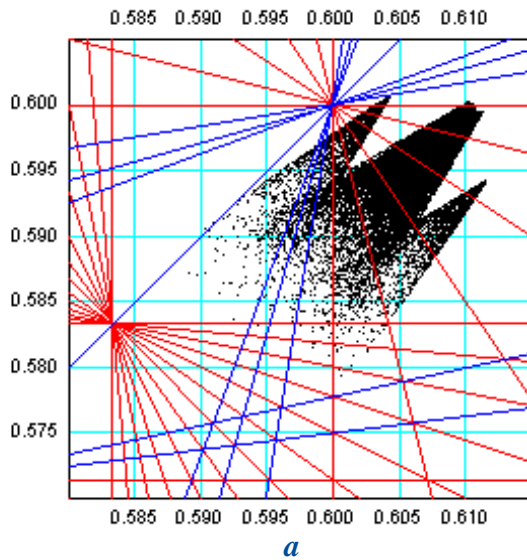


TEL2 in the Tevatron Tunnel (A11)



Compensation with Two TELs

Yu. Alexahin



- Tev Run II: 36x36 bunches in 3 trains
- compensate beam-beam tune shifts
 - a) Run II Goal
 - b) one TEL
 - c) two TELs
 - d) 2 nonlinear TELs
- requires
 - 1-3A electron current
 - stability $dJ/J < 0.1\%$
 - e-pbar centering
 - e-beam shaping

Electron Charge Distribution

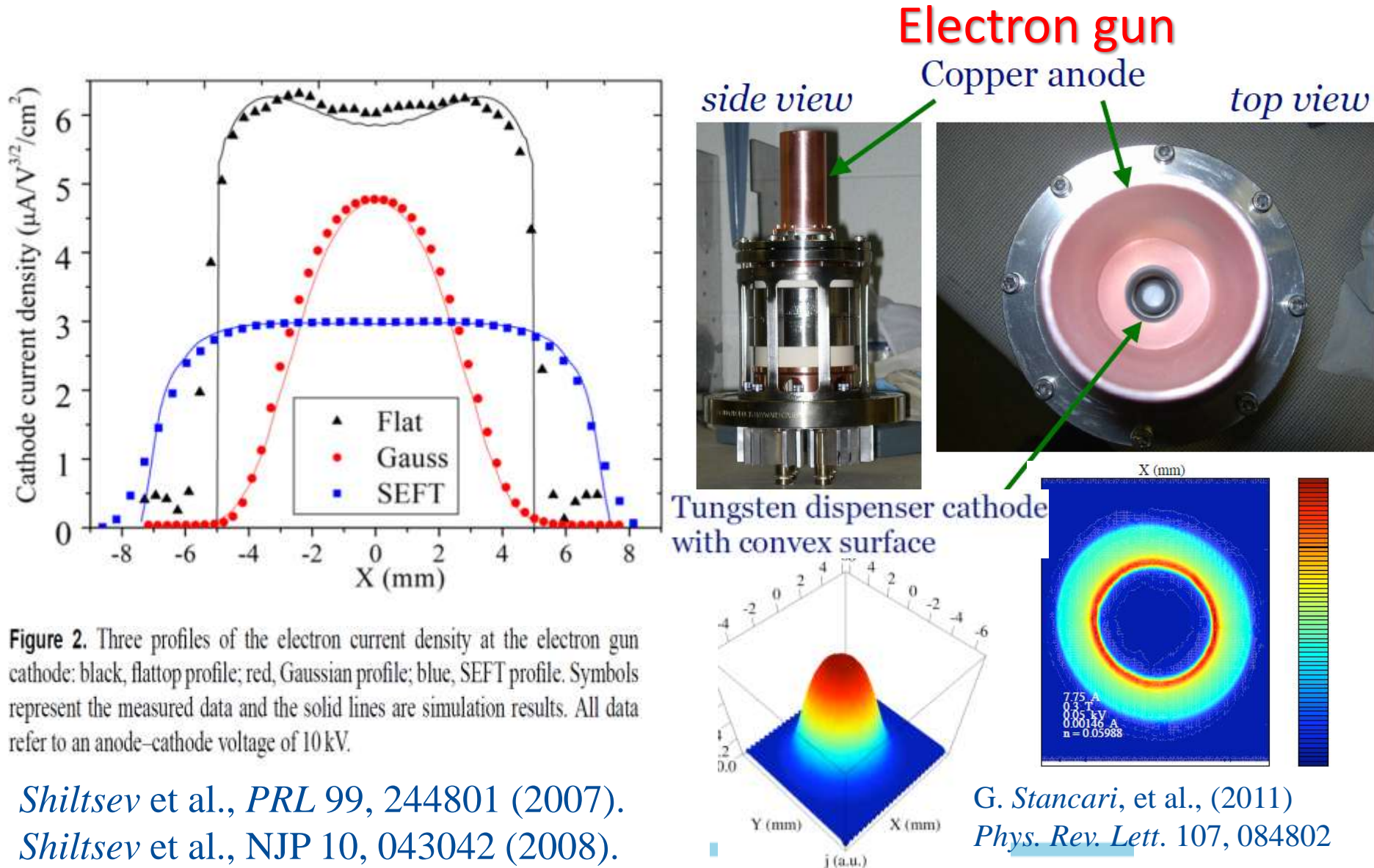


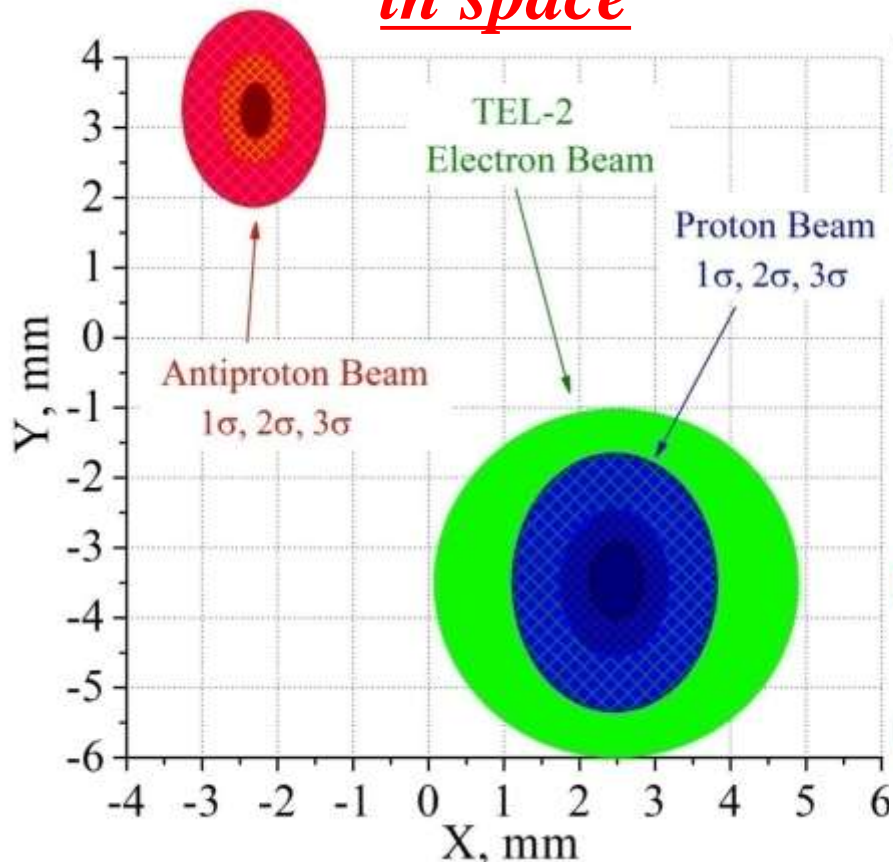
Figure 2. Three profiles of the electron current density at the electron gun cathode: black, flattop profile; red, Gaussian profile; blue, SEFT profile. Symbols represent the measured data and the solid lines are simulation results. All data refer to an anode-cathode voltage of 10 kV.

Shiltsev et al., PRL 99, 244801 (2007).
Shiltsev et al., NJP 10, 043042 (2008).

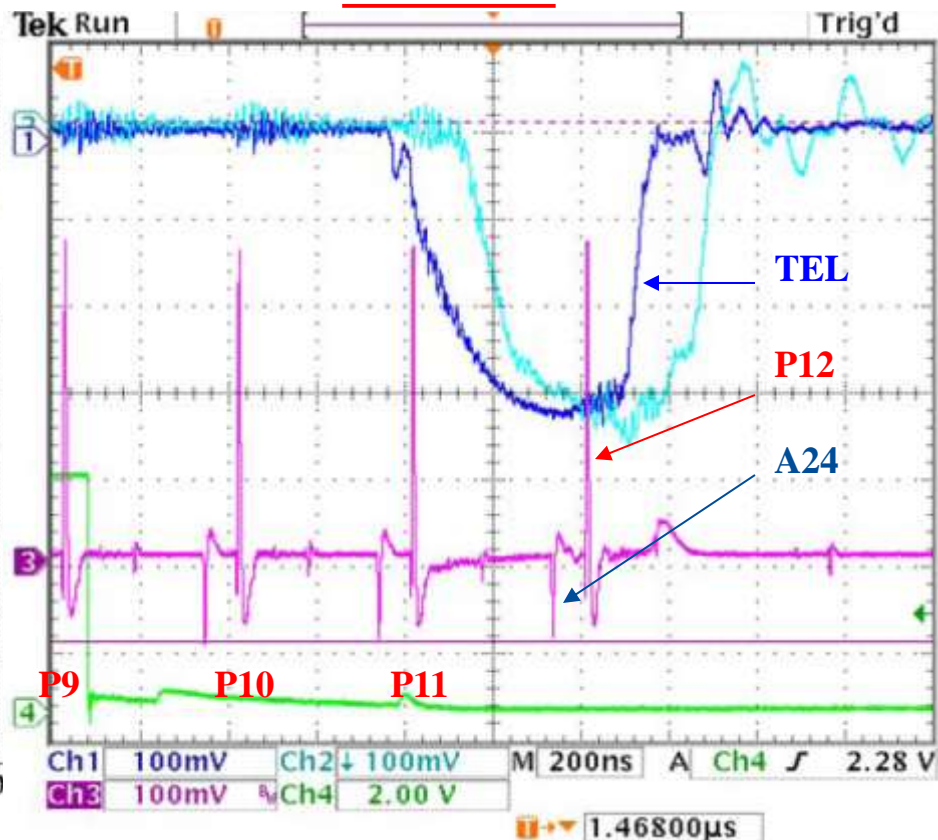
G. Stancari, et al., (2011)
Phys. Rev. Lett. 107, 084802

TEL e-beam aligned and timed on protons

in space



in time

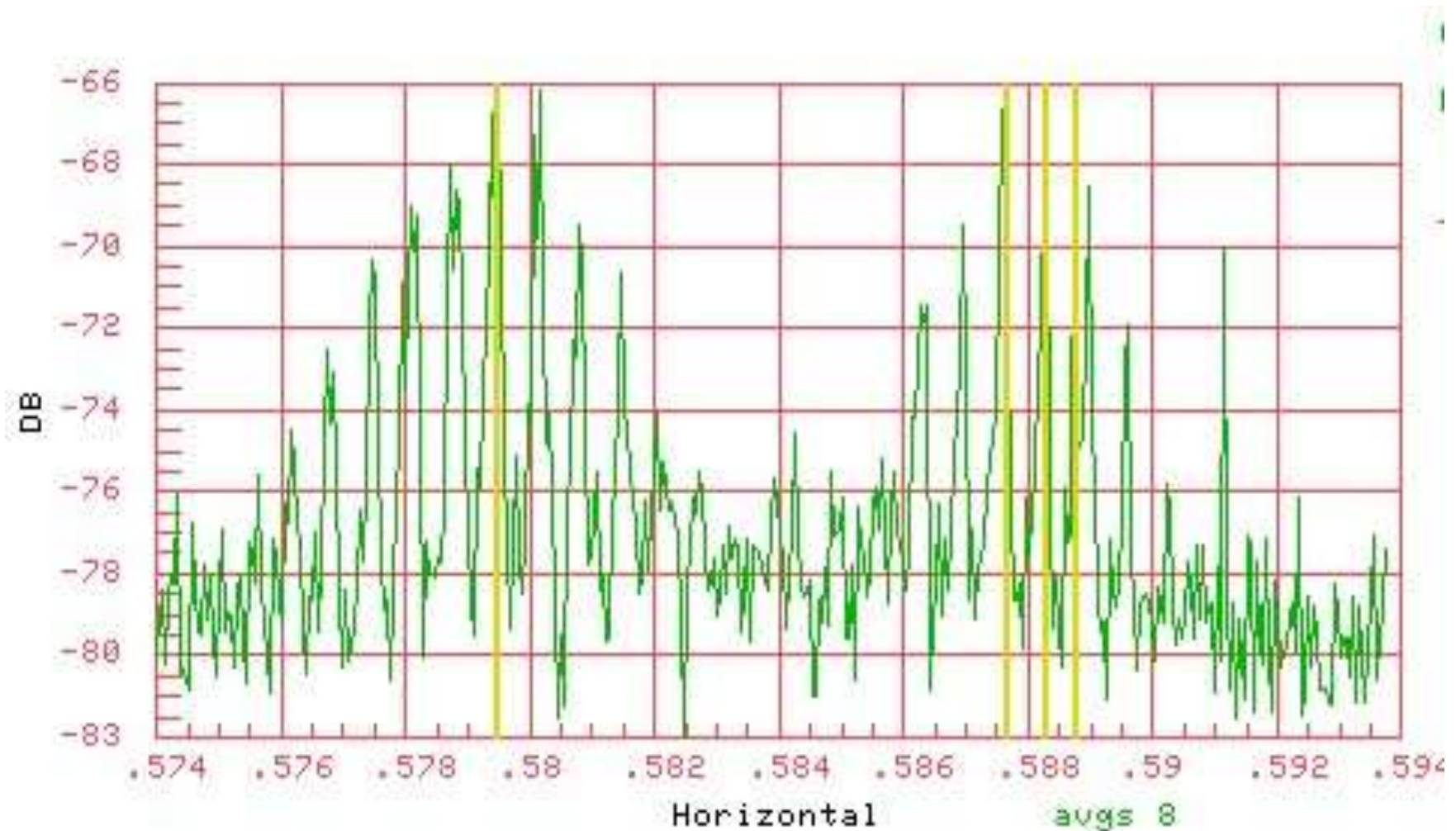


Transverse e-p alignment is very important for minimization of noise effects and optimization of positive effects due to e-beam. *Timing* is important to keep protons on flat top of e-pulse – to minimize noise and maximize tune shift.

Tevatron Electron Lenses (2001-2011)

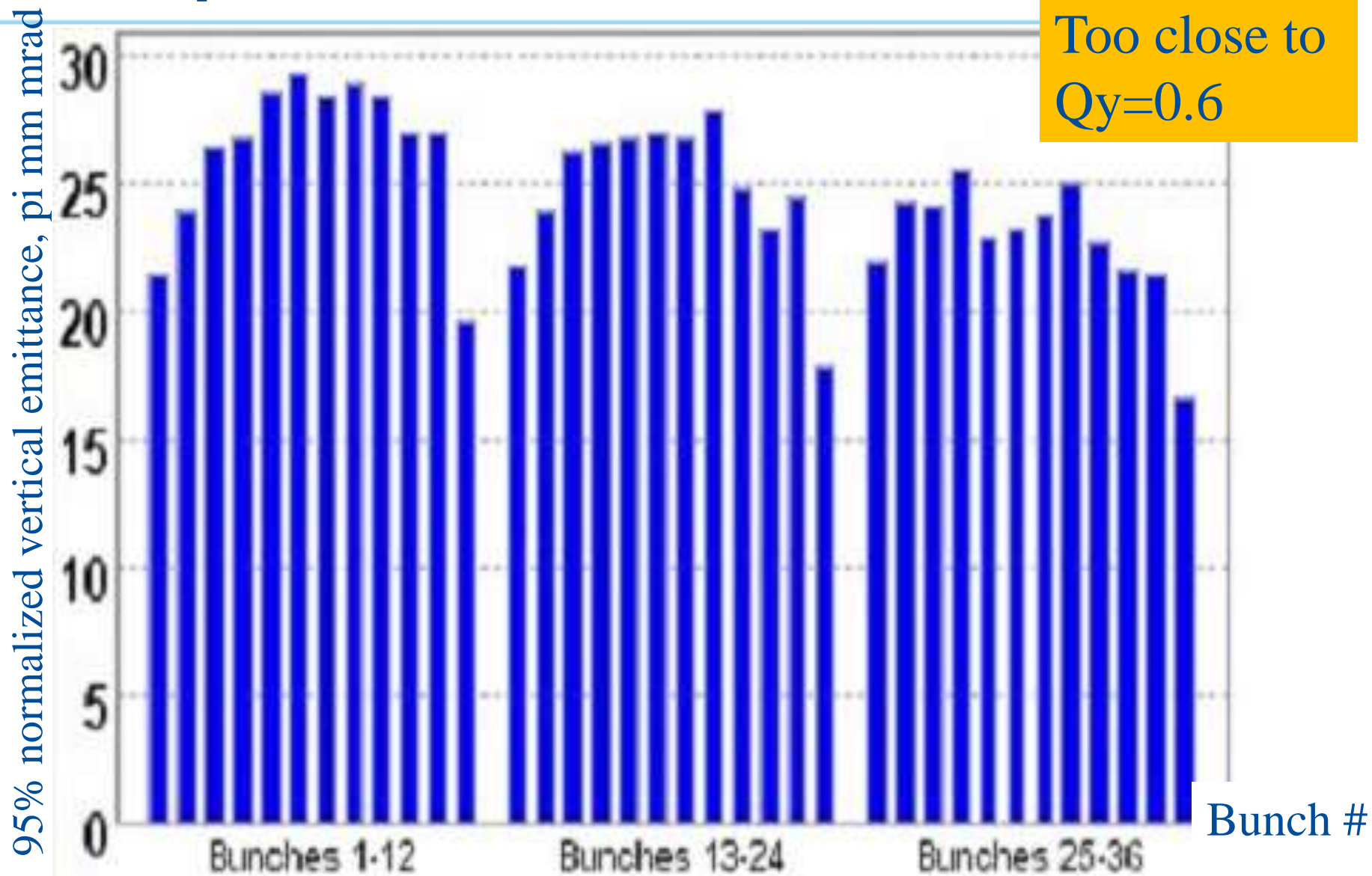
- Technology proven, tune shift ~ 0.01 demo'd
- First successful **active** compensation
- *Head on effects compensation:*
 - Reduced emittance growth of a PACMAN **antiproton** bunch (“scallop” effect)
- *Long range effects compensation:*
 - Significant (x2) improvement of the lifetime of most affected **proton** bunches
 - By shifting tunes of otherwise unfavorable bunch away from resonances

Tuneshift $dQ_{\text{hor}} = +0.009$ by TEL

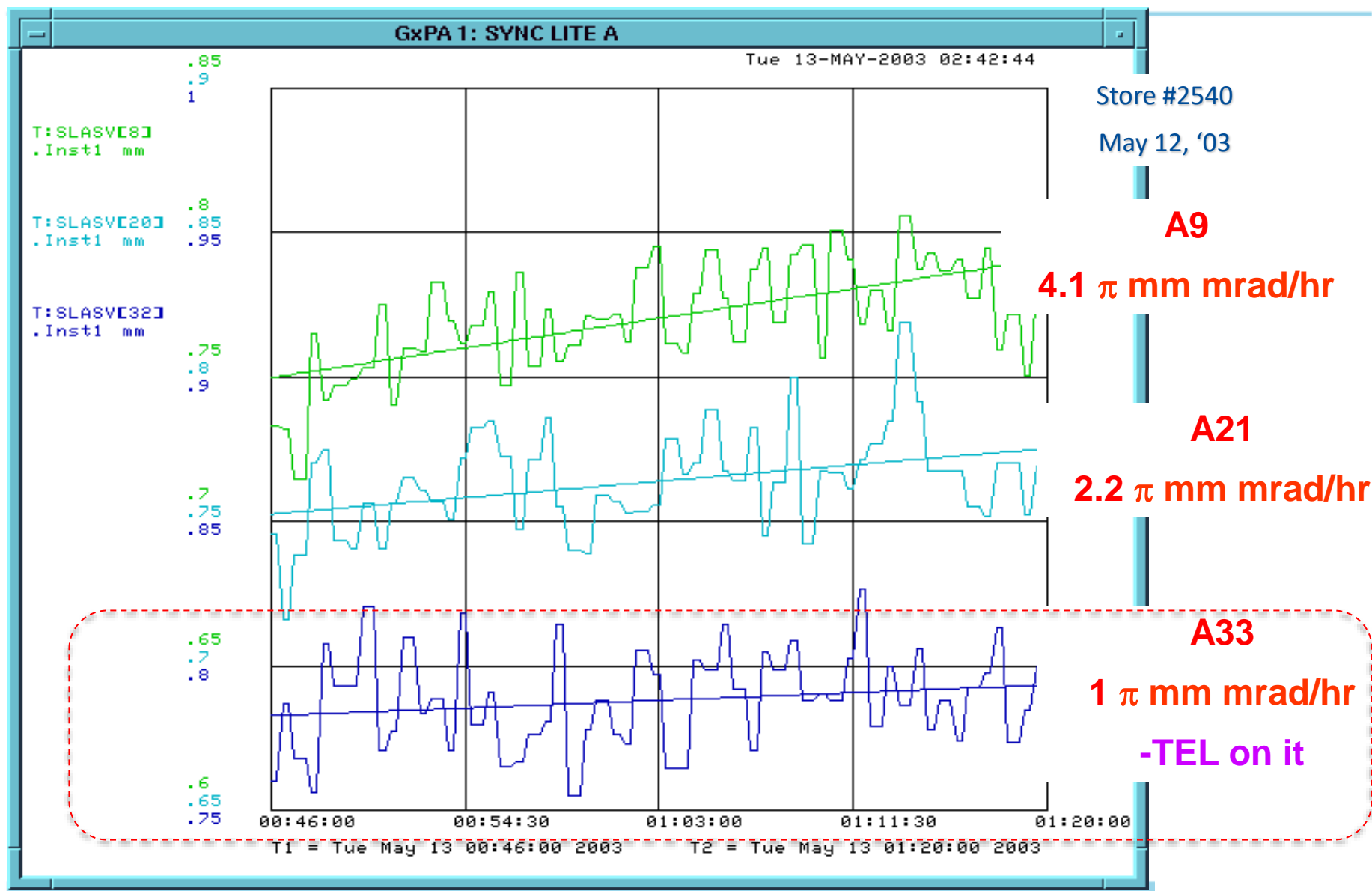


Three bunches in the Tevatron, the TEL acts on one of them

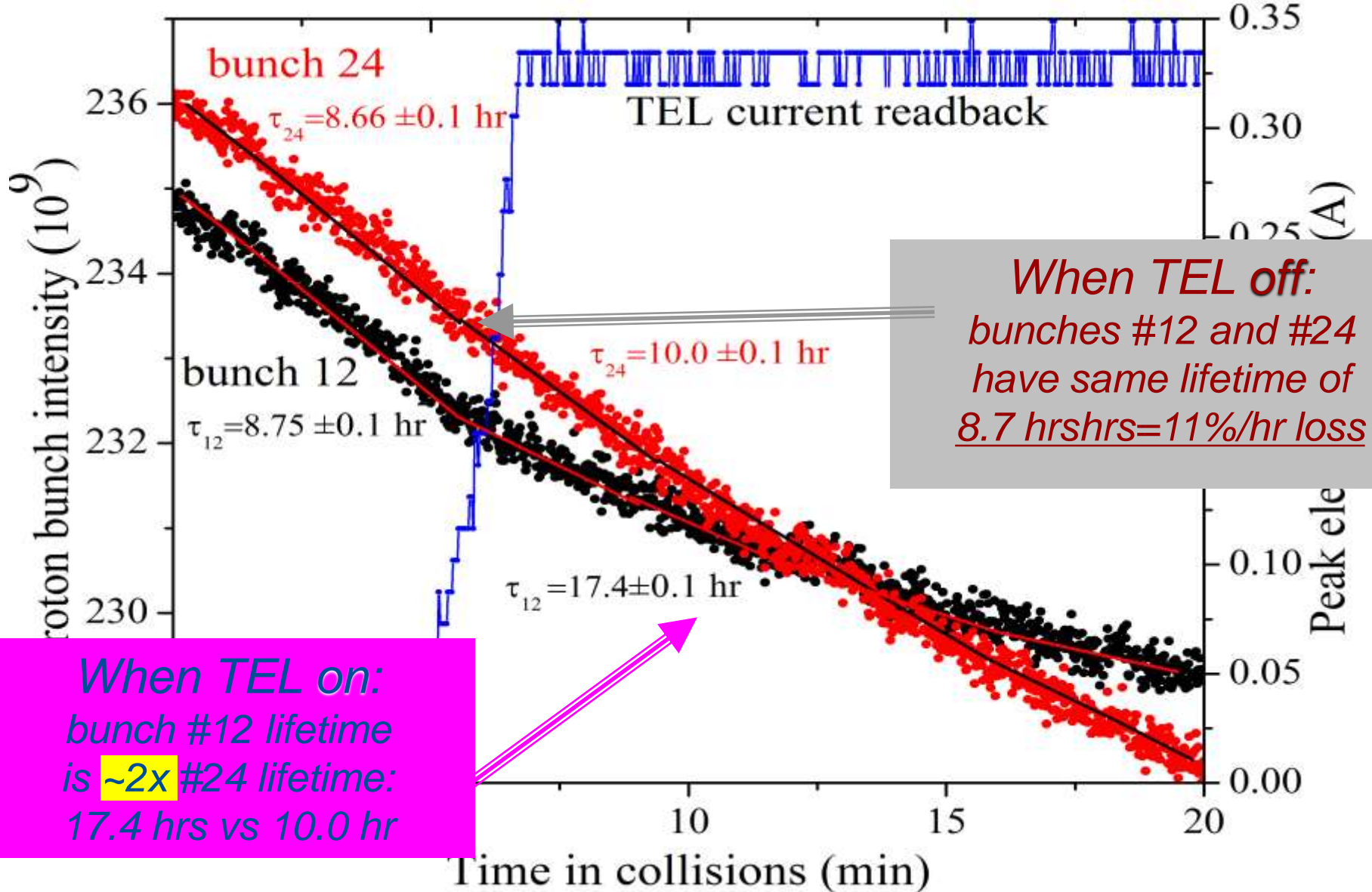
“Scallops” in Pbar Bunch Emittances



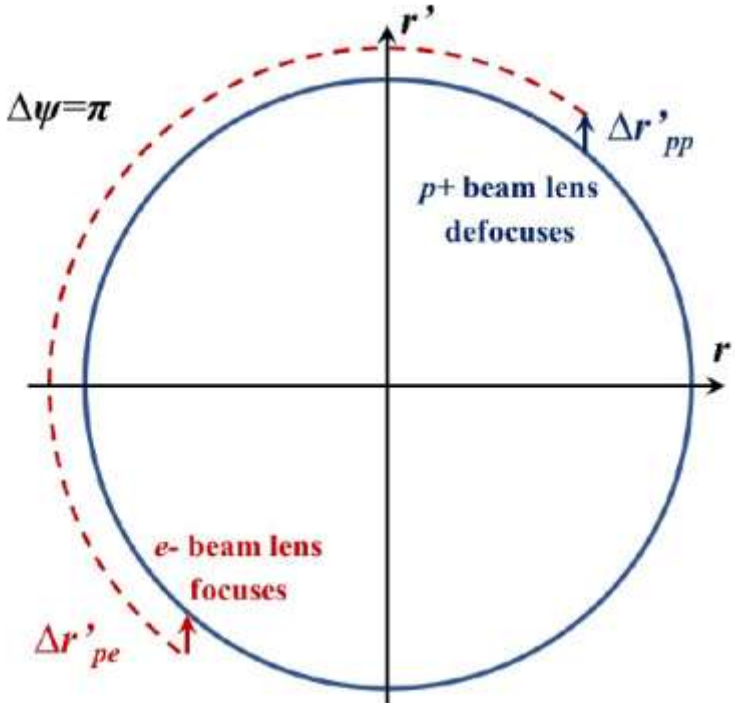
ittance Growth of A33 Suppressed by TEL



TEL2 on One Proton Bunch P12

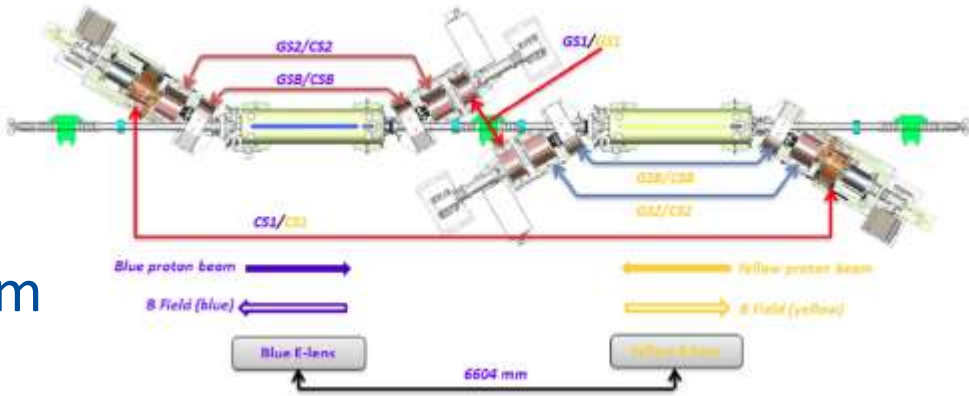


Approach #3: Head-On Comp'n in RHIC



(W.Fischer et al)

With e-lens, one can compensate Head-On effect: not only the tune footprint, but also the *resonant driving terms* if elens is placed 180 degrees (betatron phase) away from the main IP (one IP compensation)



RHIC pp 2015 elens Success

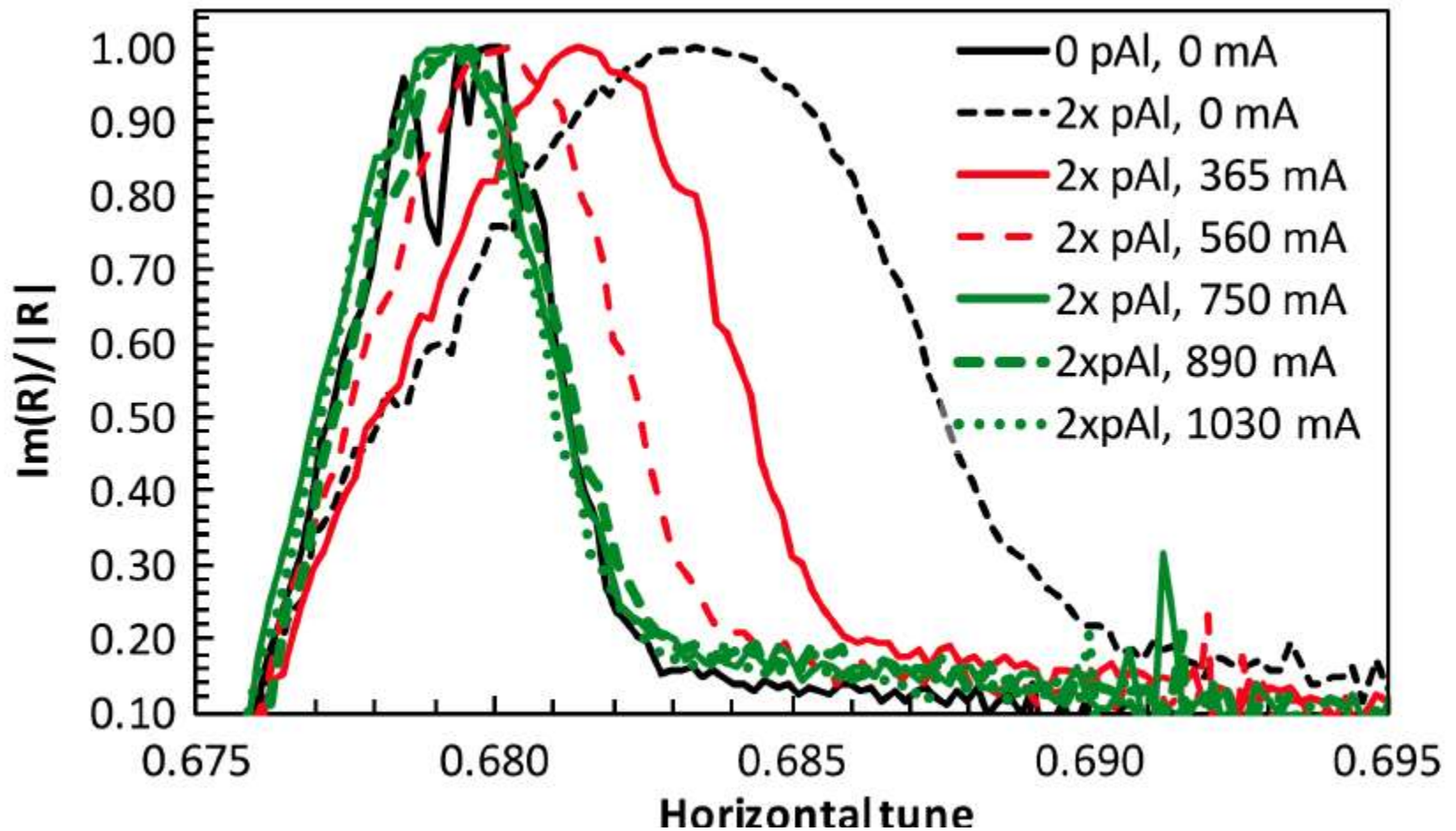
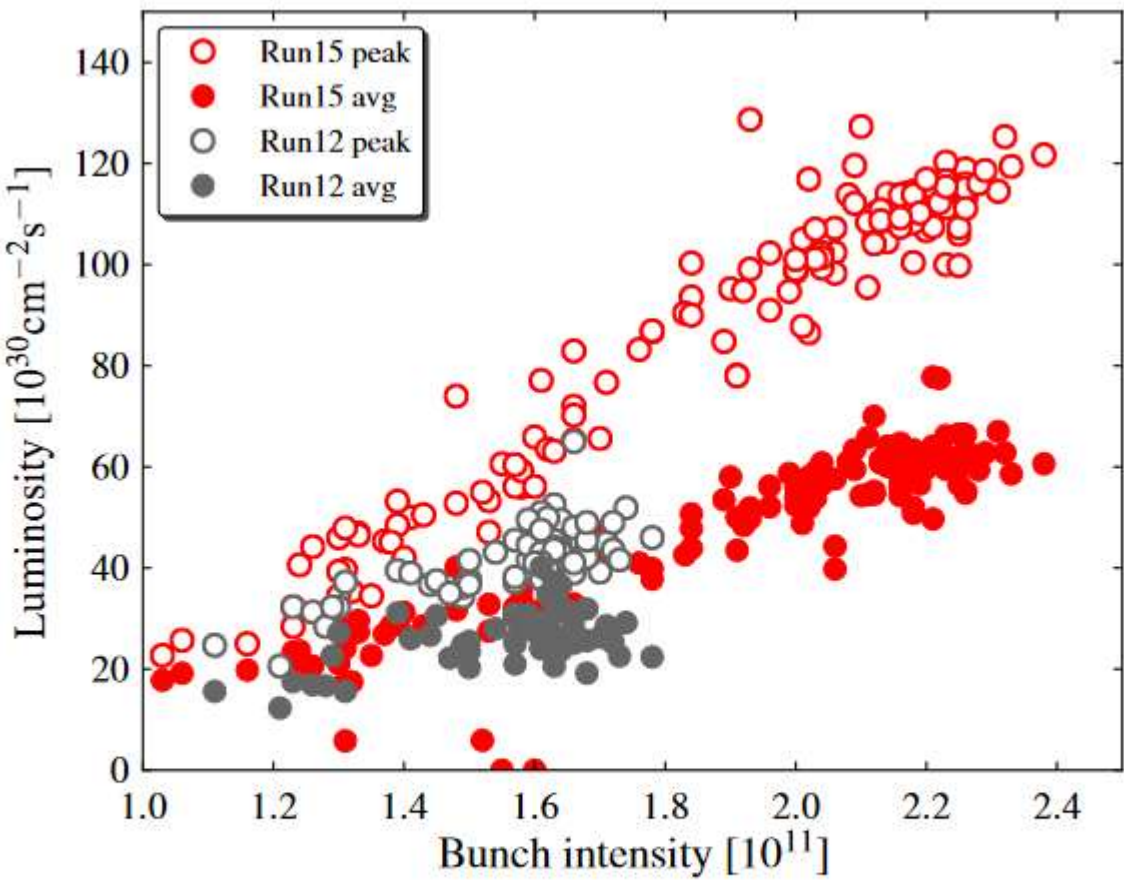


Figure 7: Tune distribution width reduction with the RHIC electron lens, measured in the proton beam with $p+Al$ collisions. The distribution widens due to two beam-beam interactions, and narrows again with increase of the electron lens current to 1.03 A [9].

RHIC pp 2015 elens in Ops

Electron lens parameters

Distance of center from IP	m	1.5	1.5
Effective length L_e	m	2.1	2.1
Kinetic energy E_e	kV	5	5
Relativistic factor β_e		0.14	0.14
Relativistic factor γ_e		1.0002	1.0002
Current I_e	A	1.0	0.43/0.60
Electron beam size at interaction	μm	350	650
Linear tune shift		0.0147	0.01



With 0.6A, 2.1m long, 5 kV e-beam, essentially:

- one out of 2 IP head-on effect cancelled,
- max allowed beam intensity increased by $\sim 40\%$,
- peak average lumi \sim tripled, averaged lumi \sim doubled

FIG. 3. Peak and average store luminosity in polarized proton operation at 100 GeV beam energy in 2012 and 2015.

Approach #4 : Wire Compensation of Long Range Beam-Beam Interactions

Fields of separated $p+$ beam:

$$E \sim N_{IPs} N_p / d$$

$$B = E$$

Field of separated **conductor** (wire):

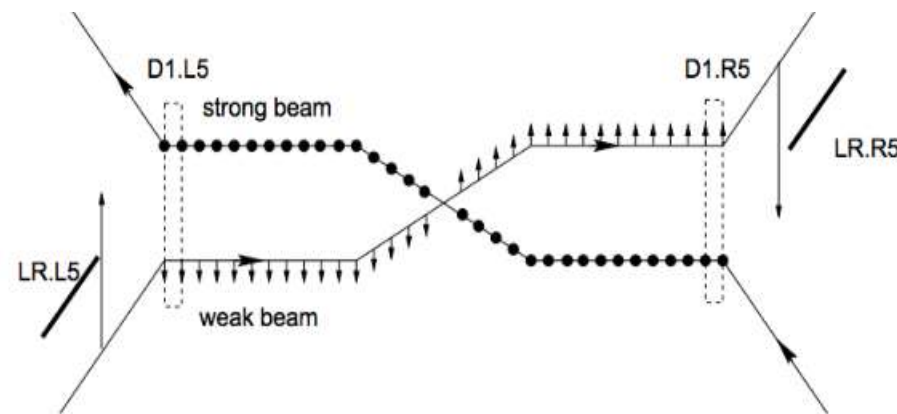
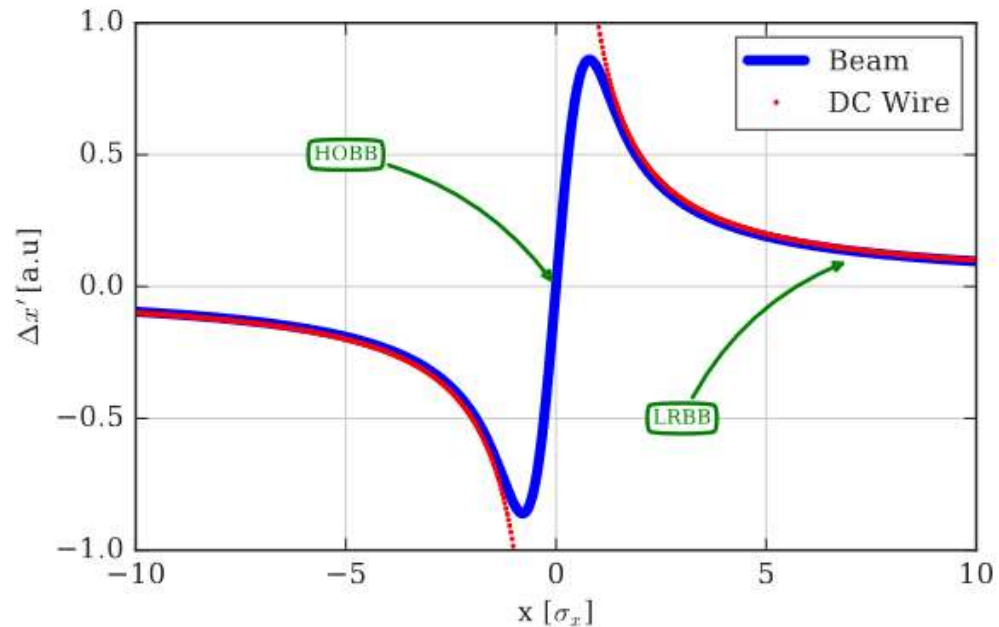
$$E = 0$$

$$B \sim 2J_e / d$$



Combined effects of $p+$ beam + $e-$ beam will cancel out if

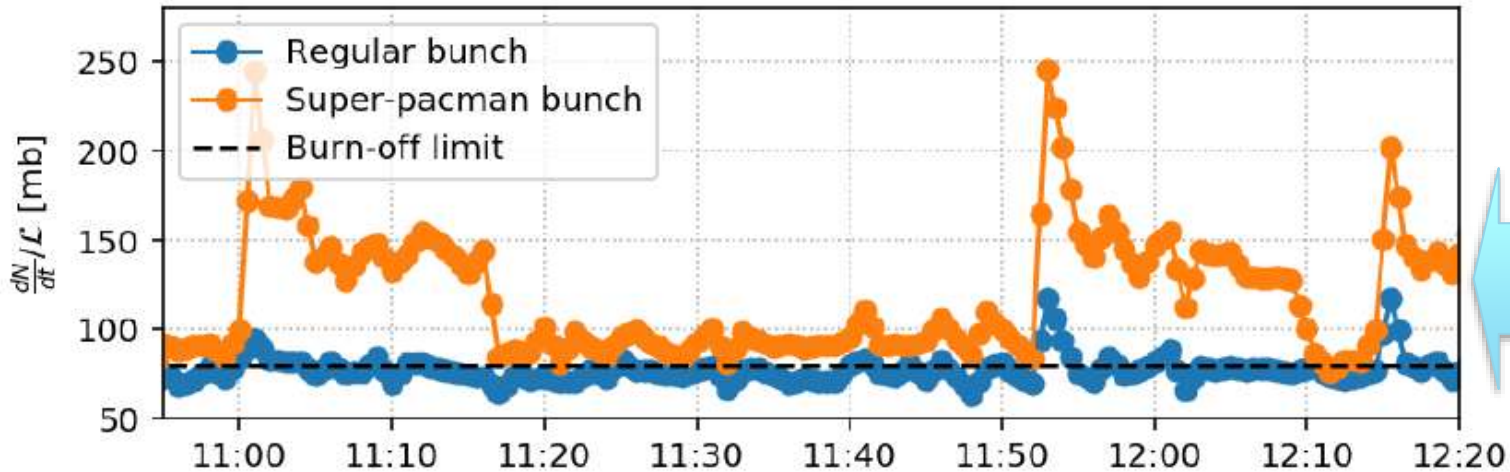
wire is placed at the same d
wire kick $J_e \times \text{length}$ matches $N_{IPs} N_p$



(J.P.Koutchouk, G.Sterbini et al)

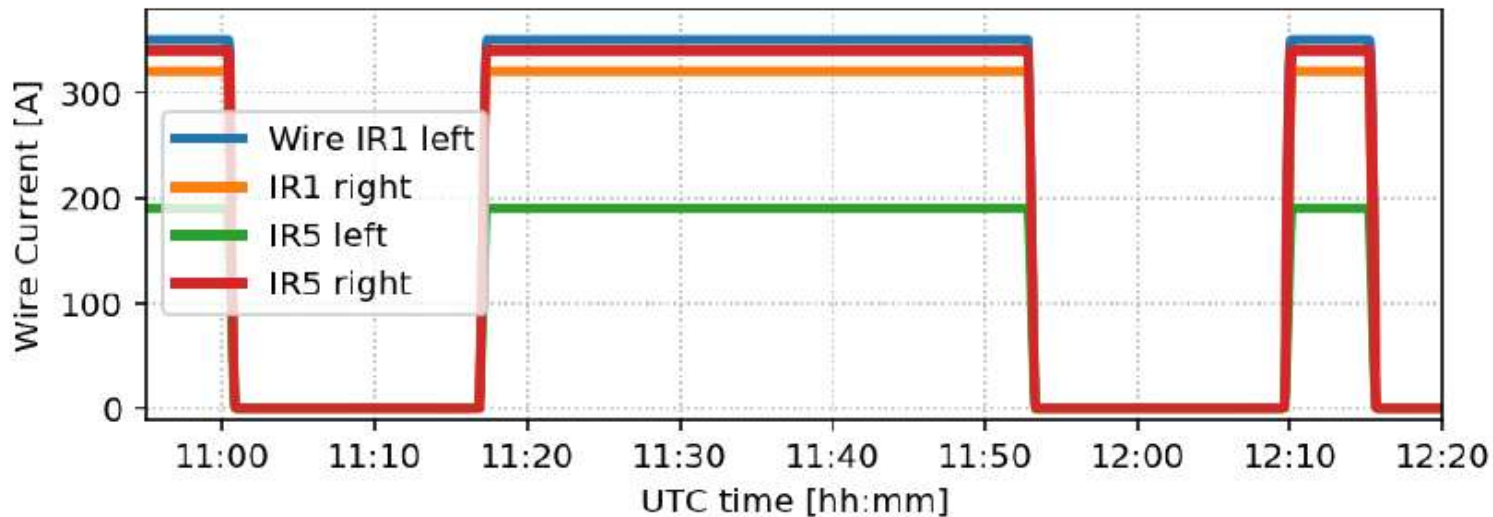
Wire Compensation in the LHC (2018)

14th September 2018 - FILL 7169



Proton losses in collisions are due to:
Luminosity burn up $\frac{dN}{dt} = -L \times 80$ mbarn

and beam-beam effects - different for regular and PACMAN bunches



So, plotted is $\frac{dN}{dt} / \text{Lumi}$ for regular and PACMAN bunches

Not mentioned here (but will be later)

- Beam-beam effects in linear colliders
 - Beamstrahlung
 - Asymmetric beams
 - Synchrotron coupling
 - Crabbed and crab-waist schemes
 - Monochromatization
 - Beam-beam simulation codes
- ... etc.

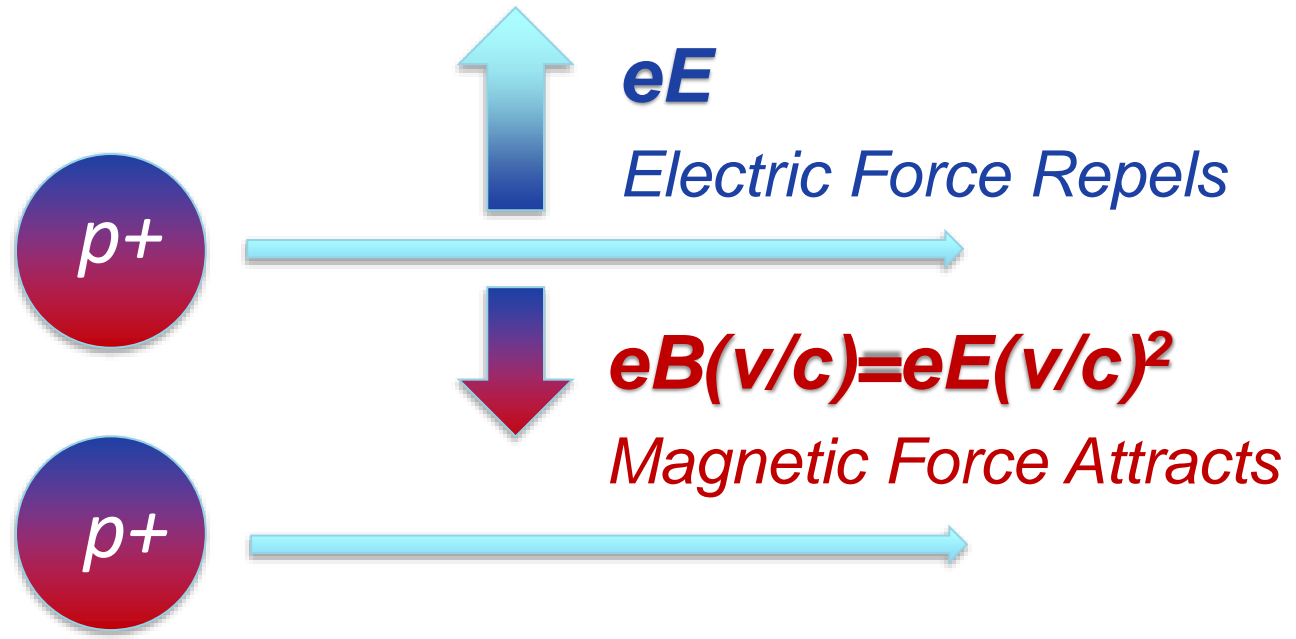
BREAK (!...?)

**OTHER
EFFECTS**

Important Effects (besides Beam-beam)

- Space-charge effects
- Instabilities
- Collimation
- Cooling (brief, see lectures VP5-6)
- Diffusion and Intrabeam scattering (see VP4)
- Beamstrahlung (see lectures VS8-9)
- Polarization (see lecture VP4)
- Synchrotron radiation (see lecture VS6)

Intense Beams : Forces and Losses (1)

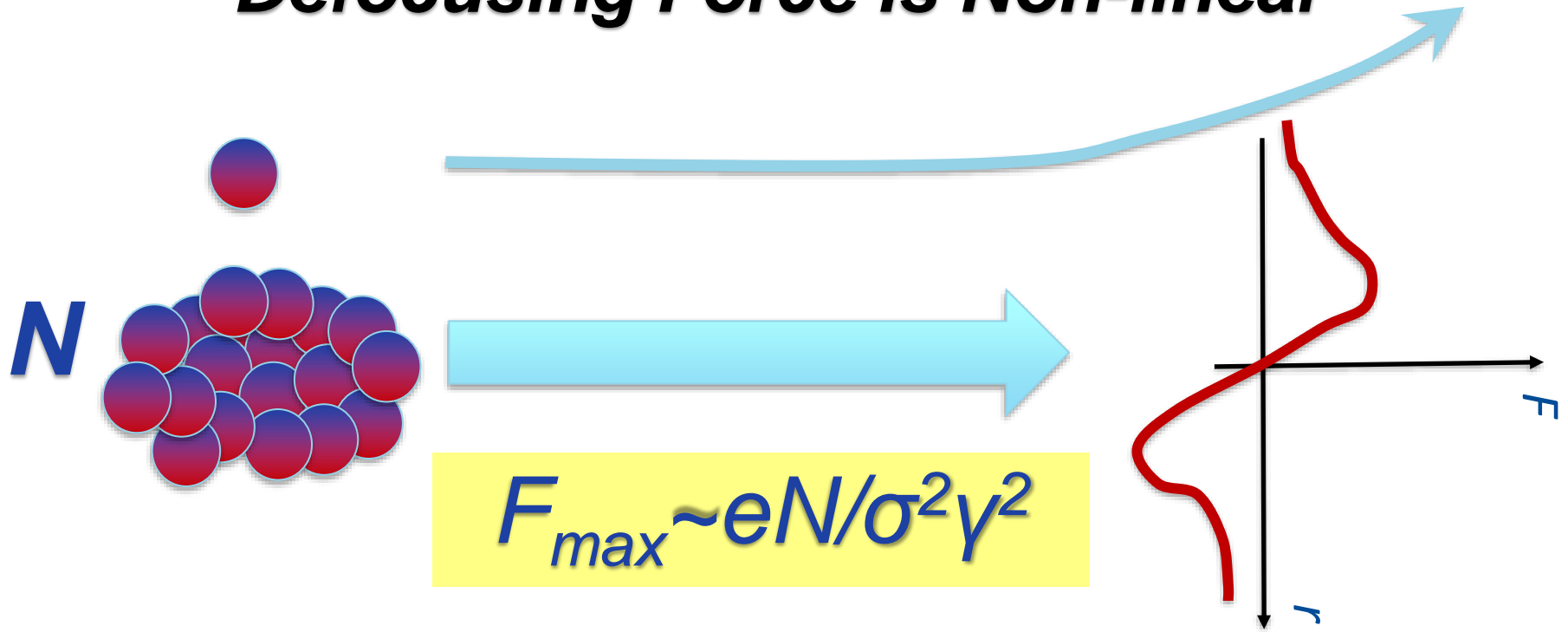


Net Force: Repels

$$eE - eE(v/c)^2 = eE(1 - \beta^2) = eE/\gamma^2$$

Intense Beams : Forces and Losses (2)

Defocusing Force is Non-linear



Space-charge effects (emittance growth, losses):

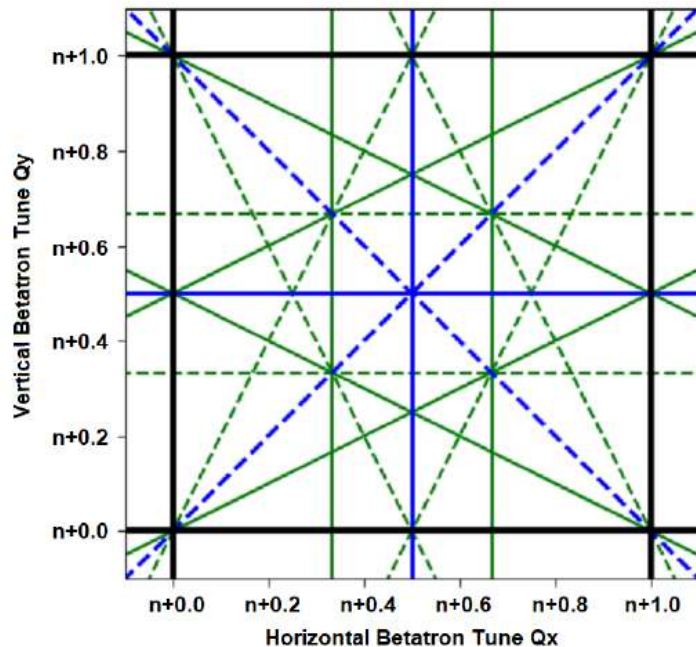
- a) proportional to current (N)***
- b) scale inversely with beam size (σ)***
- c) scale with time at low energies (γ)***

Linacs 5-20 MeV/m
Rings 0.002-0.01 MeV/m

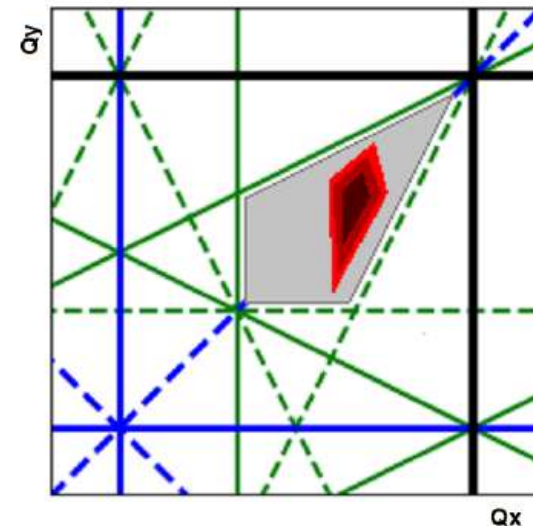
Space-charge effects: Proton Rings

- SC tune shift

$$\Delta Q_{SC} = - \frac{N_p r_p B_f}{4\pi \epsilon \beta_p \gamma_p^2}$$



resonance conditions
 - - - skew sextupole
 — sextupole
 - - - skew quadrupole
 — quadrupole
 — dipole



■ Available Tunespace
 ■ Tune Footprint
 (density of particles)

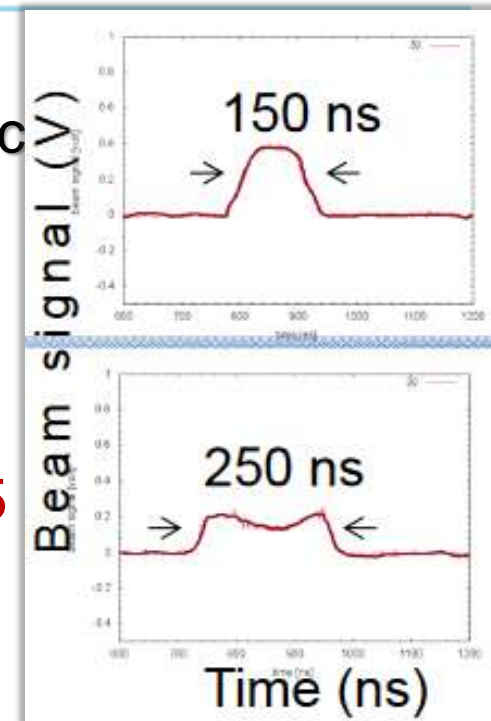
Max SC tuneshift Achieved: -0.2...-0.5

	E_i/E_p	N_p	T	P	ΔQ_{sc}	$\%_{N_p}$	$\%_{\epsilon}$	C	S	$Q_{h,v}$
ISIS	0.07/0.80	3.1	0.01 s	200	0.4	2		163	10	4.31/3.83
PS-B	0.05/1.4	0.25	1.2	n/a*	0.50	5	20	157	16	4.3/4.45
CSNS	0.08/1.6	1.6	0.02	100	0.28	1	20	228	4	4.86/4.78
J-RCS	0.4/3	4.2	0.02	500	0.35	0.3	10	348	3	6.45/6.32
FNAL-B	0.4/8	0.45	0.03	84	0.60	5	20	474	24	6.78/6.88
CERN-PS	1.4/28	1.5	3.6	n/a*	0.24	3	5	628	50	6.12/6.24
JPARC-MR	3/30	27	1.5	515	0.4	1.5	10	1568	3	21.35/21.43
FNAL-MI	8/120	5.1	0.62	803	0.09	2.5	5	3319	1	26.46/25.38
CERN-SPS	28/450	0.9	19	n/a*	0.21	5	10	6911	6	20.13/20.18
PSR	0.8	3.1	6e-4	80	0.29	0.3		90	10	3.18/2.19
SNS-R	1	14	0.001	1400	0.15	0.01		248	4	6.23/6.20
FNAL-RR	8	5.2	0.84	54	0.09	2.5	10	3319	1	25.44/24.43

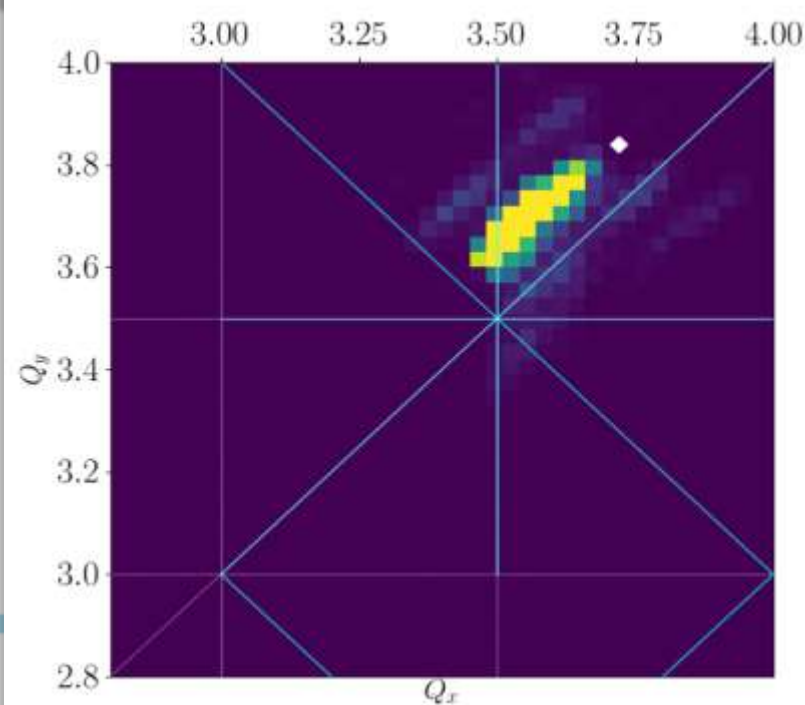
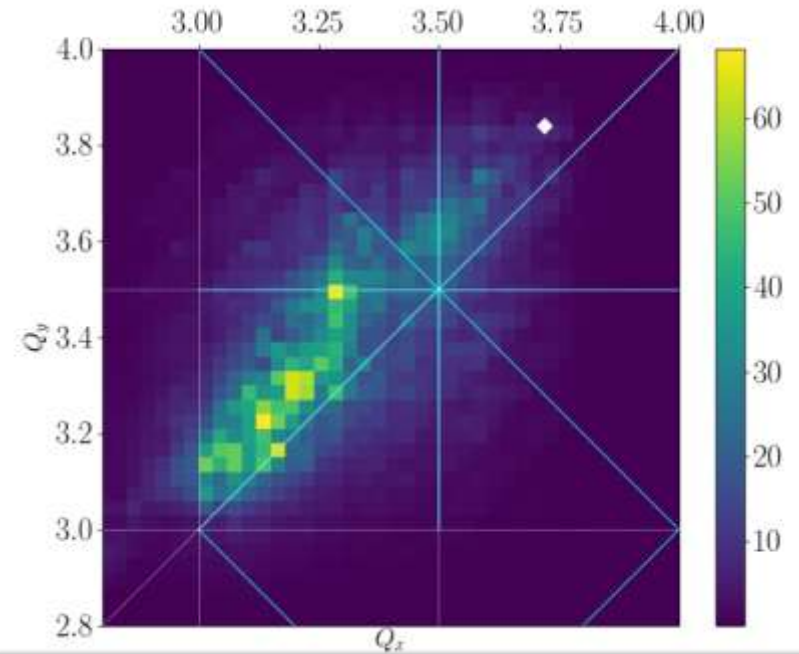
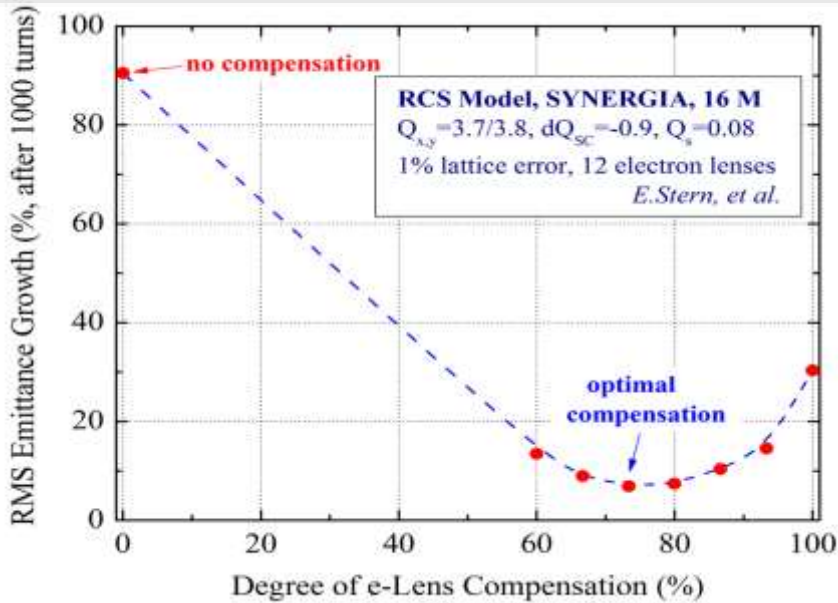
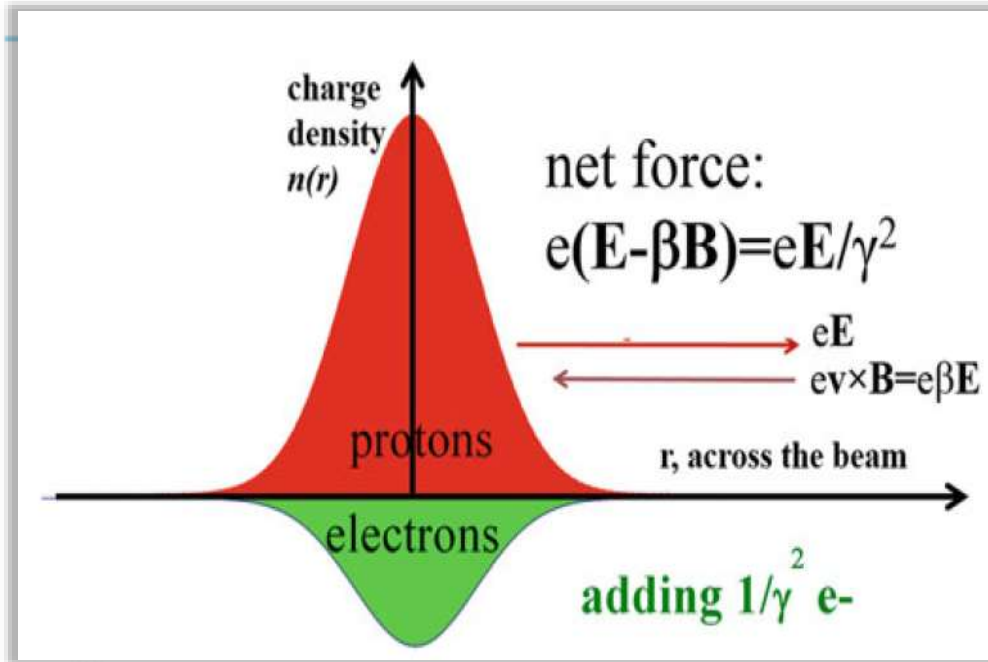
Figure 3: Operational high intensity RCSs and accumulator rings: injection/extraction kinetic energies E_i/E_p in GeV, number of protons per pulse N_p in 10^{13} , beam acceleration/storage time T in s, average beam power P in kW, maximum SC tune shift ΔQ_{sc} , fractional intensity loss $\%_{N_p} = \Delta N_p/N_p$ and emittance growth $\%_{\epsilon} = \Delta\epsilon/\epsilon$ in %, circumference C in m, lattice periodicity S and tunes $Q_{h,v}$. (* For CNGS operation in 2005-2012, the SPS delivered 510 kW average power at 400 GeV). Figure and caption from [10].

Ways to Increase “Protons Per Pulse”

- **Increase the injection energy:**
 - Gain about $N_p \sim \beta\gamma^2$, need (often - costly) linacs
- **Flatten the beams (using 2nd harm, RF) :**
 - Makes SC force uniform, $N_p \sim \times 2$
- **“Painting” beams at injection:**
 - To linearize SC force across beams $N_p \sim \times 1.5$
- **Better collimation system beams:**
 - From $\eta \sim 80\%$ to $\sim 95\%$ $N_p \sim \times 1.5$
- **Make focusing lattice perfectly periodic:**
 - Eg P=24 in Fermilab Booster, P=3 in JPARC MR $\rightarrow N_p \sim \times 1.5$
- **(to be tested) Introduce *Non-linear Integrable Optics* :**
 - May reduce the losses and allow $N_p \sim \times 1.5-2$
- **(tbt) Space-Charge Compensation by electron lenses :**
 - Electrons to focus protons, may allow $N_p \sim \times 1.5 - 2$



Space-Charge Compensation R&D



Beams Document 6790-v1 FNAL

IOTA: *Integrable Optics Test Accelerator* @ FNAL



Instabilities

- Beam instabilities are driven by the **electromagnetic interaction with the accelerator environment** (-> wakefields/impedances) and by **electron clouds**.
- Above a certain **intensity threshold** the beam's oscillation amplitude increases exponentially and the beam is either **lost at the wall** (transverse instabilities) or from the rfbucket (longitudinal) and/or the **emittance increases**.
- Presently, heat loads and instabilities are one of the **main beam quality and intensity limitation** in particle accelerators for high intensity and brightness !
- Finding “**cures**” for **instabilities** is one of the major challenges in beam physics and accelerator technology for **future machines**.
- **High energy beams**: Beam instabilities are a ‘current effect’. However, synchrotron radiation, photoelectrons or other high energy effects affect instability thresholds.

Maxwell's equations and Lorentz Force

$$\begin{aligned}\nabla \cdot \mathbf{E} &= \frac{\rho}{\epsilon_0} \\ \nabla \cdot \mathbf{B} &= 0 \\ \nabla \times \mathbf{E} &= -\frac{\partial \mathbf{B}}{\partial t} \\ \nabla \times \mathbf{B} &= \mu_0 \mathbf{j} + \frac{1}{c^2} \frac{\partial \mathbf{E}}{\partial t}\end{aligned}$$

+ boundary conditions at the walls

Impulse approximation

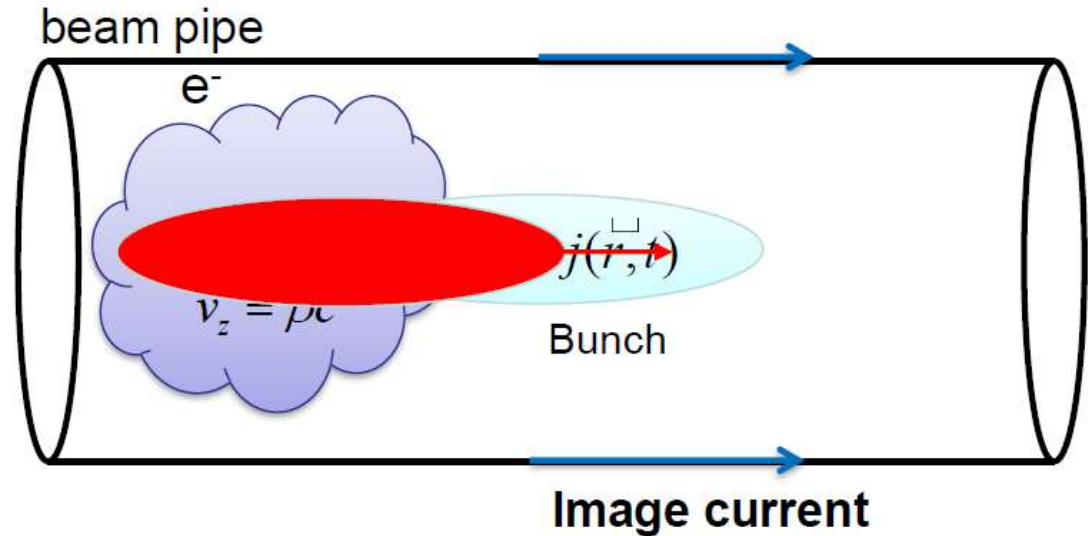
$$c\Delta p = q \int_{-\infty}^{\infty} (\mathbf{E} + \mathbf{v} \times \mathbf{B}) ds$$

The EM force continuously acting on a test charge is lumped in a single kick after the passage through the structure.

Rigid bunch approximation

$$\mathbf{j} = \beta_0 c \rho \mathbf{e}_z$$

The beam traverses the structure rigidly.



EM forces due to : a) wake fields and impedances, b) electron cloud, c) beam-beam, d) etc

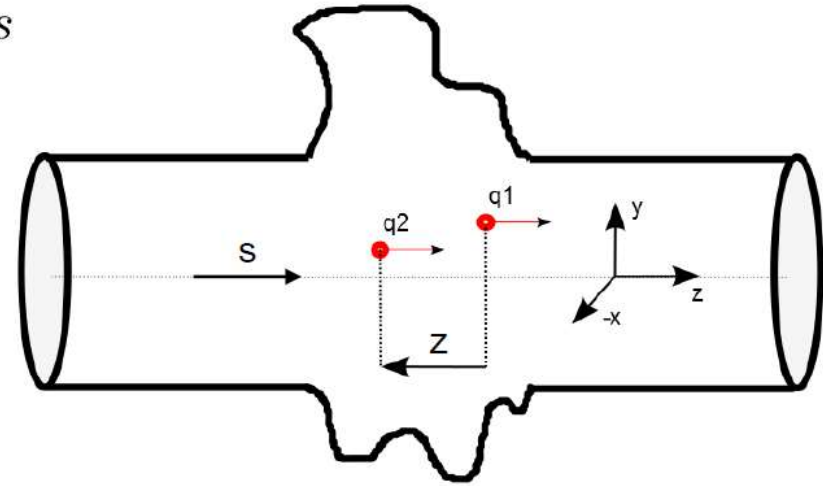
more on b) and c) in later lectures

Wake-fields

$$W(r_2, r_1, z) = -\frac{1}{q_1} \int_{-\infty}^{\infty} [\mathbf{E} + \mathbf{v} \times \mathbf{B}](r_2, z, t = \frac{z+s}{c}) ds$$

T. Weiland and R. Wanzenberg, "Wake Fields and Impedances," in CERN Accelerator School (CAS), 1993. 20, 28, 99

L. Palumbo, V. G. Vaccaro, and M. Zobov, "Wake Fields and Impedance," in Cern Accelerator School, 1994. 20



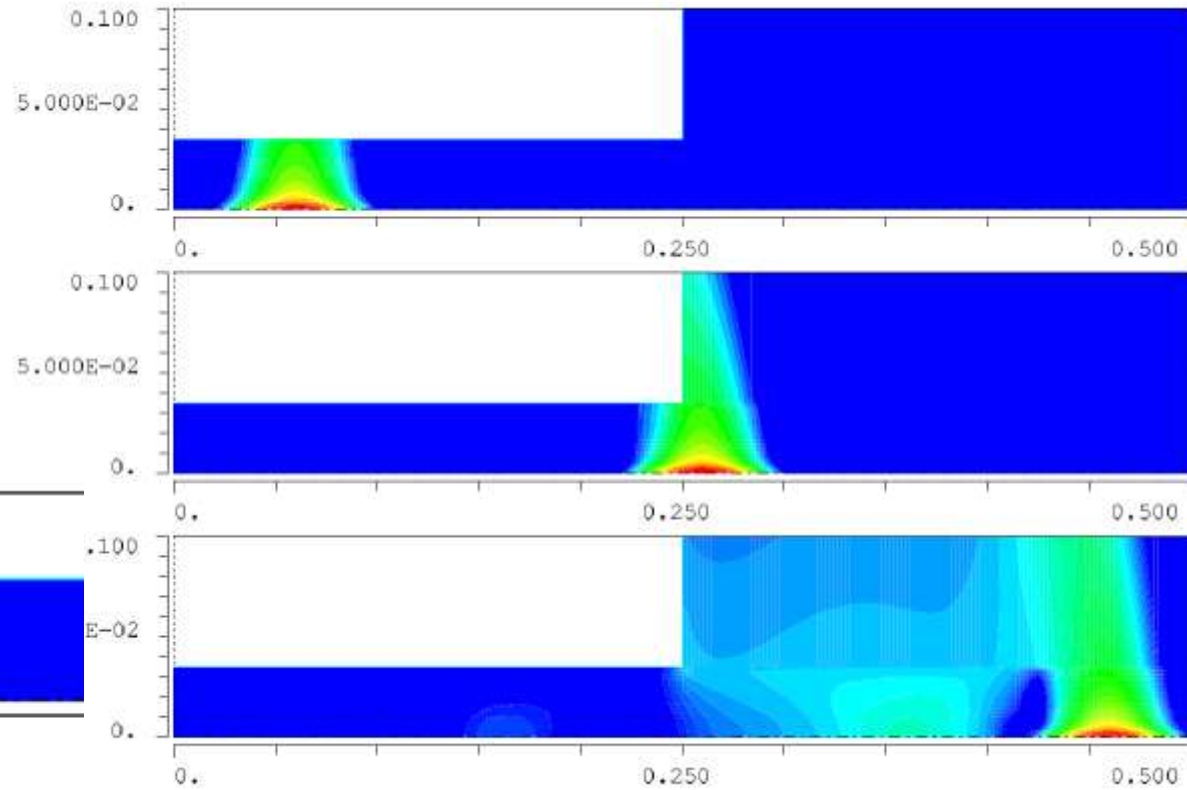
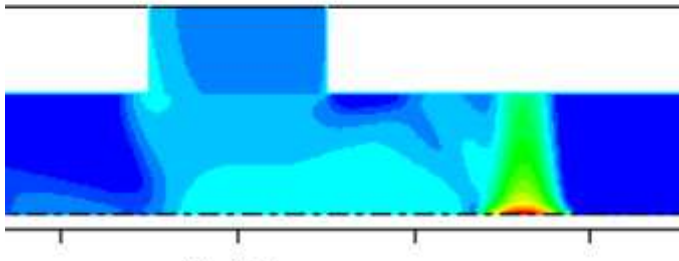
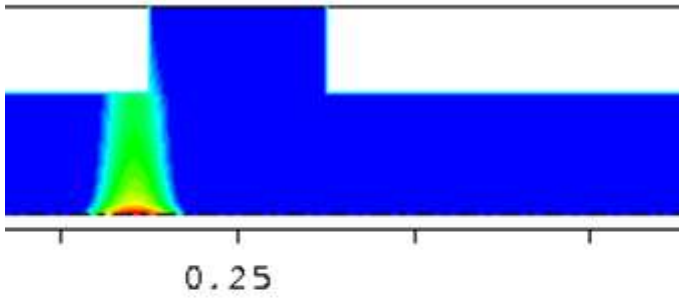
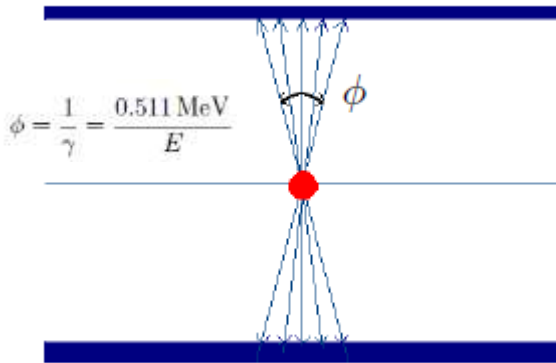
Longitudinal:

$$W_{\parallel}(z) = -\frac{1}{q_1} \int_{-\infty}^{\infty} E_z(r_2 = 0, z, t = \frac{z+s}{c}) ds$$

Transverse:

$$W_{\perp}(z) = -\frac{1}{q_1 d_1} \int_{-\infty}^{\infty} [\mathbf{E} + \mathbf{v} \times \mathbf{B}]_{\perp}(r_2 = 0, z, t = \frac{z+s}{c}) ds$$

Wake-fields - Examples



Wake fields behind a bunch generated at a step-out transition from a small to a larger beam pipe

Wake fields in a cavity

What is you have many particles

- Wake-functions

Longitudinal: $\int_0^L F_z ds = -q^2 W_{\parallel}(z)$

For a test particle in a bunch:

$$\int_0^L F_z ds = qV \quad V = -q \int W_{\parallel}(z-u) \lambda(u) du$$

(Voltage kick or Wake potential)

Line density: $\lambda(z) = \frac{dN}{dz}$

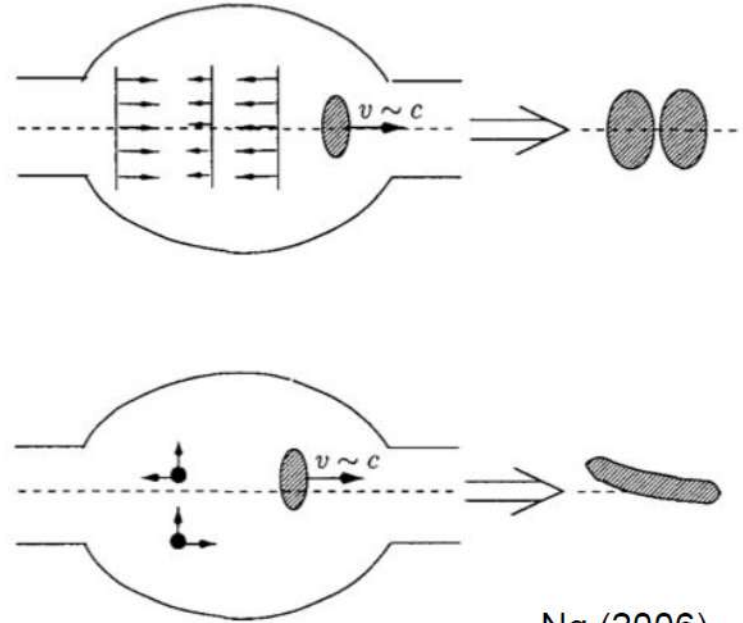
Transverse: $\int_0^L F_{\perp} ds = -q^2 r W_{\perp}(z)$

For a test particle in a bunch:

$$\frac{1}{\gamma_0 mc^2} \int_0^L F_x ds = \Delta x' \quad \Delta x' = -\frac{q^2}{\gamma_0 mc^2} \int W_{\perp}(z-u) \lambda(u) \bar{x}(u) du$$

(horizontal kick)

$\bar{x} = \langle x \rangle$: local bunch offset



Ng (2006)

Even “simple” resistive wall leaves wakes

Longitudinal: $W_{\parallel}(z) = \frac{c}{4\pi b} \sqrt{\frac{Z_0}{\pi\sigma}} \frac{L}{|z|^{3/2}}$

Transverse: $W_{\perp}(z) = \frac{c}{\pi b^3} \sqrt{\frac{Z_0}{\pi\sigma}} \frac{L}{|z|^{1/2}}$

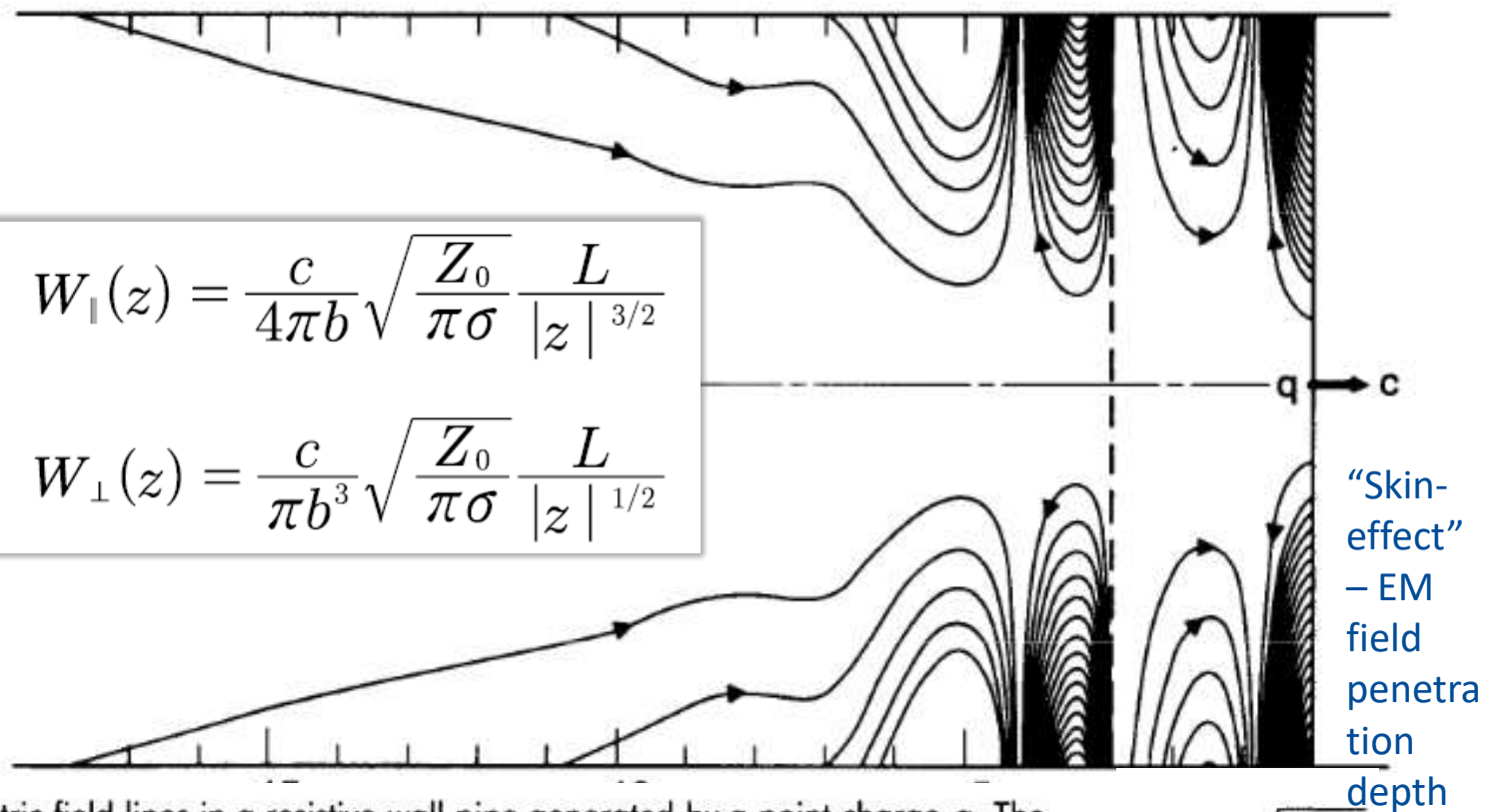
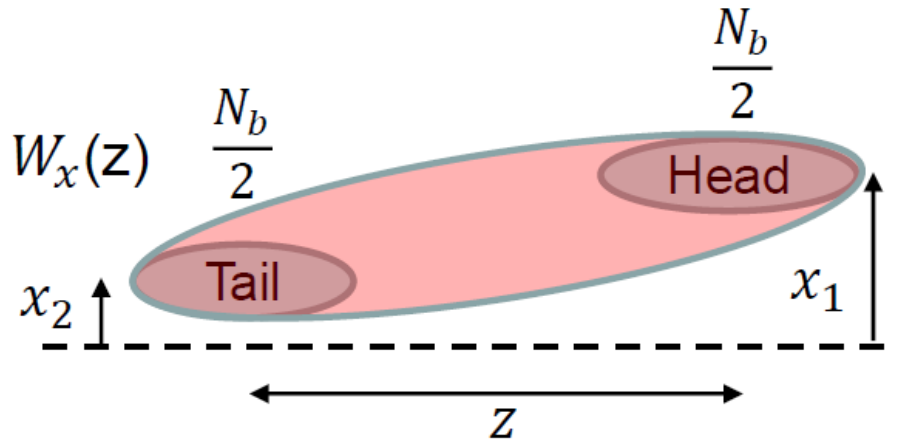


Figure 2.3. Wake electric field lines in a resistive wall pipe generated by a point charge q . The field pattern shows oscillatory behavior in the region $|z| \leq 5(2\chi)^{1/3} b$ (or $|z| \leq 0.35$ mm for an aluminum pipe with $b = 5$ cm). The field line density to the left of the dashed line has been magnified by a factor of 40. (Courtesy Karl Bane, 1991.)

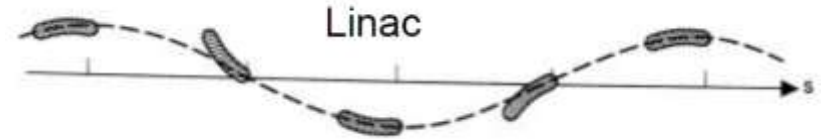
$$\delta r = \sqrt{\frac{c|z|}{\pi\sigma}}$$

Key points: a) longitudinal wakefield leads to particle energy loss and pipe heating; b) transverse wake is defocusing for vacuum beam pipe (focusing in case of electron cloud)

Consequences: two-particle model



In linacs: Beam-break up (BBU) instability



Two-particle coupled betatron oscillations:

$$x_1'' + \kappa x_1 = 0$$

$$x_2'' + \kappa x_2 = \frac{q^2 N_b W_x(z)}{2LE_0} x_1 \quad \kappa = \frac{Q_x^2}{R^2}$$

New coordinates:

$$\tilde{x}_l = x_l + i \frac{x'_l}{\kappa} \quad l = 1, 2$$

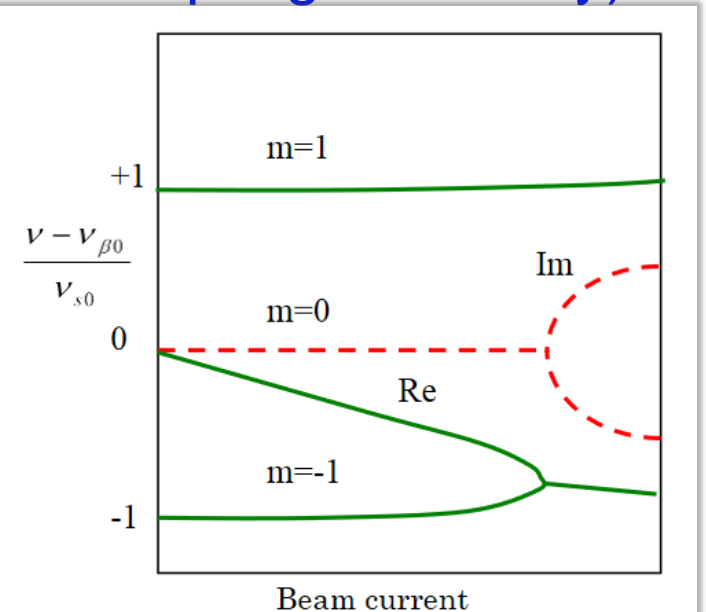
Solution:

$$\tilde{x}_1(s) = \tilde{x}_1(0) e^{-i\kappa s}$$

$$\tilde{x}_2(s) = \tilde{x}_2(0) e^{-i\kappa s} + i \frac{q^2 N_b W_x(z)}{4E_0 L \kappa} \tilde{x}_1(0) s e^{-i\kappa s}$$

Linear growth !

In rings: Head-tail instability (aka TMCI = Transverse Mode Coupling Instability)



Intensity Limits and Cures

Beampipe heating is important for cryo – may limit on $N_b I_b$

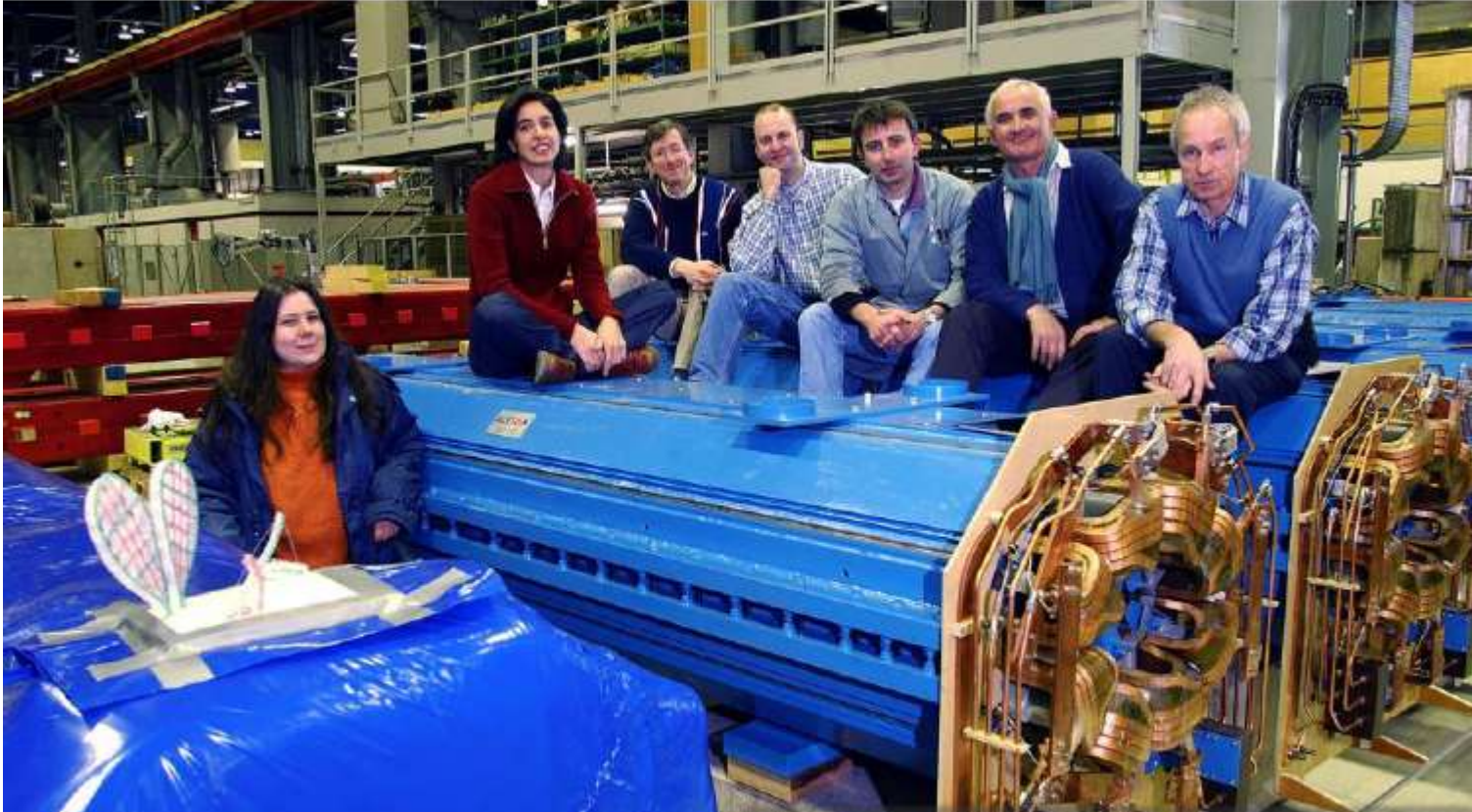
Instabilities **severely** limit either single bunch current I_b or total beam current $N_b I_b$

Cures employed so far:

- 1) Reduce wakes/impedances – no discontinuities in beam pipe, better conducting materials, etc
- 2) **In linacs** – *BNS damping* = introduce energy difference btw head and tail of the bunch (RF phase choice) leading to slight difference in the betatron oscillation frequencies
- 3) **In rings**
 - 1) Feedback dampers (might not work for single bunch instabilities)
 - 2) introduce betatron frequency spread via chromaticity $dQ=Q'(dP/P)$ (does not always work) or octupoles $dQ \sim Oct * \sigma^2$ (mostly worked so far) or electron beams for Landau damping (next gen colliders)

Intensity Limits and Cures

168 LHC octupoles for Landau Damping



Tune shifts (integrated):

$$\Delta Q_x = a_x J_x - b_{xy} J_y$$

$$\Delta Q_y = a_y J_y - b_{xy} J_x$$

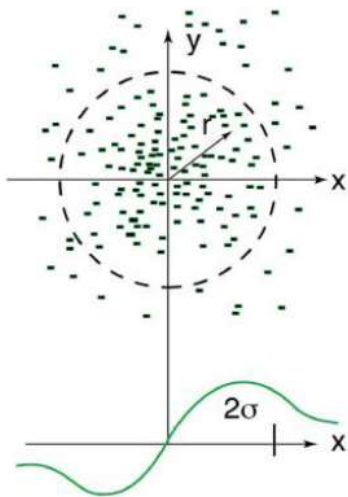
Concern is that these octupoles are so nonlinear that they reduce *Dynamic Aperture* of the collider
→ affect lifetime

Landay Damping by Electron Lenses



Matched transverse beam radii.

Gaussian

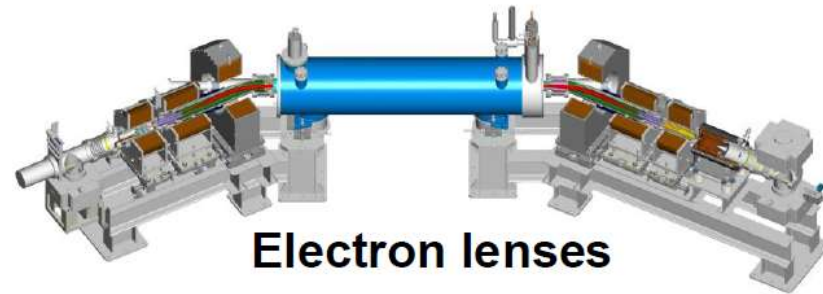


Gaussian electron beam provides a nonlinear tune shift.

V. Shiltsev et al., PRL (2017)

Example: One e-lens ($l=2$ m, $I_e=1$ A) in LHC would provide a tune spread similar to the 168 octupoles.

Similar to the beam-beam force !

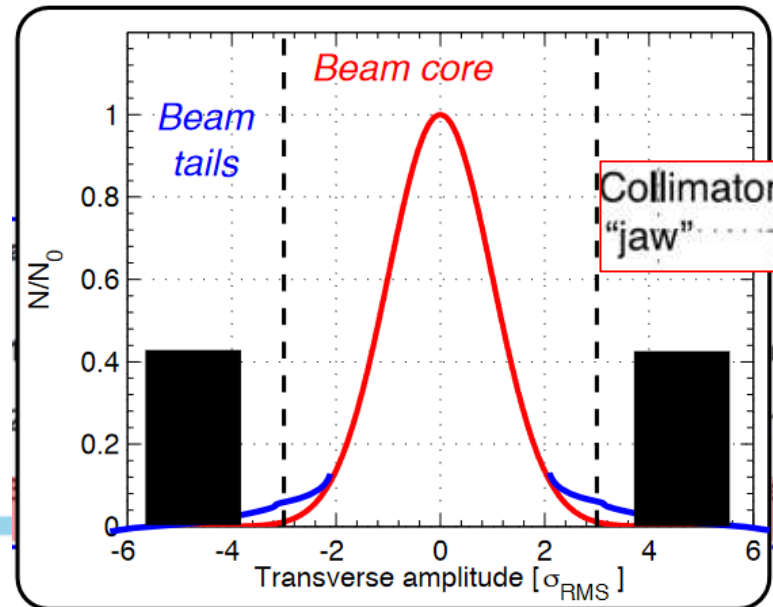
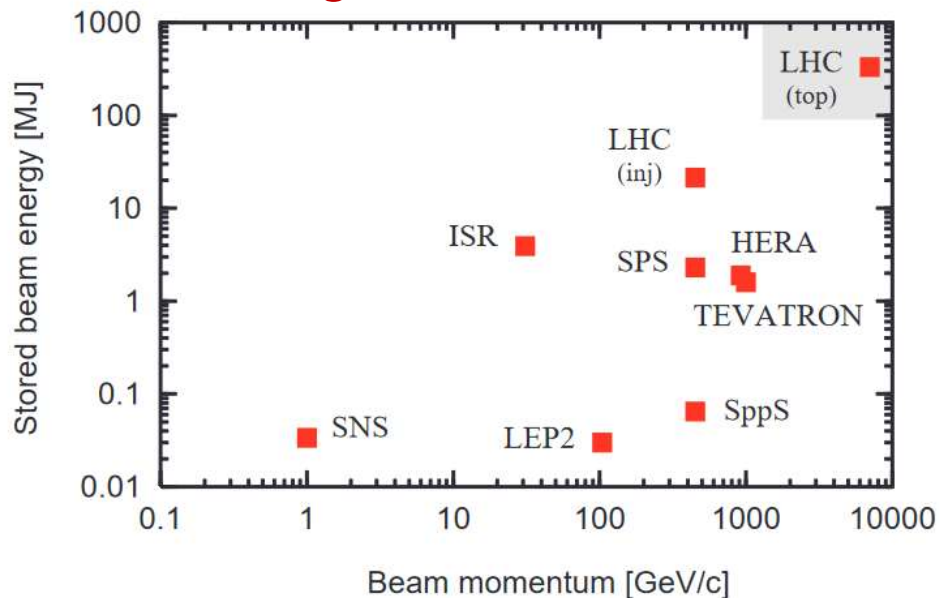


Tune shift induced by a counter-propagating electron beam:

$$\Delta Q_x^e = \frac{1 + \beta_e}{\beta_e} \frac{I_e l r_p}{2\pi e c \epsilon_x}$$

Collimation

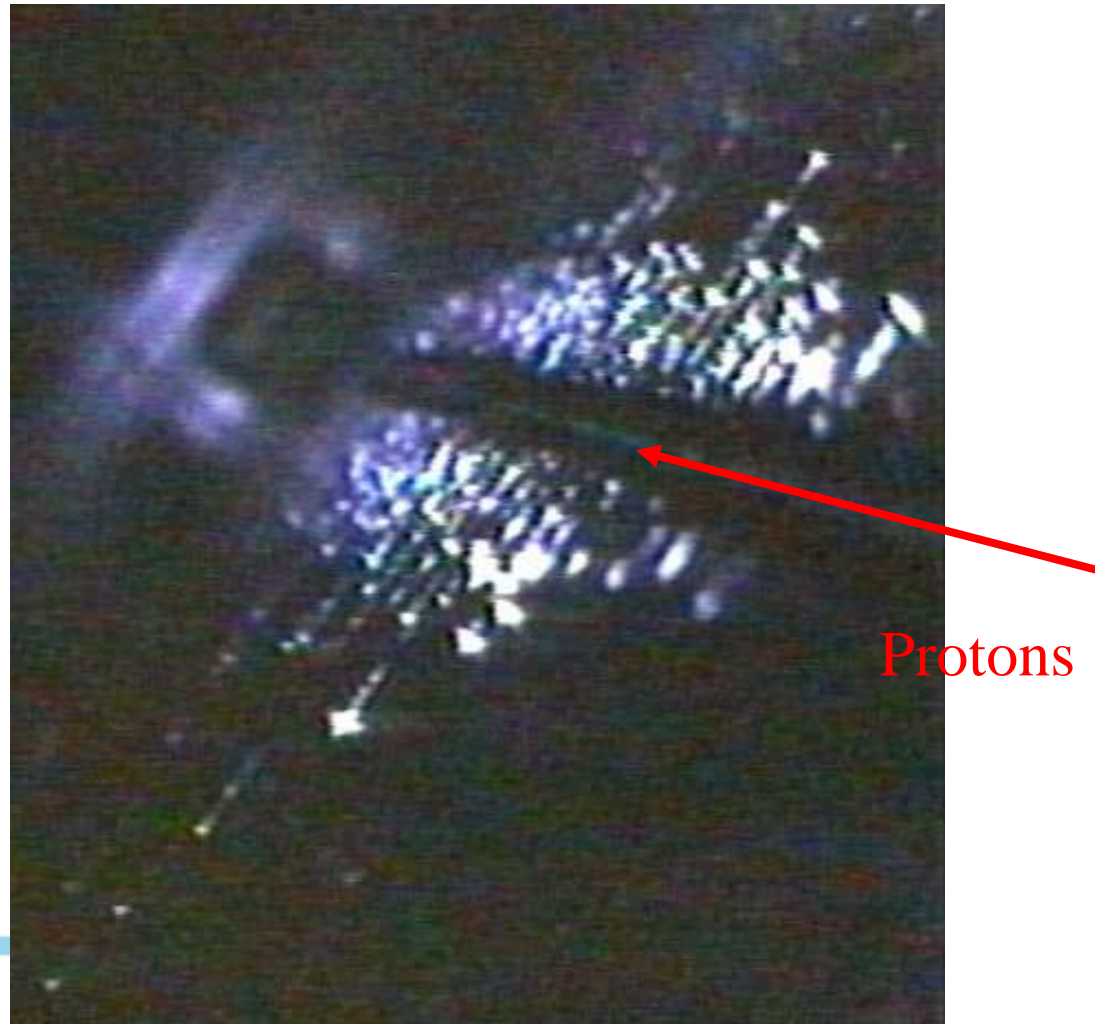
- To protect from enormous beam power (and power density) of high energy accelerators and colliders – events and processes:
 - Injection errors
 - Instabilities
 - Losses due to beam-beam, beam-gas, intrabeam scattering, etc
 - Synchrotron radiation photons
- **Protect magnets, RF and detectors !**



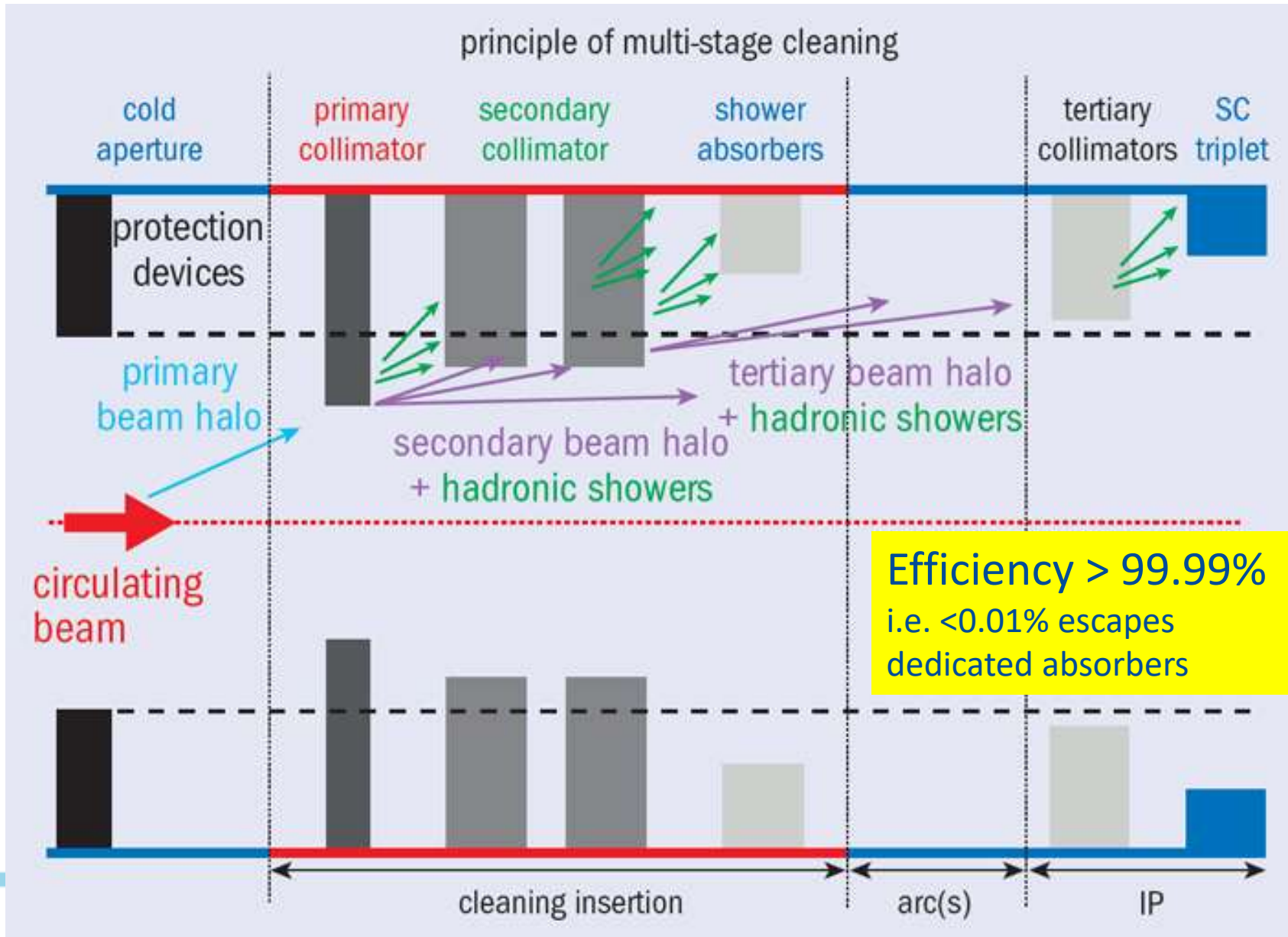
Collimators

- Tevatron 12 collimators:
 - Hor and Vert
 - Proton and antiproton
 - 4 primaries
 - 5 mm W
 - 8 secondaries
 - 1.5 m stainless steel
 - Flat to <25 micron
 - As close as few mm to the
- Efficiency 95-99%
 - reduction of background in CDF and D0 detectors x20-100

Damage to E03 1.5m Collimator



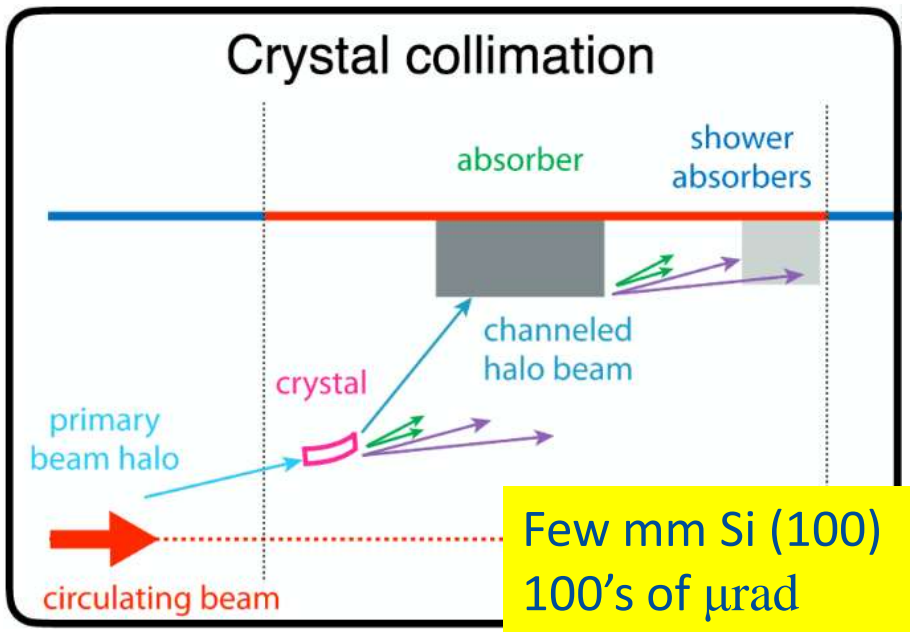
(Most Sophisticated) LHC Collimation



Collimation Challenges and Cures

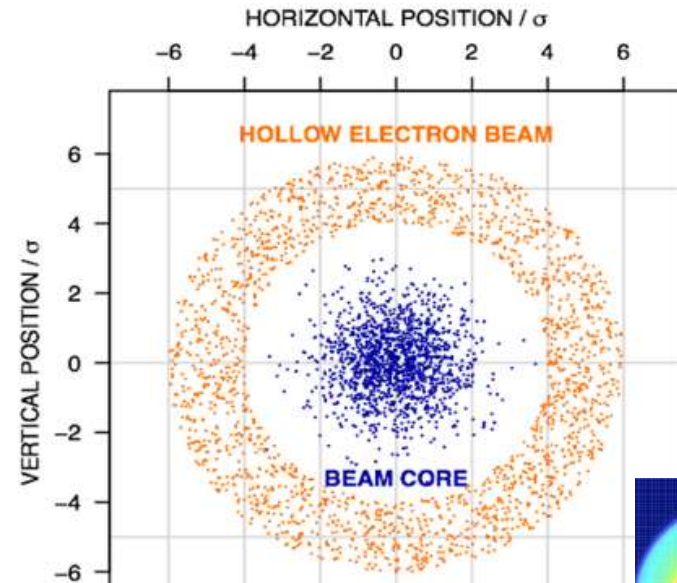
- Too many, too close to beams → large wakefields/impedance
- Can be damaged/destroyed **NEW METHODS**

Bent crystal collimation

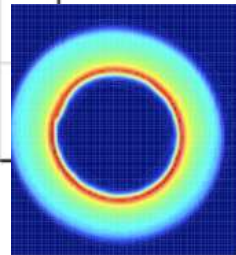


Makes bigger deflection → better interception of scattered particles
Tested at the Tevatron and LHC

Hollow e-beam collimation



Few Amperes, few mm dia, few m long e-beam



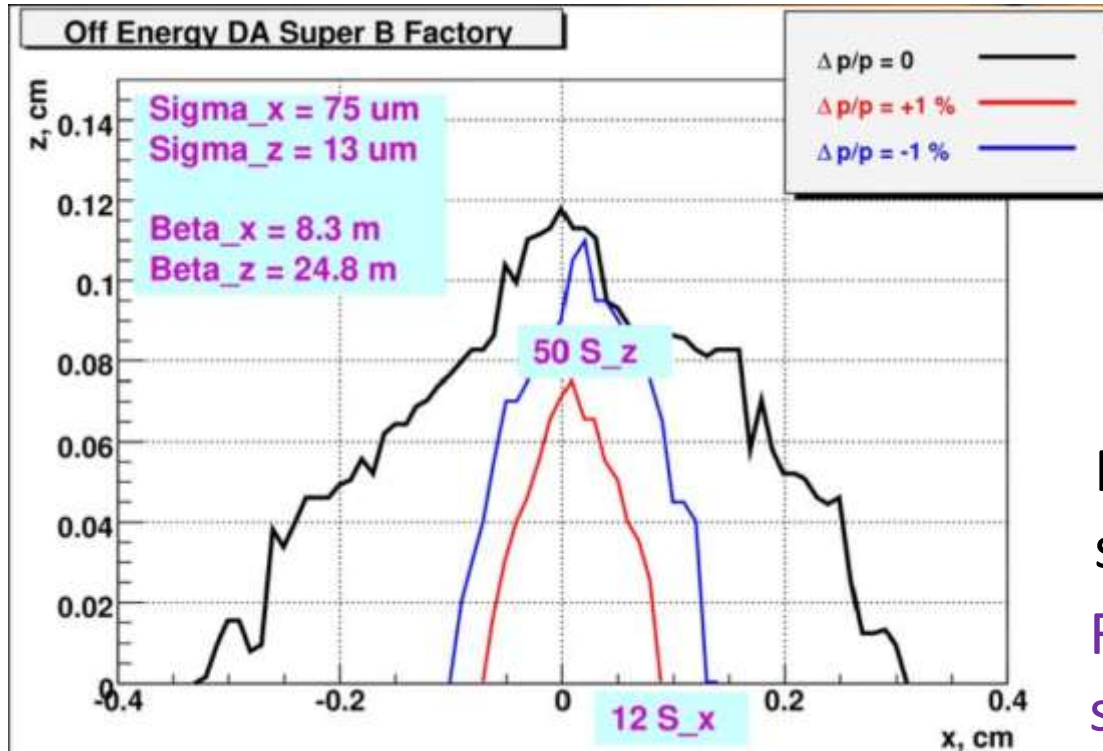
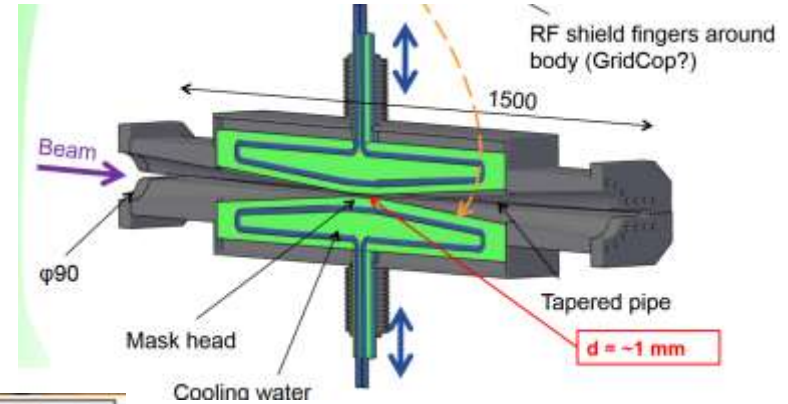
Soft "penetrable" & fast diffusor → undamageable. Tested at the Tevatron and being built for LHC

Aperture and Dynamic Aperture

Physical beam pipe ~60-100 mm ... 10's-100's σ
Often coated (eg TiN) and/or grooved (ecloud)



Collimators - closest to beam – 5-10's of σ
Often coated (eg TiN) and/or grooved (ecloud)



The **dynamic aperture** is the stability region of phase space in an accelerator – dependent on nonlinearities and chromatic effects

For proton machines - stability over $O(1e9)$ turns

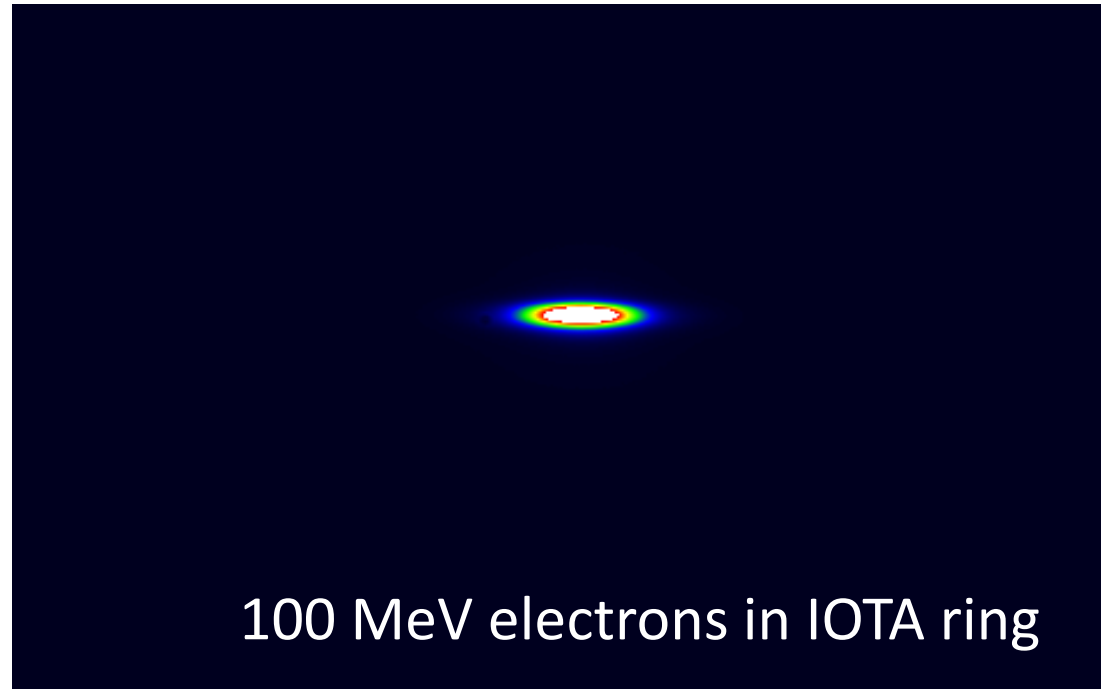
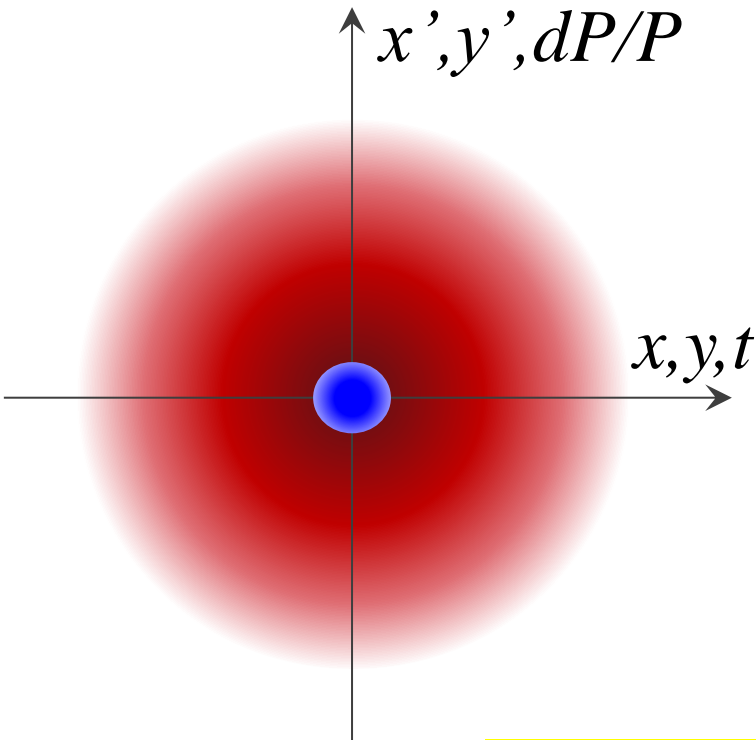
For electron/e+ machines - stability over $O(1e4)$ turns

Beam Cooling

Beam Phase Space Density Increase

- As needed for a collider
- Forbidden by the *Liouville theorem* in non-dissipative systems

$$\mathcal{L} = f_{\text{coll}} \frac{N_1 N_2}{4\pi\sigma_x^* \sigma_y^*}$$



Ideally - "6D-Cooling"

Diffusion and Cooling (1)

Diffusion equation for beam distribution function $f(J,t)$, J - action variable

$$\frac{\partial f}{\partial t} = \frac{\partial}{\partial t} \left(D(J) \frac{\partial f}{\partial J} \right)$$

In the presence of cooling:

$$\frac{d\epsilon_n}{dt} = \beta\gamma \frac{dD(J)}{dJ} - \frac{\epsilon_n}{\tau_{\text{cool}}}$$

where for example:

Lectures VL7-10

Dipole noise For a single dipole steering error randomly fluctuating each revolution of the accelerator with rms value θ_{rms} , the emittance growth rate is

$$\frac{d\epsilon_N}{dt} = \frac{1}{2} f_0 (\gamma v/c) \beta_0 \theta_{\text{rms}}^2 \quad (10)$$

where β_0 is the β -function at the location of the error, and f_0 is the revolution frequency.

Coulomb scattering If the scattering is due to small angle Coulomb interactions between the beam particles and other material in the beam chamber, then

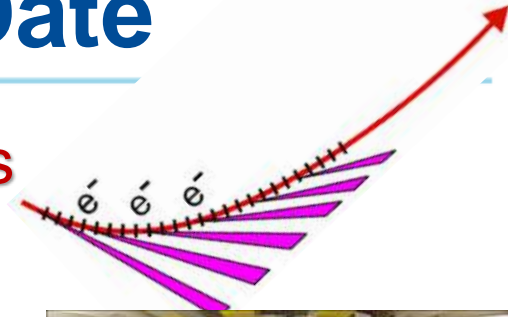
$$\frac{d\epsilon_N}{dt} = \frac{1}{2} f_0 \langle \beta \rangle \left(\frac{13.6 \text{ MeV}}{mc^2} \right)^2 \frac{z}{\gamma(v/c)^3} \frac{\ell}{X_0} \quad (12)$$

where mc^2 is the rest energy of a beam particle, z its charge, and X_0 is the radiation length of the

Beam Cooling Methods to Date

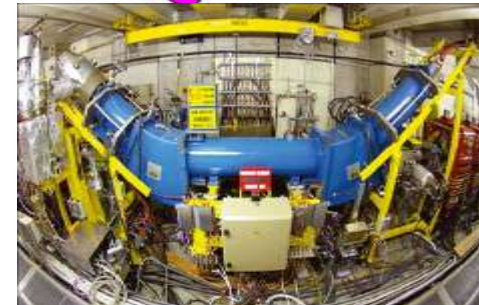
Synchrotron Radiation Damping – since 1960's

- common in all e+/e- rings



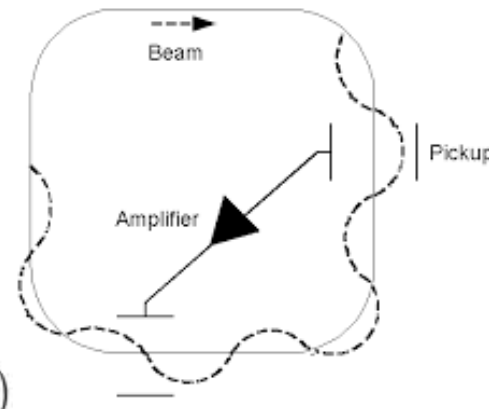
Electron Cooling – since 1970's

- Widely used to cool ions and antiprotons
- 0.1 - 8 GeV/n (50 keV – 4 MeV electrons DC)



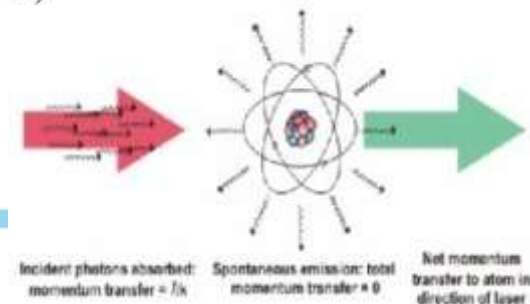
Stochastic Cooling – since 1970's

- Widely used to cool ions and antiprotons
- 0.1-100 GeV/n (up to 10 GHz feedback BW)



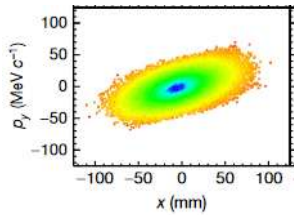
Laser Cooling – since 1990's $\Omega = \gamma\omega_{21}(1 - \beta \cos \theta)$

- Works for some highly charged ions
- 0.1-0.5 GeV/n, deep cooling, spectroscopy

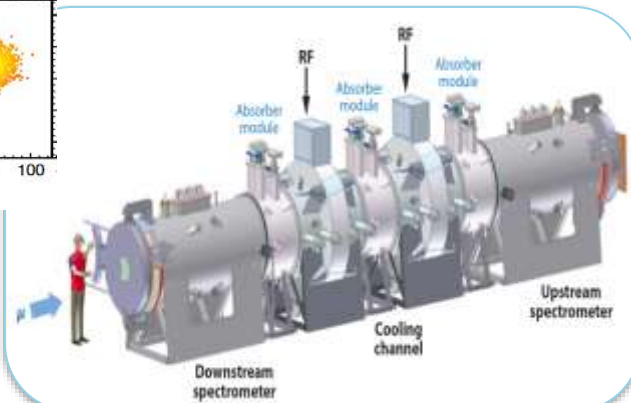


Recent Beam Cooling Breakthroughs

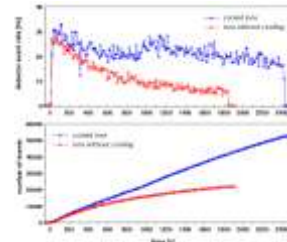
2019 - Ionization cooling of muons (140 MeV/c, RAL, UK)



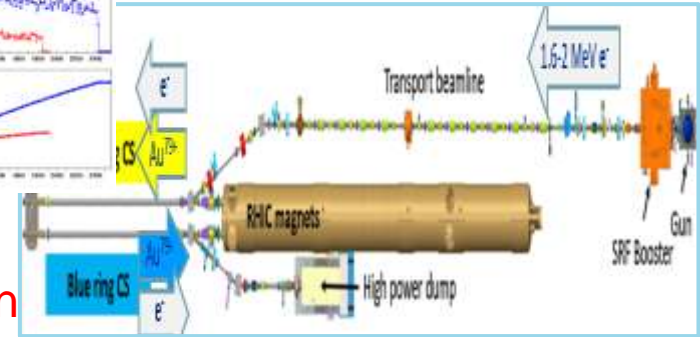
MICE
~10% in one pass



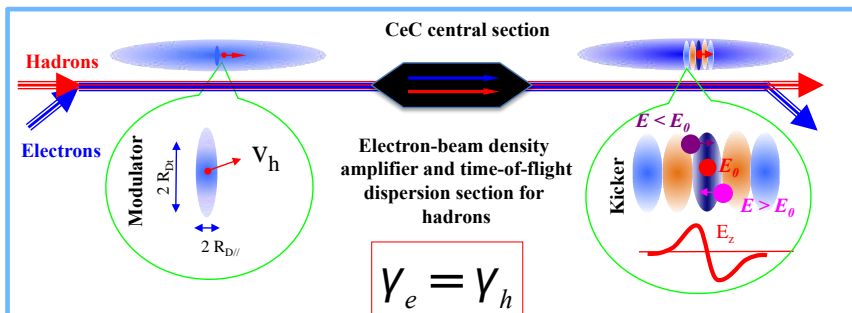
2020 – “Bunched” electron cooling of ions ($\gamma \sim 5$, BNL)



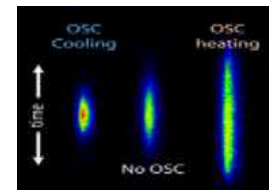
RHIC
RF e-gun



2021 – Coherent Electron cooling of ions (26.5 GeV/n, RHIC) – ongoing PoP exp't at BNL



2021 – Optical Stochastic cooling e- (100 MeV, FNAL)



IOTA
THz
bandwidth



Thanks for your Attention!

Questions !?

Literature

- W.Herr, CAS school

<https://cds.cern.ch/record/941319/files/p379.pdf>

- V.Lebedev, V.Shiltsev, Tevatron Book Ch.8

https://indico.cern.ch/event/774280/attachments/1758668/2915590/2014_Book_AcceleratorPhysicsAtTheTevatro.pdf

- Proc. 2013 ICFA mini-workshop on "Beam-Beam Effects in Hadron Colliders"

<https://indico.cern.ch/event/189544/>

- Past schools :

- A. Chao, The beam-beam instability, SLAC-PUB-3179 (1983).
- L. Evans, The beam-beam interaction, CAS Course on proton-antiproton colliders, in CERN 84-15 (1984).
- L. Evans and J. Gareyte, Beam-beam effects, CERN Accelerator School, Oxford 1985, in: CERN 87-03 (1987).
- A. Zholents, Beam-beam effects in electron-positron storage rings, Joint US-CERN School on Particle Accelerators, in Springer, Lecture Notes in Physics, 400 (1992).

Comprehensive JUAS-book (2371 pages – all topics!)
<https://doi.org/10.23730/CYRSP-2024-003>.

Instabilities:

A.Chao, *Physics of collective beam instabilities in high energy accelerators* (1993)

<https://www.slac.stanford.edu/~achao/wileybook.html>

Many useful articles:

S.Myers, H.Schopper *Accelerators and Colliders*
(2013, open access)

<https://link.springer.com/book/10.1007/978-3-030-34245-6>



U.S. Particle Accelerator School
Education in Beam Physics and Accelerator Technology



Colliders – Lectures VS6-7: Circular e^+e^- Colliders Higgs Factories Hadron Colliders (1)

Vladimir Shiltsev, Northern Illinois University

part of the “Colliders” class by V.Shiltsev, V.Ptitsyn and C. Liu

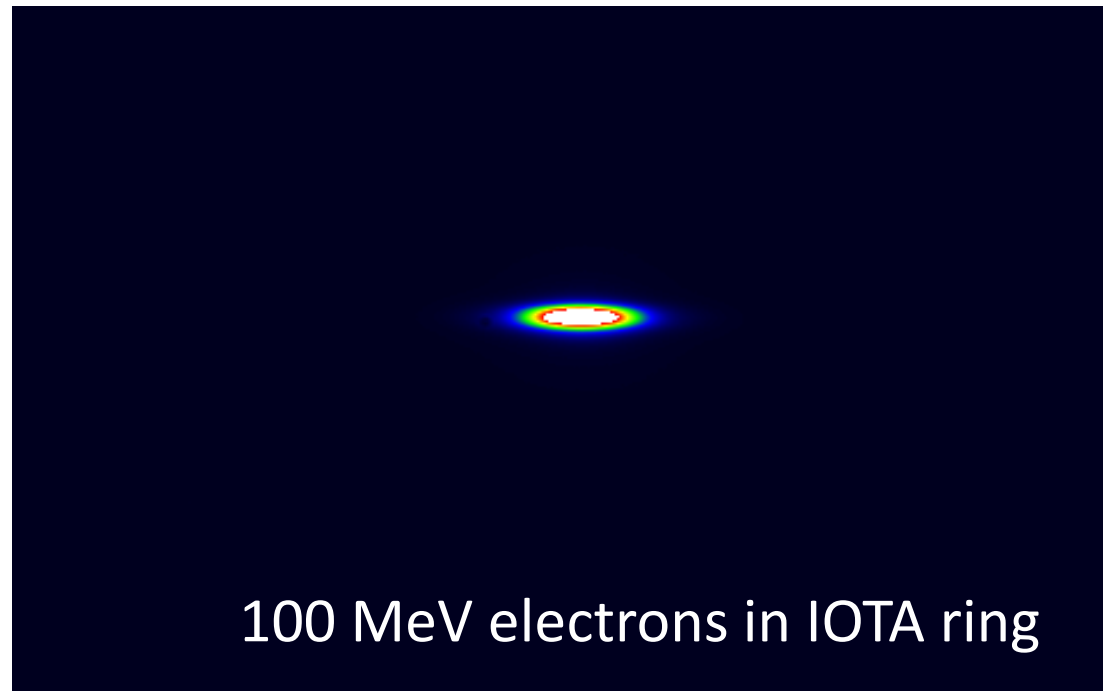
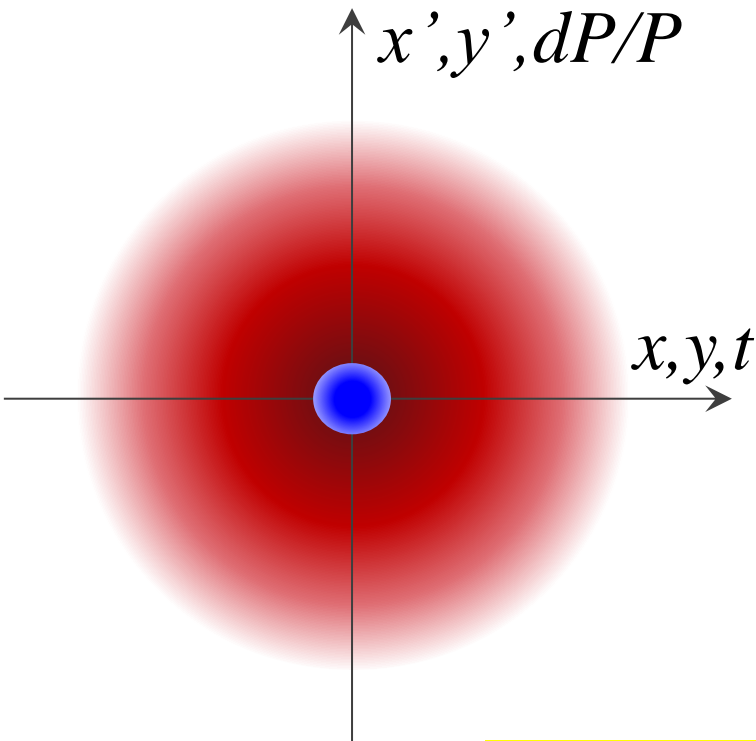
US Particle Accelerator School, Jan 27 – Jan 31, 2025

Beam Cooling

Beam Phase Space Density Increase

- As needed for a collider
- Forbidden by the *Liouville theorem* in non-dissipative systems

$$\mathcal{L} = f_{\text{coll}} \frac{N_1 N_2}{4\pi\sigma_x^* \sigma_y^*}$$



Ideally - “6D-Cooling”

Diffusion and Cooling (1)

Diffusion equation for beam distribution function $f(J,t)$, J - action variable

$$\frac{\partial f}{\partial t} = \frac{\partial}{\partial t} \left(D(J) \frac{\partial f}{\partial J} \right)$$

In the presence of cooling:

$$\frac{d\epsilon_n}{dt} = \beta\gamma \frac{dD(J)}{dJ} - \frac{\epsilon_n}{\tau_{\text{cool}}}$$

where for example:

Dipole noise For a single dipole steering error randomly fluctuating each revolution of the accelerator with rms value θ_{rms} , the emittance growth rate is

$$\frac{d\epsilon_N}{dt} = \frac{1}{2} f_0 (\gamma v/c) \beta_0 \theta_{\text{rms}}^2 \quad (10)$$

where β_0 is the β -function at the location of the error, and f_0 is the revolution frequency.

Coulomb scattering If the scattering is due to small angle Coulomb interactions between the beam particles and other material in the beam chamber, then

$$\frac{d\epsilon_N}{dt} = \frac{1}{2} f_0 \langle \beta \rangle \left(\frac{13.6 \text{ MeV}}{mc^2} \right)^2 \frac{z}{\gamma(v/c)^3} \frac{\ell}{X_0} \quad (12)$$

where mc^2 is the rest energy of a beam particle, z its charge, and X_0 is the radiation length of the

Synchrotron Radiation (1)

Average radiated power restored by RF

$$U_0 \cong 10^{-3} \text{ of } E_0$$

- Electron loses energy each turn
- RF cavities provide voltage to accelerate electrons back to the nominal energy

$$V_{RF} > U_0$$

Radiation damping

- Average rate of energy loss produces **DAMPING** of electron oscillations in all three degrees of freedom (if properly arranged!)

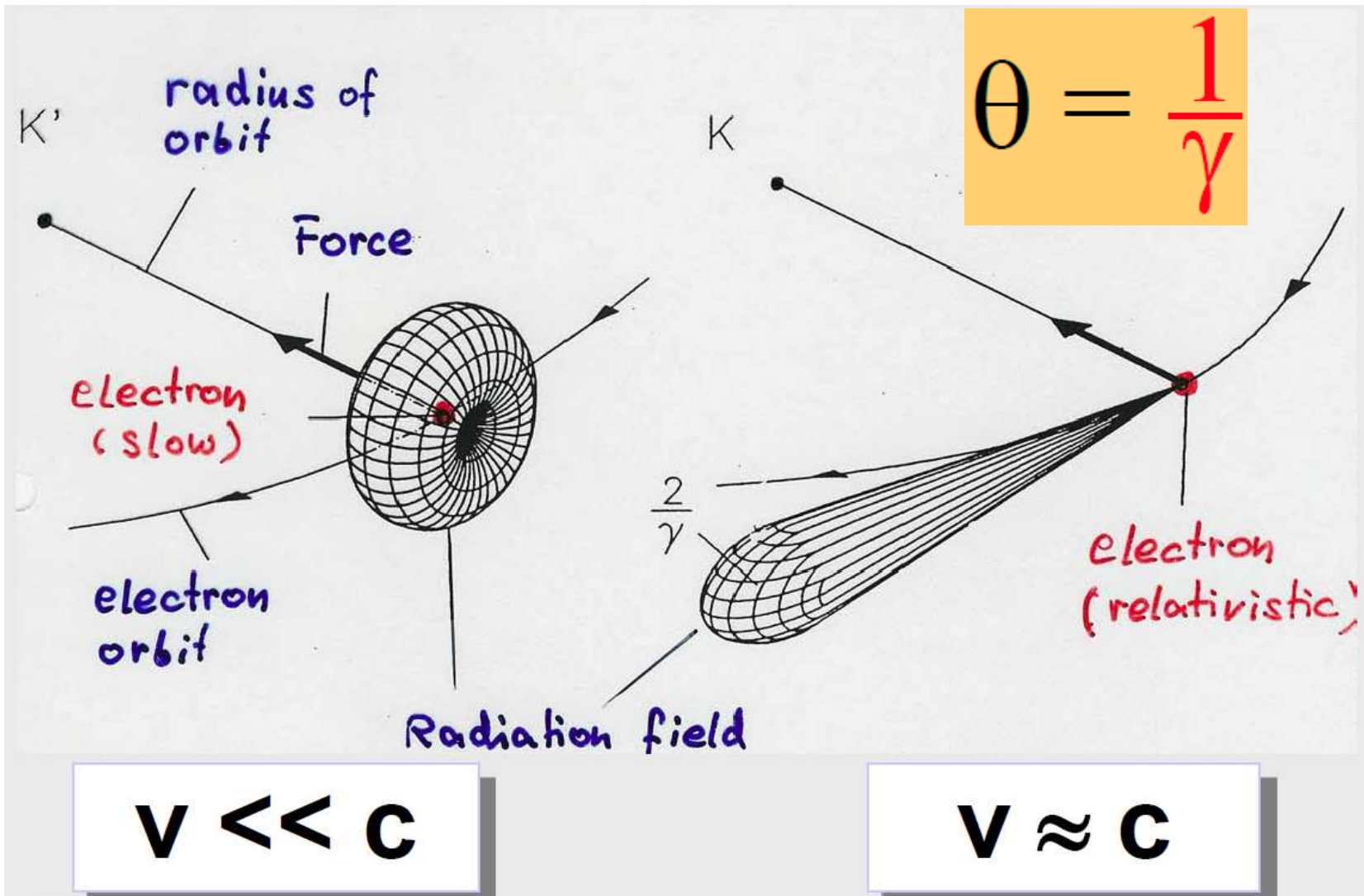
Quantum fluctuations

- Statistical fluctuations in energy loss (from quantised emission of radiation) produce **RANDOM EXCITATION** of these oscillations

Equilibrium distributions

- The balance between the damping and the excitation of the electron oscillations determines the equilibrium distribution of particles in the beam

Radiation is emitted in a narrow cone



Synchrotron radiation power

Power emitted is proportional to:

$$P \propto E^2 B^2$$

$$P_\gamma = \frac{c C_\gamma}{2\pi} \cdot \frac{E^4}{\rho^2}$$

$$P_\gamma = \frac{2}{3} \alpha \hbar c^2 \cdot \frac{\gamma^4}{\rho^2}$$

$$C_\gamma = \frac{4\pi}{3} \frac{r_e}{(m_e c^2)^3} = 8.858 \cdot 10^{-5} \left[\frac{\text{m}}{\text{GeV}^3} \right]$$

$$\alpha = \frac{1}{137}$$

$$\Delta E_{\text{SR}} = 0.089 \text{ MeV/turn } E_b^4 (\text{GeV}) / \rho (\text{m})$$

Energy loss per turn:

$$\hbar c = 197 \text{ MeV} \cdot \text{fm}$$

$$U_0 = C_\gamma \cdot \frac{E^4}{\rho}$$

$$U_0 = \frac{4\pi}{3} \alpha \hbar c \frac{\gamma^4}{\rho}$$

Diffusion and Cooling (2)

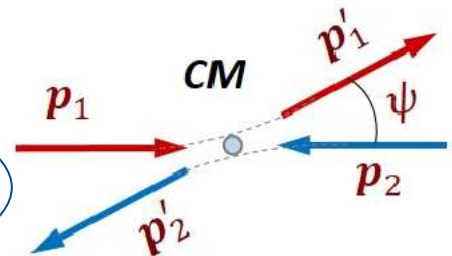
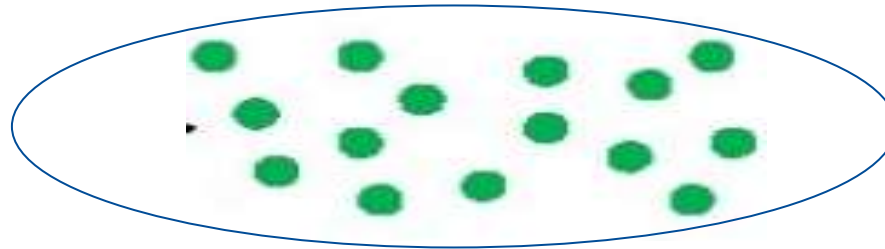
Examples

proton beam scattering with the residual gas (assumed to be air) gives

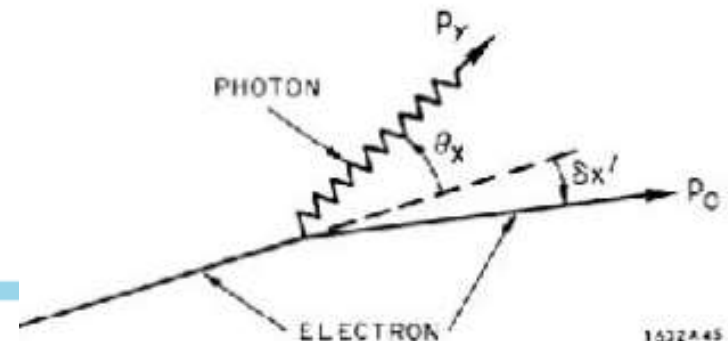
$$\frac{d\epsilon_N}{dt} = \langle \beta \rangle (1.6 \times 10^{-7} / \text{s}) \frac{P[\mu\text{Torr}]}{\gamma} \quad (13)$$

or Intrabeam Scattering:

(see lecture VP2)



or fluctuations of synchrotron radiation:

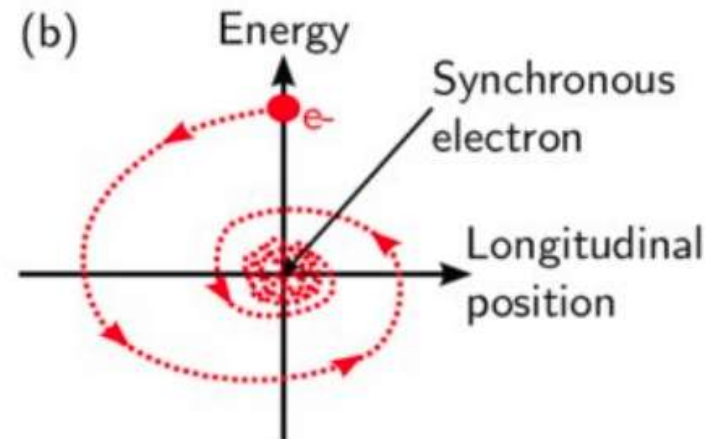
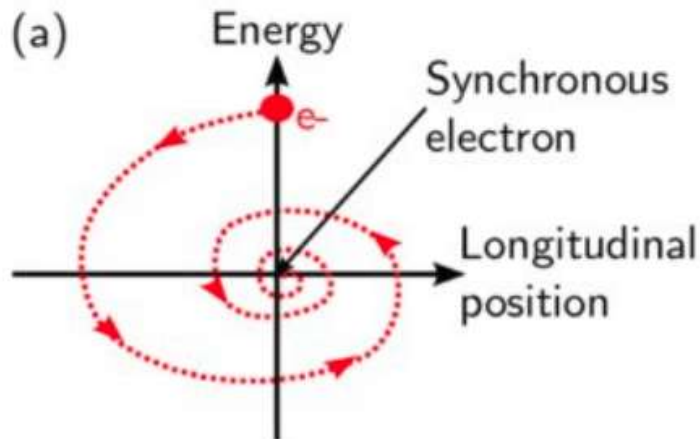


Quantum Nature of Synchrotron Radiation

Damping only: If damping was the whole story, the beam emittance (size) would shrink to microscopic dimensions! Because the radiation is emitted in quanta, radiation itself takes care of the problem! It is sufficient to use quasi-classical picture

- a) Emission time is very short
- b) Emission times are statistically independent (each emission leads to only a small change in electron energy)

→ Purely stochastic (Poisson) process



Quantum Excitation of Energy Oscillations

Photons are emitted with typical energy $u_{ph} \approx \hbar\omega_{typ} = \hbar c \frac{\gamma^3}{\rho}$
at the rate (photons/second) $\mathcal{N} = \frac{P_\gamma}{u_{ph}}$

Fluctuations in this rate excite oscillations

During a small interval Δt electron emits photons

losing energy of

Actually, because of fluctuations, the number is

resulting in **spread in energy loss**

$$N = \mathcal{N} \cdot \Delta t$$

$$N \cdot u_{ph}$$

$$N \pm \sqrt{N}$$

$$\pm \sqrt{N} \cdot u_{ph}$$

For large time intervals RF compensates the energy loss, providing damping towards the design energy E_0

Steady state: typical deviations from E_0

\approx typical fluctuations in energy during a damping time τ_e

Equilibrium energy spread

We then expect the rms energy spread to be

$$\sigma_\varepsilon \approx \sqrt{N \cdot \tau_\varepsilon \cdot u_{ph}}$$

and since

$$\tau_\varepsilon \approx \frac{E_0}{P_\gamma}$$

and

$$P_\gamma = N \cdot u_{ph}$$

$$\sigma_\varepsilon \approx \sqrt{E_0 \cdot u_{ph}}$$

geometric mean of the electron and photon energies!

Relative energy spread can be written then as:

$$\frac{\sigma_\varepsilon}{E_0} \approx \gamma \sqrt{\frac{\lambda_e}{\rho}}$$

$$\lambda_e = \frac{\hbar}{m_e c} = 4 \cdot 10^{-13} m$$

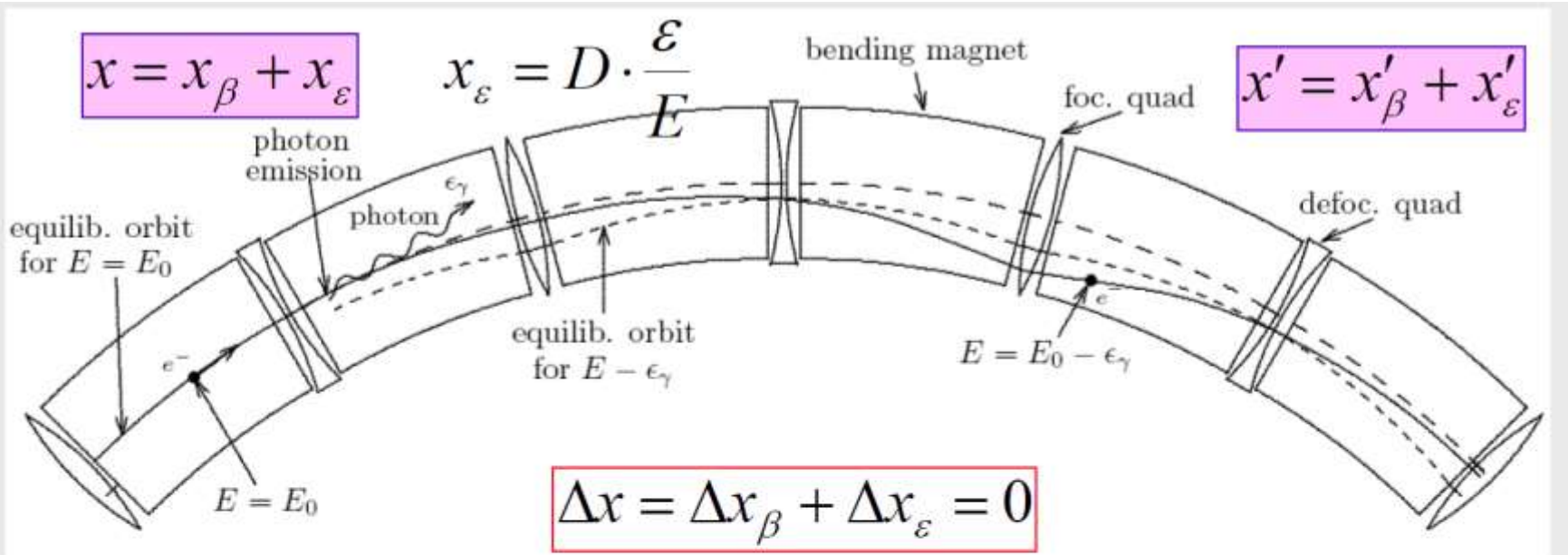
it is roughly constant for all rings

• typically

$$\rho \propto E^2$$

$$\frac{\sigma_\varepsilon}{E_0} \sim const \sim 10^{-3}$$

Excitation of Betatron Oscillations



$$\Delta x_\beta = -D \cdot \frac{\epsilon_\gamma}{E}$$

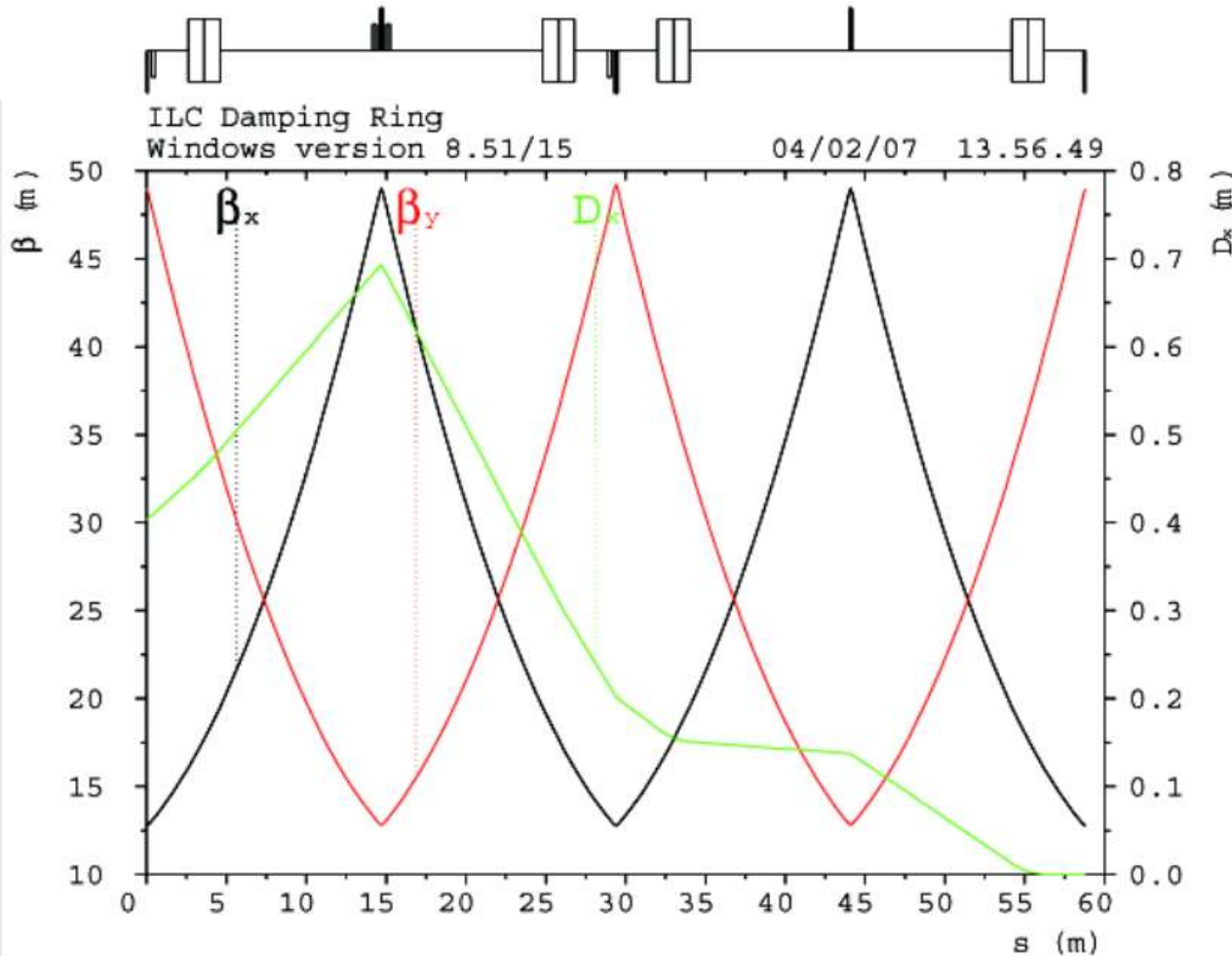
Courant Snyder invariant

$$\Delta x'_\beta = -D' \cdot \frac{\epsilon_\gamma}{E}$$

$$\Delta \epsilon = \gamma \Delta x_\beta^2 + 2\alpha \Delta x_\beta \Delta x'_\beta + \beta \Delta x'^2_\beta = \left[\gamma D^2 + 2\alpha D D' + \beta D'^2 \right] \cdot \left(\frac{\epsilon_\gamma}{E} \right)^2$$

e- Rings are All set By Optical Lattice

Five Integrals



$$I_1 = \oint \frac{D}{\rho} ds$$

$$I_2 = \oint \frac{ds}{\rho^2}$$

$$I_3 = \oint \frac{ds}{|\rho^3|}$$

$$I_4 = \oint \frac{D}{\rho} \left(2k + \frac{1}{\rho^2} \right) ds$$

$$I_5 = \oint \frac{\mathcal{H}}{|\rho^3|} ds$$

$$C_\gamma = \frac{4\pi}{3} \frac{r_e}{(m_e c^2)^3} = 8.858 \cdot 10^{-5} \left[\frac{\text{m}}{\text{GeV}^3} \right]$$

Momentum
compaction
factor

$$\alpha = \frac{I_1}{2\pi R}$$

Energy loss
per turn

$$U_0 = \frac{1}{2\pi} C_\gamma E^4 \cdot I_2$$

Summary of SR Integrals

Damping parameter

$$\mathcal{D} = \frac{I_4}{I_2}$$

Damping times, partition numbers

$$J_\varepsilon = 2 + \mathcal{D}, \quad J_x = 1 - \mathcal{D}, \quad J_y = 1$$

$$\tau_i = \frac{\tau_0}{J_i}$$

$$\tau_0 = \frac{2ET_0}{U_0}$$

Equilibrium energy spread

$$\left(\frac{\sigma_\varepsilon}{E}\right)^2 = \frac{C_q E^2}{J_\varepsilon} \cdot \frac{I_3}{I_2}$$

Equilibrium emittance

$$\varepsilon_{x0} = \frac{\sigma_{x\beta}^2}{\beta} = \frac{C_q E^2}{J_x} \cdot \frac{I_5}{I_2}$$

$$I_1 = \oint \frac{D}{\rho} ds$$

$$I_2 = \oint \frac{ds}{\rho^2}$$

$$I_3 = \oint \frac{ds}{|\rho^3|}$$

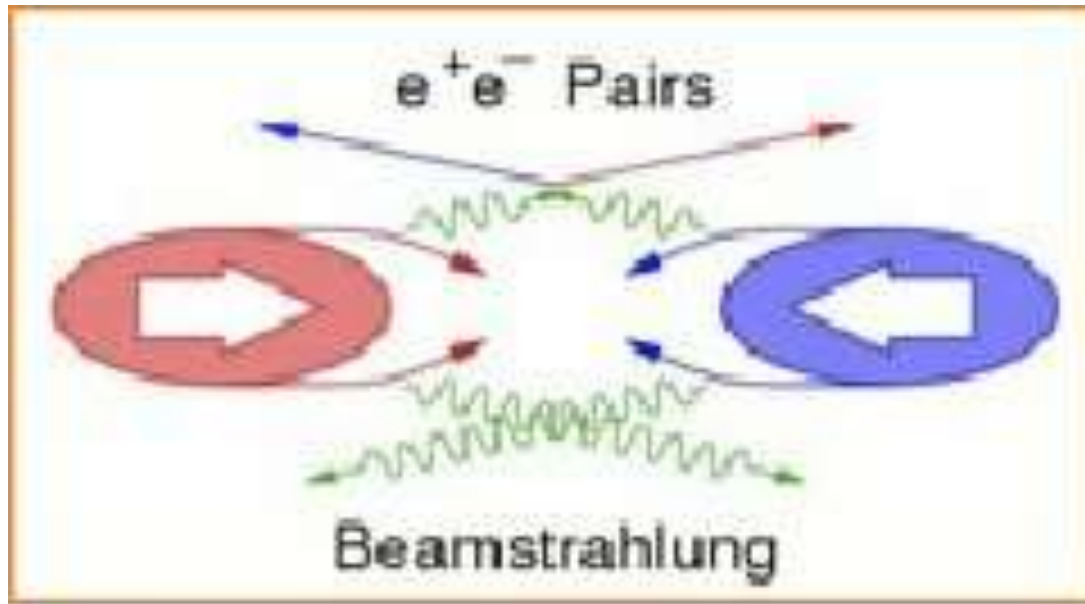
$$I_4 = \oint \frac{D}{\rho} \left(2k + \frac{1}{\rho^2}\right) ds$$

$$I_5 = \oint \frac{\mathcal{H}}{|\rho^3|} ds$$

$$C_q = \frac{55}{32\sqrt{3}} \frac{\hbar c}{(m_e c^2)^3} = 1.468 \cdot 10^{-6} \left[\frac{\text{m}}{\text{GeV}^2} \right]$$

$$\mathcal{H} = \gamma D^2 + 2\alpha DD' + \beta D'^2$$

Beamstrahlung – SR due to Opposite Bunch



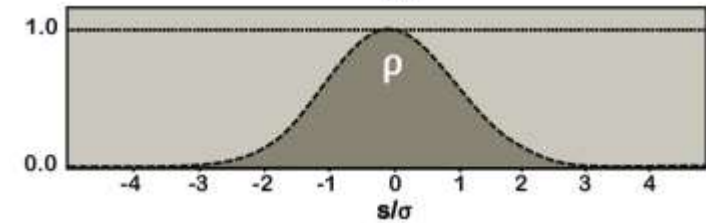
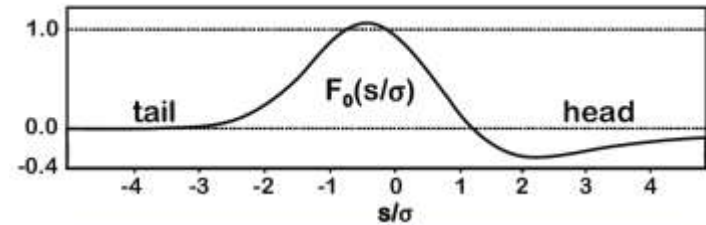
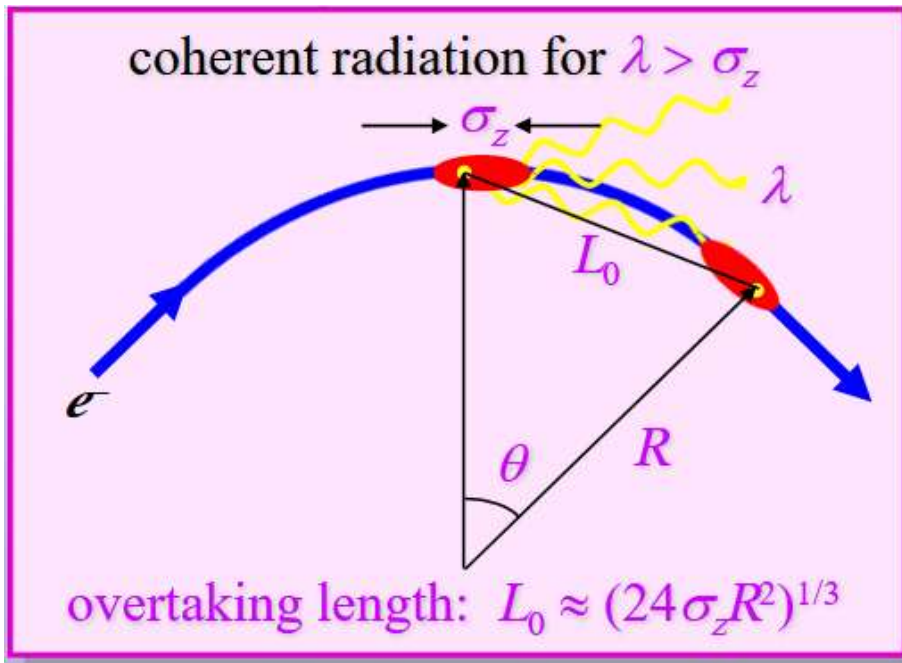
- Effect depends on the energy and field of opposite bunch approx

$$\sim \gamma^2 B^2$$

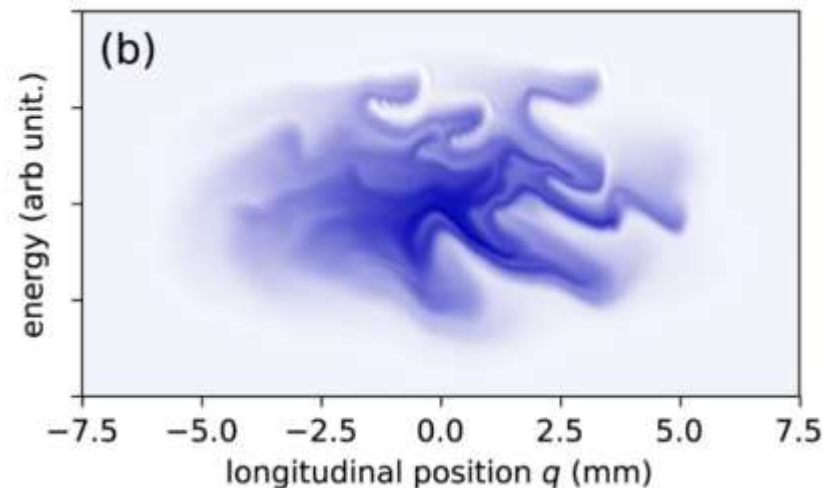
- Serious for large bunch populations (N), small hor. beam size (σ_x) & short bunches (σ_s)
- Linear colliders: 1% to 100% energy spread after 1 collision
- Circular : particles with 1-2% energy loss lost on Dynamic Aperture

Coherent Synchrotron Radiation

- In the case of short bunches with length comparable with radiation wavelength \rightarrow SR from tail decelerates head



microbunching instability (fast)



Electron-positron colliders

- Initially, e^-e^+ was effective way to save space as beams can be bent by the same set of magnets (charges in opposite directions \rightarrow same direction of motion \rightarrow same force in same B-field $q[\mathbf{v} \times \mathbf{B}]$)
- Unique need of B -physics requires relativistic boost of $e^+e^- \rightarrow B$ -meson reaction products \rightarrow need to have relativistic velocities to be detected \rightarrow need to have asymmetric energies eg $3.1+9$ GeV (SLAC P-II), $3.5+8$ GeV (e^+e^- KEKB)
- Below we consider e^+e^- colliders: VEPP-2000 (round beams), SuperKEKB (flat beams, world record holder) and FCCee & CEPC (future Linear Colliders)

SKIP VEPP-2000

VEPP-2000 Collider in Novosibirsk

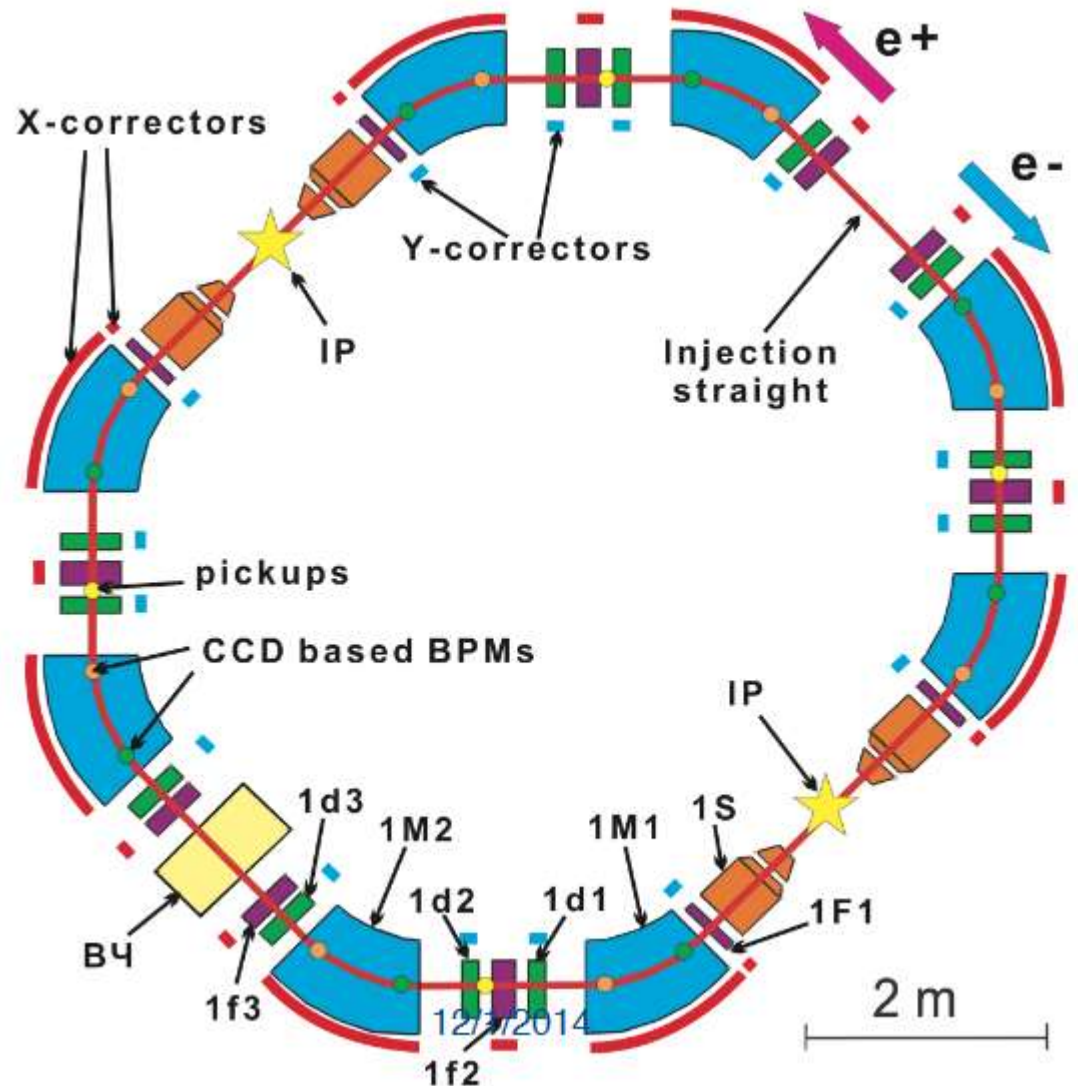
e^+e^- collider at ϕ -meson
energy $E_{cm}=0.3-2$ GeV
 $C=24.4$ m, 1+1 bunch
 $L=5e31$ at 1 GeV cme

Axially symmetric linear
focusing in arcs

Round beams at 2 IPs
with four 13 T solenoids

World record beam-beam
tune shift!

$\xi=0.34$



“Round Beams” in practice

Usually, SR-dominated beams have flat beams – large horizontal emittance and small vertical emittance. The ratio V/H is set by the coupling of x-y degrees of freedom → usually quite small ~1%, that helps to keep vertical beam-beam parameter under b-b limit ~0.05:

$$\xi_{x,y} = \frac{r_0 N \beta_{x,y}^*}{2\pi\gamma\sigma_{x,y}^*(\sigma_x^* + \sigma_y^*)} \quad \mathcal{L} = f_0\gamma \frac{I_b \xi_y}{2er_e\beta_y^*} \left(1 + \frac{\sigma_y^*}{\sigma_x^*}\right)$$

- **Round beams** boost the b-b parameter via less resonances. For that
 1. Small and equal x and y beta-functions at the IPs, head-on collision
 2. Equal beam emittances in x and y
 3. Equal betatron tunes $Q_x = Q_y$

Axial symmetry of counter beam force together with **x-y** symmetry of transfer matrix provides additional integral of motion (angular momentum $M_z = x'y - xy'$). Particle dynamics remains nonlinear, but becomes **1D** (fewer res $Q=n/m$)

Operation Modes – Polarity of Solenoids

4 solenoids in total:

2 at each IP

Equal strength:

each rotates x-y
oscillations

by 45 degrees ie

$$HL = \pi (B_{\text{ring}} \rho_{\text{ring}}) / 2$$

eg “Mobius” +--- =

+45-45+45+45=90 degrees

that is $x \rightarrow y$ flip per turn

“normal round” ++-- =

+45+45-45-45=0 degrees,

$x \rightarrow y \rightarrow x$ per turn

Recall: in solenoid

$$Force_x = e v_y \times B_z$$

i.e. coupling x-y

$$\frac{1}{f} = \frac{e^2}{4\gamma^2 m^2 v_z^2} \int B^2 dz$$

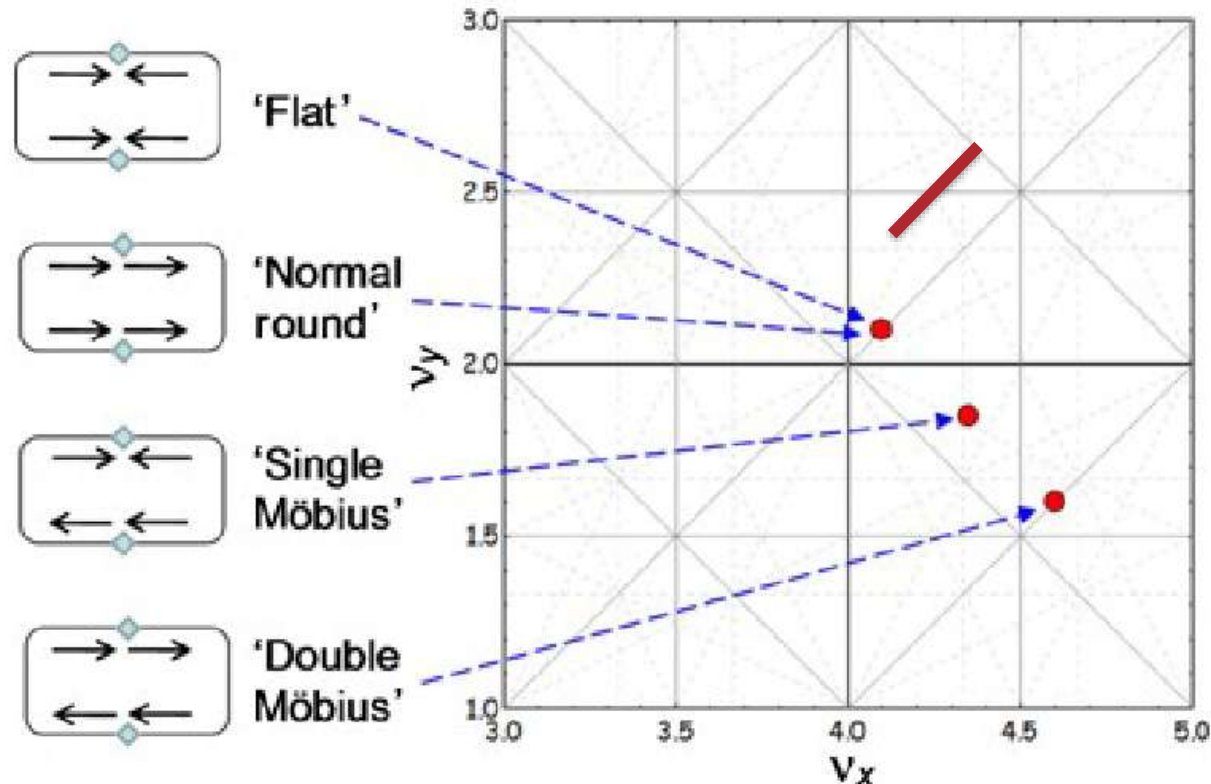
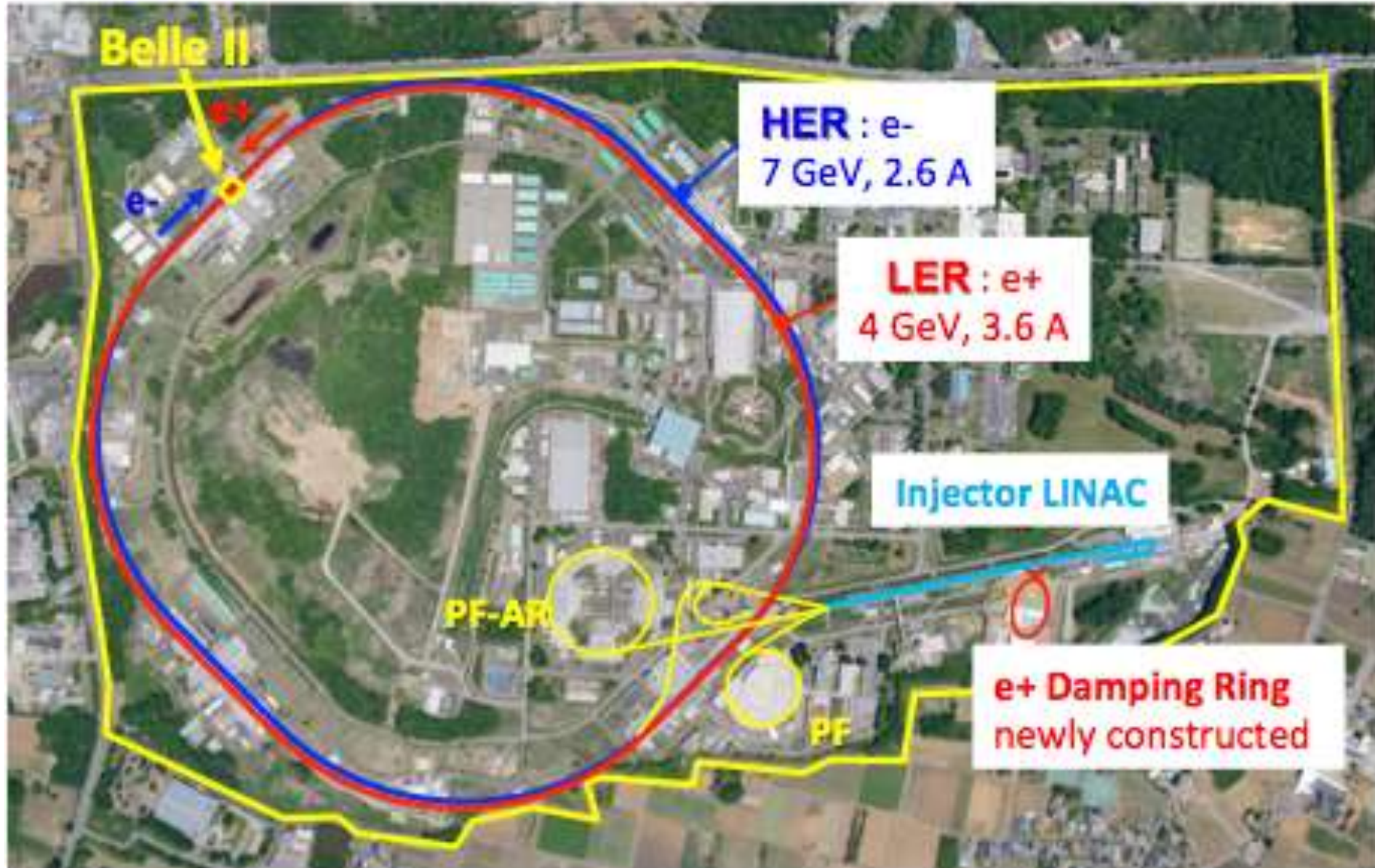
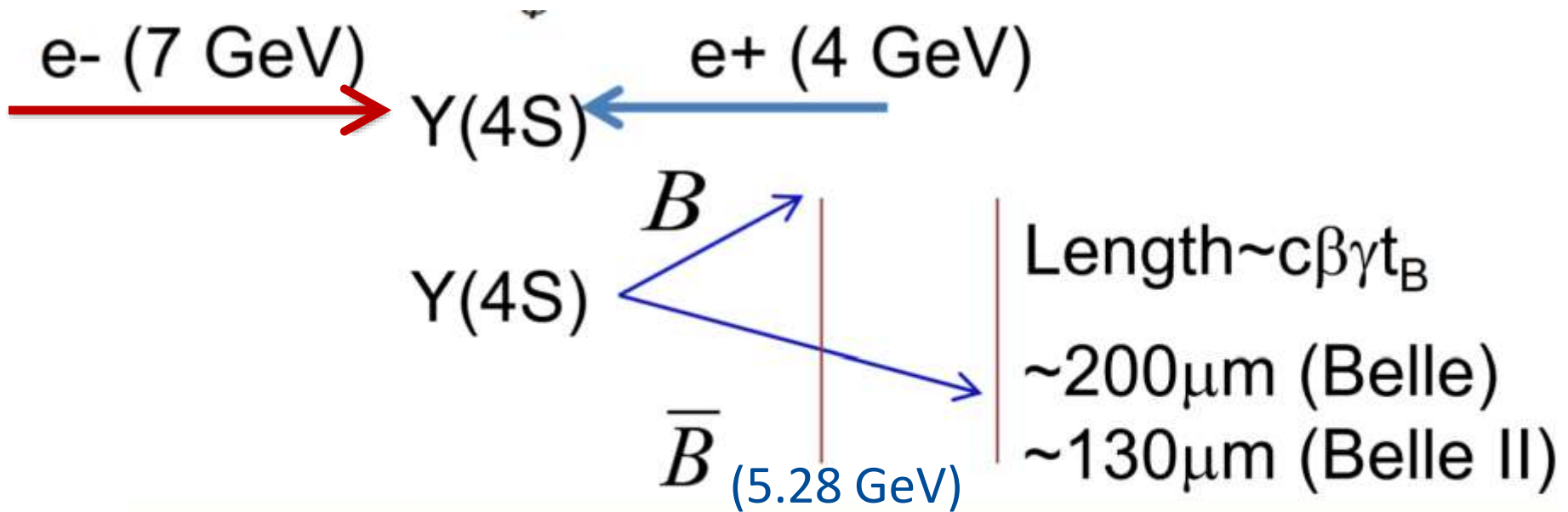


Figure 4: VEPP-2000 round beam options.

Super-KEKB – Next Gen Asymmetric B-factory



Energy Asymmetry Helps to Detect B 's



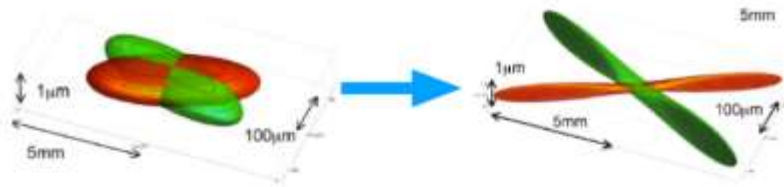
SuperKEKB $\beta\gamma=0.28$: $e^-(7\text{GeV}), e^+(4\text{GeV})$
KEKB $\beta\gamma=0.42$: $e^-(8\text{GeV}), e^+(3.5\text{GeV})$

1. Measuring CP violation with B meson
 2. Fine verification of CKM mechanism which causes CP violation
- \rightarrow Need 50 Billion B particles, therefore : “Asymmetric B -factory”

Super-KEKB Nanobeams

40x=20 from beta* and 2 from currents

To get 40x luminosity of KEKB



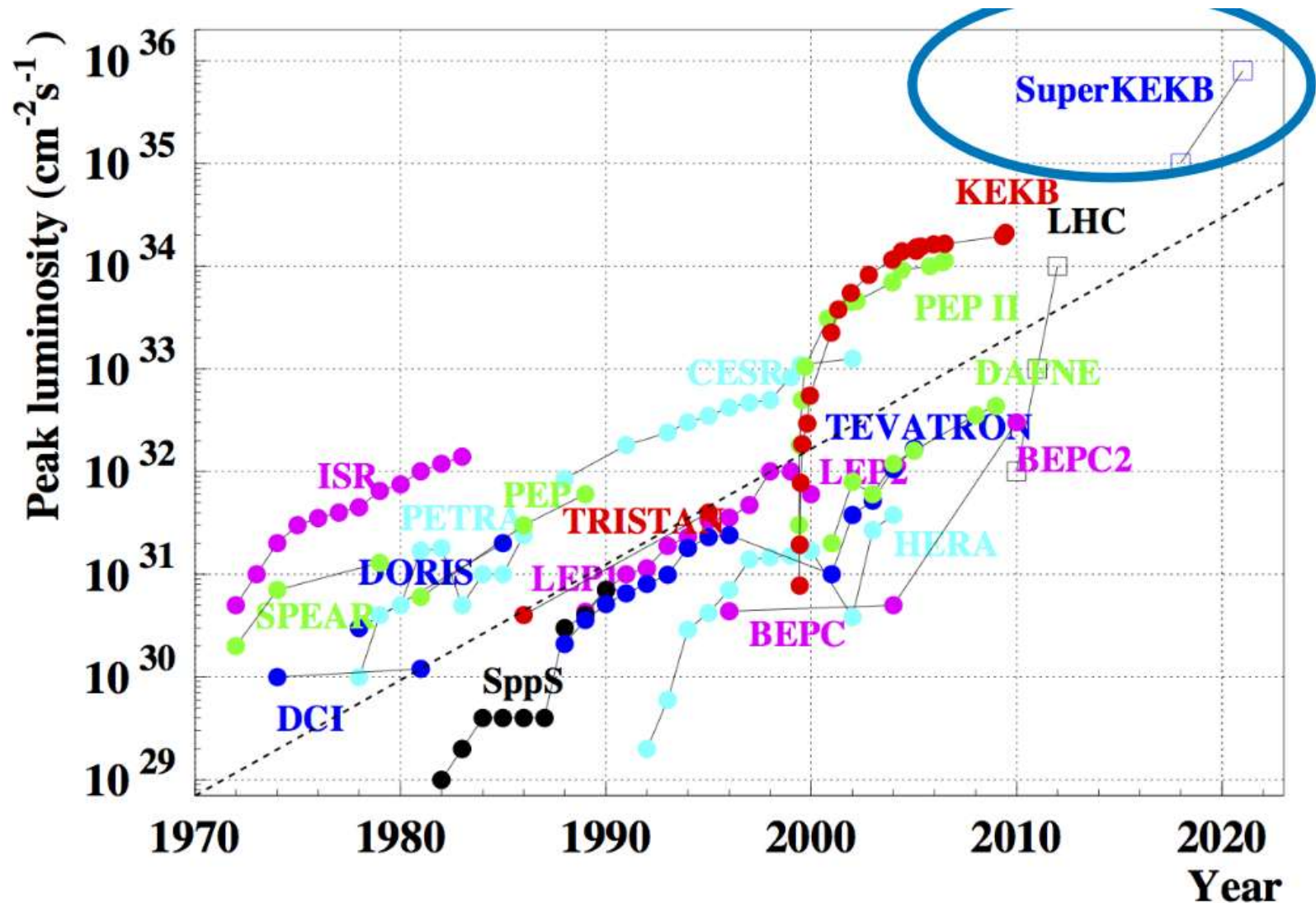
Reduce beam size to a few 100 atomic layers!

$$L = \frac{\gamma_{\pm}}{2er_e} \left(1 + \frac{\sigma_y^*}{\sigma_x^*} \right) \frac{I_{\pm} \xi_{y\pm}}{\beta_{y\pm}^*} \left(\frac{R_L}{R_{\xi_y}} \right)$$

Lorentz factor γ_{\pm}
 Beam current I_{\pm}
 Beam-Beam parameter $\xi_{y\pm}$
 Geometrical reduction factors (crossing angle, hourglass effect) $\left(\frac{R_L}{R_{\xi_y}} \right)$
 Beam aspect ratio at IP $\left(1 + \frac{\sigma_y^*}{\sigma_x^*} \right)$
 Vertical beta function at IP $\beta_{y\pm}^*$

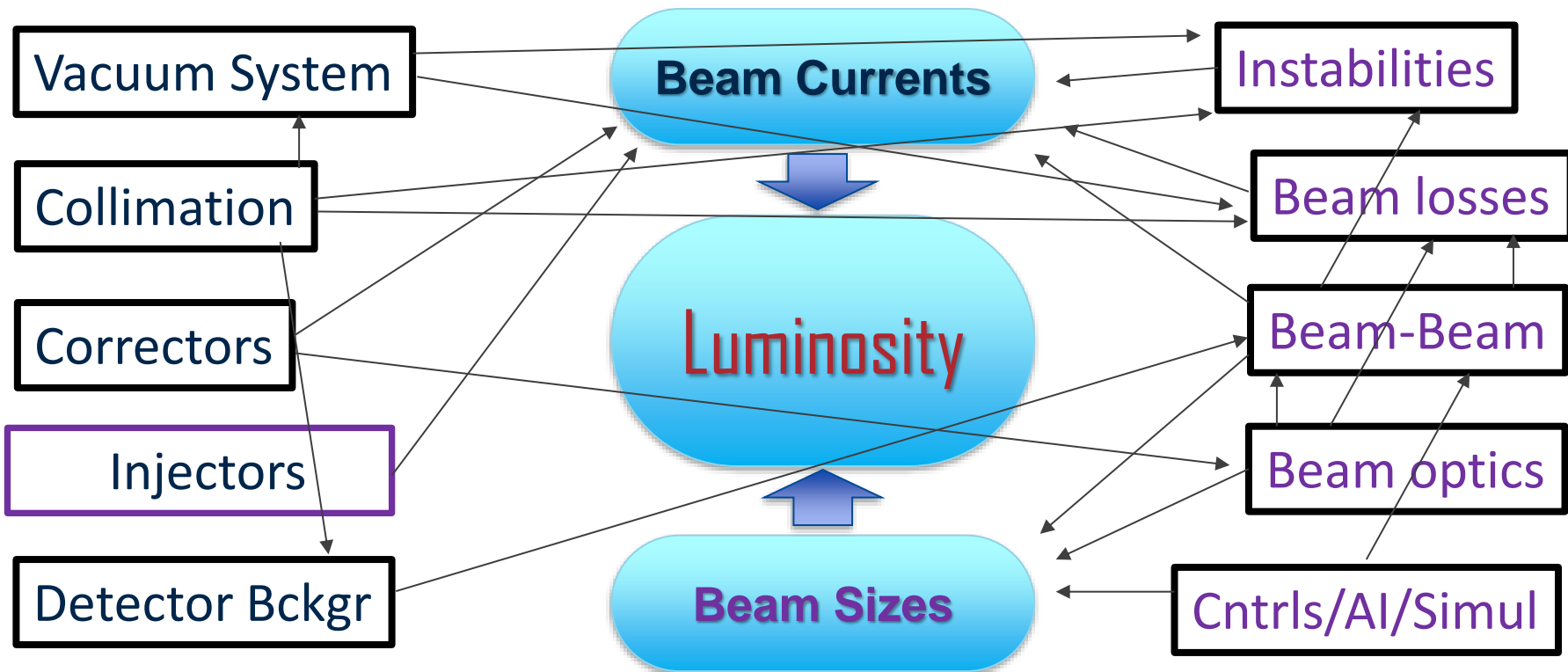
Parameter		KEKB		SuperKEKB		units
		LER	HER	LER	HER	
beam energy	E_b	3.5	8	4	7	GeV
CM boost	β_y	0.425		0.28		
half crossing angle	ϕ	11		41.5		mrad
horizontal emittance	ϵ_x	18	24	3.2	4.6	nm
beta-function at IP	β_x^*/β_y^*	1200/5.9		32/0.27	25/0.30	mm
beam currents	I_b	1.64	1.19	3.6	2.6	A
beam-beam parameter	ξ_y	0.129	0.090	0.0881	0.0807	nm
beam size at IP	σ_x^*/σ_y^*	100/2		10/0.059		μm
Luminosity	L	2.1×10^{34}		8×10^{35}		$\text{cm}^{-2}\text{s}^{-1}$

Super-KEKB – Next Gen B-factory



Super-KEKB :Status and Challenges

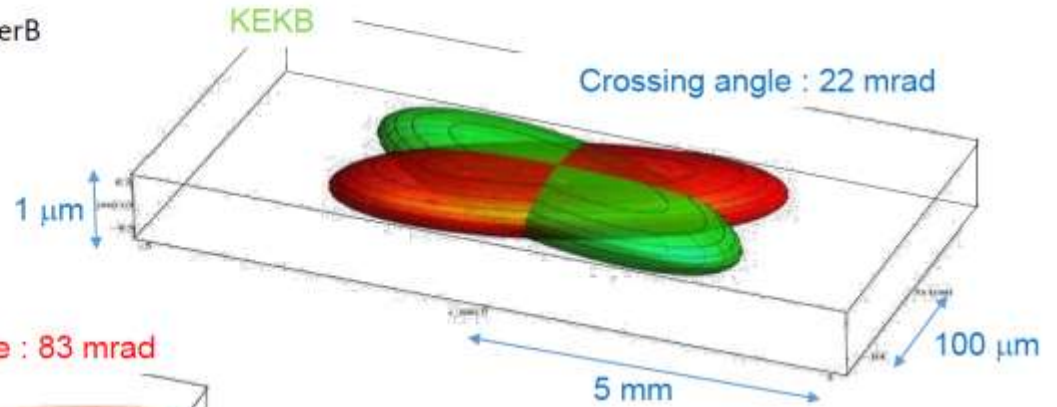
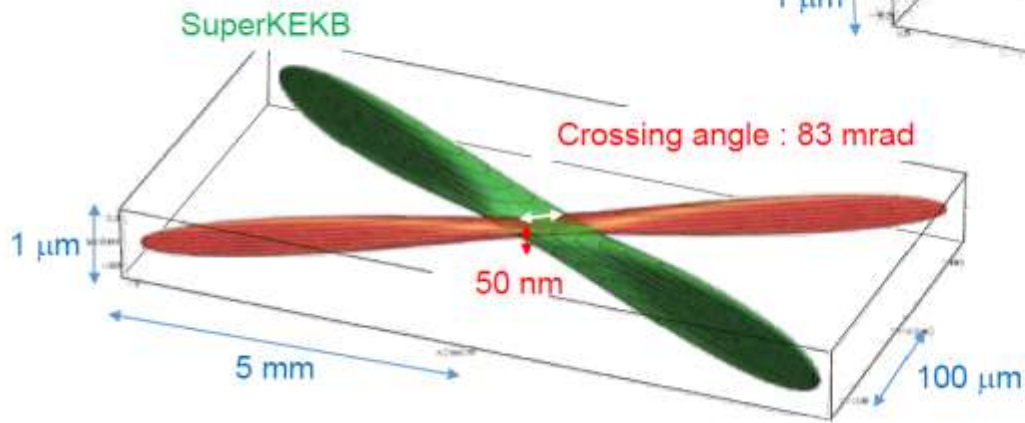
- Peak luminosity $5.1 \times 10^{34} \text{ cm}^{-2}\text{s}^{-1}$ – *collider world record*
- Design goal $80 \rightarrow (60 \dots 40?) \times 10^{34} \text{ cm}^{-2}\text{s}^{-1}$
- **Luminosity Challenge = x16** – where's the problem?
 - Beam current LER(4 GeV e+) is 1.7A vs 3.6A design, HEP(7 GeV e-) 1.3A vs 2.6A (design); beta-function 1.0mm vs 0.3mm design \rightarrow x16



Tricks and Troubles #1 : “Nano-Beams”

Nano-beam collision scheme

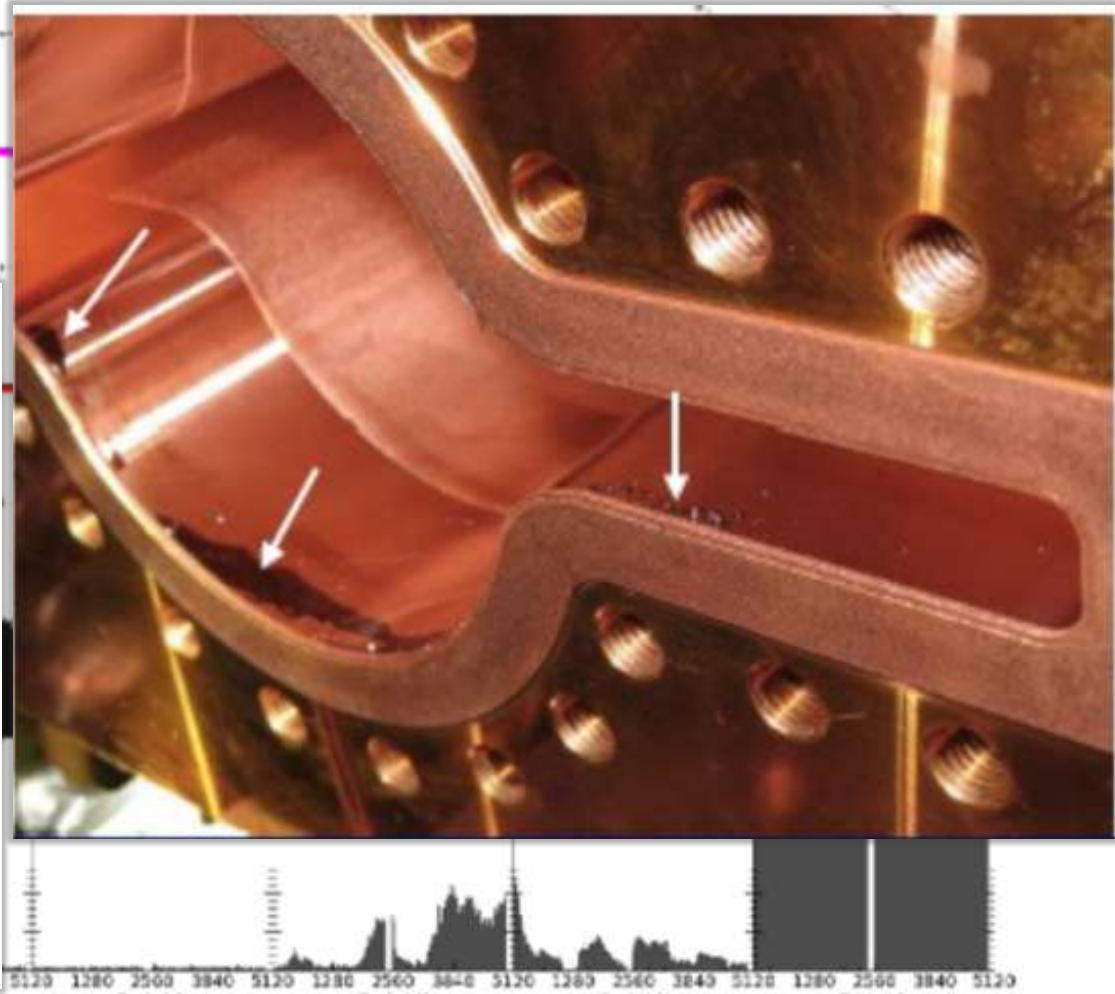
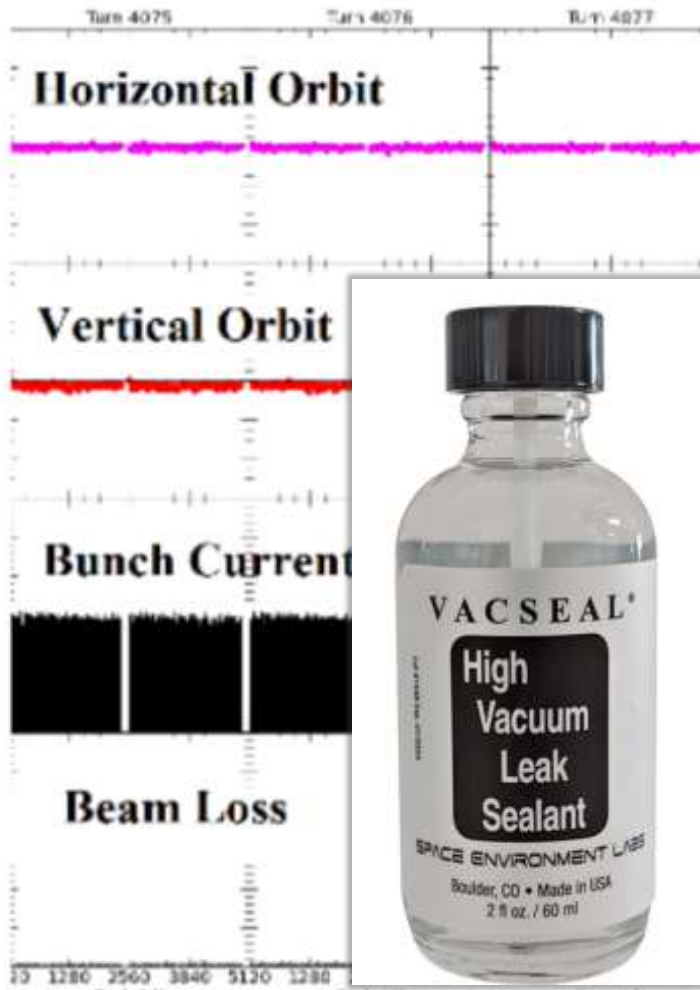
- Proposed by P. Raimondi at INFN-LNF for the Italian SuperB project around 2006 and tested successfully at DAΦNE.
- Implemented at SuperKEKB, for the first time, with low-emittance beams on a high-energy collider.



- To avoid Hourglass effect:
 - Beam bunches collide
 - ✓ With sufficiently small σ_x^* .
 - ✓ At a large horizontal crossing angle.
 - The longitudinal size of the overlap between colliding bunches is much shorter than bunch length.

* **beam-beam effects** are not as well understood in this new regime – emittances (beam sizes) are bigger than expected → as indicated by reduction in **specific luminosity (peak Lumi)/(I₊ I₋)**

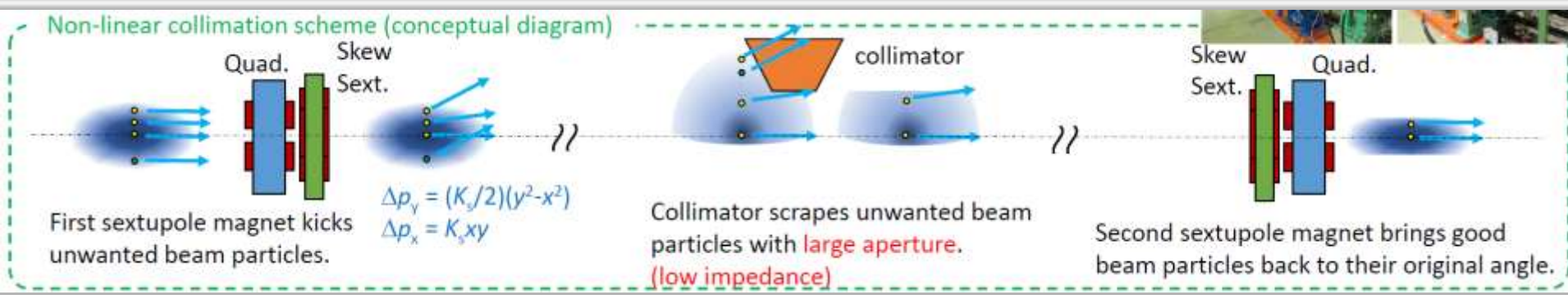
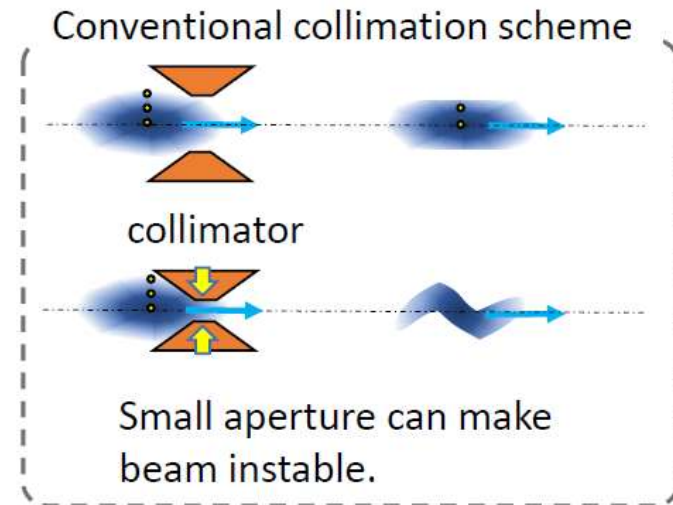
Troubles #2: SBLs - Sudden Beam Loss



SBL events not only obstruct luminosity improvement but also pose a significant risk to accelerator components, the Belle II detectors, and the superconducting focusing system,

Trick #3 : “Non-Linear Collimator”

- Beam halo, beam-beam effects and SBLs demanded better protection of detectors, smaller gaps in collimators → *Impedance* $\sim 1/\text{Gap}^2$
- Also, makes top up injection more difficult (less aperture)
- Non-linear collimation (NLC) system was installed in LER Oho straight section.
 - Impedance of NLC is much lower than that of conventional collimator due to its large aperture.
 - NLC can relax TMCI bunch current limit.
 - Oho straight section is the location where the optics satisfies the requirements for NLC.
 - A part of wiggler magnets was removed to make space for NLC.
 - New skew sextupole magnets and beam pipes in them were fabricated.
 - New power supplies, cabling works and new radiation shields were also required.



Future Circular e+e- Colliders

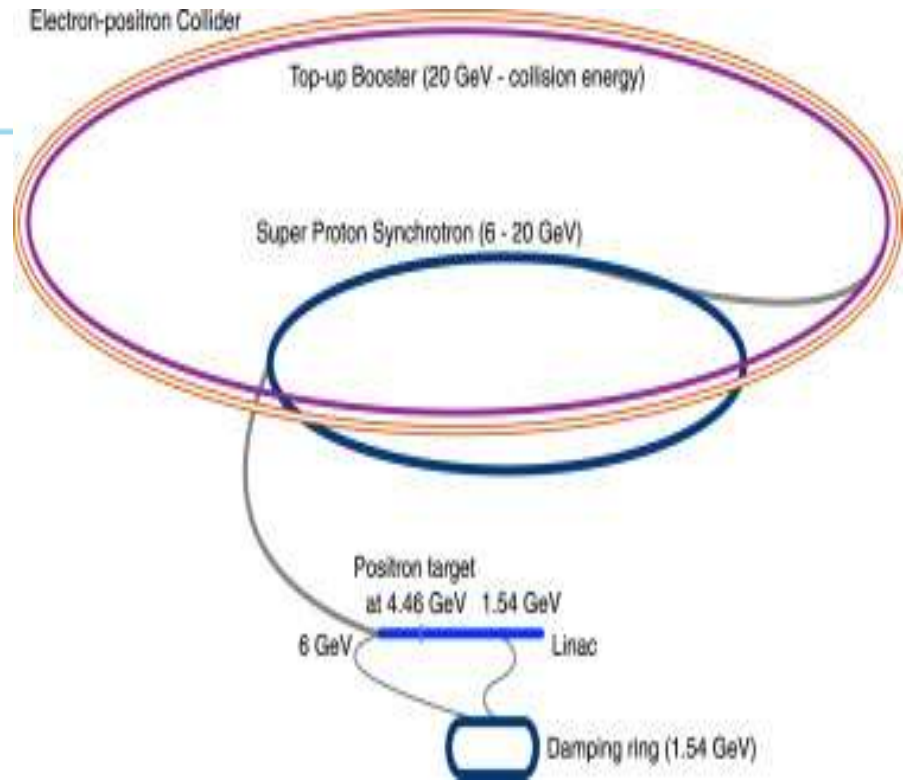
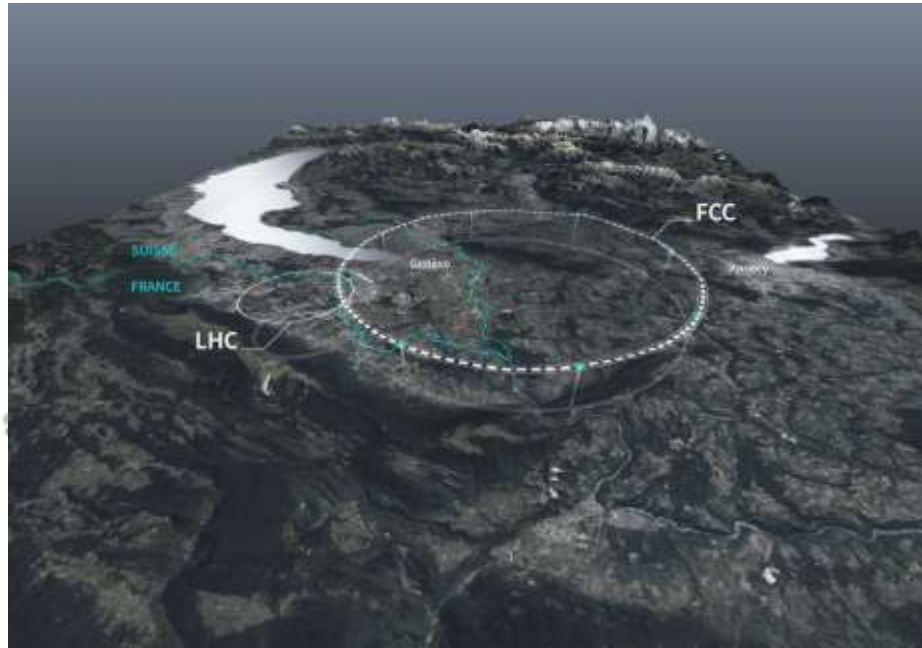
- Energy of interest – at least Higgs production (ZH, ~240 GeV)
- High luminosity $O(1e34-1e35) \dots (10^4-10^5)$ Higgses per year
- High beam energy 120 GeV \rightarrow huge SR loss/turn multi-GeV

$$U_0[\text{keV}] = 88.46 \frac{E[\text{GeV}]^4}{\rho[\text{m}]} \quad 120 \text{ GeV, } 10 \text{ km} \rightarrow 2 \text{ GeV}$$

- High lumi needs high current \rightarrow huge RF power = SR power
- As the result – large rings, 100MW power $P_{SR} = 2I \cdot \Delta E_{SR}$

$$\mathcal{L} = \frac{3}{16\pi r_0^2 (m_e c^2)} \frac{P_{SR} \xi_y \rho}{\beta_y^* \gamma^3}$$

Competing Projects



FCCee at CERN: $e+e-$

91 km, $E_{cm} = 91...365$ GeV

NC magnets and **100MW** SRF

CDR (2018): cost ~ 12 BCHF *

Two rings for $e+$ and $e-$

CEPC (China) $e+e-$

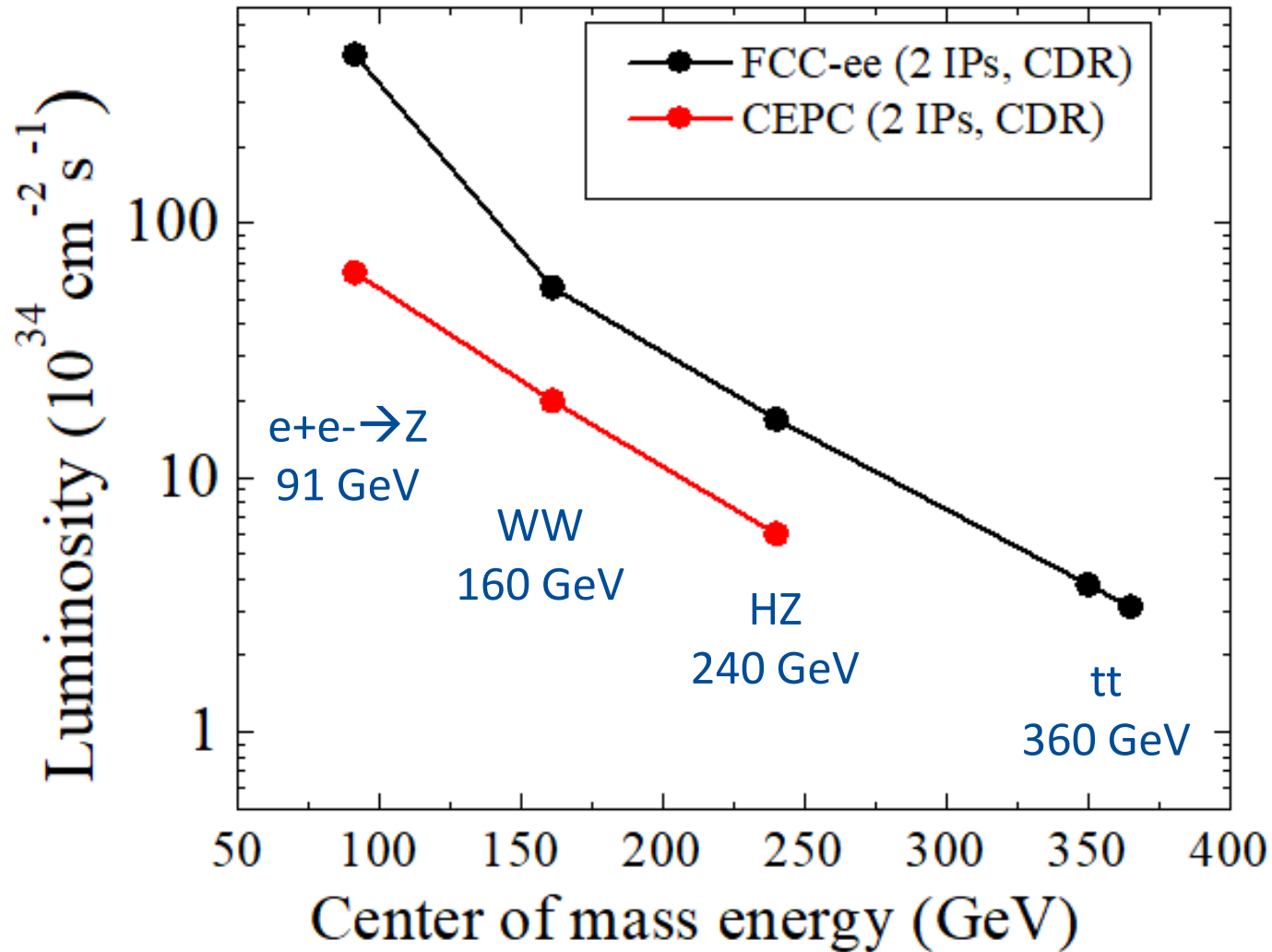
100 km, $E_{cm} = 91...360$ GeV

NC magnets and **60MW** SRF

TDR (Dec'2023): ~ 5.2 B $\$$ *

Two rings for $e+$ and $e-$

FCCee& CEPC @ Several Energies of Interest

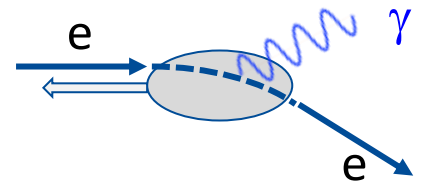


Specific Issues for FCCee and CEPC

- Wall-plug power to RF & beam efficiency (280 MW → 100MW)
- Shielding from 1 MeV SR photons
- Cost
- Beamstrahlung – emission of hard photons → beam losses

$$\tau_{bs} \propto \frac{\rho^{3/2} \sqrt{\eta}}{\sigma_s} \exp(A\eta\rho) \quad \frac{1}{\rho} \approx \frac{Nr_e}{\gamma\sigma_x\sigma_s}$$

η : ring energy acceptance



ρ : mean bending radius at the IP (in the field of the opposing bunch)

□ for acceptable lifetime, $\rho \times \eta$ must be sufficiently large

- *flat beams (large σ_x) !*
- *bunch length !*
- *large momentum acceptance: aiming for $\geq 1.5\%$ at 175 GeV*

- LEP: <1% acceptance, SuperKEKB $\sim 1.5\%$

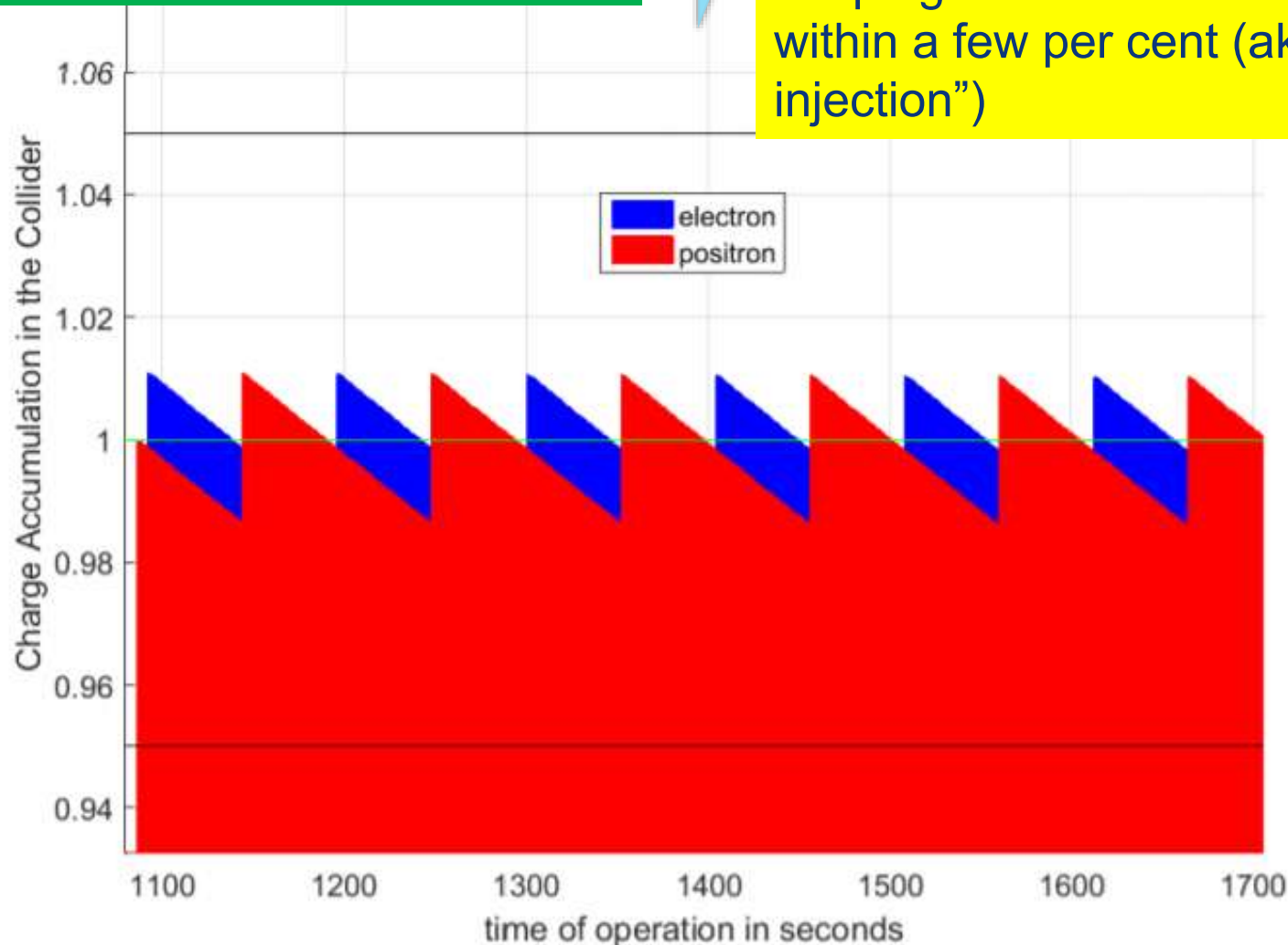
Parameter [4 IPs, 91.2 km, $T_{rev}=0.3$ ms]	Z	WW	H (ZH)	ttbar
beam energy [GeV]	45	80	120	182.5
beam current [mA]	1400	135	26.7	5.0
number bunches/beam	8800	1120	336	42
bunch intensity [10^{11}]	2.76	2.29	1.51	2.26
SR energy loss / turn [GeV]	0.0391	0.37	1.869	10.0
total RF voltage 400/800 MHz [GV]	0.120/0	1.0/0	2.48/0	4.0/7.67
long. damping time [turns]	1170	216	64.5	18.5
horizontal beta* [m]	0.15	0.2	0.3	1
vertical beta* [mm]	0.8	1	1	1.6
horizontal geometric emittance [nm]	0.71	2.17	0.64	1.49
vertical geom. emittance [pm]	1.42	4.34	1.29	2.98
horizontal rms IP spot size [μm]	10	21	14	39
vertical rms IP spot size [nm]	34	66	36	69
beam-beam parameter ξ_x / ξ_y	0.004 / 159	0.011 / 0.111	0.0187 / 0.129	0.096 / 0.138
rms bunch length with SR / BS [mm]	4.32 / 15.2	3.55 / 7.02	2.5 / 4.45	1.67 / 2.54
luminosity per IP [10^{34} cm ⁻² s ⁻¹]	181	17.3	7.2	1.25
total integrated luminosity / year [ab ⁻¹ /yr]	86	8	3.4	0.6
beam lifetime radBhabha / BS [min]	19 / ?	20 / ?	10 / 19	12 / 46

Consequence of Low Lifetime →

To keep average luminosity ~ peak luminosity



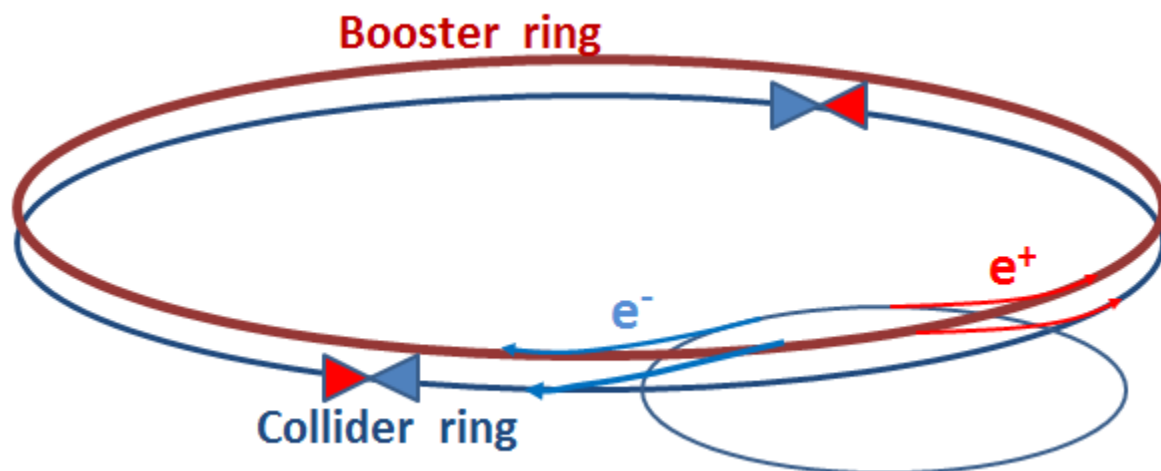
requires alternating replenishment of the two colliding beams, keeping beam currents stable within a few per cent (aka “top-up injection”)



Top-Up Injection in FCCee

beside the collider ring(s), a booster of the same size (same tunnel) must provide beams for top-up injection to sustain the extremely high luminosity

- same size of RF system, but low power (\sim MW)
- top up frequency ≈ 0.1 Hz
- booster injection energy $\approx 5-20$ GeV
- bypass around the experiments



Two separate booster rings for e^+ and e^- in the CEPC

Cost !!!

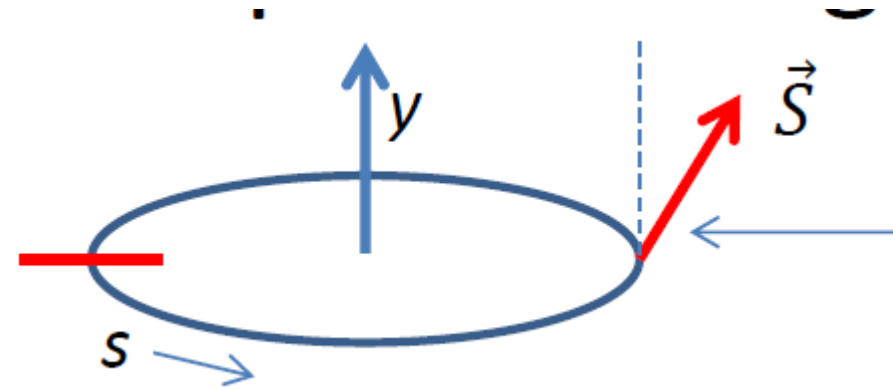
Beam Polarization and Spin Dynamics

Sokolov-Ternov effect: SR
jumps prefer spin-down

$$\xi(t) = A \left(1 - e^{-t/\tau}\right)$$

$$A = 8\sqrt{3}/15 \approx 0.924$$

$$\tau = \frac{8\hbar^2}{5\sqrt{3}mce^2} \left(\frac{mc^2}{E}\right)^2 \left(\frac{H_0}{H}\right)^3$$



$H_0 \approx 4.414 \times 10^{13}$ gauss is the Schwinger field

260 hrs at 45 GeV... at 80 GeV, this time falls as $(45/80)^5$ to 15 hrs.

45 GeV LEP: 5 hours $\rightarrow P \sim 6\%$

$$P = 92.4 (\%) / (1 + \tau_{ST} / \tau_{dep})$$

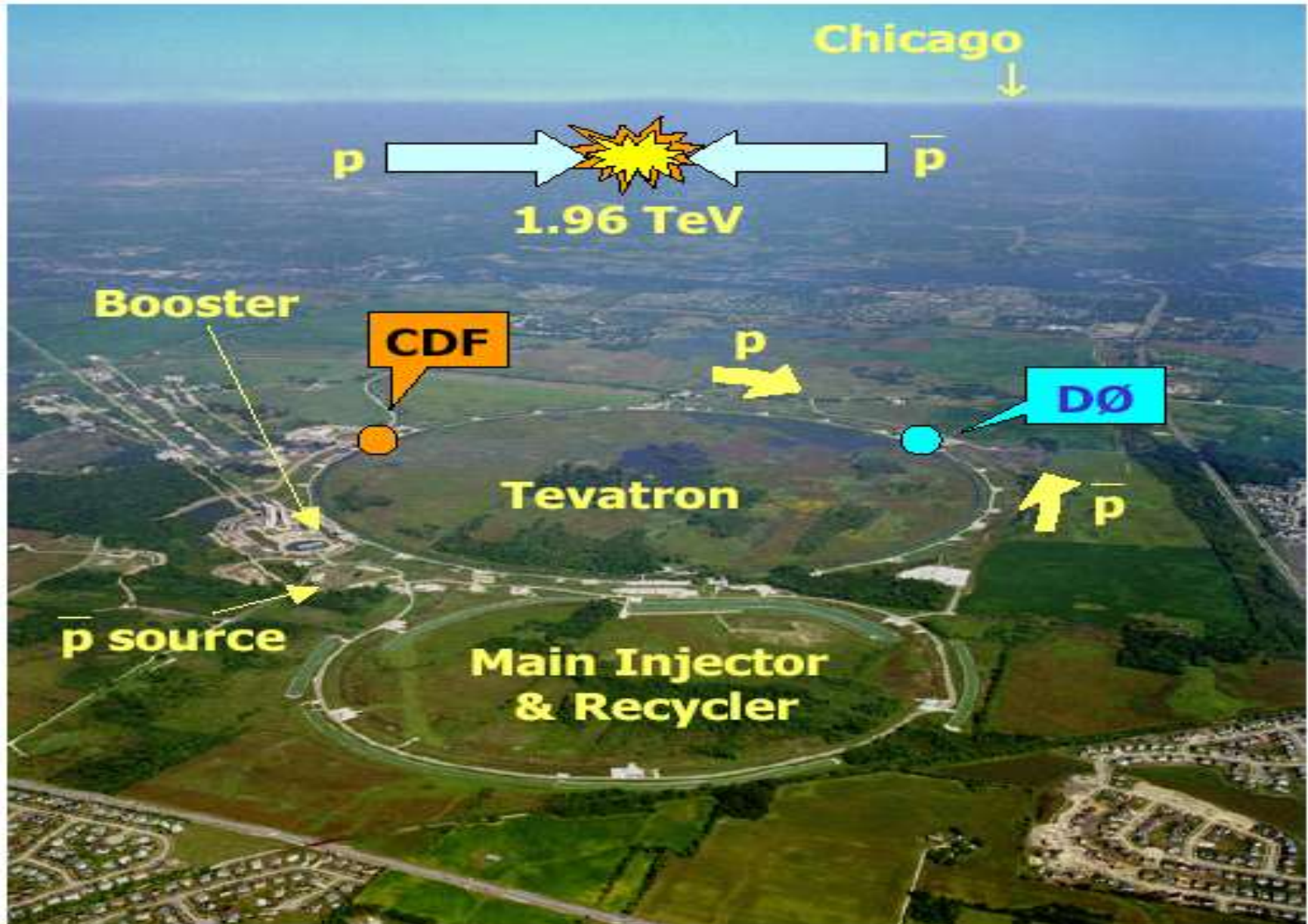
Depolarization due to vertical orbit (= B_x field in quads) and B_z in detector solenoids

Resonant spin harmonic amplitudes in orbit distortions can be compensated using special orbit bumps or global correction (in LEP $\rightarrow P \sim 40\%$)...no use in collisions but can be used for non-colliding bunches to do energy calibration to $dE/E \sim 1e-6$

BREAK (!...?)

**Circular
pp Colliders (1)**

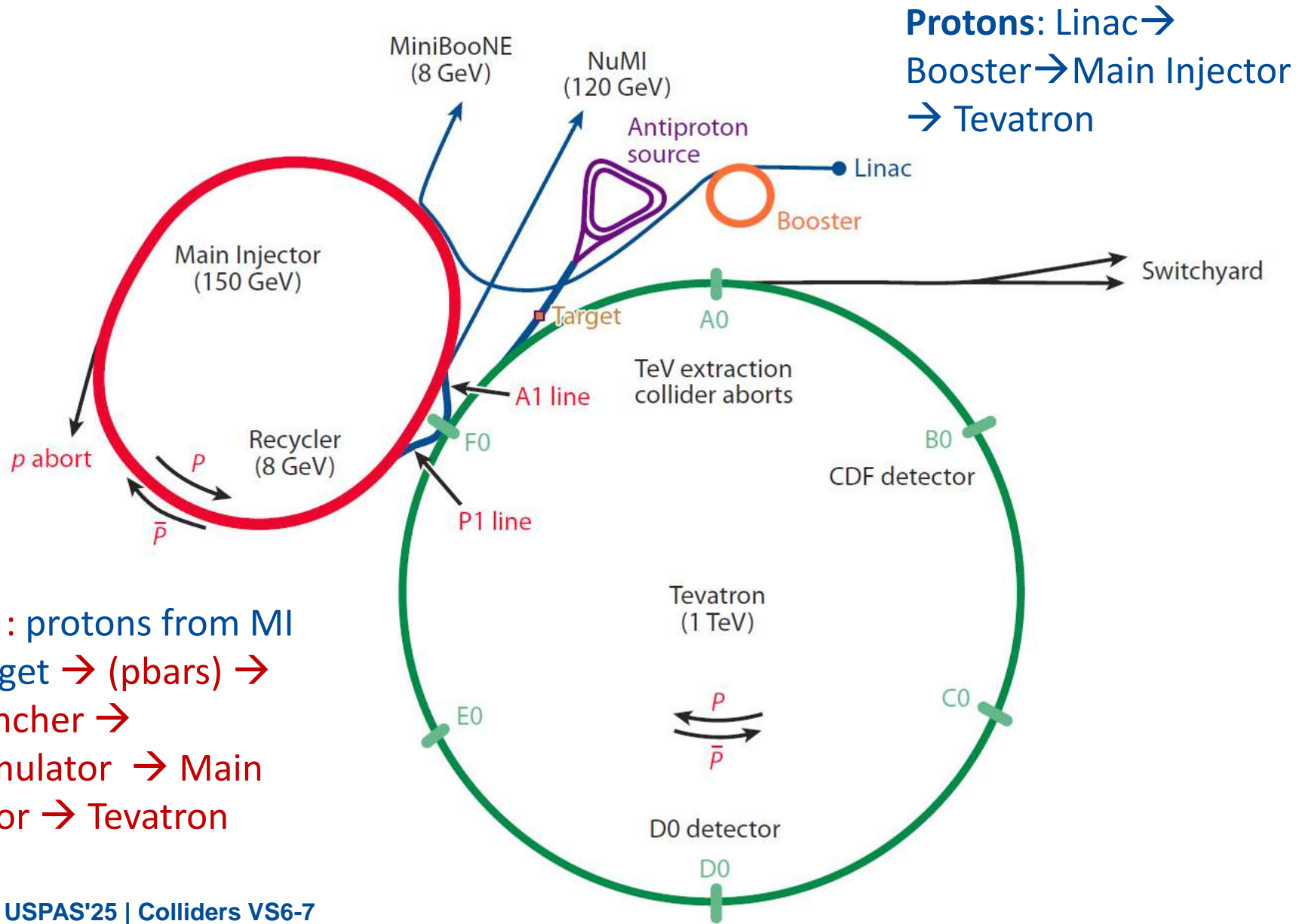
Tevatron Collider: 1.96 TeV cme, 6.3km



Tevatron: 26 yrs of colliding beams

- Jul 1983** Tevatron SC synchrotron commissioned, reached world record 512 GeV (protons)
- 1982-1985** Antiproton source construction & commissioning, installation of the B0 low beta insertion magnets
- Oct 1985** First 1.6 TeV c.o.m. p-pbar collisions in CDF
- 1987-1989** Collider Run at 1.8 TeV c.o.m., magnet leads fix
- 1990 -1992** HV separators installed, new low beta insertions at D0 and B0 interaction regions
- 1992 -1993** Collider Run Ia at 1.8 TeV c.o.m., both CDF & D0
- 1992 -1993** 400 MeV Linac construction and commissioning
- 1994 -1996** Collider Run Ib, top quark discovery
- 1993 -1999** Main Injector construction and commissioning
- 2001 - 2011** Collider Run II, 1.96 TeV c.o.m.

Tevatron Accelerator Complex



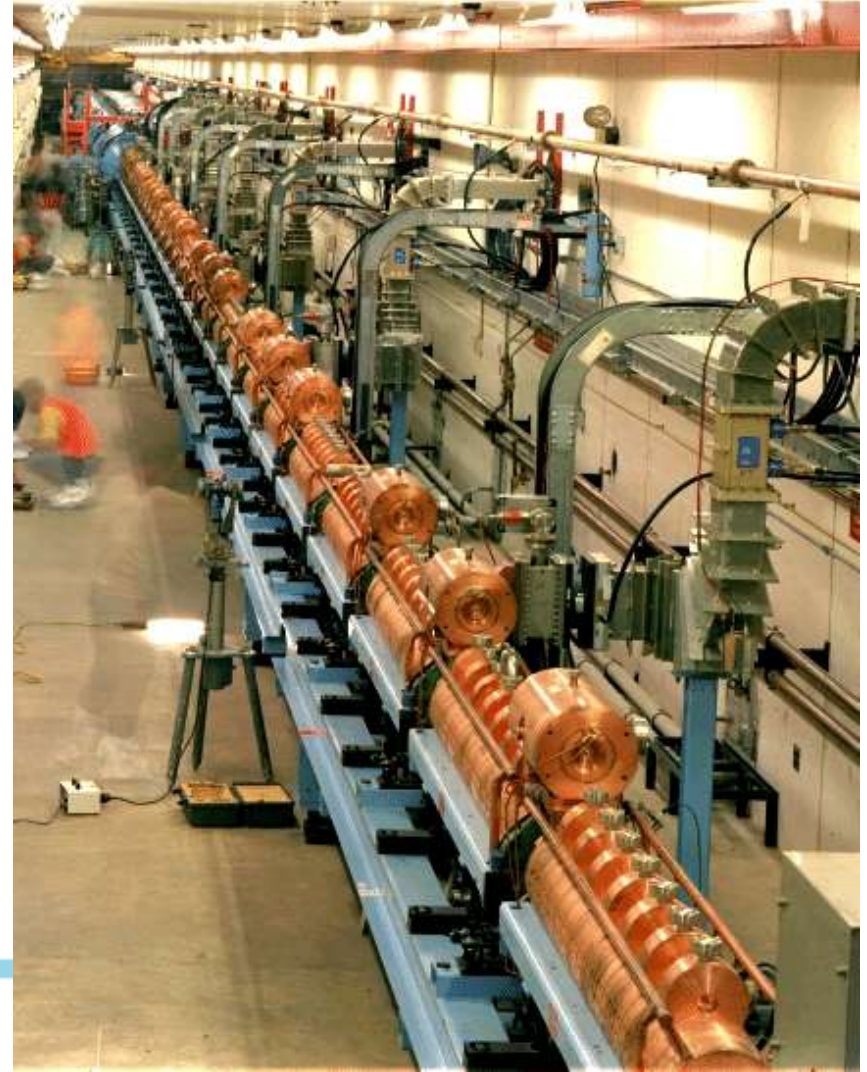
Pbars : protons from MI
 → target → (pbars) →
 Debuncher →
 Accumulator → Main
 Injector → Tevatron

Proton Source



H- ion source and 750keV
Cockcroft-Walton accelerator,
sends beam to Linac

$E_{kin}=400\text{MeV}$ H- to Booster
room temperature RF linac
400MHz



Booster, Debuncher and Antiproton Accumulator



Two 8 GeV pbar rings for stochastic cooling in one Δ -shape tunnel
Debuncher (fast cool)
Accumulator (deep cooling with stacking).. aperture



Booster: $C=480\text{m}$
15 Hz synchrotron
 $E_{inj}=400\text{ MeV}$ H-
 $E_{max}=8\text{ GeV}$ protons
 $\sim 5e12$ p/pulse max
Space charge dominated

Main Injector



$C=3.32\text{km}$

Room temperature
magnets ($<2\text{T}$)

$E_{\text{max}}=150\text{GeV}$
 $E_{\text{inj}}=8\text{ GeV}$

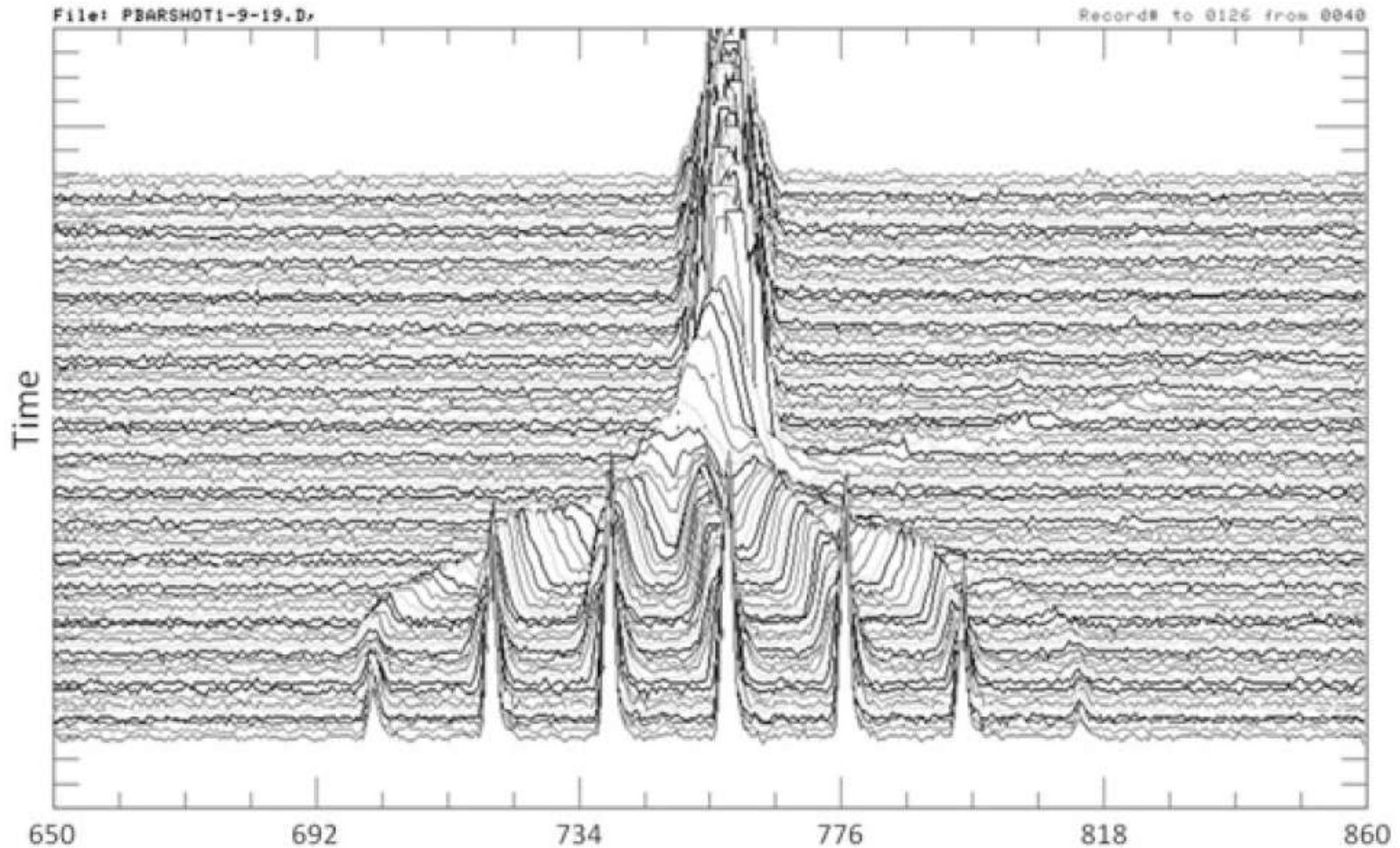
Min cycle time 1.4s

Accelerates protons
and Pbars to 150GeV
for Tevatron

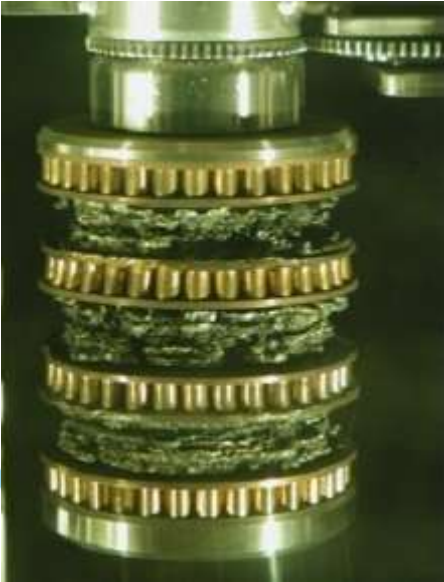
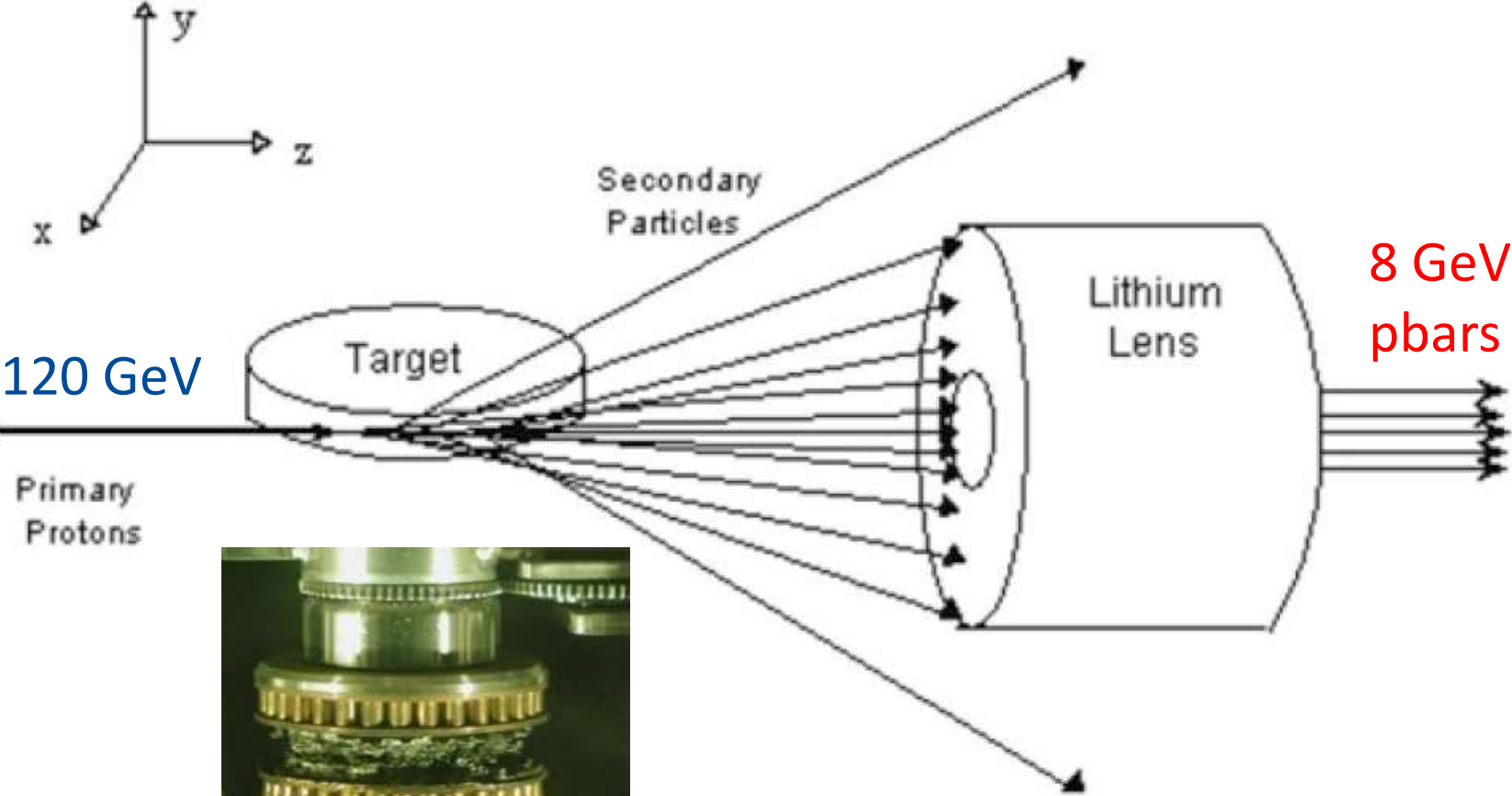
Accelerates protons
to 120 GeV for pbar
production and NuMI

Coalescing in Main Injector

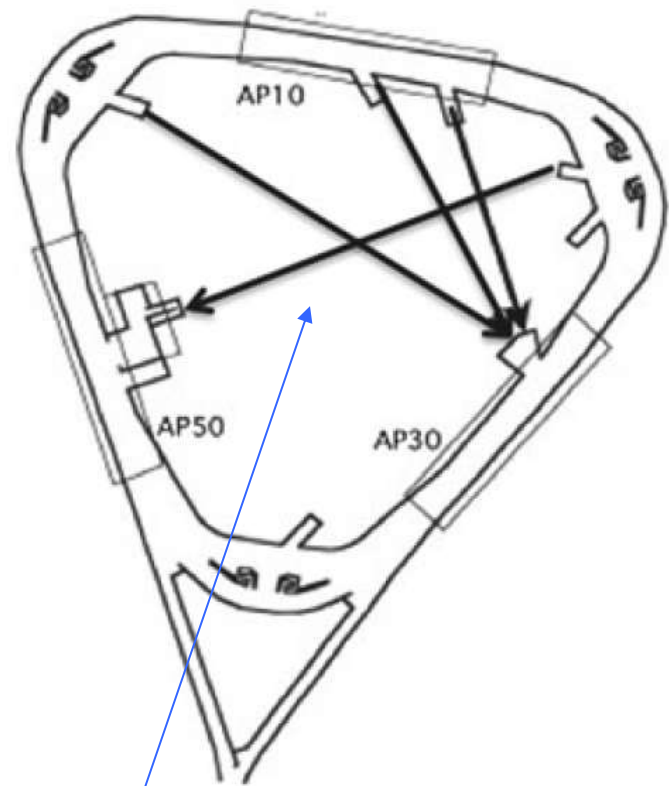
Combine 7 proton bunches in one big one to inject to the Tevatron
Requires two RF systems : 53 MHz and 2.5MHz (1/25 of 53 MHz)



Antiproton Production Target



Stochastic Cooling in Accumulator C=474 m, E=8 GeV



Stochastic Cooling
signal paths

see lectures VL13-14

How to Overcome That Transverse Emittance ?

$$\frac{d\varepsilon}{dt} = - \frac{\varepsilon}{\tau_{\text{Stoch.Cooling}}} + (\text{IBS Heating})$$

$$\varepsilon_{\text{equilibrium}} = \tau_{\text{Stoch.Cooling}} \times (\text{IBS Heating}) =$$

$$\propto \tau_{\text{Stoch.Cooling}} \times \frac{N_a}{\varepsilon_{\text{Long}}^{1/2} \varepsilon_{\text{Transv}}^{3/2}} \times \frac{D^2 + (D' \beta - D \beta' / 2 \beta)^2}{\beta}$$

Recycler Ring



Shares tunnel
with Main Injector

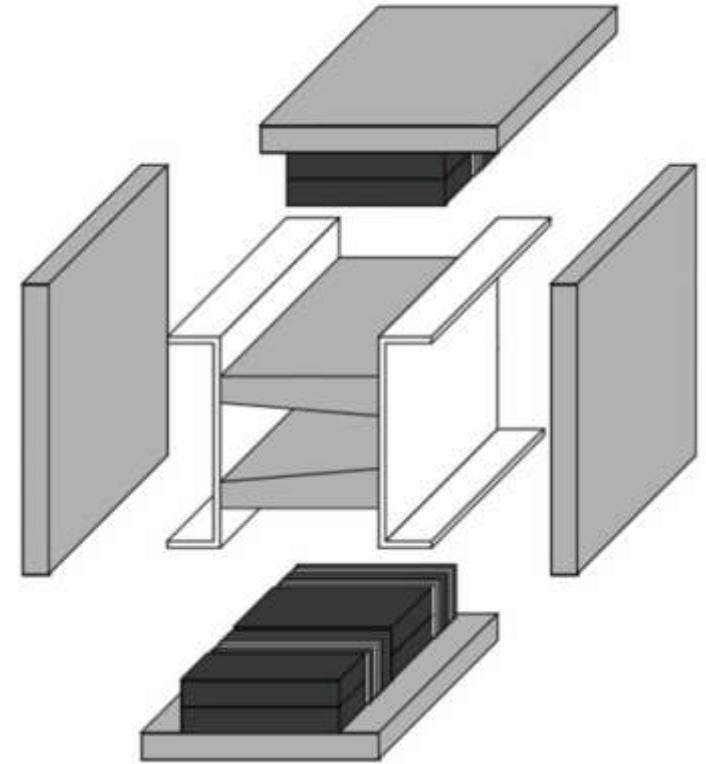
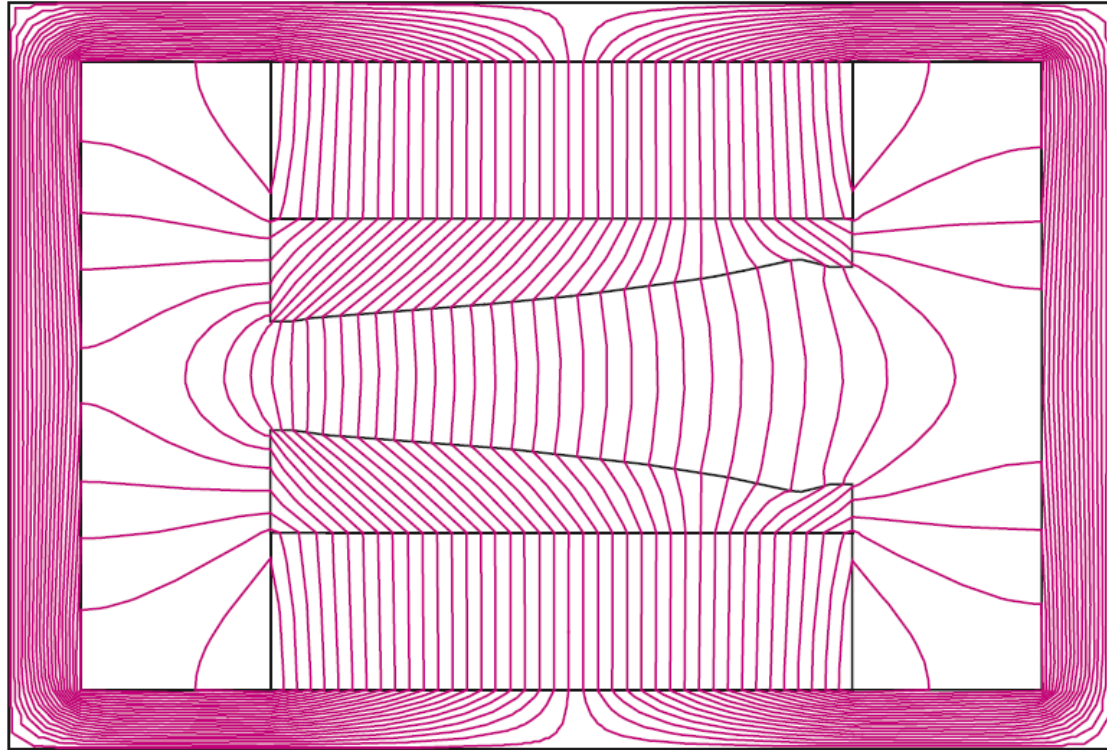
$C=3.32\text{km}$

Permanent magnets
(344, 1.45T, Sr-Fe
combined function)

$E_{\text{kin}}=8\text{ GeV}$ fixed

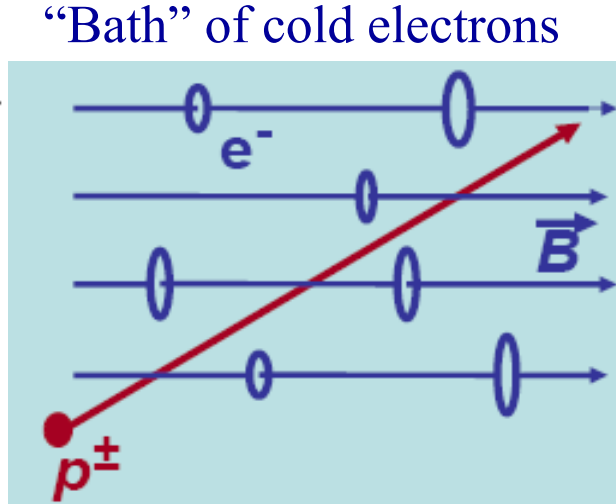
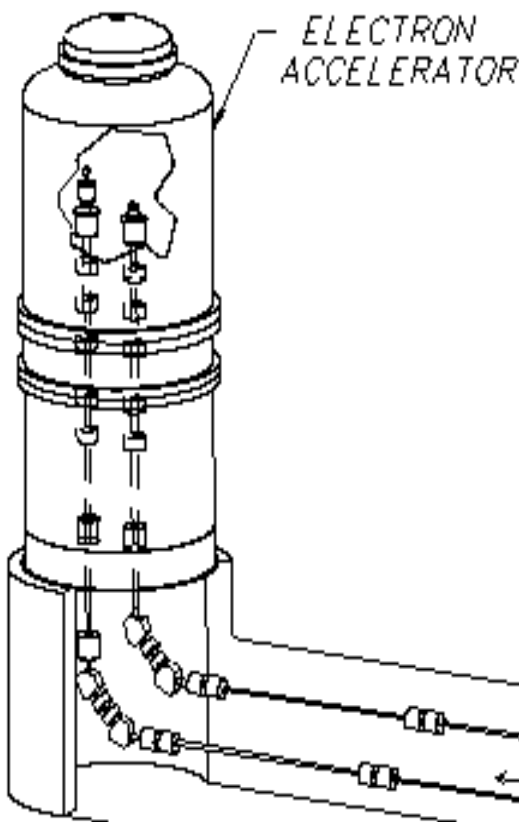
Stores and cools
antiprotons
From Antiproton
Accumulator
ring

8 GeV Recycler Ring Magnets (1.4kG)



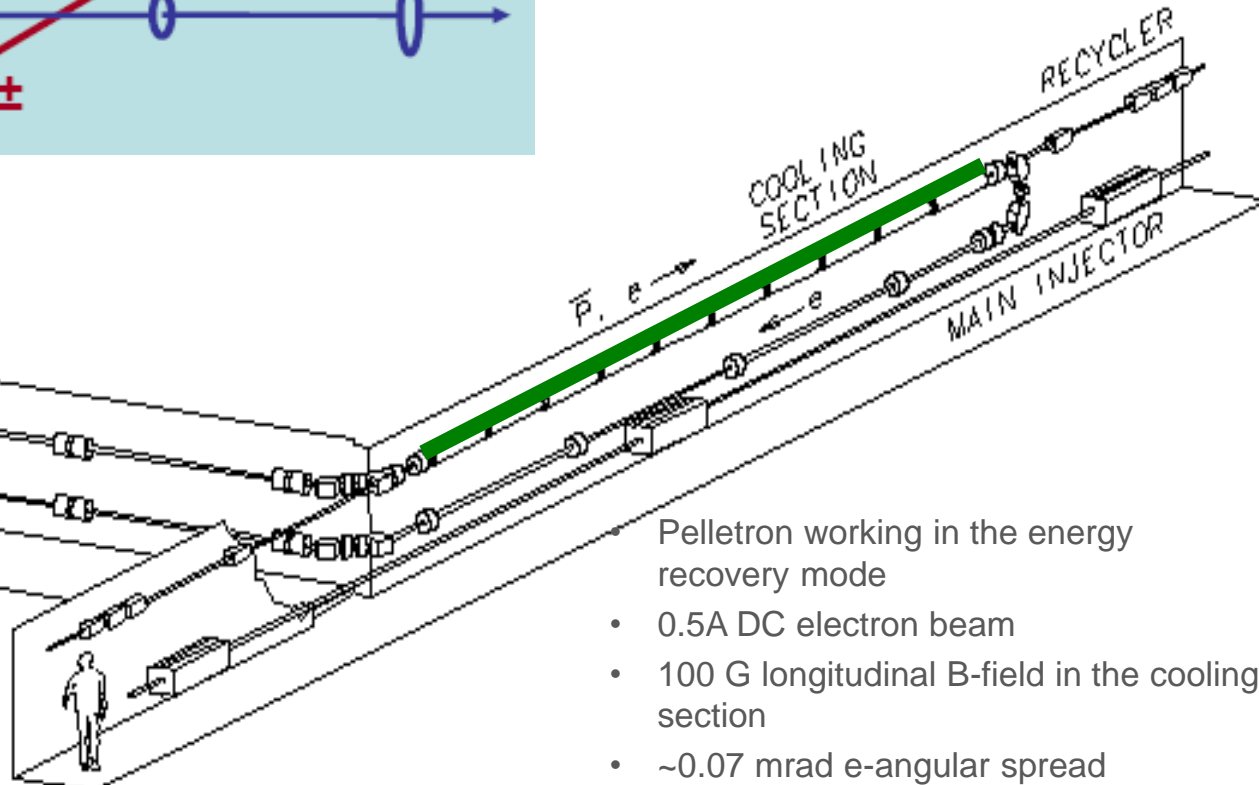
Recycler permanent magnet gradient dipole components shown in an exploded view. For every 4" wide brick there is an 0.5" interval of temperature compensator material composed of 10 strips

Electron Cooling of 8GeV Pbars in Recycler



Condition#1 for effective heat transfer: $V_e = V_{antiproton}$
4.338 MeV e- for 8.89MeV pbar

Other conditions (below)



- Pelletron working in the energy recovery mode
- 0.5A DC electron beam
- 100 G longitudinal B-field in the cooling section
- ~0.07 mrad e-angular spread

see lectures VL13-14

Electron Cooling Device



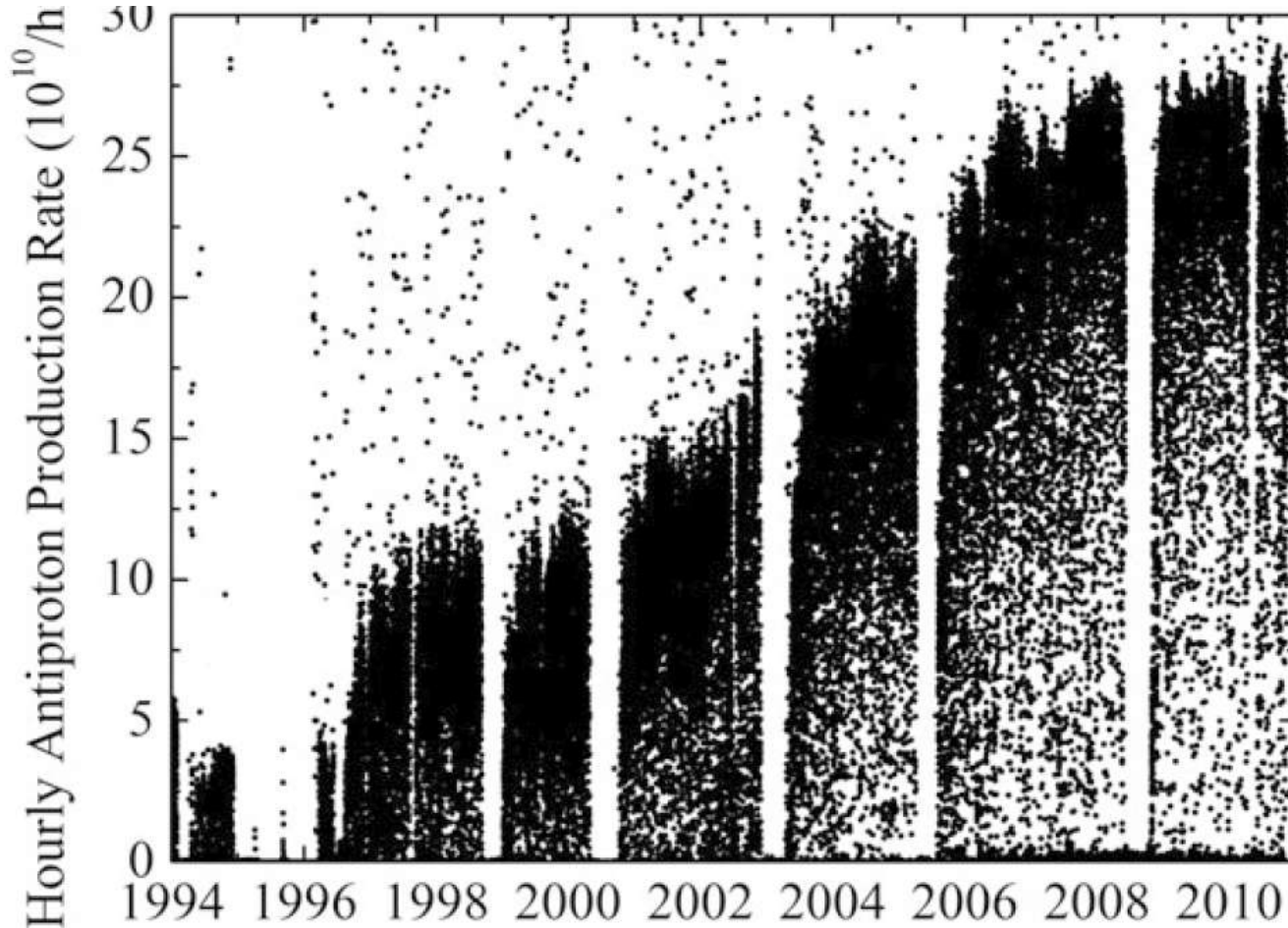
4.5MeV Pelletron=Van der Graaf

Interaction section in RR/MI tunnel



Antiproton production rate

90% of the world's total man-made nuclear antimatter (17 ng)



Average antiproton accumulation rate since 1994 and during all of Collider Run II (including production in the Antiproton Source and storage in the Recycler)

Tevatron



$C=6.28\text{km}$
 $\sim 800\text{ SC}$
Magnets ($4d+q$)
 $B_{\text{max}}=4.5\text{T}$
 $E=980\text{GeV}$
 $E_{\text{inj}}=150\text{ GeV}$
Proton clockws
Pbars counter
36+36 bunches
Same aperture
26 HV separators
2 Low-beta
insertions

Same magnets = to turn into a COLLIDER = need same direction currents as $F=J \times B$ = particles and antiparticles (p and $p\text{bars}$)

Tevatron Contributions to Science and Technology

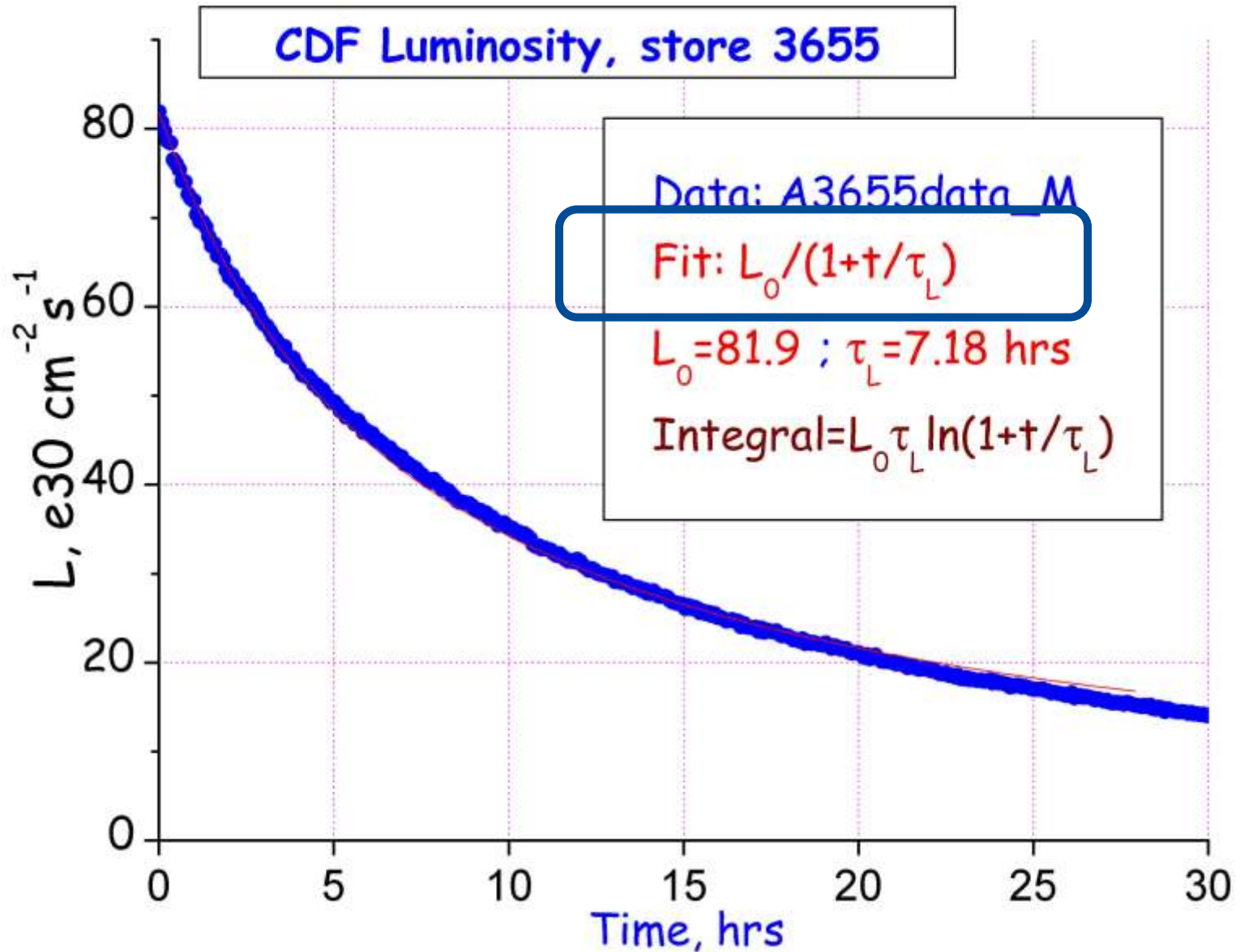
- Technology:

- 1st SC accelerator ring - NbTi magnets 4.5 T
- 1st ever permanent magnets 3.3 km 8 GeV Recycler Ring
- Record antiproton production & accumulation with stochastic and electron cooling systems in Debuncher, AA, and Recycler → 90% of the world's total man-made nuclear antimatter ever produced (17 ng)
- Two-stage collimation systems

- Beam physics advances:

- Longitudinal manipulations slip-stacking in Main Injector and momentum mining in Recycler
- Beam-beam record at $\xi_{x;y} \sim 0.025$, first successful demo b-b compensation by electron lenses,
- New collimation techniques : crystal collimation, hollow e-lens collimation and longitudinal abort gap collimation

Luminosity, Lifetime and Integral



Luminosity and Luminosity Integral

$$L = \gamma f_0 \frac{(B N_{\bar{p}}) N_p}{2\pi\beta^* (\varepsilon_p + \varepsilon_{\bar{p}})} H(\sigma_l / \beta^*)$$

$$I = \int L dt \approx N_{stores} \tau_L L_0 \ln(1 + T / \tau_L)$$

Luminosity Integral: primary factors

- Number of antiprotons: $B N_{pbar}$
- Number of protons: N_p
- Emittances $\varepsilon_p \varepsilon_{pbar}$
- Beta* at IP and bunchlength: $H(x) / \beta^{*^2}$
- Lumi-lifetime: τ_L
- Number Stores: N_{stores}

Lifetime Constituents (end of Run II)

$$\tau_L^{-1} = \tau_\varepsilon^{-1} + \tau_a^{-1} + \tau_p^{-1} + \tau_H^{-1}$$

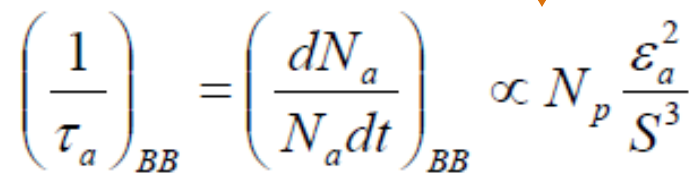
$$(9-11) + (16-18) + (25-45) + (70-80) = (5-5.5) \text{ hrs}$$

- Emittance growth = >90% IBS + <10% Beam-Beam
- Pbar lifetime = (80-85)% burnup + ~15% LR Beam-Beam
- Proton lifetime = >50% Beam-Beam + <50 % burnup
- Houghlass lifetime = >90% IBS + <10% Beam-Beam

IBS determined ~50-55% of lifetime

Burnup due to luminosity – another 30-35%

Beam-Beam Interaction reduces lumi- lifetime by 12-17 %



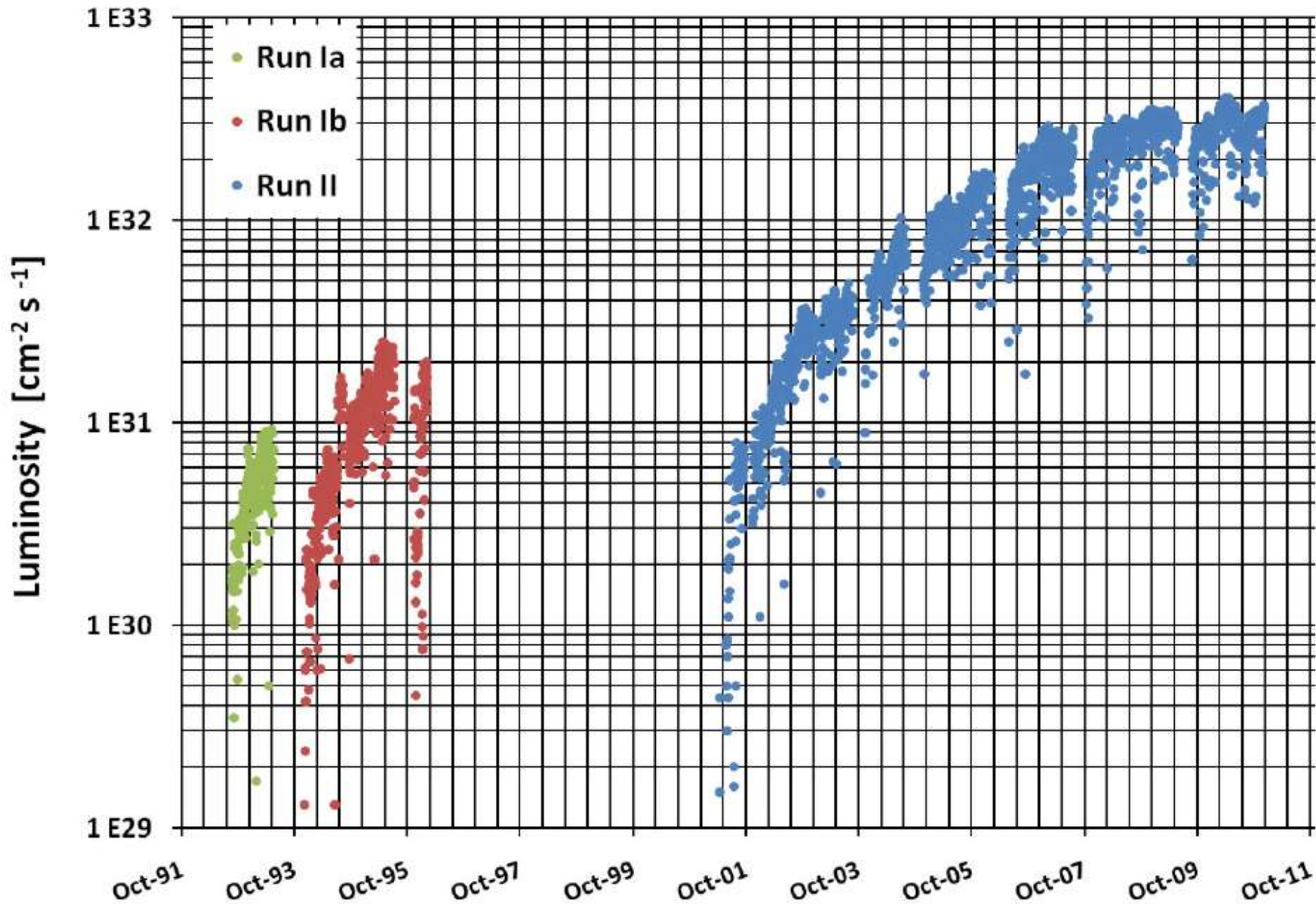
$$\left(\frac{1}{\tau_a} \right)_{BB} = \left(\frac{dN_a}{N_a dt} \right)_{BB} \propto N_p \frac{\varepsilon_a^2}{S^3}$$

Tevatron Parameters

Table 2. Design and achieved performance parameters for Collider Runs I and II (typical values at the beginning of a store).

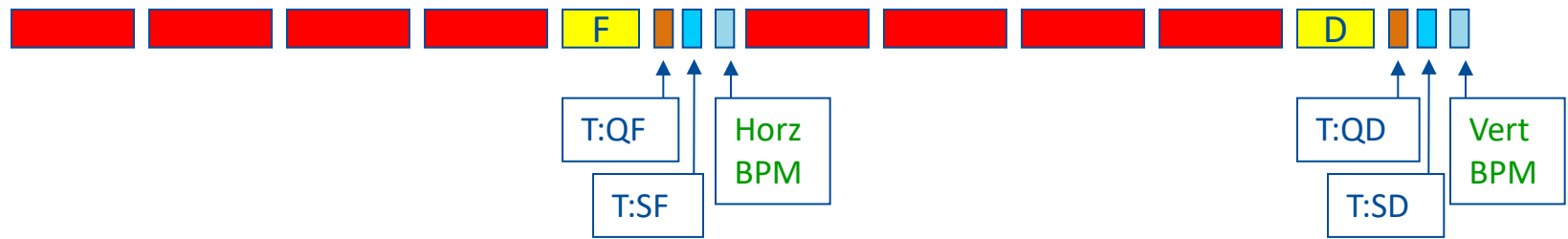
	Run Ia	Run Ib	Run II	
Energy (center-of-mass)	1800	1800	1960	GeV
Protons/bunch	1.2	2.3	2.9	$\times 10^{11}$
Antiprotons/bunch	3.1	5.5	8.1	$\times 10^{10}$
Bunches/beam	6	6	36	
Total Antiprotons	19	33	290	$\times 10^{10}$
Proton emittance (rms, normalized)	3.3	3.8	3.0	π mm-mrad
Antiproton emittance (rms, normalized)	2	2.1	1.5	π mm-mrad
β^*	35	35	28	cm
Luminosity (Typical Peak)	5.4	16	340	$\times 10^{30}$ cm ⁻² sec ⁻¹
Luminosity (Design Goal)	5	10	200	$\times 10^{30}$ cm ⁻² sec ⁻¹

Tevatron Collider Run I & II Luminosity



Tevatron Optics: FODO cells +IPs

	Dipoles	Quads	Spools
Number	772+2	90+90	88+88



Tevatron Dipole
 (There are 772 Tevatron dipoles)

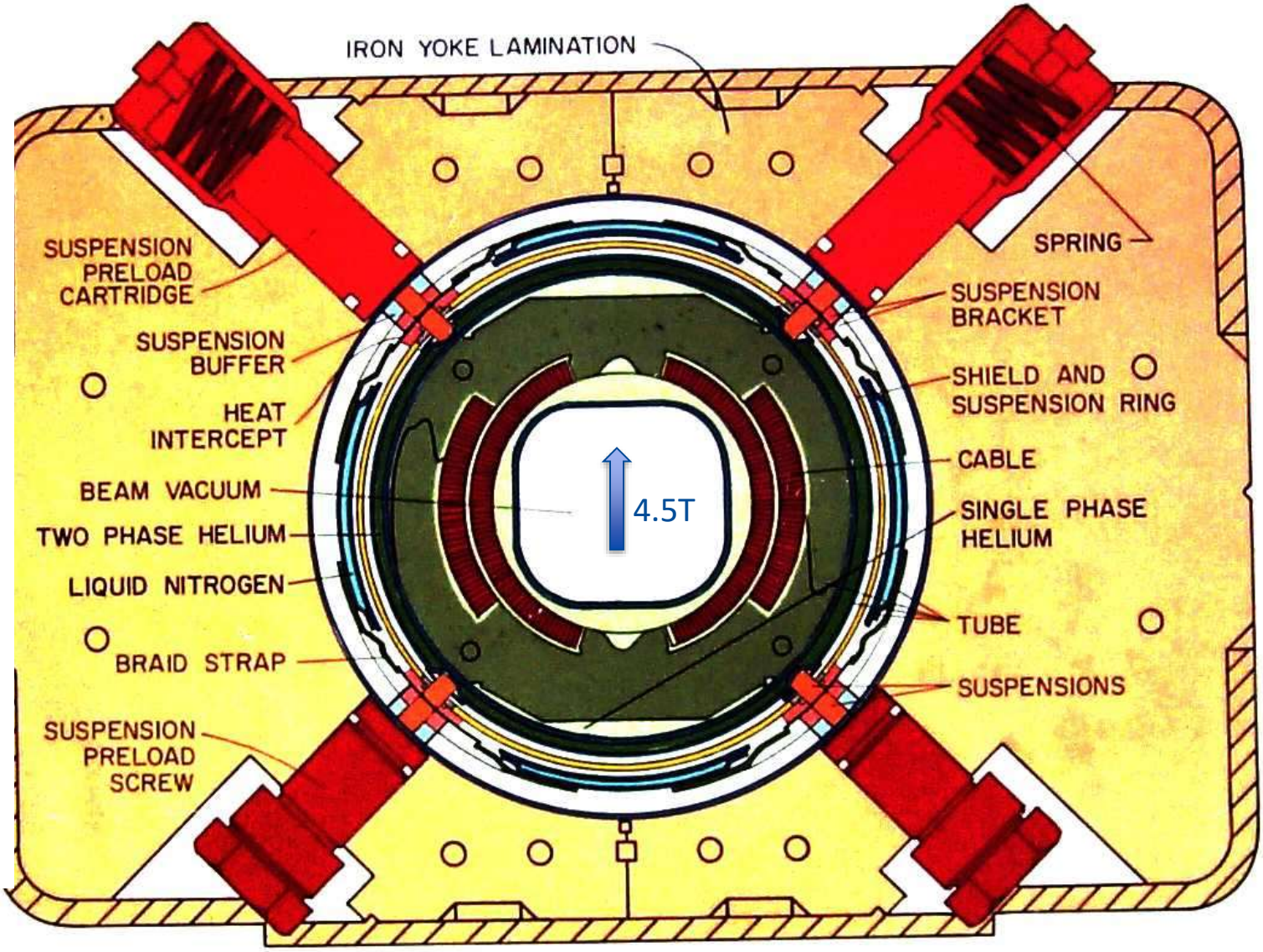
Tevatron Quadrupole

Tevatron Quad corrector
 Tevatron Sextupole corrector
 Tevatron Beam Position Monitor

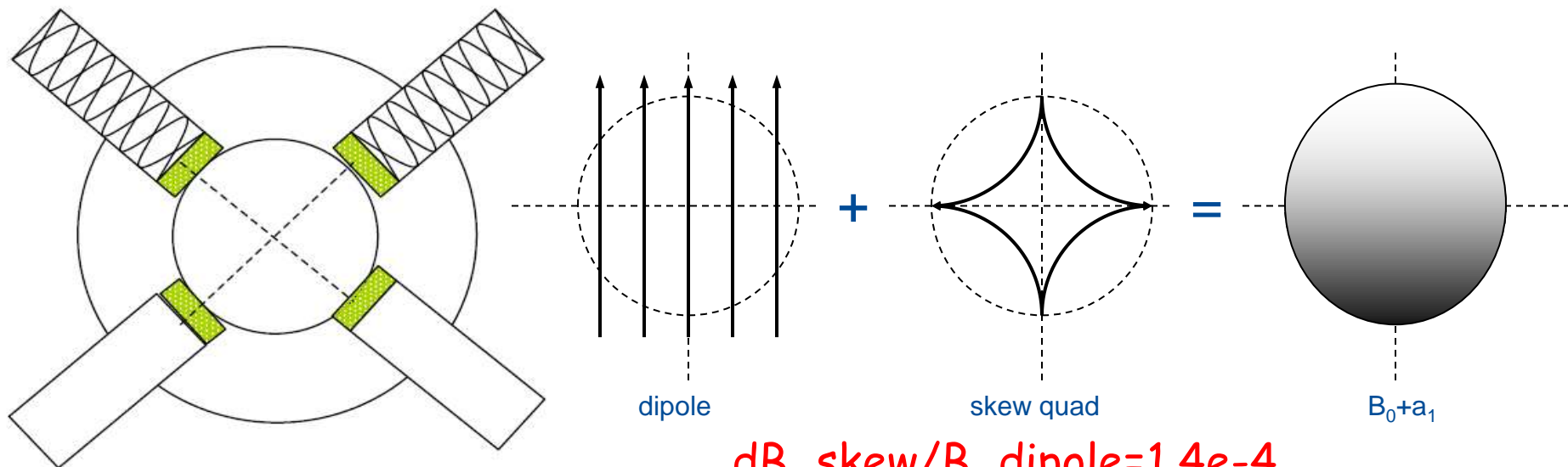
Heart of the Collider – 4.5 T SC magnets

Age Effect: SC Coils Sank wrt Iron Yoke

After ~20 years of operation, the coil block sank wrt iron yoke under strong forces of springs in "smart bolts" (smashed G10 spacers)



Reshimming=Lifting Up SC Coils



$$\frac{dB_{\text{skew}}}{B_{\text{dipole}}} = 1.4e-4$$

at 25.4 mm

Solution: add 140 micron shims to the bottom suspensions to raise the coil block. In 3 years we did it for all 774 dipoles (18 "smart" bolts and 18 lower bolts per magnet) → coupling reduced as expected and correspondingly beam size mismatch at injection

Skew quadrupole → x-y coupling

Expected Motion (and as the results – optics functions)

$$X'' + 4\pi^2 Q_x^2 x = 0$$

$$Y'' + 4\pi^2 Q_y^2 y = 0$$

“Skew” quadrupole field components add extra forces

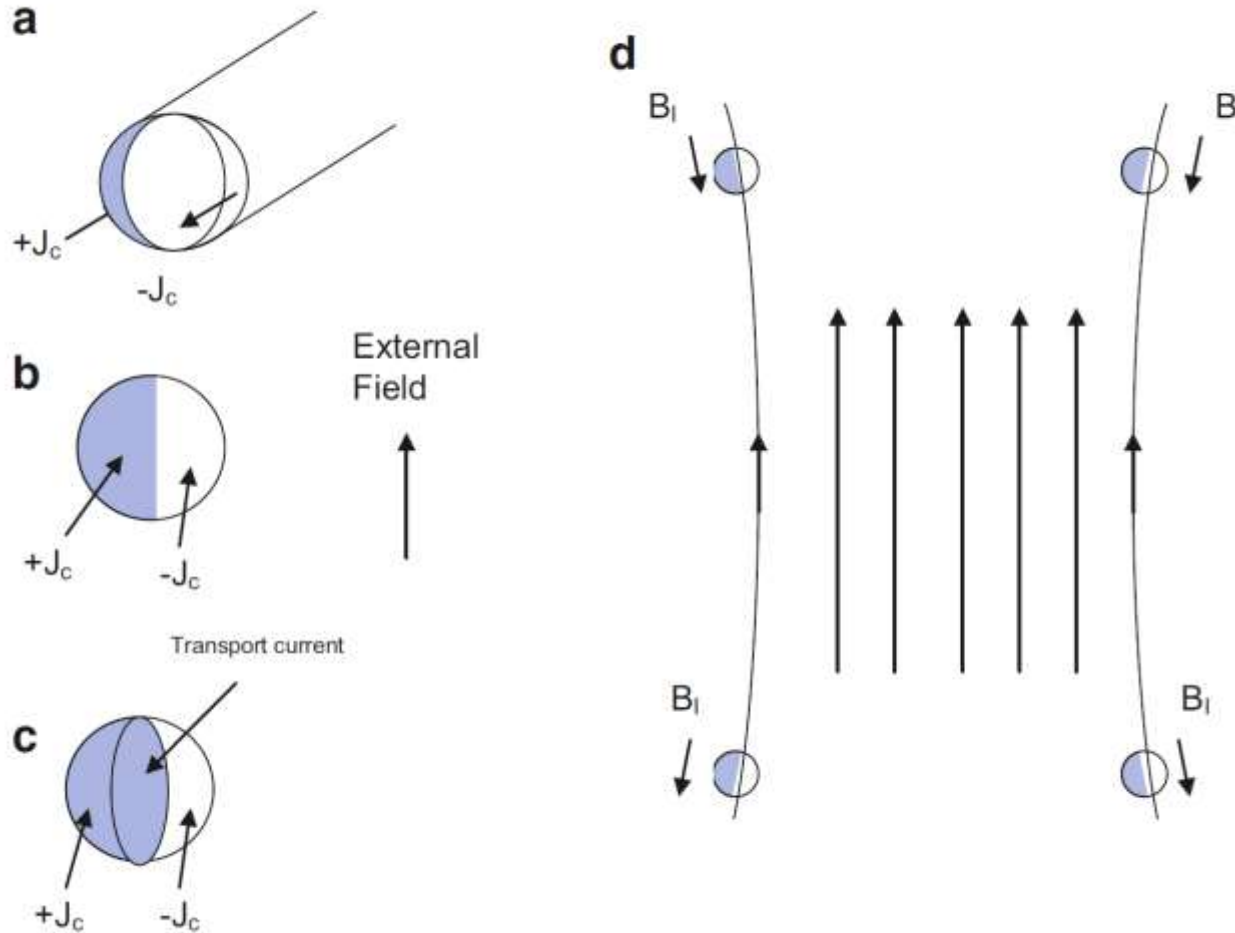
$$X'' + 4\pi^2 Q_x^2 x = +(Skew) y$$

$$Y'' + 4\pi^2 Q_y^2 y = -(Skew) x$$

(especially if strong and systematic all around the ring)

Messes up with all optics functions, orbit, separations, tunes, chromaticities, etc → lost control over beam dynamics in collider

Persistent Currents Effect

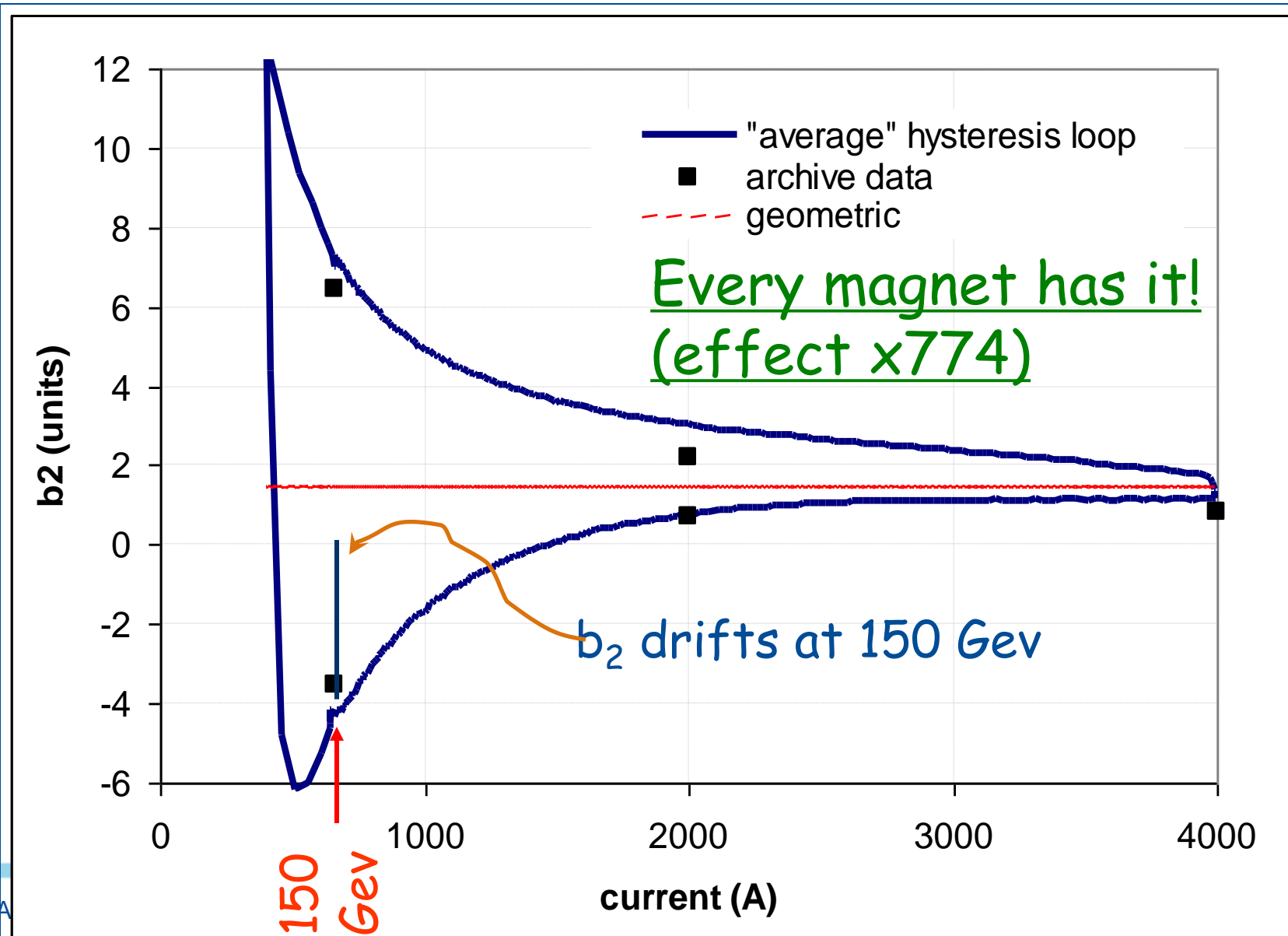


Persistent currents in SC due to Messner effect: a) shielding of external field; b) external field changes \rightarrow more shielding; c) on top of that – transport current that drives the B-field; d) appearance of sextupole field component for four symmetrical “micro-dipoles”

If the magnets are held at a fixed excitation, say, at the injection field, the persistent currents and thus the sextupole fields decay with a logarithmic dependence of time. The source of the decay is the resistive redistribution of Interstrand Coupling Currents (ISCC). These coupling currents flow through a complicated pattern in the copper strands and splices, and as they change, the magnetization of the cable decays.

Another Peculiarity of SC Magnets - Sextupole component due to so called *persistent currents* in SC

1 unit
= $1e-4$
dB/B
at $r=1''$



Sextupole Fields → Chromaticity

Expected Motion (and as the results – optics functions)

$$X'' + 4\pi^2 Q_x^2 x = 0$$

$$Y'' + 4\pi^2 Q_y^2 y = 0$$

Sextupoles result in additional forces $F_x \sim Sxy$ and $F_y \sim S(x^2 - y^2)$

In the arcs where dispersion is non-zero $x = x_\beta + D_x (dP/P)$ that leads to additional terms like

$$X'' + 4\pi^2 Q_x^2 x = -K_x S D_x (dP/P) x$$

$$Y'' + 4\pi^2 Q_y^2 y = -K_y S D_x (dP/P) y$$

Which result in tune variation with momentum $Q_x = Q_x + Q'_x (dP/P)$

Coefficient $Q'_{x,y} = dQ_{x,y} / (dP/P)$ is called chromaticity → critical!

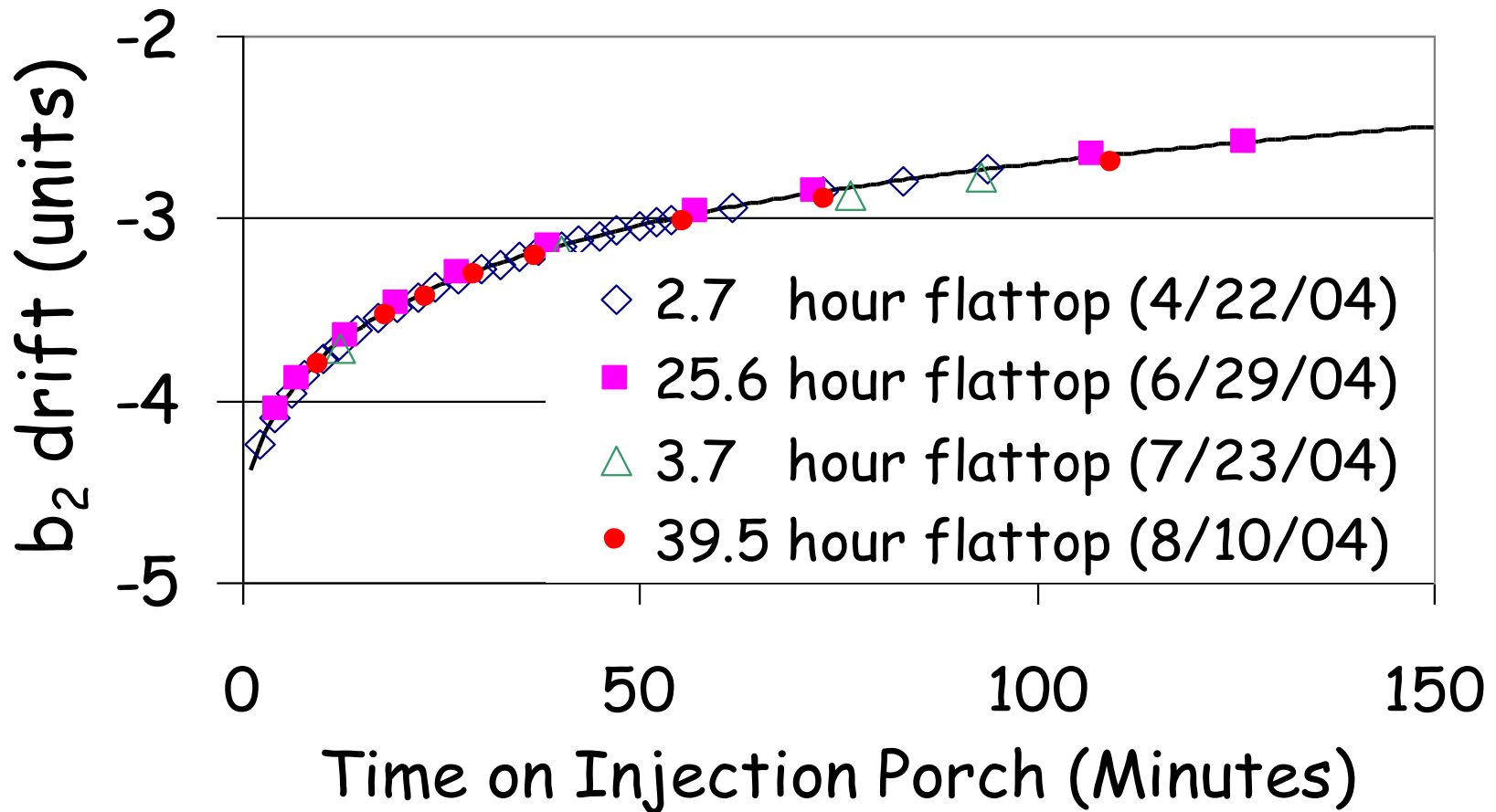
Eg spread $(dP/P) \sim 0.1\%$ and $Q'_{x,y} = 10 \rightarrow dQ_{x,y} = 0.01$

Measured b_2 Drift in Tevatron @150 GeV

Equivalent to ~ 10 units of chromaticity drift

Scale depends on the history of the Tevatron magnets ramping up and down! \rightarrow was well understood and carefully corrected

Also, seen and corrected in orbits, tunes and coupling



Tevatron Inefficiencies: 2001

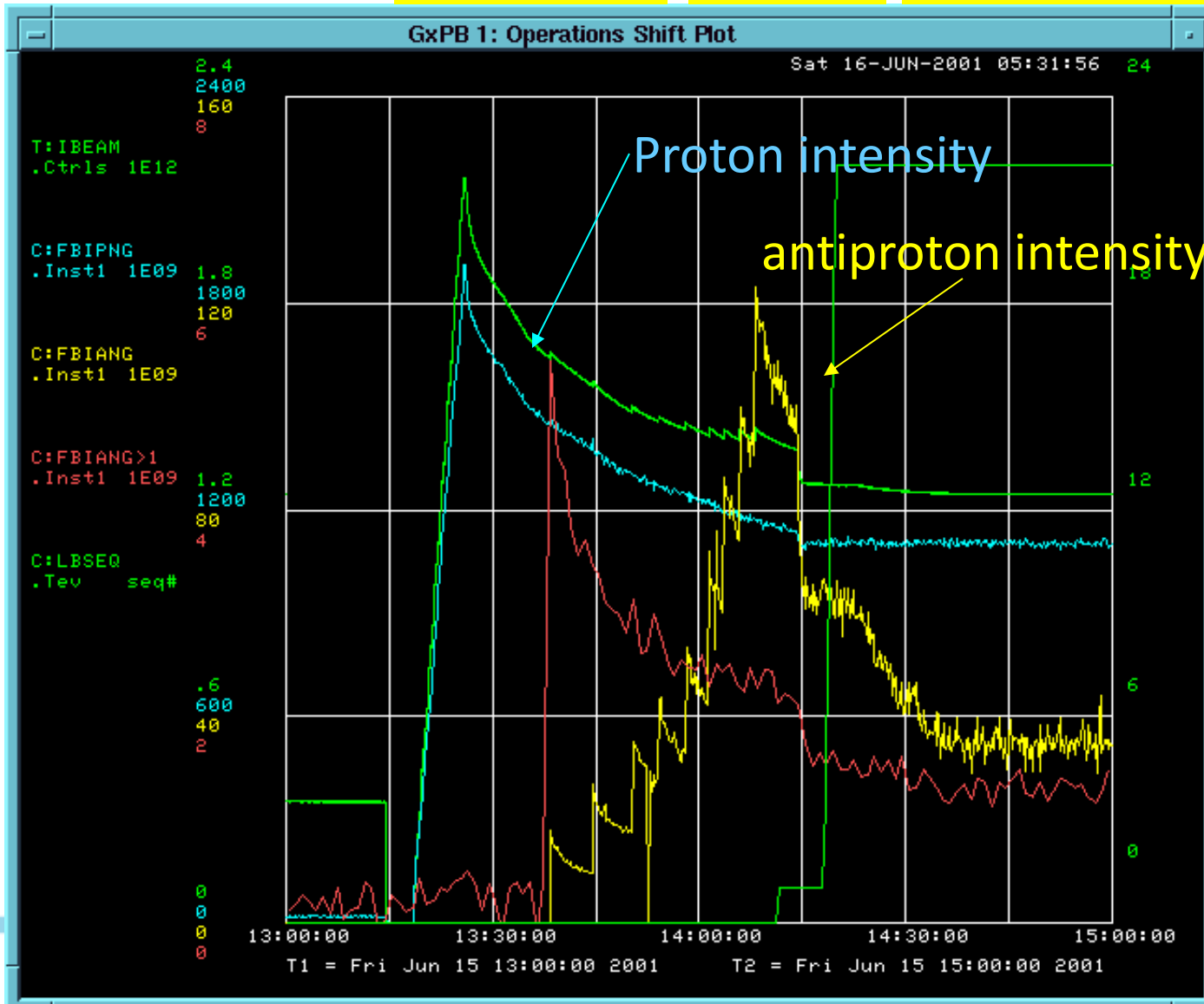
Injection E

E-ramp

Low-beta collisions

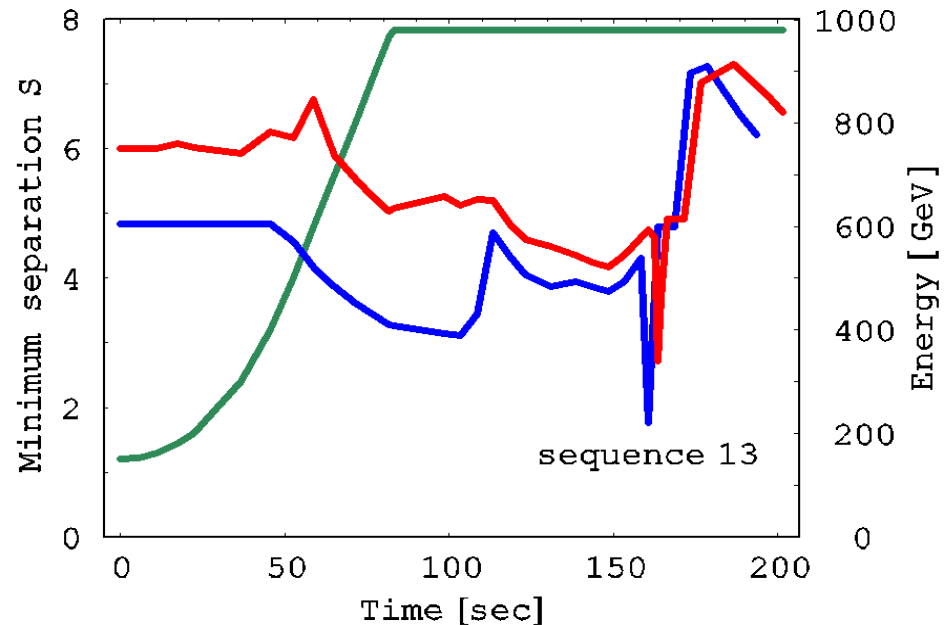
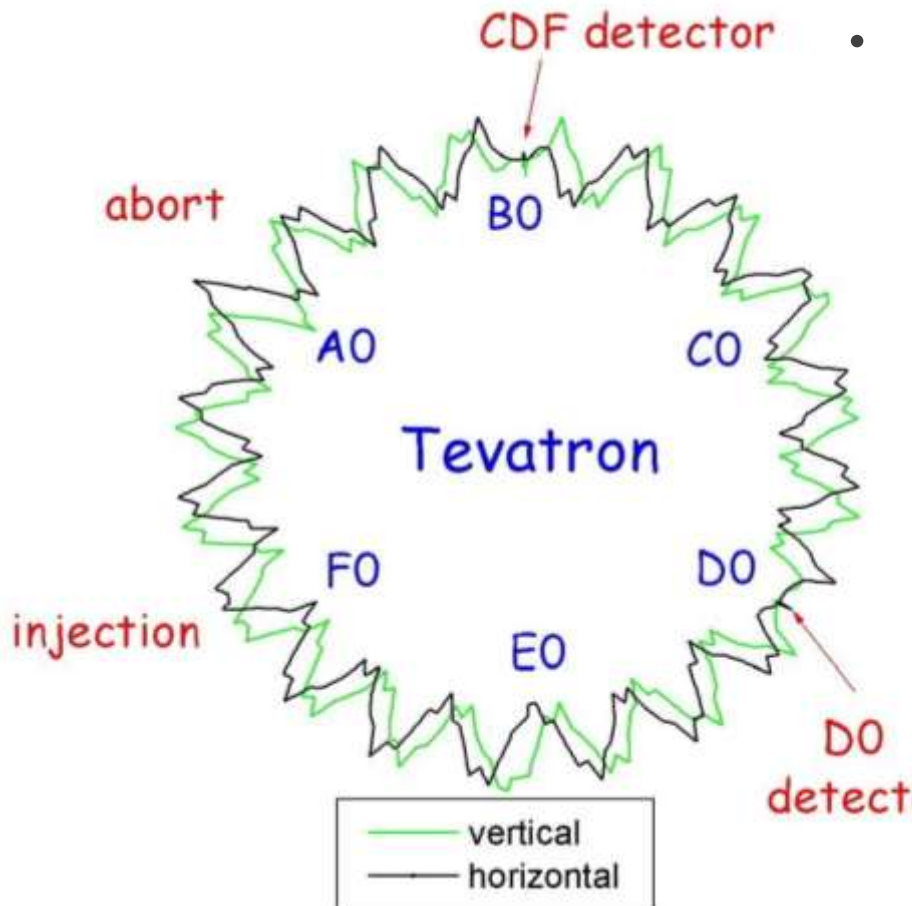
Core #535

Jun 15, 2001

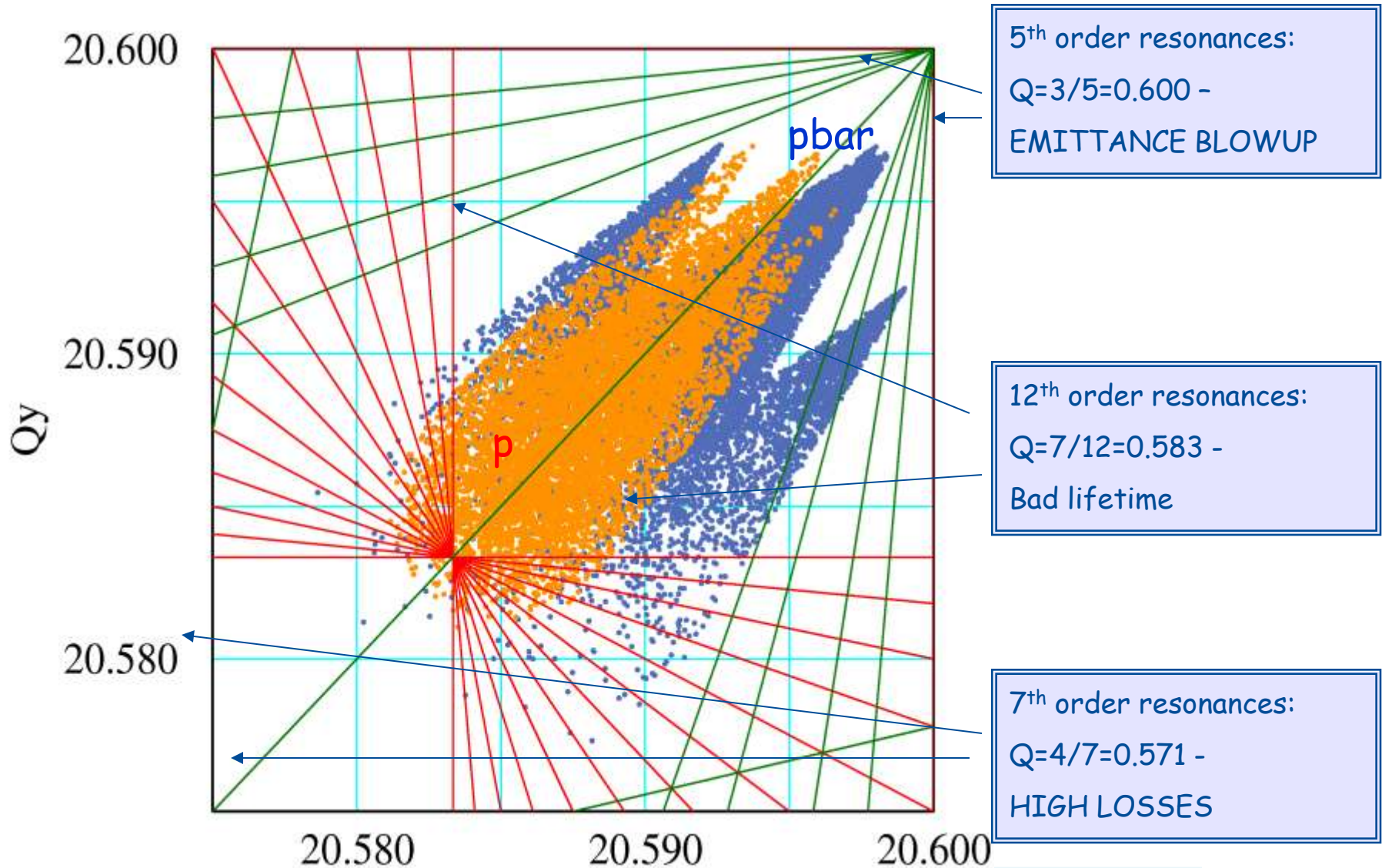


Importance of Helical Orbits

- Beams share beam pipe → be separated
 - Helical separation $\sim (10-22)$ mm at 150 GeV
 - $S \sim (3-6)$ mm at 980 GeV
- Lifetime is strong function of S
 - 30 sec at 2σ , 50 hrs at 7σ



Betatron Tunes of Tev Beams



Head-On Beam-Beam Collisions

affected mostly protons

max. tuneshift

$$2\xi_p = 0.018 - 0.022$$

rms beam size

28 microns

protons

max. tuneshift

$$2\xi_a = 0.020 - 0.026$$

rms beam size

16 microns

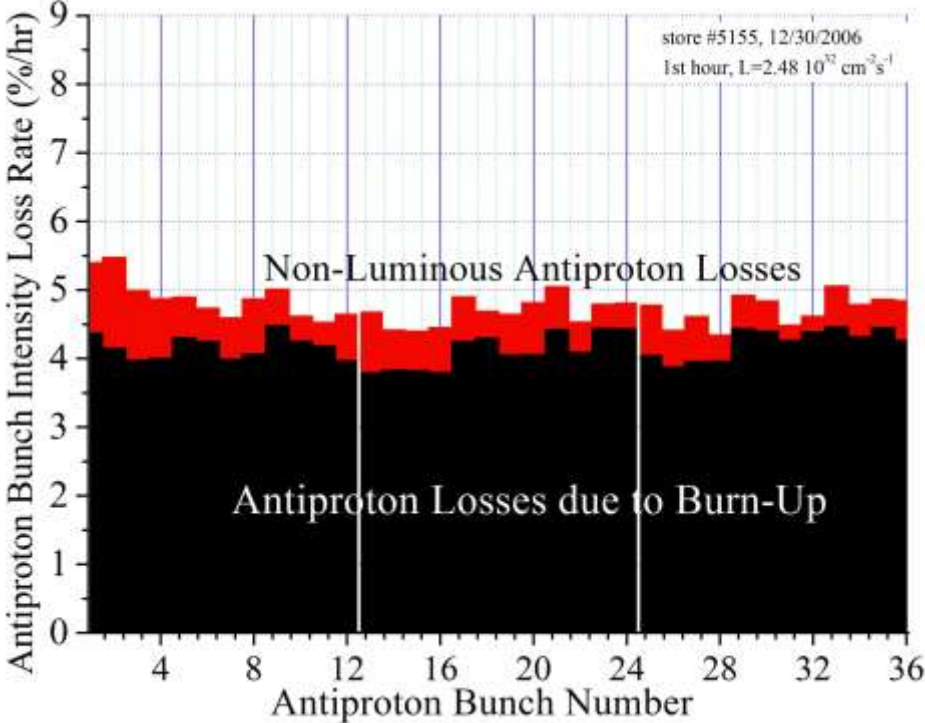
anti-
protons

emittance ratio (ϵ_p/ϵ_a) ~3

Losses of particles due to beam-beam

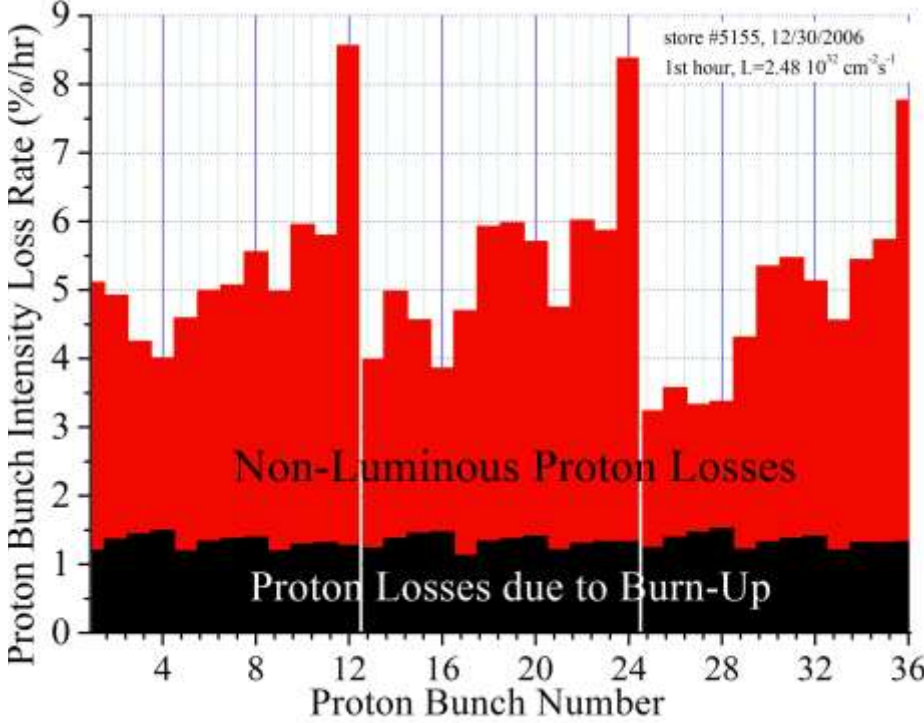
Antiprotons 980 GeV :

$$\xi_{max} = +0.024$$



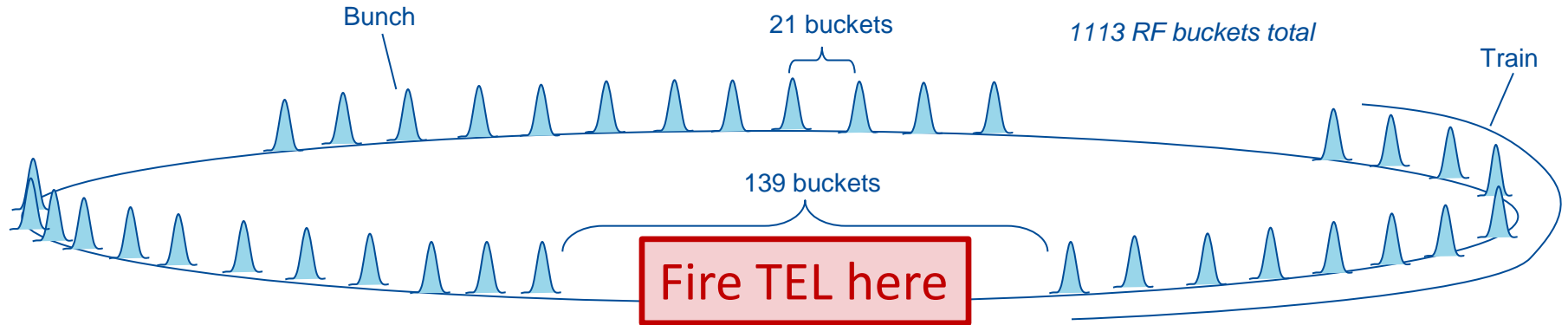
Protons 980 GeV :

$$\xi_{max} = +0.016$$



At present, beam-beam effects are relatively stronger on protons, accounting for some 10-15% loss of the integrated luminosity. Proton loss rates vary greatly from bunch to bunch.

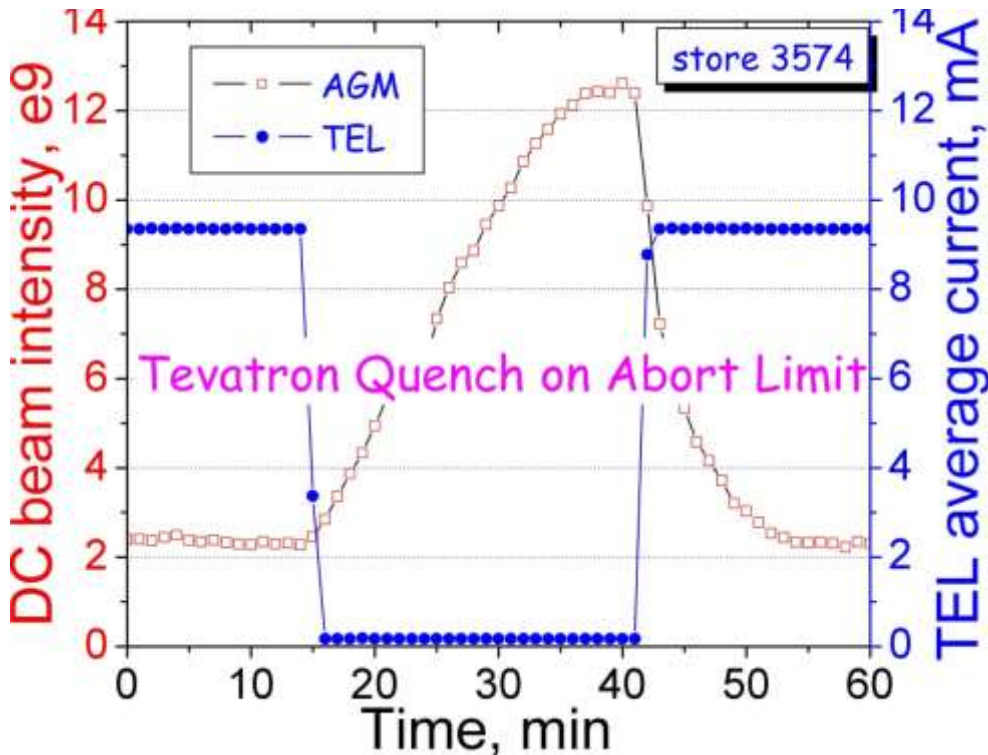
Intrabeam Scattering and Longitudinal Oscillations Lead to Generation of DC beam in Abort Gaps



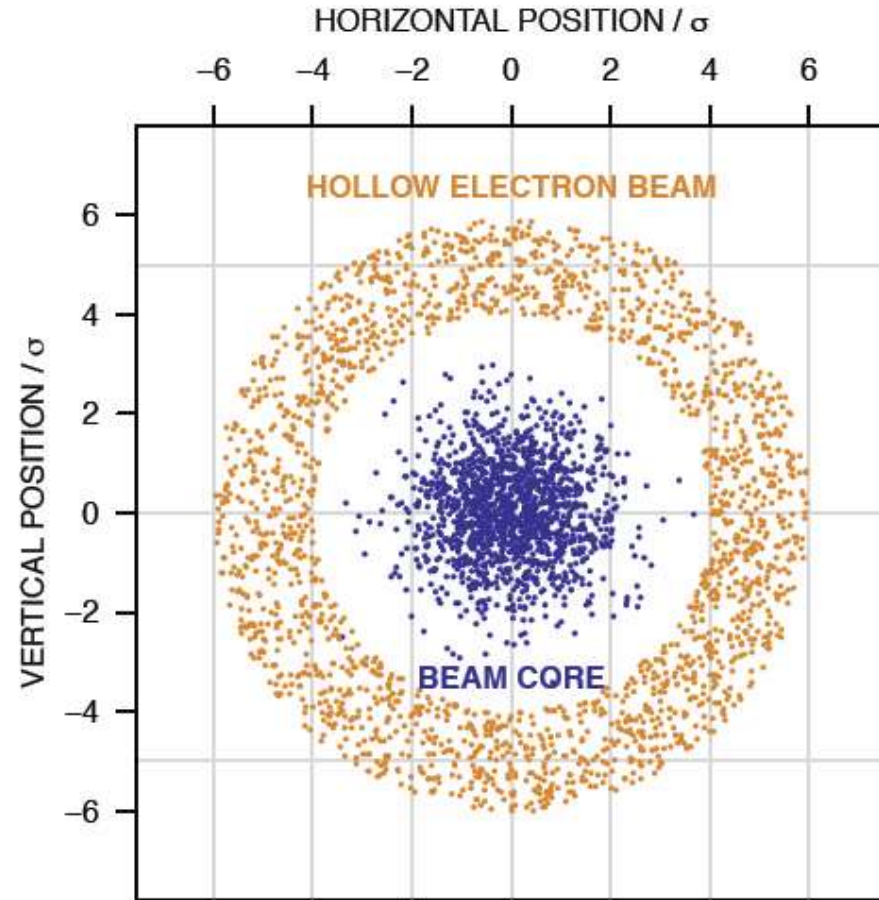
- The Tevatron operates with 36 bunches in 3 groups called trains
- Between each train there is an abort gap that is 139 RF buckets long
 - RF bucket is 18.8 ns → Abort gap is 2.6 μ s
- **Protons leak out of main bunches to the gaps.** Tevatron is sensitive to few $\times 10^9$ particles in the abort gaps (total beam $\sim 10^{13}$) as they lead to quench on beam abort (kicker sprays them)
- **Kill (diffuse)** DC beam in gaps by electron lens

e-Lenes for Beam Collimation

Pulsed e-current
in the abort gap
→ Drive out DC beam



USPAS'25 | Colliders VS6-7



Hollow-e-beam →
no EM field inside
Strong field outside

Tevatron Luminosity Progress

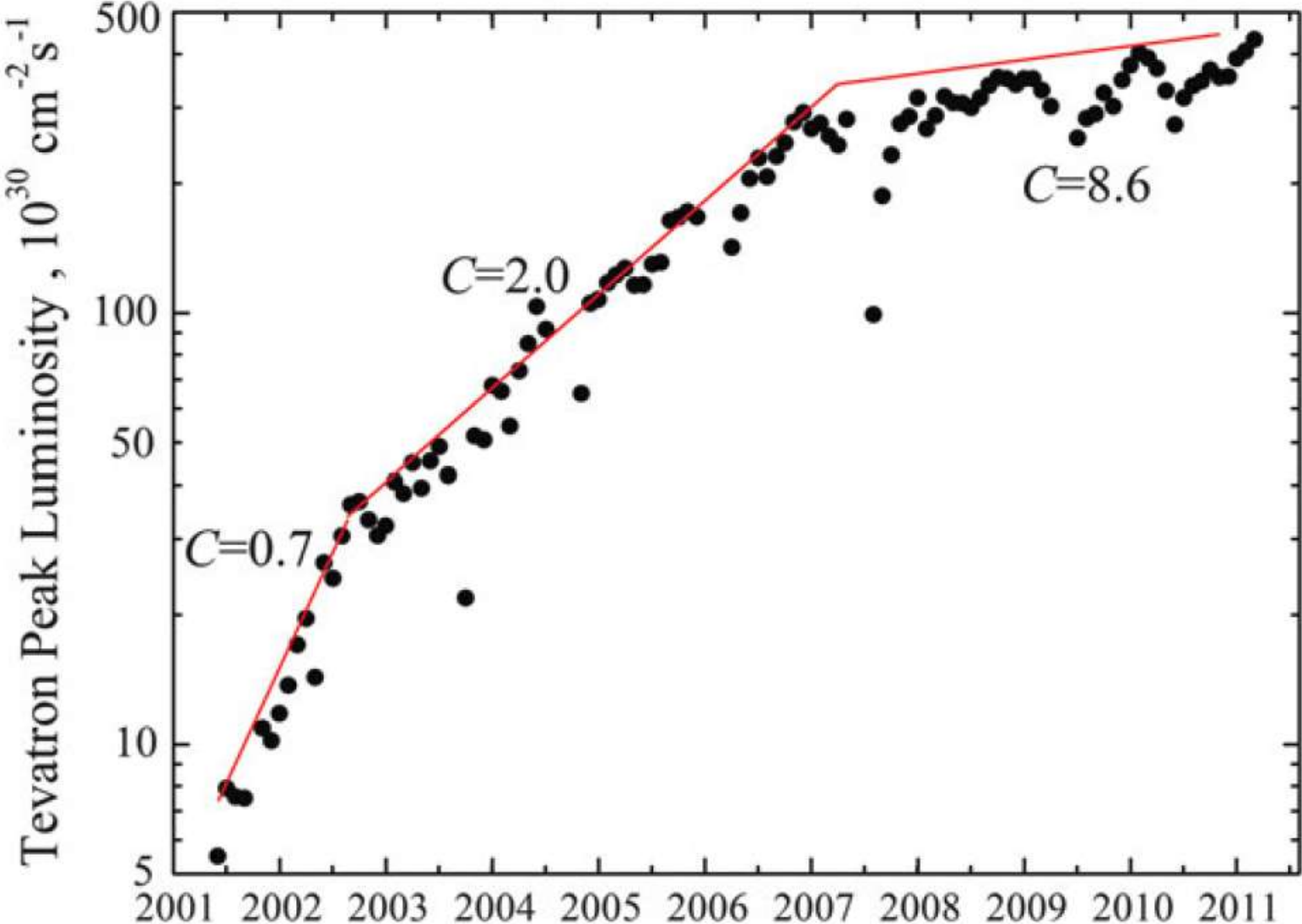


Table 3. Tevatron Collider Run II major luminosity improvements history.

Improvement	Date	Luminosity gain
Optics correction in Accumulator (AA) to Main Injector (MI) beam line	12/2001	25 %
Tevatron quenches on abort stopped by electron lens	02/2002	~ 10 % stability
Antiproton loss at the step #13 of Tevatron low-beta squeeze fixed	04/2002	~ 5 %
New Tevatron injection helix implemented	05/2002	~ 5 %
New AA lattice reduces IBS, emittances	07/2002	~ 5 %
Beam Line Tuner to reduce emittance dilution at Tevatron injection	07/2002	~ 5 %
Antiproton multi-bunch coalescing efficiency improved in MI	07/2002	~ 5 %
Small aperture Lambertson magnets removed from Tevatron C0 section	07/2002	15 %
Tevatron sextupoles tuned / SEMs taken out of antiproton beam line	07/2002	10 %
New Tevatron helix implemented on ramp to reduce beam loss	07/2003	2 %
Tevatron magnet reshimming (to center coils inside iron yokes)	07/2003	10 %
MI dampers operations / HEP store length increased	02/2004	30 %
Improved efficiency of 2.5 MHz antiproton transfer	04/2004	8 %
Reduction of Tevatron β^* to 35 cm	05/2004	20 %
Antiproton injections from both Recycler and Main Injector	07/2004	8 %
Electron cooling system in Recycler operational	01–07/2005	~ 25 %
Longitudinal slip-stacking system in Main Injector operational	03/2005	~ 20 %
Tevatron octupoles optimized at injection / 980 GeV	04/2005	~ 5 %
Further reduction of the Tevatron β^* to 28 cm	09/2005	~ 10 %
Antiproton production optimized	02/2006	~ 10 %
Tevatron helical separation improved, more protons	06/2006	~ 10 %
Tevatron collision helicity improved, better lifetime	07/2006	~ 15 %
New Recycler working point, smaller antiproton emittances	07/2006	~ 25 %
Faster antiproton transfer from AA to RR (1 hour → 1 min)	12/2006	~ 15 %
New antiproton transfer gradient Li lens operational	01/2007	~ 10 %
Tevatron sextupoles circuits set up for new working point	2007	~ 10 %
Compensation of chromaticity in Tevatron beam optics	2008	~ 5 %
Shorter bunches by multi-bunch proton injection	2008–09	~ 5 %
Better beam quality by scraping in Main Injector	2008	~ 5 %
Antiproton size dilution at collisions / B0 aperture opened up	2008	~ 5 %
Booster proton emittances reduced / tune up of P1 and A1 transfer lines	04/2010	~ 10 %
Tevatron collimators employed during low-beta squeeze, more protons	04/2011	~ 8 %

x43 in luminosity in 32 steps

Holmes, Moore, Shiltsev 2011 JINST 6 T08001

- ❑ 26 658.883 m
- ❑ 6.8 TeV x 2
- ❑ Four detectors



LHC Contributions to Science and Technology

- Technology:

- Record field NbTi magnets 8 T
- Record field Nb₃Sn magnets for IR 12T@poles – for HL-LHC
- >99.99% efficient 4-stage system of 128 collimators
- Crab-cavities to compensate crossing angle *Lumi* reduction – for HL-LHC

- Beam physics advances:

- Record pp Luminosity $2.6E34 \text{ cm}^{-2}\text{s}^{-1}$ (x2.5 over LHC design; x60 Tevatron)
- Effective electron cloud control (scrubbing, etc)
- Crystal collimation demo
- Long-range beam-beam wire compensation demo
- Hollow e-beam collimation – for HL-LHC

PROTON PHYSICS: STABLE BEAMS

Energy:

6499 GeV

I(B1):

1.56e+14

I(B2):

1.72e+14

Inst. Lumi [(ub.s)⁻¹]

IP1: 8155.99

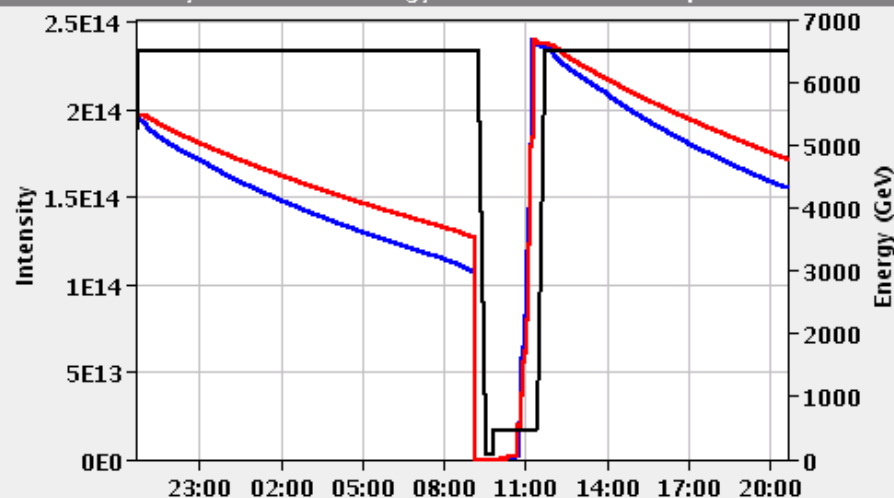
IP2: 1.76

IP5: 7827.12

IP8: 330.93

FBCT Intensity and Beam Energy

Updated: 20:38:28



Instantaneous Luminosity

Updated: 20:38:28



BIS status and SMP flags

B1

B2

Comments (01-May-2018 14:18:10)

Fill for physics (1887b)

XRPCs IN

continous crossing angle leveling in IP1/5

Link Status of Beam Permits

true true

Global Beam Permit

true true

Setup Beam

false false

Beam Presence

true true

Moveable Devices Allowed In

true true

Stable Beams

true true

AFS: 25ns_1887b_1874_1694_1772_144bpi_19inj

PM Status B1

ENABLED

PM Status B2

ENABLED

Luminosity and Burn-Up

The relationship of the beam to the rate of observed physics processes is given by the “Luminosity”

$$\text{Rate} \rightarrow R = L\sigma$$

“Luminosity” Cross-section (“physics”)

Standard unit for Luminosity is $\text{cm}^{-2}\text{s}^{-1}$

Example: total p - p inelastic+elastic cross section at 13 TeV cme is ~110 mbarn (58 inel+ 12 ssd+40 el not seen) →

~60 interactions per crossing x

40,000,000 collision/sec = **2.4e9 protons** leave each beam every second

Beam lifetime due to such “Burn up” $T=N/(dN/dt)=$
2.8e14 protons/(2.4e9/s) =32 hours

LHC Luminosity Evolution

Instantaneous Luminosity:

$$n_b \sim 2800 \quad F = 1/\sqrt{1 + \left(\frac{\sigma_z \phi}{\sigma_t/2}\right)^2} \sim 0.85 \quad L = \frac{f_{rev} \cdot n_b \cdot N_1 \cdot N_2}{2\pi \sqrt{(\sigma_{x,1}^2 + \sigma_{x,2}^2)} \cdot \sqrt{(\sigma_{y,1}^2 + \sigma_{y,2}^2)}} \cdot F \cdot H$$

Proton burn-up rate

$$dN/dt = - n_{IP} L \sigma_{tot}$$

where

$$L = L_0 (N(t)/N_0)^2$$

Solution

$$N(t) = N_0 / (1 + t/\tau)$$

$$L(t) = L_0 / (1 + t/\tau)^2$$

where

$$\tau = N_0 / n_{IP} L_0 \sigma_{tot}$$

~32 hours

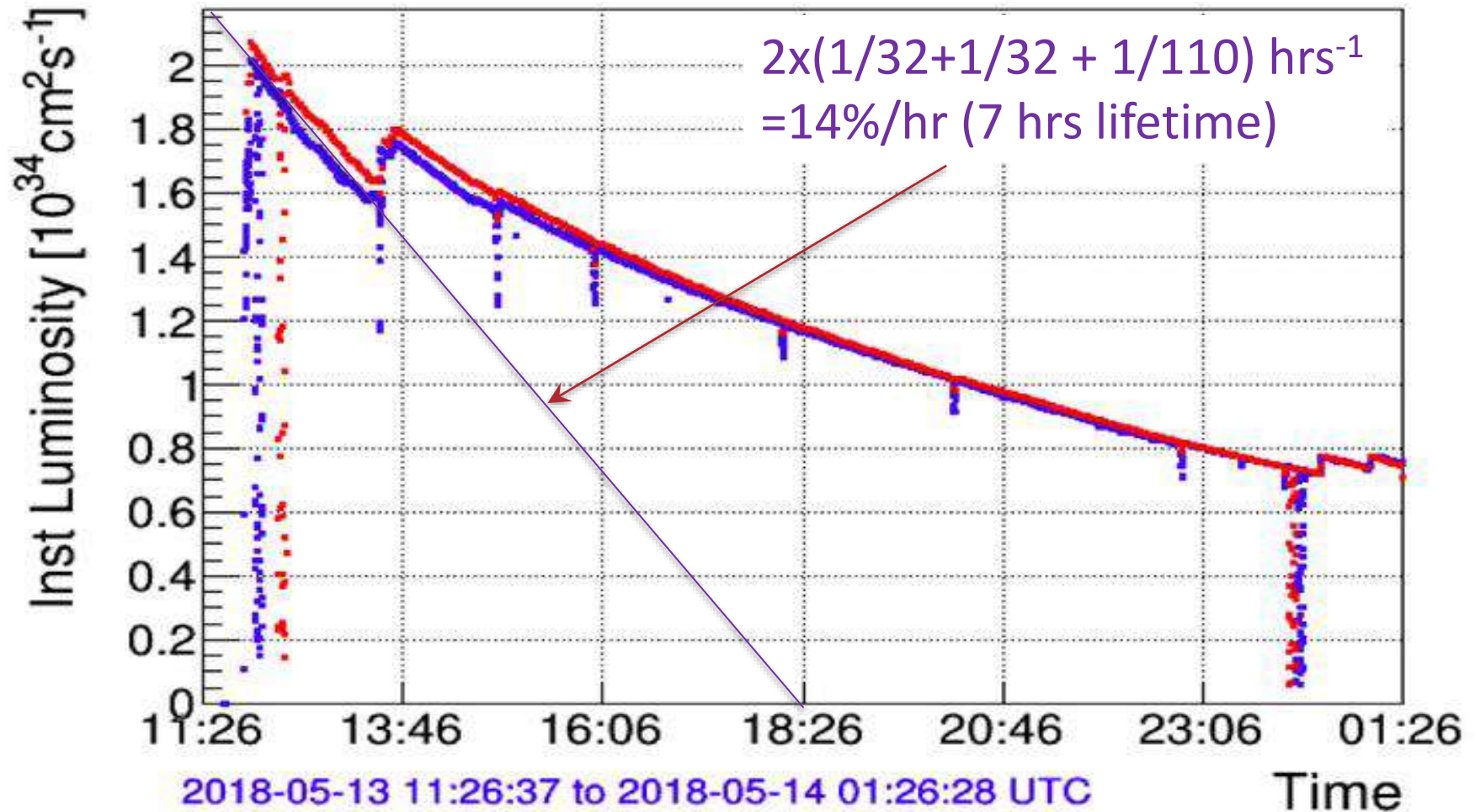
Luminosity lifetime (*eats itself*)

Take into account two IPs (ATLAS, CMS and 3% LHCb) $1/32+1/32$ hrs⁻¹

Take into account beam gas $1/110$ hrs⁻¹ and that $Lumi \sim N^2 \rightarrow \times 2$

Fill 6677 CMS/ATLAS Inst luminosity

— CMS
— ATLAS



Heart of the LHC: State-of-the-Art SC Magnets

1232 bending magnets 15m
 NbTi cables, 13 kA @ 1.9 K 10 GJ

4.5T

5.3T

3.5T

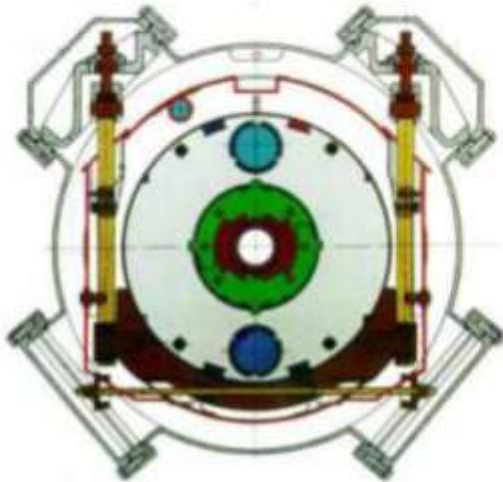
8.3T

LHC,
 15 m, 56 mm
 1276 dipoles

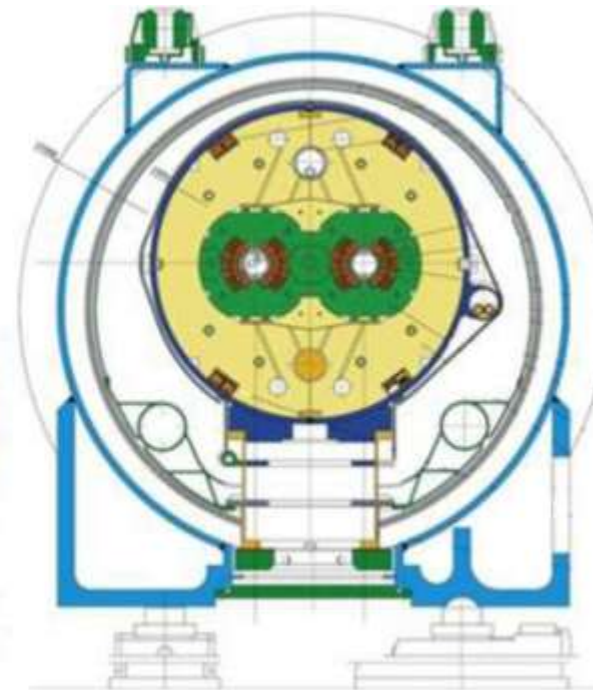
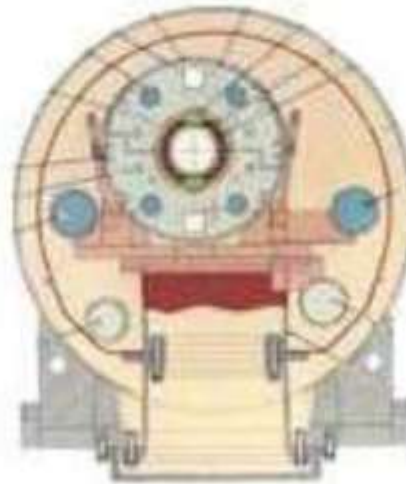
Tevatron,
 6 m, 76 mm
 774 dipoles



HERA,
 9 m, 75 mm
 416 dipoles



RHIC,
 9 m, 80 mm
 264 dipoles



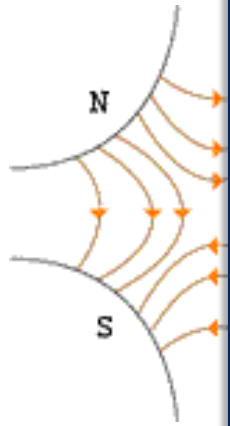
4.5 K He, NbTi
 + warm iron
 small He-plant

NbTi cable
 cold iron
 Al collar

NbTi cable
 simple &
 cheap

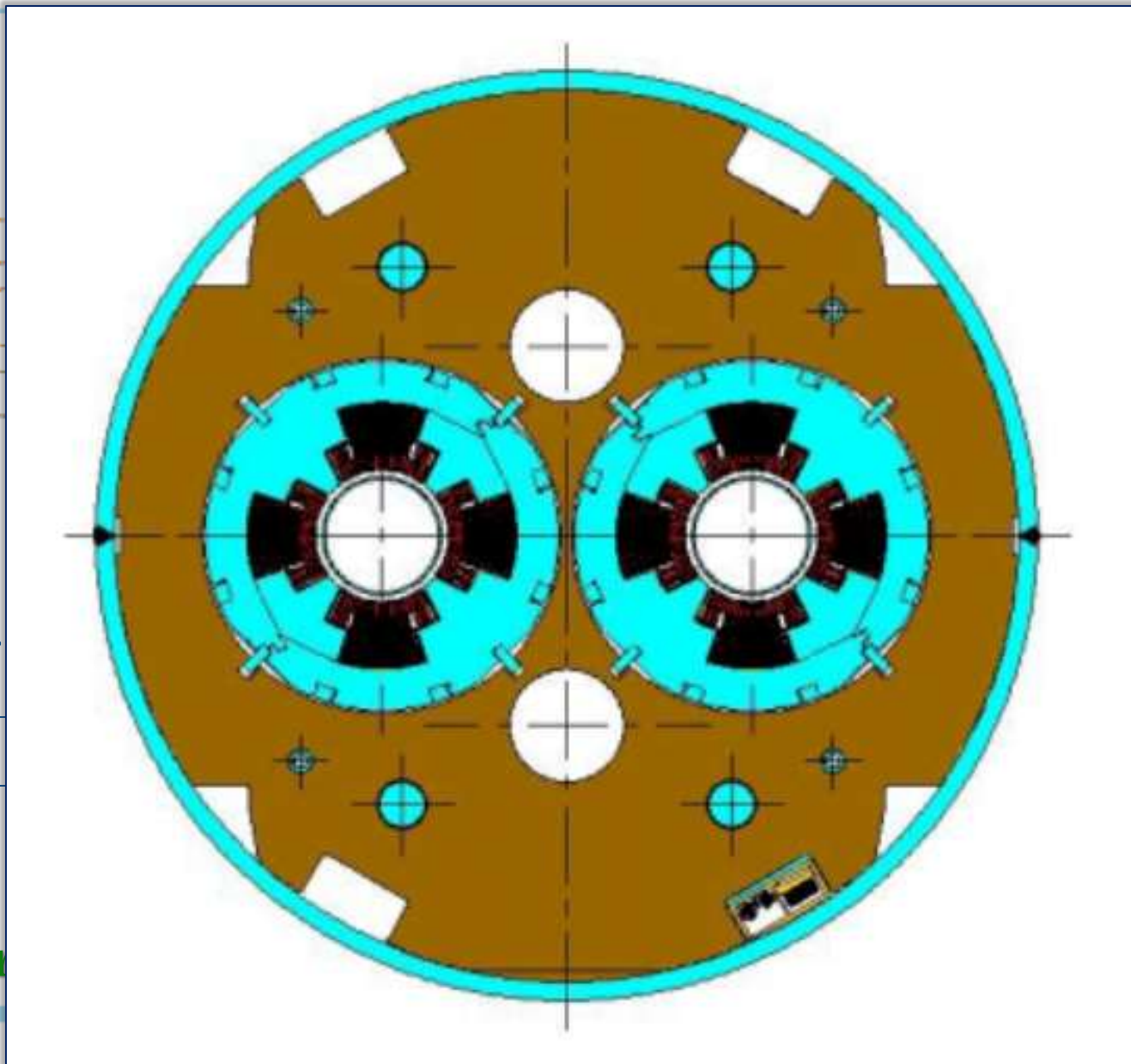
NbTi cable
 2K He
 two bores

Focusing by 2-Aperture Quadrupole Magnets



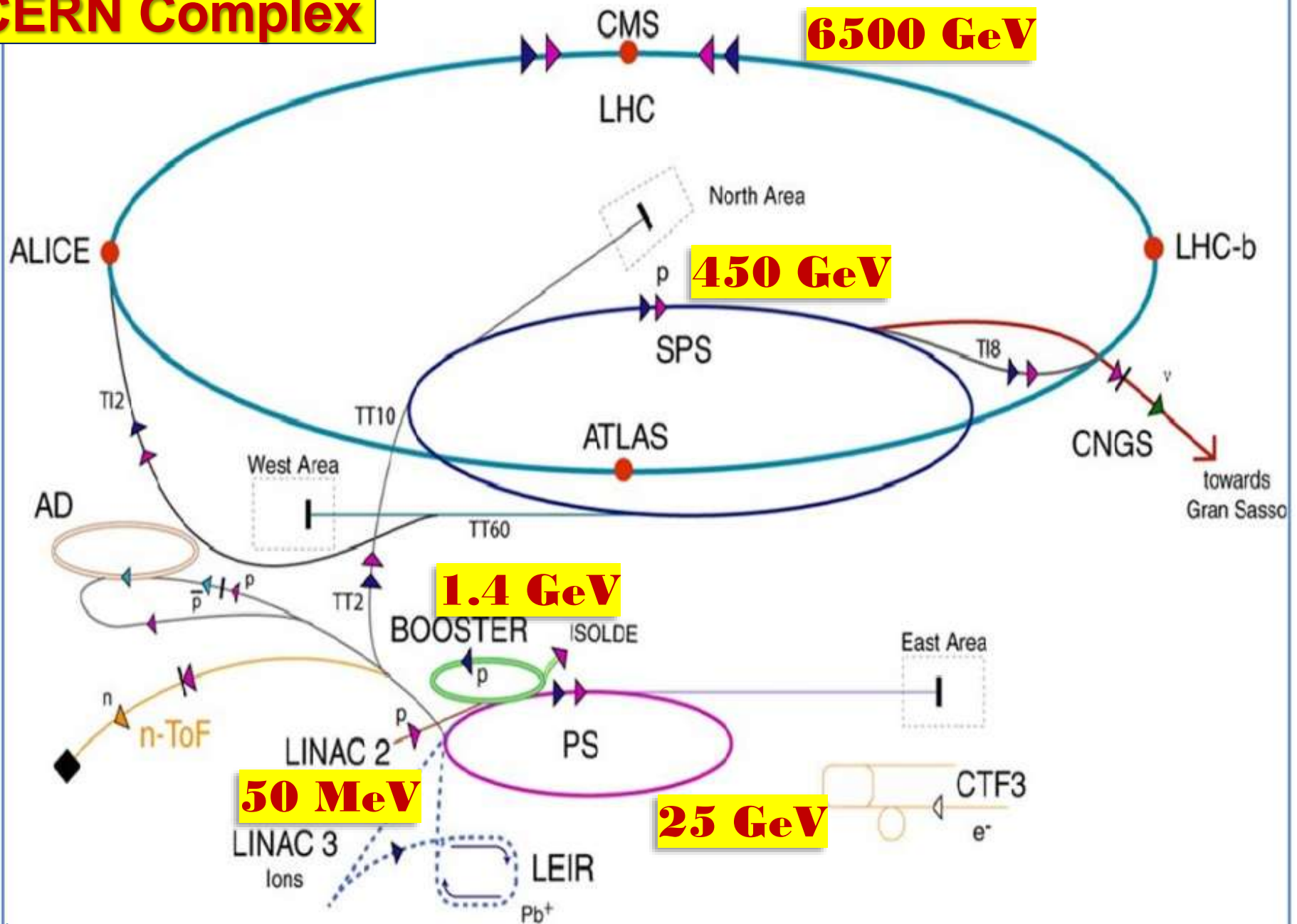
Luckily..

...pair

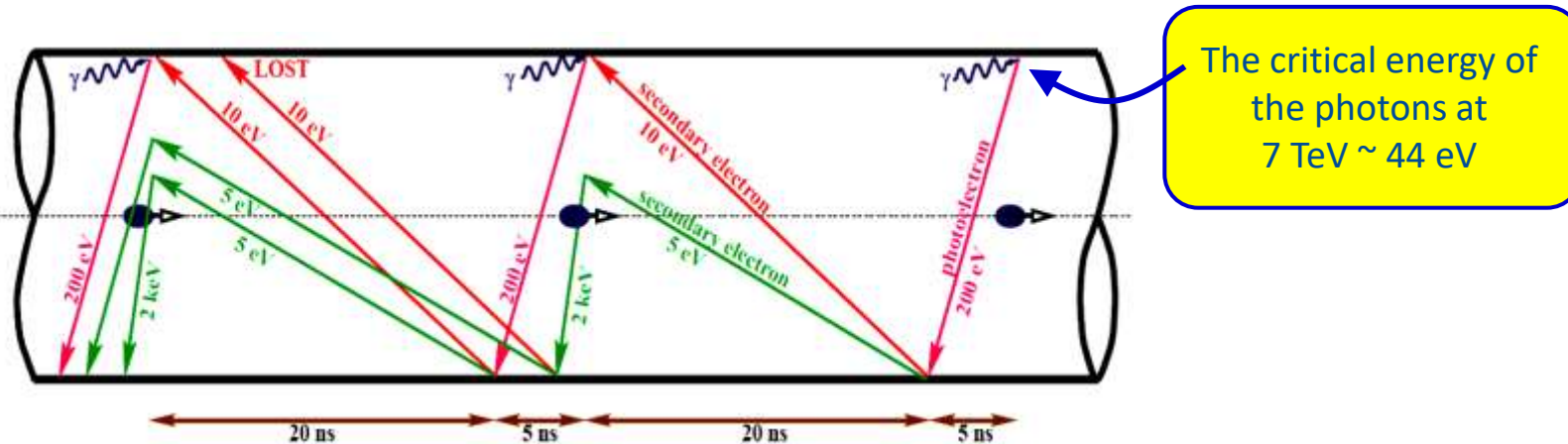


cell"

CERN Complex



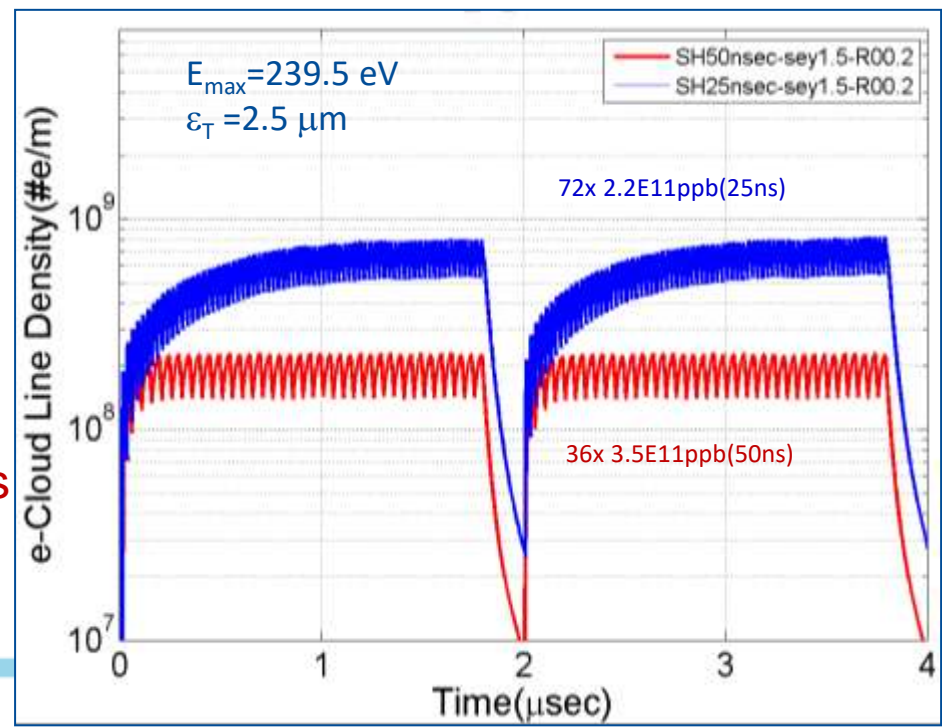
Electron Cloud & Need of Scrubbing



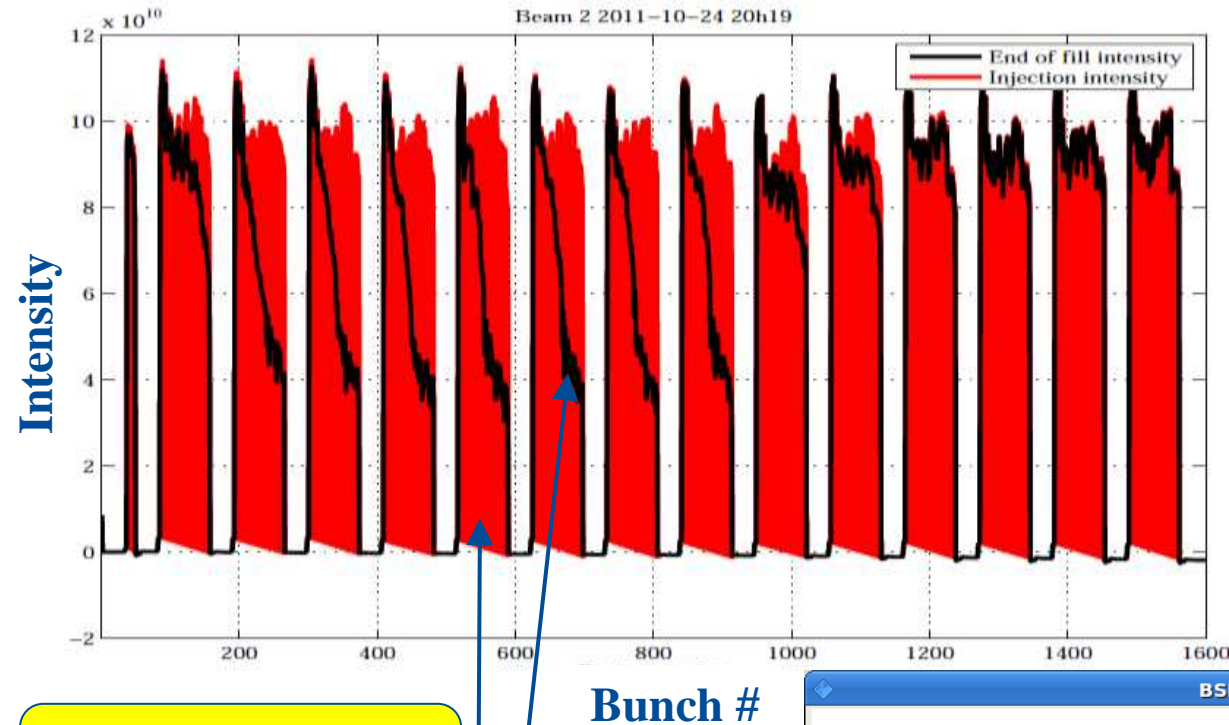
- Primary sources of electrons in the LHC
 - At Injection (450 GeV) gas ionization
 - At 7 TeV Synchrotron Radiation

Consequences:

- instabilities, emittance growth, desorption ← bad vacuum, beam loss
- excessive energy deposition in the cold sectors



What e-cloud can do to the Beam?



Injection Intensity
End of fill Intensity

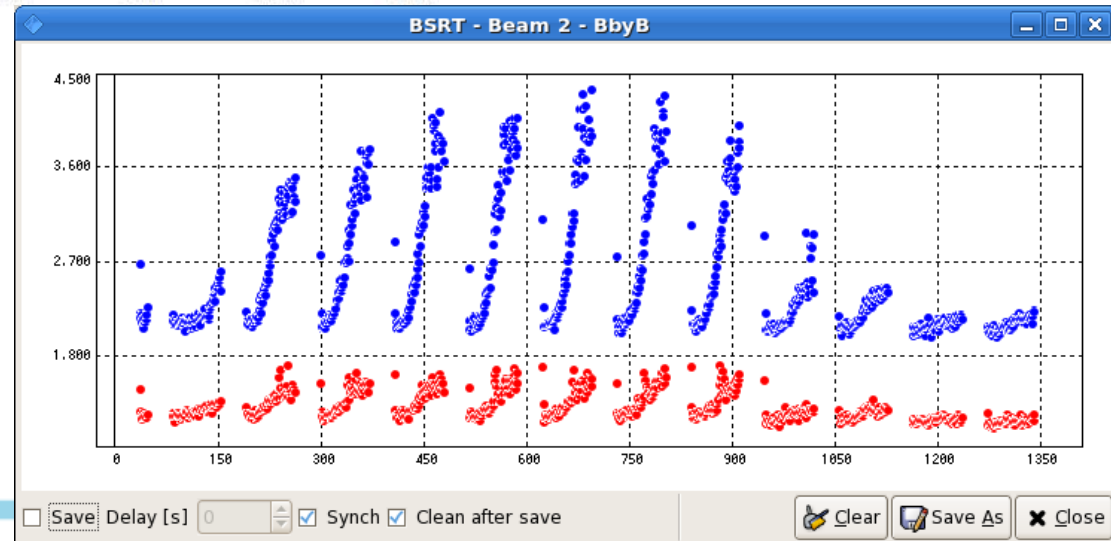
Measured Emittance Growth

~33% Horizontal

~110% Vertical

Associated beam loss

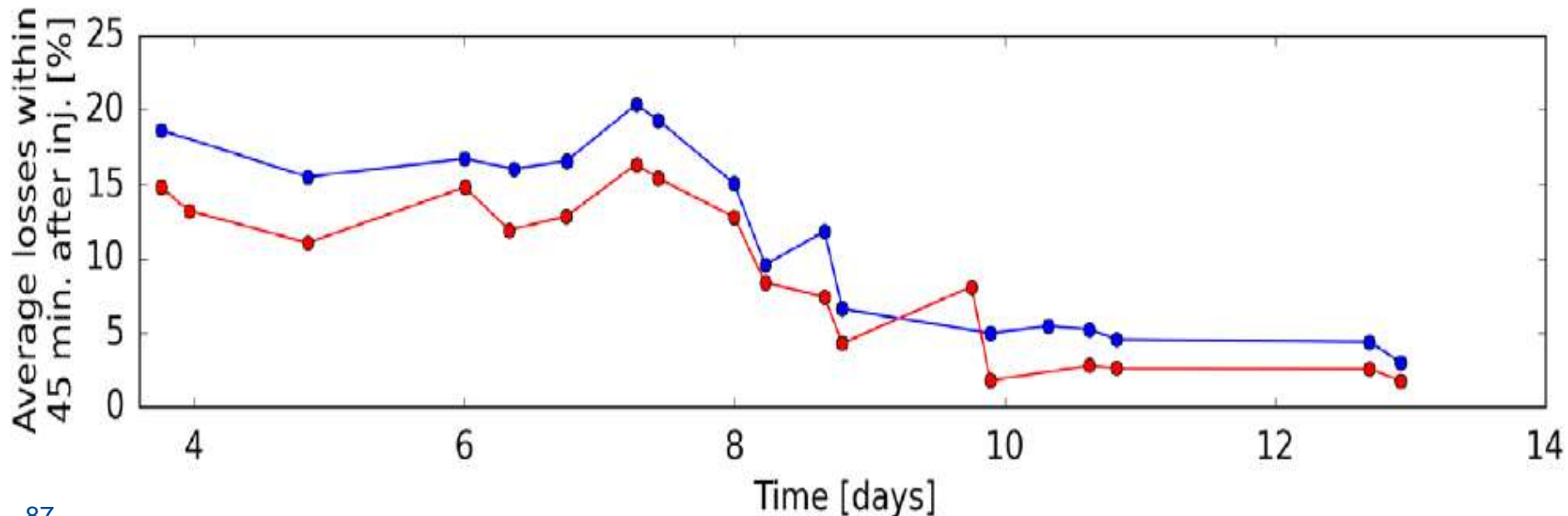
- Fill: 2249 (2011)
- 25 ns Bunch Spacing
- Energy = 450 GeV
- Time between Injection to End ~10 min
- Dumped by BPM
- 1020 Bunches



Scrubbing @ 25 ns bunch spacing

So far it is the only cure in the LHC.... Takes time to clean the surface and reduce SEY (secondary electron yield) from ~ 2.2 to ~ 1.5

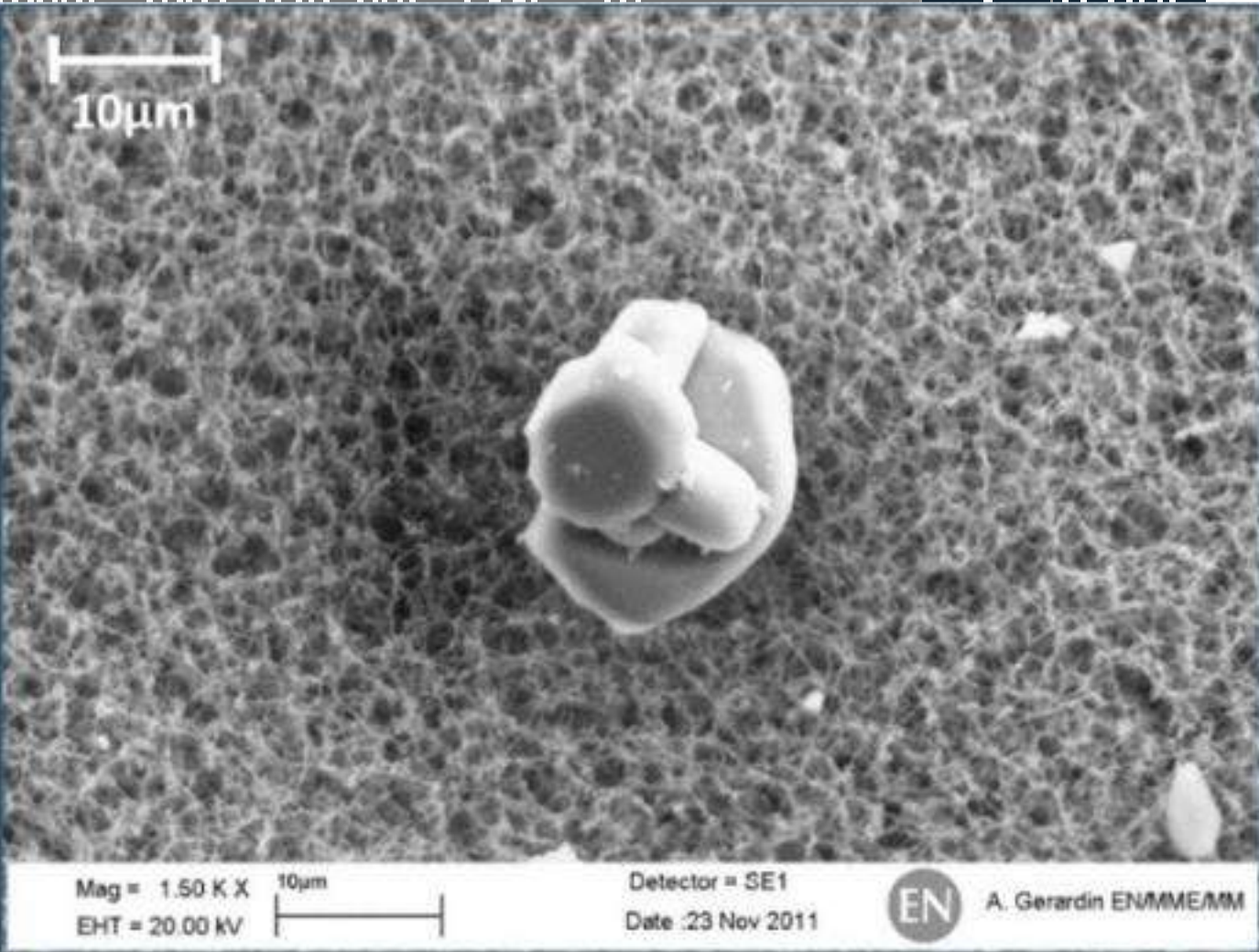
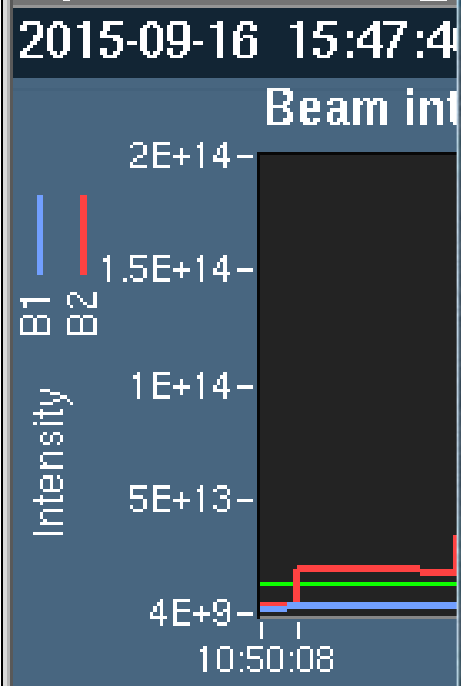
Scrubbing “memory” kept while running with 25 ns beams - **deconditioning** was observed after few weeks of low e-cloud operation



UFOs & 16L2

'Unidentified Falling Objects'

LHC FILL NUMBER: 4378 CYCLING	Beam	Intens
PROTON PHYSICS	1	0.00E
Inj. scheme: 25ns_10001_1001_070_005_141_110	2	0.00E

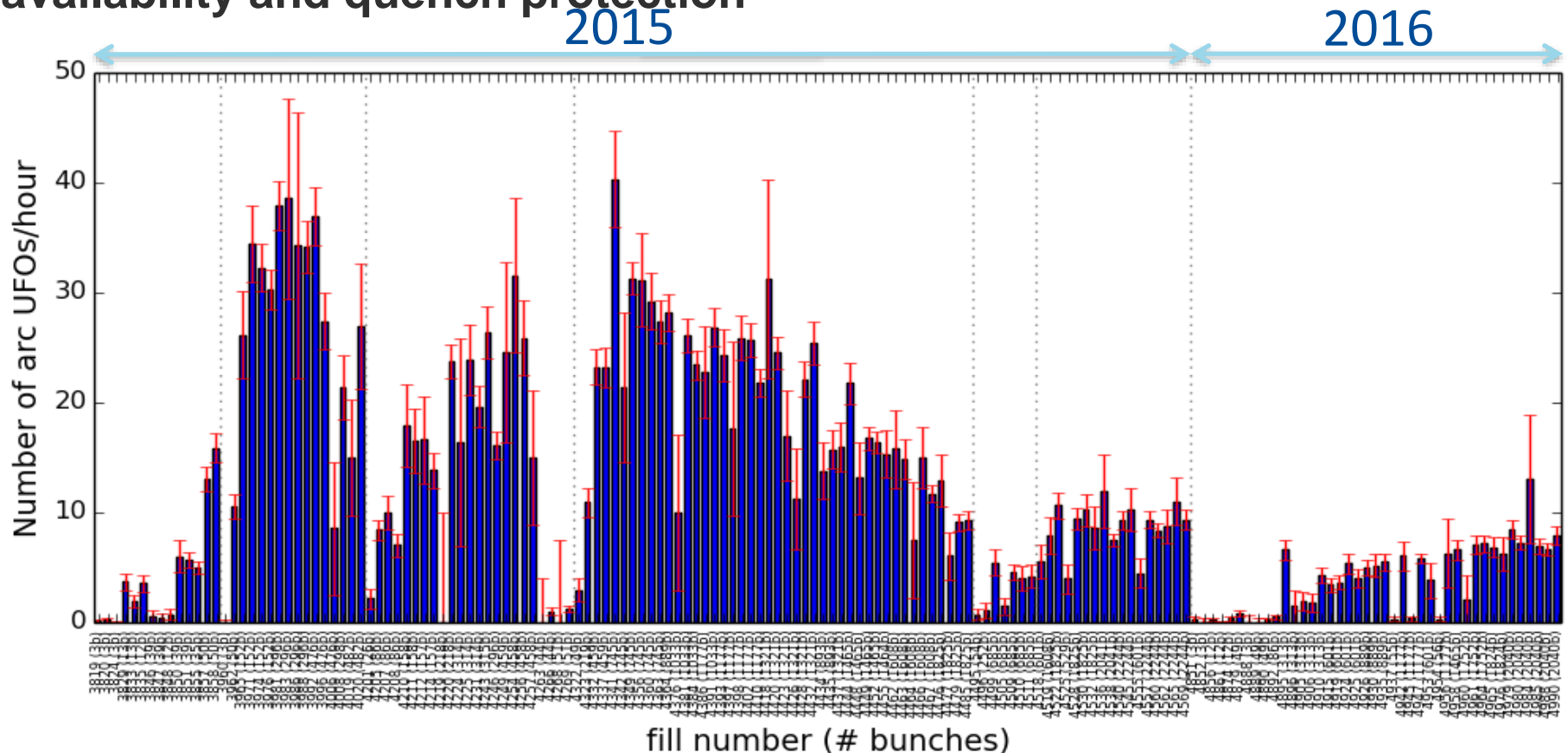


UFOs: there are many of them, they are frequent !

UFO events observed quite often during operation at 6.5 TeV

Conditioning is observed on the UFO rate in spite of the increasing number of bunches

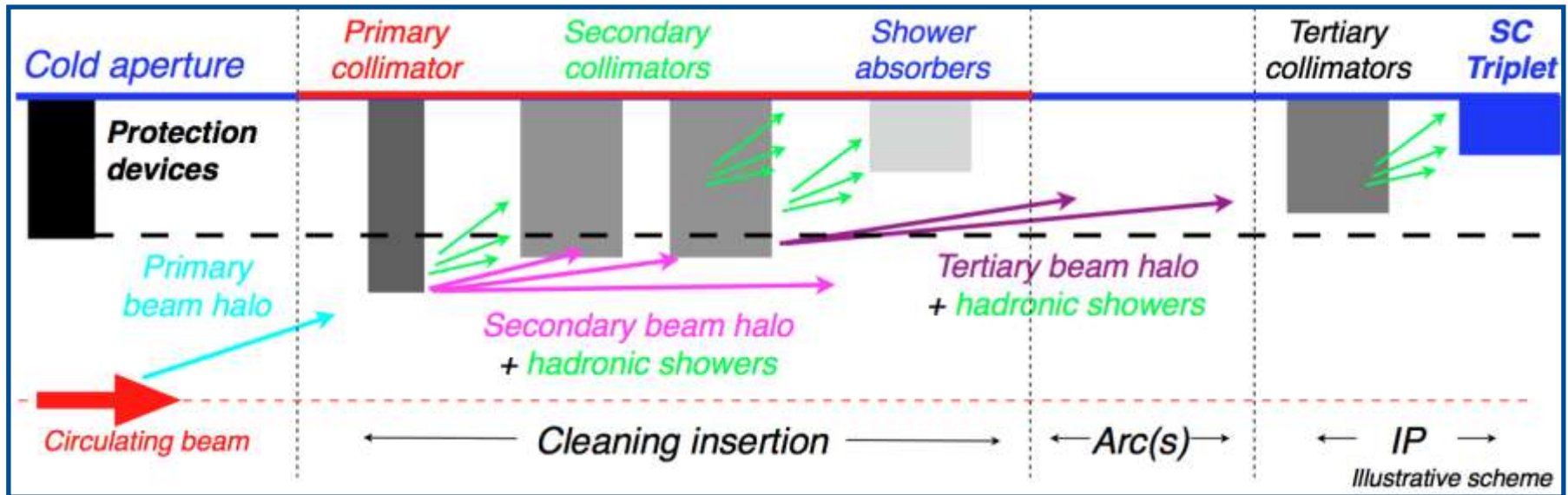
BLM thresholds being optimize to find a good compromise between availability and quench protection



- arc UFOs (cell >11): rates similar to end of 2015
 - did not lose conditioning over the Xmas stop

LHC collimation system

- LHC has **complex** and **distributed collimation** system of >100 collimators
 - several stages to protect LHC components as well as detectors



- **Collimation** is designed to provide cleaning efficiencies > 99.99%
 - need **good statistical accuracy** at limiting loss locations;
 - simulate only halo particles that interact with collimators, not the core.

LHC Collimator

- Two jaws, beam passing in between, most are 1 m long

Carbon fiber composite.

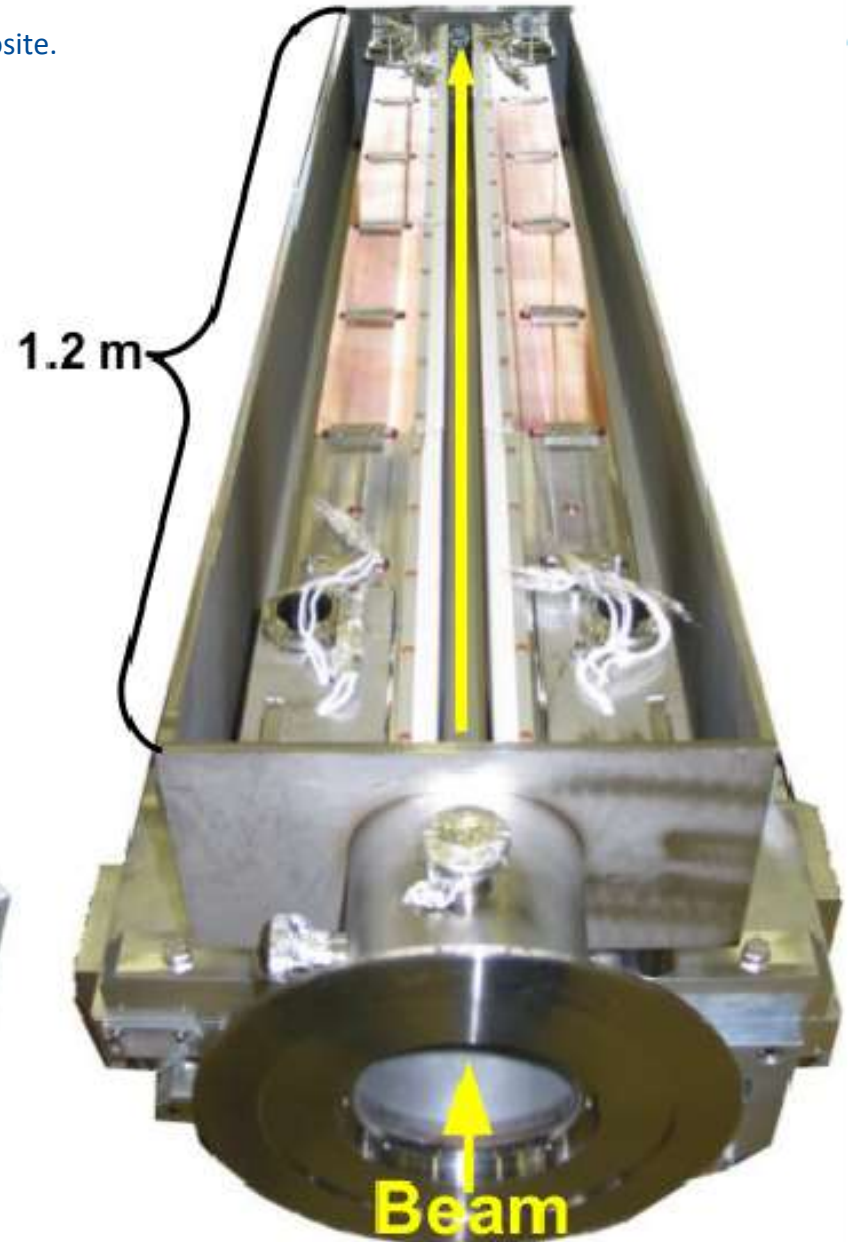
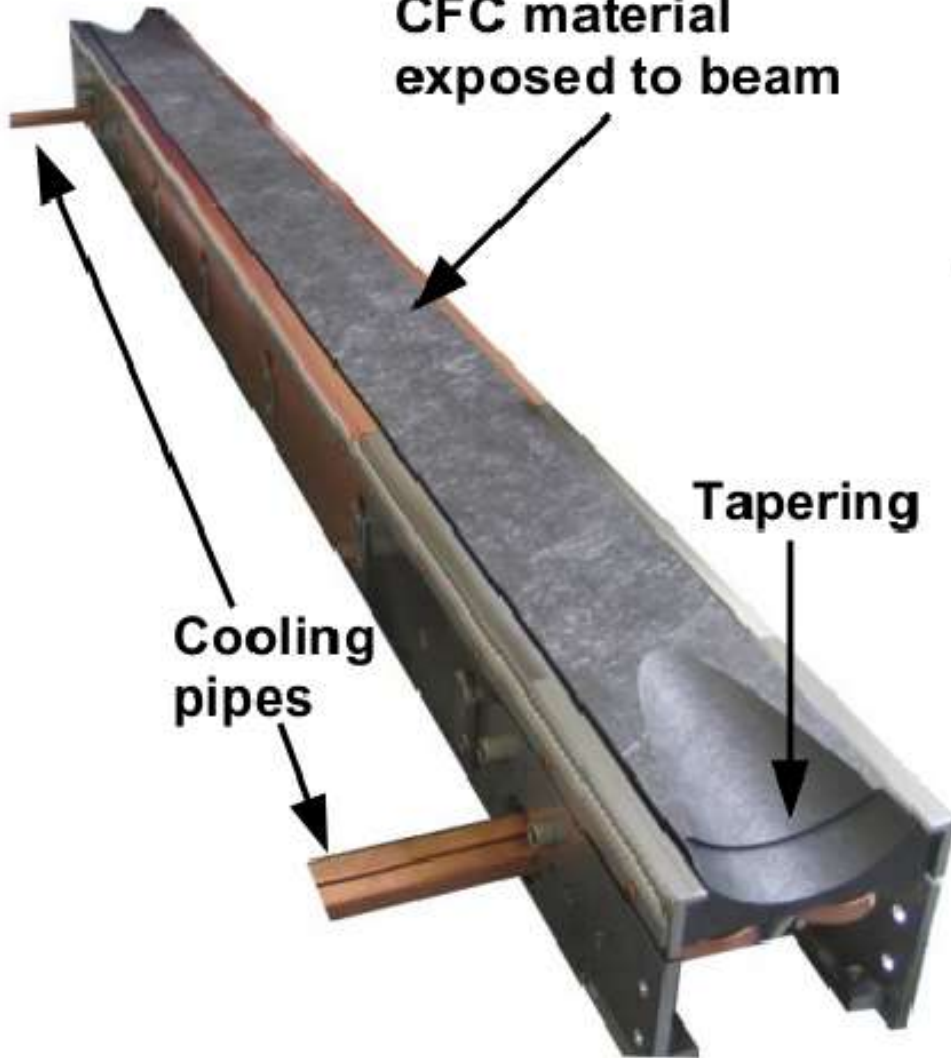
**CFC material
exposed to beam**

Tapering

**Cooling
pipes**

1.2 m

Beam



LHC Collimation System Layout

**Two warm cleaning insertions,
3 collimation planes**

IR3: Momentum cleaning

- 1 primary (H)
- 4 secondary (H)
- 4 shower abs. (H,V)

IR7: Betatron cleaning

- 3 primary (H,V,S)
- 11 secondary (H,V,S)
- 5 shower abs. (H,V)

Local cleaning at triplets

8 tertiary (2 per IP)

Passive absorbers for warm magnets

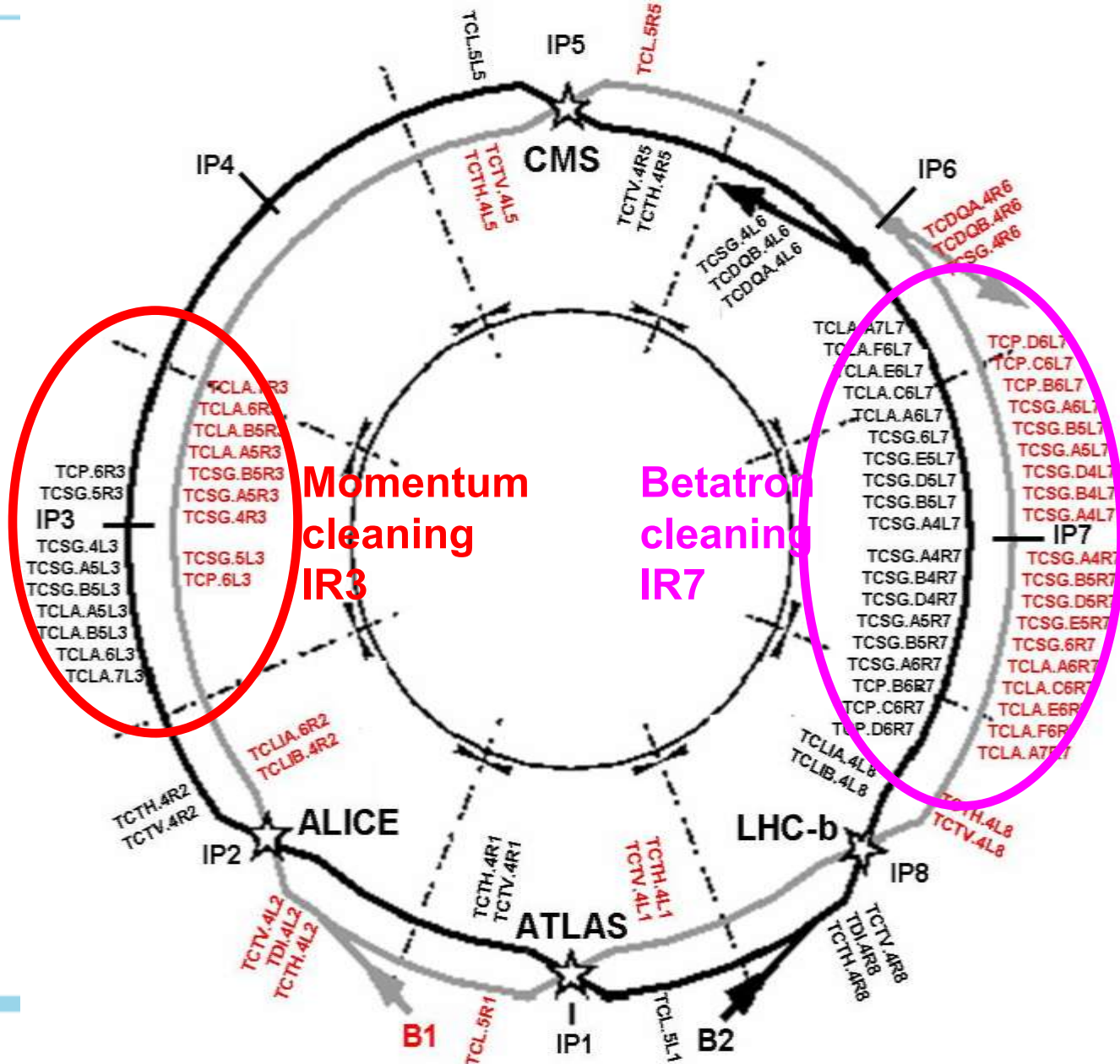
Physics debris absorbers

Transfer lines (13 collimators)

Injection and dump protection (10)

**Total of 108 collimators
(100 movable).**

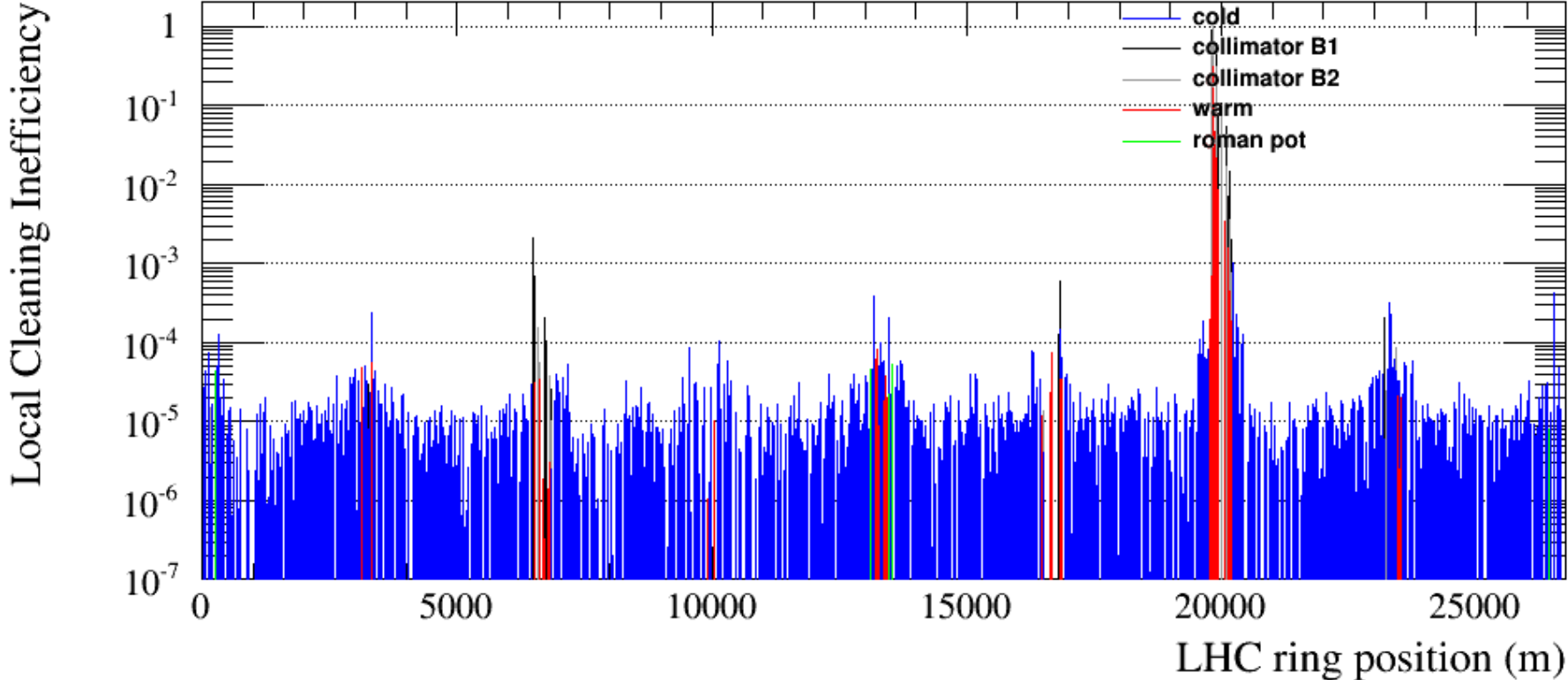
**Two jaws (4 motors)
per collimator!**



Super-Effective Halo Cleaning in LHC

- 2015

Betatron Beam 1 VER 6500GeV 2015-09-06 02:07:11



LHC Luminosity Upgrade (ca 2027): Goals

Luminosity recipe :

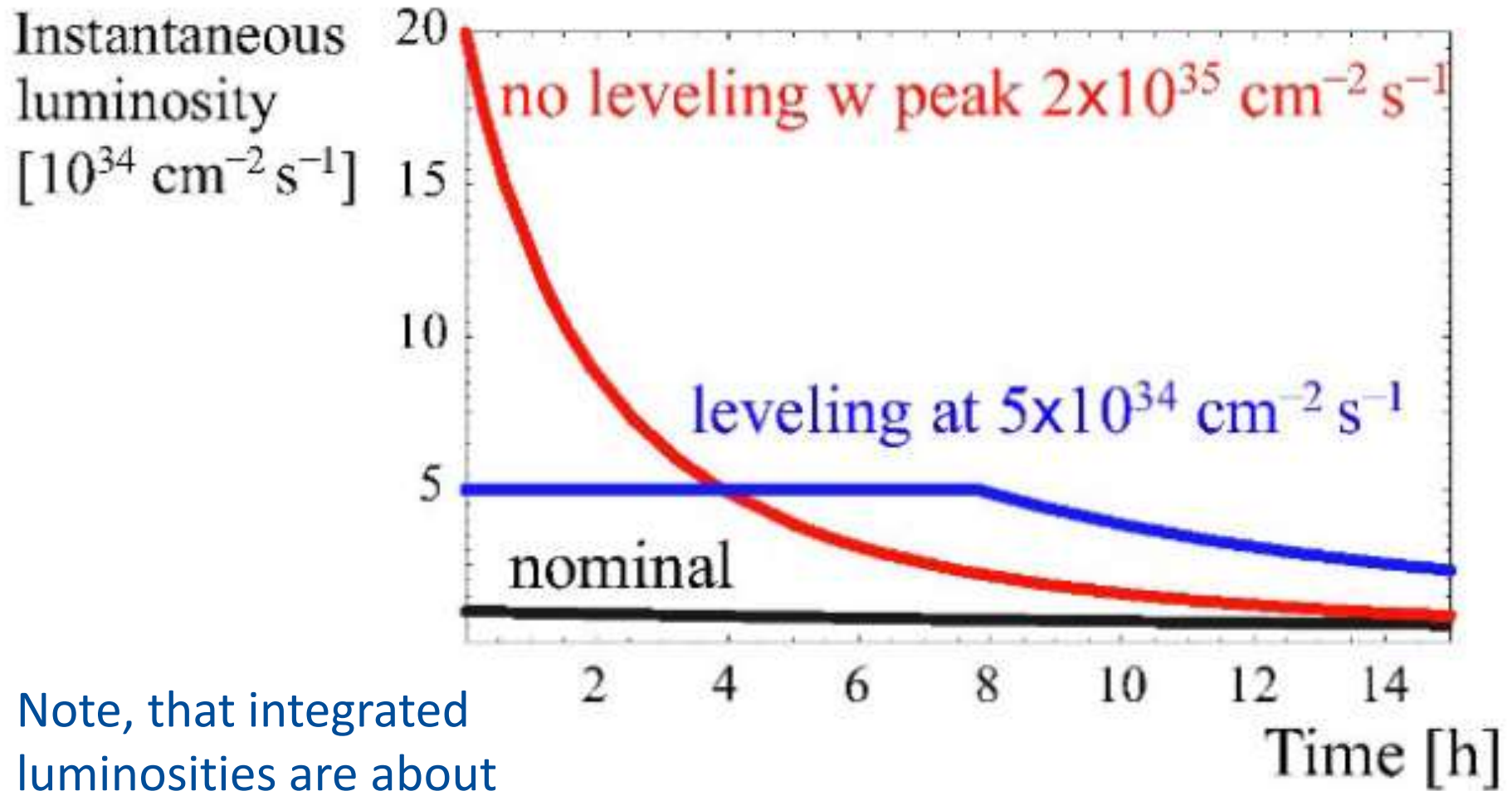
$$L = \frac{n_b \cdot N_1 \cdot N_2 \cdot \gamma \cdot f_{rev}}{4\pi \cdot \beta^* \cdot \epsilon_n} \cdot F(\phi, \beta^*, \epsilon, \sigma_s)$$

- 1) maximize bunch intensities → Injector complex **1.15 → 2.2e11**
- 2) minimize the beam emittance LIU ⇔ IBS **3.75 → 2.5 μm**
- 3) minimize beam size (constant beam power); → triplet aperture **β* 0.3 → 0.15 m**
- 4) maximize number of bunches (beam power); → 25ns **0.3 w/o Crab Cavities**
- 5) compensate for 'F'; → Crab Cavities **0.83 w. Crab Cavities**
- 6) Improve machine 'Efficiency' → minimize number of unscheduled beam aborts

With all these changes luminosity could peak at **~20e34** → 10x 2018 lumi and 10x pile up, ie $\mu > 540$ → luminosity leveling will be done at **~5e34**

HL-LHC Luminosity Leveling

-by change of the Crab-Strength or beta*

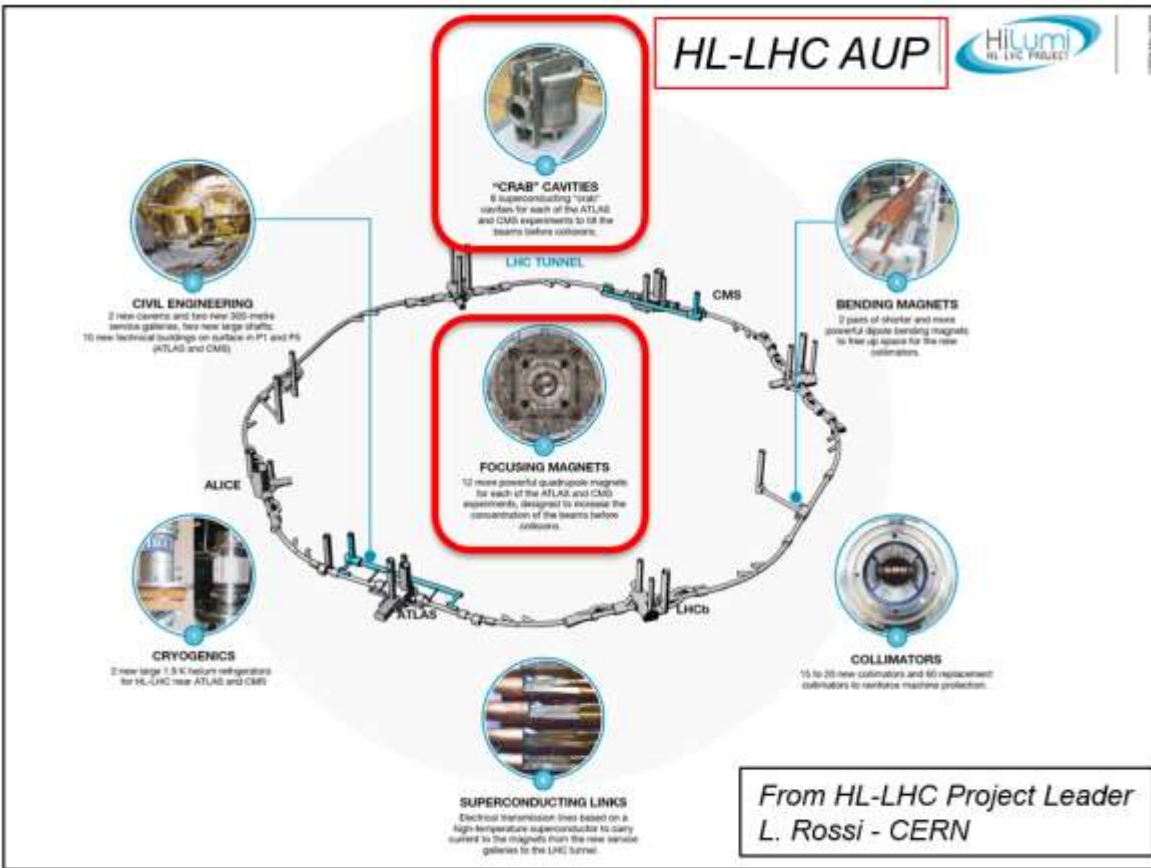


Note, that integrated luminosities are about the same in two cases

HL-LHC Scale: Hardware and Cost

The HL-LHC Project

976MCHF (-142 +208)
~2,500 man-years



- New IR-quads Nb_3Sn (inner triplets)
- New 11 T Nb_3Sn (short) dipoles
- Collimation upgrade
- Cryogenics upgrade
- Crab Cavities
- Cold powering
- Machine protection
- ...

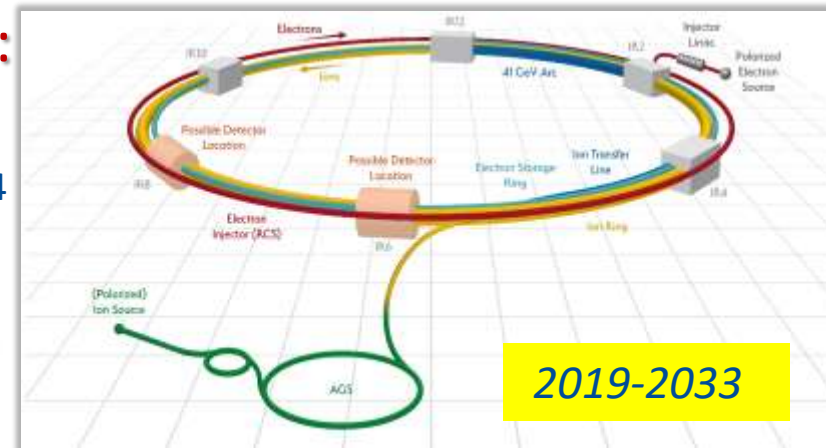
Major intervention on more than 1.2 km of the LHC

Future Hadron Colliders

NICA Collider in JINR(Dubna):
4-11 GeV cme, SC magnets; polarized
p, *d* and ions (*Au*); $L \sim 10^{27}$ w. beam
 cooling



Electron-Ion Collider EIC at BNL:
 275 GeV protons ring (RHIC) + new **10-18 GeV e- ring**, 70% polarization, $L \sim 10^{34}$
 w. cooling
 (see VP lecture 4)



Three Ideas at CERN:

High luminosity electron-proton collider LHeC
 High energy LHC (16T magnets \rightarrow 28 TeV cme)

Post-LHC: 100 TeV LHC, FCC-hh, FCC-ee, CEPC, ILC, CLIC, VCC, CERN

Other Ideas and Options for LHC

- (besides/beyond HL-LHC... ie after ~2040)
- High luminosity electron-proton collider LHeC
- **High energy LHC** (16T magnets → 28 TeV cme)
- **Injector for the future 91km ~100 TeV cme**
FCChh – see lectures VS8-9

Thanks for your Attention!

Questions !?

Literature

- V.Shiltsev, F.Zimmermann, Modern and Future Colliders (Rev.Mod.Phys., 2021)
<https://journals.aps.org/rmp/abstract/10.1103/RevModPhys.93.015006>
- V.Lebedev, V.Shiltsev, Accelerator Physics at the Tevatron Collider (Springer, 2014)
https://indico.cern.ch/event/774280/attachments/1758668/2915590/2014_Book_AcceleratorPhysicsAtTheTevatro.pdf
- S.Myers, H.Schopper, eds. Accelerator and Colliders (Springer, 2013, 2020)
<https://link.springer.com/book/10.1007/978-3-030-34245-6>
- “[Particle accelerator physics - 4th ed.](https://library.oapen.org/handle/20.500.12657/23641)” (Springer) by Wiedemann, Helmut.
<https://library.oapen.org/handle/20.500.12657/23641>
- “[Measurement and control of charged particle beams](https://library.oapen.org/handle/20.500.12657/23642)” (Springer) by Minty, Michiko G; Zimmermann, Frank
<https://library.oapen.org/handle/20.500.12657/23642>

Literature

Instabilities:

A.Chao, *Physics of collective beam instabilities in high energy accelerators* (1993)

<https://www.slac.stanford.edu/~achao/wileybook.html>

Many useful articles:

S.Myers, H.Schopper *Accelerators and Colliders* (2013, open access)

<https://link.springer.com/book/10.1007/978-3-030-34245-6>



U.S. Particle Accelerator School
Education in Beam Physics and Accelerator Technology



Colliders – Lectures VS8-9: 10+ TeV pCM colliders (hh, $\mu\mu$) Linear and Plasma Colliders

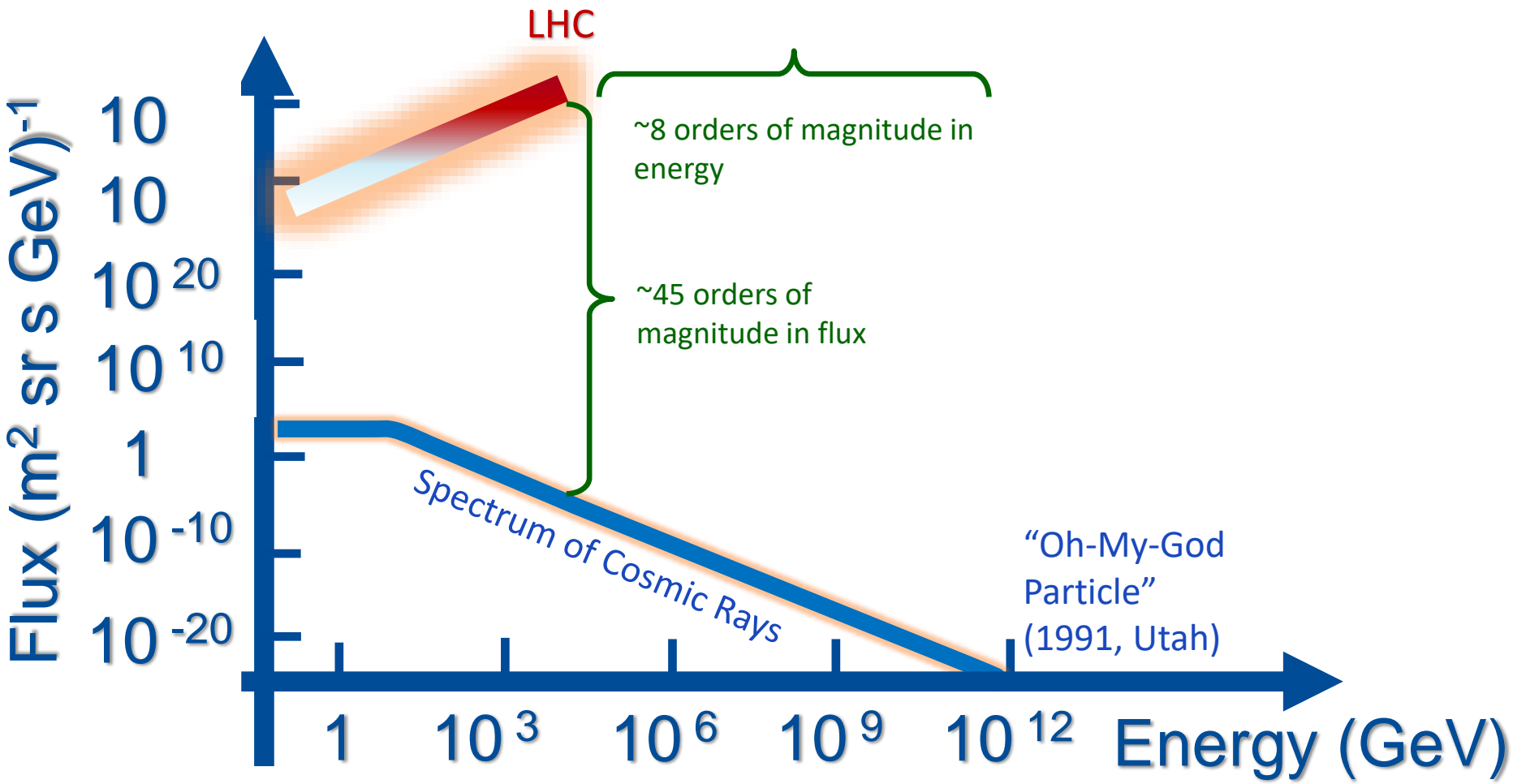
Vladimir Shiltsev, Northern Illinois University

part of the “Colliders” class by V.Shiltsev, V.Ptitsyn and C. Liu

US Particle Accelerator School, Jan 27 – Jan 31, 2025

LHC covers E_{cm} upto ~ 2 TeV... What's next?

ACCELERATORS vs COSMOS



ENERGY: Brute Force Approaches

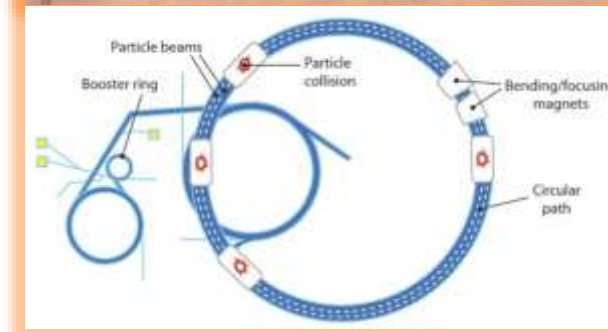
Particle Energy Increase

$$\Delta E = \text{Electric Field Gradient} \times \text{Length}$$

#1 Increase length = linac
(linear accelerator)



#2 Accelerate in a ring ($N_{\text{turns}} \Delta E$)
increase circumference as $E=0.3BR$
(synchrotrons)



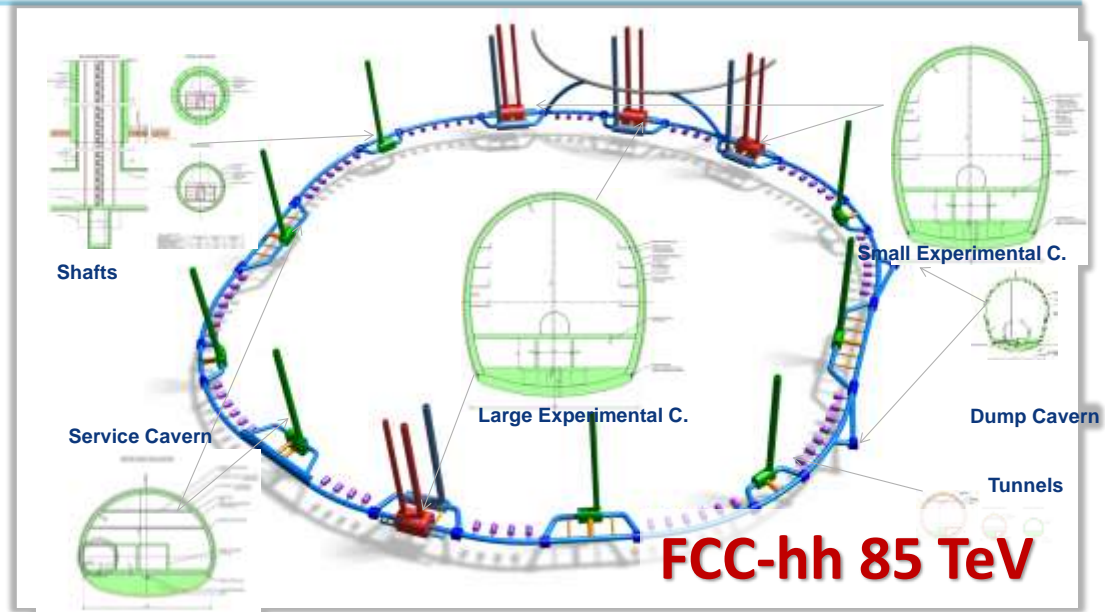
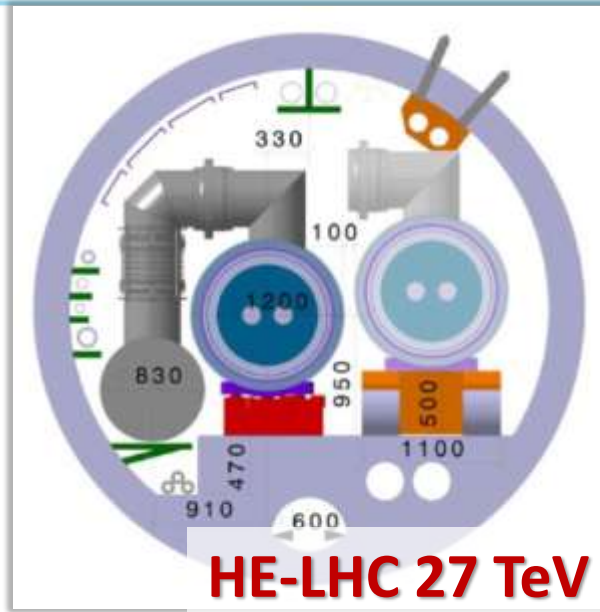
ENERGY: Three Great Ideas

#1 SuperColliders [increase $B \times R$]

#2 Different particles [to be implemented – see below]

#3 New acceleration methods [to be explored - see below]

Energy Frontier pp Colliders



Key facts: *HE-LHC / FCC-hh* / SppC**

Large tunnel – 27 / 91 / 100 km

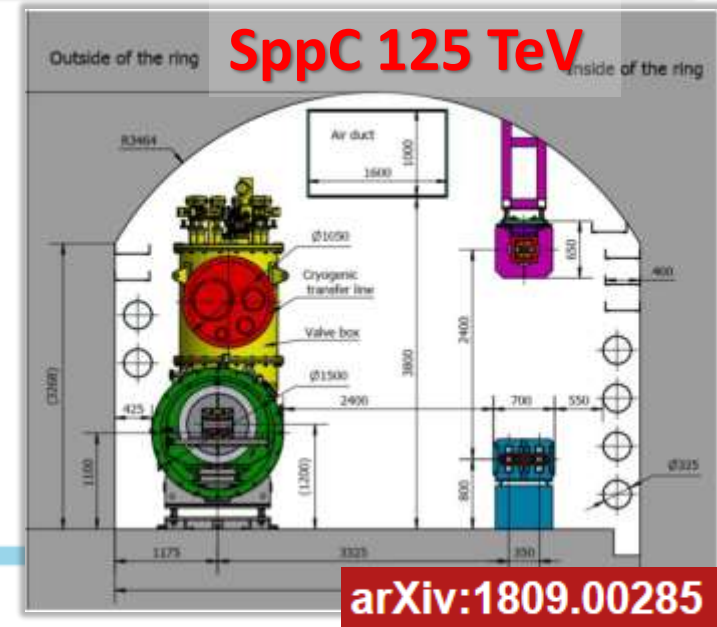
SC magnets – 16 / 14 / 20 T

High Lumi / pileup $O(10^{35})$ / $O(500)$

Site power (MW) – 200 / 500? / ?

Cost (BCHF) – 7.2 / +20*? / ?

** follow up after $e+e-$ Higgs factories*



Future pp Colliders: Parameters and Problems (1)

parameter	FCC-hh	HL-LHC	LHC
collision energy cms [TeV]	84 - 120	14	
dipole field [T]	14 - 20	8.33	
circumference [km]	90.7	26.7	
arc length [km]	76.9	22.5	
beam current [A]	0.5	1.1	0.58
bunch intensity [10^{11}]	1	2.2	1.15
bunch spacing [ns]	25	25	
synchr. rad. power / ring [kW]	1100 - 4570	7.3	3.6
SR power / length [W/m/ap.]	14 - 58	0.33	0.17
long. emit. damping time [h]	0.77 – 0.26	12.9	
peak luminosity [10^{34} cm ⁻² s ⁻¹]	~30	5 (lev.)	1
events/bunch crossing	~1000	132	27
stored energy/beam [GJ]	6.3 – 9.2	0.7	0.36
Integrated luminosity/main IP [ab^{-1}]	20	3	0.3

Reminder from Lecture 1: Key is Current *Density*

Scaling:

$$B_{max} \sim J/A_{aperture}$$

Assume all aperture A is filled with conductor \rightarrow max current is

$$J \sim j(\text{current density}) \cdot A^2$$

thus :

$$B_{max} \sim j \cdot A$$

but **Cost** $\sim A/j$ ($=A^2 \cdot \text{length}$ = cost of needed conductor)

Therefore, high(est) current density is needed to maximize B -field and minimize **Cost**

- For room temperature copper $j \sim (1-10) \text{ A/mm}^2$
- For superconductors \rightarrow kA/mm^2

Low Temperature Superconductors (LTS)

- Nb-Ti @ 1.8K

~10 T

- Plenty of experience
- May be able to increase practical field a little
- Large industrial capacity

- High Performance Nb₃Sn

~14-16 T

- Fields up to 16T in dipole configuration, but challenging
- Strain sensitive
- No significant industrial capacity
- Not inexpensive

But is that a “practical” limit?

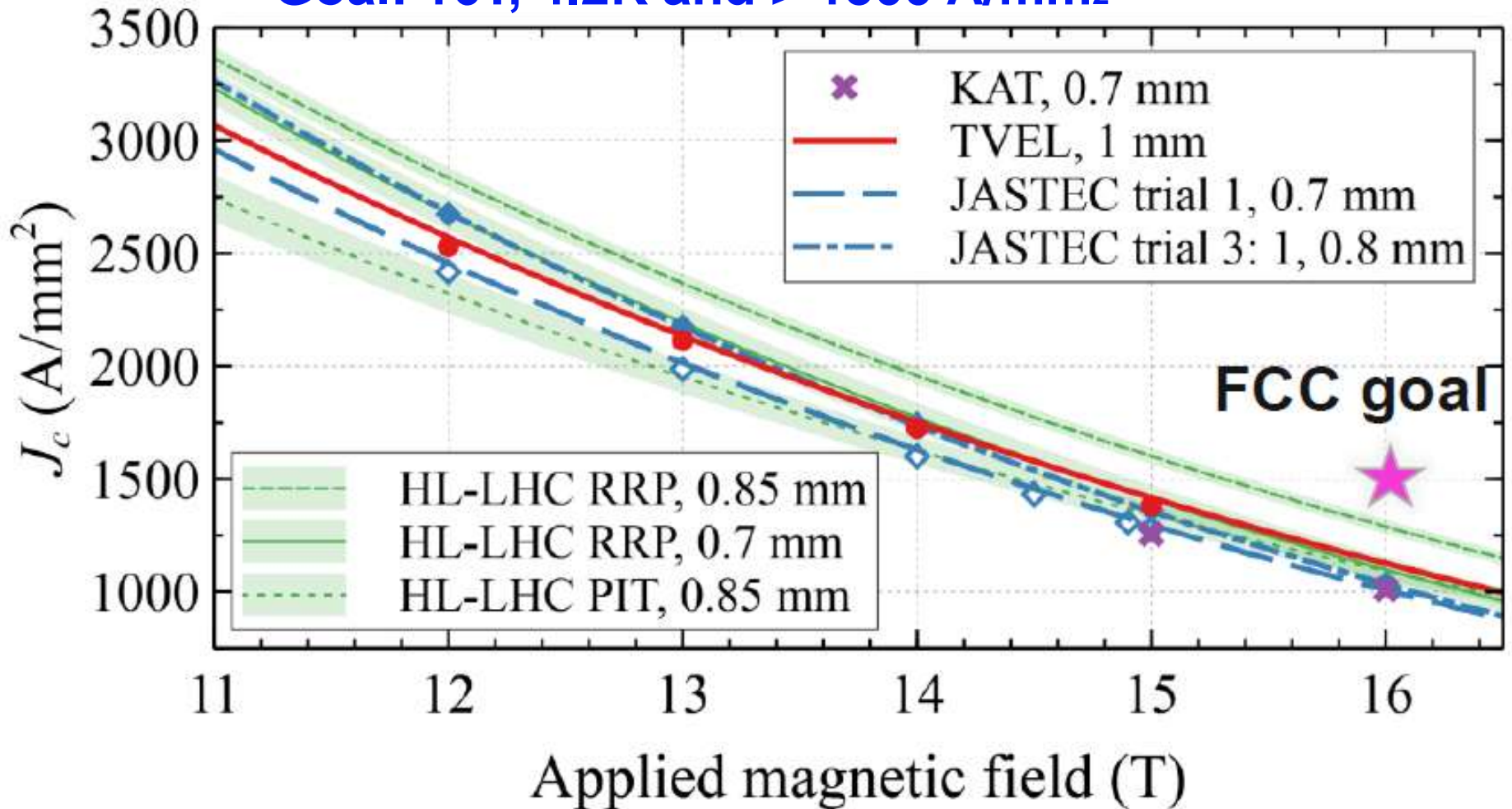
- Iron-Based Superconductor (IBS)

High risk, high potential payoff
Still much work to be done

- High field, low cost, better mechanical properties
- Successful conductor could lead to commercial demand

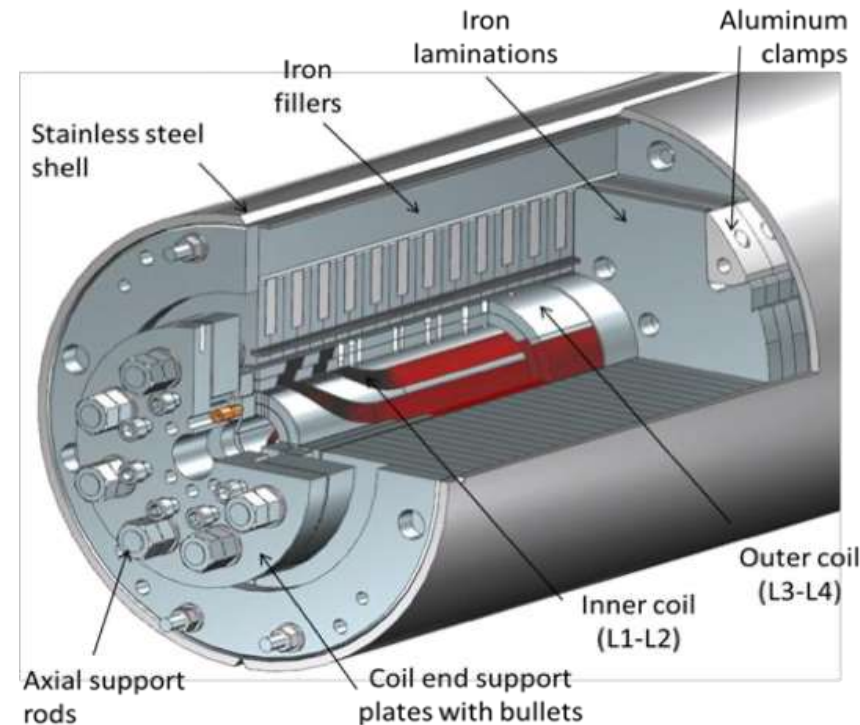
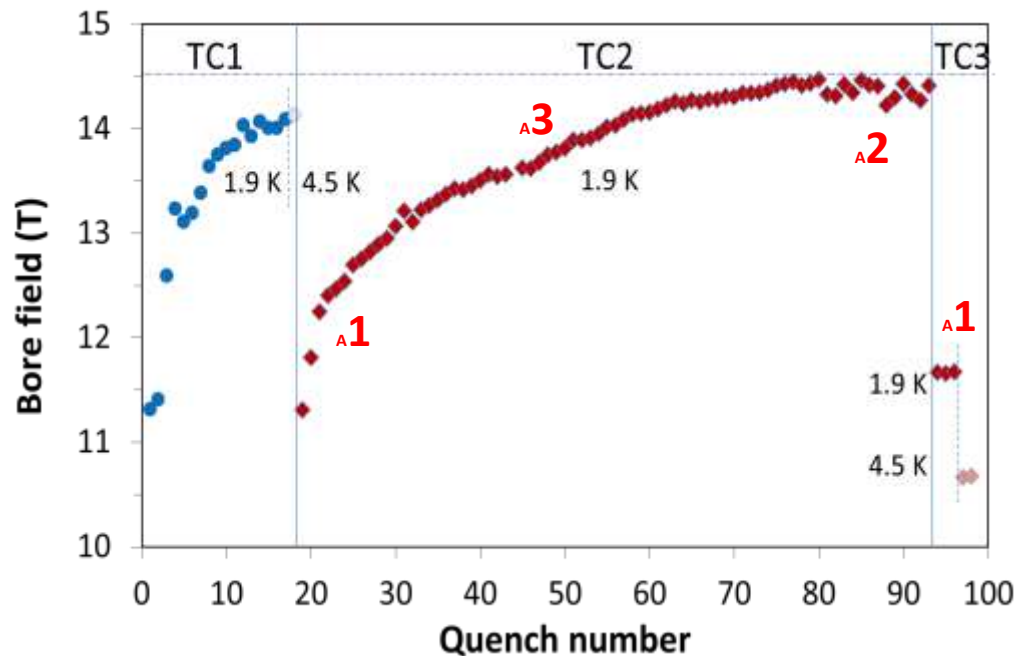
Nb3Sn Conductor R&D for FCCChh

Goal: 16T, 4.2K and $> 1500 \text{ A/mm}^2$



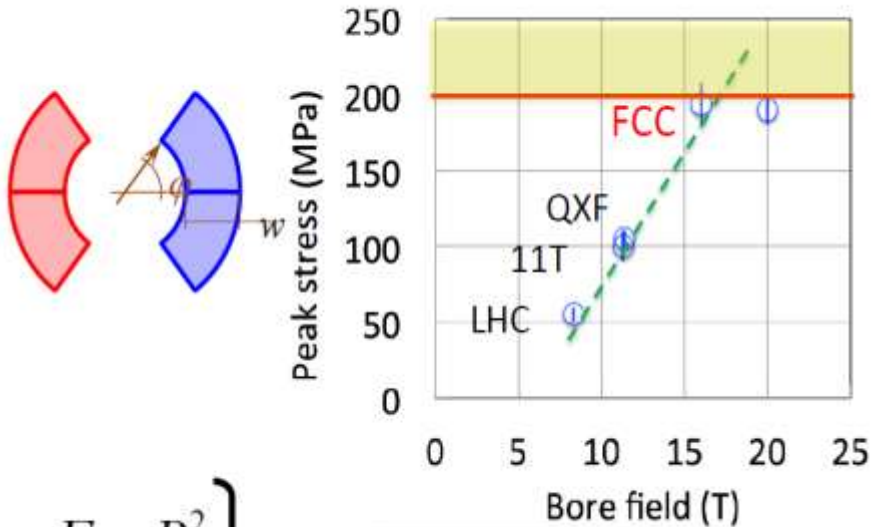
Challenges and lessons of Nb₃Sn (Hint, it's stress!!)

- MDP 15T project
 - MDPCT achieved 14.5 T at 1.9K...Degradation on subsequent thermal cycle
 - To avoid wire movements – need pre-stress ~150 Mpa
 - Field pressure scaling $P=B^2/2\mu_0$



Courtesy, A. Zlobin, FNAL

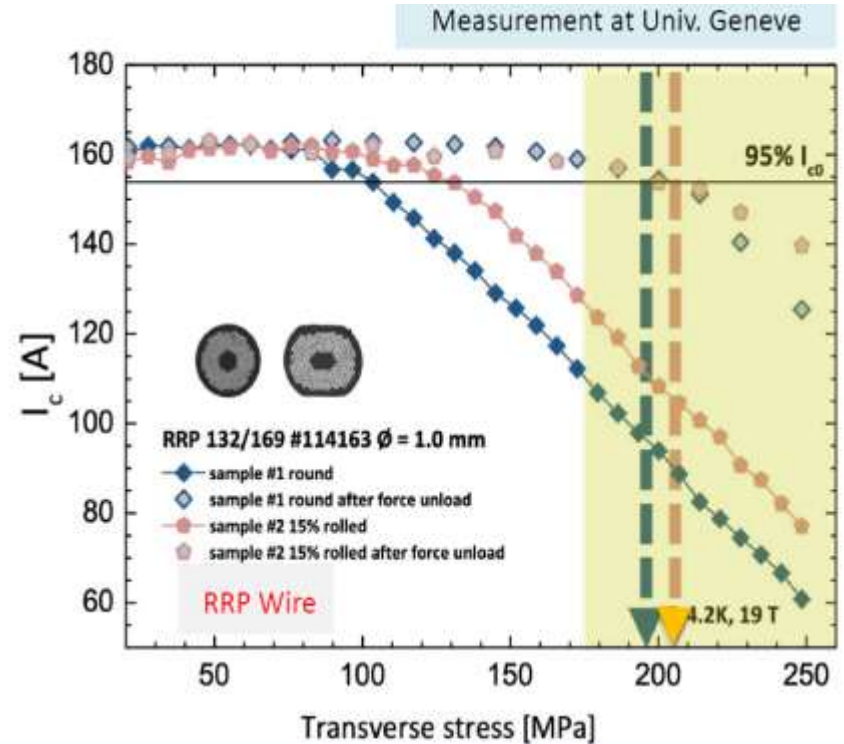
On Mechanical Stress Limit



$$\left. \begin{array}{l} F \propto B^2 \\ w \propto \frac{B}{J} \end{array} \right\} \rightarrow \sigma \propto \frac{F}{w} \propto JB$$

or

$$\rho \sim B^2$$



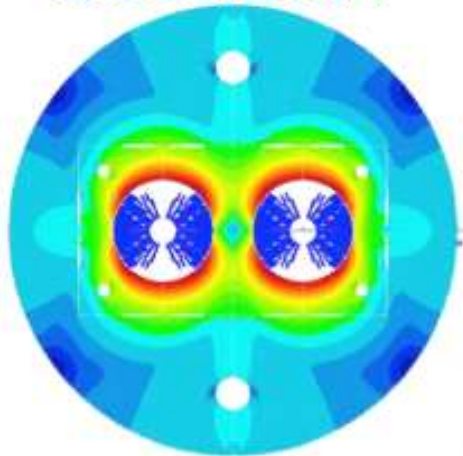
Attention, I_c (J_c) reduction:

- reversible at <150 MPa (~15% at 11.6 T),
- irreversible at >170 MPa.

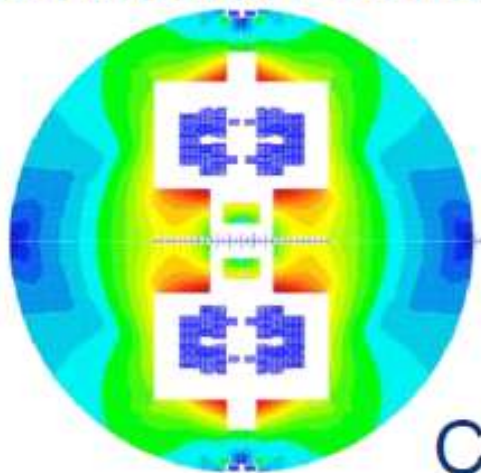
as a critical constraint because of fundamental mechanical property.

Several Design Approaches: FCChh

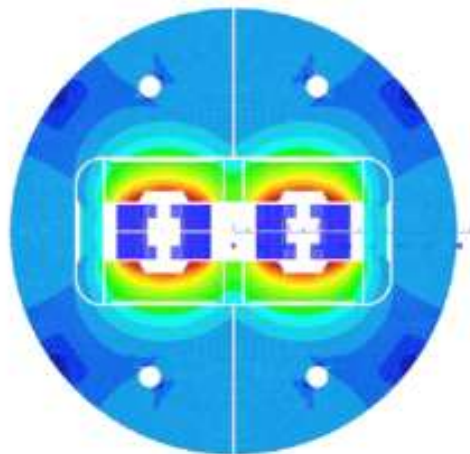
Cos-theta



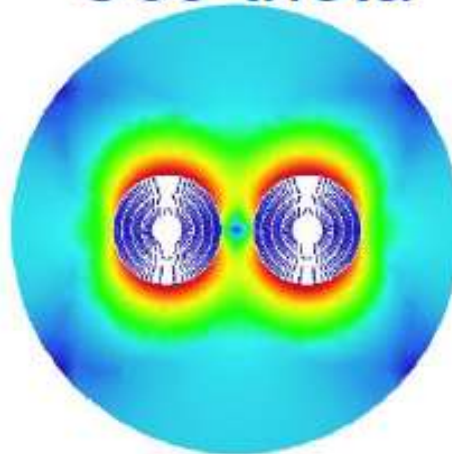
Common coils



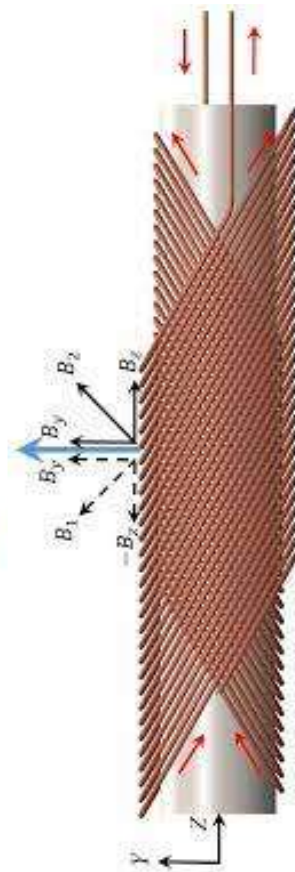
Blocks



Canted
Cos-theta



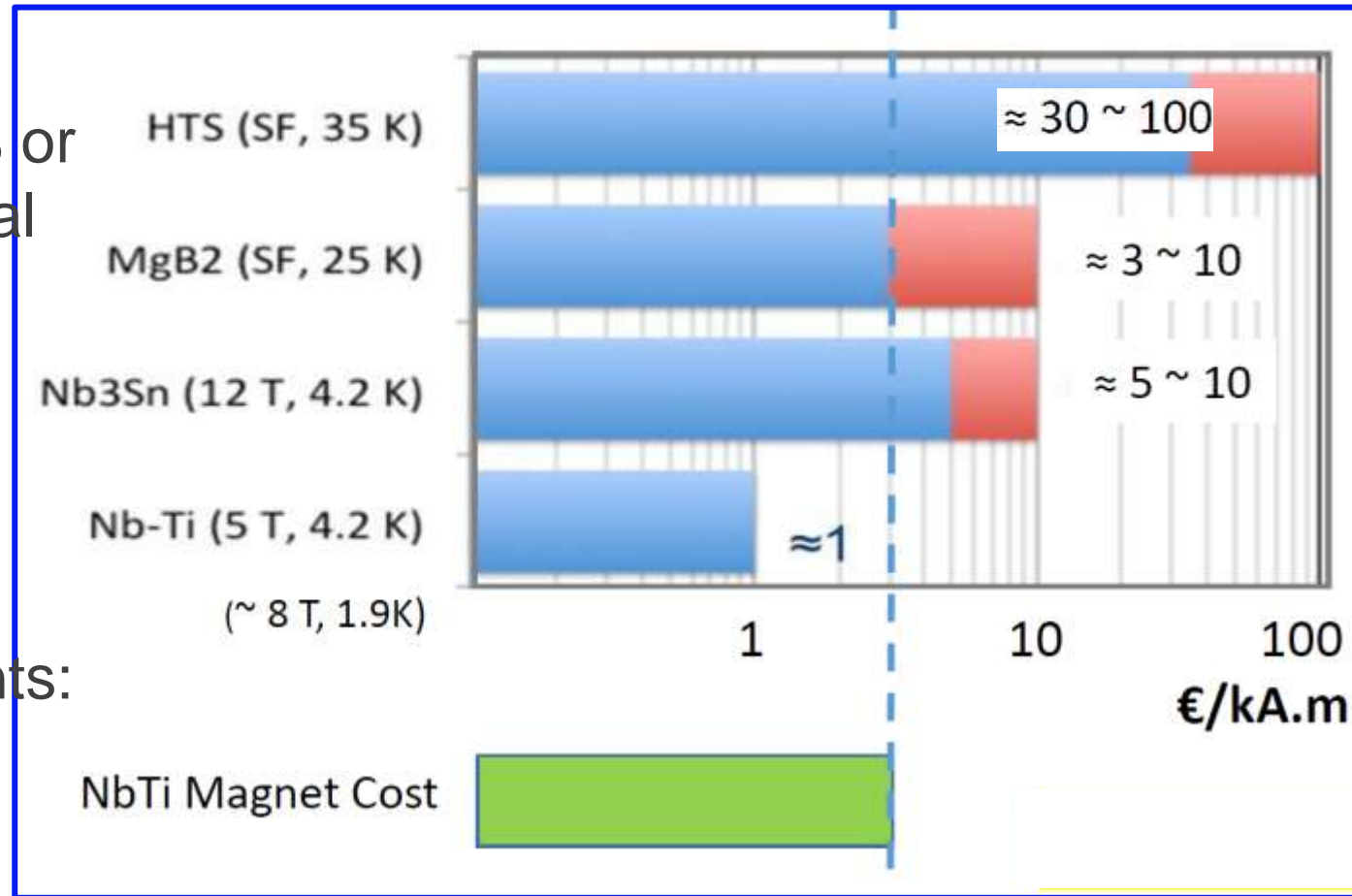
Worldwide short
model magnet
R&D → various coil
geometries (2018
–2025)



CEA,
CIEMAT,
INFN, PSI,
FNAL, LBNL,
BINP

Cost (... most important factor?)

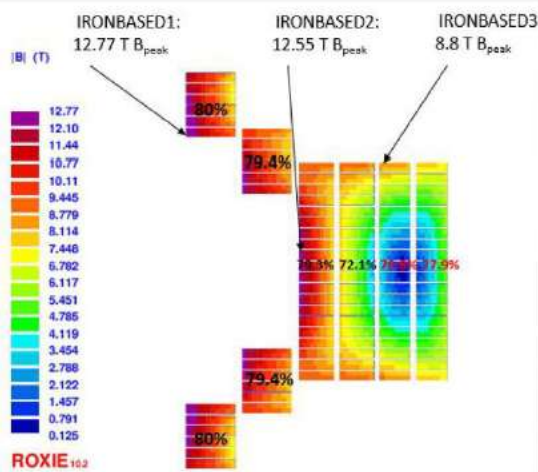
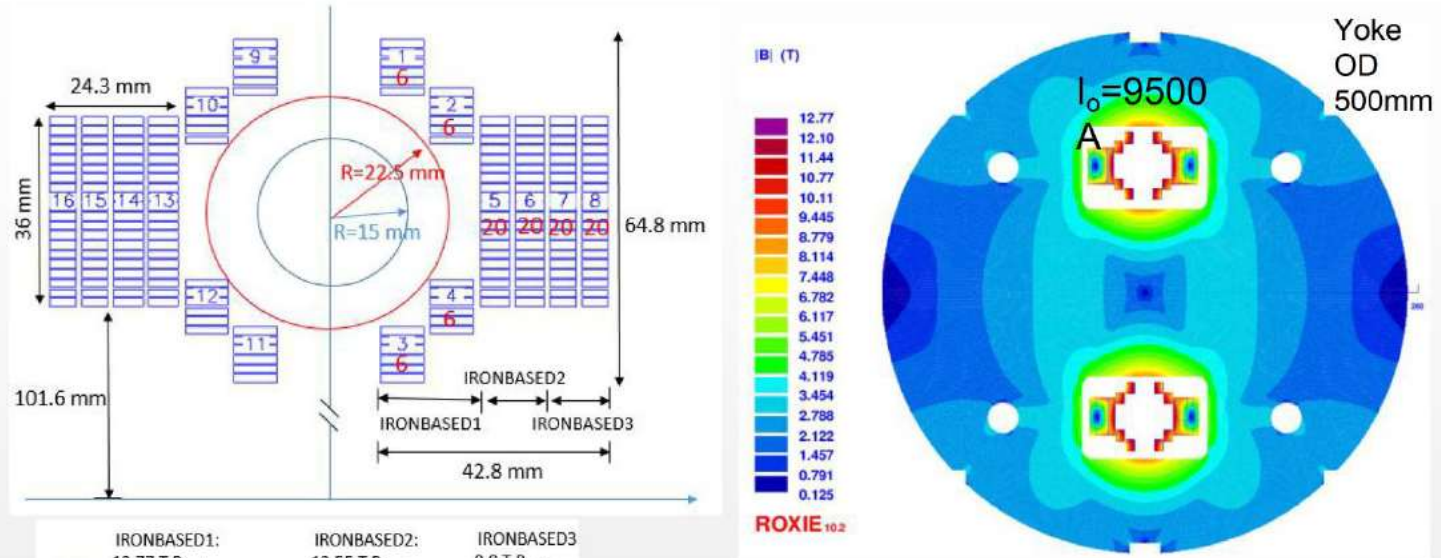
- Cost of the magnets ~50% or more of the total collider cost (~30+B\$)
- For the LHC dipoles three approx. equal cost components:
 - Cost of conductor
 - Cost of labor
 - Cost of structure



(Rough) cost of conductor per kA·m **IBS : NbTi : Nb3Sn : HTS**
 now **0.25(?) : 1 : 5 : 30**

IBS Magnet R&D in China

The 12-T Fe-based Dipole Magnet



Design with expected J_e of IBS in 2025

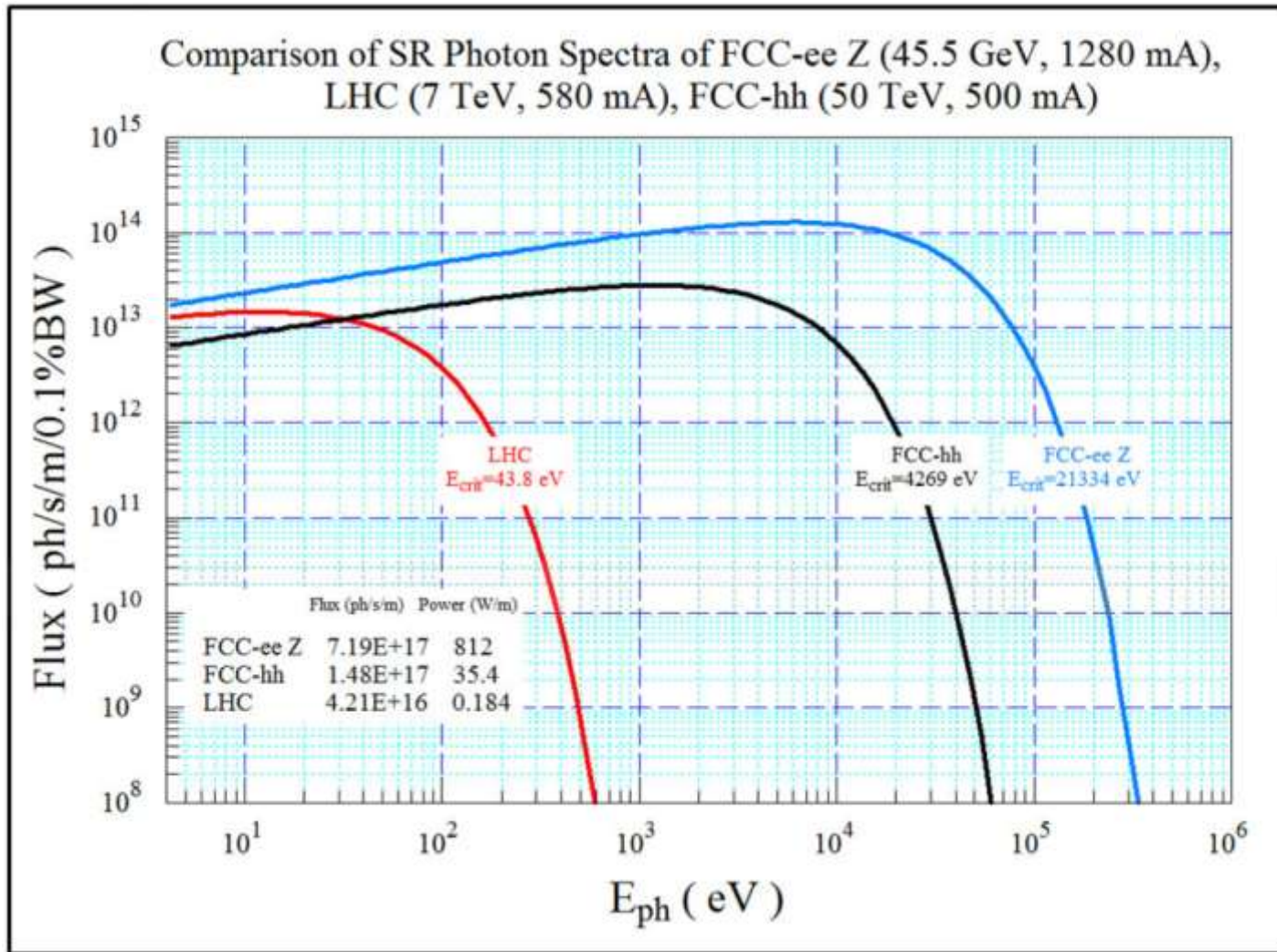
Strand	diam.	cu/sc	RRR	Tref	Bref	Jc@ BrTr	dJc/dB
IBS	0.802	1	200	4.2	10	4000	111

- For 100-km SPPC, **3000 tons of IBS** is needed
- Target cost of IBS: **20 RMB /kAm @12 T**
- Total cost for IBS conductors: **~10B RMB**

Future pp Colliders: Parameters and Problems (2)

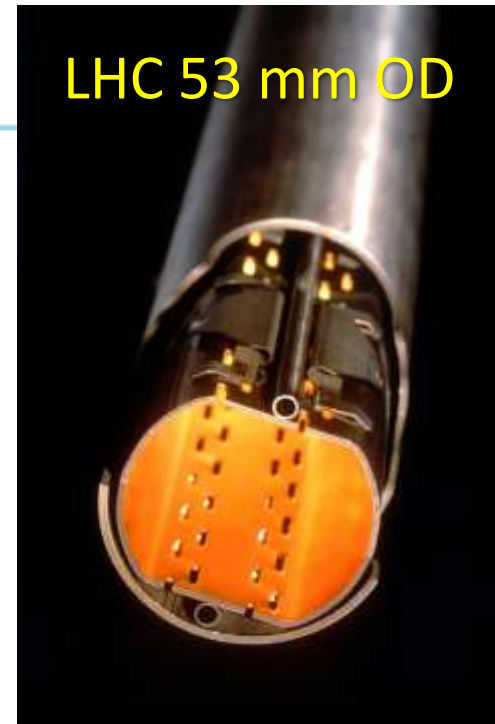
parameter	FCC-hh	HL-LHC	LHC
collision energy cms [TeV]	84 - 120	14	
dipole field [T]	14 - 20	8.33	
circumference [km]	90.7	26.7	
arc length [km]	76.9	22.5	
beam current [A]	0.5	1.1	0.58
bunch intensity [10^{11}]	1	2.2	1.15
bunch spacing [ns]	25	25	
synchr. rad. power / ring [kW]	1100 - 4570	7.3	3.6
SR power / length [W/m/ap.]	14 - 58	0.33	0.17
long. emit. damping time [h]	0.77 - 0.26	12.9	
peak luminosity [10^{34} cm ⁻² s ⁻¹]	~30	5 (lev.)	1
events/bunch crossing	~1000	132	27
stored energy/beam [GJ]	6.3 - 9.2	0.7	0.36
Integrated luminosity/main IP [ab^{-1}]	20	3	0.3

Synchrotron Radiation of Protons

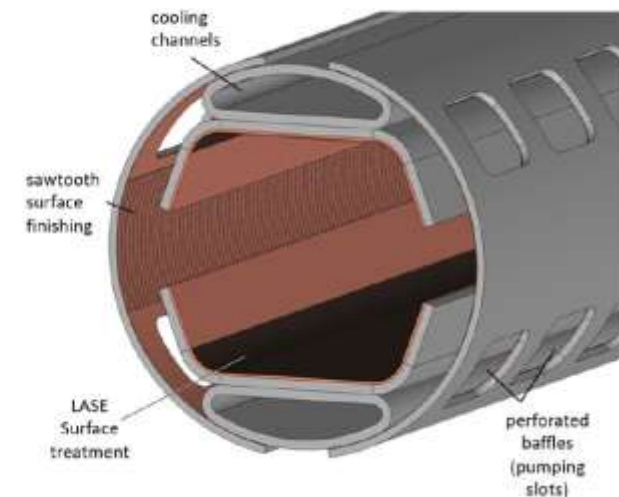
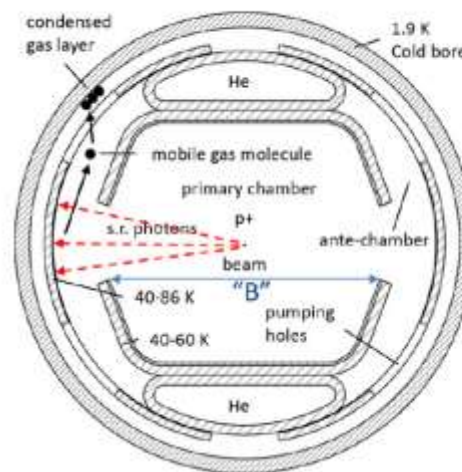


Intercept 1-5MW of SR

- While the linear photon flux for FCC-hh is only a factor of 3.5 times higher than that of LHC, the linear SR power density at 50 TeV is almost 200 times higher, ruling out a scaled version of the LHC beam-screen.
- Calculations have ruled out the possibility of using LHC-sized capillaries (<4 mm) because the supercritical helium flow rate would not be sufficient. The required number of pumping slots would also affect the impedance budget too much .

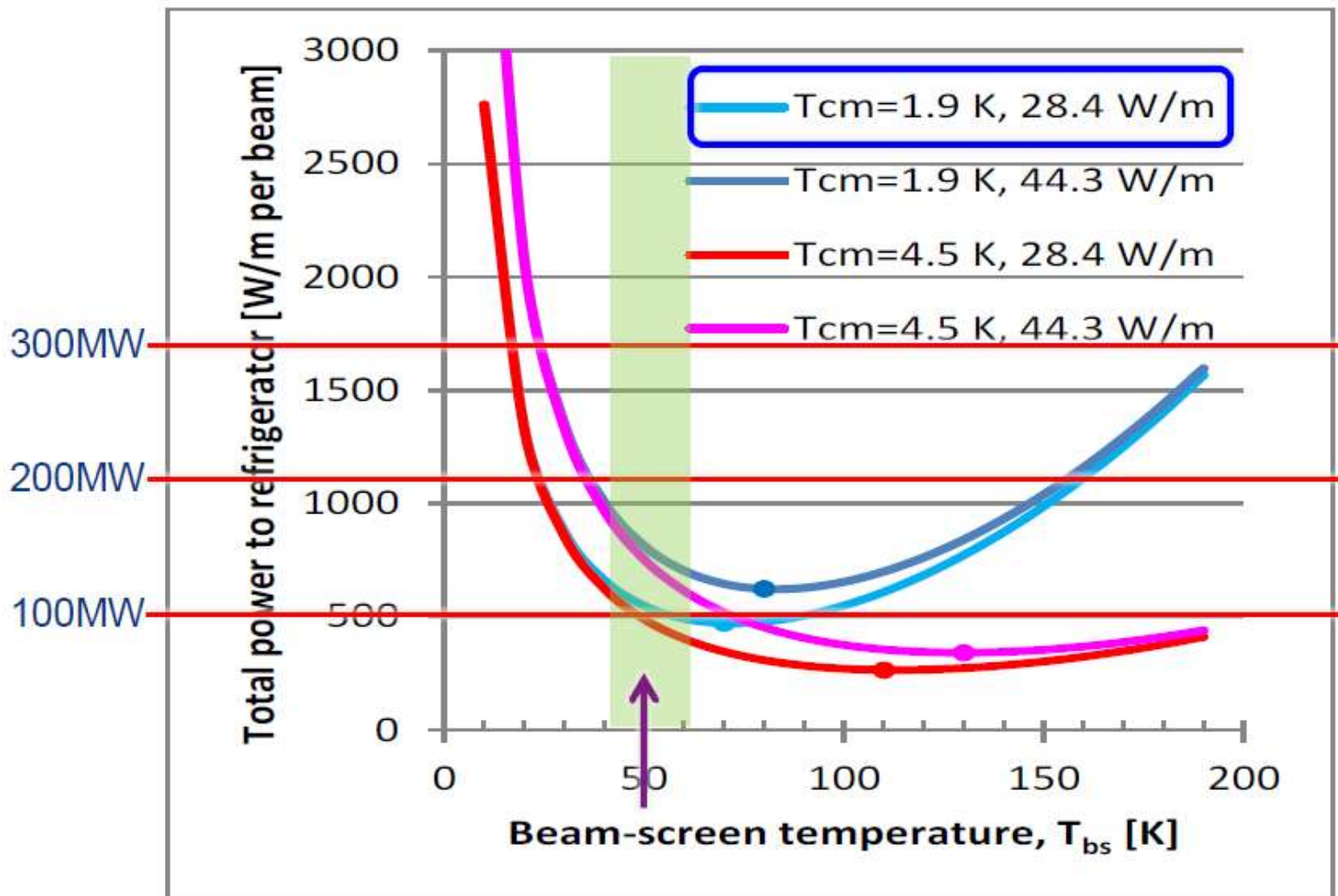


- **New type of beam pipe:**
 - Low impedance
 - Good pumping conductivity
 - Intercept SR photons at 50K
 - Avoid build up of e-cloud (a-C coating or LASE grooves)
 - Low th-conductivity 50K→2K

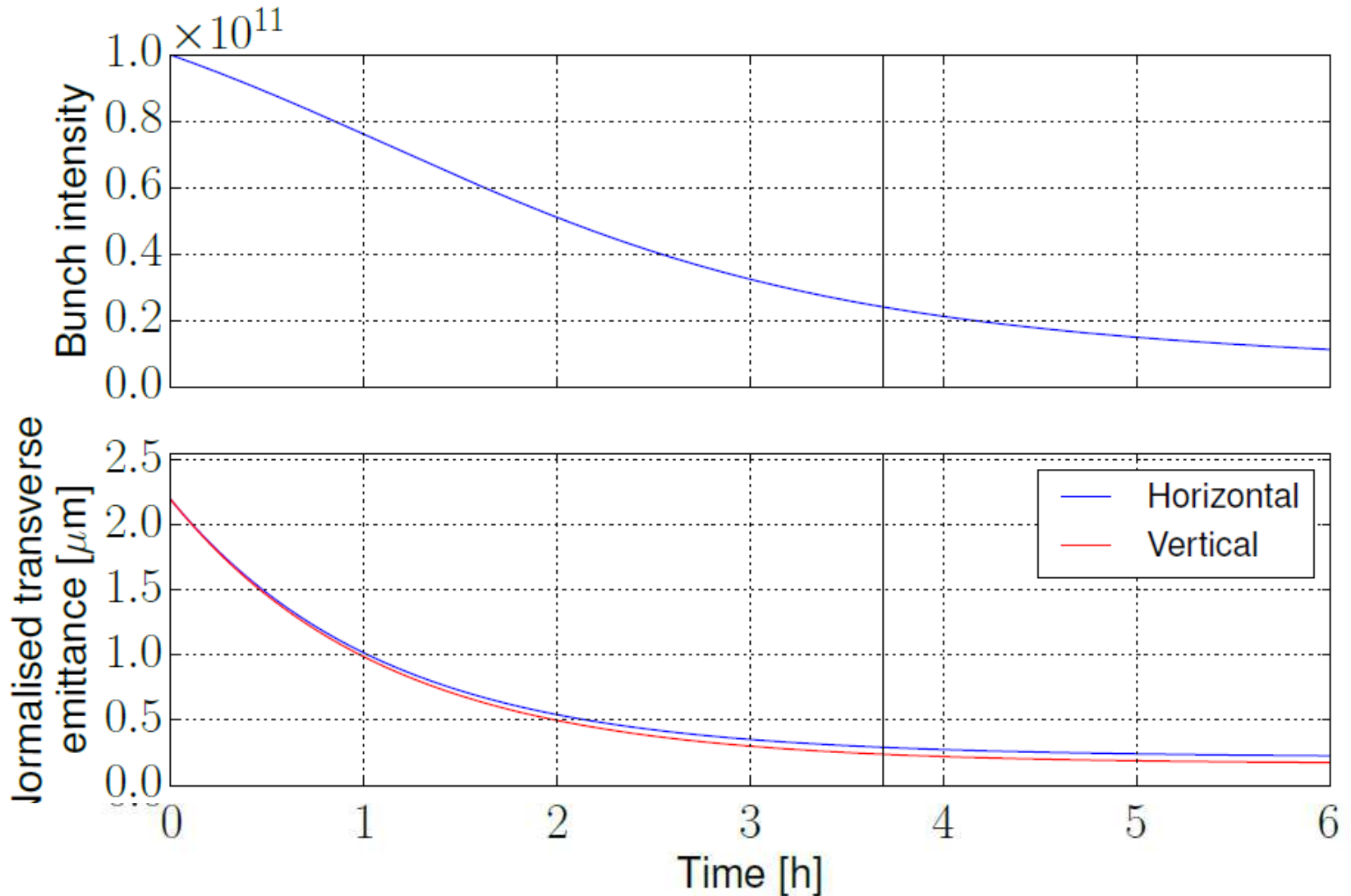


Synchrotron Radiation of Protons

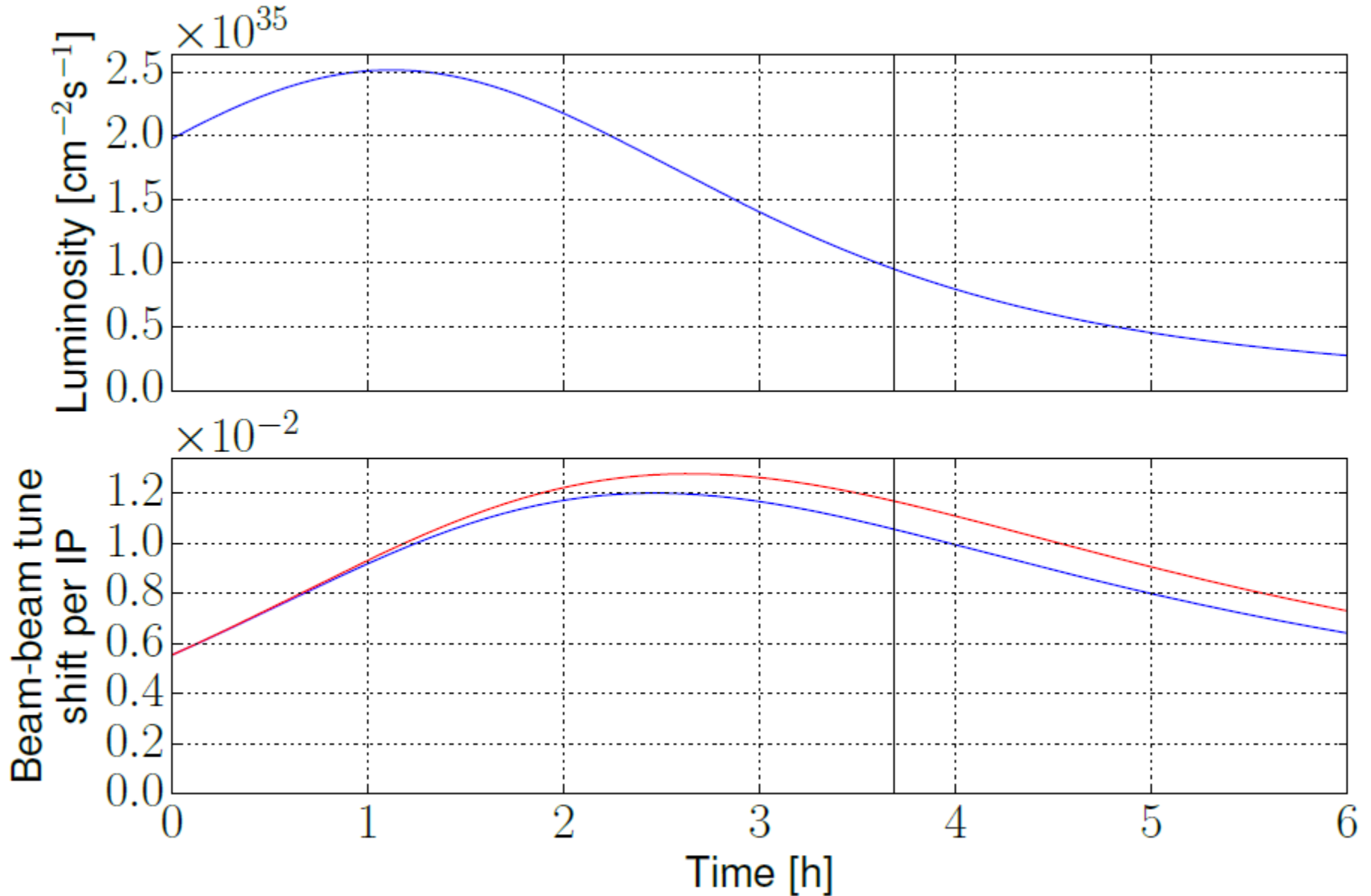
Overall optimization of cryo-power, vacuum and impedance. Contributions: beam screen (BS) & cold bore (BS heat radiation). Vacuum pumping prefers higher T. Optimum 50-100 K but impedances grow with T \rightarrow so, 50 K



“Good side” of Synchrotron Radiation



SR Cooling \rightarrow Luminosity Growth!



Future pp Colliders: Parameters and Problems (3)

parameter	FCC-hh	HL-LHC	LHC
collision energy cms [TeV]	84 - 120	14	
dipole field [T]	14 - 20	8.33	
circumference [km]	90.7	26.7	
arc length [km]	76.9	22.5	
beam current [A]	0.5	1.1	0.58
bunch intensity [10^{11}]	1	2.2	1.15
bunch spacing [ns]	25	25	
synchr. rad. power / ring [kW]	1100 - 4570	7.3	3.6
SR power / length [W/m/ap.]	14 - 58	0.33	0.17
long. emit. damping time [h]	0.77 - 0.26	12.9	
peak luminosity [$10^{34} \text{ cm}^{-2}\text{s}^{-1}$]	~30	5 (lev.)	2
events/bunch crossing	~1000	132	54
stored energy/beam [GJ]	6.3 - 9.2	0.7	0.36
Integrated luminosity/main IP [ab^{-1}]	20	3	0.3

“Pile Up”

Protons break protons

Too many events per crossing (interaction)

Makes it hard to detect and analyze

$$\text{Rate} \rightarrow R = L\sigma$$

Luminosity

Cross-section
("physics")

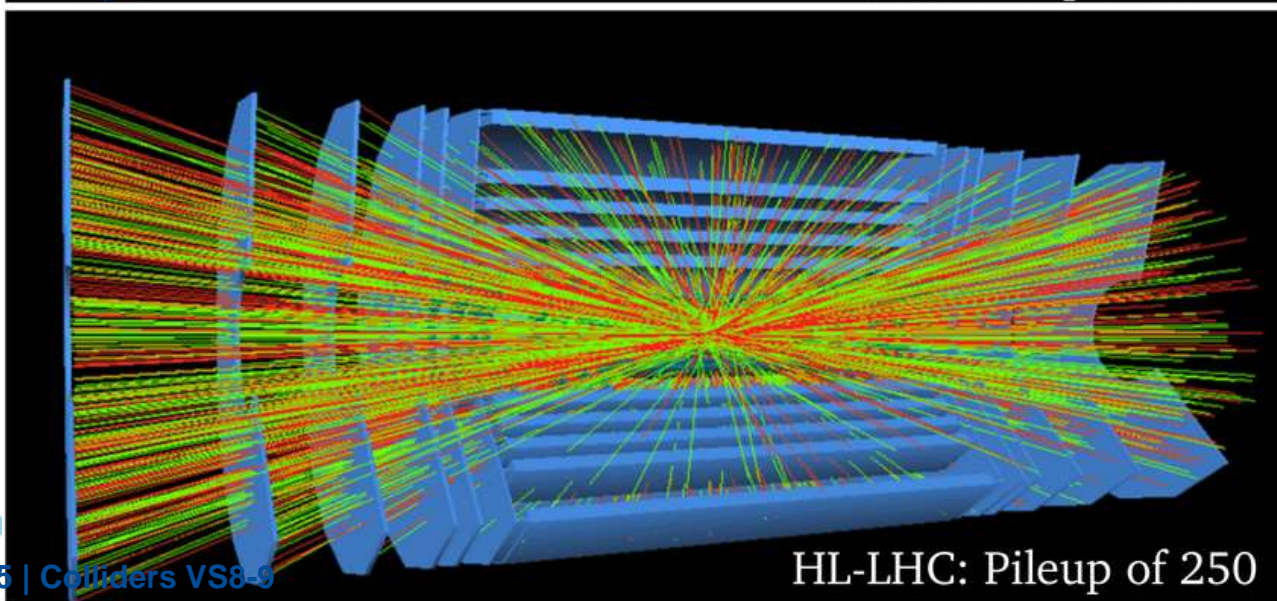
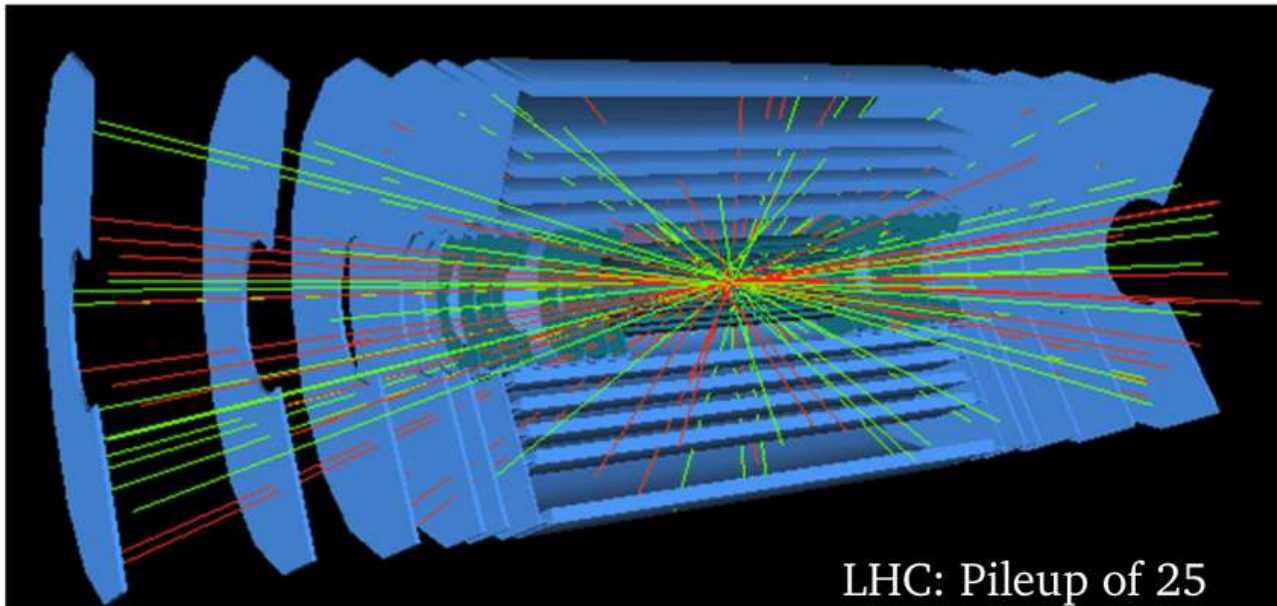
Example: LHC Luminosity is $2 \times 10^{34} \text{ cm}^{-2}\text{s}^{-1}$

p - p inelastic cross section at 13.6 TeV cme is ~ 82 mbarn
(1mbarn = $1 \times 10^{-27} \text{ cm}^{-2}$) $\rightarrow R = 1.64$ billion per second

in ~ 2800 bunches crossings per turn, 11000 turns per sec \rightarrow

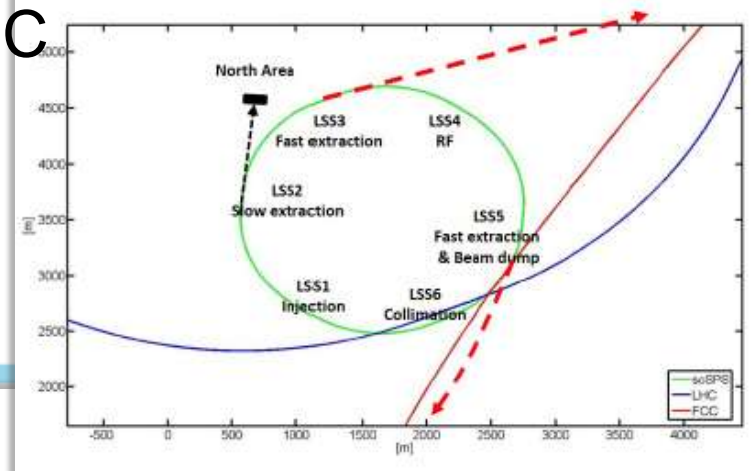
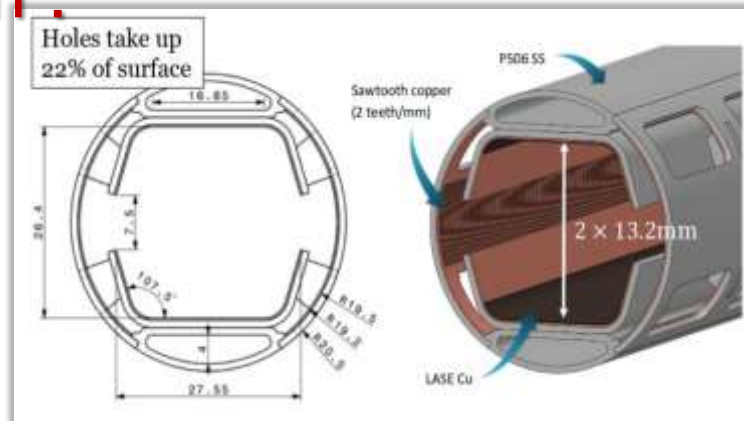
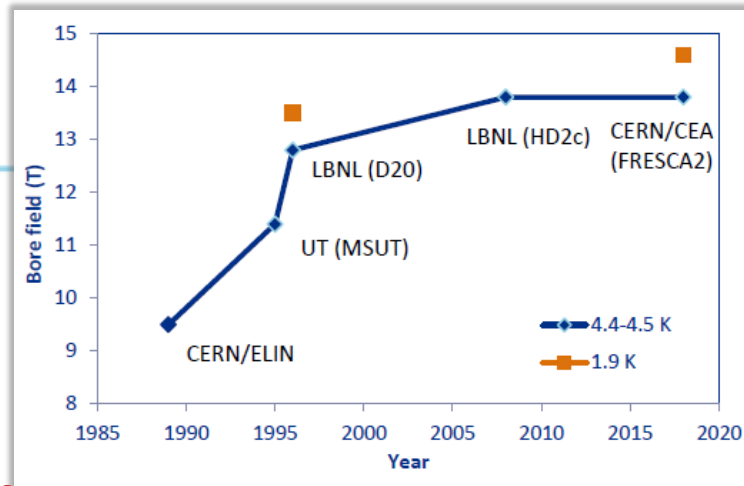
Max pile up is **54 interactions per crossing** (early in collisions)

LHC : PU=25 \rightarrow 250... FCCChh PU=1000?



Summary on R&D:

- **High field dipoles:**
 - Nb₃Sn 16 T / iron-based 12 T
 - Conductor (wire) development
- **Intercept of synchrotron radiation :**
 - 1-5 MW FCC-hh / 1 MW SppS
- **Collimation :**
 - x7 LHC circulating beam power
- **Optimal injector:**
 - 1.3TeV scSPS, 3.3 TeV in LHC/FCC
- **Overall machine design :**
 - IRs, pileup, vacuum, etc
 - Power and cost reduction



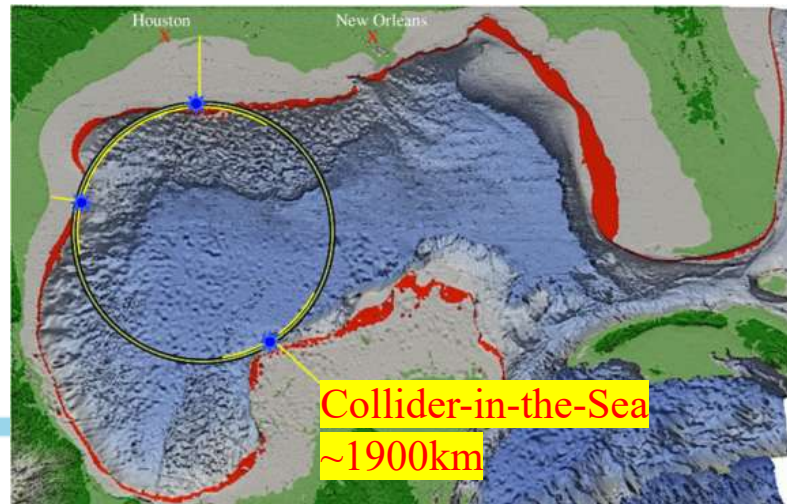
All that might take >20 years

ITF 10+ TeV pCM Colliders Summary

	CME (TeV)	Lumi per IP (10^{34})	Years, pre-project R&D	Years to 1 st physics	Cost range (2021 B\$)	Electric Power (MW)
FCChh-100	100	30	>10	>25	30-50	~560
SPPC <i>pp</i>	125	13	>10	>25	30-80	~400
Collider-in-the-Sea <i>pp</i>	500	20	>10	>25	>80	>1000

Super PP Collider (SPPC)

~100km



Collider-in-the-Sea

~1900km

10 TeV muon collider

~10km

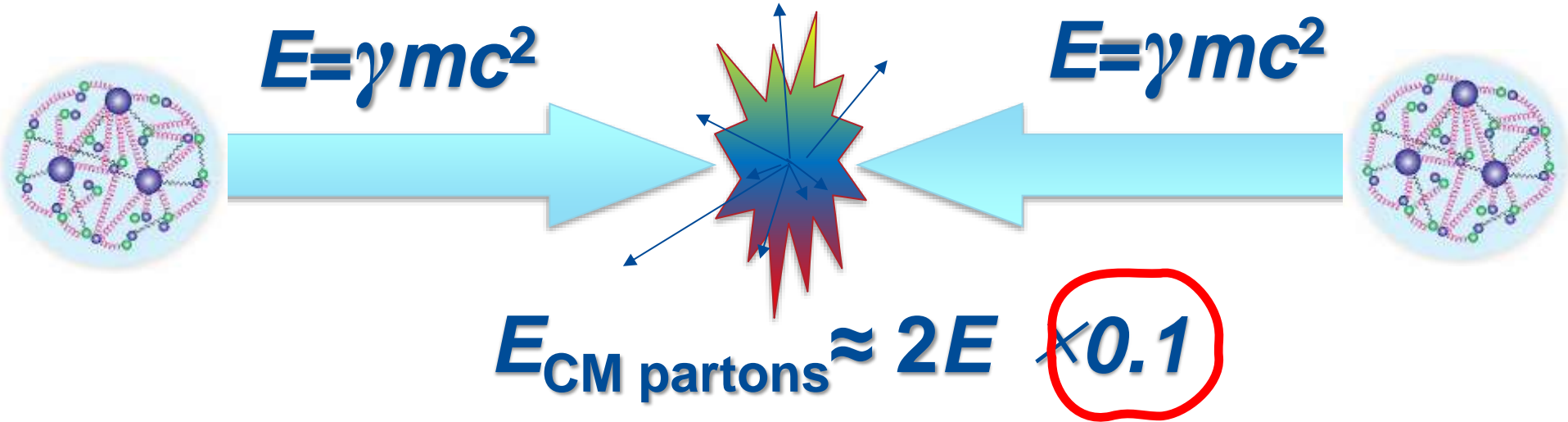


BREAK (!...?)

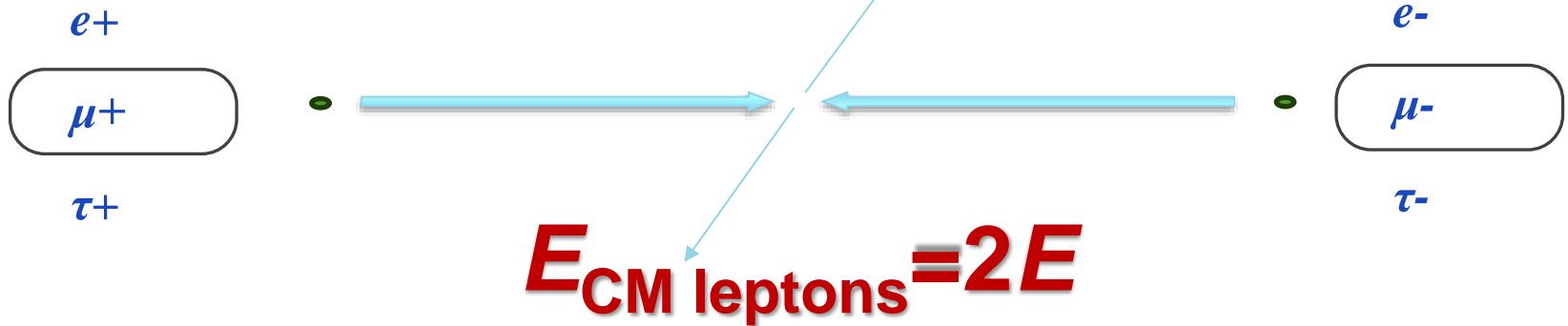
Muon Colliders (2)
Linear/Plasma
Colliders (3)

Colliding Leptons vs Hadrons

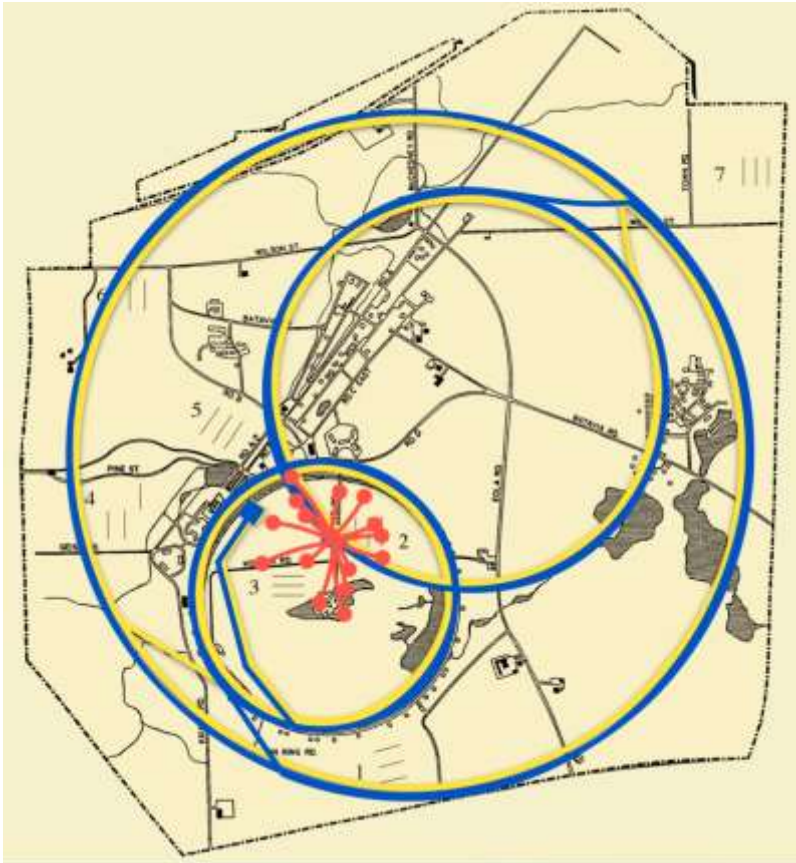
Protons



Leptons



Muon Colliders in the US



Fermilab site: about 3 x 4 miles, 6,800 acres

circular

compact

low(er) cost

low(est) power consumption

Muons decay quickly $2.2\mu s \times \gamma$

→ Fast production, cooling
(size reduction) &
acceleration

Muon Collider eg at FNAL $\mu+\mu-$

Circumference ~ 10 km, $E_{cm} = 3...10$ TeV

NC+SC magnets and SRF

Cost $\sim 12-18$ B\$ * (ITF, 2021)

20 yrs of R&D

*no labor, escalation, or contingency

Muon Colliders: Main Challenges

- Muons are not stable particles
 - Muon lifetime at rest ($mc^2=0.105$ GeV) is 2.2 microseconds
 - Muon lifetime at 5 TeV (collider $\gamma \approx 50000$) is 100 milliseconds
 - Muon can be made available only as secondary or tertiary particle products of reactions like
 - $p(\text{beam})+p(\text{target}) \rightarrow K,\pi \rightarrow \mu$
 - $e+e^- \rightarrow \mu+\mu^-$
 - $\gamma + Ze \rightarrow \mu+\mu^-$
- That usually results in large emittance (large angular spread) muon beams and requires **deep cooling for high Luminosity**
- Therefore, major challenges for High Luminosity MC are:
 - Muon production
 - Fast muon cooling
 - Fast muon acceleration
 - Neutrino flux hazard

Muon Collider Parameter Table

under development by the *International Muon Collider Collaboration*



Target integrated luminosities

\sqrt{s}	$\int \mathcal{L} dt$
3 TeV	1 ab ⁻¹
10 TeV	10 ab ⁻¹
14 TeV	20 ab ⁻¹

Reasonably conservative

- each point in 5 years with tentative target parameters
- FCC-hh to operate for 25 years
- Aim to have two detectors
- But might need some operational margins

Note: focus on 3 and 10 TeV
Have to define staging strategy

Tentative target parameters, scaled from MAP parameters

Parameter	Unit	3 TeV	10 TeV	14 TeV
L	10 ³⁴ cm ⁻² s ⁻¹	1.8	20	40
N	10 ¹²	2.2	1.8	1.8
f _r	Hz	5	5	5
P _{beam}	MW	5.3	14.4	20
C	km	4.5	10	14
	T	7	10.5	10.5
ε _L	MeV m	7.5	7.5	7.5
σ _E / E	%	0.1	0.1	0.1
σ _z	mm	5	1.5	1.07
β	mm	5	1.5	1.07
ε	μm	25	25	25
σ _{x,y}	μm	3.0	0.9	0.63

Snowmass process to give feedback on this

Average Luminosity of Muon Collider

NB: each muon makes $\sim 300B[T]$ turns in a ring with average field B

$$\langle \mathcal{L} \rangle = f_0 \gamma^2 \frac{c\tau_0}{2C} \frac{n_b N^2}{4\pi\epsilon_n \beta^*} \mathcal{F} = B P_b \frac{N r_0}{4\pi\epsilon_n} \frac{\gamma}{\beta^*} \left(\frac{c\tau_0 \mathcal{F}}{8\pi e} \right)$$



scales with B , the total beam power P_b , and the **beam brightness** (the third factor above is the beam-beam ξ)

The beta-function at the two IPs scales as $\beta^* \sim 1/\gamma$ within certain range of energies, giving overall scaling **Lumi** $\sim \gamma^2$ with other limiting parameters fixed. The main challenges to luminosity achievement with decaying particles are related to production and fast cooling and acceleration of $O(10^{12})$ muons per bunch without emittance degradation.

(Explanatory to Previous slide)

$$\Delta \int \mathcal{L} \approx \sum_{i=0}^{\infty} \frac{(N_0 e^{-i\Delta t/\gamma\tau})^2}{4\pi\sigma_x\sigma_y} \longleftarrow \sum_{i=0}^{\infty} (N_0 e^{-i\Delta t/\gamma\tau})^2 \propto N_0^2 B$$

$$\Delta \int \mathcal{L} \propto \frac{BN_0^2}{4\pi\epsilon\beta/\gamma}$$

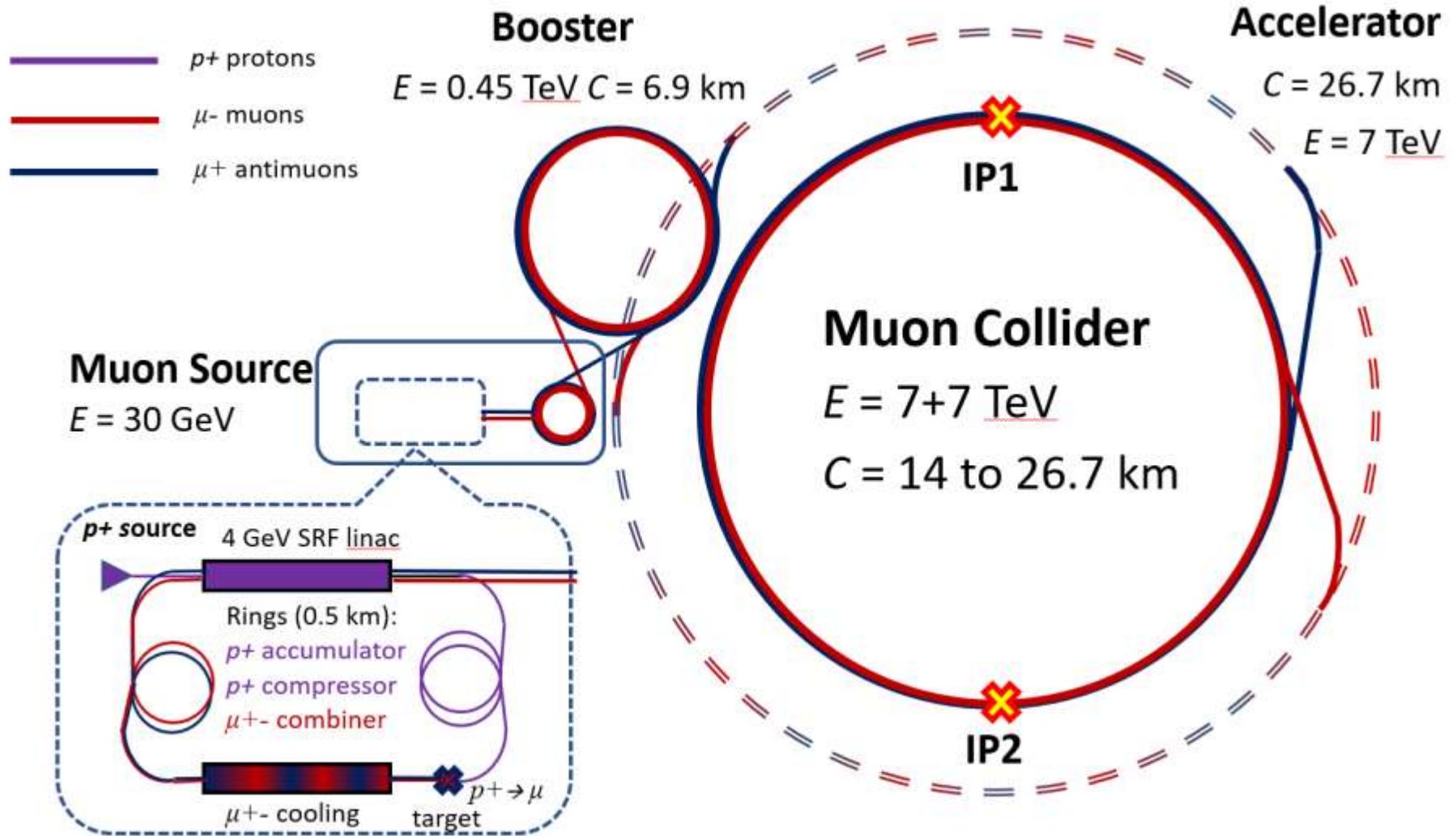
$\beta \approx \sigma_z$ $\frac{\sigma_E}{E} = \text{const}$
 $\beta \propto \frac{1}{\gamma}$ $\sigma_E \sigma_z = \text{const}$
 $\sigma_z \propto \frac{1}{\gamma}$

Note: this might be limited by technology

$$\Delta \int \mathcal{L} \propto B \frac{N_0^2 \gamma^2}{\epsilon}$$

$$\mathcal{L} \propto B \frac{N_0}{\epsilon} \gamma P_{beam}$$

O(14 TeV) Muon Collider Sub-Systems (approx. to scale)



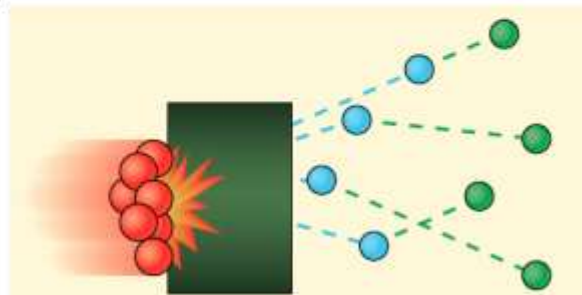
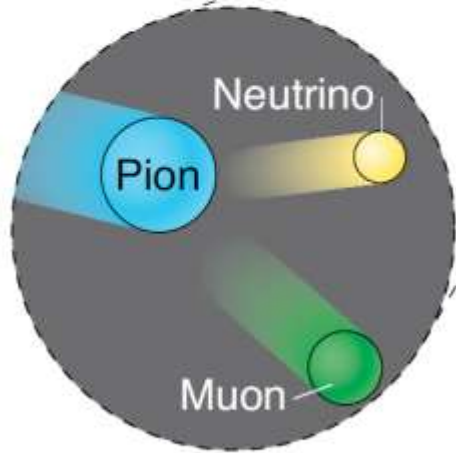
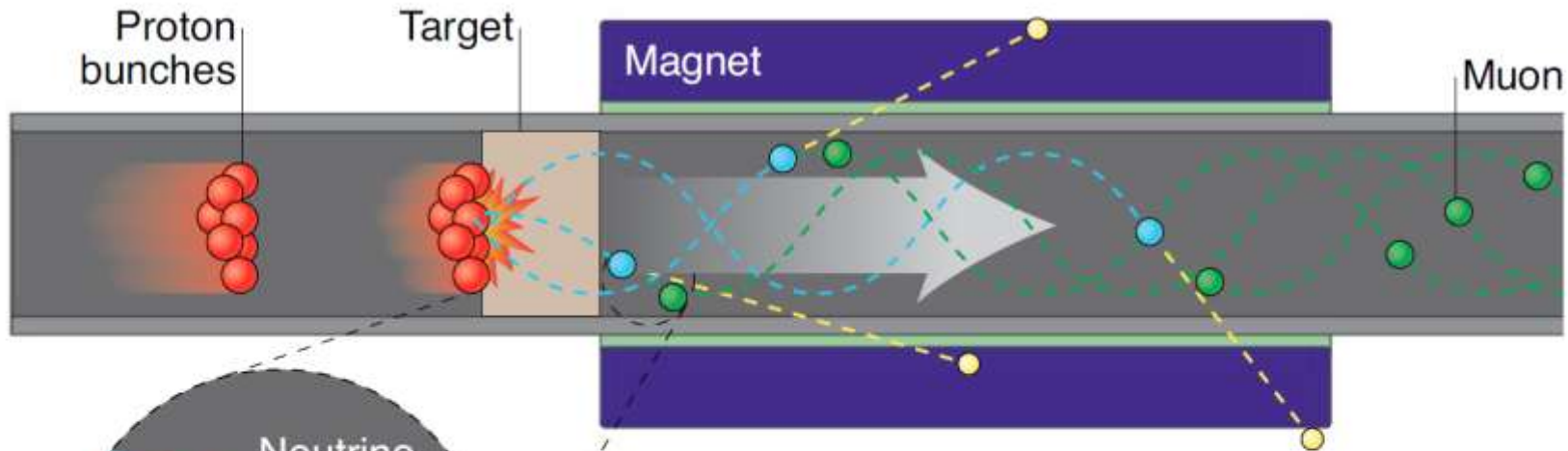
Muon Collider Subsystems

- (i) a high power **proton driver** (SRF 4 GeV 2-4 MW *H*- linac);
- (ii) pre-target **accumulation and compressor rings**, in which high-intensity 1-3 ns long proton bunches are formed;
- (iii) a liquid mercury **target** for converting the proton beam into a tertiary muon beam with energy of about 200 MeV;
- (iv) a multi-stage **ionization cooling** section that reduces the transverse and longitudinal emittances and, thereby, creates a low emittance beam;
- (v) a multistage **acceleration** (initial and main) system --- the latter employing a series recirculating rapid cycling synchrotrons (RCS) to accelerate muons in a modest number of turns up to 3-7 TeV using high gradient superconducting RF cavities;
- (vi) about 8.5 km diameter **collider ring** located some 100 m underground, where counter-propagating muon beams are stored and collide over the roughly 1000--2000 turns corresponding to the muon lifetime.

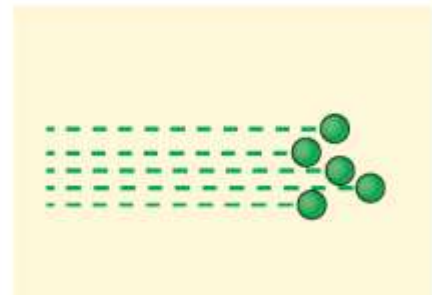
** From the point of beam physics, complexity of a Muon Collider is closer to that of the Tevatron (higher) than to that of the LHC (lower)*

Muon Production: 1-4 MW proton driver needed

Protons → Target → Pions → Muons



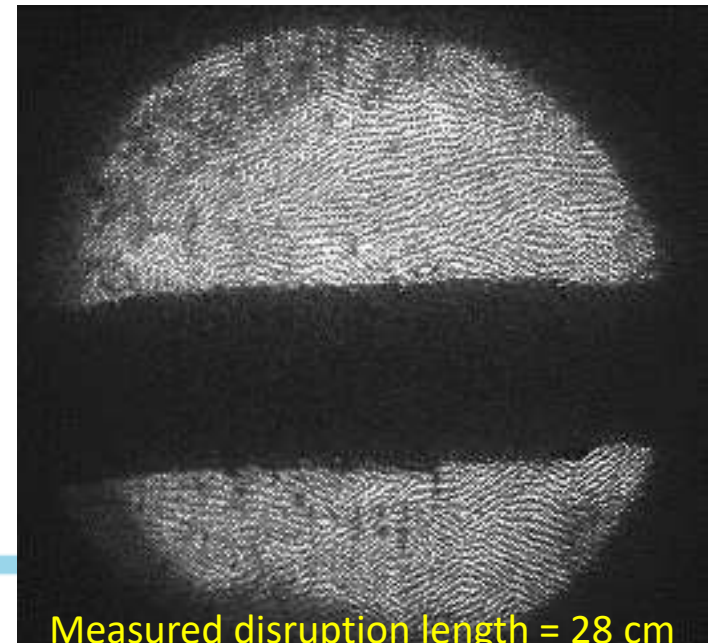
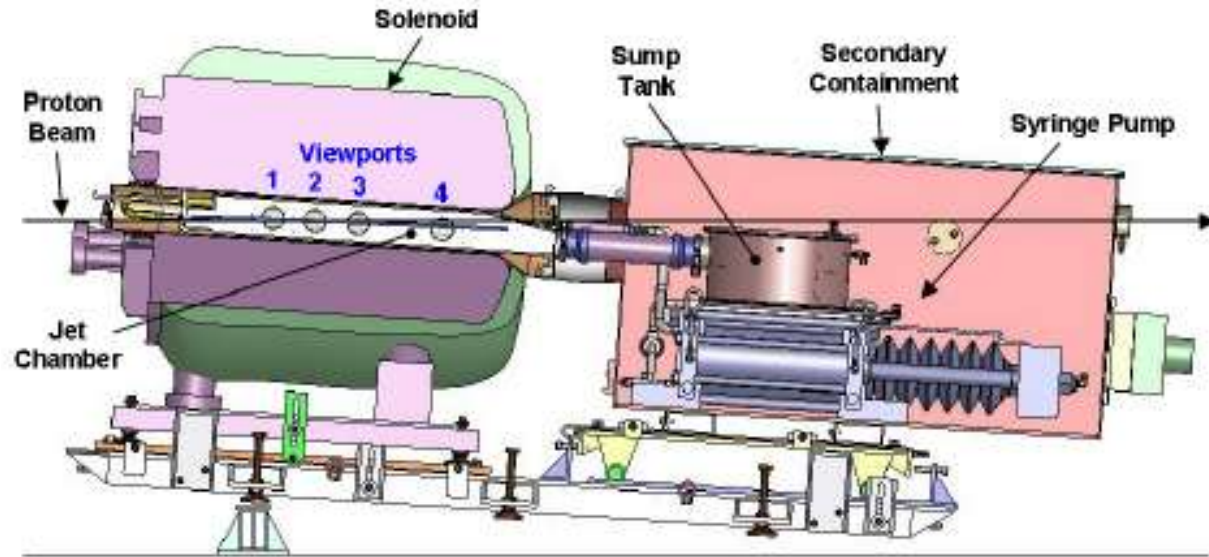
The goal is to turn a 'cloud' of muons travelling in all directions...



...into a tight beam travelling in one direction

MERIT Experiment – Demo of 4-8 MW Proton Targetry

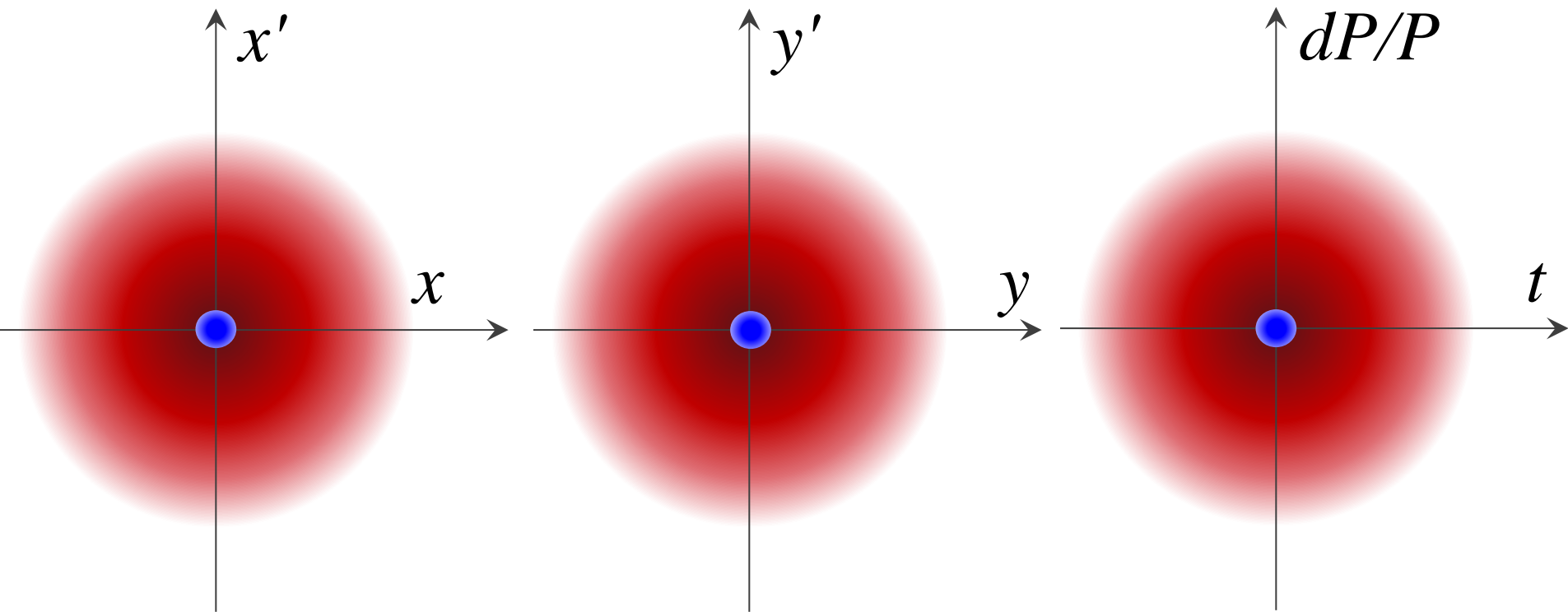
- At CERN PS
- $1e13$ protons 24 GeV (115kJ/pulse)
- Liquid Mercury target 20 m/s
- 15 T Solenoid



The Need for Muon Cooling

Muon Phase Space After Target
vs What's Needed for Collider

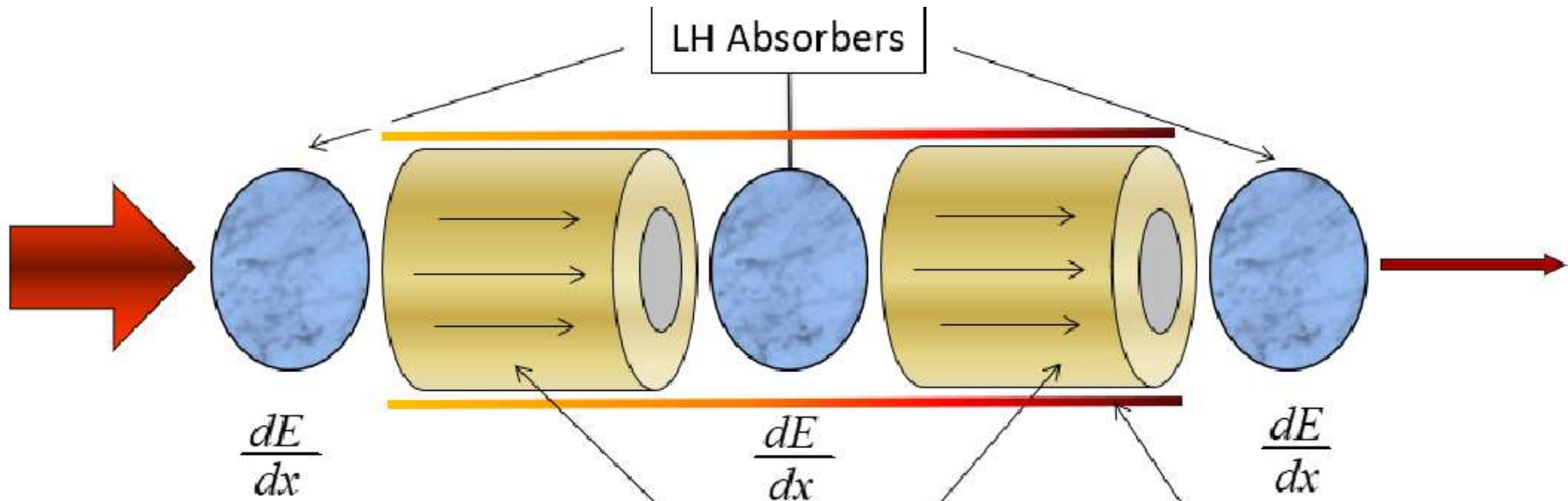
$$\mathcal{L} = f_{\text{coll}} \frac{N_1 N_2}{4\pi\sigma_x^* \sigma_y^*}$$



Need "6D-Cooling"

Fast Cooling of Muon Beams

- The desired 6D emittance for a MC is 5-6 orders of magnitude less from the emittance of the beam at the target
- How that can be done before muons decay? → ionization cooling: ionization loss *along momentum* followed by RF acceleration (*restore energy*) along longitudinal axis only (like in the Synchr Rad damping)



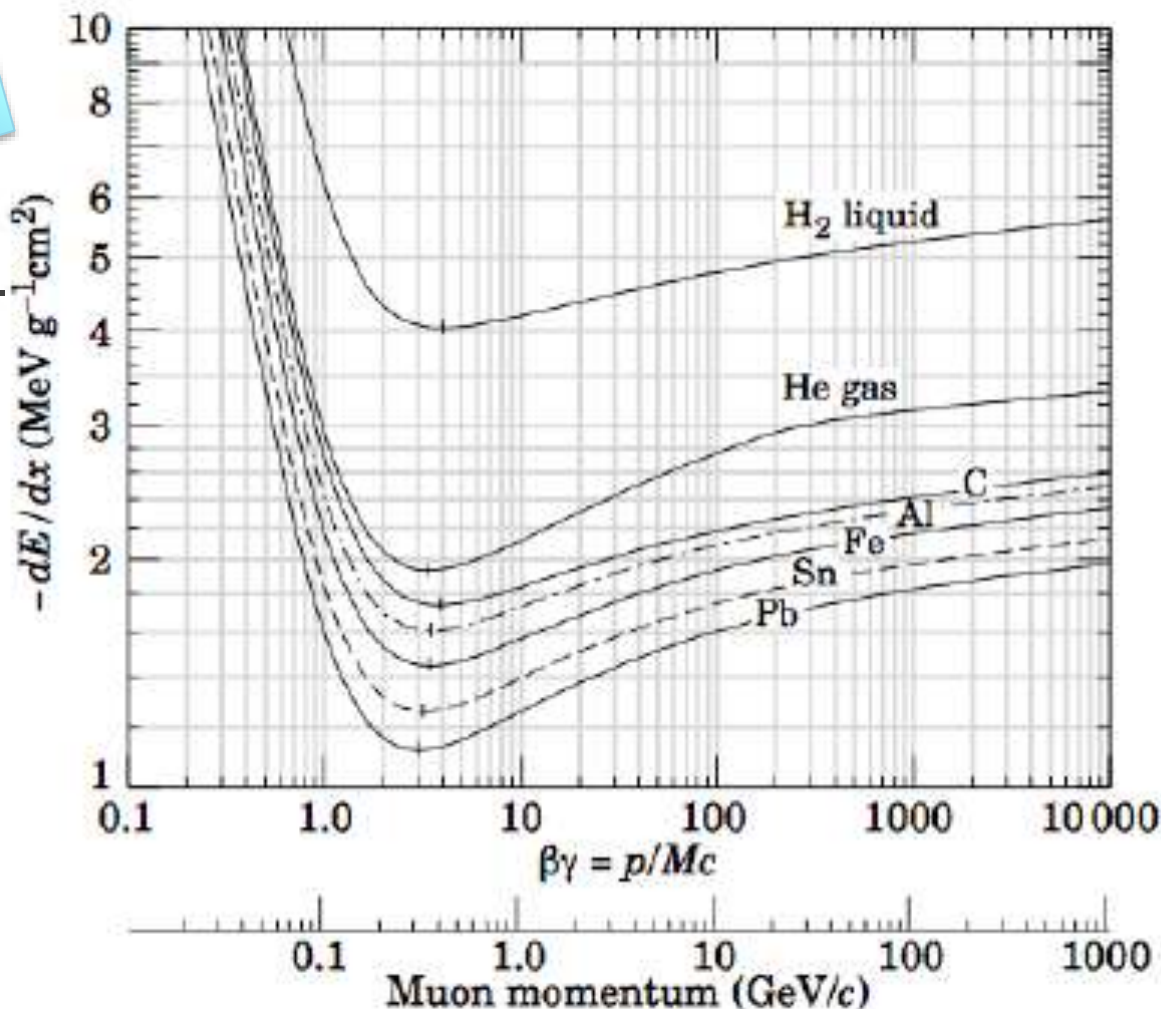
- Requires rf cavities to compensate for lost longitudinal energy
- Use strong B-fields to confine beams

$$\frac{d\epsilon_N}{ds} \approx \underbrace{-\frac{1}{\beta^2} \left\langle \frac{dE_\mu}{ds} \right\rangle \frac{\epsilon_N}{E_\mu}}_{\text{Cooling}} + \underbrace{\frac{\beta_\perp (0.014 \text{ GeV})^2}{2\beta^3 E_\mu m_\mu X_0}}_{\text{Heating}}$$

Equation:

$$\frac{d\epsilon_n}{ds} = -\frac{dE_\mu}{ds} \frac{\epsilon_n}{E_\mu} + \frac{\beta_\perp (0.014)^2}{2 E_\mu m_\mu L_R}$$

- (1st) Cooling term \sim (dE/ds) – larger the better
- (2nd) Heating/scattering term \sim beta-function at the absorber and $1/\text{radiation length}$ of the material (a low-Z preferred, *Liquid Hydrogen, Li, LiH, Be*)
- Energy of muons



Longitudinal DoF: rms E spread

cooling term

fluctuations of ionization
energy losses

$$\frac{d(\Delta E)^2}{ds} = -2 \frac{d\left(\frac{dE_\mu}{ds}\right)}{dE_\mu} \langle (\Delta E_\mu)^2 \rangle + \frac{d(\Delta E_\mu)_{straggling}^2}{ds}$$

- Cooling requires that $d(dE_\mu/ds)/dE_\mu > 0$. But at energies below about 200 MeV, the energy loss function for muons, dE_μ/ds , is decreasing with energy and there is thus heating of the beam. Above 400 MeV the energy loss function increases gently, thus giving some cooling, though not sufficient for fast cooling application (see previous slide).
- The “straggling” term

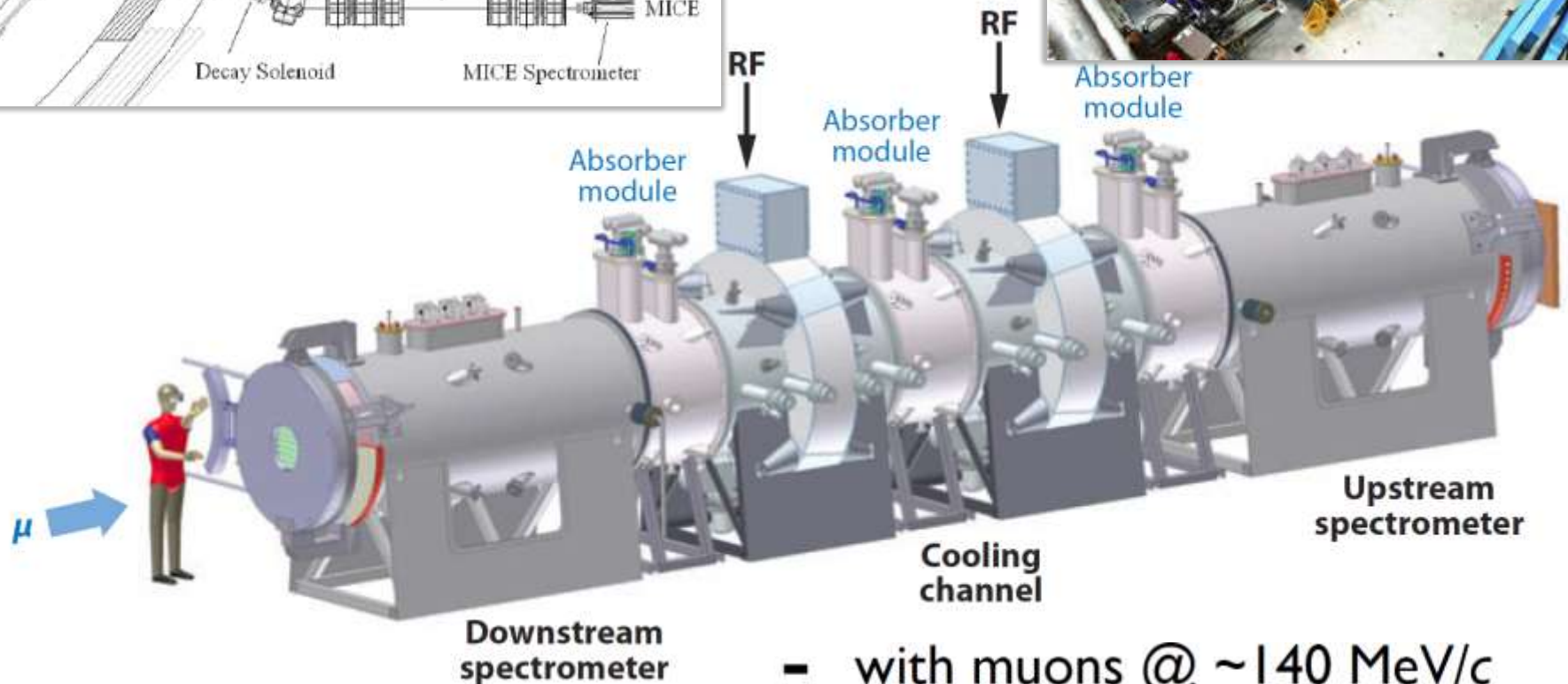
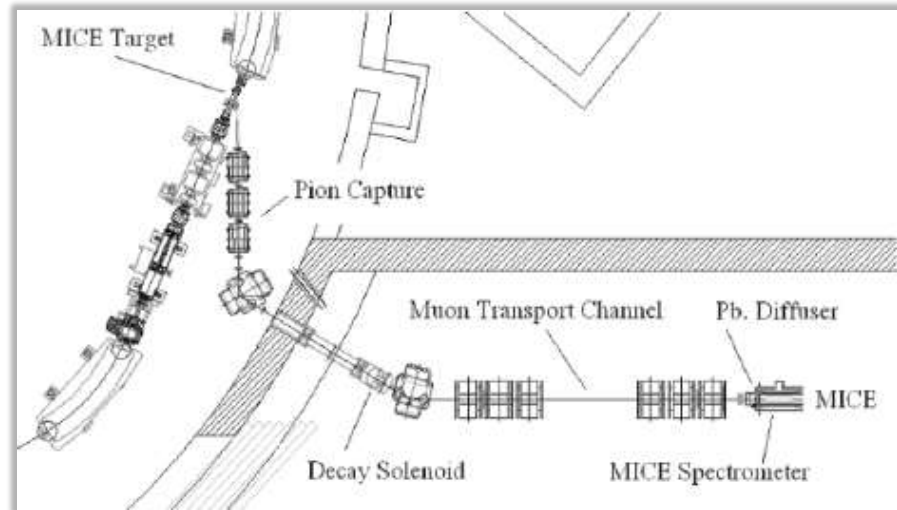
$$\frac{d(\Delta E_\mu)_{straggling}^2}{ds} = 4\pi (r_e m_e c^2)^2 N_o \frac{Z}{A} \rho \gamma^2 \left(1 - \frac{\beta^2}{2}\right)$$

increases as γ^2 , and the cooling system size scales as $\gamma \rightarrow$ cooling at low energies is desired.

- Energy spread can also be reduced by artificially increasing $d(dE_\mu/ds)/dE_\mu$ by placing a transverse variation in absorber density or thickness at a location where position is energy dependent, i.e. where there is dispersion (= emittance exchange long \rightarrow transverse)

MICE: Muon Ionization Cooling Experiment = 1 “cell”

ISIS 800 MeV
proton
synchrotron
@ RAL (UK)



- with muons @ ~ 140 MeV/c
- each muon individually measured

Muon 4D Cooling: MICE Results (2024)

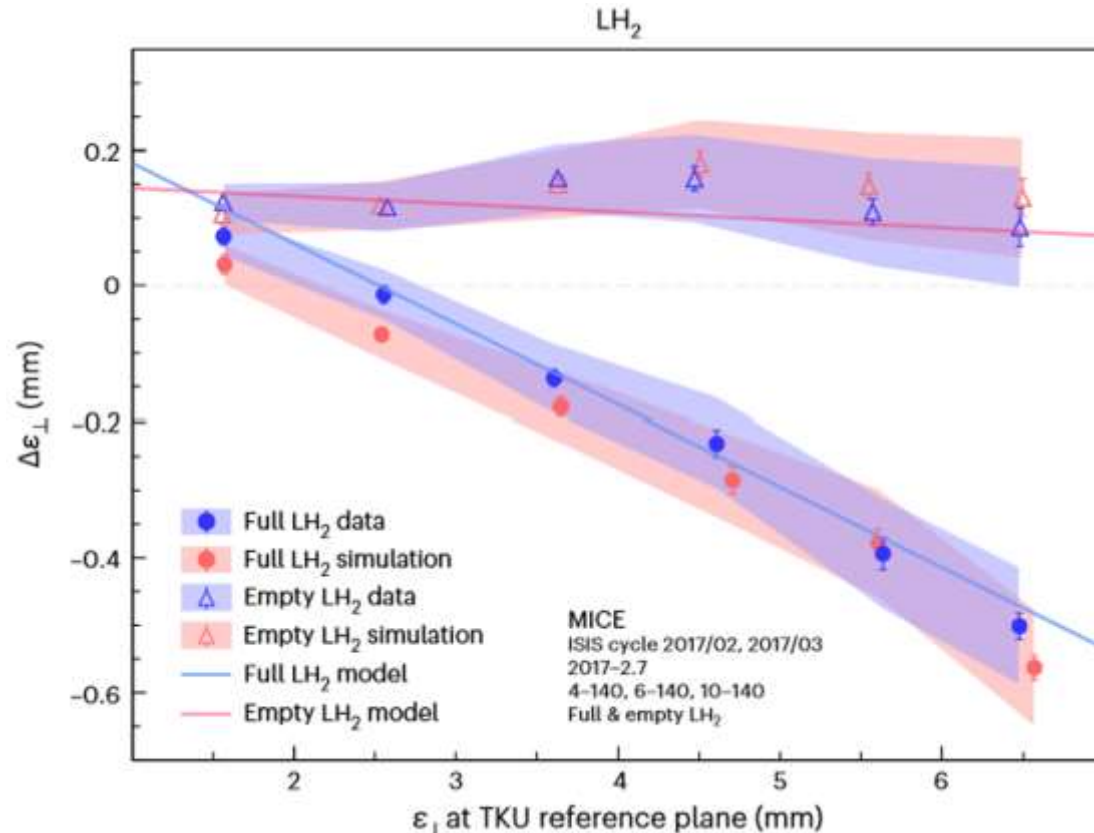
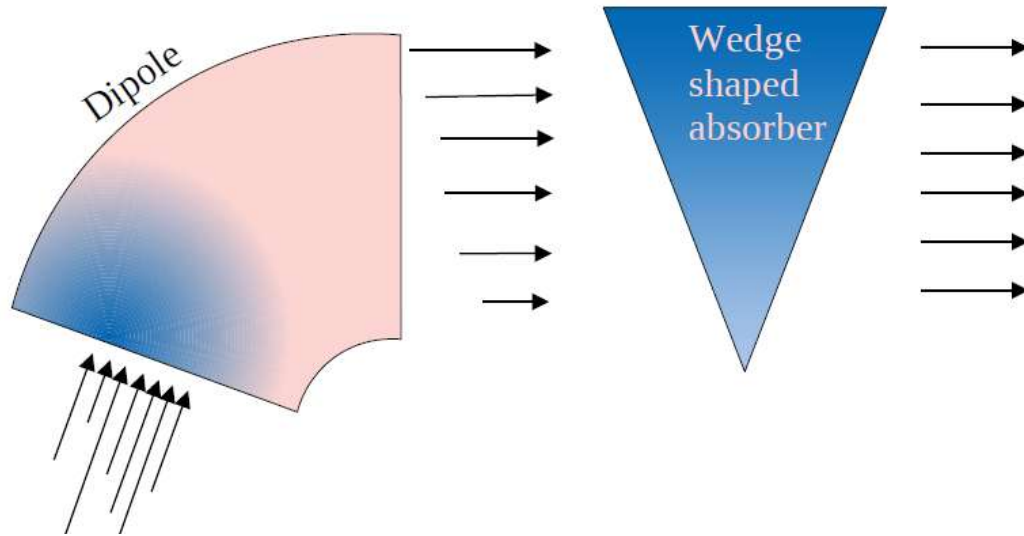


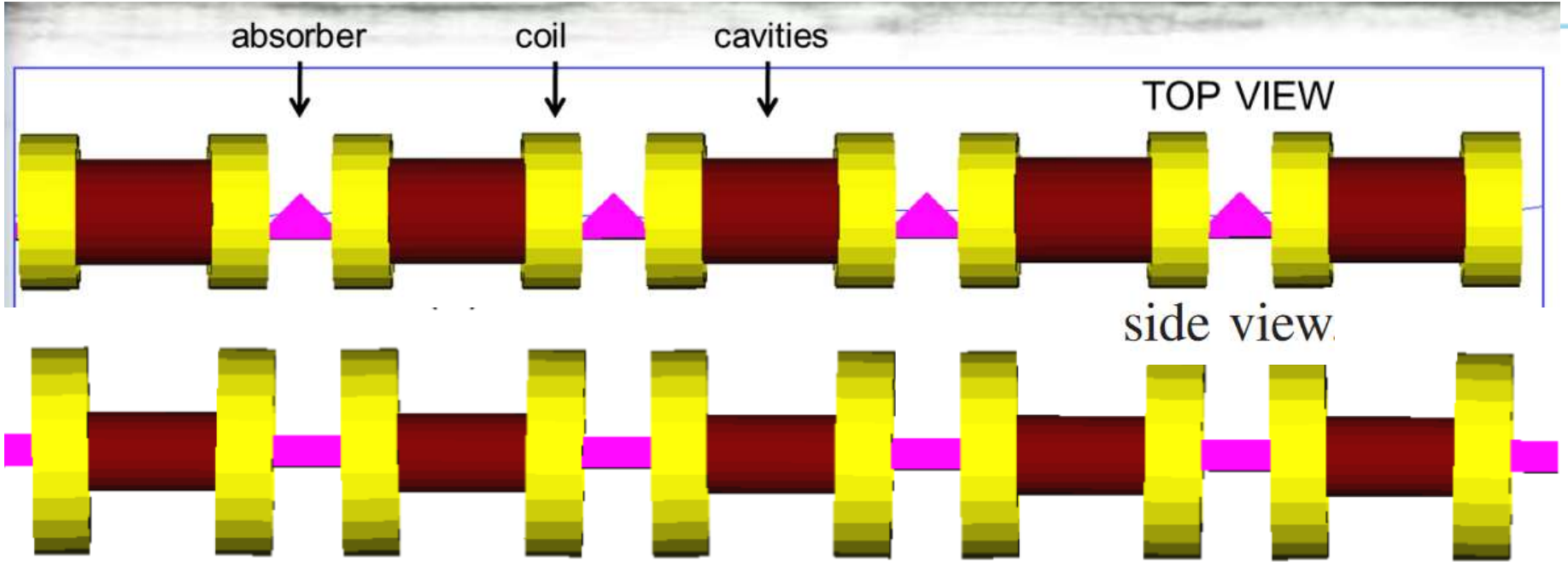
Fig. 3 | Transverse emittance change measured by MICE. Emittance change between the TKU and TKD reference planes, $\Delta\epsilon_{\perp}$, as a function of emittance at TKU for 140 MeV/c beams crossing the LH₂ MICE absorbers. Results for the empty cases, namely, No absorber and Empty LH₂, are also shown. The measured effect is shown in blue, whereas the simulation is shown in red. The corresponding semitransparent bands represent the estimated total standard error. The error bars indicate the statistical error and for some of the points, they are smaller than the markers. The solid lines represent the approximate theoretical model defined by equation (10) (Methods for the absorber (light blue) and empty (light pink) cases). The dashed grey horizontal lines indicate a scenario where no emittance change occurs.

6D Ionization Cooling



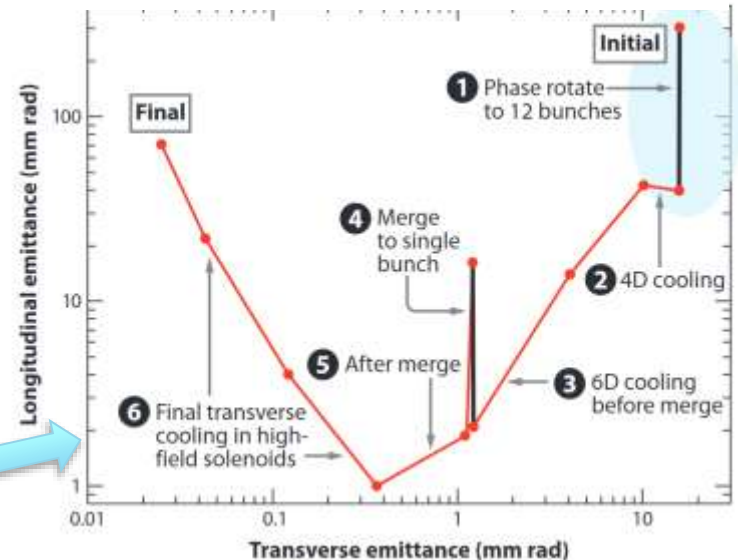
- Initial beam is narrow with some momentum spread
 - Low transverse emittance and high longitudinal emittance
- Beam follows curved trajectory in dipole
 - Higher momentum particles have higher radius trajectory
 - Beam leaves wider with energy-position correlation
- Beam goes through wedge shaped absorber
 - Beam leaves wider without energy-position correlation
 - High transverse emittance and low longitudinal emittance
- (Do transverse 4D cooling... and repeat the cycle)

Channel



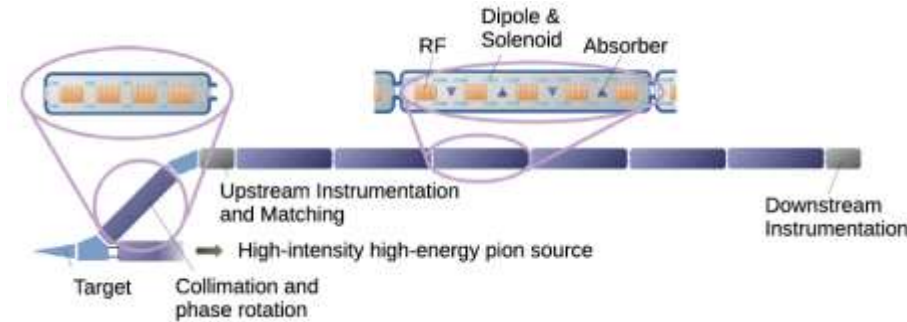
6D emittance reduction by 5 orders of magnitude (between point 2 to 5).
Length ~ 900 m

Final cooling section design requires ~30 T solenoids (point 5 to 6)



Full Ionization Cooling & Demonstrator

<https://doi.org/10.1140/epjc/s10052-023-11889-x>



Schematic of the muon cooling demonstrator

	Muon mom. MeV/c	Total length, m	Total # of cells	Total RF voltage, MV	B_max, T	6D emm. reduction	Beam loss, %
Full scale MC	200	~980	~820	~15,000	2-14	$\times 1/10^5$	~70%
Demonstrator	200	48	24	~260	0.5-7	$\times 1/2$	4-6%

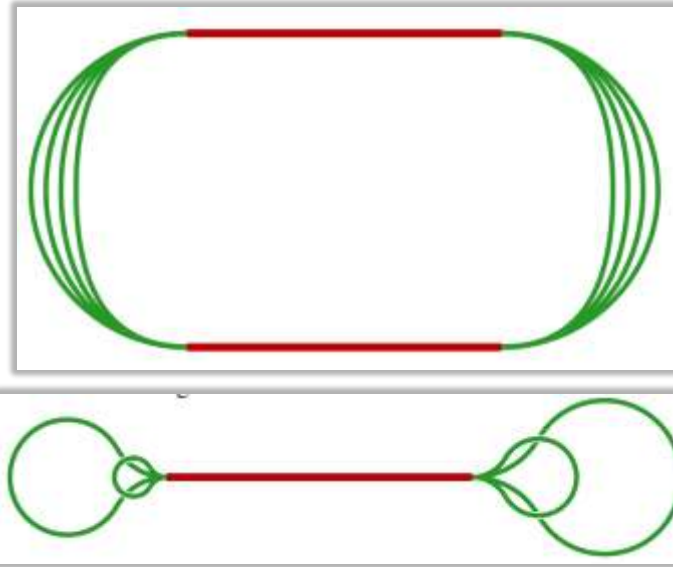
The Muon Ionization Cooling Demonstrator Experiment:

- Timeline: 2029-2034
- Location: Fermilab or CERN
- Cost: 300 ? M\$

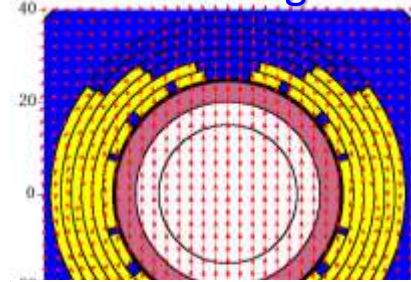
Acceleration and Collider Ring ~75% of the MC Cost

Options (high → low cost):

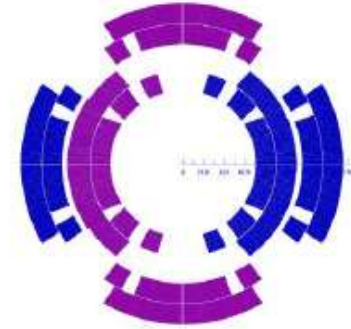
- Linac (very costly!)
- Recirculating linear accelerator (RLA)
- Fixed field alternating gradient (FFA)
- Pulsed synchrotrons



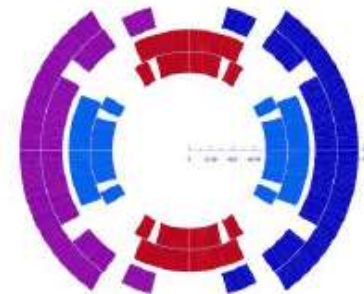
~14T Large Aperture Collider Magnets



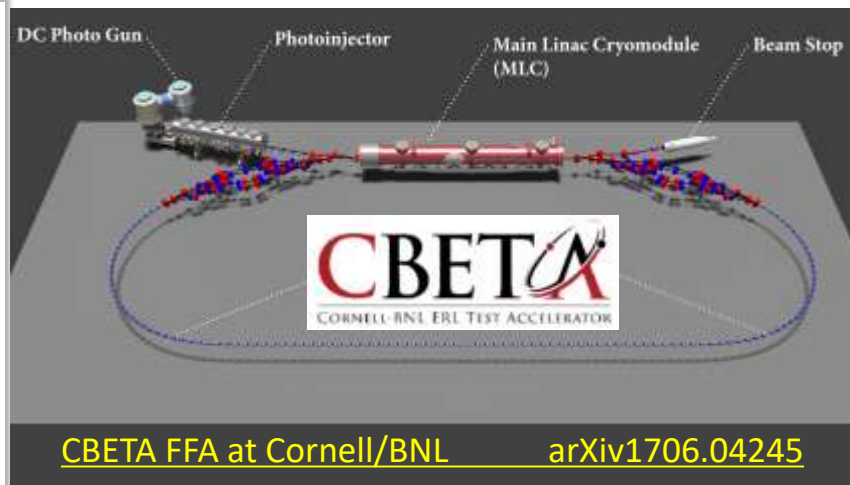
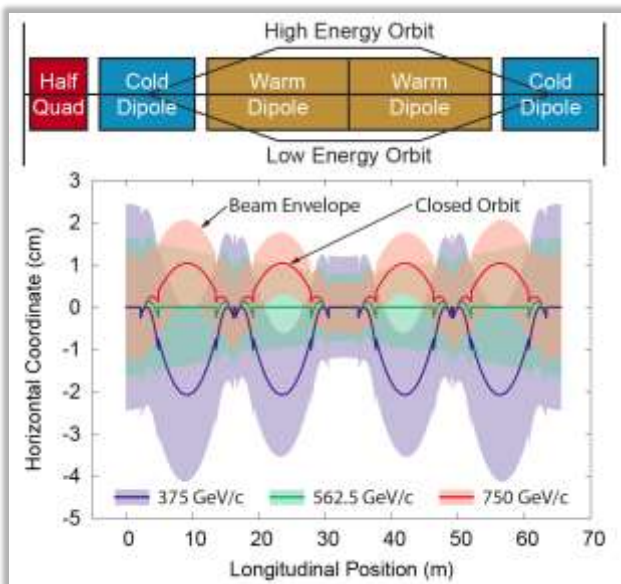
Alexahin et al 2018 JINST 13 P11002



Dipole/Quad



Quad/Dipole

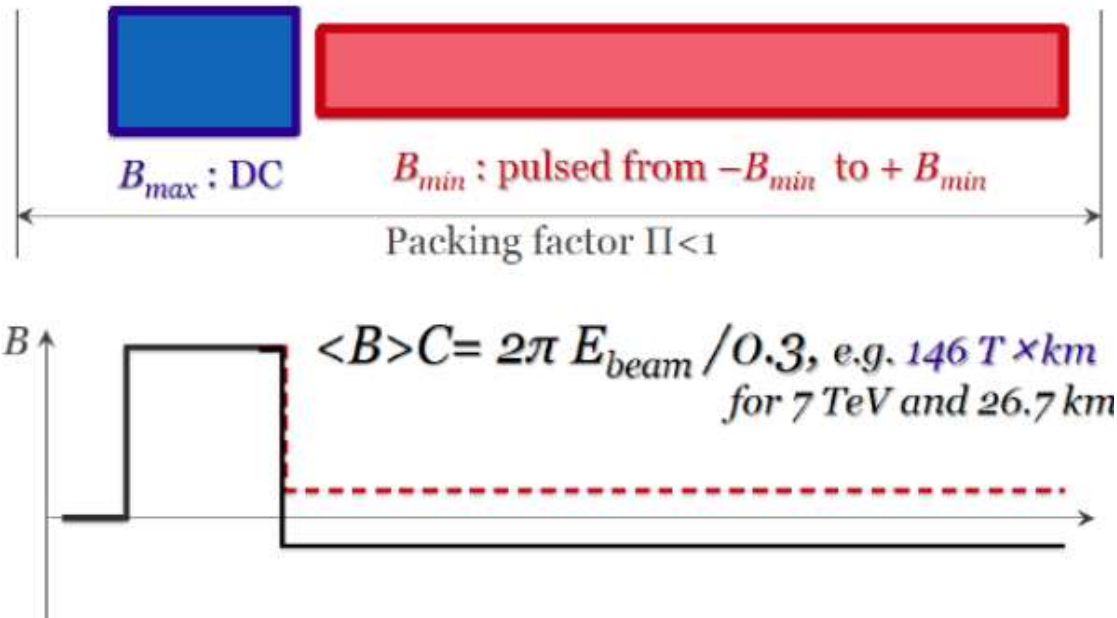


CBETA FFA at Cornell/BNL

arXiv1706.04245

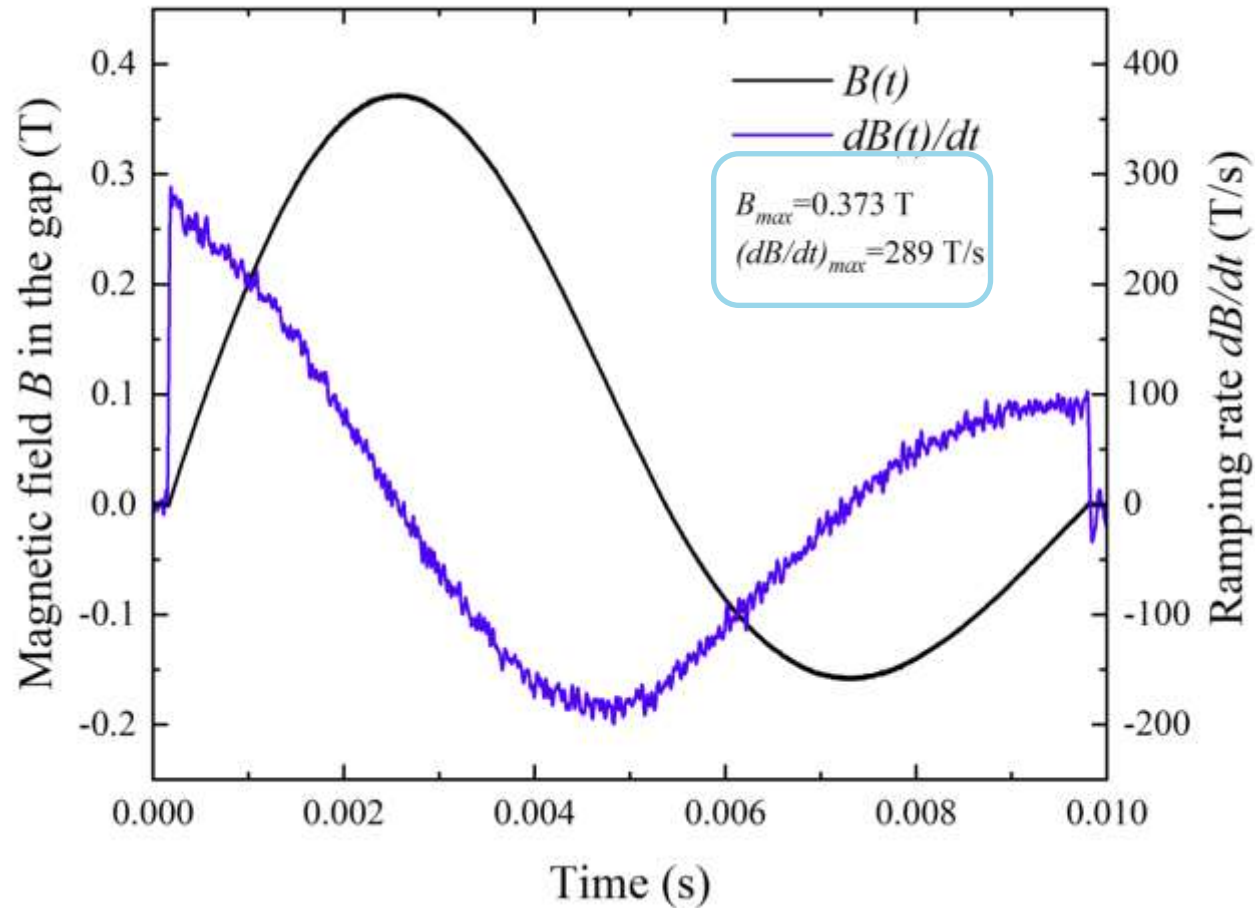
The Idea of Pulsed Muon RCS

- Rapid cycling synchrotron (RCS)
 - Potentially larger acceleration range at affordable cost
 - Could use combination of static superconducting and ramping normal-conducting or HTS magnets
 - But have to deal with energy in fast pulsing magnets



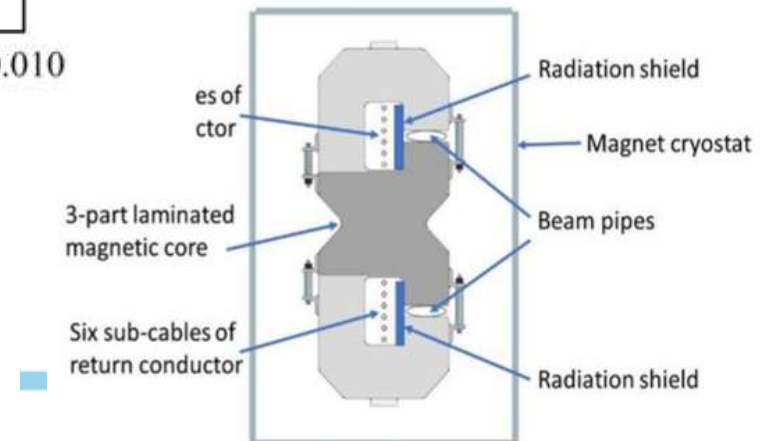
- Of course, circumference of the RCS will be larger than that of collider as **AVERAGE max B-field in RCS < AVERAGE (static) B-field collider ring**

Need pulsed magnets $dB/dt \sim 1000\text{T/s}$

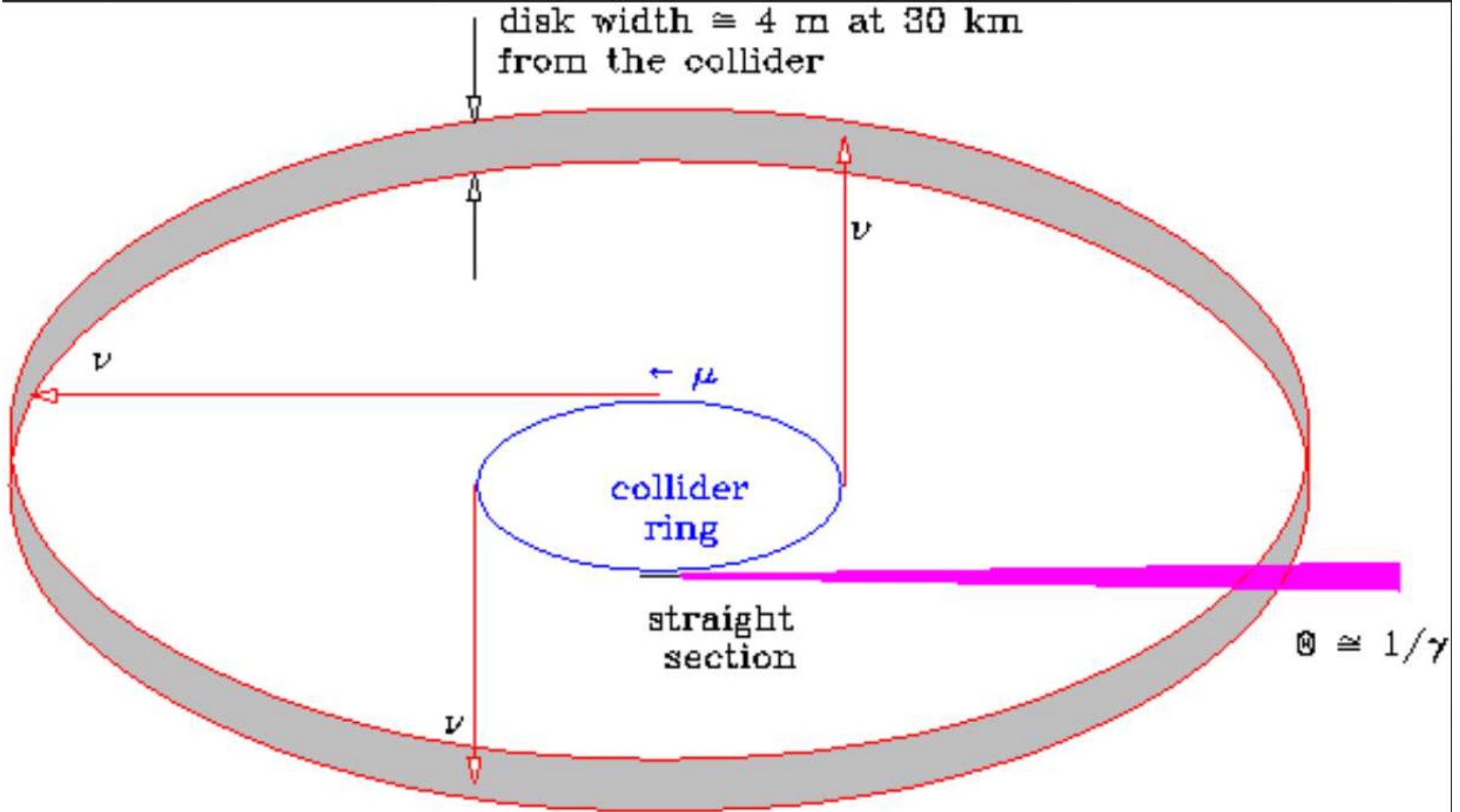


Fermilab, 2021

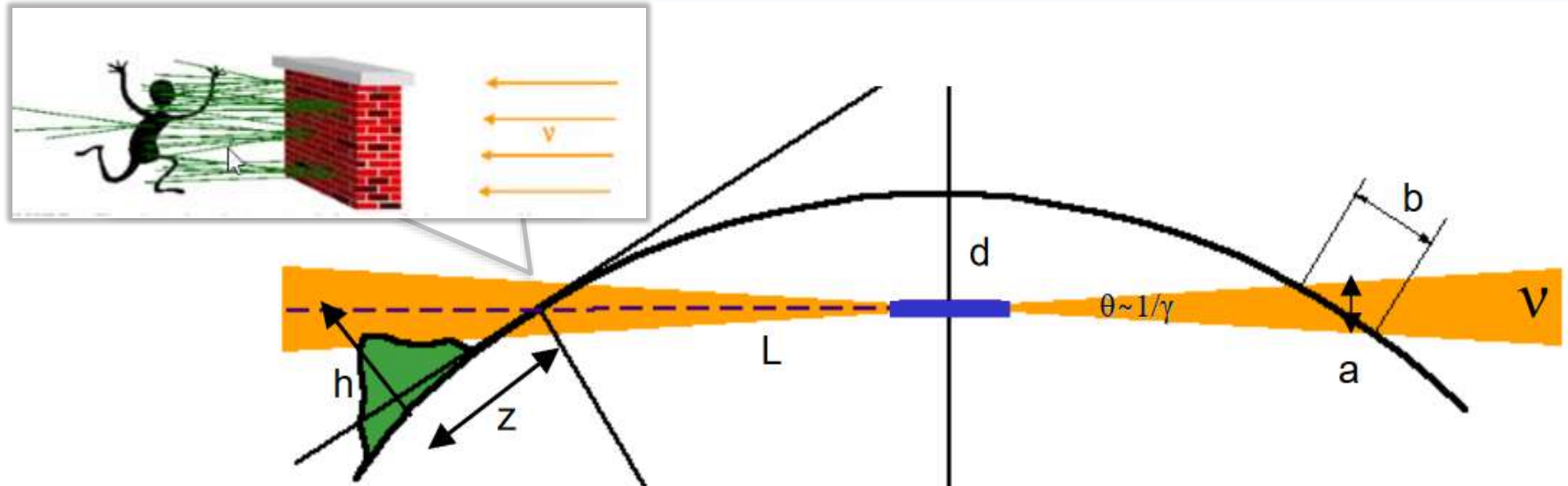
Approach to an economical magnet is to use HTS tape: very low AC losses in superconductor



Neutrino Flux (Muons decay to $e + \nu \bar{\nu}$)



Neutrino Radiation Dose & Control



Cone gets narrower with energy
 Cross section grows with energy

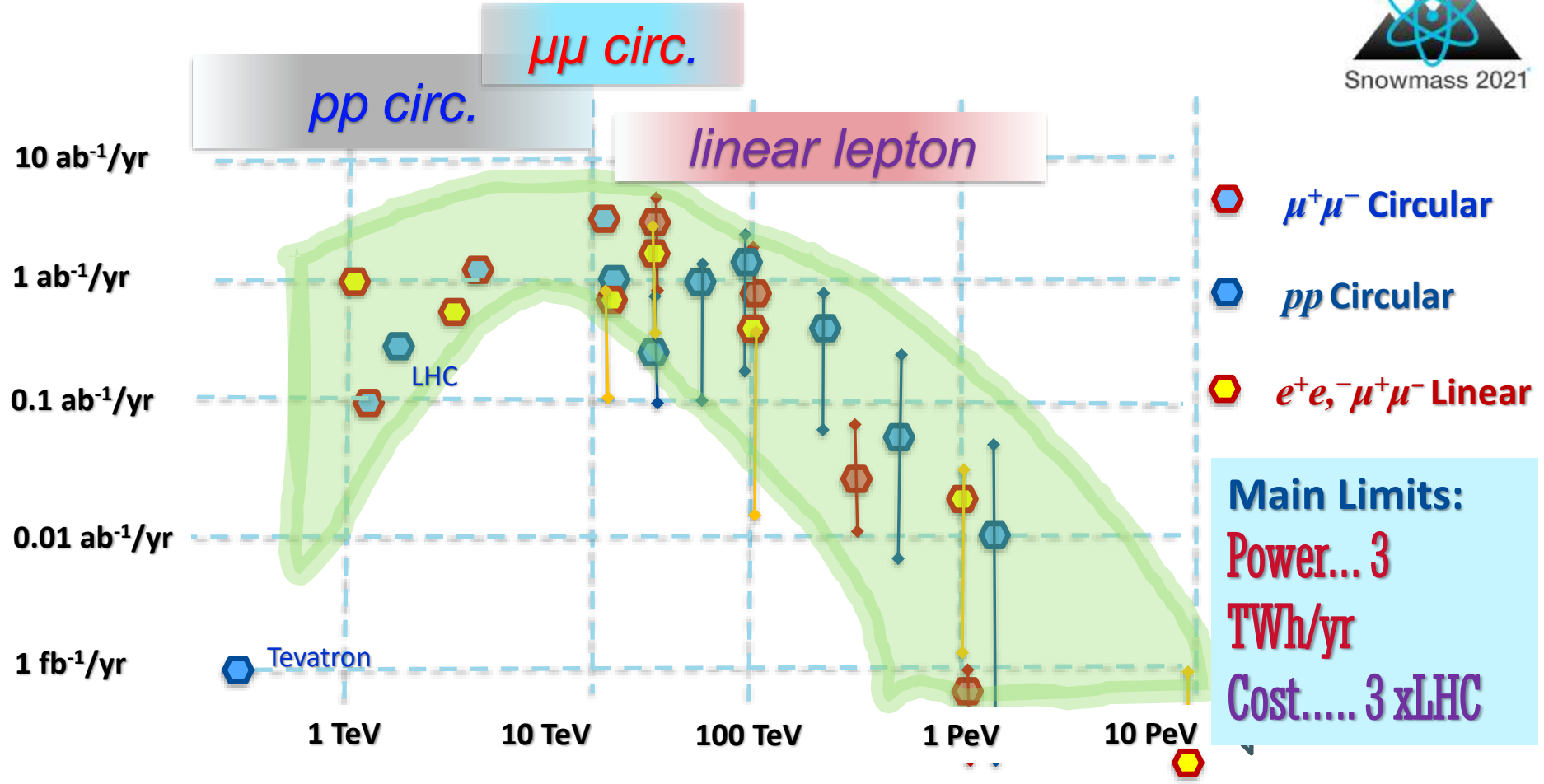
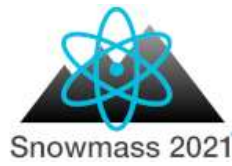
$$D^{ave}[Sv] = 3.7 \times 10^{-23} \times \frac{N_{\mu} \times (E_{\mu}[TeV])^3}{(L[km])^2}$$

- <1 mSv/yr mitigation ideas:**
- depth
 - few mm vertical collider orbit variation (next slide)
 - few cm magnet positions float (next slide)
 - less muons... =smaller emittance to keep L

On Required R&D: μ -Coll Costs and Risks

	Approx. % of the Total Cost	Approx. Luminosity Risk Factor
Proton Driver & Targetry	15 - 20 %	10^{1-2}
Muon Cooling	10 - 15 %	10^{3-4}
Acceleration	30 - 60 %	10^{1-2}
Collider	25 - 40 %	10^{0-1}
TOTAL	12 - 18 B\$ *ITF?	10^{5-9}

Ultimate Colliders *Luminosity vs Energy*



53

V.Shiltsev, "Ultimate Colliders" (Oxford Encyclopedia, 2023);
 DOI: 10.1093/acrefore/9780190871994.013

Future is “Linear”, “High Gradient”, “Muon”

- **Synchrotron radiation** defines linear vs circular if $U_{SR} < E$

$$U_{SR} = C_{\gamma} \frac{E^4}{\rho} = 88.46 \frac{r_0}{r_e} \left(\frac{m_e}{m_0}\right)^4 \frac{E^4 [GeV]}{\rho [m]}$$

- for e-/e+: $E_{cm} \leq 1 TeV \left(\frac{\rho}{10km}\right)^{\frac{1}{3}}$
- for muons: $E_{cm} \leq 1.2 PeV \left(\frac{\rho}{10km}\right)^{\frac{1}{3}}$
- for protons: $E_{cm} \leq 25 PeV \left(\frac{\rho}{10km}\right)^{\frac{1}{3}}$

- **Space limitations** call for high gradient:

Circumference 100 km, B<16 T, $E_{cm} < 100 TeV$
 Circumference 40,000 km, B=1 T, $E_{cm} < 2.5 PeV$
 Length 50 km, G<0.1 GV/m, $E_{cm} < 5 TeV$
 Length 10 km, G<1 TV/m, $E_{cm} < 10 PeV$

- **Production and survival:** unstable heavy leptons need high G too

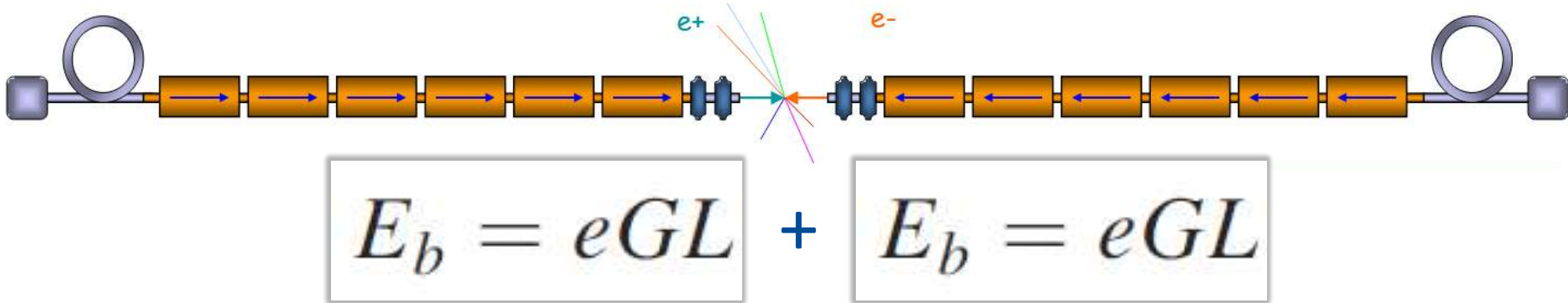
$$\frac{dN}{dt} = -\frac{N}{\gamma\tau_0}; \gamma = \gamma_i + z \frac{d\gamma}{dz}$$

where τ_0 is the lifetime, $\tau_0 \sim 2.2\mu s$ for muons...
 requires fast acceleration

for muons $G \gg 3 MeV m^{-1}$

for τ -leptons $G \gg 0.3 TeV m^{-1}$

Linear Collider vs Rings



Major advantages (wrt e^+e^- ring-ring colliders):

- No SR losses (no bending magnets... E_{cme} can go up to few TeV)
- More compact if gradient G is high
- (Somewhat) lower cost for Higgs energy $E_{cme}=250$ GeV
- Polarized beams

Major disadvantages (wrt e^+e^- ring-ring colliders):

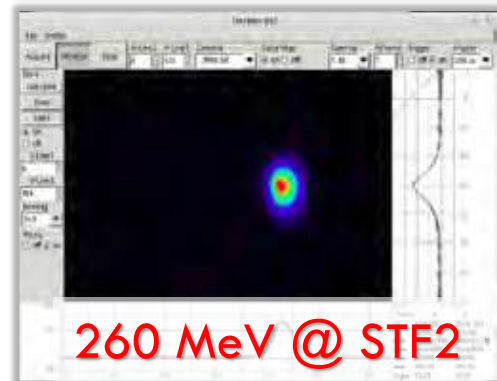
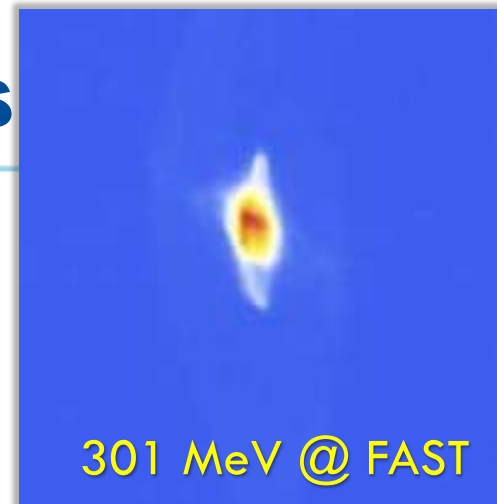
- One IP at a time (vs up to 4 in rings)
- Lower luminosity at $E_{cme} < 0.5$ TeV (lower *Lumi/Power* ratio)
- Big *Lumi* challenges: ultra low ϵ , jitters, beamstrahlung, e^+ prod'n
- Limited experience (one SLC vs dozens of e^+e^- rings)

Linear *lepton* Colliders

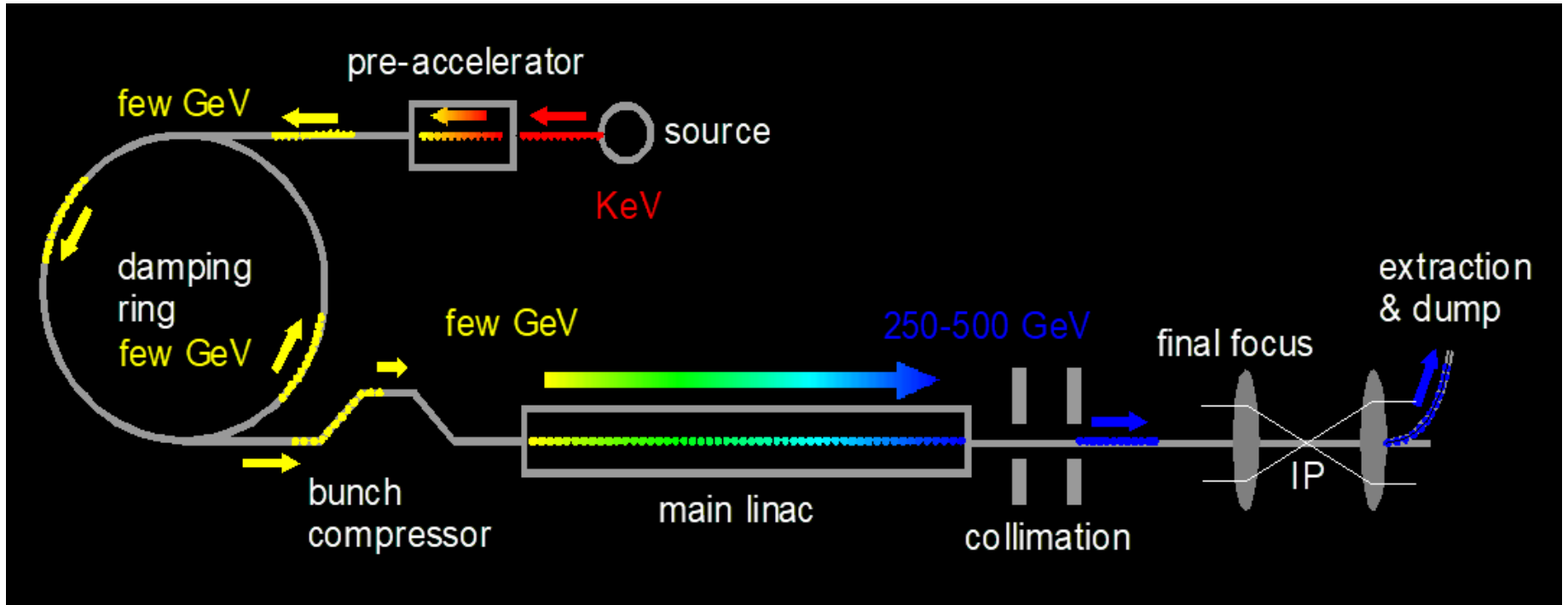
- Choice of particles :
 - Mostly e^+e^- (*till now*)
 - Muons possible, but μ -sources are expensive (and limited production rate dN/dt)
 - Protons possible, but lose factor of 7 in effective cme energy reach in hh collisions (ie need to accelerate to 7x the e^+e^- energy)
 - Interesting option $\gamma\gamma$ -colliders
 - Need two e^- linacs, few mm from IP convert $e^- \rightarrow \gamma$ and collide photons
 - Higgs production via s-channel and requires only $\sim 63\text{GeV}$ electrons! (ie factor of 2 smaller beam energy... in $e^+e^- \rightarrow ZH$ need 125 GeV)
 - Allows avoid beamstrahlung but low luminosity and broad cme dE/E
- Choice of RF technology:
 - Super-Conducting RF \rightarrow ILC
 - Room Temperature Copper NC RF \rightarrow CLIC
 - Liquid Nitrogen Temperature Copper RF \rightarrow C³
 - **[Wakefield Acceleration and Plasma \rightarrow PWFA]**

Recent progress: Linear Colliders

- Accelerating gradients demonstrated (in reasonably long RF systems):
 - ILC 31.5 MeV/m **with beam** – FNAL'17, KEK'19
 - One 12m long SRF cryomodule + 1 klystron
 - ILC needs 1000 of cryomodules +300 klystron
 - CLIC ~100 MeV/m **with beam** – CLEX@CERN
 - Several 0.25 m long structures driven by one low energy very powerful 12 GHz beam
 - CLIC needs ~15,000 structures and two “superbeam” 12 GHz 2 GeV driver beams
 - C³ 150 MeV/m **no beam** – SLAC'20
 - One ~1m long structure + 1 klystron
 - C³ needs ~1000 structures and 500 klystrons

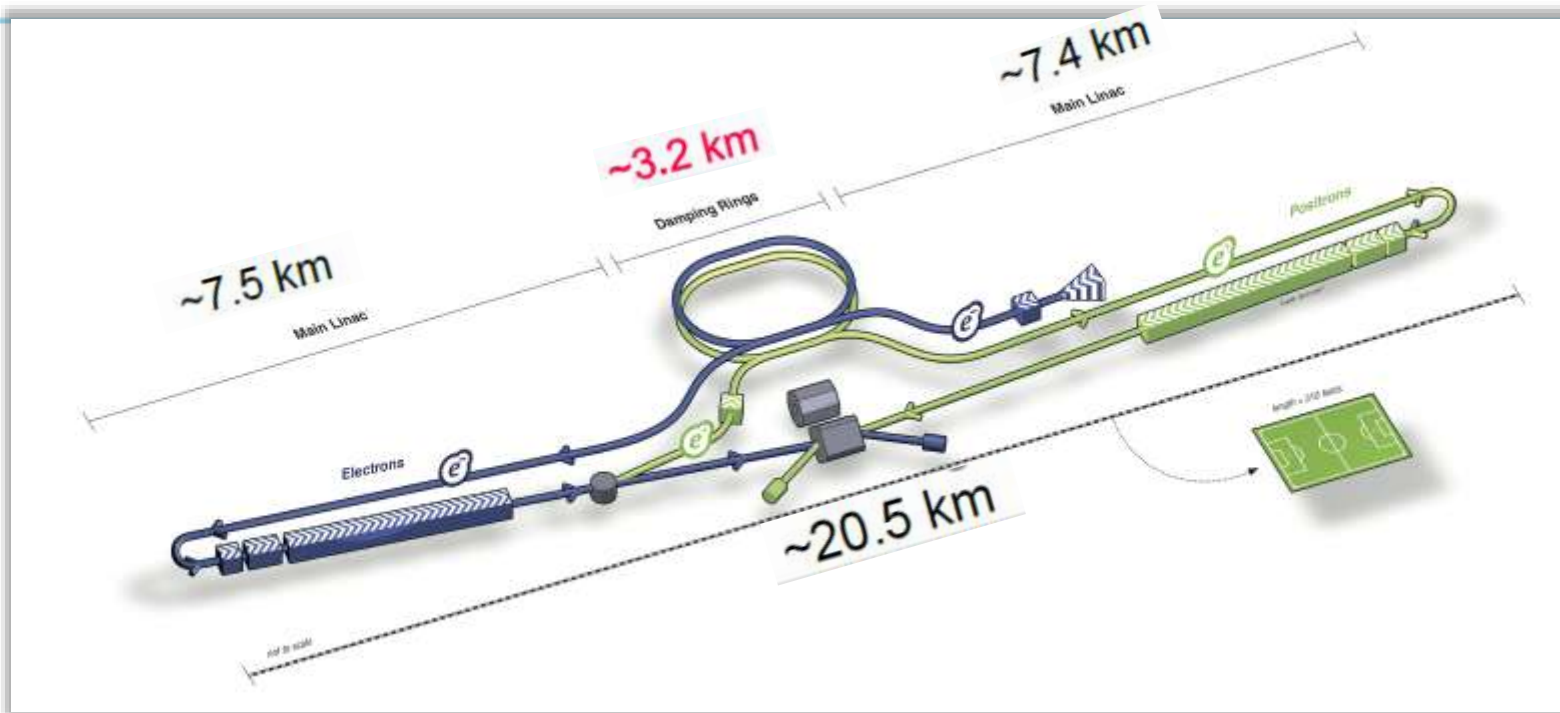


(Besides RF) Most Systems “Common”



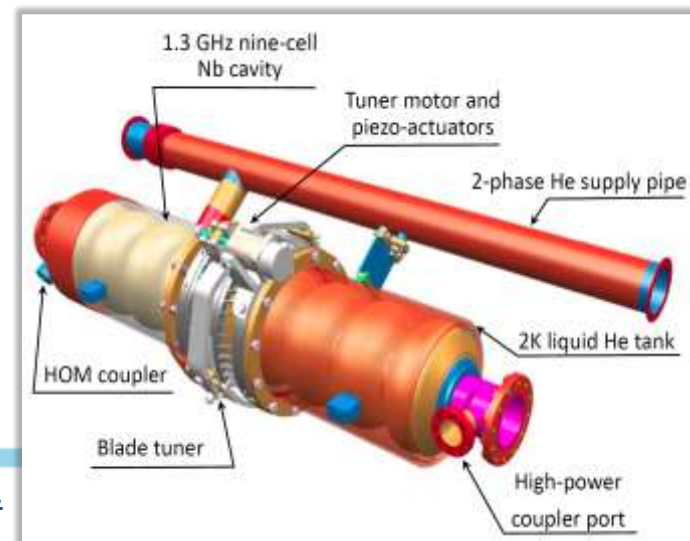
- **Electron source** → damping ring → bunch compressor
- **Positron source** → damping ring → bunch compressor
- **Acceleration**
- **Final Focus system** and beam dumps

International Linear Collider



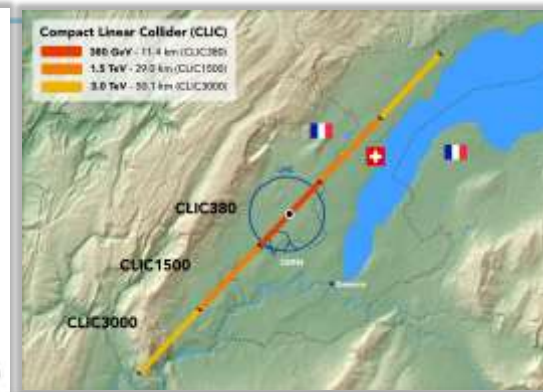
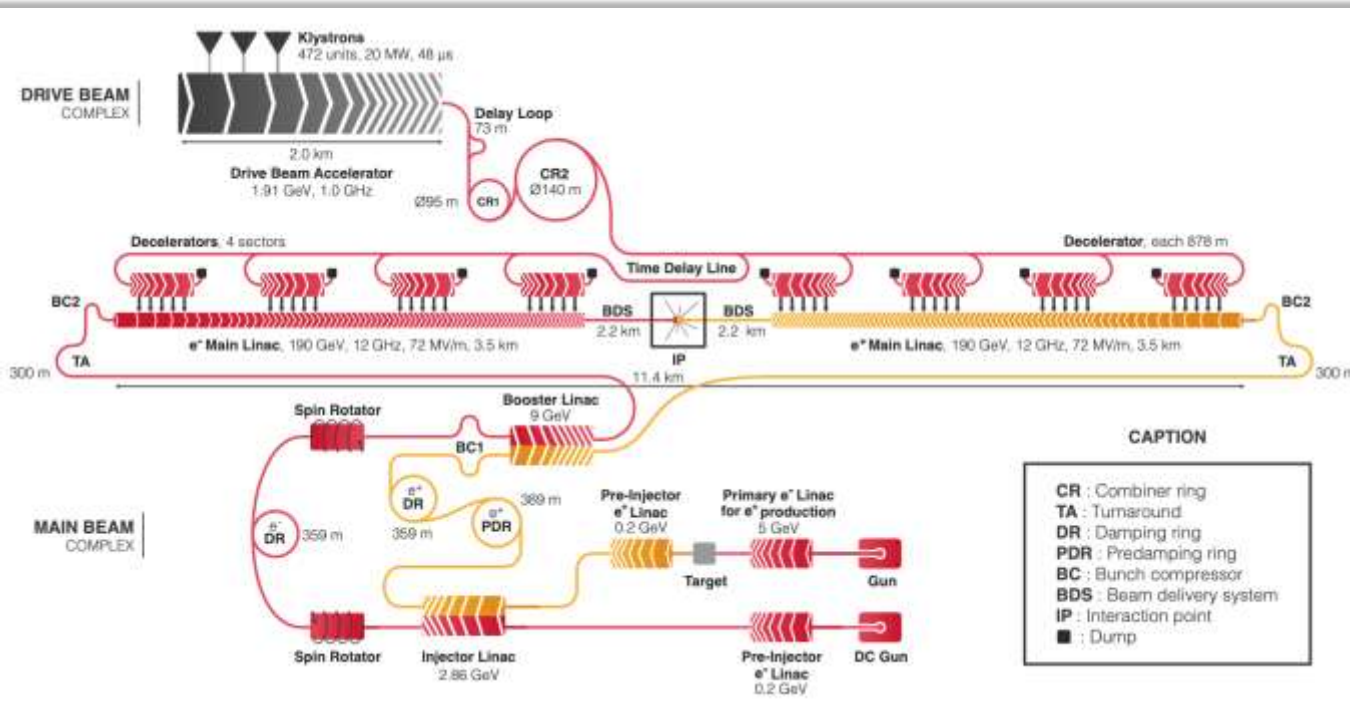
Key facts:

20 km, including 5 km of Final Focus
SRF 1.3 GHz, **31.5 MV/m**, 2 K
130 MW site power @ 250 GeV c.m.e.
Cost estimate 700 B JPY*



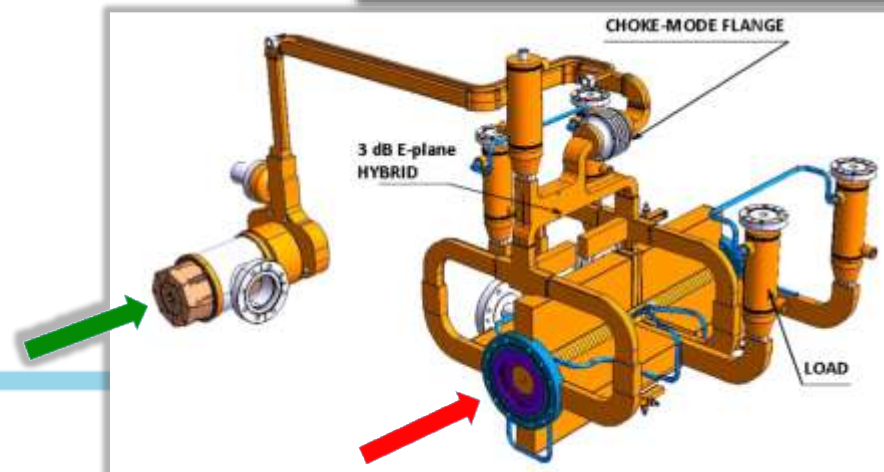
* $\pm 25\%$ err,
includes labor cost

Compact Linear Collider

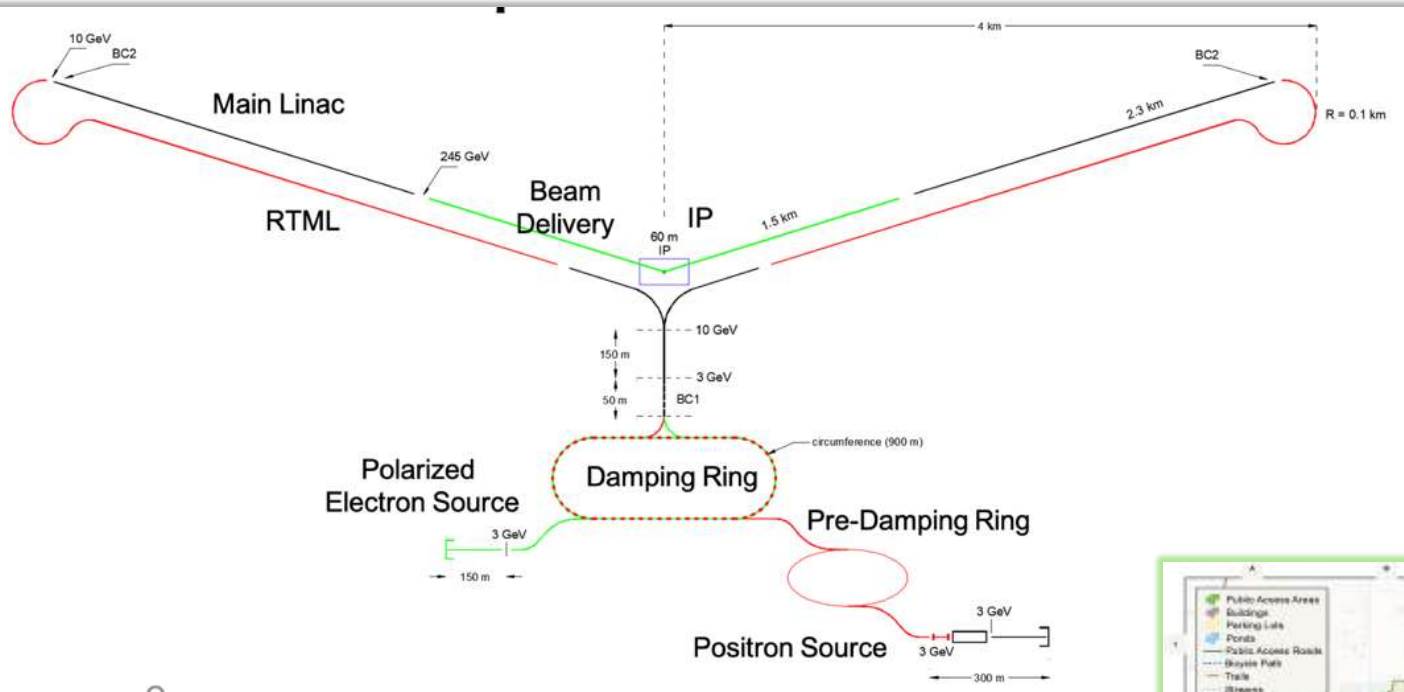
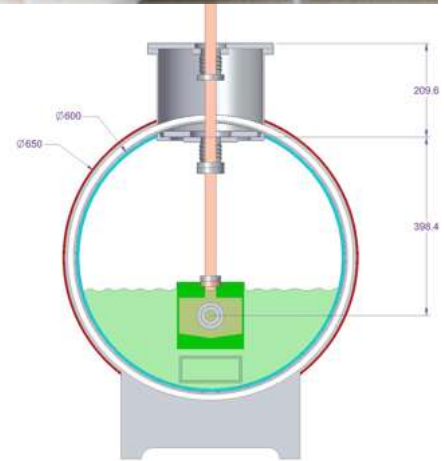


Key facts:

- 11 km main linac @ 380 GeV c.m.e.
- NC RF **72 MV/m**, *two-beam* scheme
- 168 MW site power (~9MW beams)
- Cost est. 5.9 BCHF \pm 25%



Cool Copper Collider (aka C³)



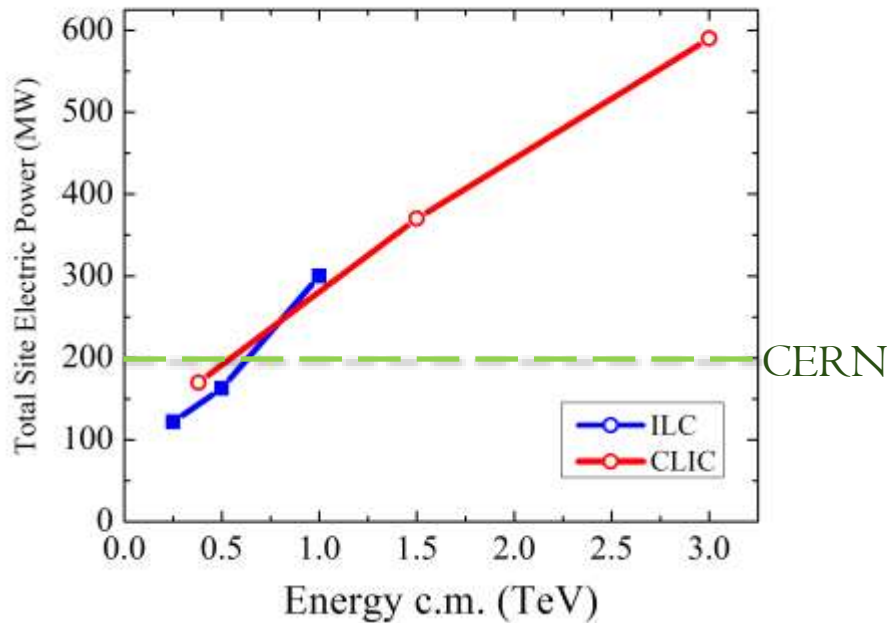
Key facts:

- 7-8 km, including 3 km of Final Focus
- NC RF 5.7 GHz, **120 MV/m**, 77 K
- 150 MW site power @ 250 GeV c.m.e.
- Cost estimate ~2/3 of ILC

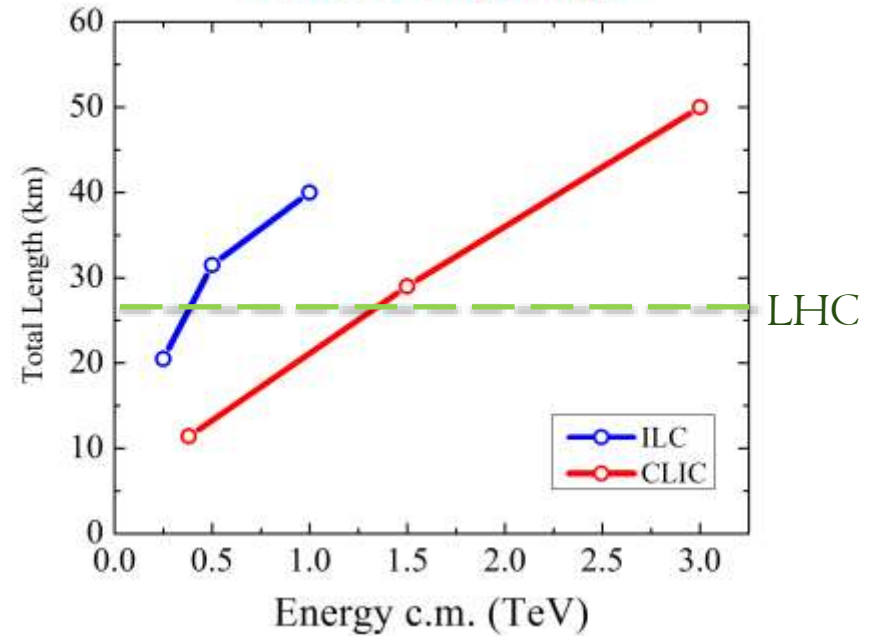


Linear e+e- Colliders Energy Limits

Total Facility Site Power Required

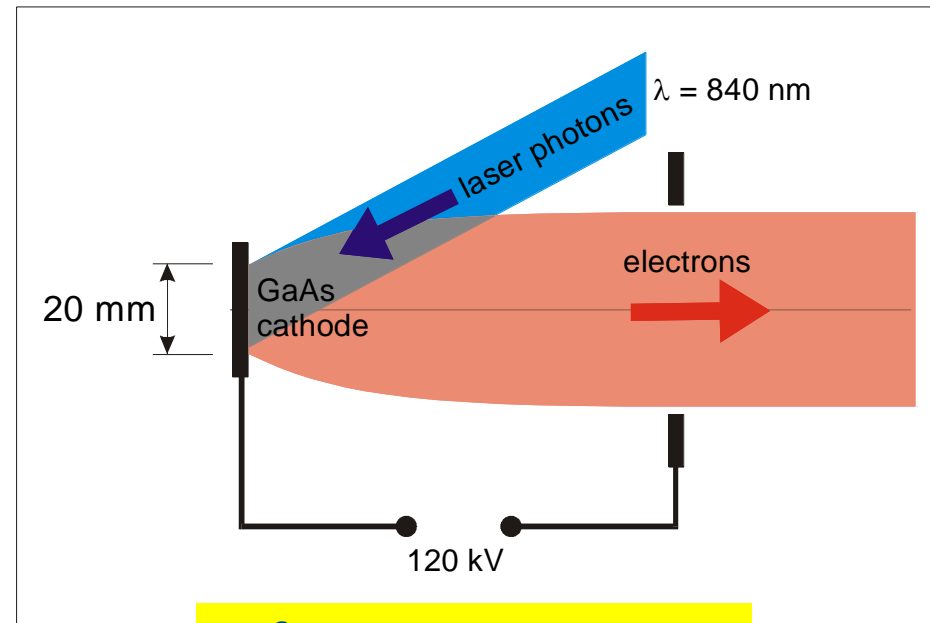


Total Facility Length



e^- Source

- laser-driven photo injector
- circ. polarised photons on GaAs cathode
→ long. polarised e^-
- laser pulse modulated to give required time structure
- very high vacuum requirements for GaAs ($<10^{-11}$ mbar)
- beam quality is dominated by space charge
(note $v \sim 0.2c$)



or few MeV in RF gun

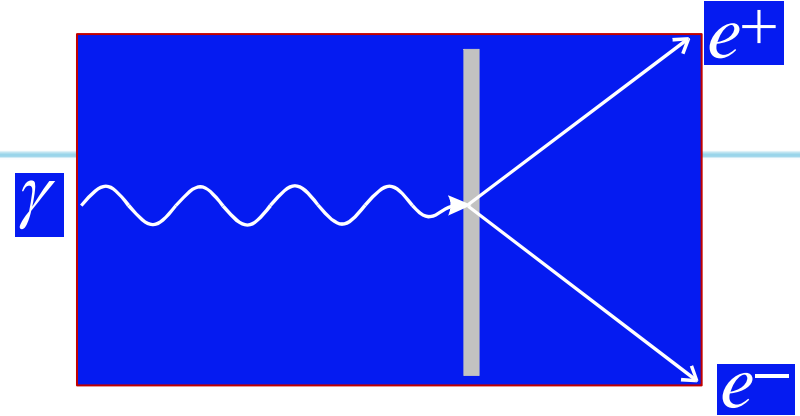
$$\epsilon_n \approx 10^{-5} m$$

factor 10 in x plane

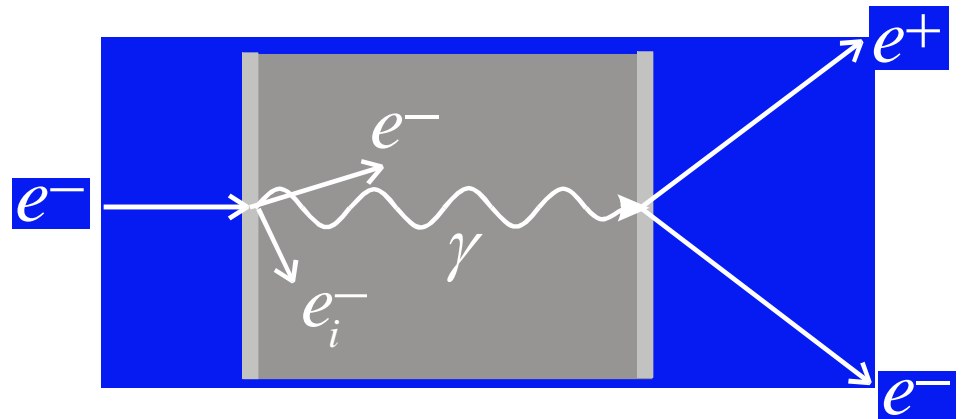
factor ~ 500 in y plane

e^+ Source

Photon conversion to e^\pm pairs in target material



Standard method is e^- beam on 'thick' target (em-shower)



Undulator based

SR radiation from undulator generates photons

no need for 'thick' target to generate shower

thin target reduces multiple-Coulomb scattering: hence better emittance (but still much bigger than needed)

less power deposited in target (no need for mult. systems)

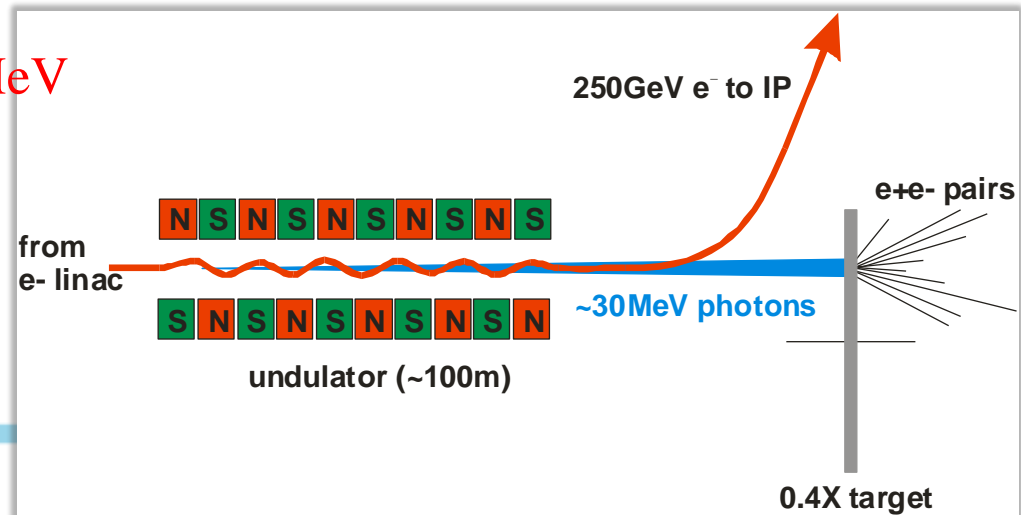
Achilles heel: needs initial electron energy > 150 GeV!

~ 30 MeV

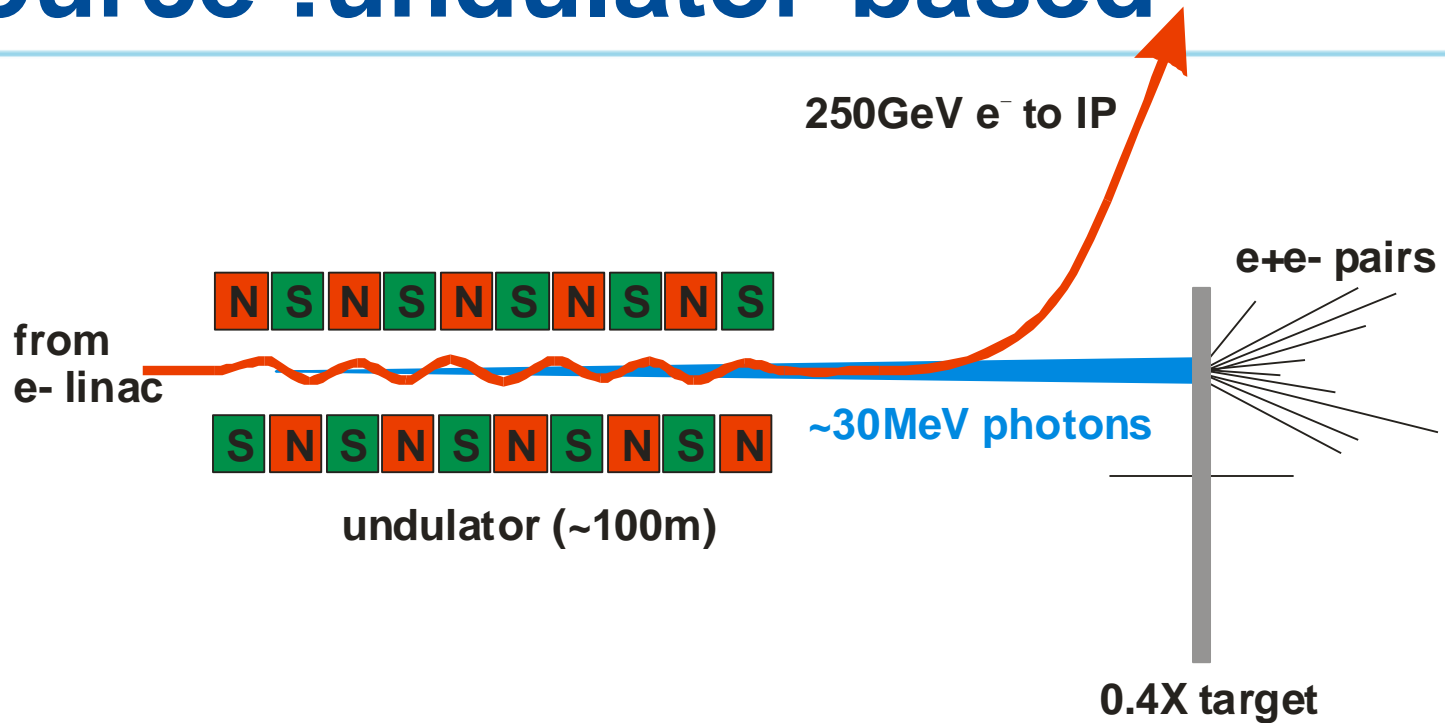
$0.4X_0$

10^{-2} m

5 kW

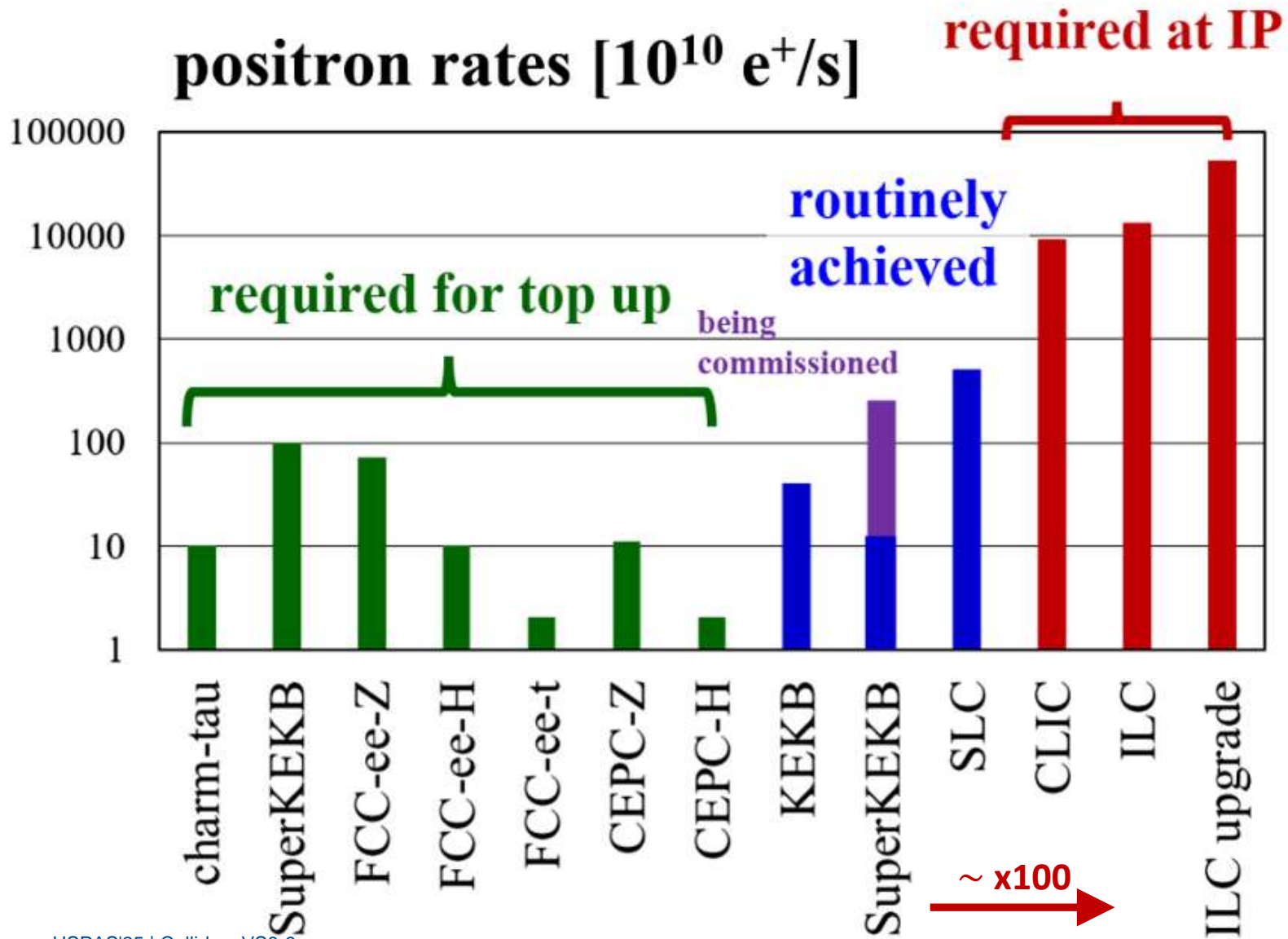


e^+ Source : undulator-based



- SR radiation from undulator generates photons ~ 30 MeV
- no need for 'thick' target to generate shower 0.4 X_0
- thin target reduces multiple-Coulomb scattering: hence better emittance (but still much bigger than needed) 10⁻² m
- less power deposited in target (no need for mult. systems) 5 kW
- Achilles heel: needs initial electron energy > 150 GeV!

(Technology) Challenge of e^+ Production



Damping Rings

- (storage) ring in which the bunch train is stored for $T_{store} \sim 20\text{-}200$ ms
- emittances are reduced via the interplay of synchrotron radiation and RF acceleration

initial emittance
($\sim 0.01\text{m}$ for e^+)

$$\varepsilon_f = \varepsilon_{eq} + (\varepsilon_i - \varepsilon_{eq}) e^{-2T/\tau_D}$$

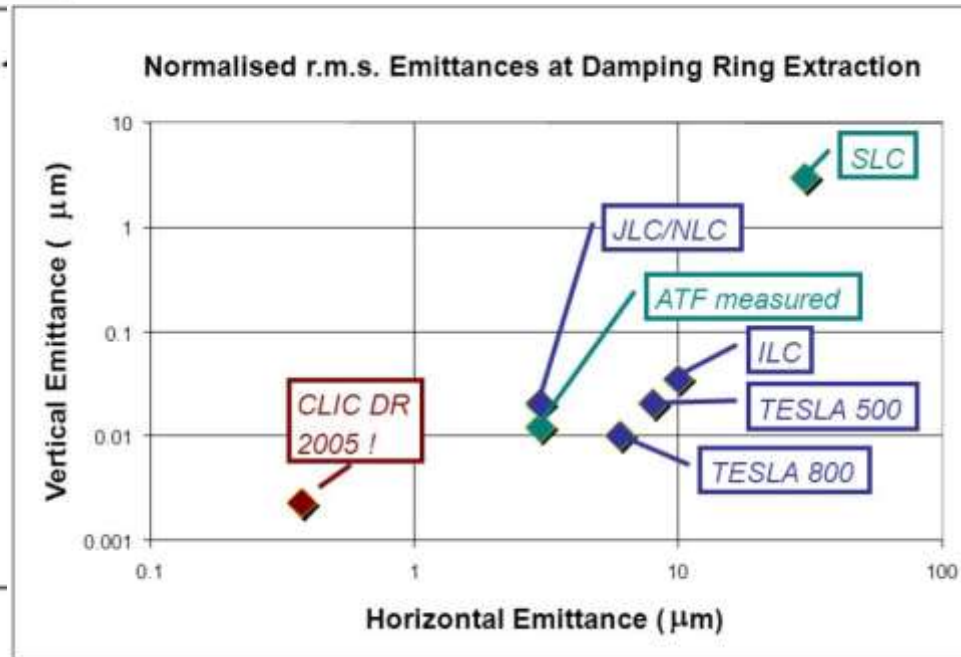
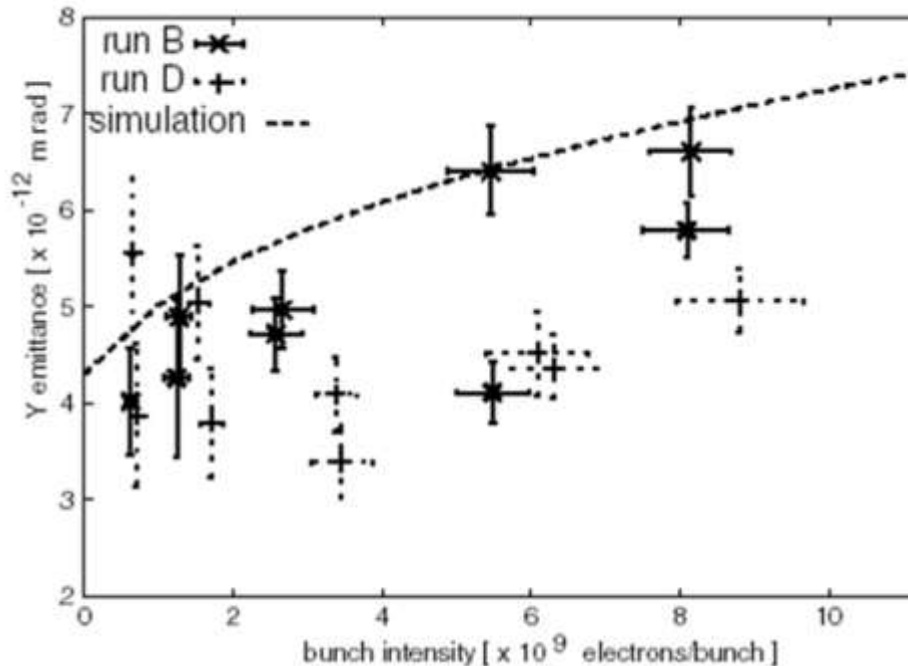
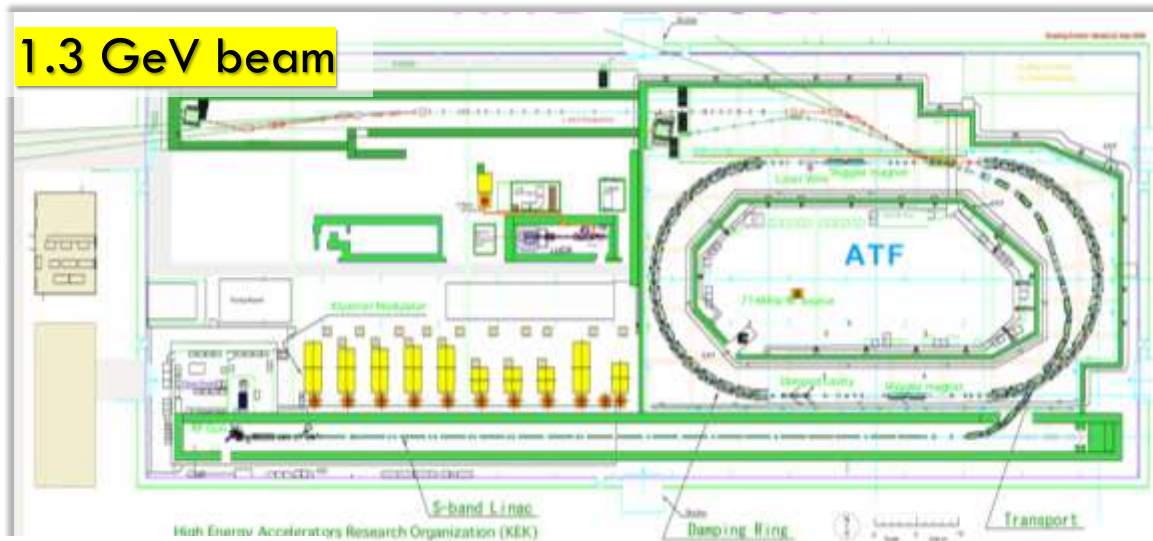
final emittance

equilibrium emittance

damping time

Damping Rings for Linear Colliders : ATF at KEK

- **DR emittances demonst'd**
 - Wigglers, instabilities, IBS ε growth, coupling
- **IP beam focusing methods**
 - 40 nm V beam size ATF2@KEK'16
 - ATF2 Goal : 37 nm \rightarrow 7.7nm@ILC250GeV



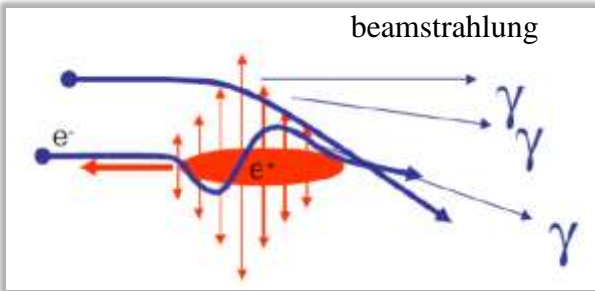
Linear e+e- Colliders: Parameters and Challenges

Collider	NLC[28]	CLIC[29]	ILC[5]	C ³	C ³
CM Energy [GeV]	500	380	250 (500)	250	550
σ_z [μm]	150	70	300	100	100
β_x [mm]	10	8.0	8.0	12	12
β_y [mm]	0.2	0.1	0.41	0.12	0.12
ϵ_x [nm-rad]	4000	900	500	900	900
ϵ_y [nm-rad]	110	20	35	20	20
Num. Bunches per Train	90	352	1312	133	75
Train Rep. Rate [Hz]	180	50	5	120	120
Bunch Spacing [ns]	1.4	0.5	369	5.26	3.5
Bunch Charge [nC]	1.36	0.83	3.2	1	1
Beam Power [MW]	5.5	2.8	2.63	2	2.45
Crossing Angle [rad]	0.020	0.0165	0.014	0.014	0.014
Crab Angle	0.020/2	0.0165/2	0.014/2	0.014/2	0.014/2
Luminosity [$\times 10^{34}$]	0.6	1.5	1.35	1.3	2.4
	(w/ IP dil.)	(max is 4)			
Gradient [MeV/m]	37	72	31.5	70	120
Effective Gradient [MeV/m]	29	57	21	63	108
Shunt Impedance [$\text{M}\Omega/\text{m}$]	98	95		300	300
Effective Shunt Impedance [$\text{M}\Omega/\text{m}$]	50	39		300	300
Site Power [MW]	121	168	125	~ 150	~ 175
Length [km]	23.8	11.4	20.5 (31)	8	8
L* [m]	2	6	4.1	4.3	4.3

Luminosity Challenges of Linear Colliders

$$\mathcal{L} = \frac{H_D}{4\pi} \frac{N}{\sigma_x} N n_b f_r \frac{1}{\sigma_y} \sim 10^{34}$$

Luminosity Spectrum (Physics)



- $\delta E/E \sim 1.5\%$ in ILC
- Grows with E : 40% of CLIC lumi **1% off** \sqrt{s}

Beam Current (RF power limited, beam stability)

- Challenging e+ production (two schemes)
- CLIC high-current drive beam bunched at 12 GHz
- Many high-power klystrons for C^3

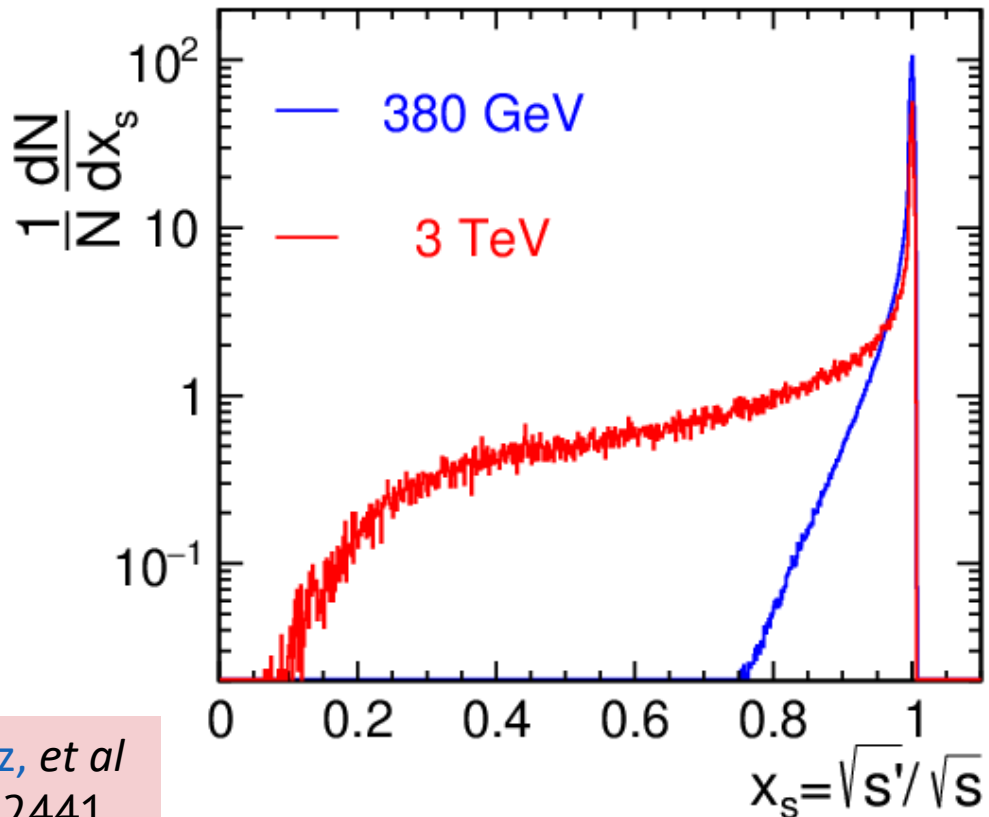
Beam Quality (Many systems)

- Record small DR emittances
 - 0.1 μm BPMs
 - IP beam sizes
- | | |
|------|-----------|
| ILC | 8nm/500nm |
| CLIC | 3nm/150nm |
| C^3 | 4nm/180nm |

BeamStrahlung at IP

linear colliders

synchrotron radiation in the strong field of the opposing beam (=“beamstrahlung”) degrades the luminosity spectrum



CLIC at 380 GeV: 60% of total luminosity within 1% of target energy

CLIC at 3 TeV: only 33% of total luminosity within 1% of target

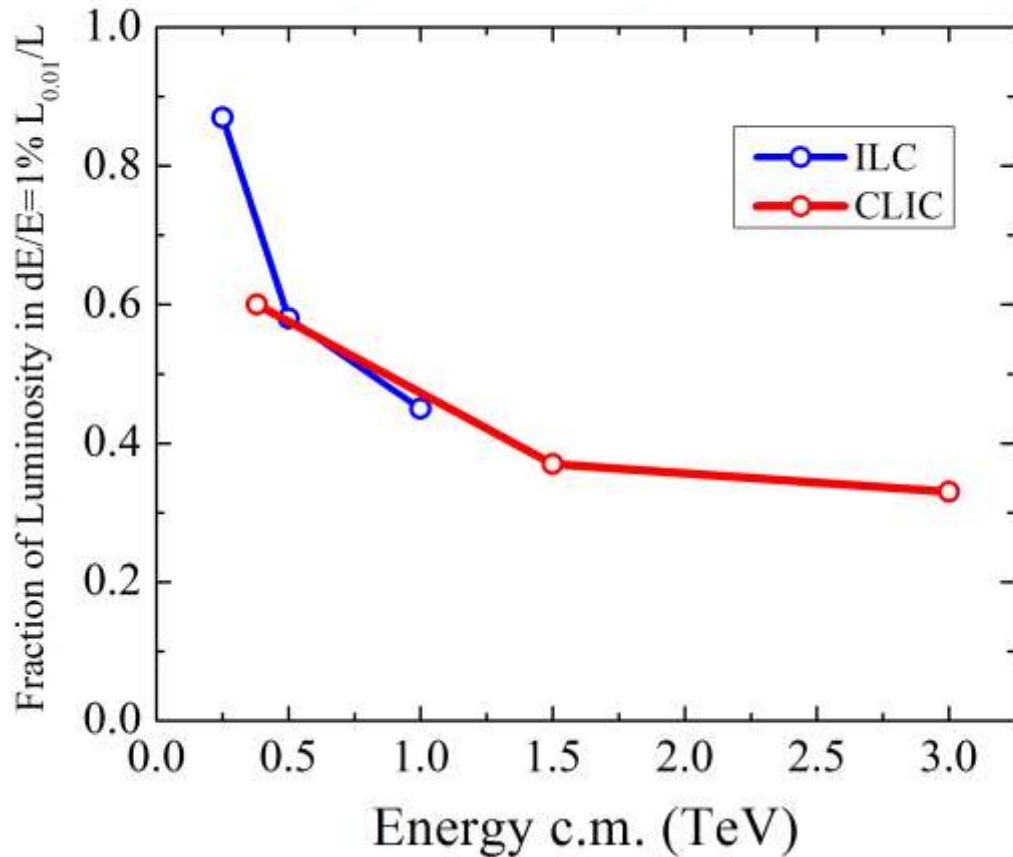
e^+e^- collisions in linear colliders lose their distinct energy precision

D. Schulte

H. Abramowicz, *et al*
- arXiv:1807.02441

Beamstrahlung Kills High- E ee LCs

Luminosity Dilution by Beamstrahlung



Beamstrahlung rms energy spread :

$$\delta_{BS} \propto \left(\frac{E_{cm}}{\sigma_z} \right) \frac{N^2}{\sigma_x^2}$$

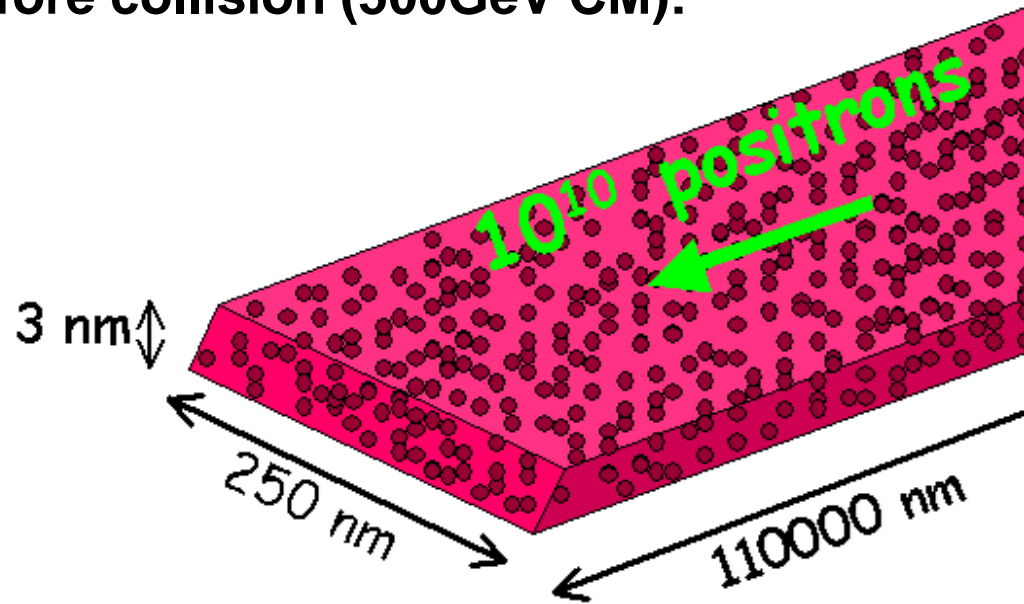
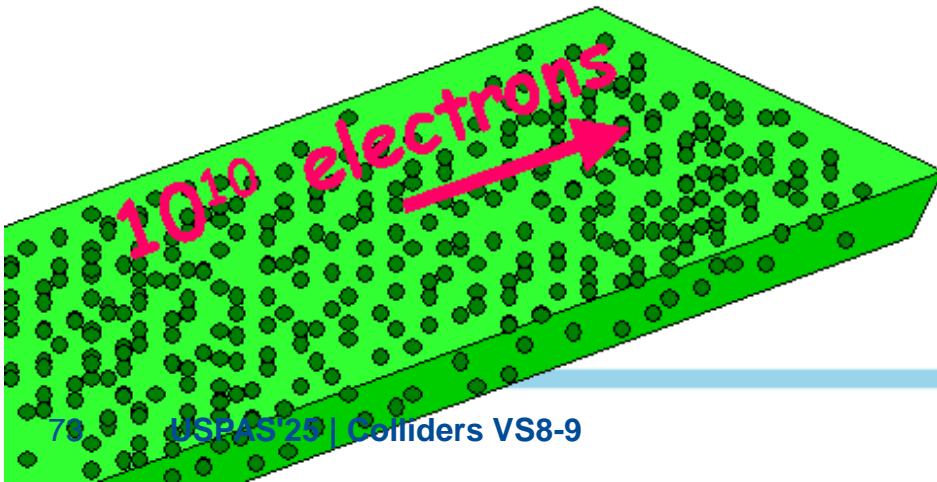
→ Luminosity :

$$L \propto P_{beam} \sqrt{\frac{\delta}{\gamma \epsilon_y}} H_D$$

How to get Luminosity

- To increase probability of direct e^+e^- collisions (luminosity) and birth of new particles, beam sizes at IP must be very small
- Exemplary beam sizes just before collision (500GeV CM):
250 * 3 * 110000 nanometers
(x y z)

↑
Vertical size
is smallest



$$L = \frac{f_{rep}}{4\pi} \frac{n_b N^2}{\sigma_x \sigma_y} H_D$$

Disruption parameter

- Strong fields will distort the opposing beam
- Normalized beam-beam focusing force at the IP:

$$K_{x,y} = \frac{2\lambda r_e}{\gamma\sigma_{x,y}(\sigma_x + \sigma_y)} \quad x'' + Kx = 0$$

- Disruption parameter defined using thin lens approximation and comparing focal to bunch length

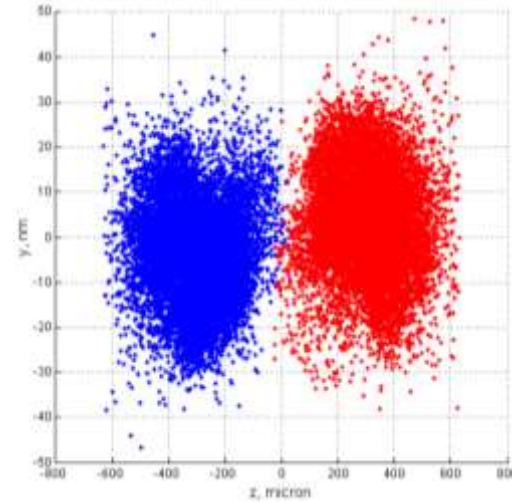
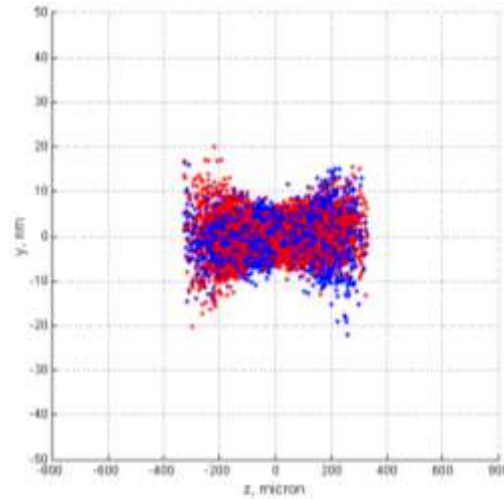
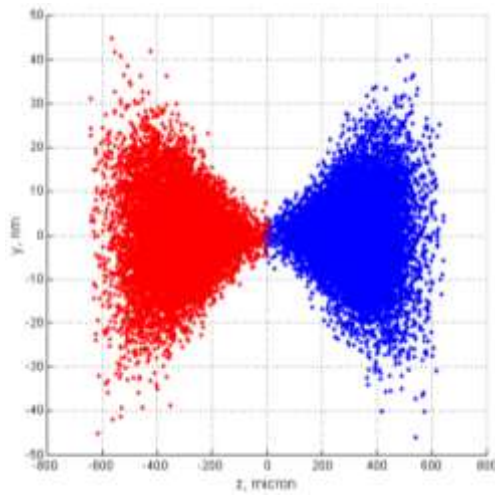
$$D_{x,y} \equiv \frac{\sigma_z}{f_{x,y}} = \frac{2Nr_e\sigma_z}{\gamma\sigma_{x,y}(\sigma_x + \sigma_y)} = 2\pi\xi_y\sigma_z/\beta^*_y$$

- Assume a rectangular distribution \rightarrow number of oscillations in opposing bunch:

$$n \approx 1.3 \frac{\sqrt{D}}{2\pi}$$

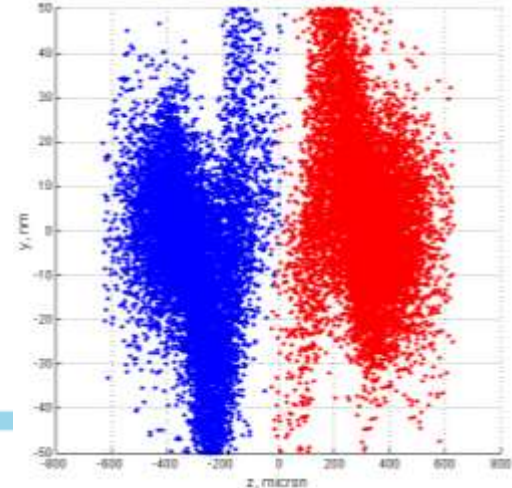
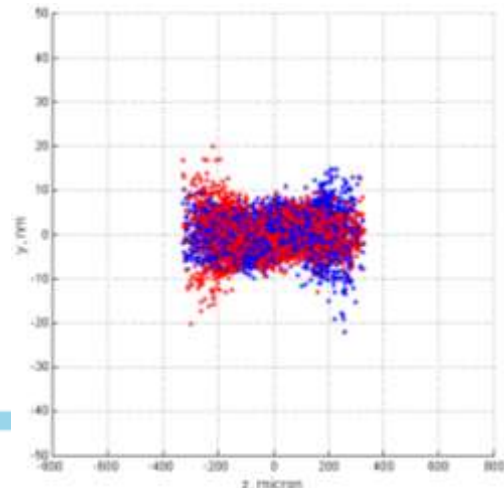
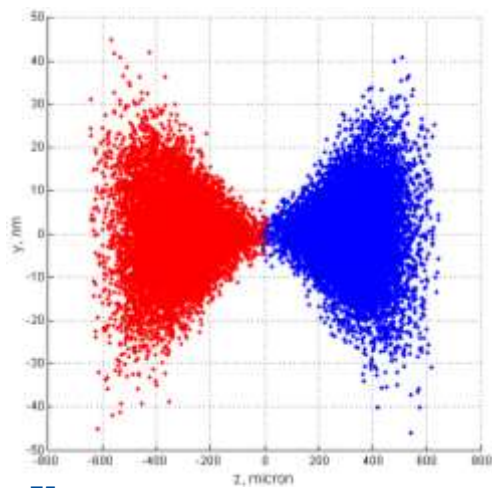
Disruption Parameter D_y and “Travelling Focus”

At modest $D \sim 3-10 \rightarrow$ luminosity enhancement due to “traveling focus”



$D_y \sim 12$

At large $D > 15 \rightarrow$ luminosity destruction by “kink instability”

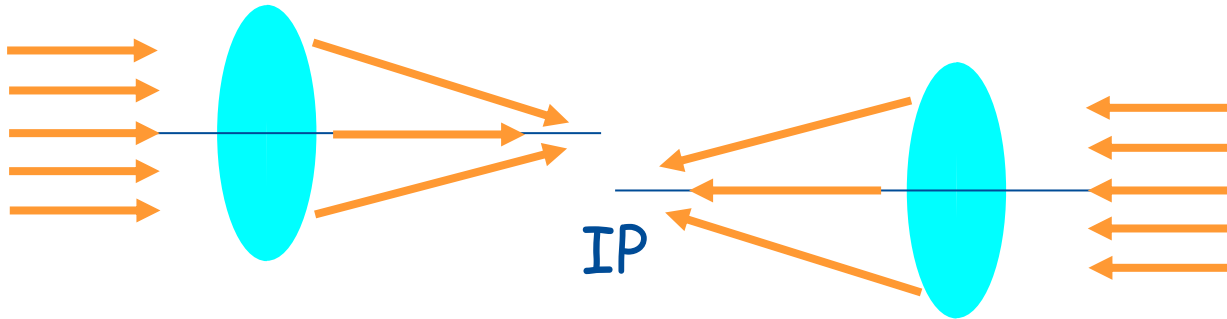


$N \times 2$
 $D_y \sim 24$

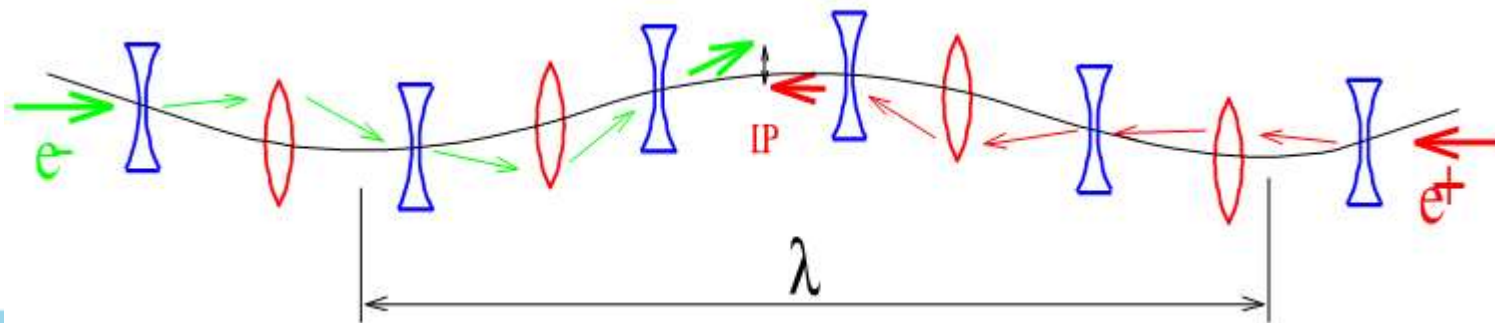
Trajectory Stability and Control

- Two effects due to ground motion, vibrations, jitter and other mechanical and EM noises:
 - Two beams get separated at the IP (rms Y size few nm)
 - Each beam goes thru not ideal trajectory along its linac and experiences either dipole kicks due to displacement in quadrupoles $\text{Kick} \sim \text{B-Gradient} \times \text{Position}$ or a kick in RF cavity due to a wakefield or (if the cavity is tilted) $\text{Kick} \sim \text{E-Gradient} \times \text{Tilt} \rightarrow$ *beam-beam separation @IP and emittance growth*
- Ways to counteract (if necessary) are:
 - Mechanical stabilization of most important elements (eg FF)
 - Beam-based feedback systems acting either from pulse to pulse or (if bunch train is long) from bunch-to-bunch
 - Note that FB systems also introduce “noise” if eg BPMs have position measurement error $O(1 \text{ micron})$

Stability – tolerance to Final Doublet motion

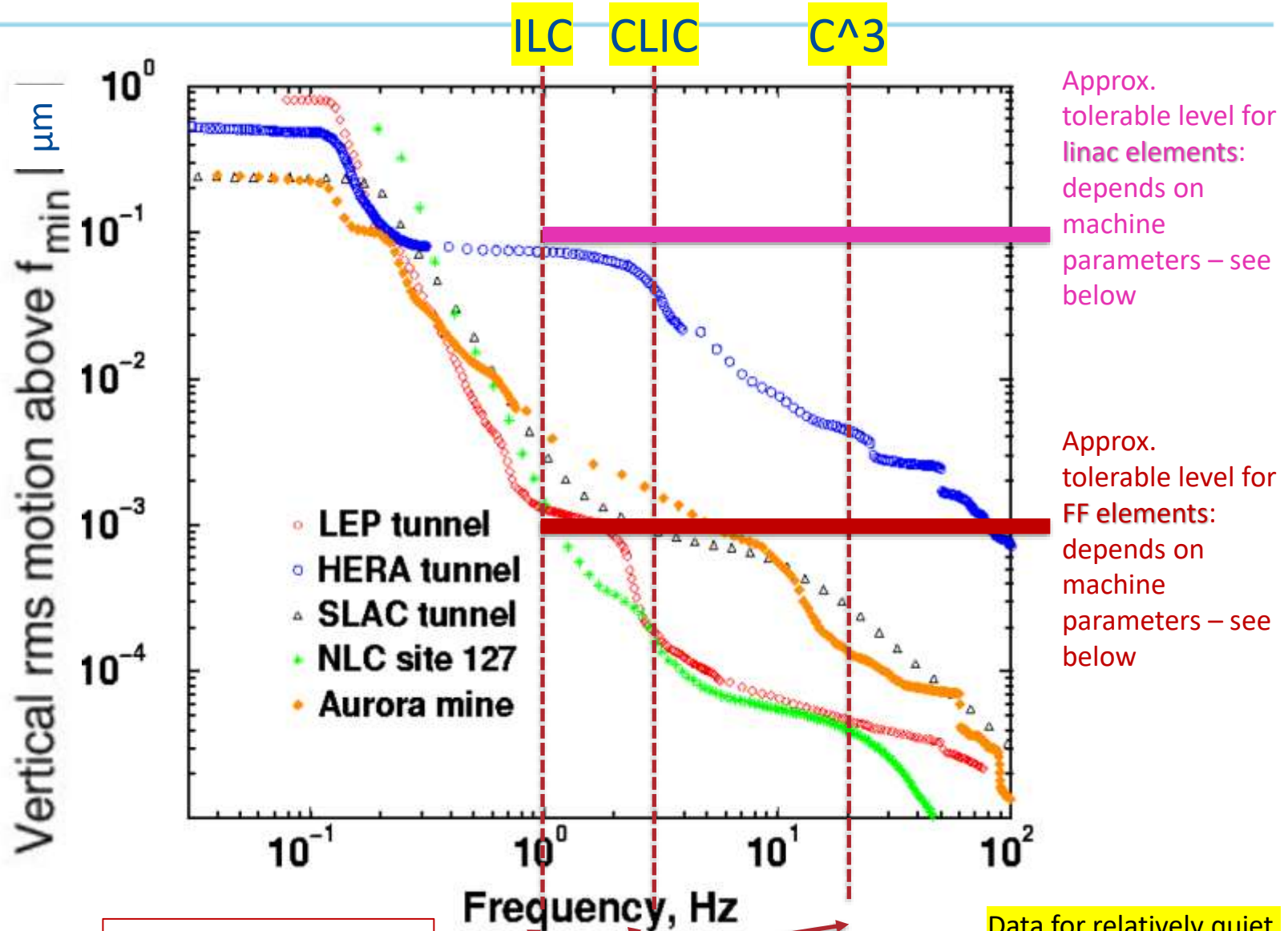


- Displacement of FD by dY cause displacement of the beam at IP by the same amount \rightarrow Therefore, stability of FD need to be maintained with a fraction of nanometer accuracy
- Such small offsets of FD or beams can be detected using beam-beam deflection
- Linac misalignments affect dY as well:



Of course, what matters is differential motion with wavelength $<$ betatron one (i.e. differential quad-to-quad motion)

Fast Vibrations ($f > f_{rep}/6$)



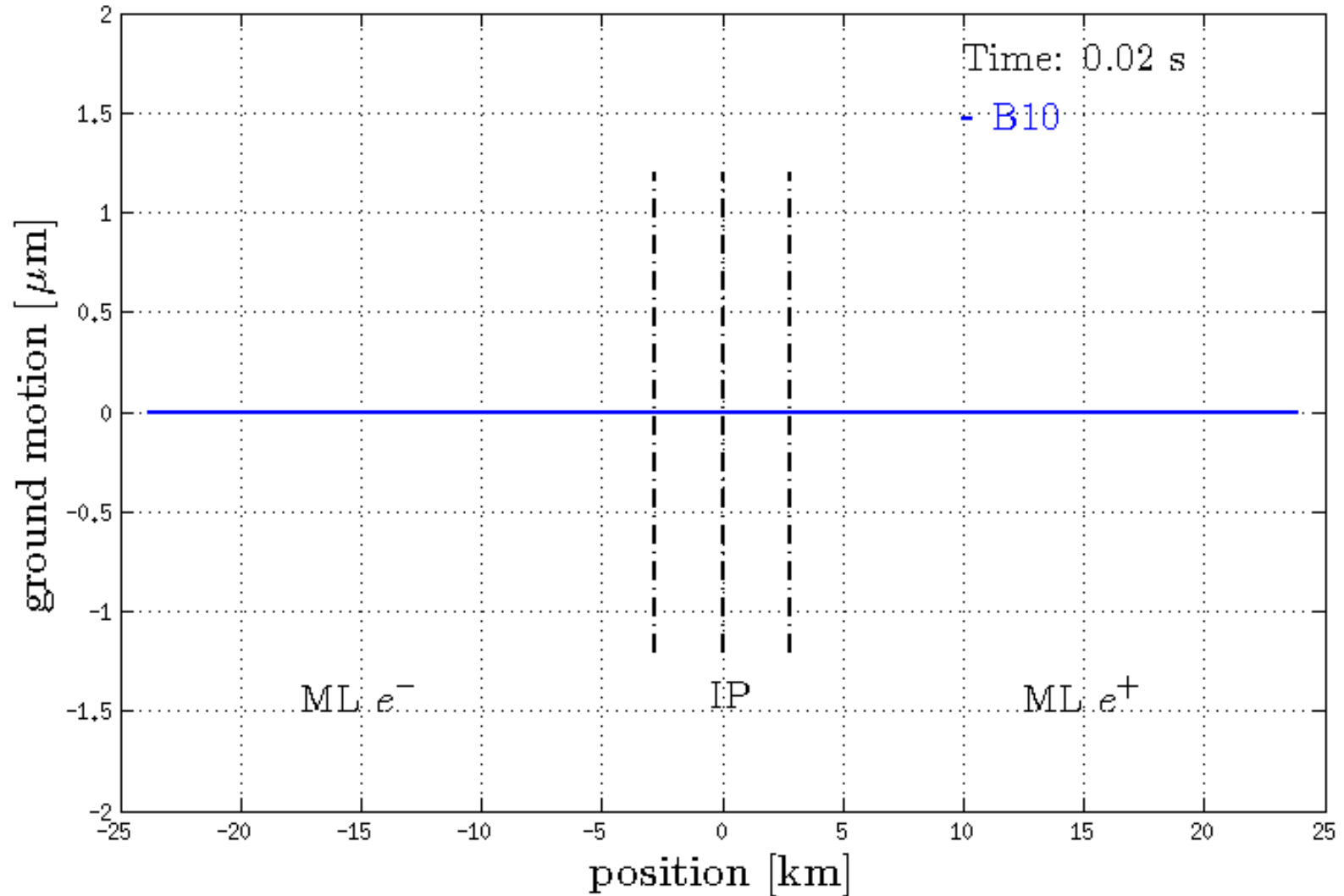
Approx. tolerable level for linac elements: depends on machine parameters – see below

Approx. tolerable level for FF elements: depends on machine parameters – see below

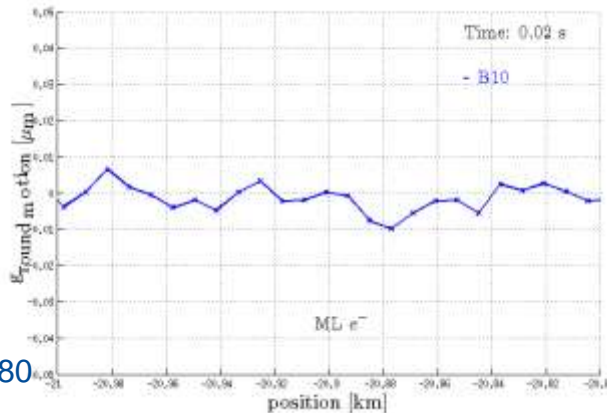
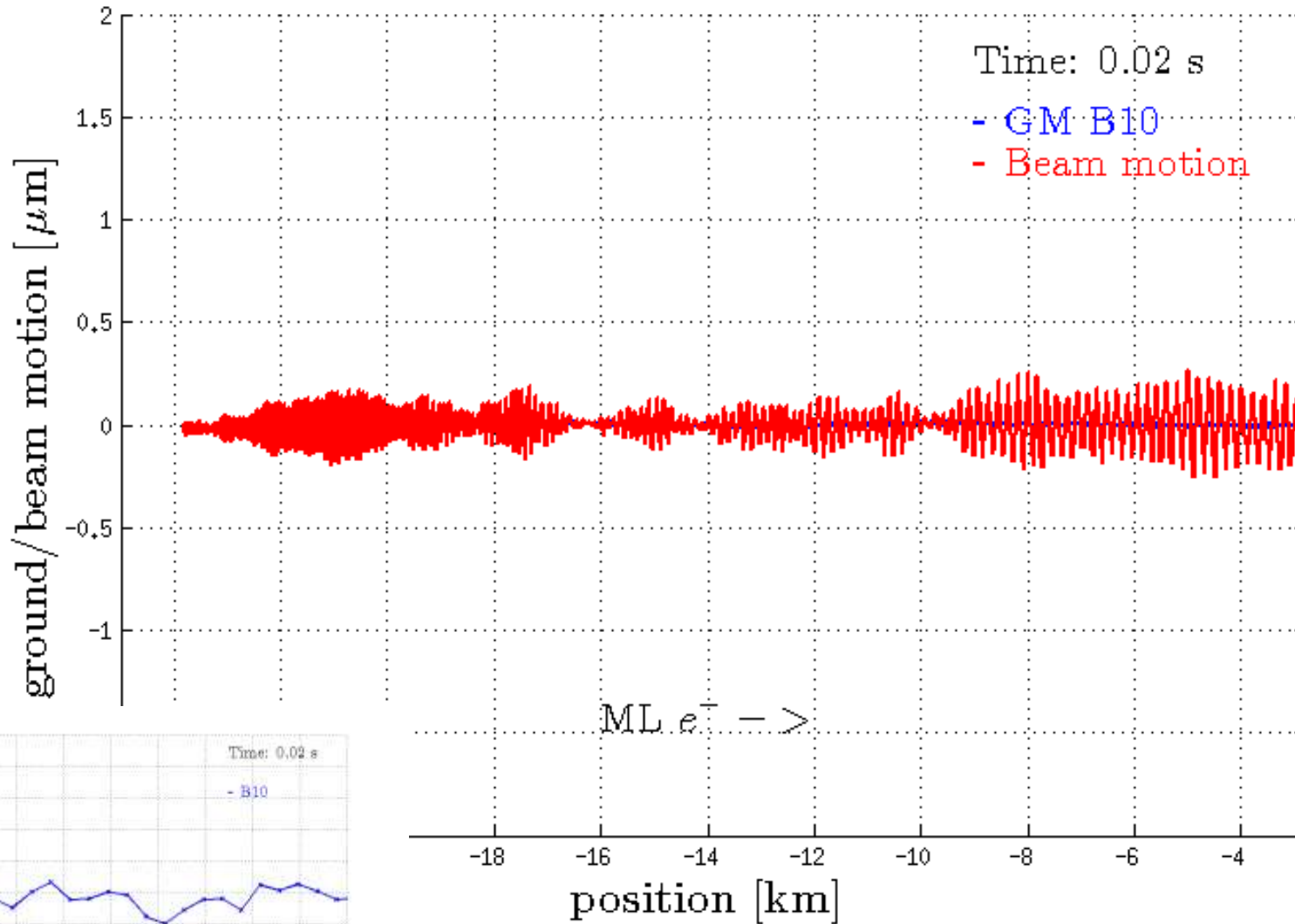
Below these frequencies FB systems can possibly control GM effects

Data for relatively quiet conditions on tunnel floors (“ground motion”)

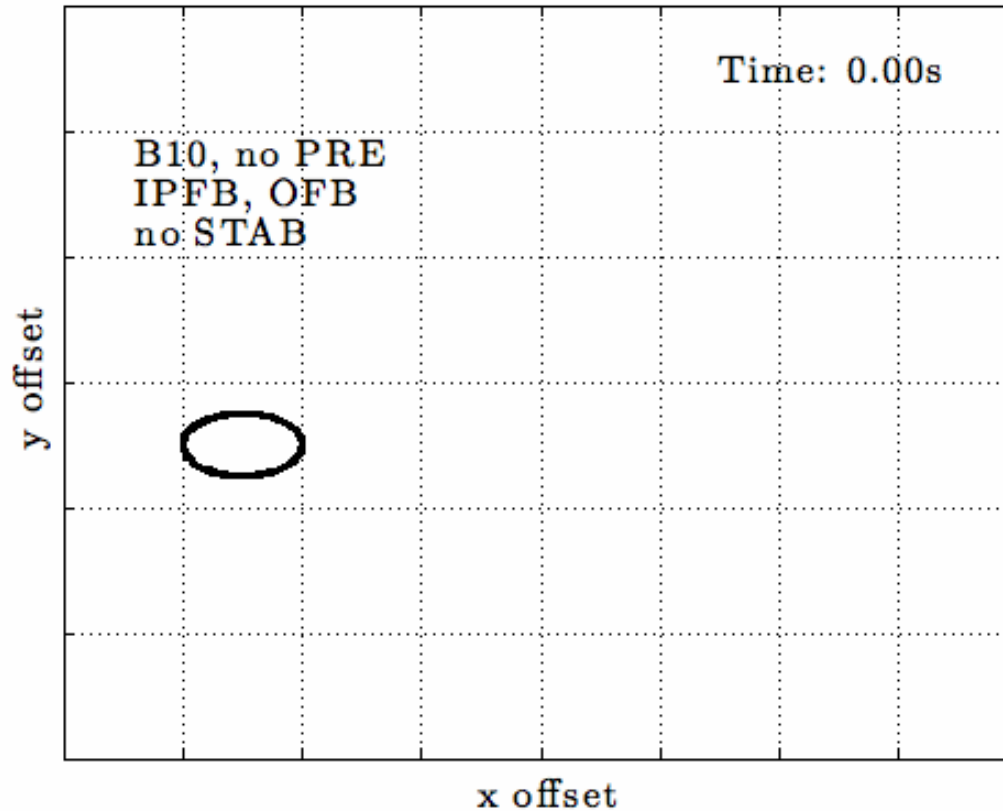
Example Issue: Ground Motion at CLIC



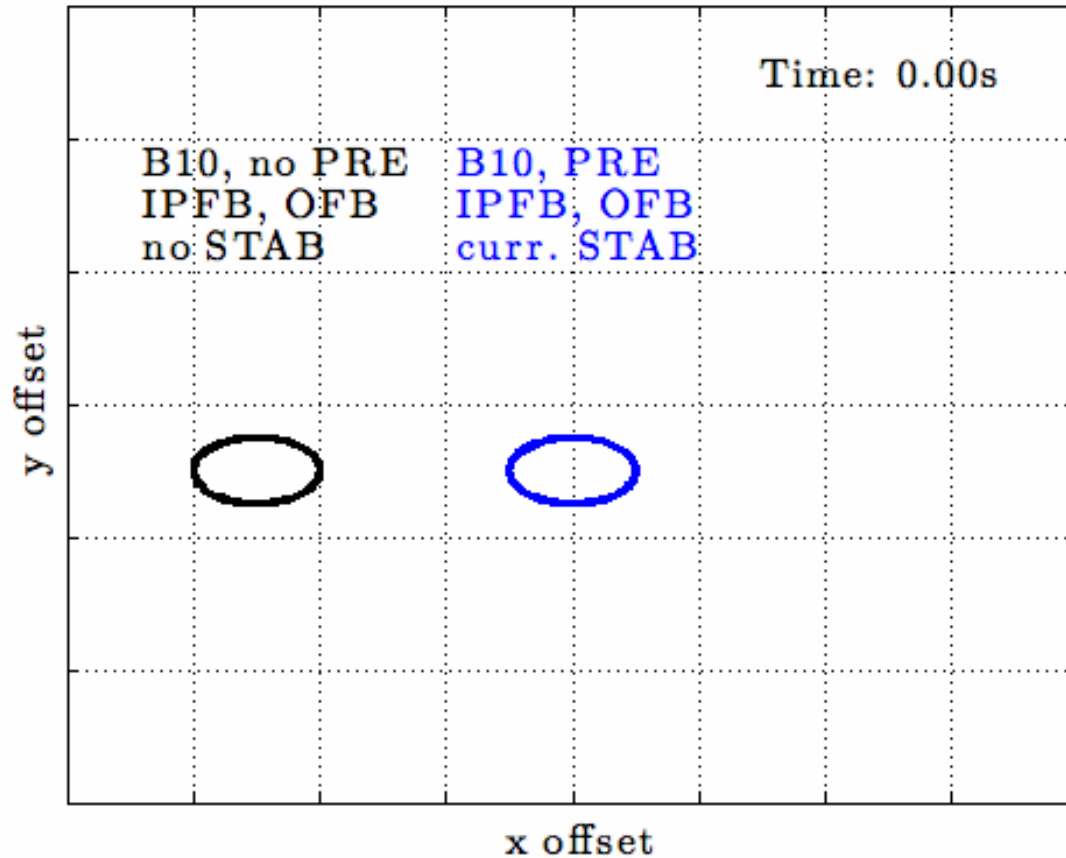
Resulting Beam Jitter (CLIC)



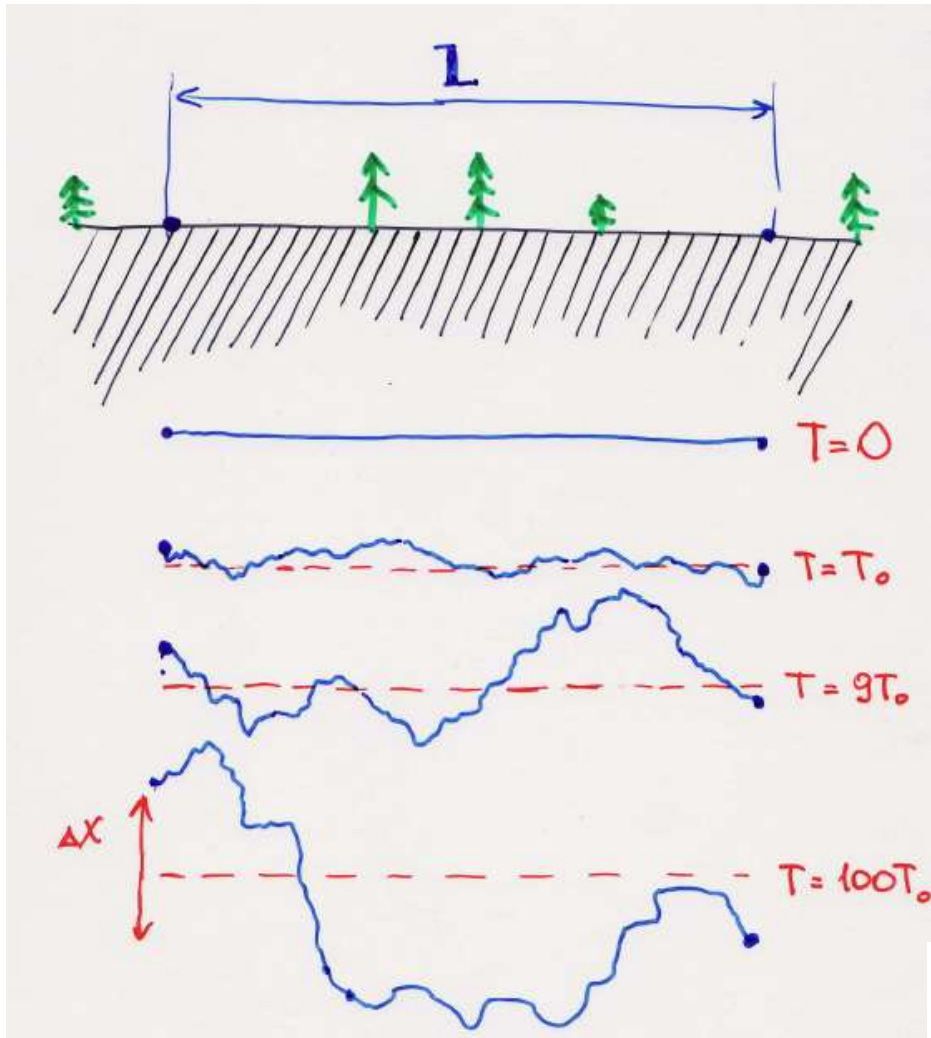
Beams at Collision (CLIC)



Beams at Collision + Feedback (CLIC)



Diffusive Ground Motion: ATL Law



Diffusive ground motion is an indication of fractal dynamics of ground/tunnel elements at the scale of min to years, m to 10's km
Observed essentially at all accelerators

MEAN IN TIME+SPACE

TIME INTERVAL

← 1991

$$\langle\langle \Delta X^2 \rangle\rangle = A \cdot T \cdot L$$

relative displacement (μ,v)
 $\Delta X = X_2 - X_1$

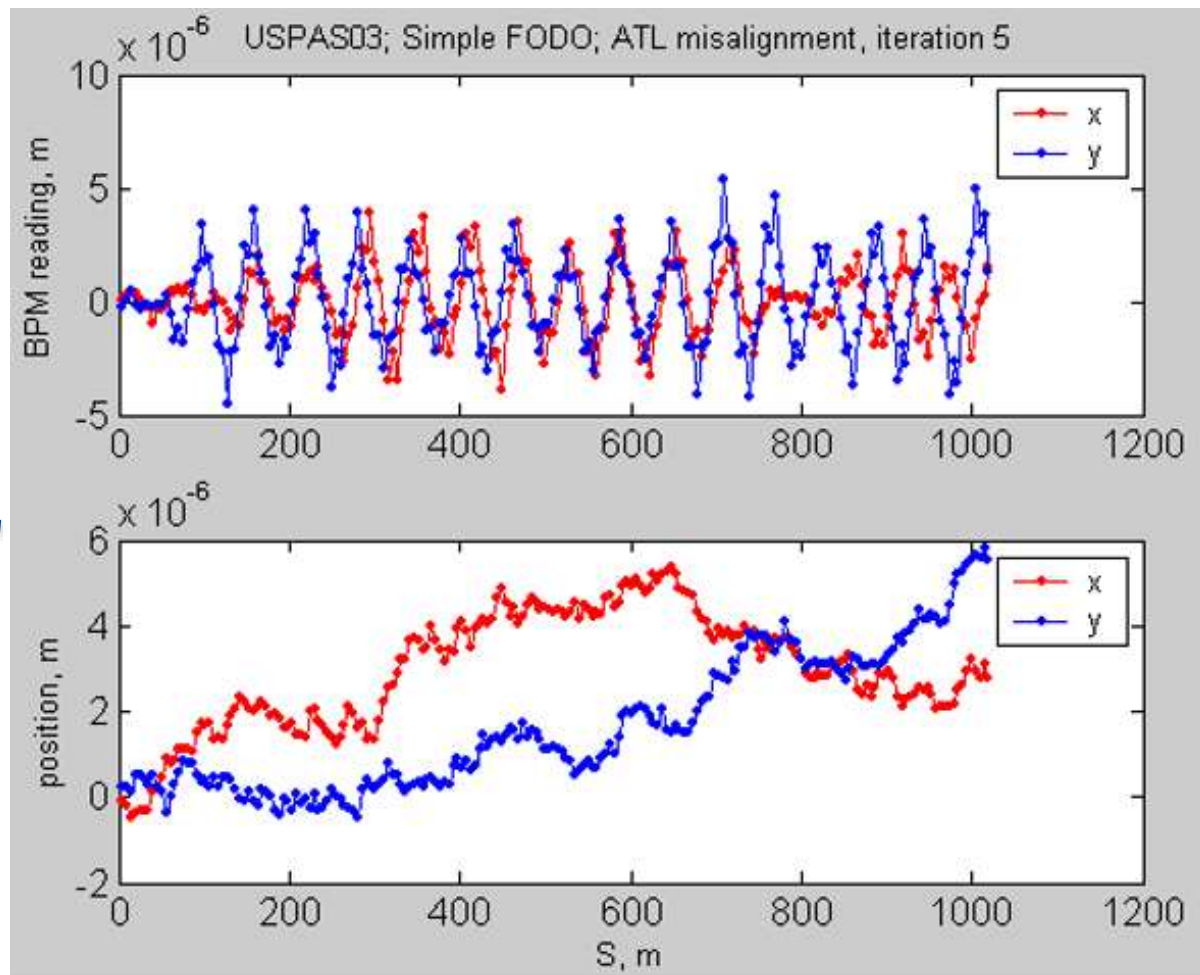
DIFFUSIVE COEFFICIENT
~10⁻⁵ ± 1 $\frac{\mu\text{m}^2}{\text{s} \cdot \text{m}}$

SPATIAL INTERVAL

Diffusion coefficient **A** is dependent on site geology, depth and tunnel construction technique

In linear colliders – Diffusion of trajectories

ATL diffusion of
quadrupole positions -
simulations for ILC
and
X, Y beam trajectories
in BPMs along the linac

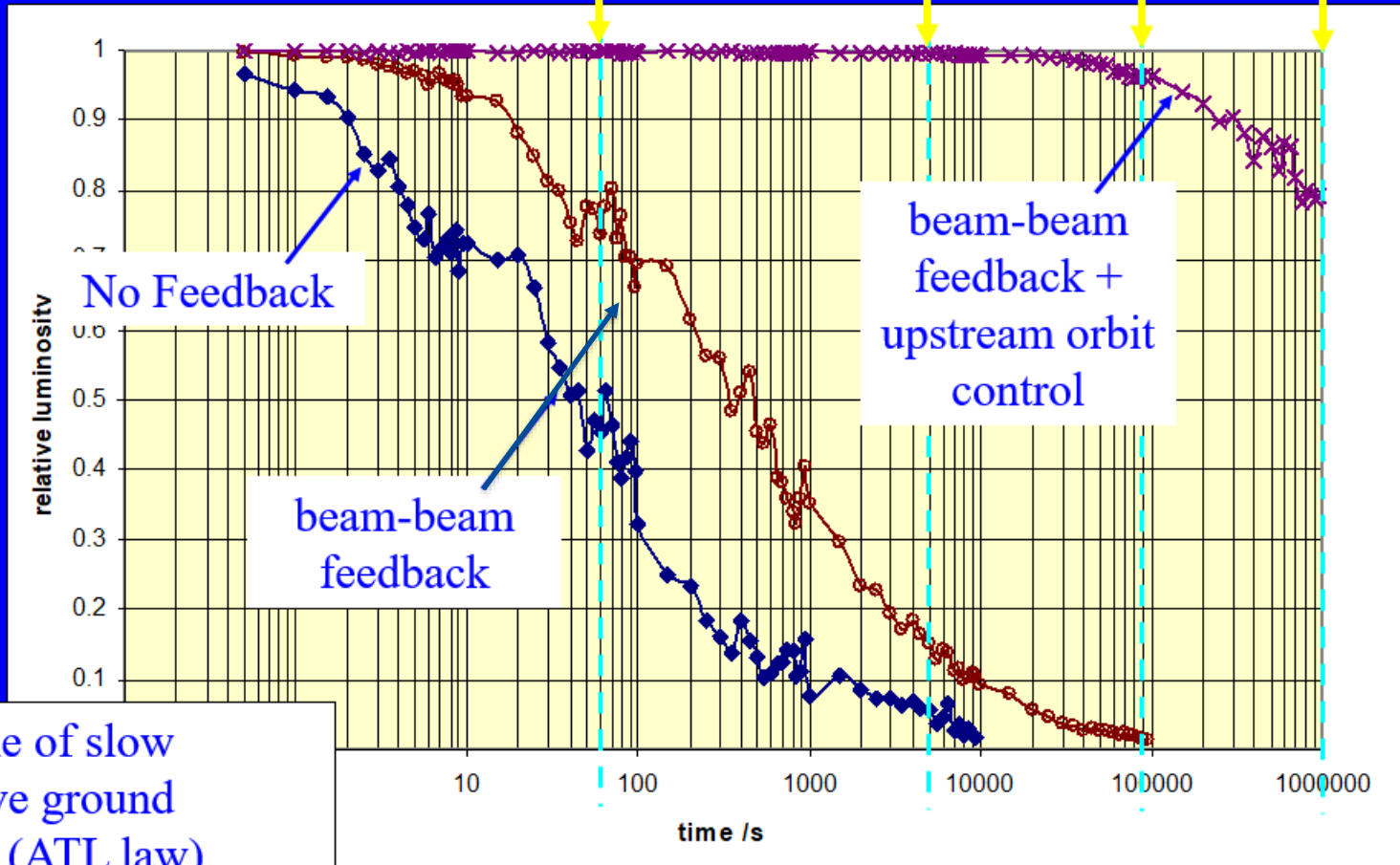


ATL+vibrations require continuous corrections by
high resolution feedback systems (BPMs+correctors)

LC: Long-Term Stability and Correction

understanding of ground motion and vibration spectrum important

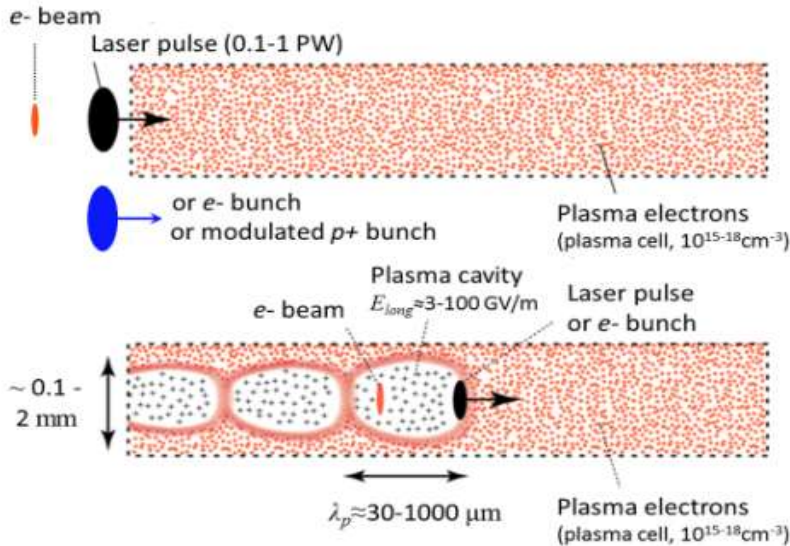
1 minute 1 hour 1 day 10 days



example of slow diffusive ground motion (ATL law)

“Hope”: Ultra-High Fields in Plasma

$$E_0 = \frac{m_e c \omega_p}{e} \approx 100 \left[\frac{\text{GeV}}{m} \right] \cdot \sqrt{n_0 [10^{18} \text{cm}^{-3}]}$$



From 0.1 GV/m (in traditional RF accelerators) to 10-100 GV/m in plasma

Three ways to excite plasma (drivers)

laser $dE \sim 10 \text{ GeV}$ ($6 \cdot 10^{17} \text{ cm}^{-3}$ 0.1 m)

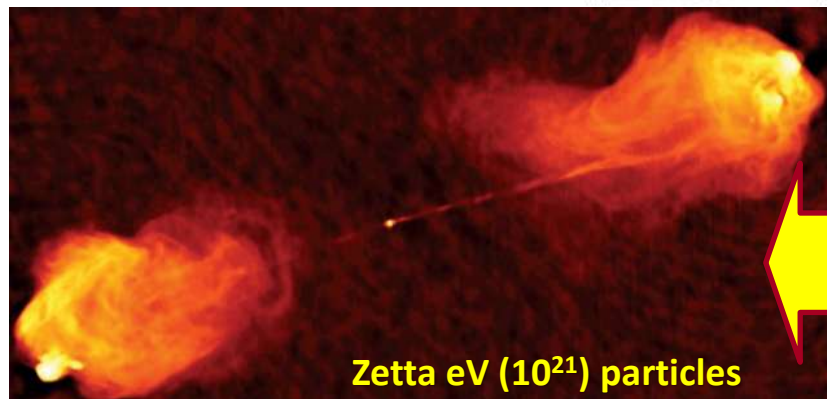
e- bunch $dE \sim 9 \text{ GeV}$ ($\sim 10^{17} \text{ cm}^{-3}$ 1.3 m)

p+ bunch $dE \sim 2 \text{ GeV}$ ($\sim 10^{15} \text{ cm}^{-3}$ 10 m)

Impressive proof-of-principle demos!

In principle, plasma **PeV** $\mu+\mu-$ colliders could be feasible...staging, cost and power of such TBD

UHECRs from EM shock waves in the ultra-dense jets of accreting magnetized black holes



Zetta eV (10^{21}) particles



Thanks for your Attention!

Questions !?



Literature

- V.Shiltsev, F.Zimmermann, Modern and Future Colliders (Rev.Mod.Phys., 2021)
<https://journals.aps.org/rmp/abstract/10.1103/RevModPhys.93.015006>
- V.Lebedev, V.Shiltsev, Accelerator Physics at the Tevatron Collider (Springer, 2014)
https://indico.cern.ch/event/774280/attachments/1758668/2915590/2014_Book_AcceleratorPhysicsAtTheTevatro.pdf
- S.Myers, H.Schopper, eds. Accelerator and Colliders (Springer, 2013, 2020)
<https://link.springer.com/book/10.1007/978-3-030-34245-6>
- “[Particle accelerator physics - 4th ed.](https://library.oapen.org/handle/20.500.12657/23641)” (Springer) by Wiedemann, Helmut.
<https://library.oapen.org/handle/20.500.12657/23641>
- “[Measurement and control of charged particle beams](https://library.oapen.org/handle/20.500.12657/23642)” (Springer) by Minty, Michiko G; Zimmermann, Frank
<https://library.oapen.org/handle/20.500.12657/23642>

Literature

- V.Shiltsev, F.Zimmermann, Modern and Future Colliders (Rev.Mod.Phys., 2021)
<https://journals.aps.org/rmp/abstract/10.1103/RevModPhys.93.015006>

Also:

1. Nature Physics MC – K.Long, et al, *Nature Physics* 17, 289–292 (2021)
2. RMP Colliders – V.Shiltsev, F.Zimmermann, *Rev.Mod.Phys.* 93, 015006 (2021)
3. 1998 PhysicsToday – A.Sessler, *Physics Today* 51(3), 48-53 (Mar.1998)
4. 1999 Design – C.Ankenbrandt, *Phys.Rev.ST-Accel.Beams* 2, 081001 (1999)
5. $\alpha\beta\gamma$ cost model – V.Shiltsev, *JINST* 9 T07002 (2014)
6. Alvin Tollestrup Book – FERMILAB-BOOK-2021-001 (2021)
7. Muon-Proton Collider – V.Shiltsev, *Proc. IEEE PAC'97*, FNAL-Conf-97/114 (1997)
8. MC and Neutrino Factory - S.Geer, *Annu. Rev. Nucl. Part. Sci.* 59:347–65 (2009)
9. Tevatron - S.Holmes, V.Shiltsev, *Annu. Rev. Nucl. Part. Sci.* 63:435-465 (2013)
10. Muon Colliders - R.B. Palmer, *Rev. Accel. Sci. Tech.* 7, 137–159 (2014)
11. 14 TeV MC in LHC tunnel - D. Neuffer and V. Shiltsev, *JINST* 13, T10003 (2018)
12. USMAP - M. Boscolo, J.-P. Delahaye, M. Palmer, *Rev.Accel.Sci.Tech.* 10, 189 (2019)
13. 2020 European Strategy <https://cds.cern.ch/record/2721370/files/CERN-ESU-015-2020%20Update%20European%20Strategy.pdf>
14. JINST Special Issue on Muon Accelerators <https://iopscience.iop.org/journal/1748-0221/page/extraproc46>
15. Muon Collider Collaboration <https://muoncollider.web.cern.ch/>

U.S. Particle Accelerator School

Education in Beam Physics and Accelerator Technology



Brookhaven
National Laboratory



U.S. DEPARTMENT OF
ENERGY

Linear Optics, Imperfection, Measurement, Correction

Chuyu Liu, Brookhaven National Lab

Part of the lectures for the "Colliders for High Energy and Nuclear Physics" course by V. Shiltsev (NIU), V. Ptitsyn (BNL) and C. Liu (BNL).



Winter 2025 USPAS Session

Knoxville, Tennessee, USA
January 27 - February 7, 2025



@BrookhavenLab

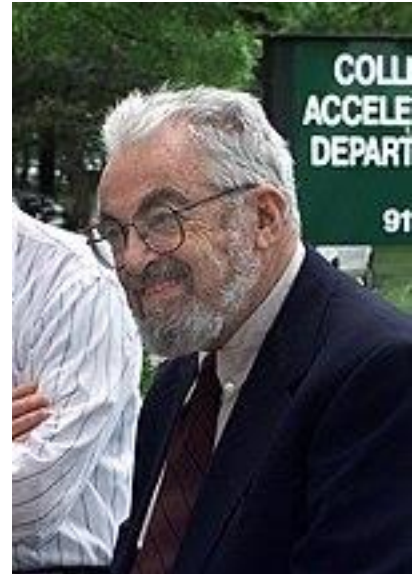
The Outline

- FODO lattice
- Dipole Error & Orbit Correction
- Gradient Errors
- Optics Measurement and Correction
- Dispersion Suppressor
- Low Beta Insertions
- Chromaticity Measurement and Correction
- Beam Coupling, Measurement and Correction

FODO lattice

Alternating Gradient

- Alternating Gradient (strong focusing) lattice is critical for modern accelerators (regardless they are small or large, linear or circular, light sources or colliders)
- It enables smaller magnets, smaller footprint, higher intensity and improved beam stability.
- A common design of Alternating Gradient (strong focusing) is so-called FODO lattice, where "F" represents a focusing quadrupole magnet, "O" is a drift space, and "D" is a defocusing quadrupole magnet

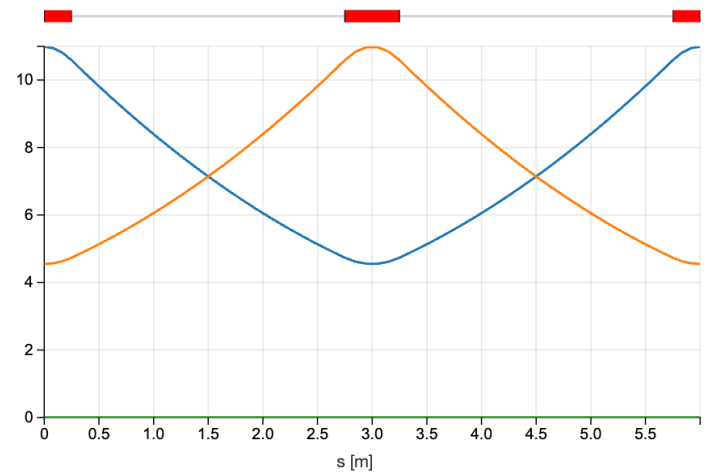


First conceived by Nicholas Christofilos, later independently developed by Courant and colleagues

FODO cell transfer matrix

Transfer matrix $M = \begin{pmatrix} 1 & 0 \\ -\frac{1}{2f} & 1 \end{pmatrix} \begin{pmatrix} 1 & L \\ 0 & 1 \end{pmatrix} \begin{pmatrix} 1 & 0 \\ \frac{1}{f} & 1 \end{pmatrix} \begin{pmatrix} 1 & L \\ 0 & 1 \end{pmatrix} \begin{pmatrix} 1 & 0 \\ -\frac{1}{2f} & 1 \end{pmatrix}$

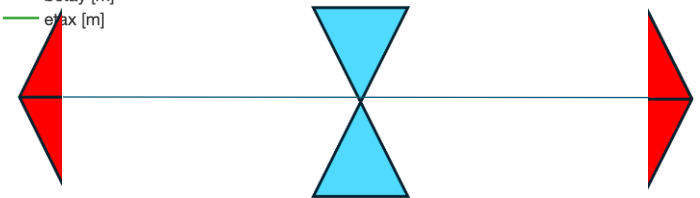
$$= \begin{pmatrix} 1 - \frac{L^2}{2f^2} & 2L\left(1 + \frac{L}{2f}\right) \\ -\frac{L}{2f^2} + \frac{L^2}{4f^3} & 1 - \frac{L^2}{2f^2} \end{pmatrix}$$



Stability criteria $Tr(M) \leq 2$

$$\text{abs}\left(2 - \left(\frac{L}{f}\right)^2\right) \leq 2 \Rightarrow L \leq 2f$$

betax [m]
betay [m]
exax [m]



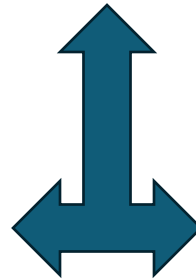
FODO cell phase advance

Transfer matrix in Twiss Parameterization

$$\mathbf{M} = \begin{pmatrix} M_{11} & M_{12} \\ M_{21} & M_{22} \end{pmatrix} = \begin{pmatrix} \cos\mu + \alpha \sin\mu & \beta \sin\mu \\ -\gamma \sin\mu & \cos\mu - \alpha \sin\mu \end{pmatrix}$$

$$\cos\mu = \frac{1}{2} \text{Tr}(\mathbf{M}) = \frac{1}{2} (M_{11} + M_{22})$$

$$\sin\mu = \text{sign}(M_{12}) \sqrt{1 - \cos^2\mu}$$



$$\beta = \frac{M_{12}}{\sin\mu}$$

$$\alpha = \frac{M_{11} - \cos\mu}{\sin\mu}$$

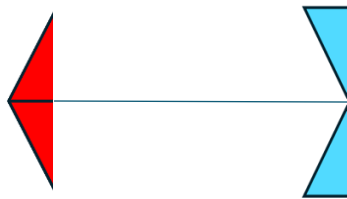
$$\gamma = \frac{1 + \alpha^2}{\beta}$$

FODO cell phase advance

$$\left| \sin\left(\frac{\mu}{2}\right) \right| = \frac{L}{2f}$$

FODO cell beta max & min

Half FODO



$$M_{half} = \begin{pmatrix} 1 & 0 \\ \frac{-1}{2f} & 1 \end{pmatrix} \begin{pmatrix} 1 & L \\ 0 & 1 \end{pmatrix} \begin{pmatrix} 1 & 0 \\ \frac{1}{2f} & 1 \end{pmatrix}$$

$$M_{half} = \begin{pmatrix} 1 + \frac{L}{2f} & L \\ -\frac{L^2}{4f^2} & 1 - \frac{L}{f} \end{pmatrix}$$

In comparison to the Twiss Parameterization

$$M = \begin{pmatrix} \sqrt{\frac{\beta_s}{\beta_0}} (\cos \Delta\psi + \alpha_0 \sin \Delta\psi) & \sqrt{\beta_s \beta_0} \sin \Delta\psi \\ \frac{(\alpha_0 - \alpha_s) \cos \Delta\psi - (1 + \alpha_0 \alpha_s) \sin \Delta\psi}{\sqrt{\beta_s \beta_0}} & \sqrt{\frac{\beta_0}{\beta_s}} (\cos \Delta\psi - \alpha_s \sin \Delta\psi) \end{pmatrix}$$

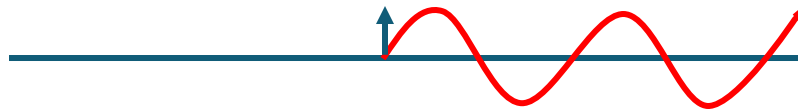
where $\alpha_0 = \alpha_s = 0$, $\Delta\psi = \frac{\mu}{2}$

$$\beta_{max,min} = 2L \frac{1 \pm \sin \frac{\mu}{2}}{\sin \mu}$$

Dipole Error

Dipole errors in linear beamline

A kick in matrix form $\begin{bmatrix} 1 & \theta \\ 0 & 1 \end{bmatrix}$

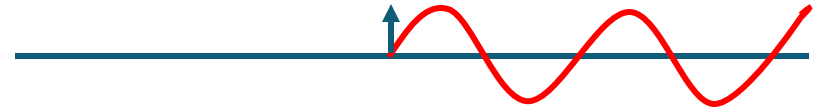
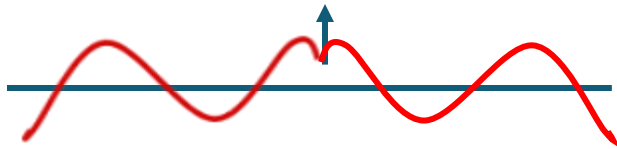


No impact on x and x' to any point upstream of the kick

For a point s at downstream

$$x(s) = M_{12} * \theta = \sqrt{\beta(s)\beta} \cdot \theta \cdot \sin(\varphi(s) - \varphi)$$

Dipole errors in a storage ring



Unlike in linear beamline, a kick in a storage ring would affect x and x' everywhere

Construct a new one-turn transfer matrix by including the kick, one would be able to calculate the equilibrium x and x' at the location of the kick, then one can propagate it to the rest of the ring

$$x(s) = \frac{\sqrt{\beta(s)\beta} \cdot \theta}{2\sin(\pi\nu)} \cos(|\varphi(s) - \varphi| - \pi\nu)$$

Build the Orbit Response Matrix (ORM)

The orbit response at all BPMs to a deflection at one particular corrector:

$$x(s)/\theta = \frac{\sqrt{\beta(s)\beta}}{2\sin(\pi\nu)} \cos(|\varphi(s) - \varphi| - \pi\nu)$$

These values make up the first column of the ORM:

$$\begin{pmatrix} \Delta x_1 \\ \Delta x_2 \\ \vdots \\ \Delta x_m \end{pmatrix} = \begin{bmatrix} R_{11} & R_{12} & \dots & R_{1n} \\ R_{21} & R_{22} & \dots & R_{2n} \\ \vdots & \vdots & \dots & \vdots \\ R_{m1} & R_{m2} & \dots & R_{mn} \end{bmatrix} \begin{pmatrix} \theta_1 \\ \theta_2 \\ \vdots \\ \theta_n \end{pmatrix}$$



Orbit Correction

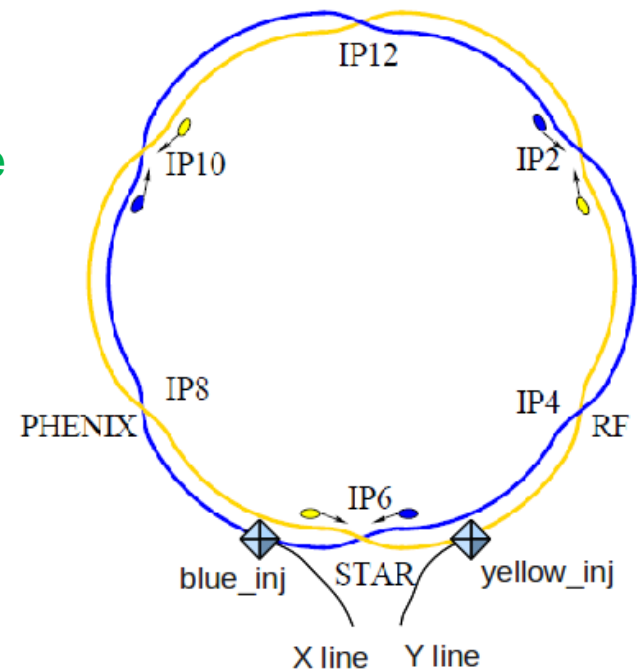
A case of orbit correction: injection steering at RHIC

When first inject beam to a storage ring, the beam may not survive more than 1 turn, then the recorded orbit can be corrected using the one pass orbit response matrix

$$R_{ij} = \begin{cases} \sqrt{\beta_i \beta_j} * \sin \phi_{ij} & \text{if } \phi_j(\text{monitor}) > \phi_i(\text{corrector}), \\ 0 & \text{if } \phi_j(\text{monitor}) < \phi_i(\text{corrector}). \end{cases}$$

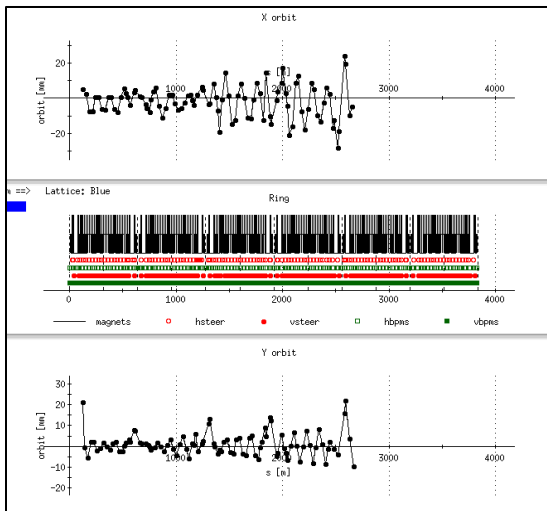
Once the beam survives multiple turns, the recorded orbit can be averaged, and the ring orbit response matrix can be used

$$x(s) = \frac{\sqrt{\beta(s)\beta} \cdot \theta}{2\sin(\pi\nu)} \cos(|\varphi(s) - \varphi| - \pi\nu)$$

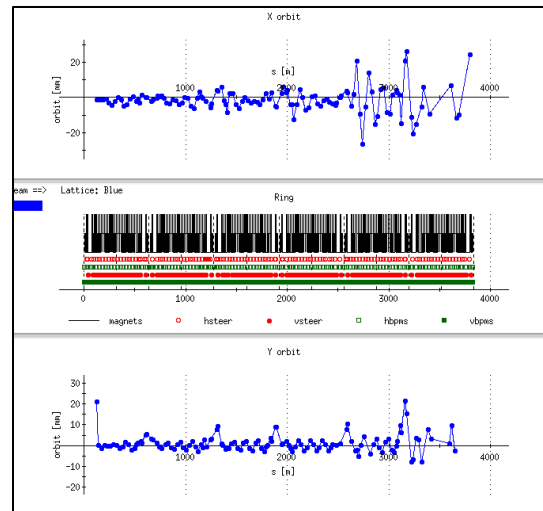


Multiple iteration of orbit correction

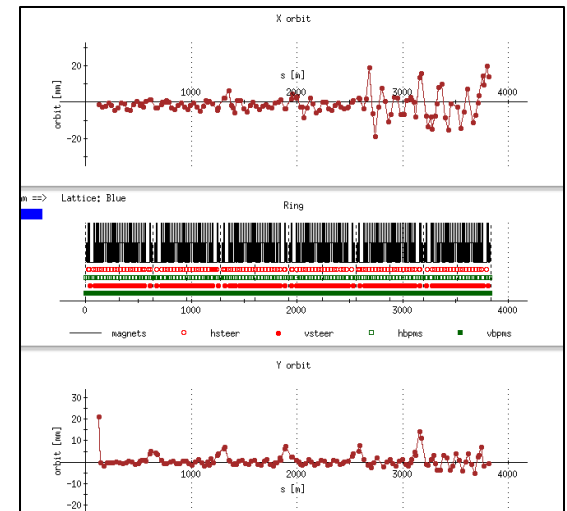
First attempt of injection



First round of correction



Second round of correction



Gradient Error

Gradient error induced tune change

Thin-lens representation of gradient error

$$M_{error} = \begin{pmatrix} 1 & 0 \\ \Delta k ds & 1 \end{pmatrix}$$

One-turn matrix including gradient error

$$\tilde{M} = \begin{pmatrix} 1 & 0 \\ \Delta k ds & 1 \end{pmatrix} \cdot \begin{pmatrix} \cos \mu_0 + \alpha_0 \sin \mu_0 & \beta_0 \sin \mu_0 \\ -\gamma_0 \sin \mu_0 & \cos \mu_0 - \alpha_0 \sin \mu_0 \end{pmatrix}$$

Trace of the one-turn matrix

$$Tr(\tilde{M}) = 2 \cos(\mu) = 2 \cos(2\pi(\nu_0 + d\nu))$$

Tune change

$$d\nu = \frac{\Delta k \beta ds}{4\pi}$$

Gradient error induced beta beat

Reconstruct the one-turn matrix

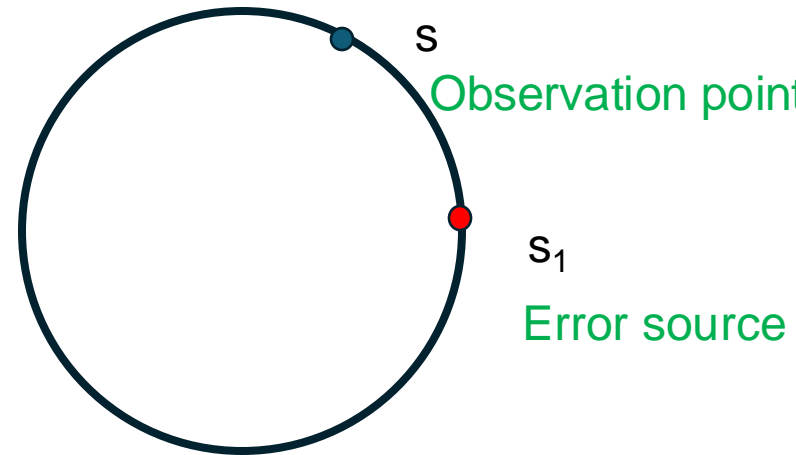
$$\tilde{M} = M_{s \rightarrow s_1} M_{error} M_{s \rightarrow s_1}$$

Apply the following constraint

$$\tilde{M}_{12} = (\beta + d\beta) \sin 2\pi(v + dv)$$

One get the beta beat

$$d\beta/\beta = \frac{-1}{2 \sin 2\pi v} \beta(s_1) \Delta k \cos\{2|\varphi(s_1) - \varphi(s)| - 2\pi v\}$$



Universal correction scheme

Use gradient errors induced beta beat correction as an example

Beta beat caused by multiple error sources

$$\frac{d\beta}{\beta} = \frac{-1}{2\sin 2\pi\nu} \sum_i \beta(s_i) \Delta k_i \cos\{2|\varphi(s_i) - \varphi(s)| - 2\pi\nu\}$$

Matrix form

$$\frac{d\beta}{\beta}_1 = R[1, :] \cdot \begin{pmatrix} \Delta k_1 \\ \Delta k_2 \\ \vdots \\ \Delta k_n \end{pmatrix}$$

Multi sources, multi observation points

$$\begin{pmatrix} \frac{d\beta}{\beta}_1 \\ \frac{d\beta}{\beta}_2 \\ \vdots \\ \frac{d\beta}{\beta}_m \end{pmatrix} = R_{m,n} \cdot \begin{pmatrix} \Delta k_1 \\ \Delta k_2 \\ \vdots \\ \Delta k_n \end{pmatrix}$$

Corrections:

$$\begin{pmatrix} \Delta k_1 \\ \Delta k_2 \\ \vdots \\ \Delta k_n \end{pmatrix} = R_{-(m,n)}^{-1} \begin{pmatrix} \frac{d\beta}{\beta}_1 \\ \frac{d\beta}{\beta}_2 \\ \vdots \\ \frac{d\beta}{\beta}_m \end{pmatrix}$$



Optics Measurement and Correction

Optics Measurement--Turn by Turn BPM data

Excite beam turn by turn oscillation with a fast kick by fast kicker/pinger
BPMs turn-by-turn data capture amplitude and phase oscillation, and are used for linear optics measurement and correction

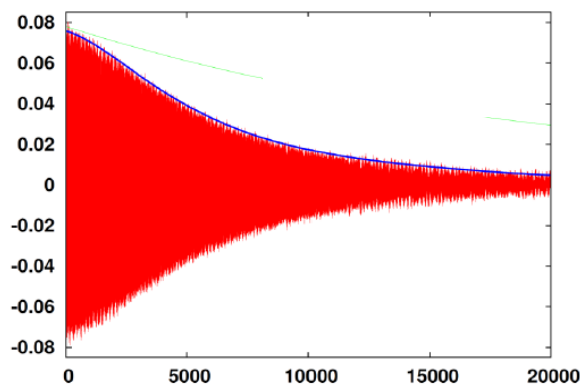
m_{th} BPM at n_{th} turn's position:

$$y_m(n) = \sqrt{2J\beta_m} \cos(2\pi\nu n + \psi_m + \chi),$$

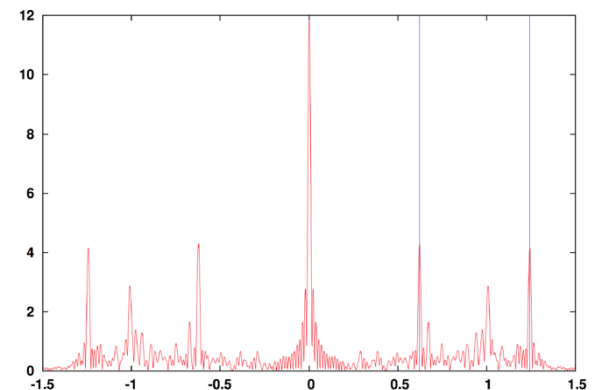
TbT BPM data includes

- Oscillation frequency: tune measurement
- Amplitude: beta function measurement
- Phase: phase advance function measurement
- BPMs around the ring: local beta function and phase advance measurement

Excited beam TBT data



FFT for tune measurement



Turn by Turn BPM data processing

Precise tune measurement

- NAFF (numerical analysis of fundamental frequency)
- Interpolated FFT

With the measured tune, amplitude and phase of the frequency component can be obtained by

$$C = \sum_n x(n) \cos 2\pi n\nu, \quad S = \sum_n x(n) \sin 2\pi n\nu$$

Then amplitude and phase are

$$A = \frac{2\sqrt{C^2+S^2}}{N}, \quad \text{and} \quad \psi = -\cot^{-1} \frac{S}{C}$$

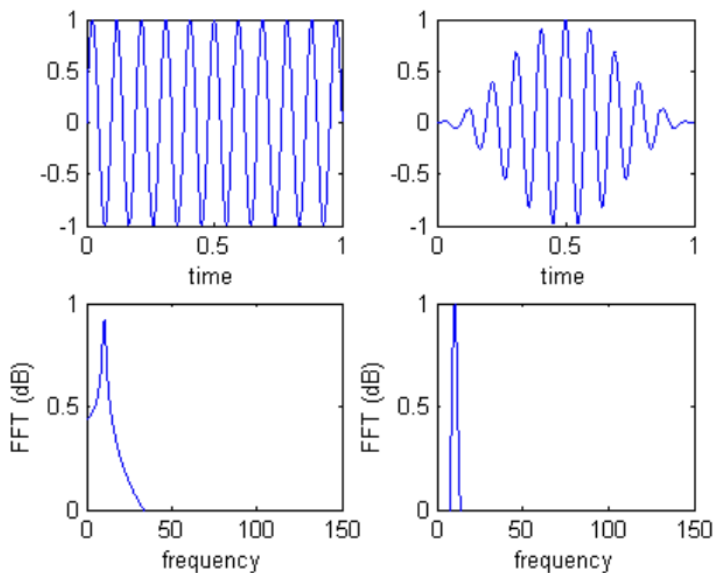
N is the number of turns

Interpolated FFT

The spectrum you get for a finite length oscillation by using a FFT, is not the actual spectrum of the original signal, but a **smear**ed version.

Applying a window minimizes the effect of spectral leakage.

List of common window types and performance



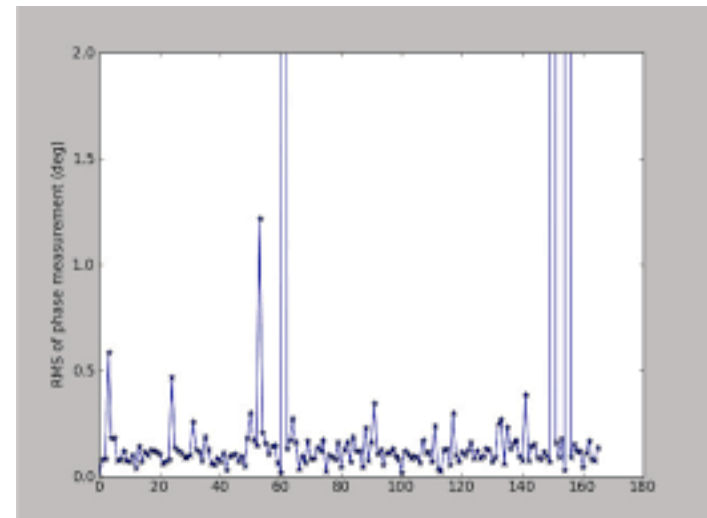
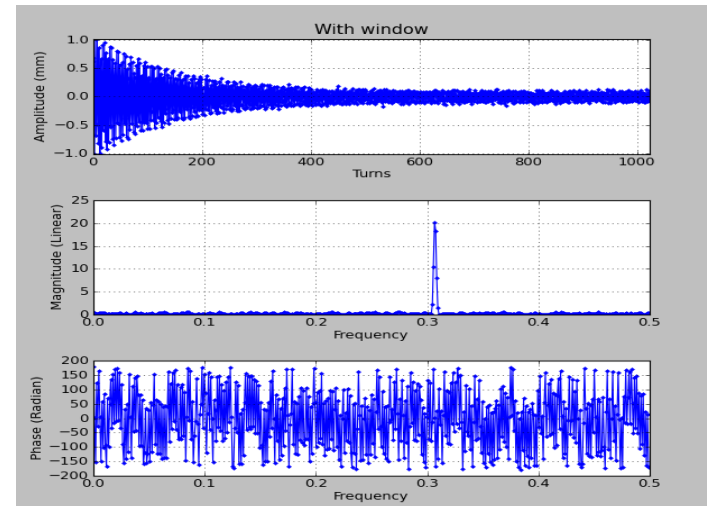
Window	Best for these Signal Types	Frequency Resolution	Spectral Leakage	Amplitude Accuracy
Barlett	Random	Good	Fair	Fair
Blackman	Random or mixed	Poor	Best	Good
Flat top	Sinusoids	Poor	Good	Best
Hanning	Random	Good	Good	Fair
Hamming	Random	Good	Fair	Fair
Kaiser-Bessel	Random	Fair	Good	Good
None (boxcar)	Transient & Synchronous Sampling	Best	Poor	Poor
Tukey	Random	Good	Poor	Poor
Welch	Random	Good	Good	Fair

Window selection for FFT

Gaussian window for RHIC TBT data

A recipe for window selection:

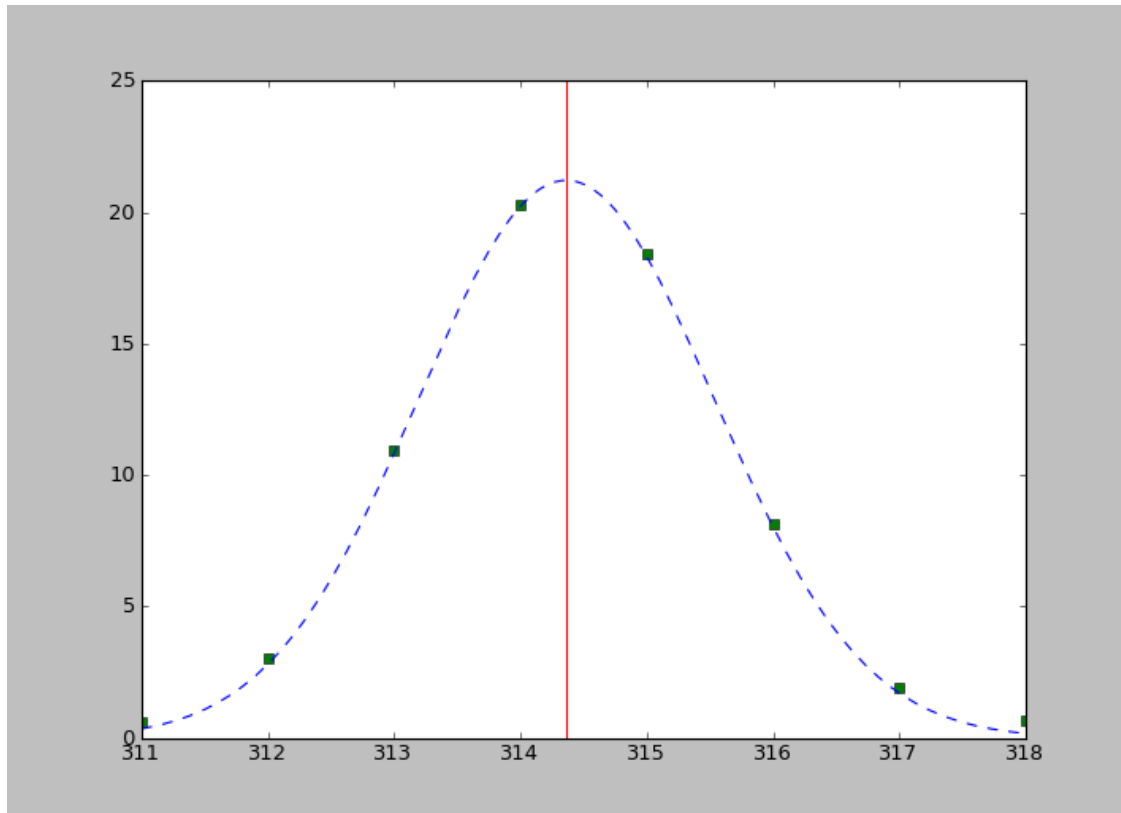
- Be clear what you care the most. For turn-by-turn data analysis, it is the precision of tune measurement, which is the basis of a precision phase and beta function measurement.
- Select a set of TBT data, apply various windows and compare the precision of tune measurement.



Phase measurement precision

Interpolated FFT cont'd

Zoom in the tune peak and perform a Gaussian fit



CFT, continuous Fourier transform

$$X(\nu) = \frac{1}{N} \sum_{n=1}^N e^{-2\pi i \nu \cdot n} x_n$$

Phase = angle(X)

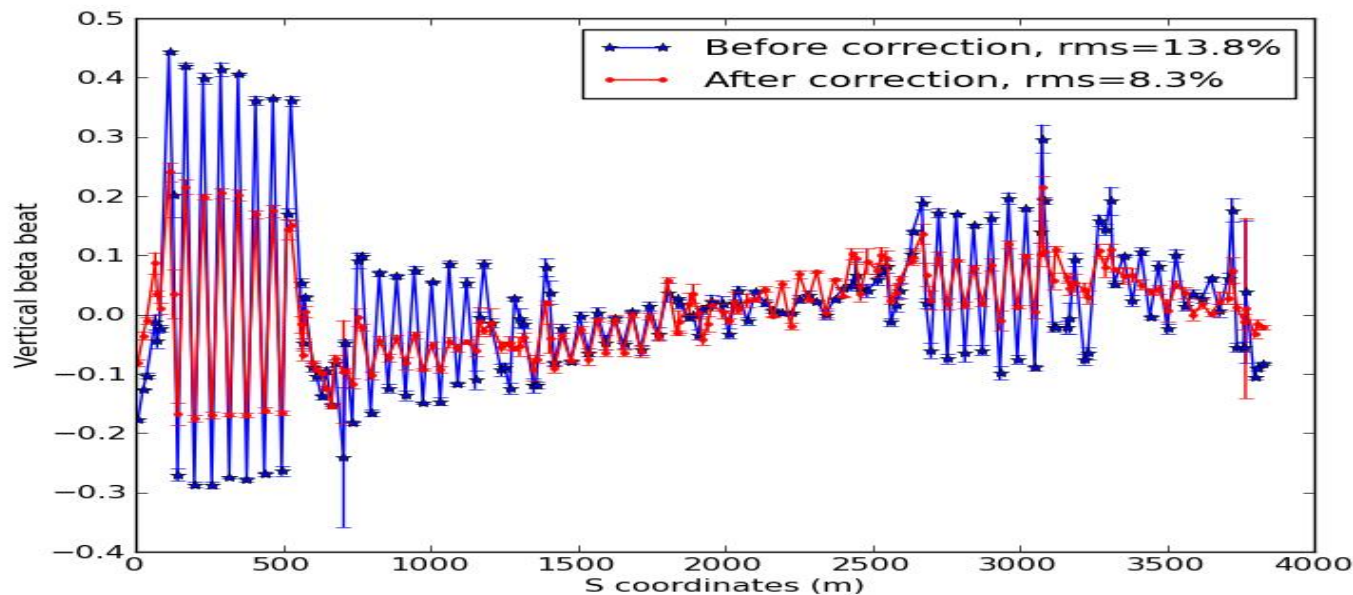
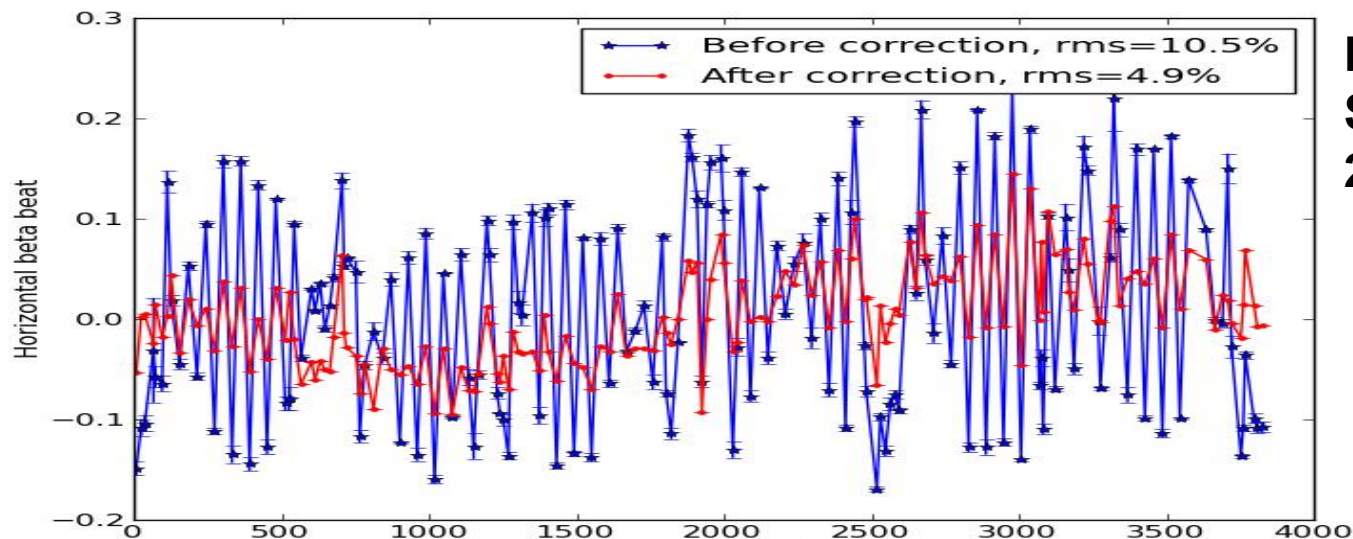
RHIC Optics Correction #1

Two independent methods were both implemented

- SVD based correction based on beta-beat from free oscillation, implemented by C. Liu
 - Beta-beat response matrix based
 - Use all the independent quadrupoles in the IR
 - Applied with RHIC tune/coupling feedback

Free Oscillation Based Optics Correction Result

Blue Ring at
Store energy of
255GeV

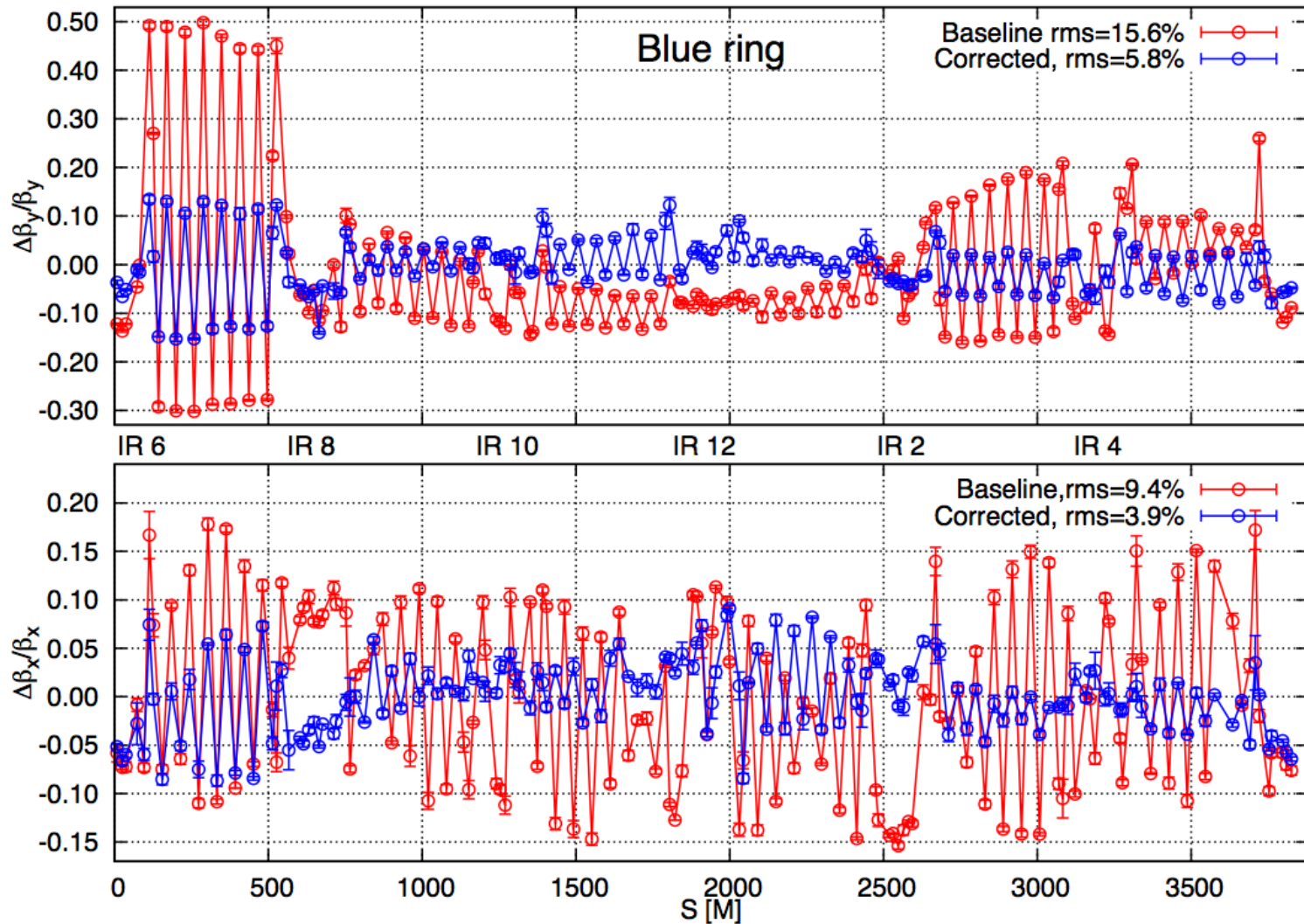


RHIC Optics Correction #2

Two independent methods were both implemented

- Optimum global optics correction(OGOC) based on beta-beat measured by AC dipoles: implemented by X. Shen
 - Beta-beat and betatron tune response matrix based
 - Use all the independent quadrupoles in the IR including triplets as well as all arc quadrupoles.
 - Minimize beta-beat without changing tune

OGOC results



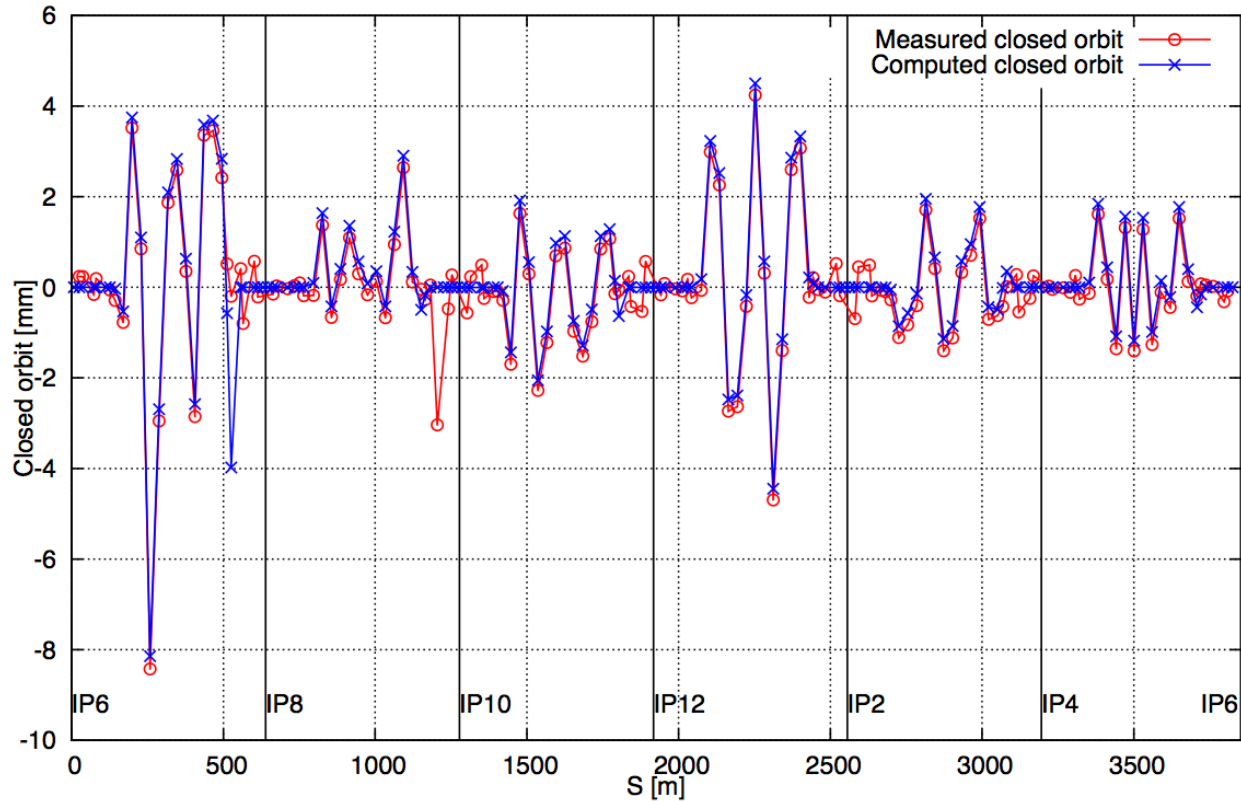
Proof-of-Principle Arc Beta-Beat Correction using Arc Sextupoles with Orbit Bumps

RHIC quadrupoles in the arc don't have their own individual power supplies. Not possible to have independent knobs in these areas

Proposed by R. Tomas and S. White to construct independent beta-beat knobs using arc sextupoles with their localized orbit bumps

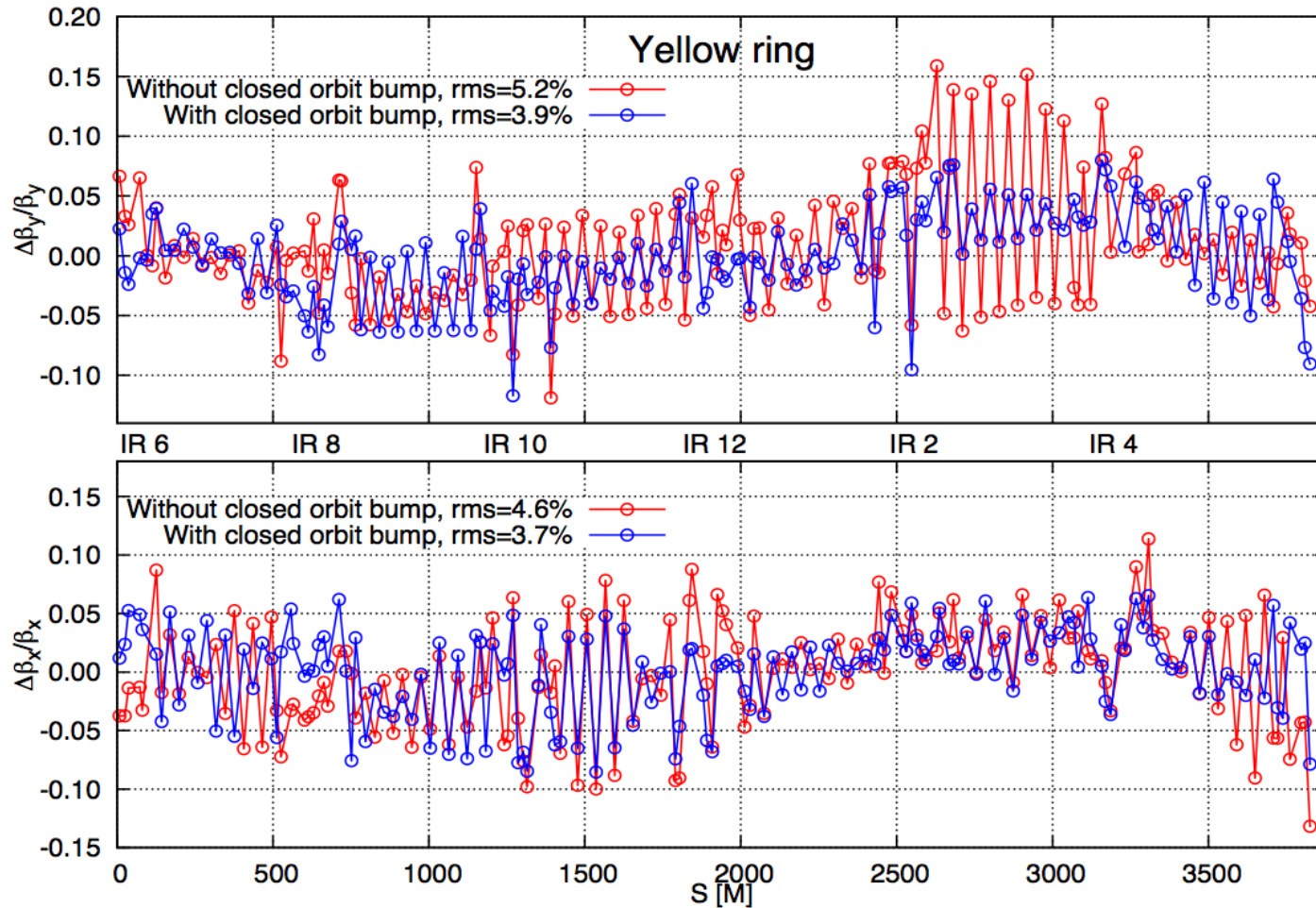
If demonstrated, this allows one to have much better control of the phase advance in the arcs for applications which desire specific requirements on optics

Orbit Bumps at Arc Sextupoles



The orbit bump was first generated based on the model. They are implemented with the orbit feedback[X. Shen and A. Marusic].

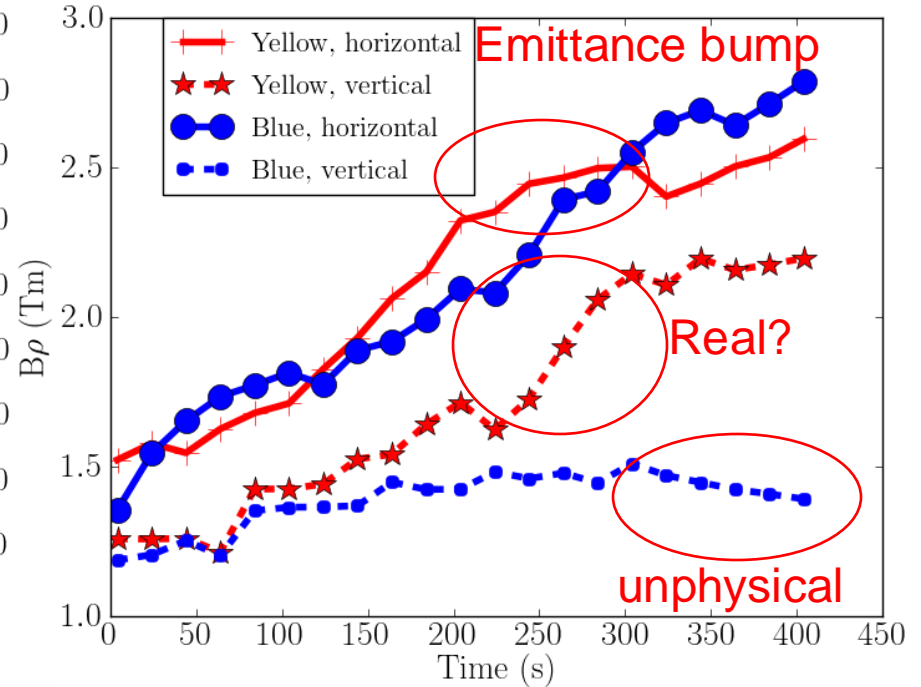
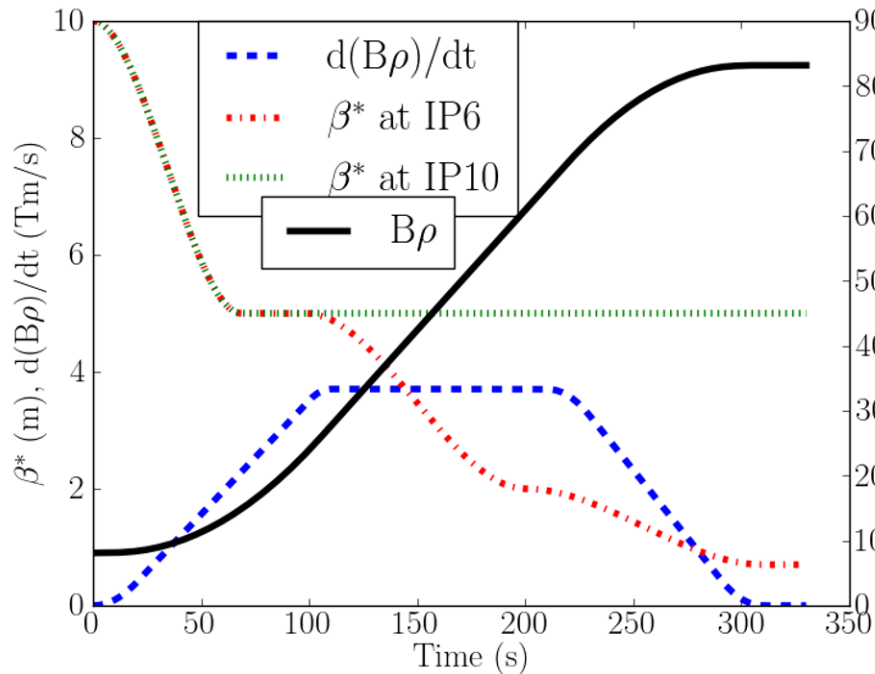
Proof-of-Principle Arc Beta-Beat Correction using Arc Sextupoles with Orbit Bumps



Ramp Optics Motivation

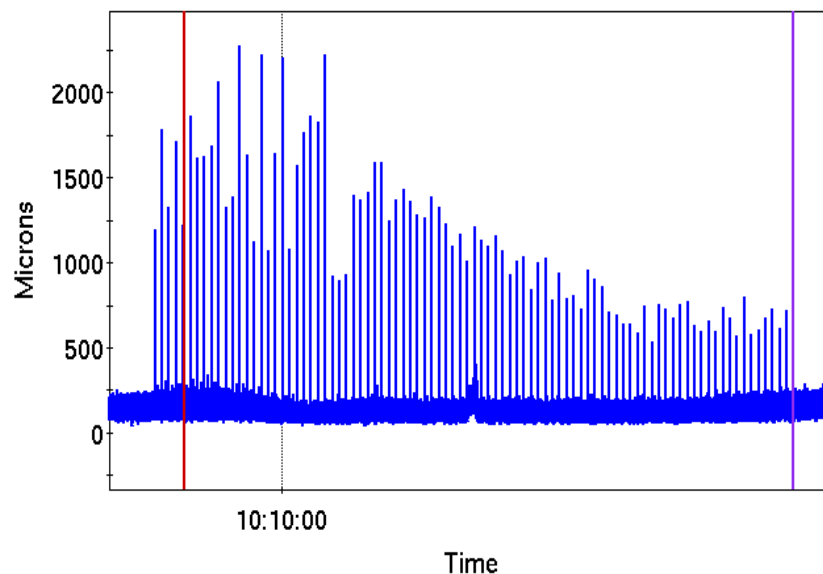
- Improves the understanding of the evolution of beam parameters (e.g. beam emittances). provides improved beam control since model-dependent beam-based feedbacks are used during acceleration.
- Improve the dynamic aperture for heavy ions and reduce the strengths of depolarization resonances for the polarized proton program.
- Time-consuming to pause at intermediate energies to allow measurement and correction of the optics, quasi-continuous, minimally invasive ramp optics measurement/correction

RHIC ramp and emittance revolution

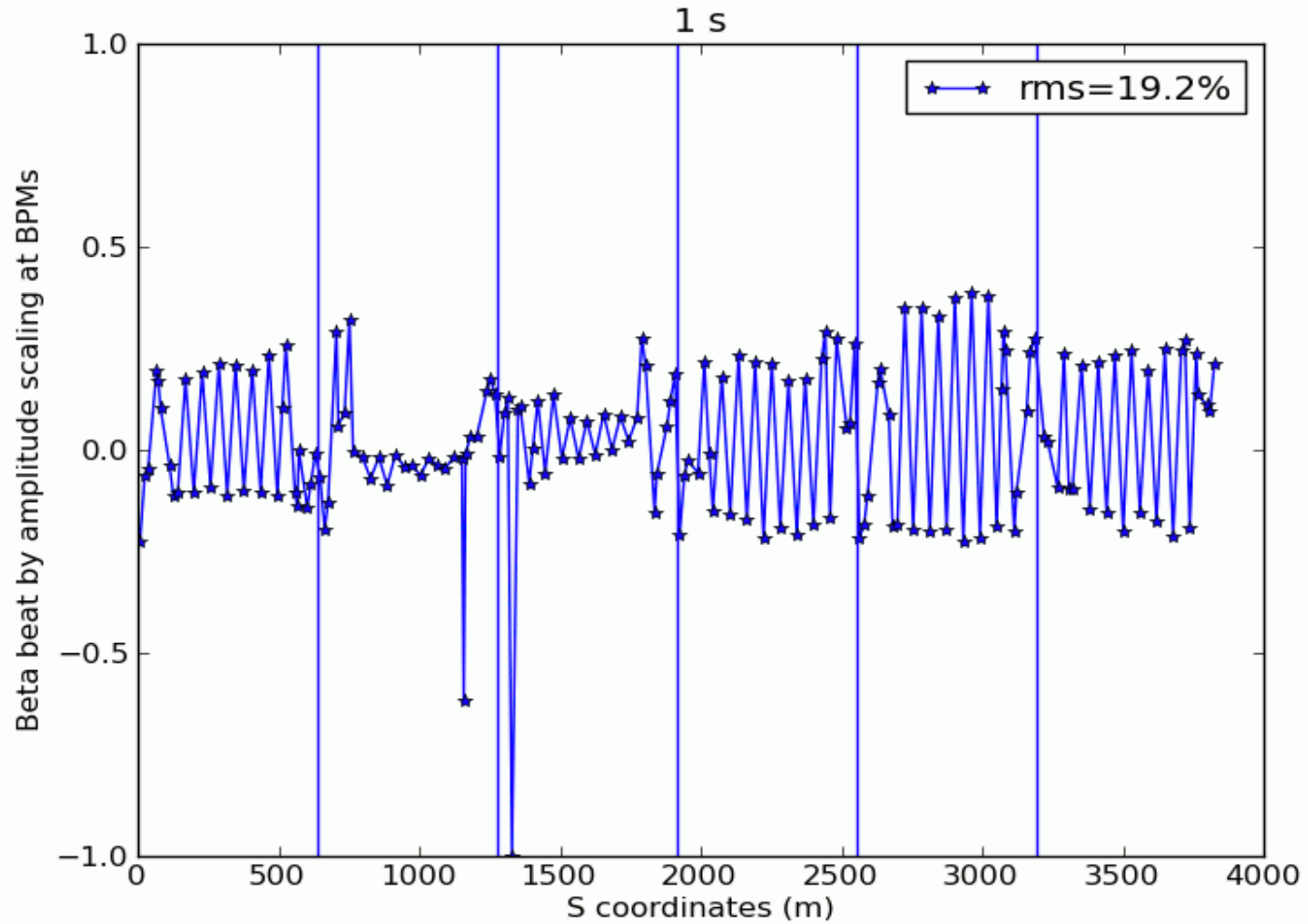


Ramp Optics Measurement recipe

- Tune meter kicker is used to excite coherent betatron motion.
- Measurements were taken every 4 second during acceleration.
- Proper staggering of delivery of the average and turn-by-turn beam position allows normal orbit feedback.
- Switch bunch if intensity is below the set threshold.

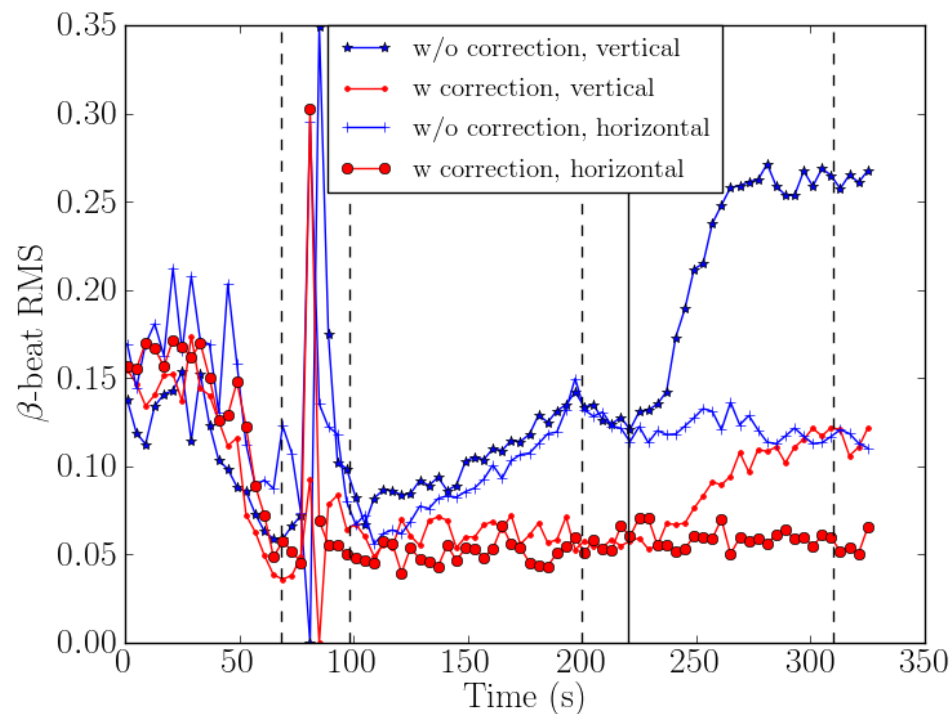


Optics measurements during RHIC ramp

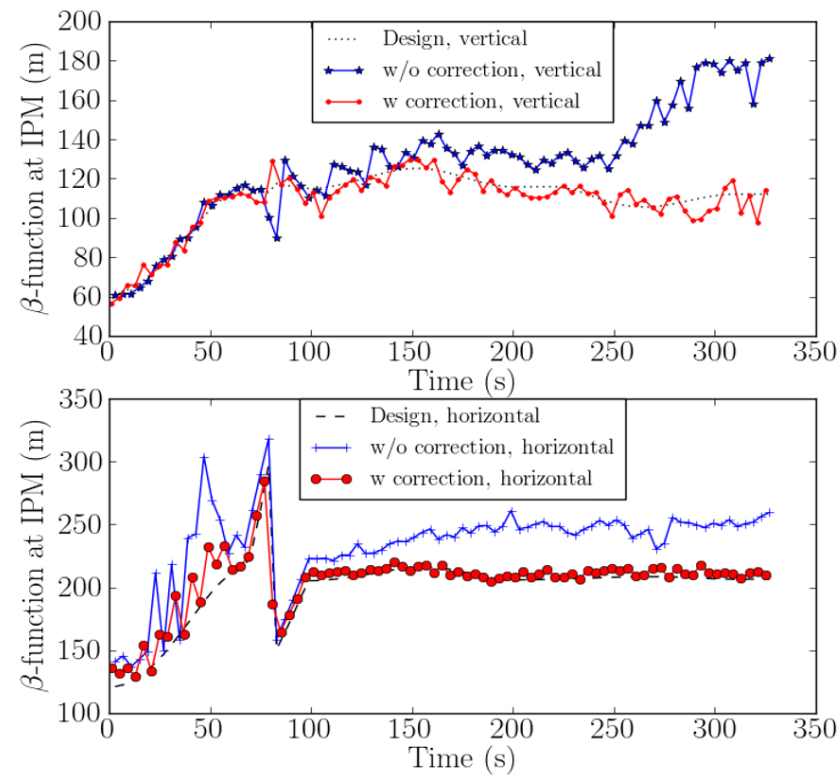


Ramp optics correction

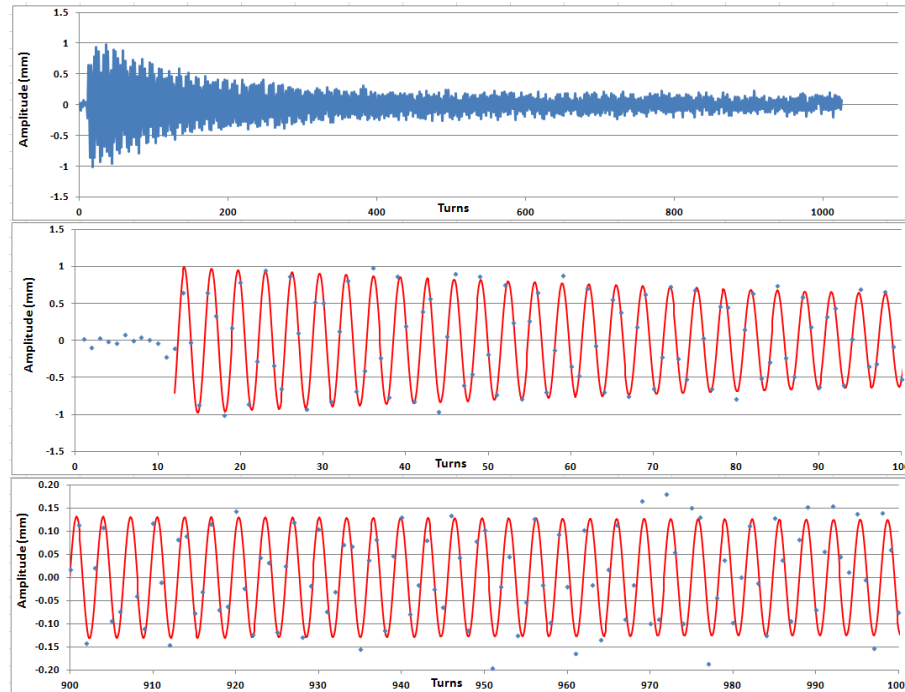
Correction of beta beat



Correction of beta at IPMs



TBT data processing: Time-domain analysis



The decay of oscillation amplitude (decoherence) is due to the tune spread, mainly caused by chromaticity and amplitude dependent tune for single beam. For RHIC beam, the decay is better characterized by double exponential decay

$$x = [A1 * \exp(-at) + A2 * \exp(-bt)] \cos(2\pi ft + \phi)$$

Optics measurement and correction with ORM: LOCO

Quadrupole errors affect orbit response matrix (ORM)

ORM consists of thousands of data points (# of BPMs × # of correctors) and reflecting the ring's linear optics at BPM i , and corrector j

$$R_{ij} = \frac{\beta_i \beta_j}{2 \sin \pi \nu} \cos(\pi \nu - |\psi_i - \psi_j|)$$

LOCO (linear optics from close orbit) fits response matrix to the lattice model to uncover lattice errors

The Parameters in a computer model of a storage ring are varied to minimize the χ^2 deviation between the model and measured ORM

$$\chi^2 = \sum_{i,j} \frac{1}{\sigma_i^2} [R_{ij}^{\text{meas}} - R_{ij}^{\text{model}}(\Delta \mathbf{K})]^2$$

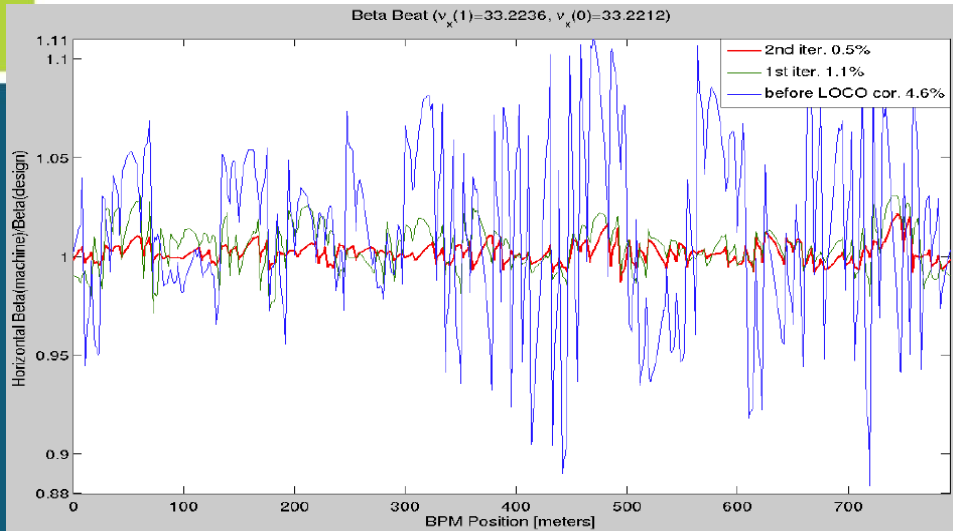
Data typically includes horizontal, vertical, cross-plane matrix, and measured dispersion

Fitted parameters include quadrupole gradients, BPM gains and coupling, and corrector gains and coupling

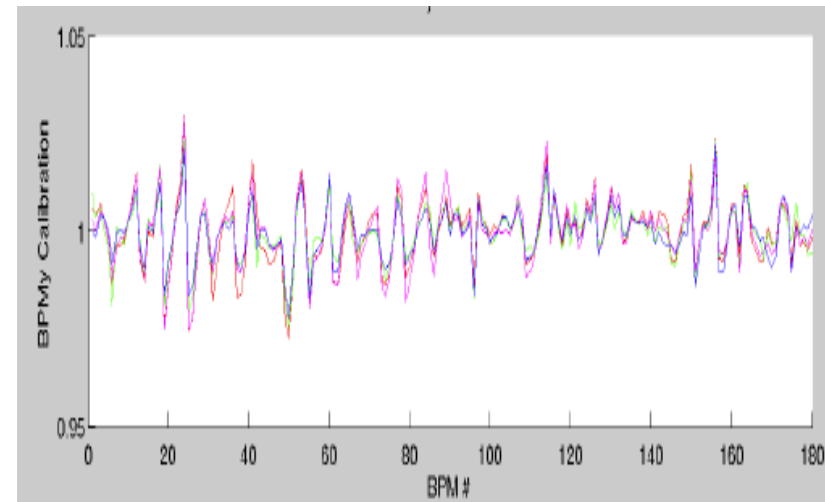
LOCO, one of the most successful optics and coupling correction method. Very timing consuming → AC-LOCO (NSLS-II: 1 hr → 2 minutes)

LOCO application example at NSLS-II

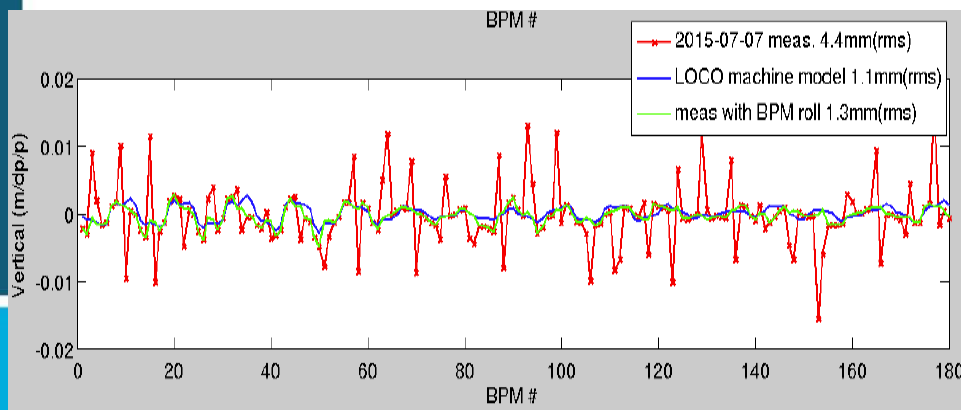
Horizontal beta beating: 4.6% \rightarrow 0.5%



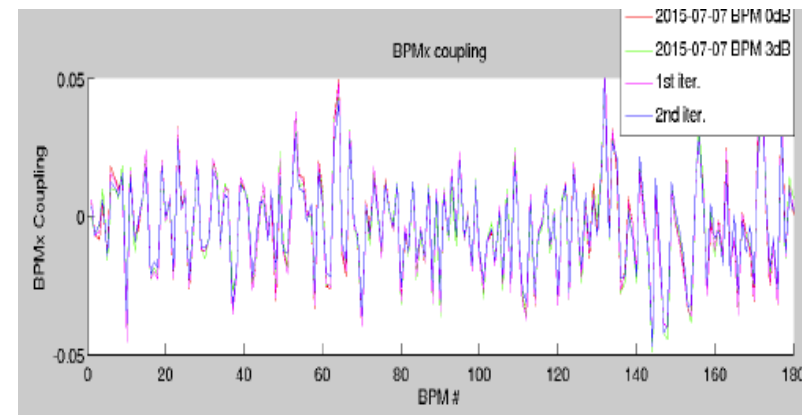
BPM gain calibration



Vertical dispersion: 4.4 \rightarrow 1.3mm



BPM rolls error





Dispersion Suppressor

FODO Dispersion

Dispersion transfer matrix

$$\begin{pmatrix} D_x(s) \\ D'_x(s) \\ 1 \end{pmatrix} = \begin{pmatrix} m_{11} & m_{12} & d(s) \\ m_{21} & m_{22} & d'(s) \\ 0 & 0 & 1 \end{pmatrix} \begin{pmatrix} D_x(0) \\ D'_x(0) \\ 1 \end{pmatrix}$$

FODO cell Dispersion transfer matrix

$$\mathbf{M} = \begin{pmatrix} 1 & 1 & 0 \\ -\frac{1}{2f} & 1 & 0 \\ 0 & 0 & 1 \end{pmatrix} \begin{pmatrix} 1 & L & \frac{L\theta}{2} \\ 0 & 1 & \theta \\ 0 & 0 & 1 \end{pmatrix} \begin{pmatrix} 1 & 1 & 0 \\ \frac{1}{f} & 1 & 0 \\ 0 & 0 & 1 \end{pmatrix} \begin{pmatrix} 1 & L & \frac{L\theta}{2} \\ 0 & 1 & \theta \\ 0 & 0 & 1 \end{pmatrix} \begin{pmatrix} 1 & 1 & 0 \\ -\frac{1}{2f} & 1 & 0 \\ 0 & 0 & 1 \end{pmatrix} = \begin{pmatrix} 1 - \frac{L^2}{2f^2} & 2L\left(1 + \frac{L}{2f}\right) & 2L\theta\left(1 + \frac{L}{4f}\right) \\ -\frac{L}{2f^2} + \frac{L^2}{4f^3} & 1 - \frac{L^2}{2f^2} & 2\theta\left(1 - \frac{L}{4f} - \frac{L^2}{8f^2}\right) \\ 0 & 0 & 1 \end{pmatrix}$$

Applying the periodic condition,
one obtains

$$D_{F,D} = \frac{\theta L \left(1 \pm \frac{1}{2} \sin \frac{\mu}{2}\right)}{\sin^2 \frac{\mu}{2}}; \quad D'_{F,D} = 0$$

Dispersion suppressor

Let's modify the bending angles of two FODO cells, so the dispersion and its derivative get suppressed

$$\begin{pmatrix} 0 \\ 0 \\ 1 \end{pmatrix} = \mathbf{M}(\theta = \theta_2) \mathbf{M}(\theta = \theta_1) \begin{pmatrix} D_m \\ D'_m \\ 1 \end{pmatrix}$$

One would get the bending angles as follows

$$\theta_1 = \theta \left(1 - \frac{1}{4 \sin^2 \frac{\mu}{2}} \right); \theta_2 = \theta \frac{1}{4 \sin^2 \frac{\mu}{2}}$$

Half dipole dispersion suppressor

- Solution:

$$\theta_1 = \theta \left(1 - \frac{1}{4 \sin^2 \frac{\mu}{2}} \right); \theta_2 = \theta \frac{1}{4 \sin^2 \frac{\mu}{2}}$$

- For $\mu = 90^\circ$, we get

$$\theta_1 = \theta_2 = \frac{\theta}{2}$$

Missing dipole dispersion suppressor

- Solution:

$$\theta_1 = \theta \left(1 - \frac{1}{4 \sin^2 \frac{\mu}{2}} \right); \theta_2 = \theta \frac{1}{4 \sin^2 \frac{\mu}{2}}$$

- For $\mu = 60^\circ$, we get

$$\theta_1 = 0, \quad \theta_2 = \theta$$



Low Beta Insertion, Chromatic Effect and Correction

Natural chromaticity

Focusing depends on the momentum

$$k = -\frac{eg}{p_0 + \Delta p} \approx -\frac{e}{p_0} \left(1 - \frac{\Delta p}{p_0}\right)g = k_0 - \Delta k$$



$$\Delta k = \frac{\Delta p}{p_0} k_0$$

Result in tune change of

$$\Delta \nu = \frac{\Delta p}{p} \frac{-1}{4\pi} \oint k(s) \beta(s) ds$$

Natural chromaticity

$$\xi = \frac{\Delta \nu}{\frac{\Delta p}{p}} = \frac{-1}{4\pi} \oint k(s) \beta(s) ds$$

Chromaticity correction

Goal: introduce gradient dependence on offset using sextuples to compensate focusing dependence on momentum


$$\frac{\partial B_x}{\partial z} = \frac{\partial B_z}{\partial x} = \tilde{g}x$$
$$k_{sext} = \frac{\tilde{g}x}{p/e} = m_{sext.}x$$
$$k_{sext} = m_{sext.}D \frac{\Delta p}{p}$$

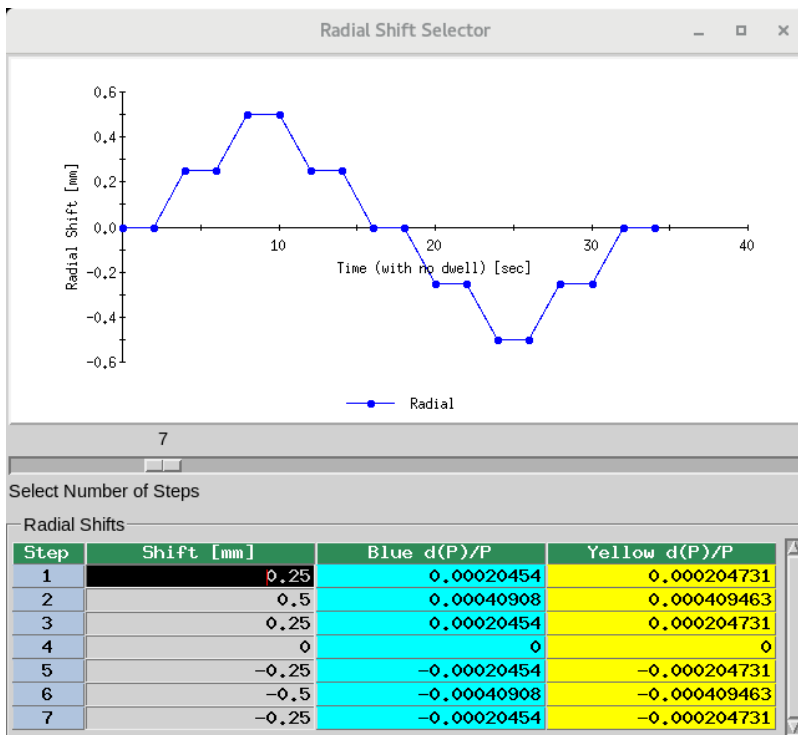
Chromaticity with compensation

$$\xi = \frac{-1}{4\pi} \oint \{k(s) - mD(s)\} \beta(s) ds$$

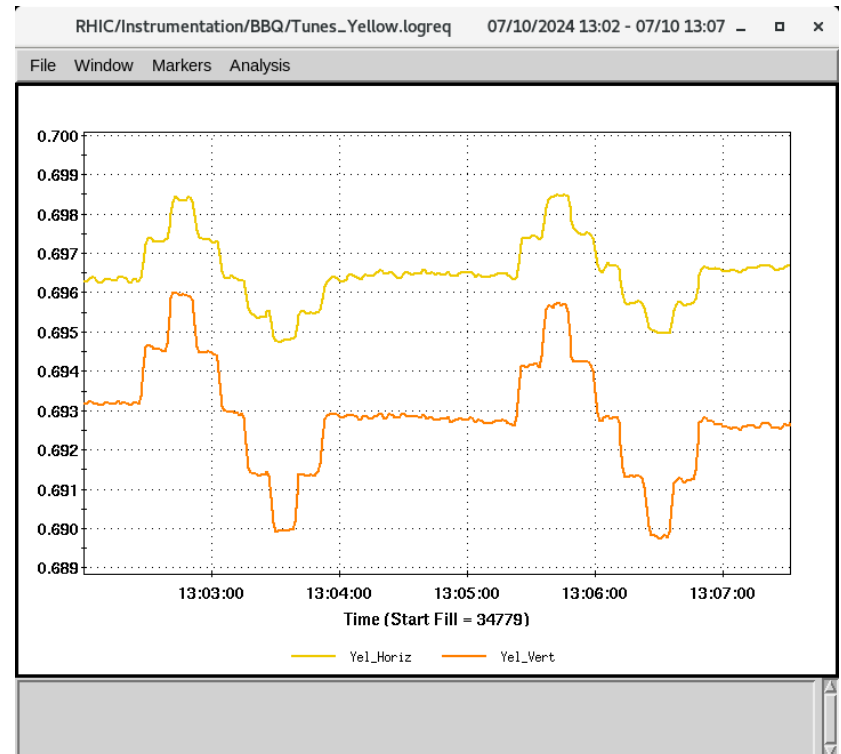
Usually, sextuples in the dispersive arcs are split in two families for the chromatic compensation

Dispersion and Chromaticity Measurement

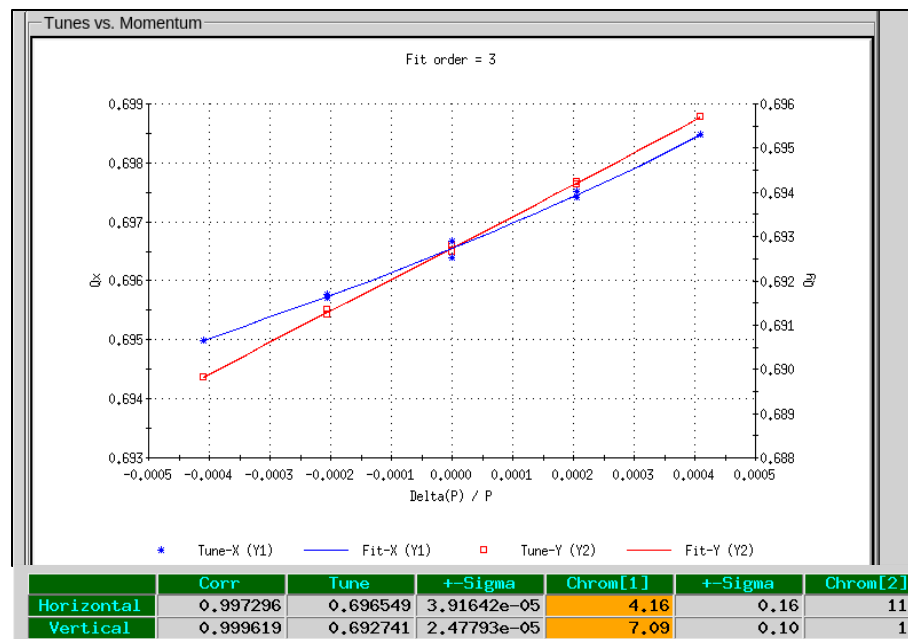
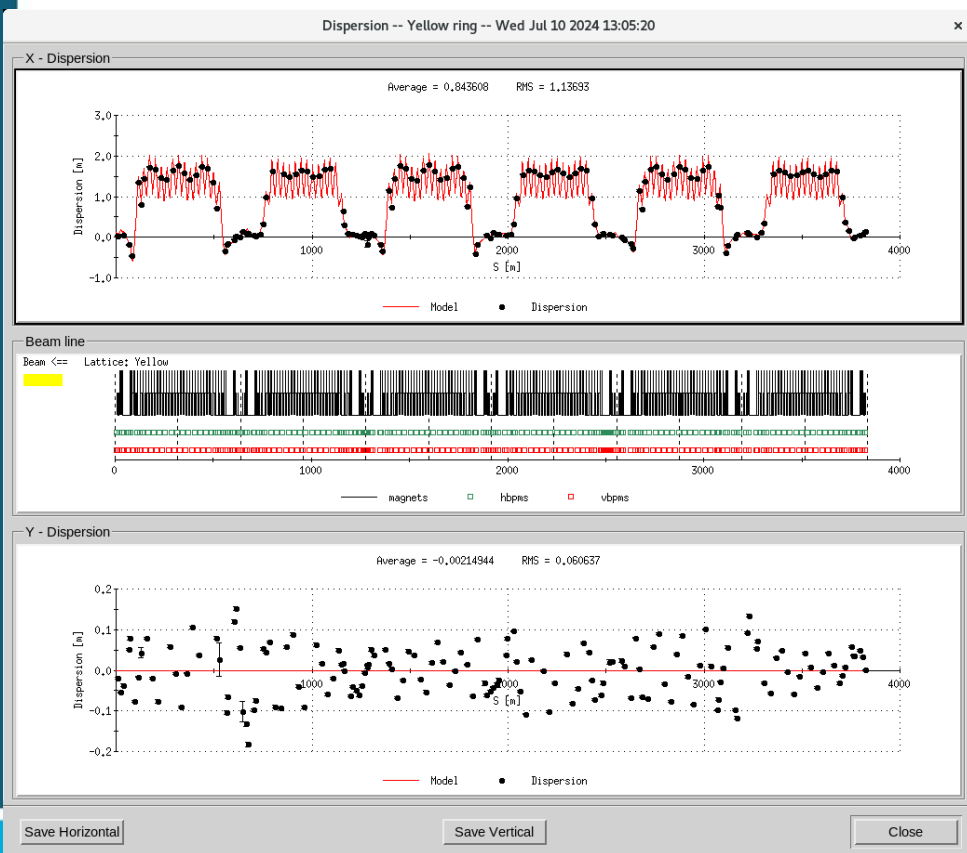
Request a radial shift by changing RF frequency



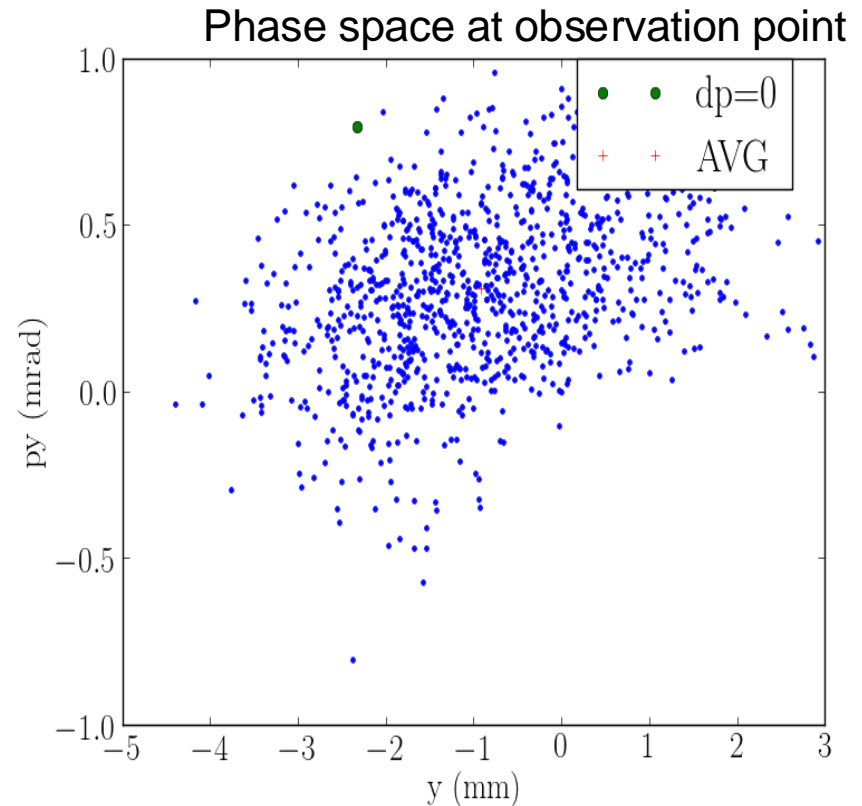
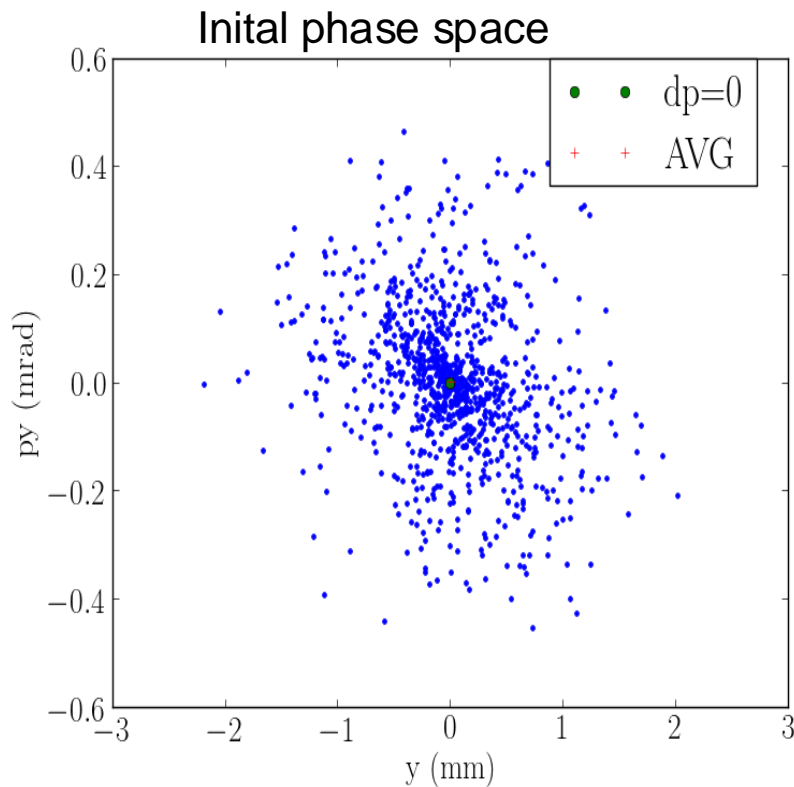
Measure tune changes



Measurement results



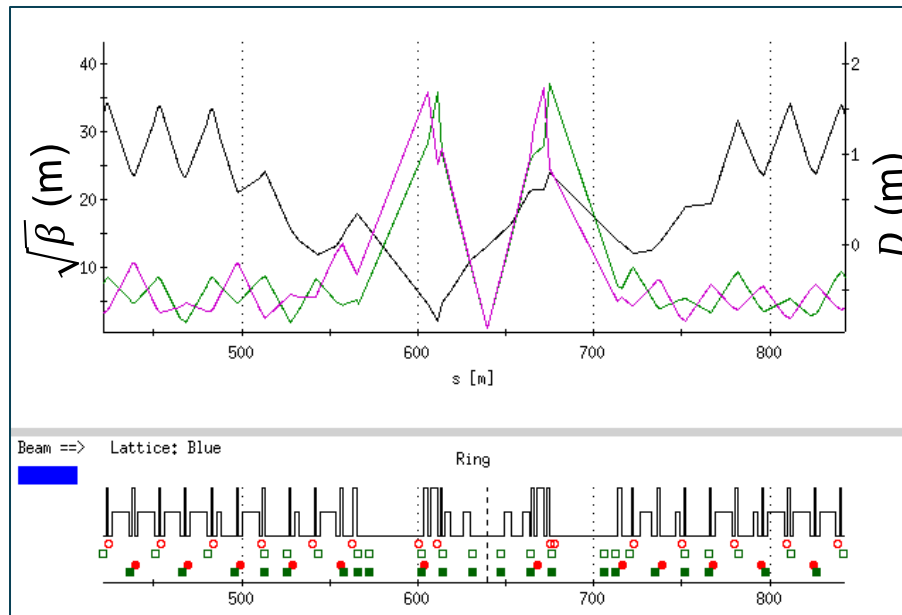
Chromatic effect on orbit response



Measured beam position (red +) deviate substantially from the on-momentum particle position (green dot) due to chromatic effect.

Low β Insertion

- In a collider, one needs to focus the beam in both planes at the collision point to boost luminosity.
- This can be done with an asymmetric pair of focusing triplets, matched to the lattice functions
- These low insertion quadrupoles contribute to chromaticity and its higher orders significantly.



At the IP:

$$\beta = \beta^* ; \alpha = 0$$

- The beta function between triplets is

$$\beta(s) = \beta_0 - 2\alpha_0 s + \gamma_0 s^2 = \beta^* + \frac{s^2}{\beta^*}$$

Chromatic beta beat

Focusing elements, especially the final focusing quads, introduce chromatic beta beat which results in reduced momentum aperture.

$$d\beta = \frac{-\beta(s)}{2\sin 2\pi\nu} \int \beta(s_1) \Delta k \cos\{2|\varphi(s_1) - \varphi(s)| - 2\pi\nu\} ds$$

$$d\beta/d\delta = \frac{-\beta(s)}{2\sin 2\pi\nu} (kl - mlD) \beta(s_1) \cos\{2|\varphi(s_1) - \varphi(s)| - 2\pi\nu\}$$

Unlike chrom, chromatic beta beat is distributed all around the machine. Therefore, the compensation needs more than 2 families of sextuples.

The Montague Formalism

The following chromatic variables are defined to characterize the off-momentum beam envelope

$$a = \lim_{\delta \rightarrow 0} \frac{1}{\delta} \frac{(\alpha_1 \beta_0 - \alpha_0 \beta_1)}{(\beta_0 \beta_1)^{1/2}}$$
$$b = \lim_{\delta \rightarrow 0} \frac{1}{\delta} \frac{(\beta_1 - \beta_0)}{(\beta_0 \beta_1)^{1/2}}$$

The index 0 will refer to the parameters for design energy and the index 1 will refer to the perturbed optics due to energy offset.

W vector

$$\mathbf{W} = b + ia.$$

W function

$$|\mathbf{W}| = \sqrt{a^2 + b^2}$$

The formalism is implemented in the MAD-X and Bmad program.

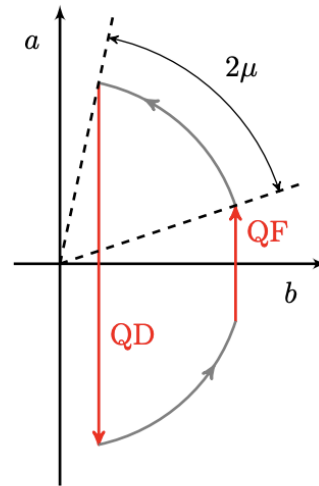
W vector in a FODO

$$\Delta a = -(\beta_0\beta_1)^{1/2}\Delta k_n\Delta s \simeq \beta_0 k_1 L_q$$

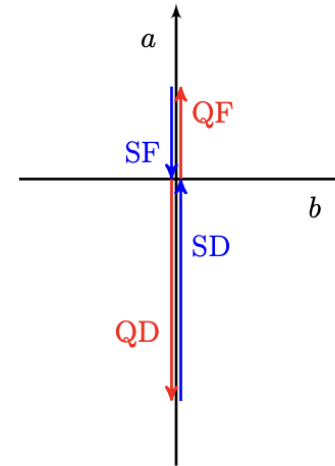
for quadrupole

$$\Delta a = -(\beta_0\beta_1)^{1/2}\Delta k_n\Delta s \simeq -\beta_0 D_x k_2 L_s$$

for sextupole



(a)



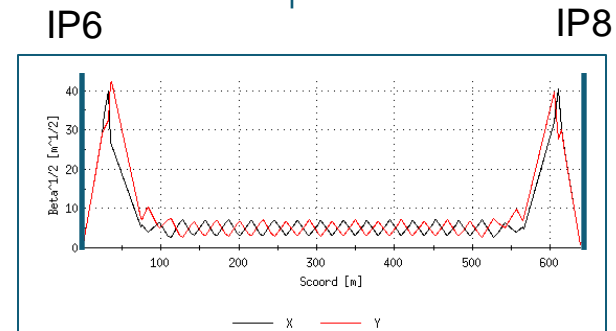
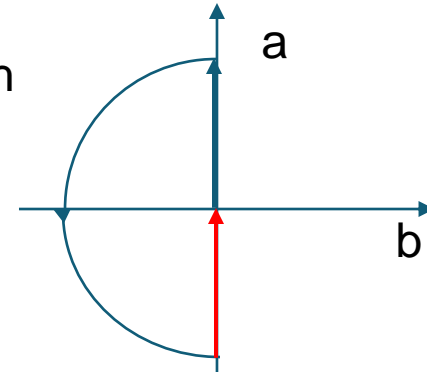
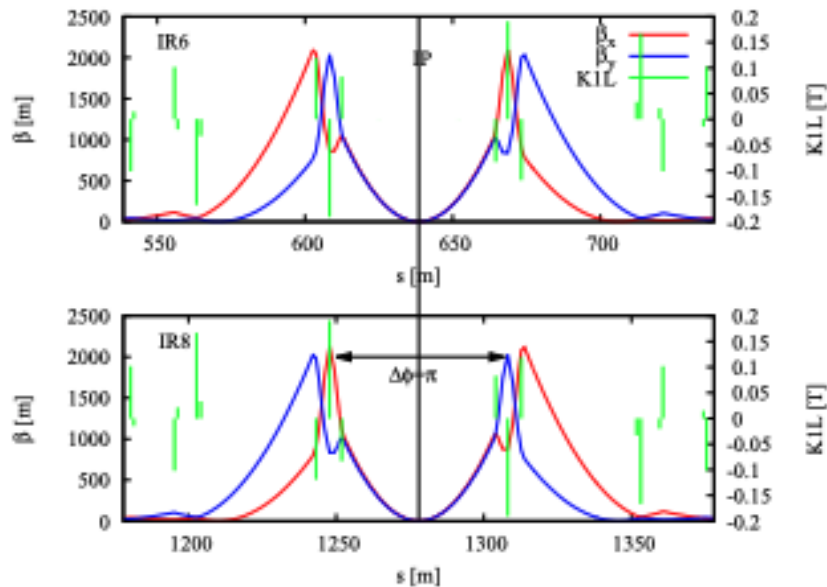
(b)

No compensation in a 60 deg FODO

Compensated case starting with zero

Passive compensation for 2 low beta insertions

RHIC IR6 and IR8 beta functions and quad strength



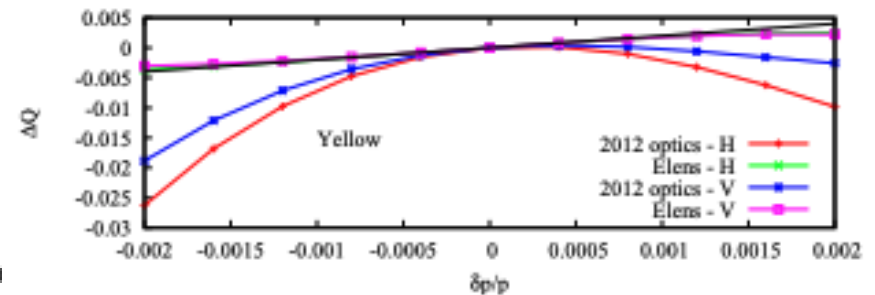
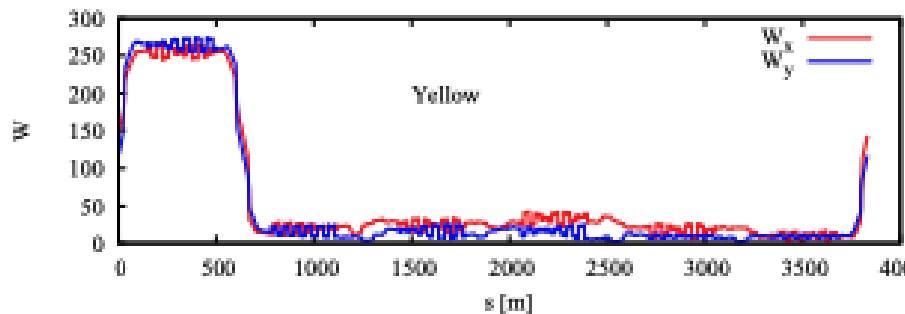
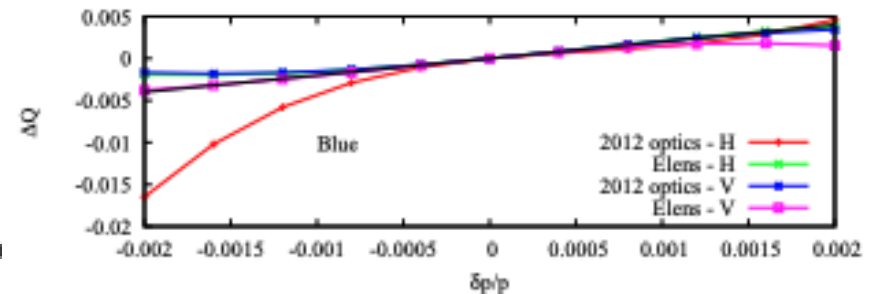
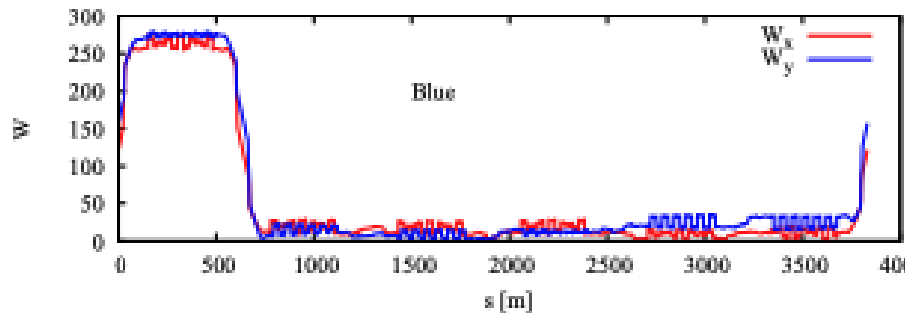
Conditions for a perfect passive compensation of chromatic aberration:

$$\Delta\phi_{L6 \rightarrow R8} = k \frac{\pi}{2},$$

$$\Delta\phi_{R6 \rightarrow L8} = k \frac{\pi}{2},$$

k is an odd integer

W-function and chromaticity with passive compensation



W function perfectly cancelled outside of the IR6-IR8 region, and the higher order chromaticity are significantly reduced.

Chromatic beta beat correction

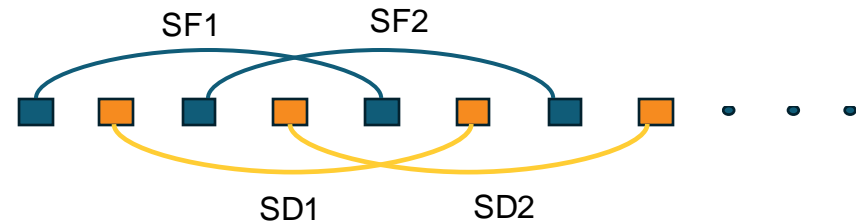
Wiring of sextuples for chromaticity correction:



Wiring of sextuples for chromatic beta beat correction (W function) for a 90 deg lattice:

$$I_{sf1} + I_{sf2} = 2I_{sf}$$

$$I_{sd1} + I_{sd2} = 2I_{sd}$$

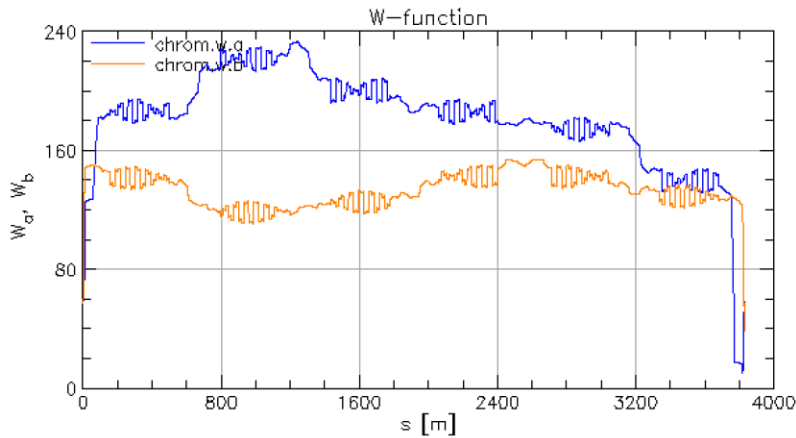


Constraints for keeping linear chromaticity constant

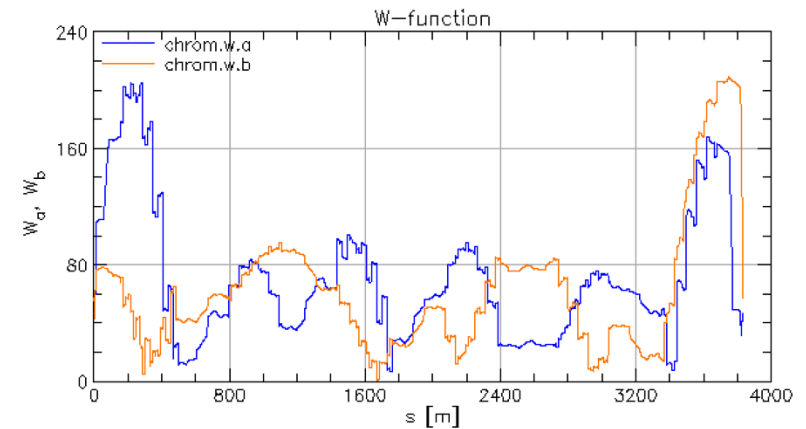
180 deg between SFs → cancellation of geometric aberration
iterative reduction of W function

W function reduction in EIC HSR

There are 6 arcs in RHIC/HSR, each with 4 families of sextupoles. In total, there are 24 chromatic sextupole families in each RHIC (HSR) ring.



W/O W function compensation



With W function compensation

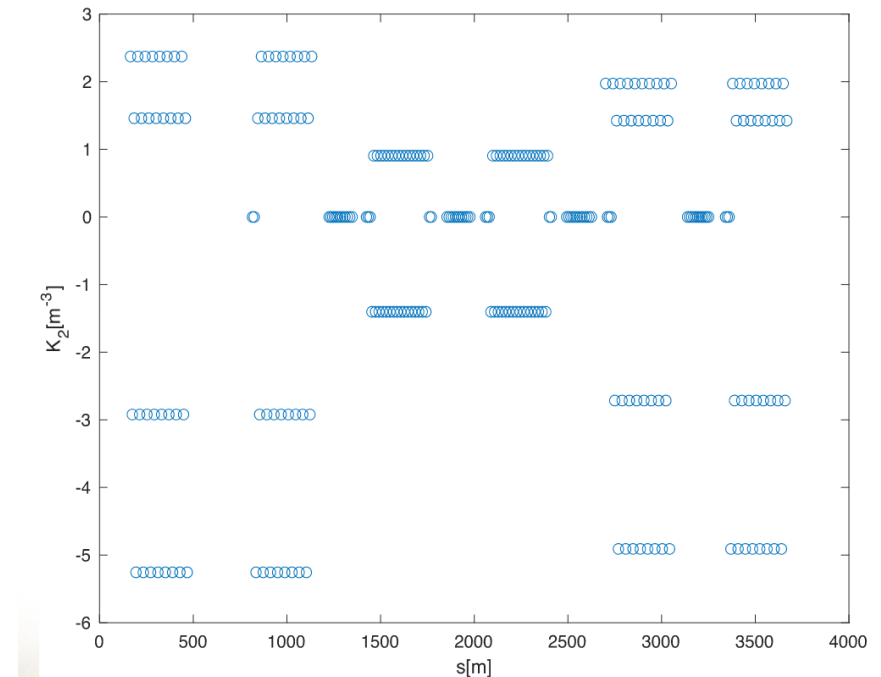
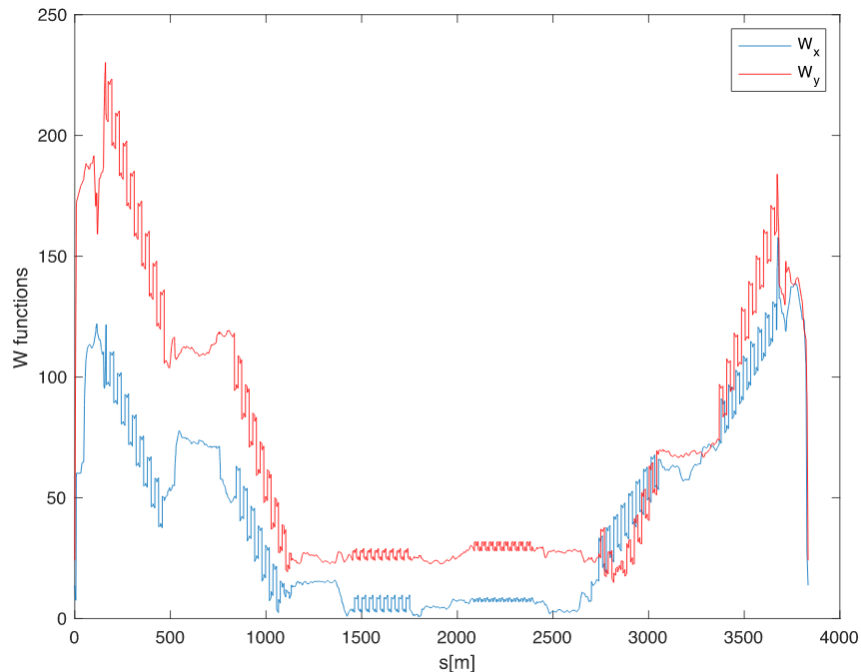
Further improvement is possible with adjustment of the phase advance of each straight section.

EIC ESR lattice parameters

Parameter	60°	90°
Beam energy, E_0 [GeV]	10	18
Circumference, C [m]	3834	3834
Emittance, ϵ_x [nm]	24.0	28.3
Energy spread, σ_δ [10^{-4}]	5.54	9.83
Betatron tunes, ν_x/ν_y	45.12/36.1	48.12/43.1
Chromaticity, ξ_{0x}/ξ_{0y}	-83/ -91	-85/ -94
IP betas, β_x^*/β_y^* [m]	0.42/0.05	0.42/0.05
Distance from IP to quad, L^* [m]	5.3	5.3

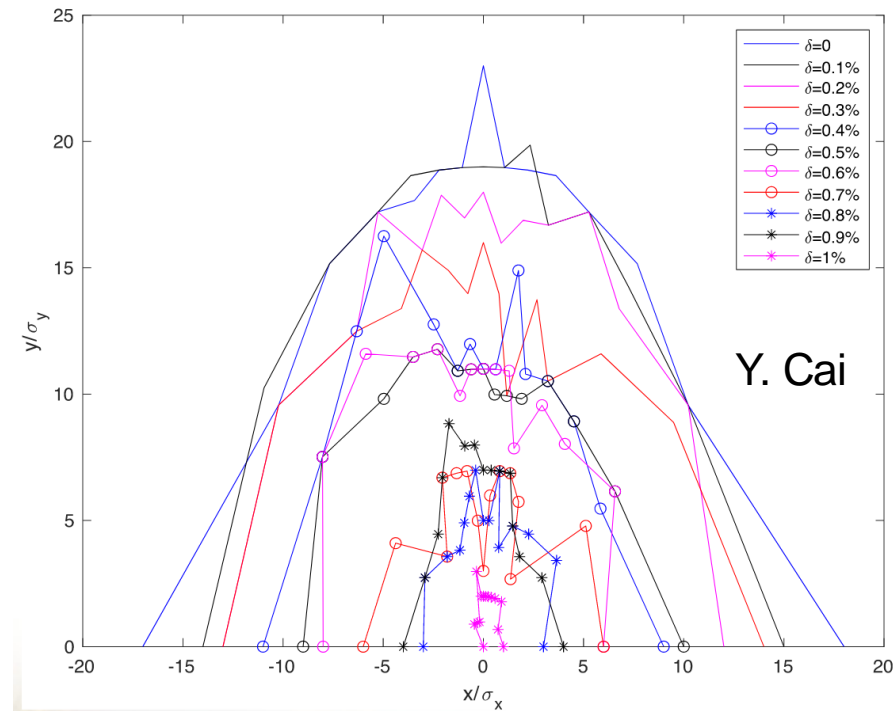
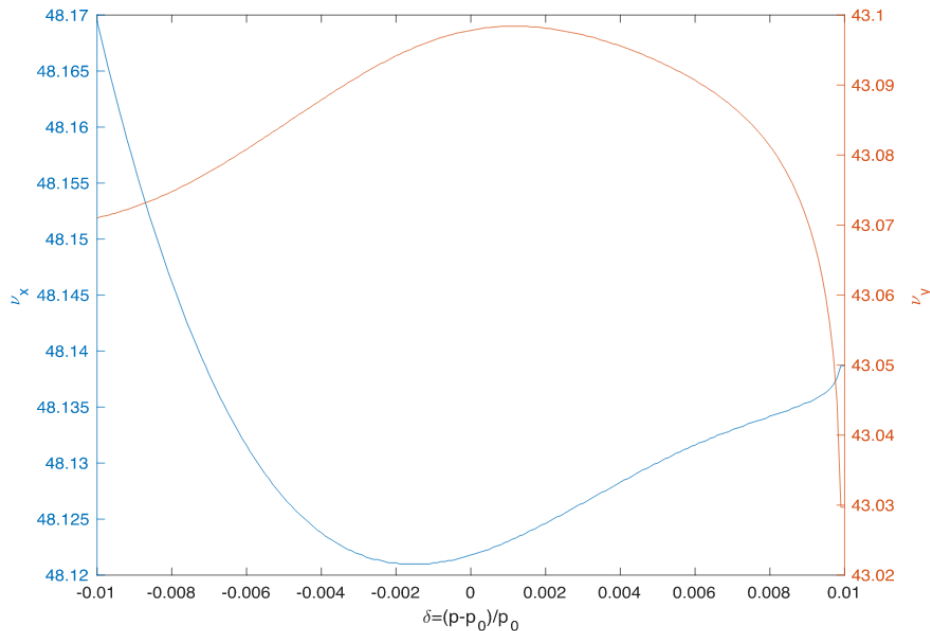
Sextupole configuration for 90 deg ESR

Dynamic aperture at 18 GeV, 90° lattice, 1IP
After a lot of work: 10 families of sextupoles



Chromaticity and dynamics aperture

Dynamic aperture at 18 GeV, 90° lattice, 1IP
10 families of sextupoles





Betatron Coupling

Coupled Transfer Matrix

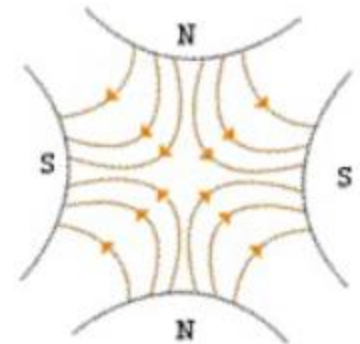
- Skew quadrupole fields generate betatron coupling between horizontal and vertical equations of motion

$$\begin{aligned}x'' + K_x(s)x &= a_1(s)y \\ y'' + K_y(s)y &= a_1(s)x.\end{aligned}$$

- 4x4 transfer matrix for a quadrupole tilted in a small angle φ ($a_1 = K_x\varphi$)

$$\begin{pmatrix} x \\ x' \\ y \\ y' \end{pmatrix}_{\text{final}} = \begin{pmatrix} 1 & 0 & 0 & 0 \\ -k & 1 & -2k\varphi & 0 \\ 0 & 0 & 1 & 0 \\ -2k\varphi & 0 & k & 1 \end{pmatrix} \begin{pmatrix} x \\ x' \\ y \\ y' \end{pmatrix}_{\text{initial}}$$

Skew quad



$$k = K_x L_q$$

Coupled One-turn matrix

One turn map (T) transformation into normal mode:

$$\mathbf{T} = \mathbf{VUV}^{-1},$$

Normal mode matrix

$$\mathbf{U} = \begin{pmatrix} \mathbf{A} & \mathbf{0} \\ \mathbf{0} & \mathbf{B} \end{pmatrix},$$

Matrix V

$$\mathbf{V} = \begin{pmatrix} \gamma\mathbf{I} & \mathbf{C} \\ -\mathbf{C}^+ & \gamma\mathbf{I} \end{pmatrix},$$

$C = 0$, then T is decoupled; $C \neq 0$ when T is coupled. $C(s)$ is a measure of local coupling.

Measuring one turn map

Calculating x' and y' based on position measurements at nearby dual plane BPMs:

$$\begin{pmatrix} x^{(n)} \\ p_x^{(n)} \\ y^{(n)} \\ p_y^{(n)} \end{pmatrix}_{i+1} = \mathbf{M}_{i,i+1} \begin{pmatrix} x^{(n)} \\ p_x^{(n)} \\ y^{(n)} \\ p_y^{(n)} \end{pmatrix}_i .$$

Calculating the one turn map based on the turn-by-turn 2D phase space coordinates:

$$\begin{pmatrix} x^{(n)} & \dots & x^{(2)} \\ p_x^{(n)} & \dots & p_x^{(2)} \\ y^{(n)} & \dots & y^{(2)} \\ p_y^{(n)} & \dots & p_y^{(2)} \end{pmatrix}_i = \mathbf{R}_i \begin{pmatrix} x^{(n-1)} & \dots & x^{(1)} \\ p_x^{(n-1)} & \dots & p_x^{(1)} \\ y^{(n-1)} & \dots & y^{(1)} \\ p_y^{(n-1)} & \dots & p_y^{(1)} \end{pmatrix}_i .$$

Electron Vertical emittance from coupling

- Difference coupling resonance strength

$$\kappa = \frac{1}{4\pi} \int ds K_s \sqrt{\beta_x \beta_y} e^{i\phi_D}$$

$$\frac{\phi_D}{2\pi} = \mu_x(s) - \mu_y(s) - \frac{s}{C} \Delta_r$$

- Vertical emittance from coupling

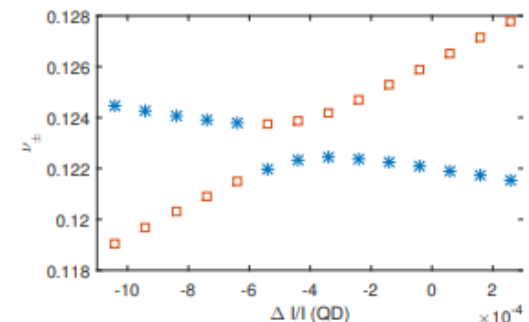
$$\frac{\varepsilon_y}{\varepsilon_x} = \frac{|\kappa|^2}{|\kappa|^2 + \Delta_r^2 / 2}$$

$$\Delta_r = (v_x - v_y - N)$$

κ is resonance strength, Δ_r is distance from resonance.

- Measure coupling strength with minimum tune split

Tune scan for coupling strength measurement



Vertical dispersion

- Vertical dispersion directly causes increase of the vertical emittance by quantum excitation
- Two main terms driven the vertical dispersion:

$$\eta_y'' + K\eta_y = \frac{1}{\rho_y} - K_s\eta_x$$

- Dipole field from vertical corrector, dipole tilt, vertical orbit offset in quadrupoles
 - Skew quadrupole field located in horizontal dispersive regions from quadrupole tilts, or vertical offsets in sextupoles
- Dispersive location skew quads for vertical dispersion correction

Correction of coupling and vertical dispersion

Both coupling and vertical dispersion contribute to the vertical emittance

Skew quadrupoles to correct coupling and vertical dispersion

Distribute skew quads at non-dispersive and dispersive location

- Non-dispersive skew quads: control coupling
- Dispersive skew quads: control both coupling and vertical dispersion

Correction methods include global or sequential correction (first dispersion, then coupling)

- **LOCO**: fit the orbit response matrix and vertical dispersion to the model
- **Coupling RDTs**: derive linear coupling resonance-driven terms (RDTs) from TBT data and minimize them terms using the response matrix over skew quads
- **ICA**: extract amplitude and phase of normal modes from TBT data and fit the data to the model
- **Vertical Beam Size Correction**: Minimize the vertical beam size at observed locations
- **Online optimization**: optimize skew quadrupoles to minimize Touschek lifetime or vertical beam size

Coupling and vertical dispersion sources in RHIC

- Coupling: The roll errors of normal quadrupoles and the vertical closed orbits in the normal sextupoles are the main sources of the betatron coupling in RHIC
- Vertical dispersion: The source of vertical dispersion is divided into two categories :
 - • Non coupling contribution: vertical offset in quadrupoles..., dipole kick
 - • Coupling contribution: all coupling errors (quads roll, solenoids, snake alignment errors, offsets in sextuples, pitch of main dipole magnets, multipole errors...) and skew quadrupoles at locations with non-zero horizontal dispersion
- Analysis pointed to global skew quads as the dominant contributor for vertical dispersion

RHIC Triplet rolls

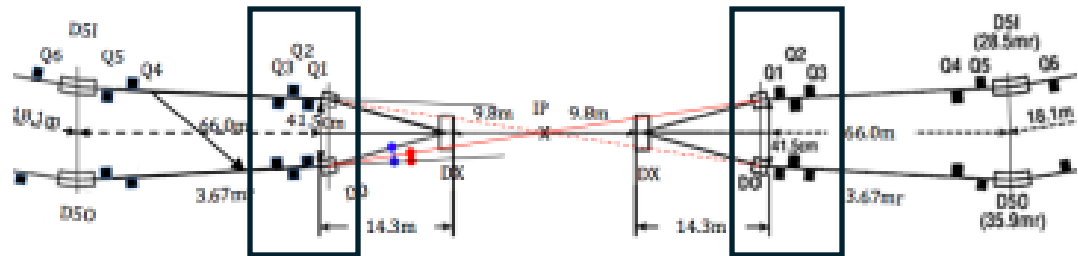
The skew quadrupole strength from a normal quadrupole with a roll angle θ is given by $-2\theta K_1$ when $\theta \ll 1$.

Skew quadrupoles are installed as part of the triplet package. The required strength can be calculated as below for each sector

$$\sum_{i=1}^N \sqrt{\beta_{x,s}\beta_{y,s}} K_{1s,s} = 0.$$

Table 1: Triplets roll errors [mrad] after 2004 adjustment

Sector	Triplet	Blue Ring	Yellow Ring
5	Q1	1.35	-4.91
	Q2	1.33	-2.35
	Q3	1.37	-2.15
6	Q1	1.59	-0.55
	Q2	-1.63	-0.10
	Q3	-3.69	1.00
7	Q1	-0.89	-
	Q2	1.23	-
	Q3	-1.32	-
8	Q1	4.67	1.02
	Q2	-2.10	-1.89
	Q3	0.17	1.37
1	Q1	4.72	6.97
	Q2	2.40	2.01
	Q3	1.38	-0.70
2	Q1	1.26	3.27
	Q2	3.21	-1.65
	Q3	-0.87	-0.69



Triplet cryostat

Local coupling measurement

A vertical offset in a skew quadrupole will generate a horizontal closed orbit in the ring,

$$x_s = -\frac{\sqrt{\beta_{x,s}\beta_{x,0}}}{2 \sin(\pi Q_x)} (\Delta y K_{1s}) \cos(\pi Q_x - |\Phi_{x,s} - \Phi_{x,0}|).$$



Local bump

Closed orbit

To compensate, add skew quad so that

$$\sum_{i=1}^N \sqrt{\beta_{x,s}} \Delta y(s) K_{1s} = 0.$$

Local Coupling Results

Local coupling measurement with local bump

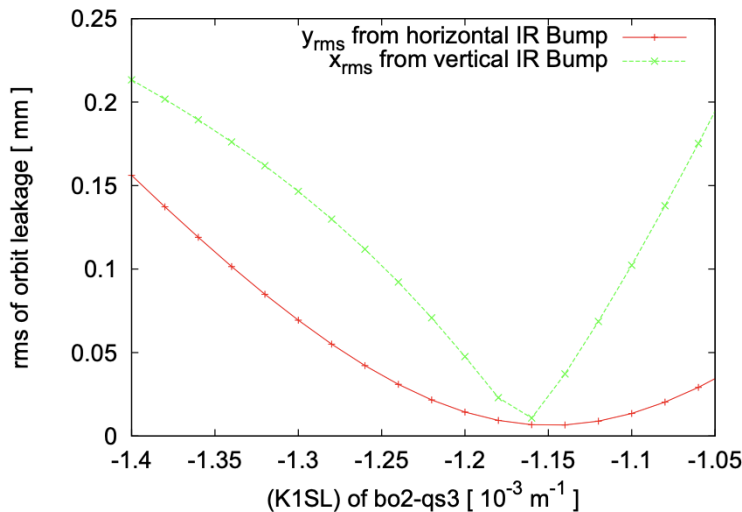


Table 3: Correction strengths [10^{-3} m^{-1}] with the Blue ring store lattice for the 2011 RHIC 250 GeV p-p runs.

Corr.	Anal.	H-Bump	V-Bump	Avg.	Contr.
bi5qs3	0.04	0.02	-0.08	-0.03	0
bo6qs3	0.04	0.02	0	0.01	0.1
bo7qs3	0.83	0.92	0.88	0.90	0.9
bi8qs3	-1.45	-1.40	-1.48	-1.44	-1.4
bi1qs3	0.08	0.06	0.10	0.08	0.2
bo2qs3	-1.23	-1.14	-1.16	-1.15	-1.2

H-bump and V-bump measurements are close, with reasonable agreement with analytical calculation based on magnet rolls. When coupling is small, V-bump is less accurate, due to the fact that sextupole components of DX and D0 magnet contribute to coupling when beam has vertical offset.

Coupling angle modulation

Eigentunes with coupling

$$Q_1 = Q_{x,0} - \frac{\Delta}{2} + \frac{1}{2}\sqrt{\Delta^2 + |C^-|^2},$$

$$Q_2 = Q_{y,0} + \frac{\Delta}{2} - \frac{1}{2}\sqrt{\Delta^2 + |C^-|^2},$$

where $\Delta = Q_{x,0} - Q_{y,0} - p,$

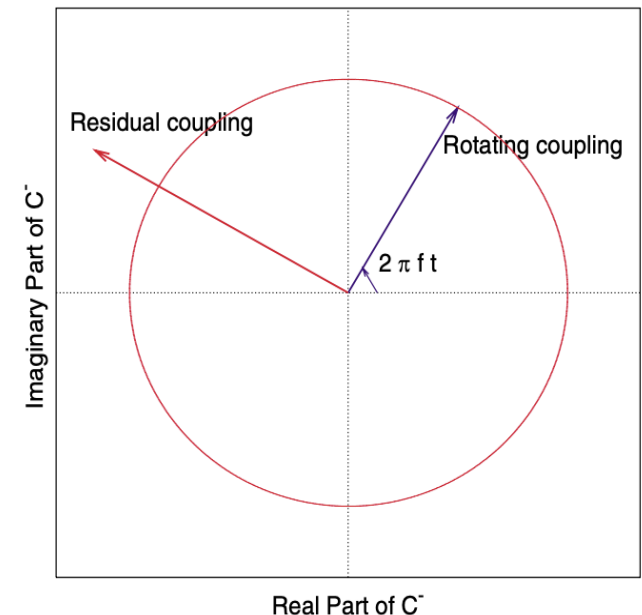
Measured tune split

$$|\Delta Q| = |Q_1 - Q_2 - p| = \sqrt{\Delta^2 + |C^-|^2}.$$

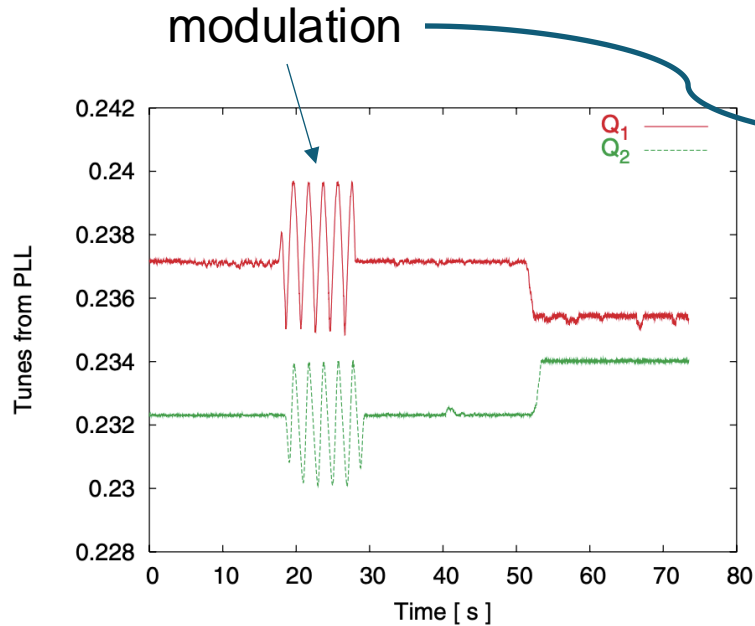
Measured tune split with modulated coupling source

$$|\Delta Q|^2 = \Delta^2 + |C_{\text{res,amp}}^-|^2 + |C_{\text{rot,amp}}^-|^2 + 2|C_{\text{res,amp}}^-||C_{\text{rot,amp}}^-| \cos(2\pi f t - \phi_{\text{res}}).$$

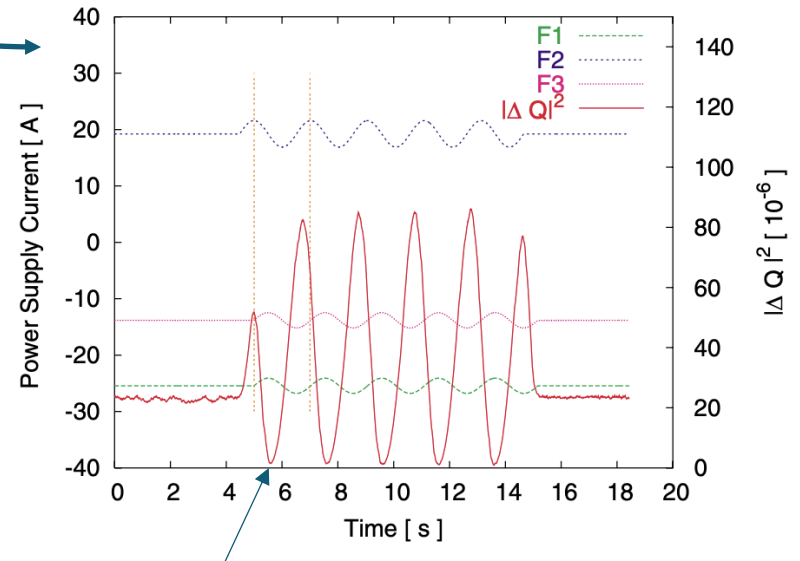
Introduce coupling with modulated phase



Measurement and correction



Tune measurement during modulation



$|\Delta Q|$ minimum

References

- Courant, E. D.; Snyder, H. S. (Jan 1958). "Theory of the alternating-gradient synchrotron" (PDF). *Annals of Physics*. 3 (1): 360–408. Bibcode:2000AnPhy.281..360C. doi:10.1006/aphy.2000.6012.
- Bernhard Holzer, <https://cas.web.cern.ch/sites/default/files/lectures/warsaw-2015/holzerinsertions.pdf>, <https://cas.web.cern.ch/sites/default/files/lectures/baden-2004/holzer-3.pdf>
- Oliver Bruning, <https://cas.web.cern.ch/sites/default/files/lectures/baden-2004/bruning1.pdf>
- J. Laskar, et al, 1990, Icarus 88, 266-291
- R. Bartolini, et al, EPAC 96
- Haerer, Bastian, Lattice design and beam optics calculations for the new large-scale electron-positron collider FCC-ee, <https://cds.cern.ch/record/2271820>
- Eric Prebys, <https://eprebys.faculty.ucdavis.edu/accelerator-physics-fundamentals-online-course/>
- https://www.egr.msu.edu/classes/me451/me451_labs/Fall_2013/Understanding_FFT_Windows.pdf
- M. Bai, RHIC Optics Status, LHC optics review 2013
- X. Yang, PRAB 20, 054001 (2017)
- D. Marks, <https://toddsatogata.net/2021-USPAS/lectures/2021-02-10-SextChromPart2.pdf>
- LATTICE DESIGN IN HIGH-ENERGY PARTICLE ACCELERATORS B. J. Holzer DESY, Hamburg, Germany <https://cds.cern.ch/record/941323/files/p31.pdf>
- Bryant, P J (CERN) Planning sextupole families in a circular collider <https://cds.cern.ch/record/302490>
- Y. Cai, Optimization of chromatic optics in the electron storage ring of the Electron-Ion Collider, <https://doi.org/10.1103/PhysRevAccelBeams.25.071001>
- Y. Luo, Re-visit local coupling correction in the interaction regions of RHIC, <https://www.osti.gov/servlets/purl/1061989>
- Y. Luo, Fast and robust global decoupling with coupling angle modulation, <https://journals.aps.org/prab/pdf/10.1103/PhysRevSTAB.8.074002>

Sextupole wiring dependence on phase advance

Different solutions are required for 60° and 90° lattices

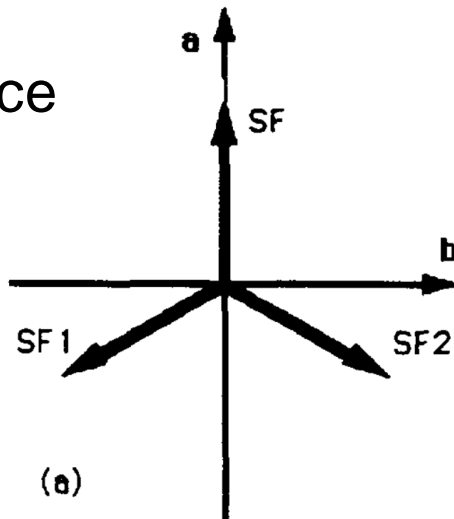
- For 60° lattice can use 6 families (3 families per plane)
- For 90° lattice can use 4 families (2 families per plane)

-

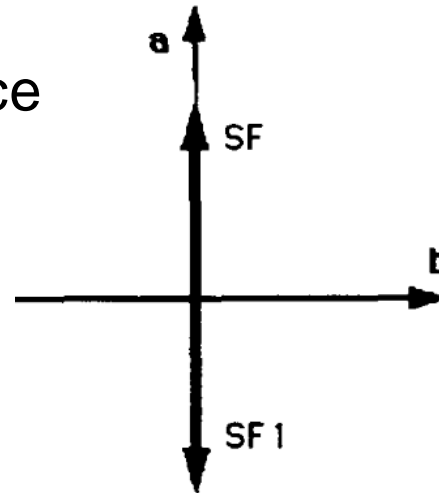
90° lattice is most challenging:

- Additional constraints on phase advance to first sextupoles in arcs
- Larger rms momentum spread

60°
lattice



90°
lattice



Bryant,
1995

Longitudinal Motion

Vadim Ptitsyn
EIC Project, BNL

(This lecture uses materials from V. Lebedev's USPAS 2022 lectures)

In This Lecture

1. We introduce you to basics of linear optics for longitudinal degree of freedom which includes:

- Connection between horizontal and longitudinal motions
- The longitudinal equation of motion in the presence of RF cavities
- Concepts of synchrotron tune and separatrix.

2. We also consider the effect of RF noise, which, if not properly addressed, may result in unacceptably large longitudinal emittance growth.

In a collider the beam should stay for a long time

⇒ The growth rates for beam emittances and bunch length should be sufficiently small

Longitudinal Motion

Connection Between Horizontal and Longitudinal Matrix

- The particle transport through the magnet beamline in linear approximation is described by transfer matrix. Here we use 4D matrix, which includes horizontal and longitudinal degrees of freedom. No RF cavities.

$$\mathbf{x}_2 = \mathbf{M}\mathbf{x}_1 \quad , \quad \mathbf{M} = \begin{bmatrix} M_{11} & M_{12} & 0 & M_{16} \\ M_{21} & M_{22} & 0 & M_{26} \\ M_{51} & M_{52} & 1 & M_{56} \\ 0 & 0 & 0 & 1 \end{bmatrix} \quad , \quad \mathbf{x} \equiv \begin{bmatrix} x \\ \theta_x \\ s \\ \theta_s \end{bmatrix} \quad , \quad \theta_s = \frac{\Delta p}{p}$$

Longitudinal displacements are counted relative to the reference particle.

- Trajectory of particle having momentum deviation θ_s can be expressed as the sum of betatron oscillation and θ_s dependent terms:

$$x = x_\beta + D \cdot \theta_s$$

where D is called the dispersion function.

- Elements M_{16} and M_{26} are directly related to dispersion

$$\begin{bmatrix} D_2 \\ D'_2 \\ \dots \\ 1 \end{bmatrix}^T = \begin{bmatrix} M_{11} & M_{12} & 0 & M_{16} \\ M_{21} & M_{22} & 0 & M_{26} \\ M_{51} & M_{52} & 1 & M_{56} \\ 0 & 0 & 0 & 1 \end{bmatrix} \begin{bmatrix} D_1 \\ D'_1 \\ \dots \\ 1 \end{bmatrix}, \quad \begin{cases} D_2 = M_{11}D_1 + M_{12}D'_1 + M_{16} \\ D'_2 = M_{21}D_1 + M_{22}D'_1 + M_{26} \end{cases} \xrightarrow[\substack{D_2=D_1 \\ D'_2=D'_1}]{\text{Forring}} \begin{cases} M_{16} = D(1 - M_{11}) - D'M_{12} \\ M_{26} = -M_{21}D + D'(1 - M_{22}) \end{cases}$$

- Elements M_{51} and M_{52} are bound to others by symplecticity condition

$$\hat{\mathbf{M}}^T \mathbf{U} \hat{\mathbf{M}} = \mathbf{U} \Rightarrow \begin{cases} M_{51} = M_{21}M_{16} - M_{11}M_{26} \\ M_{52} = M_{22}M_{16} - M_{12}M_{26} \end{cases} \xrightarrow[\substack{D_2=D_1 \\ D'_2=D'_1}]{\text{Forring}} \begin{cases} M_{51} = DM_{21} + D'(1 - M_{11}) \\ M_{52} = -D(1 - M_{22}) - D'M_{12} \end{cases}$$

where we accounted that $M_{11}M_{22} - M_{12}M_{21} = 1$

- i.e. for a ring without RF M_{16} , M_{26} , M_{51} and M_{52} can be expressed through dispersion and its derivative. M_{56} is independent on other elements

Equations of Longitudinal Motion

- Let's consider particle beam circulating in a collider ring. First, we define a reference particle which travel on the ring design closed orbit and has a constant momentum p .

Then, a particle with momentum deviation $\Delta p/p$ with respect to a reference particle will change its longitudinal position (either fall behind or go forward) in one turn:

$$\begin{bmatrix} \dots \\ \dots \\ \Delta s \\ \dots \end{bmatrix}^T = \begin{bmatrix} M_{11} & M_{12} & 0 & M_{16} \\ M_{21} & M_{22} & 0 & M_{26} \\ M_{51} & M_{52} & 1 & M_{56} \\ 0 & 0 & 0 & 1 \end{bmatrix} \begin{bmatrix} D \\ D' \\ \dots \\ 1 \end{bmatrix} \frac{\Delta p}{p} \Rightarrow \Delta s = (M_{51}D + M_{52}D' + M_{56}) \frac{\Delta p}{p} = \alpha C \frac{\Delta p}{p}$$

- Momentum compaction α describes the change of revolution time period with $\Delta p/p$:

$$\frac{\Delta C}{C} = \alpha \frac{\Delta p}{p}, \quad \alpha = \frac{M_{51}D + M_{52}D' + M_{56}}{C}$$

- Slip-factor η describes the change of revolution time period with $\Delta p/p$:

$$\frac{\Delta T}{T} = \frac{\Delta C}{C} - \frac{\Delta v}{v} = \eta \frac{\Delta p}{p} \quad \begin{matrix} \frac{\Delta v}{v} = \frac{1}{\gamma^2} \frac{\Delta p}{p} \\ \frac{\Delta C}{C} = \alpha \frac{\Delta p}{p} \end{matrix} \rightarrow \left(\alpha - \frac{1}{\gamma^2} \right) \frac{\Delta p}{p} \Rightarrow \eta = \alpha - \frac{1}{\gamma^2}$$

$\eta = 0$ defines the transition energy $\gamma_t = \frac{1}{\sqrt{\alpha}}$

- Now, let's introduce an RF cavity with RF frequency $f_{RF} = qf_0$ (or several RF cavities of the same frequency) into the ring. Here, f_0 is the revolution frequency and q is called RF harmonic number.
- A particle passing the cavity will experience the energy gain (or loss) according to:

$$\Delta E = -eV_0 \cdot \sin 2\pi f_{RF} t$$

- We will use phase φ defined in units of RF phase as a coordinate describing a longitudinal position of a particle along the bunch. There is a reference particle which energy stays constant during circulations.
- The change of φ with time is described as:

$$\frac{d\varphi}{dt} \approx \frac{\varphi_{n+1} - \varphi_n}{T} = 2\pi q f_0 \eta \theta_s$$

- The change of $\theta_s = \Delta p/p$ with time is described as:

$$\frac{d}{dt} \theta_s \approx \frac{\theta_{sn+1} - \theta_{sn}}{T} = -\frac{1}{\beta^2 E} eV_0 f_0 \sin \varphi$$

- Thus, we've got the system of equations describing longitudinal motion:

$$\begin{cases} \frac{d\varphi}{dt} = 2\pi q f_0 \eta \theta_s \\ \frac{d}{dt} \theta_s = -\frac{1}{\beta^2 E} e V_0 f_0 \sin \varphi \end{cases}$$

- From here one gets:

$$\frac{d^2 \varphi}{dt^2} = -\Omega_s^2 \sin \varphi$$

where the parameter $\frac{\Omega_s}{2\pi} = f_0 \sqrt{\frac{eV_0 q \eta}{2\pi \beta^2 E}}$ is called the synchrotron frequency,

and $\nu_s = \sqrt{\frac{eV_0 q \eta}{2\pi \beta^2 E}}$ is called the synchrotron tune.

Effect of Synchrotron Radiation on Longit. Motion

- Due to the synchrotron radiation all particles in the beam lose the energy equal to eV_{SR} . We will neglect the radiation damping at this point.

In order to keep its energy constant the reference particle must gain the energy equal to eV_{SR} when passing the RF cavity. Thus, it must pass the cavity not at $\varphi = 0$, but at some phase φ_0 .

- Then the motion equation transforms to:

$$\frac{d^2\varphi}{dt^2} = -\Omega_s^2 (\sin\varphi + \sin\varphi_0), \quad \sin\varphi_0 = \frac{V_{SR}}{V_0}$$

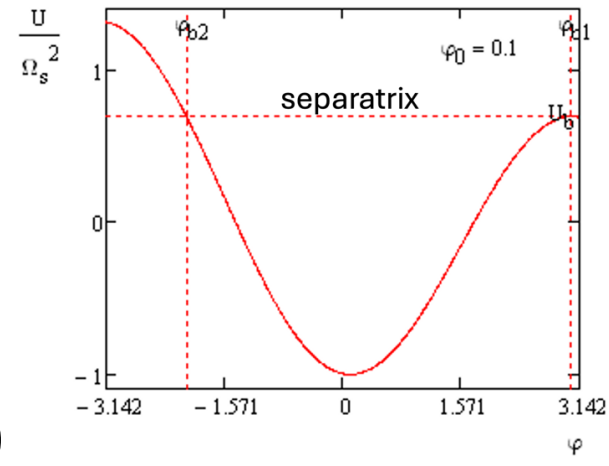
- At this point we would like to switch to variable set $(\varphi, \hat{p} = \dot{\varphi})$.
- Making transformation of differentials:

$$\frac{d^2\varphi}{dt^2} = \frac{d\varphi}{dt} \frac{d}{d\varphi} \frac{d\varphi}{dt} = \hat{p} \frac{d\hat{p}}{d\varphi} = \frac{d}{d\varphi} \left(\frac{\hat{p}^2}{2} \right) = -\Omega_s^2 (\sin \varphi + \sin \varphi_0)$$

- And doing integration one gets:

$$\frac{\hat{p}^2}{2} = \Omega_s^2 (\cos \varphi + \varphi \sin \varphi_0) + C$$

- Different values of constant C correspond to different trajectories in (φ, \hat{p}) phase space.
- On this basis one can introduce Hamiltonian and the potential energy



$$H = \frac{p^2}{2} + U(\varphi), \quad U(\varphi) = -\Omega_s^2 (\cos \varphi + \varphi \sin \varphi_0)$$

The motion is bounded when it is inside of the potential well.

- Separatrix boundaries

$$\sin \varphi_{b1} = \sin \varphi_0 \Rightarrow \varphi_{b1} = \pi - \varphi_0$$

$$\Rightarrow C = \Omega_s^2 (\cos \varphi_0 - \varphi_0 \sin \varphi_0)$$

Thus, in the presence of SR the size of the bounded motion area (RF bucket) shrinks.

- Without SR:

above transition the stable point is $\phi=0$, the bucket spans from $-\pi$ to π

below transition the stable point is $\phi=\pi$, the bucket spans from 0 to 2π

Longitudinal Emittance Growth due to RF Noise

In the absence of perturbations the longitudinal motion equation:

$$\frac{d^2 \varphi}{dt^2} + \Omega_s^2 \sin \varphi = 0, \quad \Omega_s^2 = \frac{eV_0 \eta q}{2\pi m c^2 \gamma \beta^2}$$

Fluctuations of RF phase and amplitude result in:

$$\frac{d^2 \varphi}{dt^2} + \Omega_s^2 \left(1 + \frac{\delta V(t)}{V_0} \right) \sin(\varphi - \psi(t)) = 0 \quad \xrightarrow[u(t) \equiv \delta V(t)/V_0]{\text{expanding}} \quad \frac{d^2 \varphi}{dt^2} + \Omega_s^2 \sin \varphi = -\Omega_s^2 (\sin(\varphi)u(t) + \cos(\varphi)\psi(t))$$

First, we consider the small amplitude (i.e.) linear motion and RF phase fluctuations. Then

$$\frac{d^2\varphi}{dt^2} + \Omega_s^2\varphi = -\Omega_s^2\psi(t)$$

The solution is well-known

$$\varphi(t) = -\Omega_s \int_0^t \psi(t') \sin(\Omega_s(t-t')) dt'$$

The rms particle deviation is

$$\overline{\varphi^2(t)} = \Omega_s^2 \int_0^t \int_0^t \overline{\psi(t_1)\psi(t_2)} \sin(\Omega_s(t-t_1)) \sin(\Omega_s(t-t_2)) dt_1 dt_2$$

Noise properties are characterized by the correlation function

$$K(\tau) = \overline{\psi(t)\psi(t+\tau)} \Rightarrow K(t_1 - t_2) = \overline{\psi(t_1)\psi(t_2)}$$

Or by the spectral density which is related with the correlation function through the Fourier transform:

$$K(\tau) = \int_{-\infty}^{\infty} P(\omega)e^{i\omega\tau} d\omega, \quad P(\omega) = \frac{1}{2\pi} \int_{-\infty}^{\infty} K(\tau)e^{-i\omega\tau} dt$$

$$\overline{\psi(t_1)\psi(t_2)} = K(t_1 - t_2) \Rightarrow \overline{\psi^2} = K(0) = \int_{-\infty}^{\infty} P(\omega)d\omega$$

Often white noise is used for initial evaluation of noise related effects:

$$K(t_1 - t_2) = \delta(t_1 - t_2), \quad P(\omega) = \text{const},$$

Usually the white noise considered in some practical frequency band.

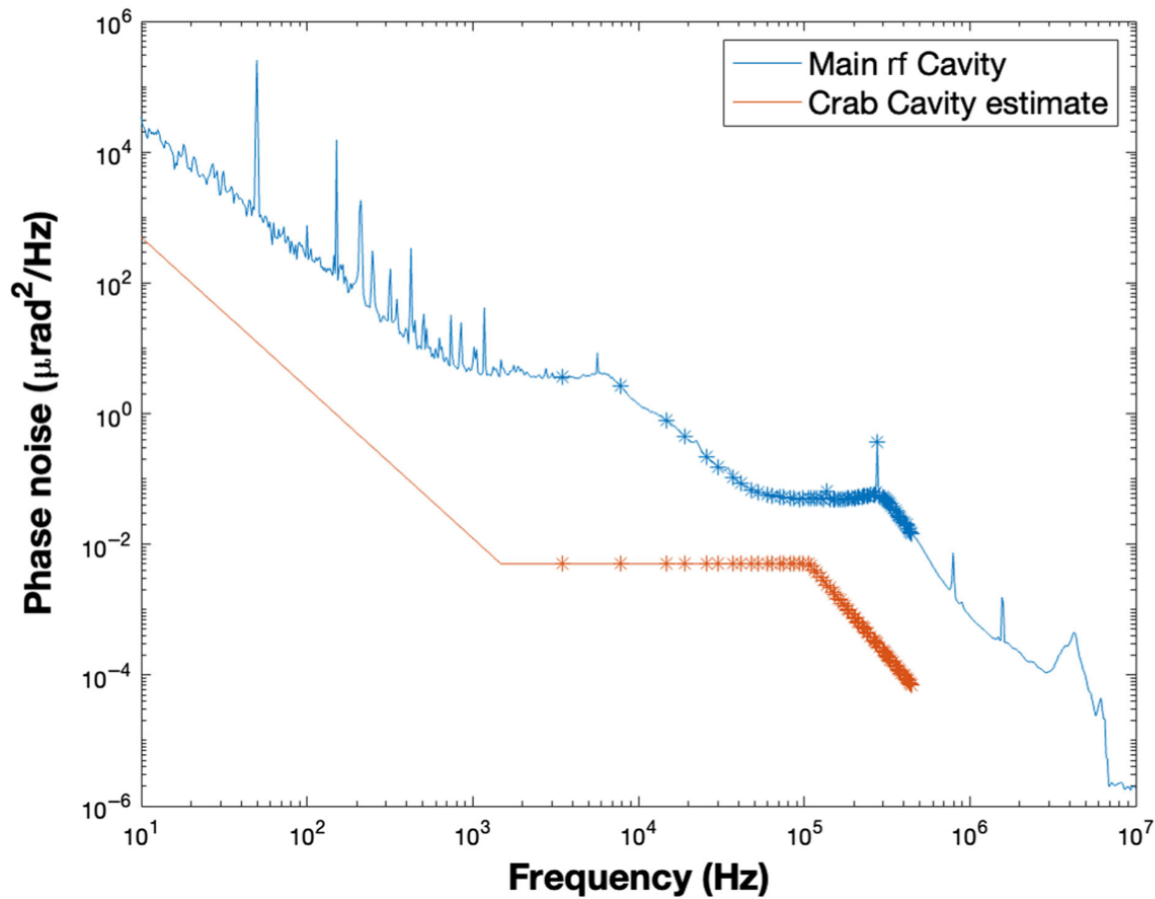


FIG. 5. LHC main accelerating cavity (measured) and crab cavity (estimated) phase noise.

P. BAUDRENGHIEN and T. MASTORIDIS

PHYS. REV. ACCEL. BEAMS **27**, 051001 (2024)

Thus, particle motion under random phase fluctuations

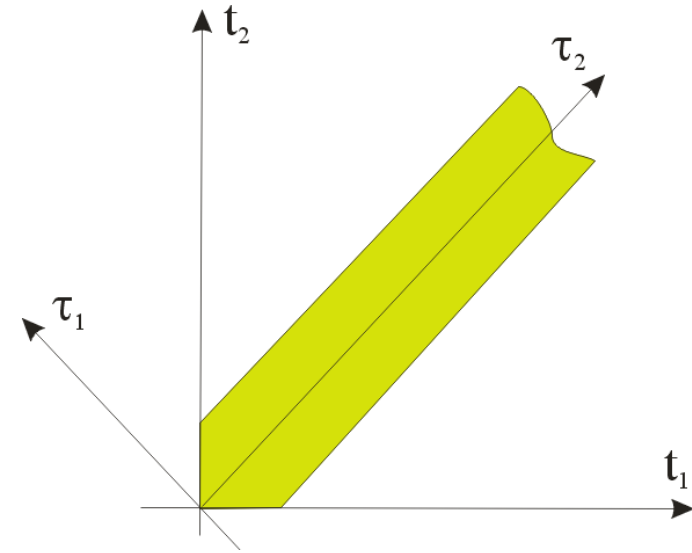
$$\begin{aligned}\overline{\varphi^2(t)} &= \Omega_s^2 \int_0^t \int_0^t \overline{\psi(t_1)\psi(t_2)} \sin(\Omega_s(t-t_1)) \sin(\Omega_s(t-t_2)) dt_1 dt_2 \\ &= \Omega_s^2 \int_0^t \int_0^t K_\psi(t_1-t_2) \sin(\Omega_s(t-t_1)) \sin(\Omega_s(t-t_2)) dt_1 dt_2\end{aligned}$$

Computation of integral

Make substitution $\begin{cases} \tau_1 = t_1 - t_2 \\ \tau_2 = t_1 + t_2 \end{cases} \quad \begin{cases} t_1 = (\tau_1 + \tau_2) / 2 \\ t_2 = (\tau_2 - \tau_1) / 2 \end{cases}$

Corresponding Jacobian is: $\frac{\partial(t_1, t_2)}{\partial(\tau_1, \tau_2)} = \begin{bmatrix} 1/2 & 1/2 \\ -1/2 & 1/2 \end{bmatrix} = \frac{1}{2}$

Then we have



$$\begin{aligned} \overline{\varphi^2(t)} &= \Omega_s^2 \int_0^t \int_0^t \overline{\psi(t_1)\psi(t_2)} \sin(\Omega_s(t-t_1)) \sin(\Omega_s(t-t_2)) dt_1 dt_2 \\ &= \Omega_s^2 \int_0^t \int_0^t K_\psi(t_1 - t_2) \left[\frac{\cos(\Omega_s(t_1 - t_2)) + \cos(\Omega_s(2t - t_1 - t_2))}{2} \right] \left(\frac{1}{2} \right) dt_1 dt_2 \\ &\approx \frac{\Omega_s^2}{4} \int_{-\infty}^{\infty} d\tau_1 \int_0^{2t} K_\psi(\tau_1) [\cos(\Omega_s \tau_1) + \cos(\Omega_s(2t - \tau_2))] d\tau_1 d\tau_2 \xrightarrow[\text{oscillating term}]{\text{drop fast}} \\ &\approx \frac{\Omega_s^2}{2} t \int_{-\infty}^{\infty} K_\psi(\tau) \cos(\Omega_s \tau) d\tau \end{aligned}$$

Recollecting connection between the correlation function and the spectral

density we finally obtain:

$$\frac{d}{dt} \overline{\varphi^2(t)} = \pi \Omega_s^2 P_\psi(\Omega_s)$$

Bunch Lengthening due to Amplitude Noise

Let's consider the small amplitude RF voltage fluctuations: $\frac{d^2\varphi}{dt^2} + \Omega_s^2\varphi = -\Omega_s^2\varphi u(t)$

In perturbation theory we replace j in RH side by $\varphi_0 \sin(\Omega_s t)$

$$\Rightarrow \overline{\varphi^2(t)} \approx \Omega_s^2 \varphi_0^2 \int_0^t \int_0^t \overline{u(t_1)u(t_2)} \sin(\Omega_s t_1) \sin(\Omega_s t_2) \sin(\Omega_s(t-t_1)) \sin(\Omega_s(t-t_2)) dt_1 dt_2$$

\Rightarrow

Similar to the calculations done for the case of phase noise one gets:

$$\overline{\varphi^2(t)} \approx \frac{\Omega_s^2}{4} t \varphi_0^2 \int_{-\infty}^{\infty} K_u(\tau) \cos(2\Omega_s \tau) d\tau$$

Accounting also $\overline{\varphi^2(t)} = \varphi_0^2 / 2$ we finally obtain

$$\frac{d}{dt} \overline{\varphi^2(t)} = \pi \Omega_s^2 \overline{\varphi^2(t)} P_u(2\Omega_s)$$

Practical Estimate

- Let's consider Tevatron: $f_s = \Omega_s / 2\pi = 35$ Hz, initial bunch length 35 cm and RF bucket length of 5.65 m (53.1 MHz)
- Require the bunch lengthening 5% after in 10 hours

$$\varphi_{fin} = \sqrt{\varphi_0^2 + T \frac{d\overline{\varphi^2}}{dt}} \approx \varphi_0 + \frac{T}{2\varphi_0} \frac{d\overline{\varphi^2}}{dt}$$

$$\Rightarrow \frac{d\overline{\varphi^2}}{dt} = \frac{\varphi_{fin} - \varphi_0}{\varphi_0 T} 2\varphi_0^2 = \frac{0.05}{10 \cdot 3600} 2 \left(2\pi \frac{35}{565} \right)^2 = 6.5 \cdot 10^{-7} \frac{\text{rad}^2}{\text{s}}$$

⇒ Corresponding spectral densities

$$\Rightarrow P_\psi = 4.3 \cdot 10^{-12} \text{s}^{-1}, \quad P_u = 3.8 \cdot 10^{-11} \text{s}^{-1}$$

⇒ Corresponding rms fluctuations for the white noise in 100 Hz band

$$\Rightarrow \sqrt{\psi^2} = \sqrt{4\pi P_\psi \Delta f} = 7.3 \cdot 10^{-5} \text{rad}, \quad \sqrt{u^2} = \sqrt{4\pi P_u \Delta f} = 2.2 \cdot 10^{-4} \text{rad}$$

Final Remarks about the RF noise

- To prevent longitudinal emittance growth a hadron collider requires high quality RF, both in the RF phase and the RF amplitude
- Microphonics in RF cavities as well as noise in power amplifiers may excite RF noise to unacceptable level
- RF feedbacks are used to stabilize the RF phase and/or amplitude to acceptable levels.
- Also the longitudinal damper may be helpful to reduce effect of phase noise
- Since proton and ion beams usually fill large part of the buckets, further consideration of noise effect, related with evaluation of diffusion at higher harmonics of synchrotron frequency is required.
- Noise in the bending magnetic field at synchrotron frequency harmonics works the same way as RF

Emittance Growth

Vadim Ptitsyn

BNL

(This lecture uses materials from V. Lebedev's USPAS 2022 lectures)

Initial notes:

- The growth rates for beam emittances and bunch length should be sufficiently small, in order to maximize the average luminosity or to minimize requirements for hadron cooling in the store.
- **The noise in bending magnetic field and transverse dampers** leads to transverse emittance growth
 - ◆ Proton colliders have larger circumference => small revolution frequency => more susceptible to noise due to its fast growth with frequency decrease
- In a properly built machine **the Intra Beam Scattering (IBS)** typically dominates the emittance growth

Transverse Emittance Growth due to Noise in Magnets

Sources of Dipole Field Noise

1. Dipole field fluctuations in bending magnets.
2. Random vibrations of the quadrupoles.
It can be caused by ground motion or by technical reasons (vacuum pumps, coolant flow).

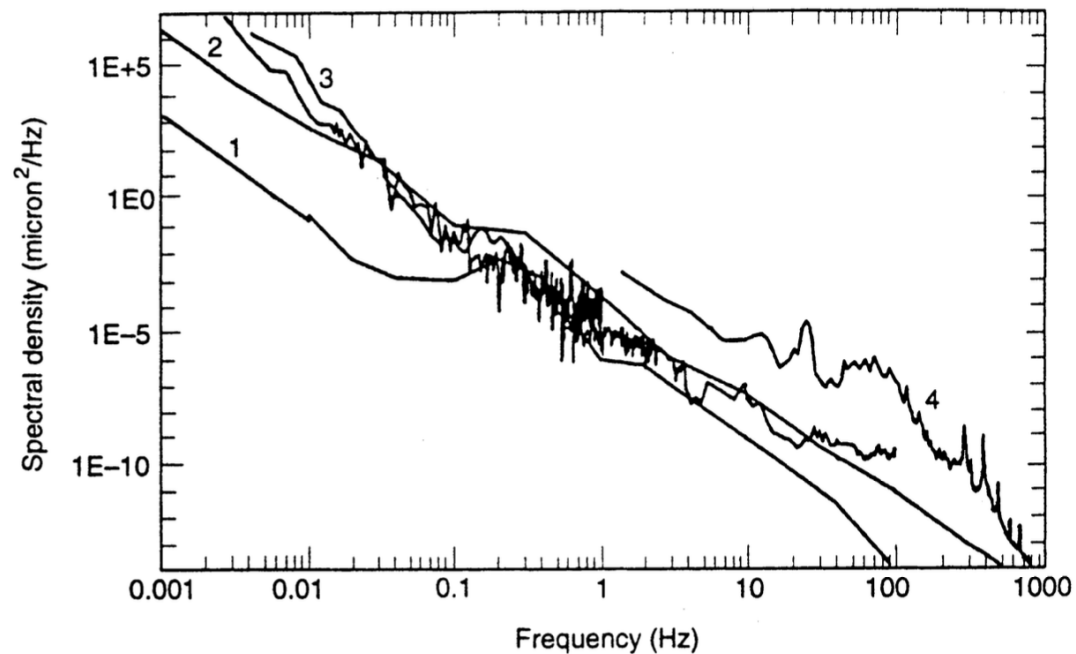
Equations of Motion and their Solution

- First, let's consider one point-like dipole field perturbation, producing dipole kicks θ_n on the beam, where n is the turn number
- The particle position after N turns is:

$$x_N = x_0 \cos(\mu N + \psi_0) + \sum_{n=0}^{N-1} \Delta p_n \sin(\mu(N-n)), \quad \Delta p_n = \sqrt{\beta} \theta_n$$

- Random noise is characterized by the correlation function K_p and the spectral density $P_p(\omega)$, which are connected by the Fourier transform.

$$\Delta p_n = p(nT), \quad \overline{p(t_1)p(t_2)} = K_p(t_1 - t_2), \quad K_p(\tau) = \int_{-\infty}^{\infty} P_p(\omega) e^{i\omega\tau} d\omega$$



Spectra of ground motion at different accelerator sites

- Then the effect of the dipole field noise on the particle trajectory is characterized by:

$$\begin{aligned}\overline{x_N^2} &= x_0^2 \cos^2(\mu N + \psi_0) + \sum_{n,m=0}^{N-1} \overline{\Delta p_n \Delta p_m} \sin(\mu(N-n)) \sin(\mu(N-m)) \\ &= x_0^2 \cos^2(\mu N + \psi_0) + \sum_{n,m=0}^{N-1} K(T(n-m)) \sin(\mu(N-n)) \sin(\mu(N-m))\end{aligned}$$

- Using the spectral density:

$$\overline{x_N^2} = x_0^2 \cos^2(\mu N + \psi_0) + \int_{-\infty}^{\infty} d\omega \sum_{n,m=0}^{N-1} P(\omega) e^{i\omega T(n-m)} \sin(\mu(N-n)) \sin(\mu(N-m))$$

- Performing summation leads us to the following result:

$$\overline{X_N^2} = X_0^2 \cos^2(\mu N + \psi_0) + \frac{N\omega_0\beta^2}{4} \sum_{n=-\infty}^{\infty} (P_\theta(\omega_0(n+\nu)) + P_\theta(\omega_0(\nu-n)))$$

Averaging over all particles and accounting that both terms make equal contribution we finally obtain

$$\varepsilon_N = \frac{1}{\beta} \left[\overline{X_N^2} \right]_{part}^{all} = \varepsilon_N + \frac{N\omega_0\beta}{2} \sum_{n=-\infty}^{\infty} P_\theta\left(\frac{2\pi n - \mu}{T}\right)$$

- If all sources of perturbation are statistically independent then for the entire ring we obtain

$$\frac{d\varepsilon}{dn} = \frac{\omega_0}{2} \sum_k^{\text{all sources}} \beta_k \sum_{n=-\infty}^{\infty} P_{\theta k} \left(\frac{2\pi n - \mu}{T} \right)$$

The average square of the single-particle displacement grows linearly with time. The only spectral components that contribute to the growth of the amplitude have a frequency equal to that of the betatron sidebands.

Mitigation of the emittance growth:

- If the emittance growth is unacceptable a **transverse damper** can be used to suppress the emittance growth
- In a collider different particles have different betatron tunes and therefore beam decoheres with typical decoherence time ~ 1000 turns.
- Therefore, to prevent the emittance growth the damper should damp the beam faster than it decoheres.

References

1. V. Lebedev, et.al. “Emittance growth due to noise and its suppression with feedback system in large hadron colliders”, SSCL-Preprint-188, (1993);
https://inis.iaea.org/collection/NCLCollectionStore/_Public/26/066/26066808.pdf
2. “Accelerator Physics at the Tevatron Collider”, edited by V. Lebedev and V. Shiltsev, Springer, 2014.

Intra-Beam Scattering

- Intra-beam scattering is Coulomb scattering of particles inside the beam on each other

- Conventionally, divided in two types:
 - ◆ **Multiple scattering:** sufficiently small changes of particle momenta in one scattering act. Multiple scattering acts produce IBS transverse/longitudinal emittance growth on large time scale.
Multiple scattering can be precisely described by Fokker-Planck equation with Landau collision integral.

 - ◆ **Single scattering:** larger change of particle momenta, bringing the particles into the tails of beam distribution or outside of dynamic/physical apertures.
Touschek effect, important for evaluating beam lifetime.

- In a “properly built machine” the IBS typically represents the main source of emittance growth, both transverse and longitudinal

Interactions in Nonrelativistic Beam Gas

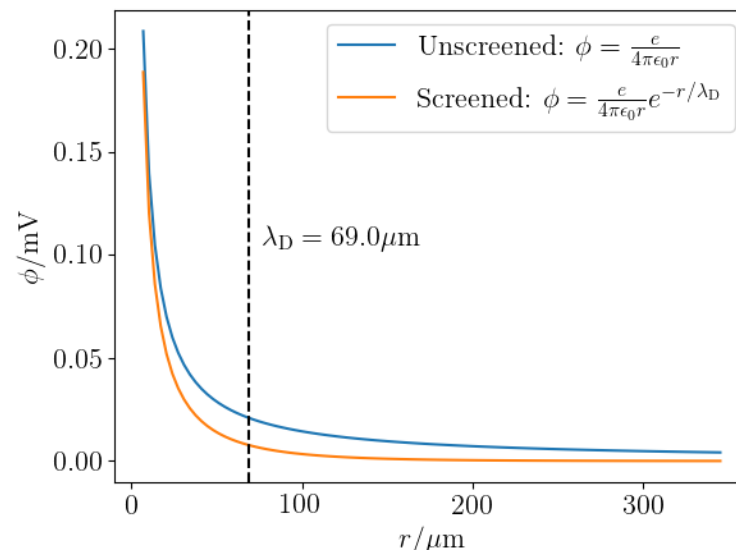
Multiple Scattering in Beam Gas (or Plasma)

- First, we consider the effect of electromagnetic (Coulomb) scattering in the beam frame (rest frame of the beam). The particle velocities are all non-relativistic, and scattering cross-section formulas are simpler, then in relativistic case.
- Each scattering act calculation involves two particles. Although, as you will see below other particles in the vicinity also play a role.
- As an example, Rutherford formula for nonrelativistic scattering of moving charge particle on unmovable charge:

$$d\sigma(\theta) = \sigma(\theta)d\Omega = \left(\frac{\alpha}{2mv^2}\right)^2 \frac{d\Omega}{\sin^4 \theta/2}.$$

- If you try to integrate to evaluate the total Rutherford cross section, the integral diverges at small scattering angle θ , which related with interaction at large distances.

- The common issue with Coulomb scattering: its cross-section diverges at larger interaction distances.
- But! Since scattering happening inside the beam the field divergence is limited by other particles screening effect (Debye length).



- Beam distribution function is governed by the Fokker-Plank equation with a collision integral in logarithmic approximation for plasma with Coulomb interaction between two particles: Landau collision integral (1936).

$$\frac{df}{dt} = -2\pi n r_0^2 c^4 L_c \frac{\partial}{\partial v_i} \int \left(f \frac{\partial f'}{\partial v'_j} - f' \frac{\partial f}{\partial v_j} \right) \frac{(\mathbf{v} - \mathbf{v}')^2 \delta_{ij} - (v_i - v'_i)(v_j - v'_j)}{|\mathbf{v} - \mathbf{v}'|^3} d^3 v'$$

- It can be re-written with friction (F) and diffusion (D) terms:

$$\frac{df}{dt} = -\frac{\partial}{\partial p_i} (F_i f) + \frac{1}{2} \frac{\partial}{\partial p_i} \left(D_{ij} \frac{\partial f}{\partial p_j} \right), \quad \begin{cases} F_i(\mathbf{v}) = -\frac{4\pi n e^4 L_c}{m} \int f(\mathbf{v}') \frac{u_i}{|\mathbf{u}|^3} d^3 v', \\ D_{ij}(\mathbf{v}) = 4\pi n e^4 L_c \int f(\mathbf{v}') \frac{u^2 \delta_{ij} - u_i u_j}{|\mathbf{u}|^3} d^3 v', \end{cases} \quad \mathbf{u} = \mathbf{v} - \mathbf{v}'$$

where

$$L_c = \ln(\rho_{\max} / \rho_{\min}), \quad \rho_{\min} = r_0 c^2 / \overline{v^2}, \quad r_0 = \frac{e^2}{mc}, \quad \int f(\mathbf{v}) d^3 v = 1$$

$$\rho_{\max} = \sqrt{\overline{v^2} / 4\pi n r_0 c^2}, \quad \overline{v^2} = \sigma_{vx}^2 + \sigma_{vy}^2 + \sigma_{vz}^2,$$

Typically, Coulomb logarithm $L_c \sim 15-20$.

Temperature Exchange in Plasma

- Consider 3 temperature Gaussian distribution

$$f = \frac{1}{(2\pi)^{3/2} \sigma_{vx} \sigma_{vy} \sigma_{vz}} \exp\left(-\frac{1}{2}\left(\frac{v_x^2}{\sigma_{vx}^2} + \frac{v_y^2}{\sigma_{vy}^2} + \frac{v_z^2}{\sigma_{vz}^2}\right)\right)$$

- Integration leads to following result for horizontal growth rate (and similar in other planes):

$$\frac{d}{dt} \frac{1}{V_x^2} = \frac{(2\pi)^{3/2} e^4 n L_c}{\sqrt{\sigma_x^2 + \sigma_y^2 + \sigma_z^2} m^2} \psi(\sigma_x, \sigma_y, \sigma_z)$$

$$\psi(\sigma_x, \sigma_y, \sigma_z) = \frac{\sqrt{\sigma_x^2 + \sigma_y^2 + \sigma_z^2}}{\sqrt{2\pi} \sigma_x \sigma_y \sigma_z} \int_0^\infty \left(\frac{\left(\frac{1}{\sigma_x^2} - \frac{1}{\sigma_y^2}\right)}{\lambda + \frac{1}{\sigma_y^2}} + \frac{\left(\frac{1}{\sigma_x^2} - \frac{1}{\sigma_z^2}\right)}{\lambda + \frac{1}{\sigma_z^2}} \right) \frac{\sqrt{\lambda} d\lambda}{\left(\lambda + \frac{1}{\sigma_x^2}\right)^{3/2} \sqrt{\lambda + \frac{1}{\sigma_y^2}} \sqrt{\lambda + \frac{1}{\sigma_z^2}}}$$

- Function $\psi(x,y,z)$ can be reduced to the sum of symmetric elliptic integrals

$$\psi(x,y,z) = \frac{\sqrt{2}r}{3\pi} \left(y^2 R_D(z^2, x^2, y^2) + z^2 R_D(x^2, y^2, z^2) - 2x^2 R_D(y^2, z^2, x^2) \right)$$

where: $R_D(x,y,z) = \frac{3}{2} \int_0^\infty \frac{dt}{\sqrt{(t+x)(t+y)(t+z)^3}}, \quad r = \sqrt{x^2 + y^2 + z^2}$

Such presentation in the form of elliptical integral is extremely useful for numerical calculations and allows for efficient numerical valuation using recursive method (B.C.Carlson) significantly reducing the computing time of the IBS growth rates (S.Nagaitsev*).

*PHYSICAL REVIEW SPECIAL TOPICS - ACCELERATORS AND BEAMS **8**, 064403 (2005)

Intrabeam Scattering in a Storage Rings

In order to translate the IBS rates from the beam frame to the laboratory frame in the case of the storage ring two major factors must be taken into account:

1. Relativistic velocity transformations between beam and laboratory frames:

$$\sigma_{vx} = \gamma\beta c \cdot \sigma_{\theta x}$$

$$\sigma_{vy} = \gamma\beta c \cdot \sigma_{\theta y}$$

$$\sigma_{vs} = \beta c \cdot \sigma_{\theta s}$$

2. Connection between horizontal and longitudinal motion in the laboratory frame.

The connection comes because of the presence of the dispersion.

For simplicity we just consider the smooth lattice approximation case.

We use constant beta-functions, dispersion for further calculations:

$$\beta_x = \frac{R_0}{v_x}, \beta_y = \frac{R_0}{v_y}, D = \frac{R_0}{v_x^2}, \alpha = \frac{1}{v_x^2}$$

■ RMS velocities and angles:

◆ Vert. plane is trivial: $\theta_y = \sqrt{\varepsilon_y / \beta_y}$, $v_y = \theta_y \beta \gamma c$

◆ Radial and horizontal planes are coupled

$$f \propto \exp\left(-\frac{1}{2}\left(\frac{(x - D\theta_s)^2}{\varepsilon_x \beta_x} + \frac{\beta_x}{\varepsilon_x} \theta_x^2 + \frac{\theta_s^2}{\sigma_p^2}\right)\right)$$

For Gaussian distribution temperatures across the beam do not depend on location. So, one can just look at the temperature at the beam center

$$f \propto \exp\left(-\frac{1}{2}\left(\left(\frac{D^2}{\varepsilon_x \beta_x} + \frac{1}{\sigma_p^2}\right)\theta_s^2 + \frac{\beta_x}{\varepsilon_x} \theta_x^2\right)\right) = \exp\left(-\frac{\theta_x^2}{2\sigma_{\theta_x}^2} - \frac{\theta_s^2}{2\sigma_{\theta_s}^2}\right)$$

where $\sigma_{\theta_x} = \sqrt{\frac{\varepsilon_x}{\beta_x}}$, $\sigma_{\theta_s} = \sqrt{\frac{\varepsilon_x \beta_x}{\varepsilon_x \beta_x + D^2 \sigma_p^2}} \sigma_p$

◆ In the beam frame: $\sigma_{vx} = \gamma \beta c \sqrt{\frac{\varepsilon_x}{\beta_x}}$, $\sigma_{vs} = \beta c \sqrt{\frac{\varepsilon_x \beta_x}{\varepsilon_x \beta_x + D^2 \sigma_p^2}} \sigma_p$

■ Thermal equilibrium in the beam frame implies

$$\sigma_{vx} = \sigma_{vs} \Rightarrow \gamma \sqrt{\frac{\epsilon_x}{\beta_x}} = \sqrt{\frac{\epsilon_x \beta_x}{\epsilon_x \beta_x + D^2 \sigma_p^2}} \sigma_p \Rightarrow \gamma^2 (\epsilon_x \beta_x + D^2 \sigma_p^2) = \beta_x^2 \sigma_p^2$$

⇒ Momentum spread in equilibrium:

$$\sigma_p = \gamma \sqrt{\frac{\epsilon_x \beta_x}{\beta_x^2 - \gamma^2 D^2}}$$

◆ Denominator equal to zero at

$$\gamma = \frac{\beta_x}{D} = \frac{v_x^2 R_0}{R_0 v_x} = \frac{1}{\sqrt{\alpha}} = \gamma_{tr}$$

i.e. at the transition energy

The thermal equilibrium impossible above transition!

- For the emittance growth rates for coasting beam in the lab frame one gets:

$$\frac{d}{dt} \begin{bmatrix} \varepsilon_x \\ \varepsilon_y \\ \sigma_p^2 \end{bmatrix} = \frac{\sqrt{\pi}}{2\sqrt{2}} \frac{e^4 N L_c}{M^2 c^3 \sigma_x \sigma_y C \beta^3 \gamma^5 \sqrt{\theta_x^2 + \theta_y^2 + \theta_p^2}} \begin{bmatrix} \beta_x \psi(\theta_x, \theta_y, \theta_p) + \gamma^2 \frac{D^2}{\beta_x} \psi(\theta_p, \theta_x, \theta_y) \\ \beta_y \psi(\theta_y, \theta_x, \theta_p) \\ 2\gamma^2 \psi(\theta_p, \theta_x, \theta_y) \end{bmatrix}$$

where

$$\sigma_x = \sqrt{\varepsilon_x \beta_x + D^2 \sigma_p^2}, \quad \sigma_y = \sqrt{\varepsilon_y \beta_y}, \quad \theta_x = \sqrt{\frac{\varepsilon_x}{\beta_x}}, \quad \theta_y = \sqrt{\frac{\varepsilon_y}{\beta_y}}, \quad \theta_p = \sqrt{\frac{\varepsilon_x \beta_x}{\varepsilon_x \beta_x + D^2 \sigma_p^2}} \frac{\sigma_p}{\gamma} \equiv \frac{\sqrt{\varepsilon_x \beta_x}}{\sigma_x} \frac{\sigma_p}{\gamma}$$

- For the bunched beam with linear RF one needs just to replace

$$\frac{1}{C} \rightarrow \frac{1}{\sqrt{2}} \frac{1}{\sqrt{2\pi}\sigma_s}$$

and $2\gamma^2 \rightarrow \gamma^2$ in the bottom row of the matrix (because the energy is equally divided between potential and kinetic energies)

For ultra relativistic beams ($\gamma \gg 1$):

- In the beam frame one can neglect the longitudinal temperature and set it to zero.
- In the laboratory the vertical emittance growth is suppressed as $(n_x/g)^2$ and is negligible in comparison to the horizontal and vertical emittance growth, (Unless there is a betatron coupling).

In the beam frame scatterings direct the energy from transverse to longitudinal direction, and in the laboratory frame this energy is distributed between the horizontal and longitudinal directions, coupled by dispersion.

A. Fedotov et al, HB2006, p. 259

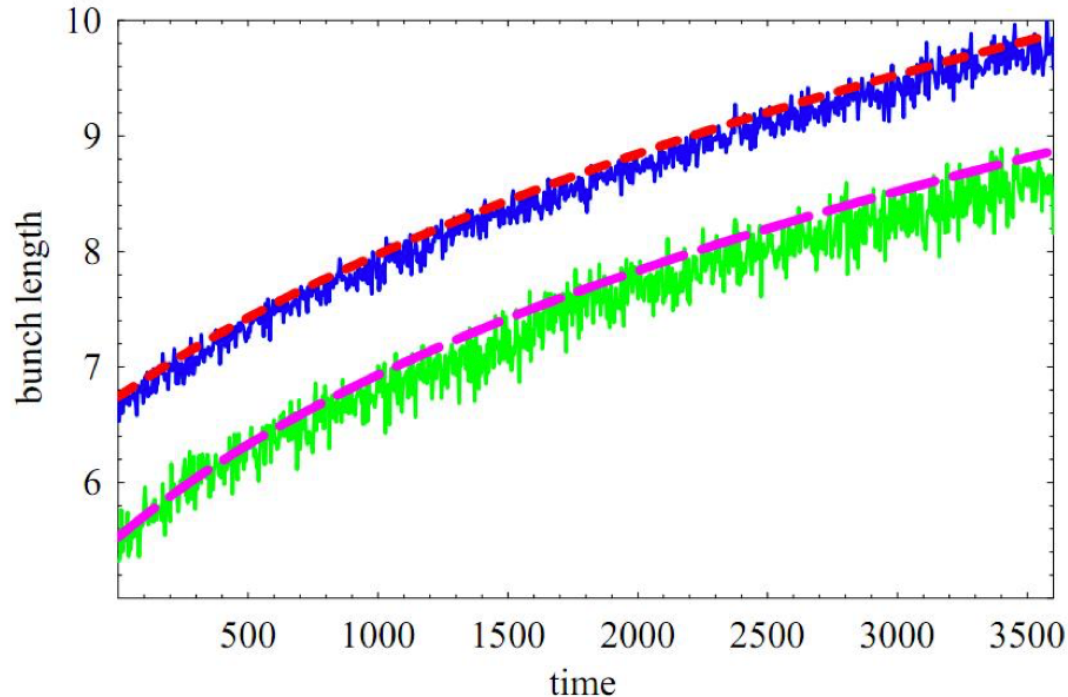


Figure 3: Growth of FWHM bunch length [ns] vs time [sec] for two bunch intensities: 2.9×10^9 (upper curve) and 1.4×10^9 (lower curve) Cu ions. Dash lines - simulations.

Lecture VP3: Luminosity Evolution Model

Vadim Ptitsyn

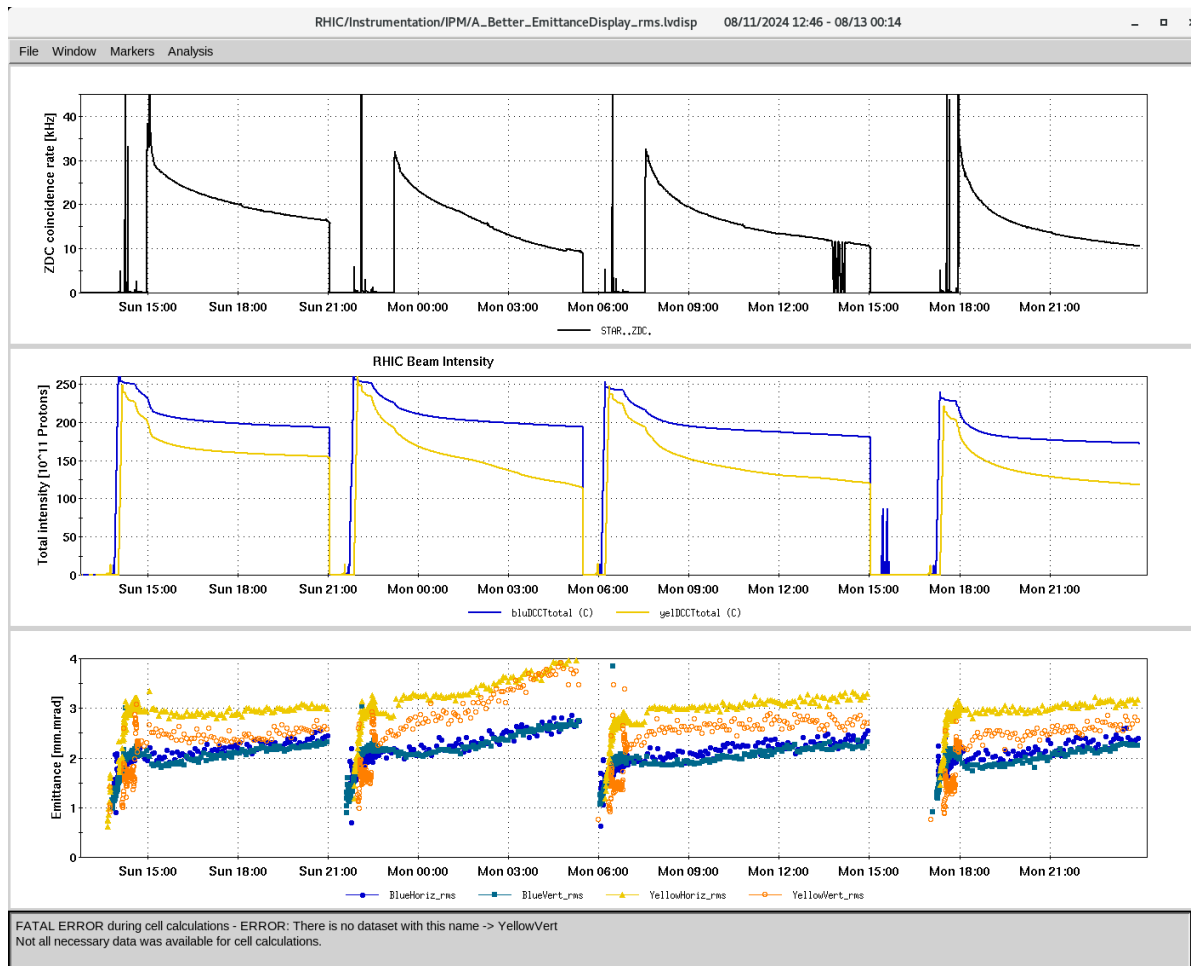
EIC Project

Brookhaven National Laboratory

USPAS, January 2025

(This lecture uses materials from V. Lebedev's USPAS 2022 lectures)

- The most important collider parameter is the integrated luminosity
 - ◆ It is determined by following major contributions
 - Uptime and downtime
 - Collider filling time
 - **Luminosity decay during the store**

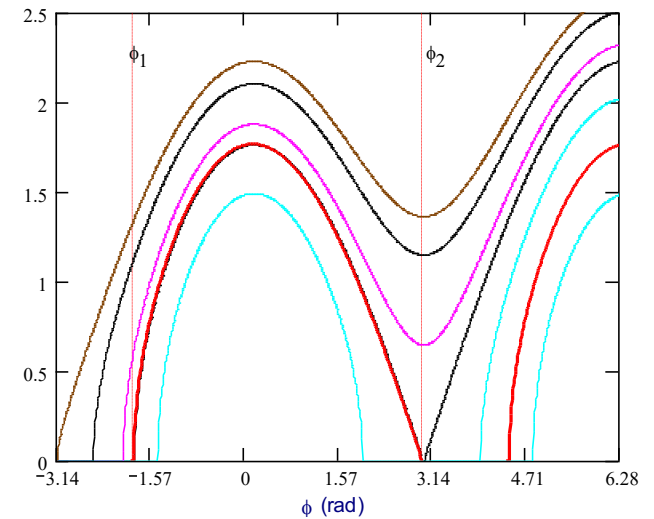


A store sequence
in RHIC in Run-24

- In this lecture we go through major effects which determine the luminosity decay time:
- Emittance growth due to different diffusion mechanisms:
 - IBS
 - multiple scattering in IP and on the residual gas,
 - different noises resulting minor beam shaking with subsequent emittance growth
- Particle loss due to:
 - scattering on residual gas,
 - Touschek effect

Longitudinal Diffusion and Particle Loss

- There are three main mechanisms creating the uncaptured beam and subsequent loss:
 - ◆ diffusion due to amplitude and phase RF noises
 - ◆ diffusion due to multiple intrabeam scattering
 - ◆ single intrabeam scattering (Touschek effect)
- At the beginning of store particles are sufficiently far from the separatrix and single scattering mechanism (Touschek) dominates losses out of the RF bucket
- With time the bunch core achieves the separatrix resulting in large acceleration of particle loss

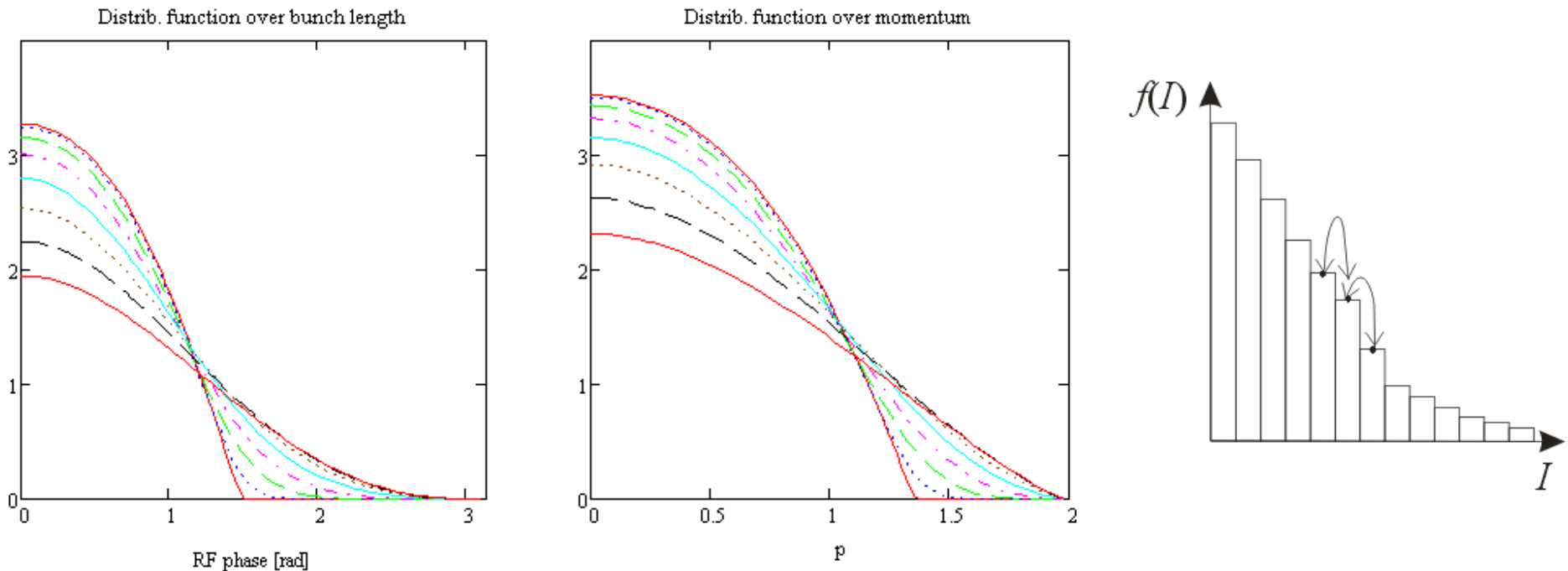


Touschek effect

- IBS scattering to large angles (in the beam frame)
- As we considered in the IBS lecture yesterday in the beam frame the velocity distribution is a pancake-like, with coldest longitudinal temperature.
- Strong scattering creates considerable longitudinal velocities in the beam frame, resulting in large $\Delta p/p$ particle change in the laboratory frame.
- As result of Touschek scattering two particles with large momentum deviation ($+\Delta p/p$) and ($-\Delta p/p$) are produced, which can go outside of the RF bucket or exceed the dynamic aperture limit of the collider ring.
- Most accelerator design code have Touschek lifetime scattering calculations included.

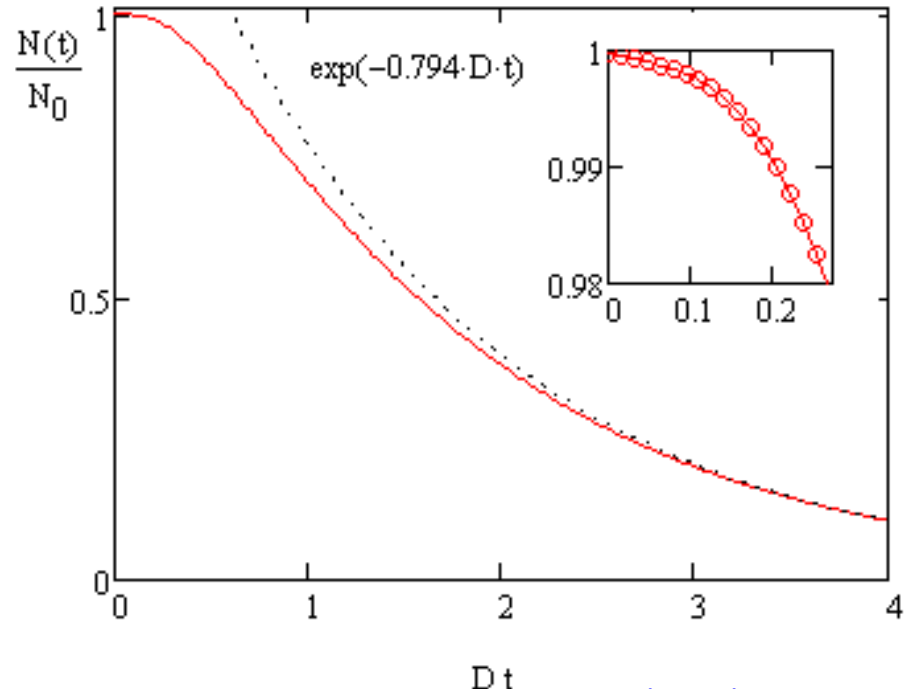
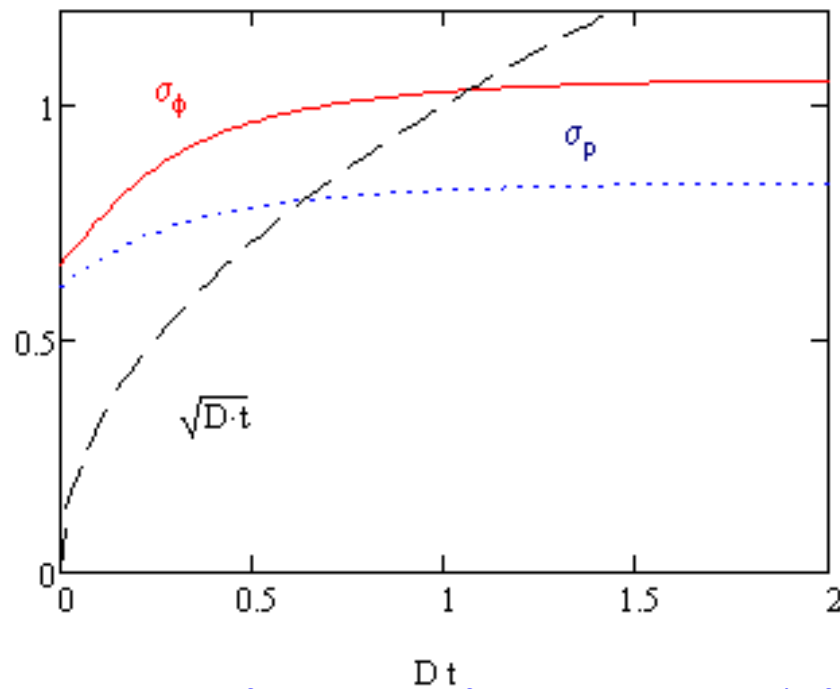
Combined single and multiple IBS

- Bunches in proton colliders take large fraction of RF bucket and standard formulas for Touschek effect become not accurate.
- Algorithm to evaluate the IBS effect without separating into single and multiple parts was developed by V. Lebedev (HB-2004 Proceedings).
- Evaluating diffusion term in FP-equation probabilities of particle transfer between different bins of longitudinal distribution function is obtained numerically, and the distribution function evolution can be followed in time.



Simulations of longitudinal distribution function for Tevatron

- Touschek scattering creates considerable beam loss at the very beginning but its overall effect is relatively small
- On larger timescale the bunch length and momentum spread are do not change but intensity exponentially decays as function of dimensionless time



Simulation of distribution function evolution: (left) rms bunch length and momentum spread, (right) relative particle number on time .

Gas Scattering

Gas scattering results may be described by three phenomena

- ◆ Particle loss due to nuclear scattering (elastic and non-elastic)

$$\tau_{scat}^{-1} \equiv \frac{1}{N} \frac{dN}{dt} = \sum_{\substack{\text{over} \\ \text{species}}} n_k \sigma_k \beta c$$

- ◆ Electromagnetic (Rutherford) scattering – above ~ 10 - 100 GeV is much smaller than nuclear scattering

$$\tau_{scat}^{-1} = \frac{2\pi c r_p^2}{\gamma^2 \beta^3} \left(\sum_i Z_i (Z_i + 1) \left(\frac{\overline{\beta_x n_i}}{\epsilon_{mx}} + \frac{\overline{\beta_y n_i}}{\epsilon_{my}} \right) \right) + \sum_i n_i \sigma_i c \beta$$

- ◆ Emittance growth due to multiple scattering

$$\frac{d\epsilon_{x,y}}{dt} = \frac{2\pi c r_p^2}{\gamma^2 \beta^3} \left(\sum_i \overline{\beta_{x,y} n_i} Z_i (Z_i + 1) L_c \right)$$

Burn-off in the IP

- Burn-off accounts for particle losses happening from collisions in the interaction point(s). The burn-off is defined by total cross section of all processes happening in the collisions:

$$\frac{dN}{dt} = L \sum_{\substack{\text{over} \\ \text{processes}}} \sigma_k$$

- Tevatron total loss cross-section is ~68 mbarn.
- RHIC 100 GeV Au beam total collision cross-section: 218 barns.

1 barn = 10^{-24} cm²

Burn-off plays considerable role in beam intensity losses in heavy ion collisions, which have very large cross-section.

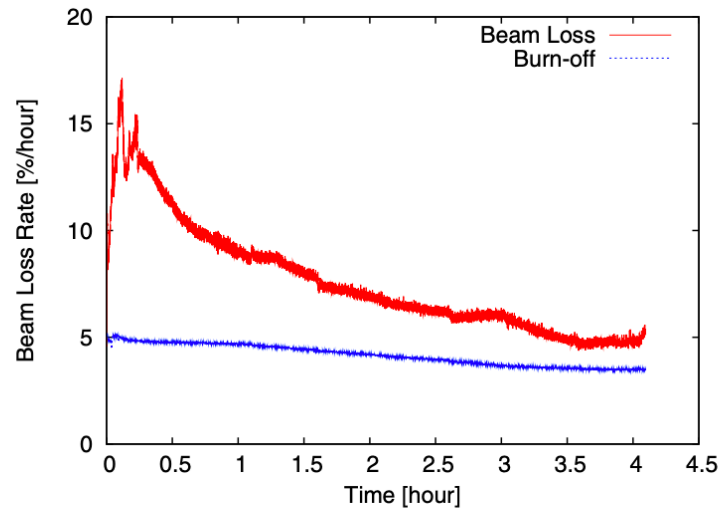


FIG. 2. One example of nonluminous beam loss of the Au beam with longitudinal and vertical cooling in the Yellow ring in the 2011 100 GeV Au-Au run.

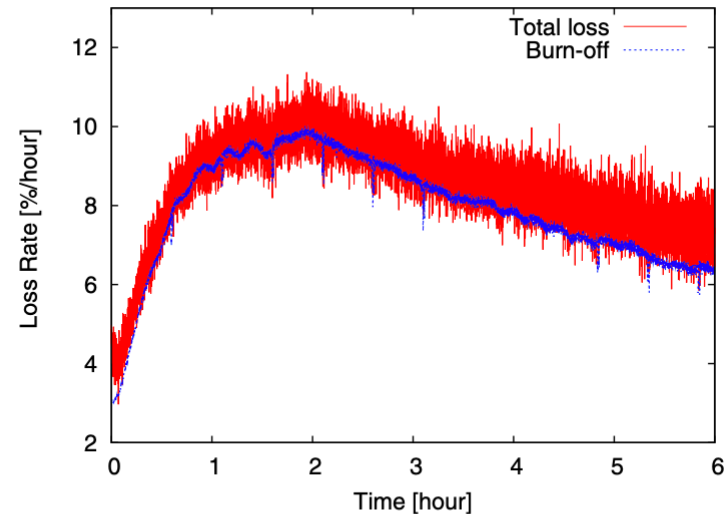


FIG. 10. The beam loss rate and burn-off contribution with 3-d cooling in the 2012 RHIC 96.4 GeV U-U run. Almost all beam loss was from burn-off.

Y. LUO et al. Phys. Rev. ST Accel. Beams 17, 081003 (2014)

Luminosity Evolution Model

$$L = \frac{f_0 n_b N_p N_a}{2\pi\beta^* \sqrt{(\varepsilon_{px} + \varepsilon_{ax})(\varepsilon_{py} + \varepsilon_{ay})}} H\left(\frac{\sqrt{\sigma_{sp}^2 + \sigma_{sp}^2}}{\sqrt{2}\beta^*}\right)$$

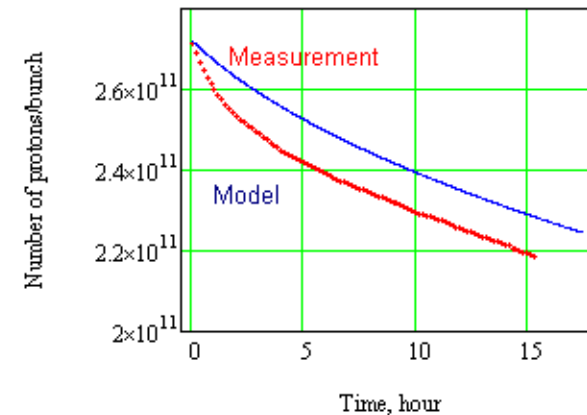
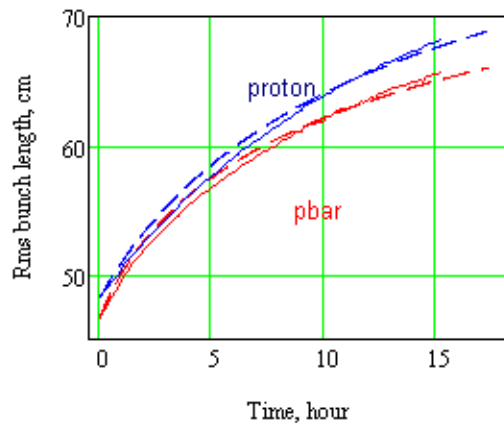
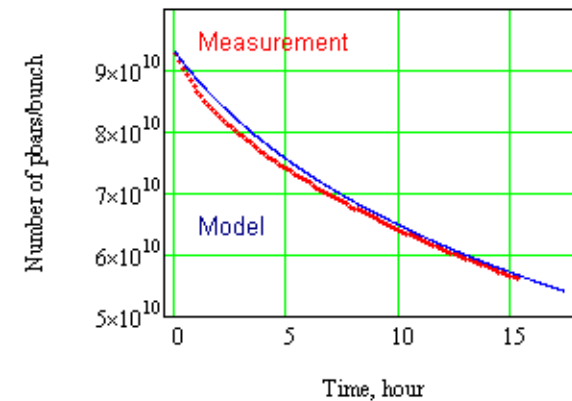
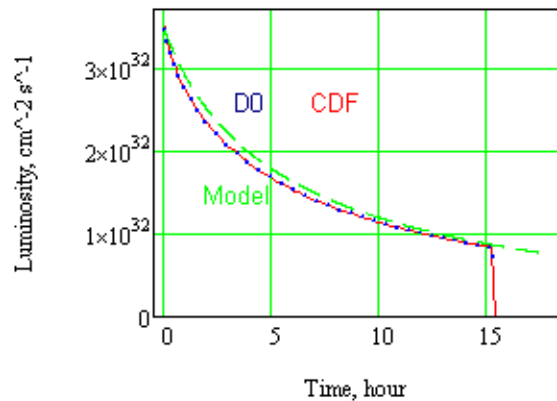
Hourglass effect

$$H(x) = \frac{2}{\sqrt{\pi}} \int_0^{\infty} \frac{e^{-y^2}}{1+x^2y^2} dy \xrightarrow{x \leq 3} \approx \frac{1}{\sqrt[3]{1+1.3x^2}}$$

The luminosity model calculates the time evolution of all beam parameters which contribute to the luminosity, and then the time evolution of the luminosity itself.

$$\frac{d}{dt} \begin{bmatrix} \varepsilon_{px} \\ \varepsilon_{py} \\ \sigma_{pp}^2 \\ N_p \\ \varepsilon_{ax} \\ \varepsilon_{ay} \\ \sigma_{pa}^2 \\ N_a \end{bmatrix} = \begin{bmatrix} 2 d\varepsilon_{px}/dt|_{BB} + d\varepsilon_{px}/dt|_{IBS} + d\varepsilon_{px}/dt|_{gas} \\ 2 d\varepsilon_{py}/dt|_{BB} + d\varepsilon_{py}/dt|_{IBS} + d\varepsilon_{py}/dt|_{gas} \\ d\sigma_{pp}^2/dt|_{total} \\ -N_p \tau_{scat}^{-1} - dN_p/dt|_L - 2L\sigma_{p\bar{p}}/n_b \\ 2 d\varepsilon_{ax}/dt|_{BB} + d\varepsilon_{ax}/dt|_{IBS} + d\varepsilon_{ax}/dt|_{gas} \\ 2 d\varepsilon_{ay}/dt|_{BB} + d\varepsilon_{ay}/dt|_{IBS} + d\varepsilon_{ay}/dt|_{gas} \\ d\sigma_{pa}^2/dt|_{total} \\ -N_a \tau_{scat}^{-1} - dN_a/dt|_L - 2L\sigma_{p\bar{p}}/n_b \end{bmatrix}$$

Luminosity Evolution for Tevatron Store 6950



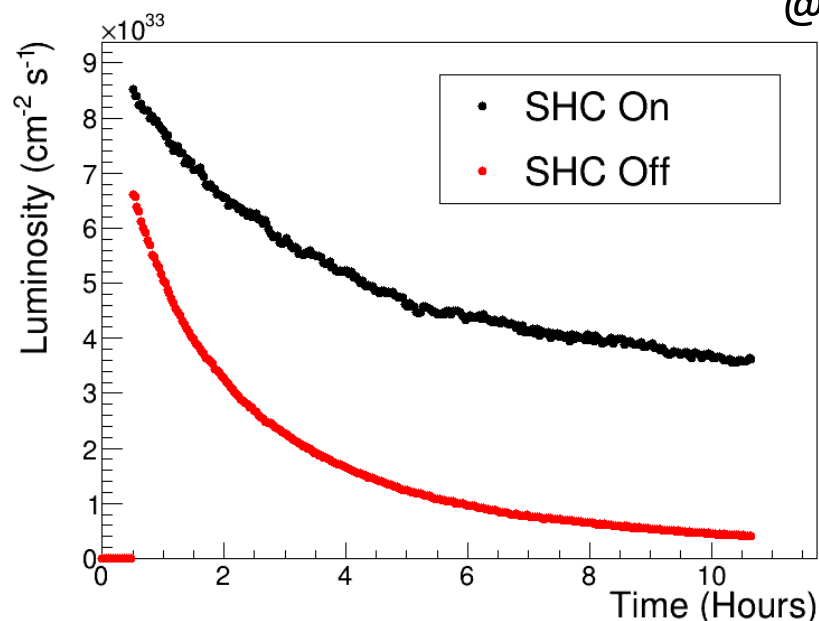
$\tau_{\text{gas}}=530$ hour, $\tau_{\text{Lum}}=4.9$ hour, $\kappa_{\text{beam-beam}}=1.3$, $\kappa_{xy}=0.95$, 38% of pbars burned in luminosity

- Clearly seen excessive beam loss in proton beam

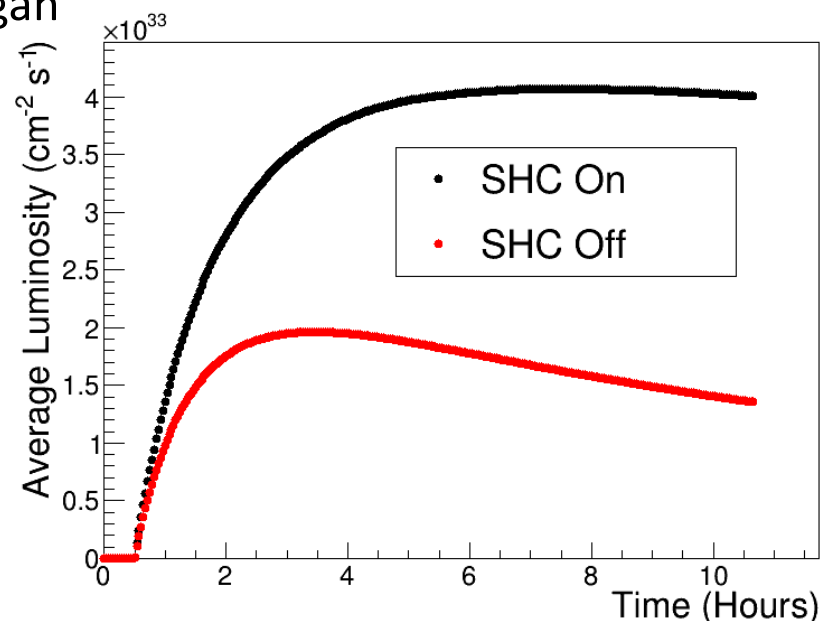
- Antiproton beam sizes are smaller than proton ones. Therefore, the proton beam is more susceptible to the beam-beam effects.

Luminosity Evolution in EIC (model)

@W.Bergan



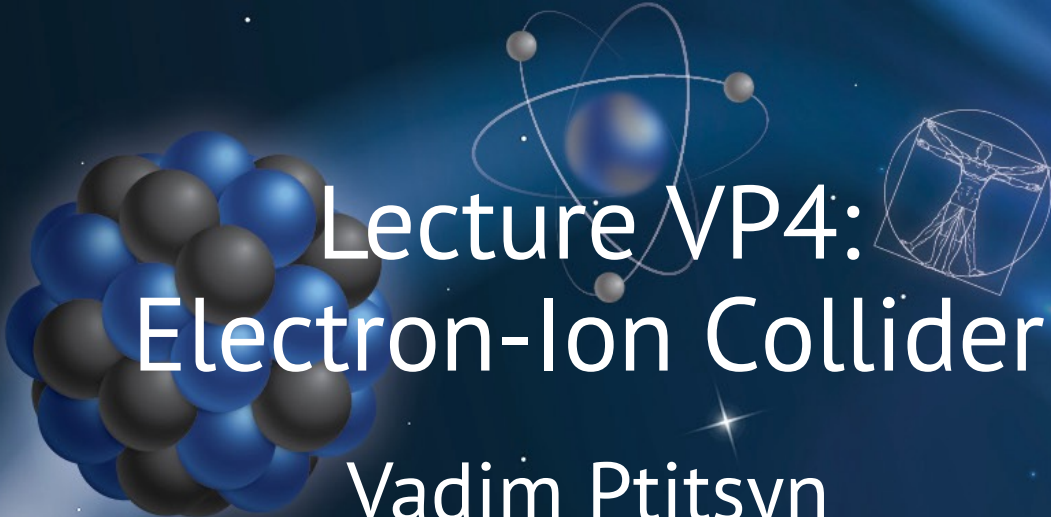
The luminosity evolution in the EIC store with and without Strong Hadron Cooling



The average luminosity vs store length for EIC stores with and without Strong Hadron Cooling

This model includes also beam-beam induced emittance growth, although the dominating effect still IBS.

Thank you for your attention!



Lecture VP4: Electron-Ion Collider

Vadim Ptitsyn
EIC Project
BNL

USPAS, January 2025

Electron-Ion Collider

BROOKHAVEN
NATIONAL LABORATORY

Jefferson Lab

 U.S. DEPARTMENT OF
ENERGY | Office of
Science

Lecture Outline

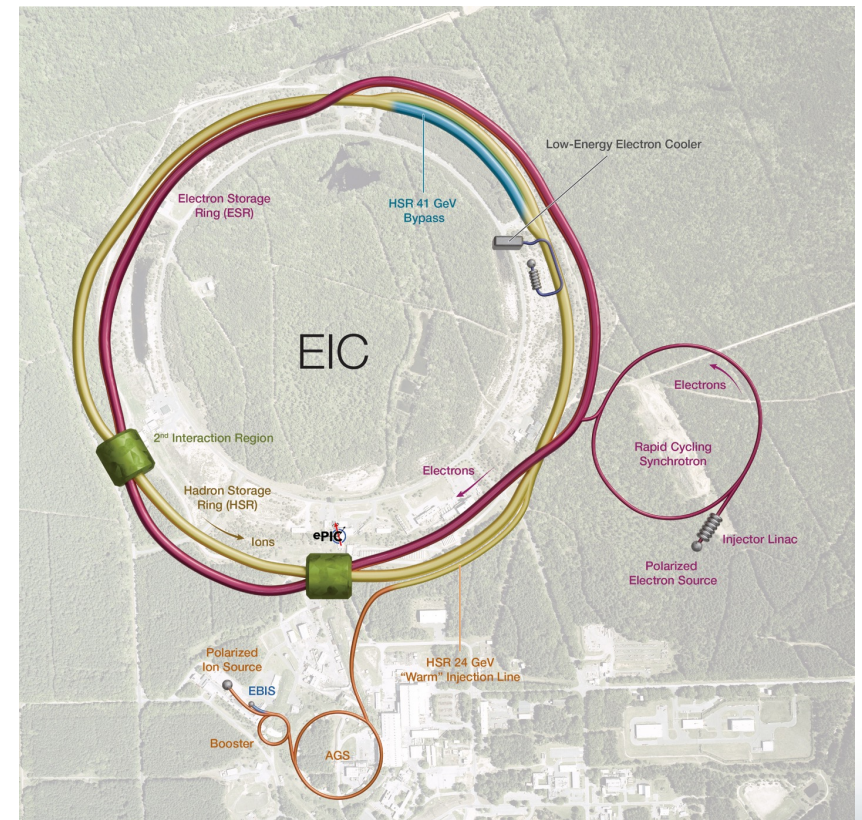
- Overview
 - Electron-Ion Collider at BNL
 - Luminosity
- Major Accelerator Physics/Design Topics
 - Interaction Region
 - Hadron Emittance and Hadron Cooling
 - Beam-Beam Interactions
 - High Beam Intensity
 - Dynamic Aperture
 - Beam Polarization
- Summary

Electron-Ion Collider at BNL

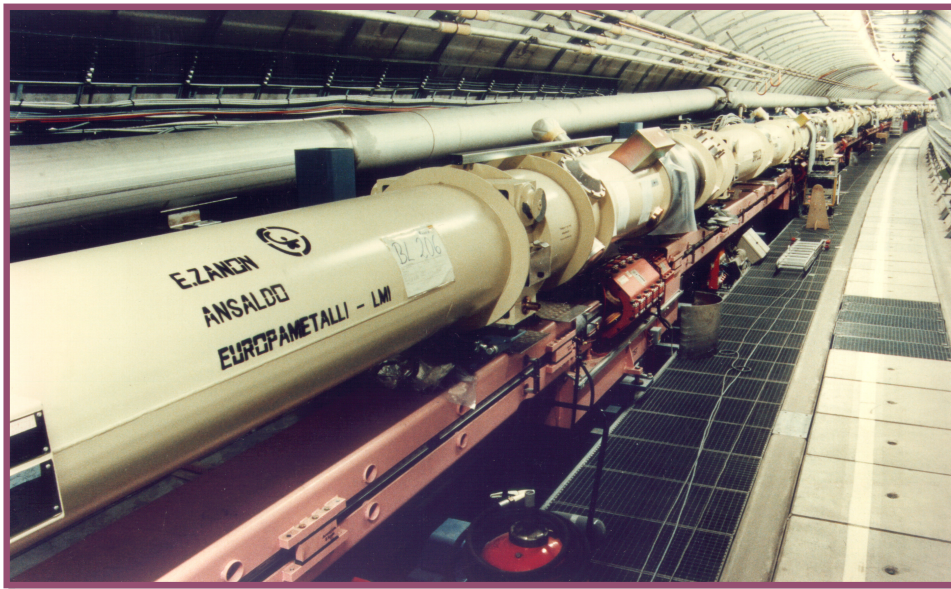
Requirements outlined in the White Paper:

- High Luminosity: $L=(0.1-1)\cdot 10^{34}\text{cm}^{-2}\text{sec}^{-1}$, need 10 -100 fb^{-1}
- Collisions of highly polarized e and p (& light ion) beams with flexible bunch by bunch spin patterns : 70%
- Large range of center of mass energies: $E_{\text{cm}} = (20-140) \text{ GeV}$
- Large range of Ion Species: Protons – Uranium
- Ensure Accommodation of a second IR
- Large detector acceptance
- Good background conditions (hadron particle loss and synchrotron radiation in the IR)

EIC is designed and constructed in full partnership between BNL and TJNAF



HERA – first lepton-proton collider



Double ring collider (6.3 km)

920 GeV (p) X 27.5 GeV (e^- , e^+)

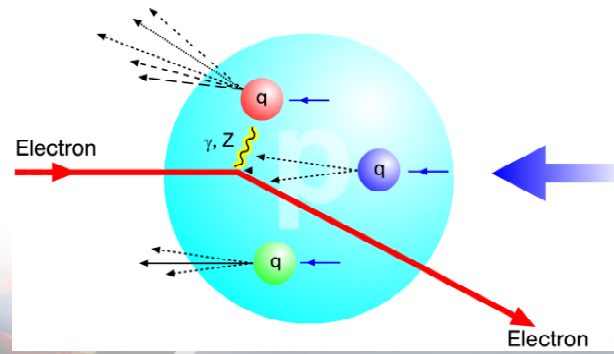
320 GeV center-of-mass energy

Longitudinal lepton polarization

Superconducting proton ring

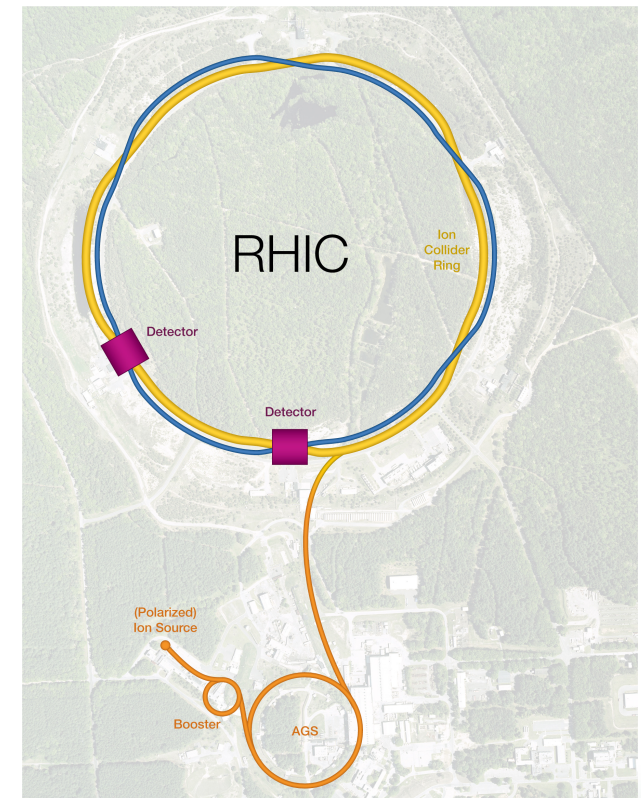
Operation: 1992 - 2007

Luminosity: $7.5 \cdot 10^{31} \text{ cm}^{-2} \text{ s}^{-1}$

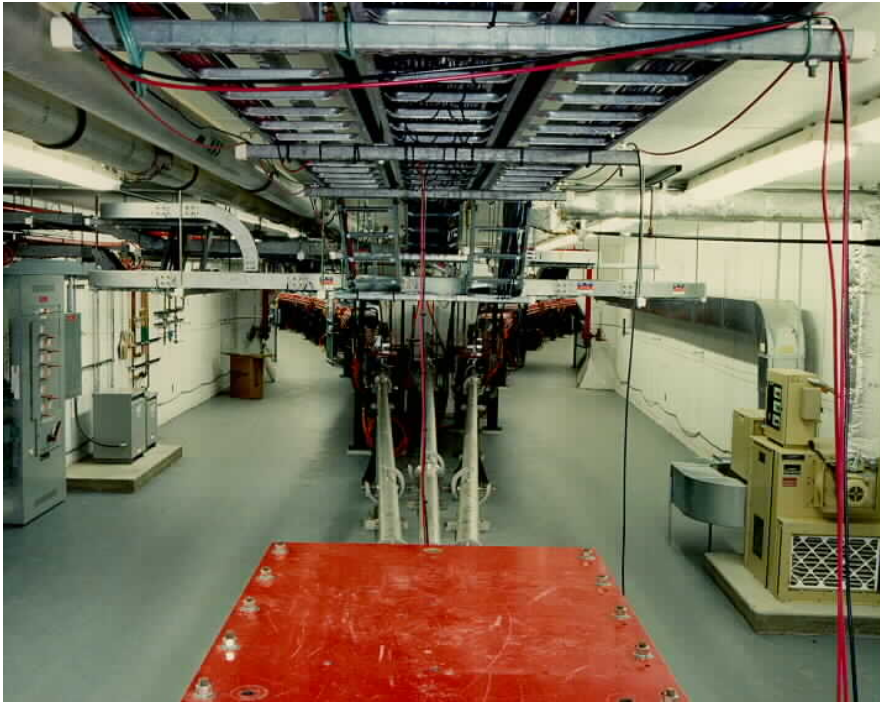


Relativistic Heavy Ion Collider (RHIC)

- Existing tunnel and infrastructure
- Two SC storage rings
 - 3.8km circumference
- Energy up to 255 GeV protons, or 100 GeV/n gold
- 110 bunches/beam
- Ion species from protons to uranium
- 60% proton polarization – world's only polarized proton collider
- Exceeded design luminosity by a factor of 44
- 6 interaction regions, 2 detectors
- In operation since 2001; operations will end in 2025



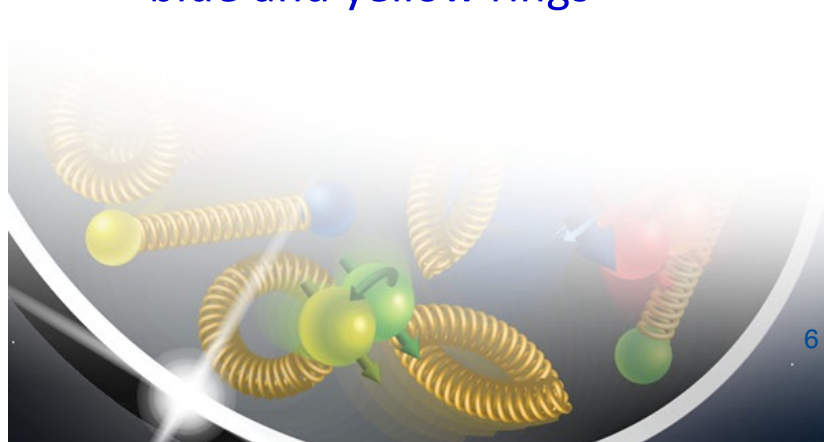
Inside RHIC



Injection arcs to
blue and yellow rings



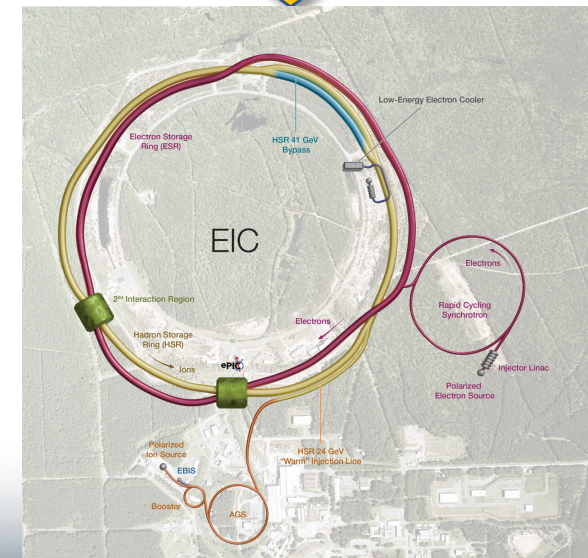
Blue and yellow rings



EIC Collider Concept

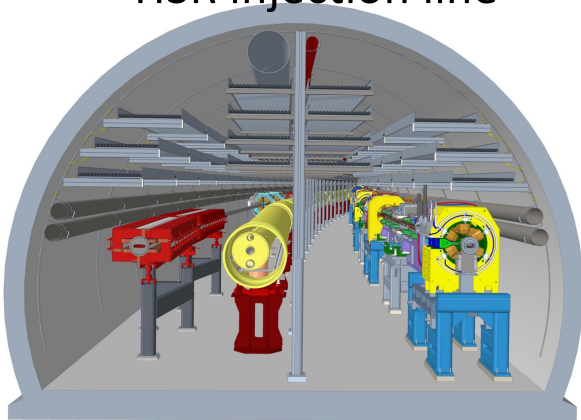
Design based on **existing** RHIC, RHIC is well maintained, operating at its peak

- **Hadron storage ring 40-275 GeV (existing)**
 - Many bunches
 - Bright beam emittance
 - Need strong cooling **or** frequent injections
- **Electron storage ring (2.5–18 GeV (new))**
 - Many bunches,
 - Large beam current (2.5 A) → 10 MW S.R. power
- **Electron rapid cycling synchrotron (new)**
 - 1 Hz repetition rate
 - Spin transparent due to high periodicity
- **High luminosity interaction region(s) (new)**
 - $L = 10^{34} \text{cm}^{-2}\text{s}^{-1}$
 - Superconducting magnets
 - 25 mrad Crossing angle with crab cavities
 - Spin Rotators (longitudinal spin)
 - Forward hadron instrumentation

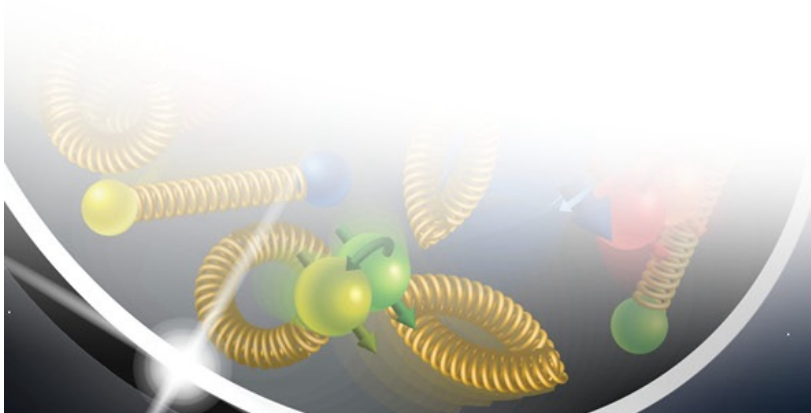
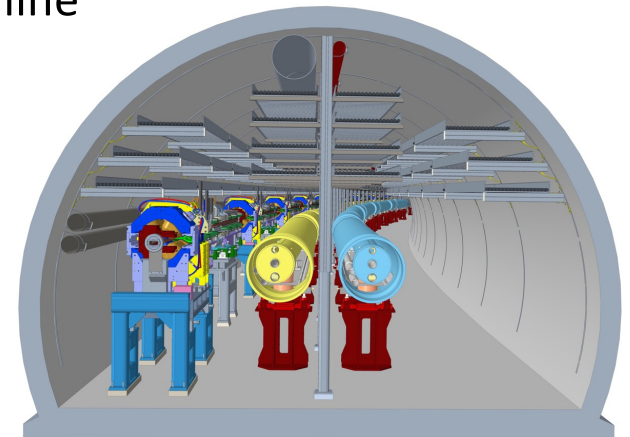
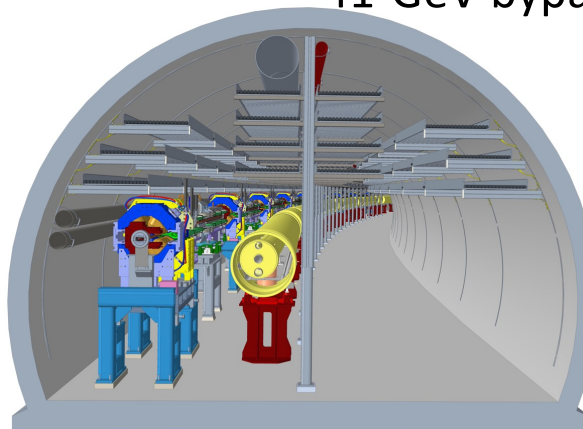


EIC magnets in tunnel in Sectors 1 and 5

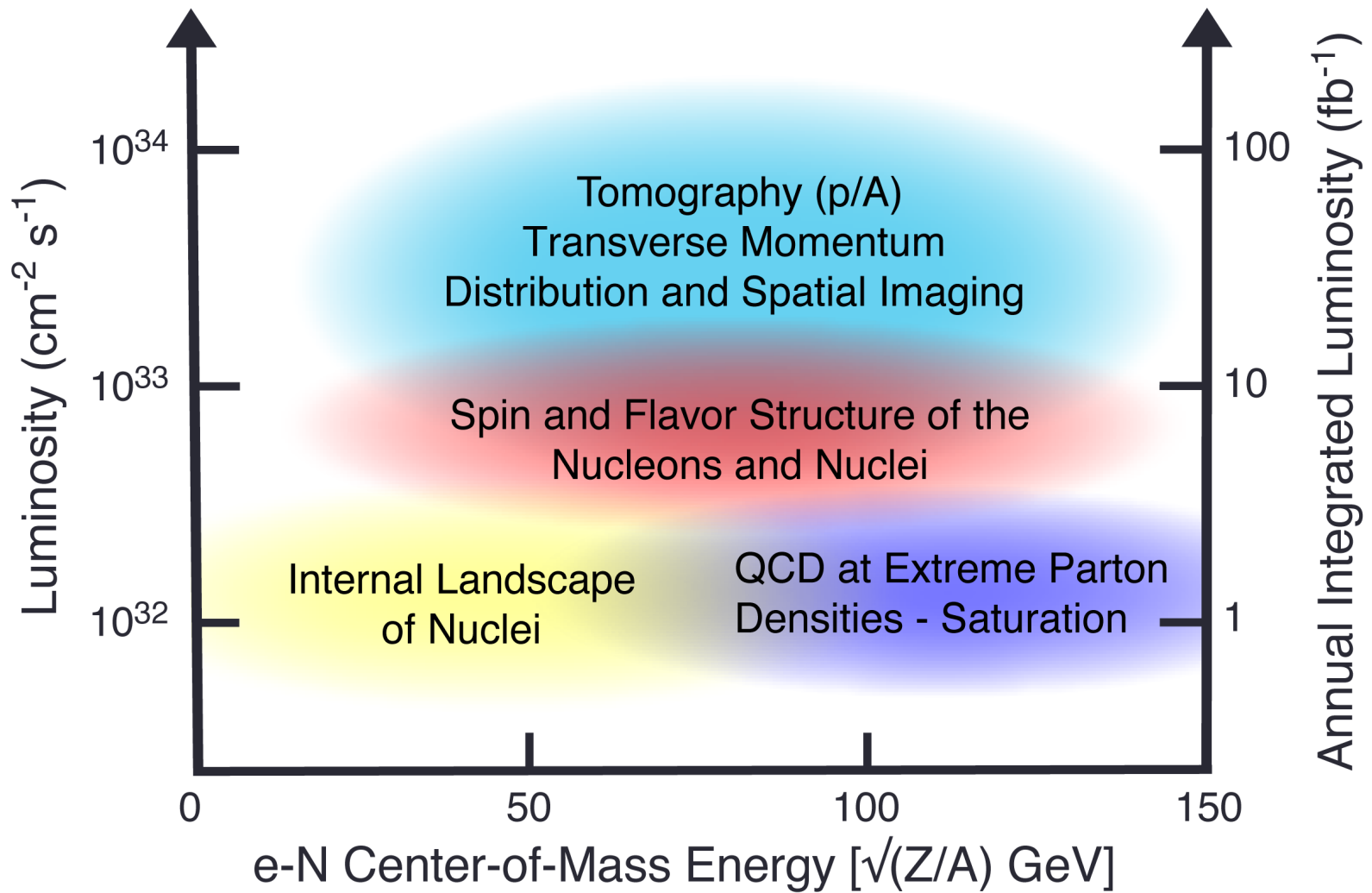
Sector 5 with a new HSR injection line



Sector 1 without and with the 41-GeV bypass line

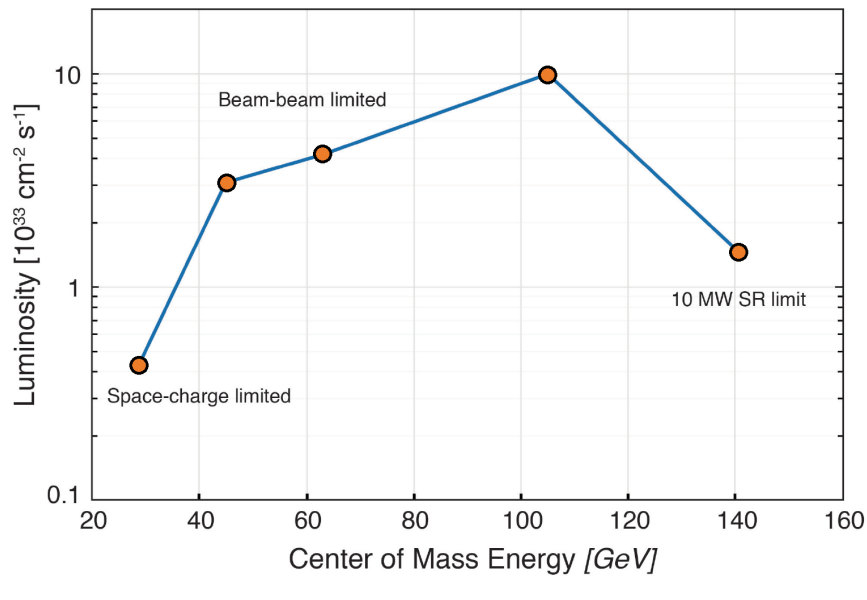


EIC Physics



EIC Luminosity

Optimization yields $10^{34} \text{ cm}^{-2} \text{ sec}^{-1}$ luminosity at 105 COM GeV (275 GeV p x 10 GeV e)



$$L = f_b \frac{\pi \gamma_e \gamma_h}{r_{0e} r_{0h}} \cdot (\xi_h \sigma'_h) \cdot (\xi_e \sigma'_e) \frac{(1 + K)^2}{K} \cdot H,$$

$K = \sigma_y / \sigma_x$, H -hourglass and crab-crossing factor

ξ is beam-beam parameter

σ' is beam angular spread in the IP

High luminosity ingredients:

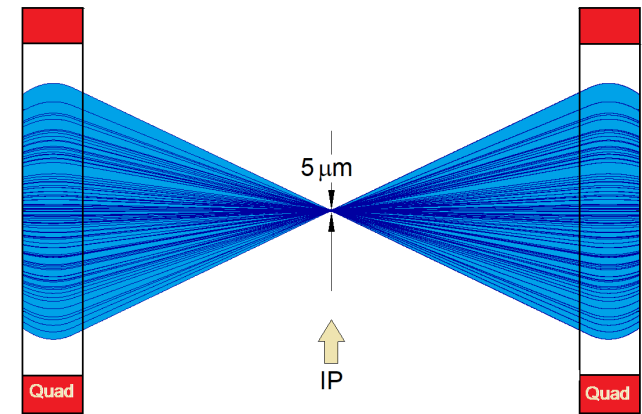
- high beam-beam parameters
- flat beams at the IP
- high number of bunches
(at fixed optimized single bunch collision parameters)

$$E_{COM} \approx 2\sqrt{E_e E_h}$$

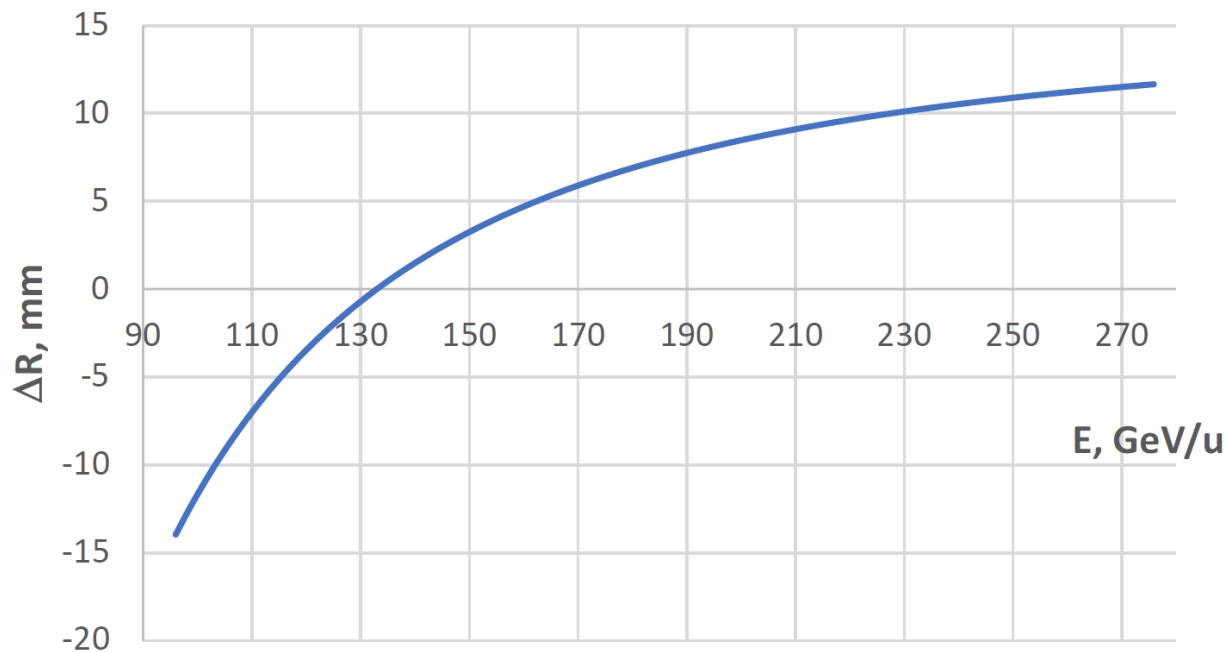
EIC achieves high luminosity $L = 10^{34} \text{ cm}^{-2}\text{s}^{-1}$

- **Large bunch charges** $N_e \leq 1.7 \cdot 10^{11}$, $N_p \leq 0.69 \cdot 10^{11}$
- **Many bunches**, $n_b=1160$ (vs 110 in RHIC)
 - crossing angle collision geometry
 - large total beam currents (x3 RHIC)
 - limited by installed RF power of **10 MW**
- **Small beam size** at collision point achieved by
 - small emittance, requiring either:
 - strong hadron cooling to prevent emittance growth **or**
 - frequent hadron injection
 - and strong focusing at interaction point (small β_y)
 - flat beams $\sigma_x/\sigma_y \approx 11$
- **Strong, but previously demonstrated beam-beam interaction**
 - $\xi_p = 0.015$ demonstrated in RHIC
 - $\xi_e = 0.1$ demonstrated in B-factories

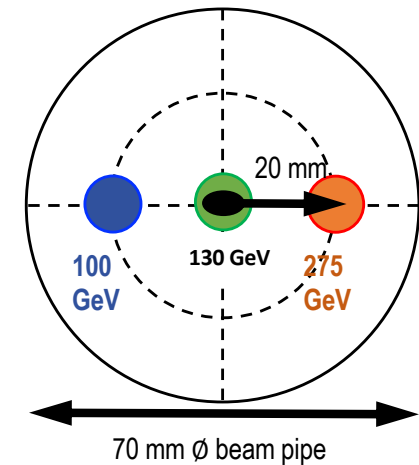
Strong focusing $\beta_y = 5 \text{ cm}$



Hadron Beam Energy and Average Orbit Radius in the HSR



Average radius of the horizontal orbit depends on the operation energy.



Since the electron revolution frequency is fixed, the hadron orbit must be adjusted with energy to keep the collisions in sync.

Beam Parameters at $E_{\text{cm}} = 105 \text{ GeV}$

	Electrons	Protons
Beam energies	10 GeV	275 GeV
Center of mass energy	$E_{\text{cm}} = 20\text{-}140 \text{ GeV}$	
Number of bunches	1160	
Crossing angle	25 mrad	
Bunch intensity	$1.7 \cdot 10^{11}$	$0.7 \cdot 10^{11}$
Total beam current	2.5 A	1 A
Beam emittance, horizontal	20 nm	11 nm
Beam emittance, vertical	1.3 nm	1 nm
β^* function at IP, horizontal	45	80
β^* function at IP, vertical	5.5	7
Beam-beam tunes shift, horizontal	0.07	0.012
Beam-beam tunes shift, vertical	0.1	0.012
Luminosity	$1 \cdot 10^{34} \text{ cm}^{-2} \text{ s}^{-1}$	

!

!

$K = 0.09$!

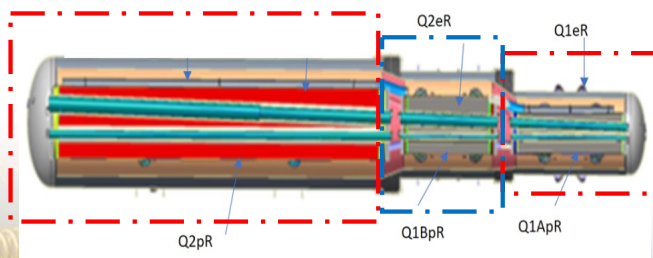
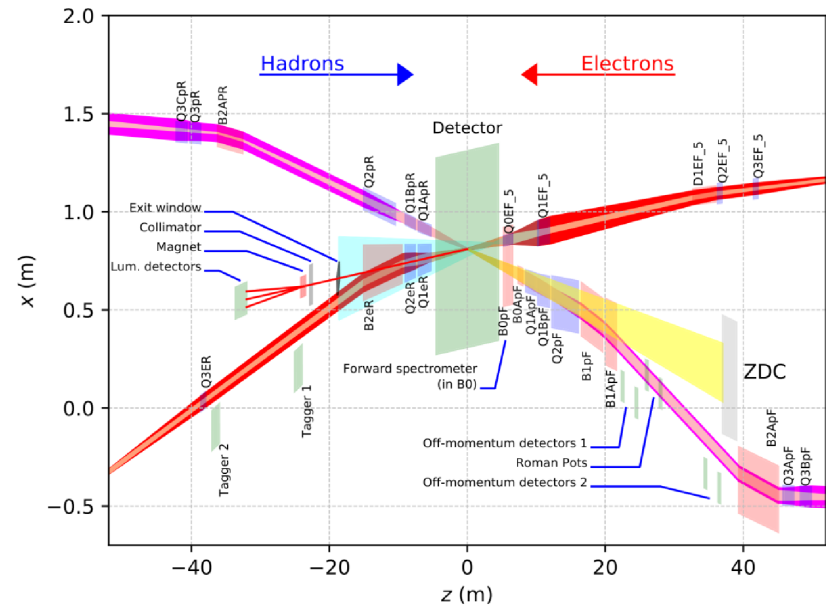
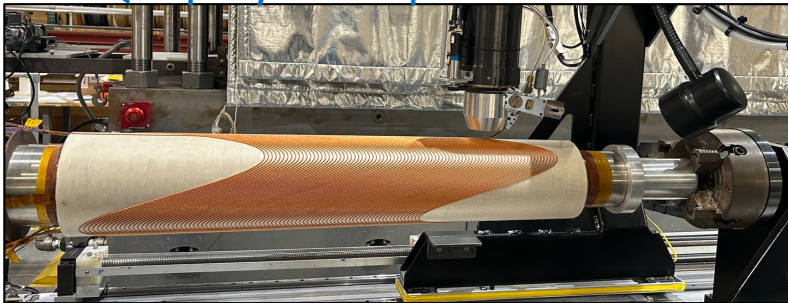
!

!

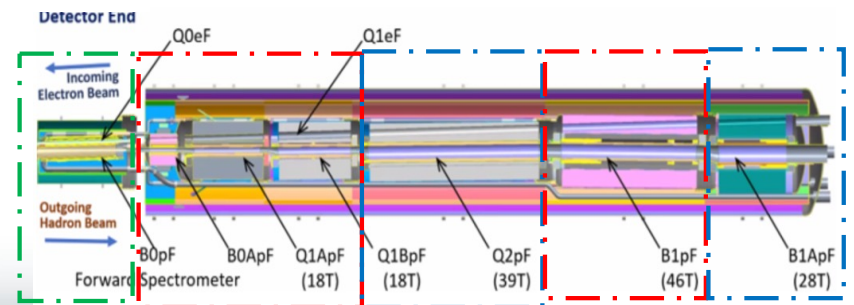
Interaction Region

- 25 mrad crossing angle
- Large aperture superconducting IR magnets
- Spin rotators: strong solenoids for e, helical magnets for p
- Large acceptance for forward scattered hadrons

Q1ABpF layer 10 completed at B-902

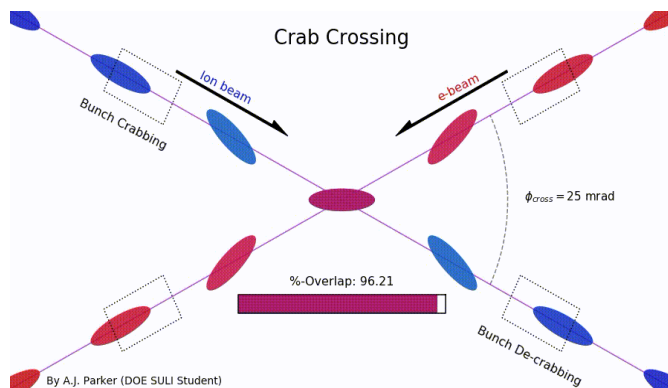


Detector Here



Crab-crossing

Crab-crossing scheme (local)



Crab cavities → quasi head on collisions

For hadrons:

Second harmonic cavity to minimize synchro-betatron resonances.

Not fully local. 175° phase advance between cavities on left and right sides of the IP.



197 MHz crab-cavity

Crab-crossing (2)

Crab-cavity produce transverse kick which varies along the bunch:

- The head of the bunch is kicked in one direction
- The center of the bunch is not affected by the cavity
- The tail of the bunch is kicked in the opposite direction

Crab-cavity kick along position z in the bunch :

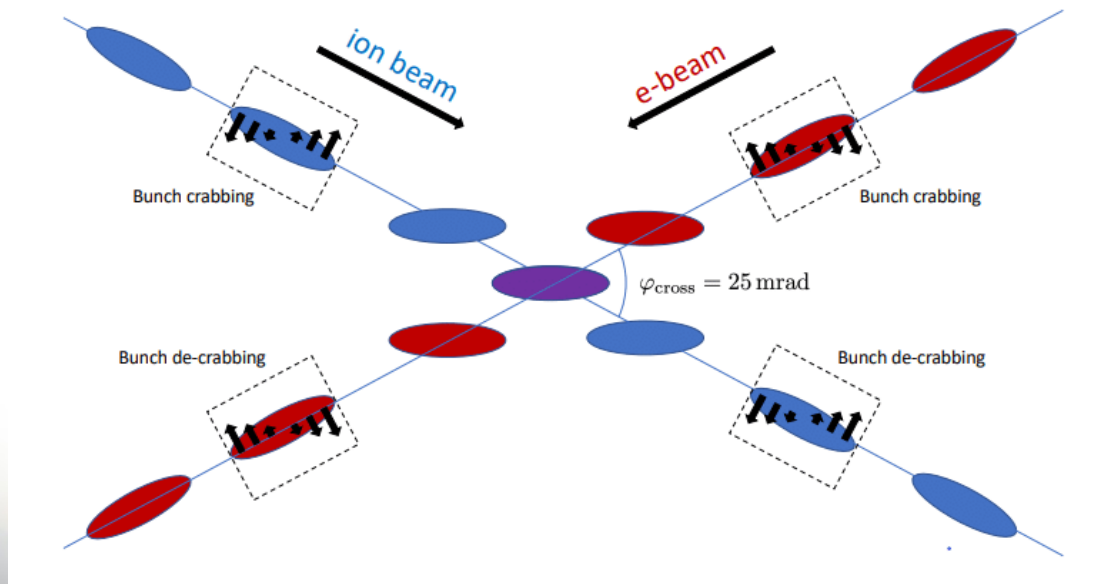
$$\theta_{cc}(z) = r \cdot \sin kz$$

where

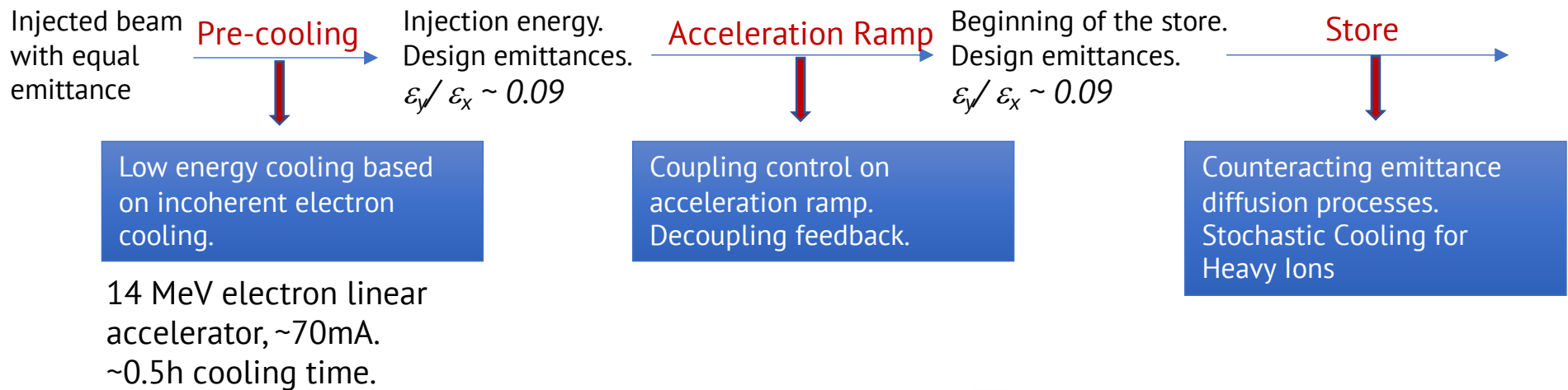
$$k = \frac{2\pi}{\lambda} \text{ and } \lambda = c/f_{RF}$$

Bunch head and tail oscillation propagate downstream forming at the IP 12.5 mrad angle between the bunch axis and the longitudinal direction.

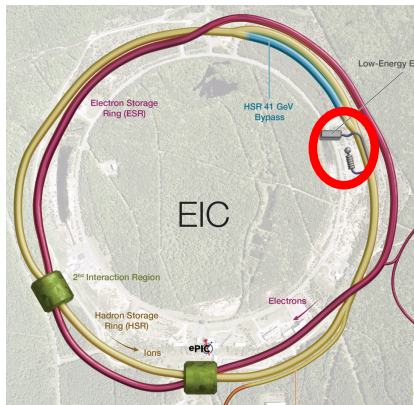
Another crab-cavity on the opposite side of the IR cancel the head and tail orbit distortion with another crab kick.



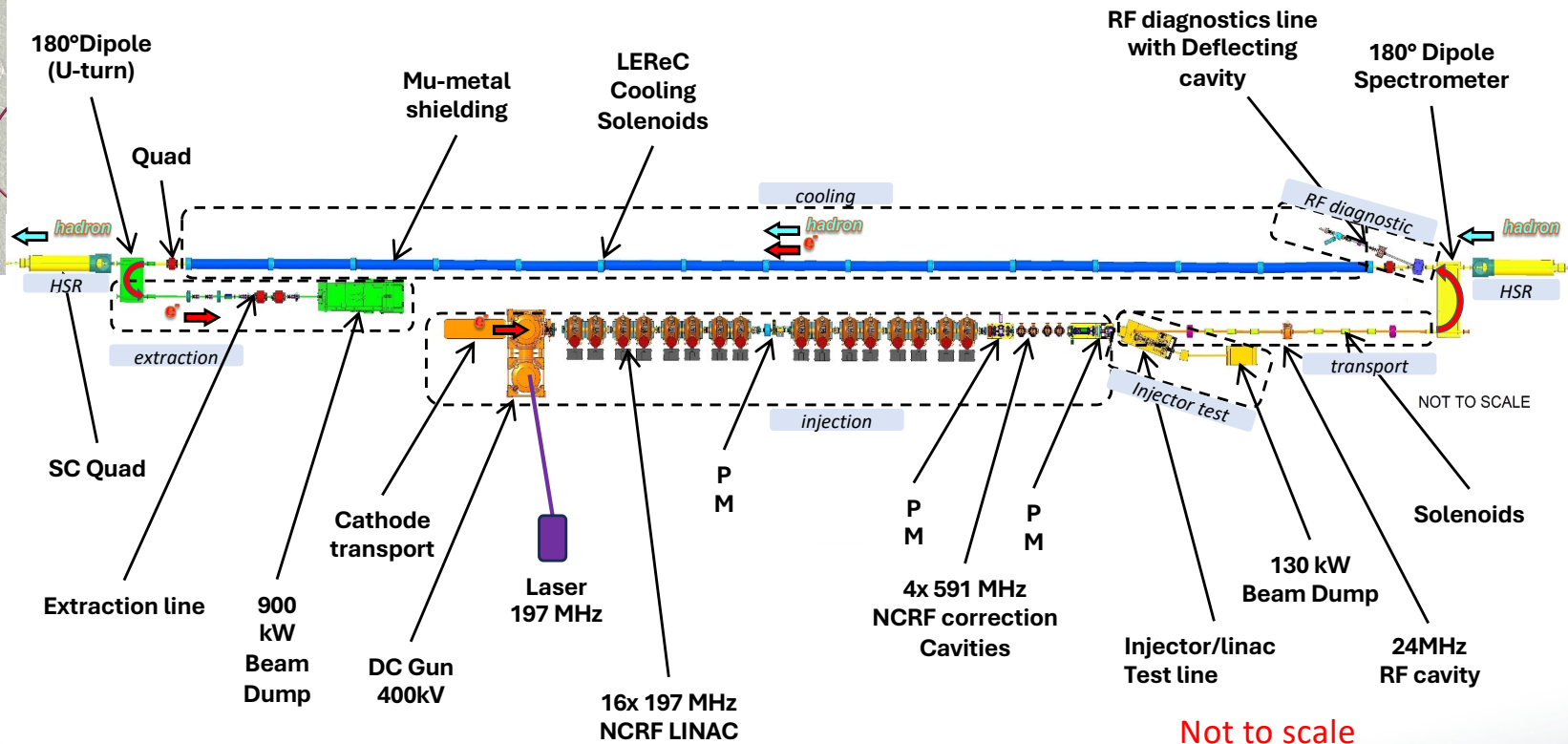
HSR emittance formation



'Flat' Proton Bunches are produced by the Low Energy Cooler



12.5 MeV electron accelerator

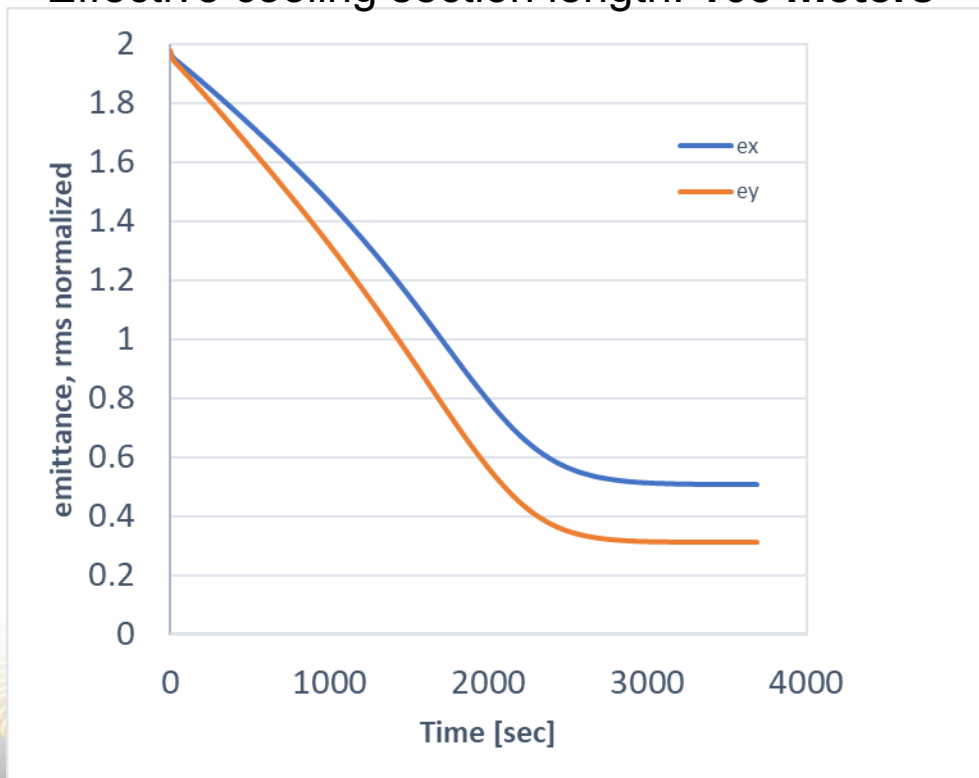


Cooling emittances by the Low Energy Cooler

Average current of electrons: $I_{av}=74\text{mA}$

Electrons rms angles in the cooling section: **25 urad**

Effective cooling section length: **168 meters**



Horizontal emittance needs to be increased after cooling by the emittance dilution to produce 10:1 emittance ratio.

Flat beams

- Emittance ratio of 11:1 is required for reaching design luminosity with equal proton beam divergencies at the IP.
- Required emittances are formed at 24 GeV with by using the Injection cooler.
- The HSR will reuse the RHIC decoupling system, adding new skew-quadrupoles in the IR6 area to help with the detector solenoid compensation.
- On the HSR acceleration ramp, the coupling feedback will be used, a routine operation tool used to maintain good decoupling on RHIC ramps.

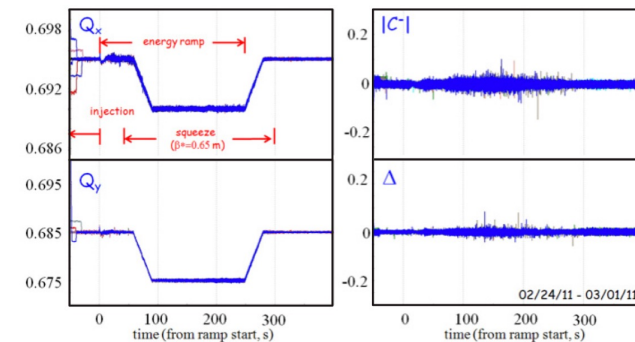
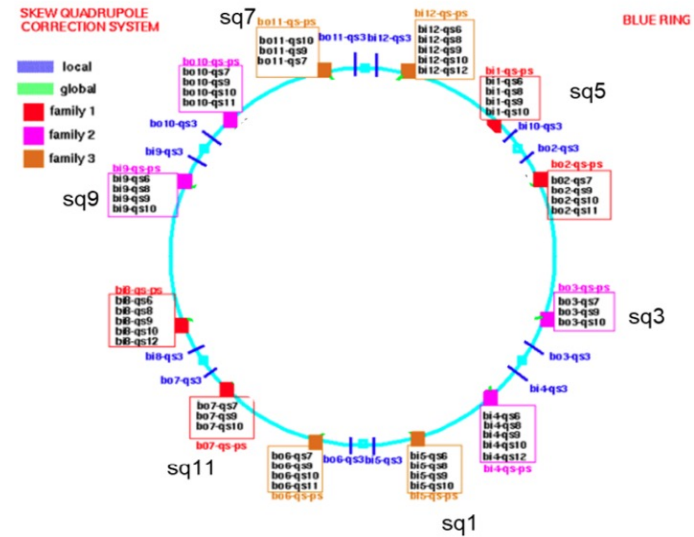
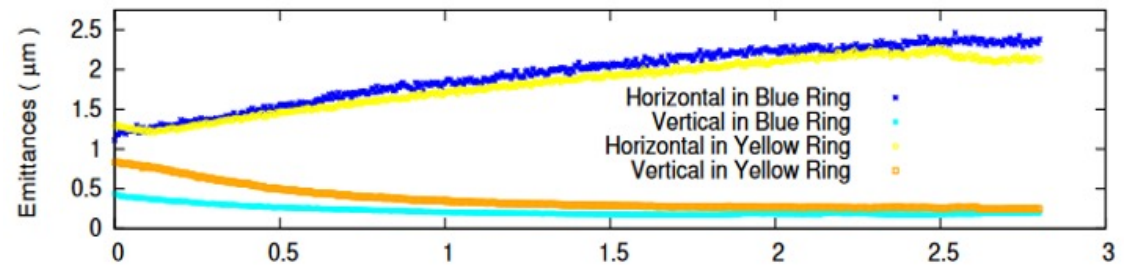
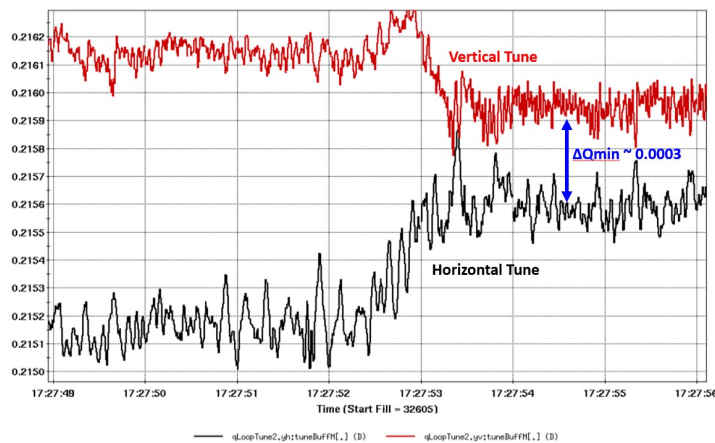


Figure 3: Superposition of measurements from multiple ramps of the betatron tunes (left) and coupling (right) measured with tune/coupling feedback in run-11.

Experiments to Demonstrate Flat Beams

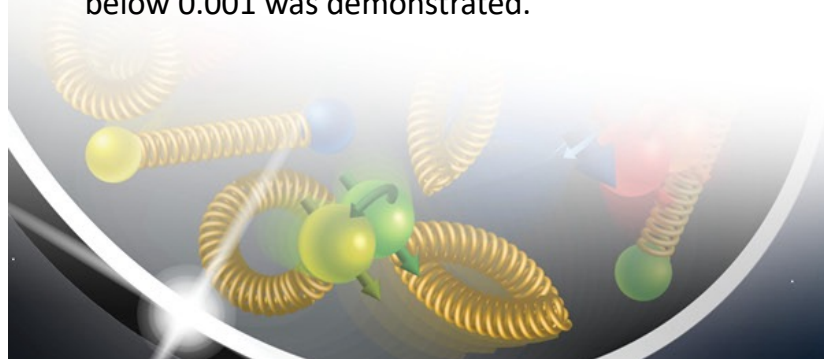
- A series of experiments have been performed in RHIC to verify the capability of reaching the flat beam.
- Preserving flat beam during acceleration will be studied in a beam experiment in the coming RHIC run: stochastic cooling will be used on Au ion beam at 31 GeV/u, followed by the acceleration to 100 GeV/u.



Beam experiment in 2023 demonstrated the emittance ratio 11:1 with Au ions at 100 GeV with the help of vertical stochastic cooling.

Simulation studies concluded that at the HSR design tunes (0.228,0.210), one needs $|C| = \Delta Q_{\min} < 0.002$ to reach and maintain the required emittance ratio.

During beam experiment in 2017, reaching ΔQ_{\min} well below 0.001 was demonstrated.

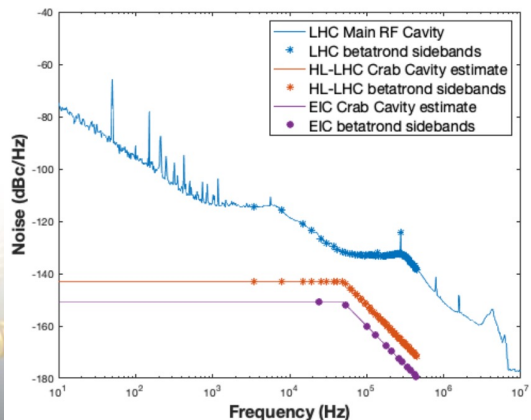


Crab-Cavity RF Noise

The RF phase and amplitude noise tolerances for EIC and HL-LHC crab- cavities.

	$\sigma_{\Delta\phi}$ (μrad)	$\sigma_{\Delta A}$ (1e-6)
HL-LHC	8.17	13.30
ESR 5 GeV	805	12700
ESR 10 GeV	860	13600
ESR 18 GeV	548	7060
HSR 41 GeV	3.09	10.1
HSR 100 GeV	2.69	9.36
HSR 275 GeV	<u>1.75</u>	<u>7.07</u>
Au 41 GeV	18.7	39.4
Au 110 GeV	5.12	17.8

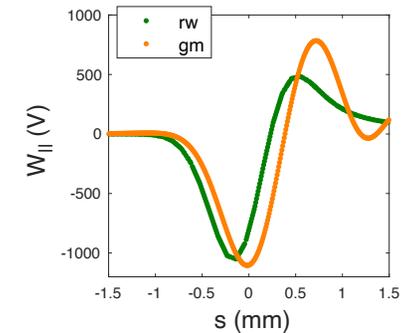
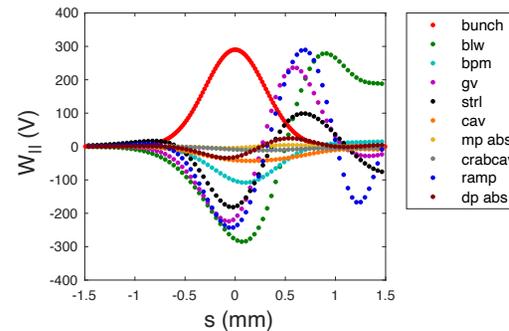
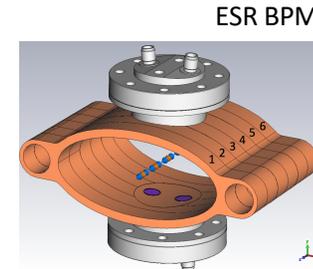
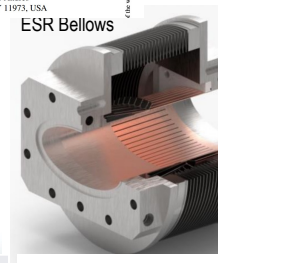
Estimated spectral noise in EIC and HL-LHC crab-cavity RF in comparisons with measured noise spectra data for the main LHC RF cavity:



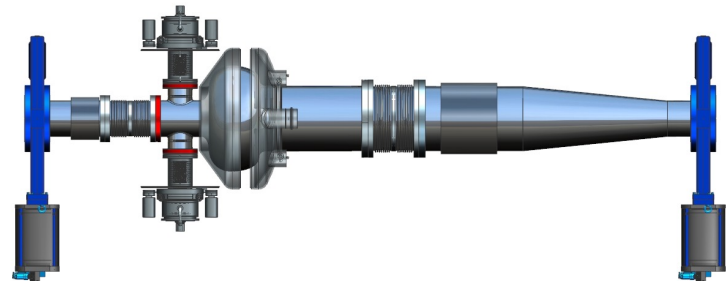
- Crab-cavity RF noise is a strong source of emittance growth.
- Issue for crab-cavities in both EIC and HL-LHC.
- Mitigations are being developed in EIC:
 - By LLRF design
 - Beam-based feedback
- Minimizing the pickup measurement noise is of critical importance.

High Beam Intensity : ESR

- **ESR Beam Current:** 2.5 A (at 10 GeV and below).
- Preliminary design of vacuum and beam instrumentation is underway.
- **ESR impedance budget** is already quite comprehensive. Design bunch parameters are **well below instability thresholds**.



591 MHz single cell SRF cavity with high power beam line HOM absorbers.



The ESR RF cavity system:

- making up for 9 MW synchrotron radiation losses
- deal with considerable HOM loads (more than 40 kW per cavity).

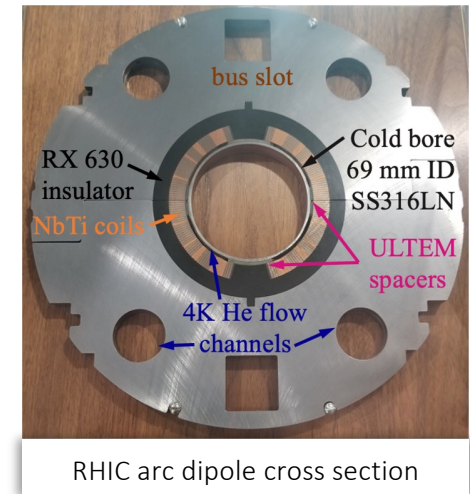
Unacceptable resistive-wall impedance of RHIC vacuum chamber for EIC hadron beams

- Beam-induced currents on resistive walls of vacuum chamber dissipate heat.

$$P'_{RW} = \Gamma \left(\frac{3}{4} \right) \frac{Q^2 M}{4\pi^2 b T_0} \left(\frac{\mu\rho}{2} \right)^{\frac{1}{2}} \left(\frac{1}{\sigma_t} \right)^{\frac{3}{2}}$$

: resistive-wall (RW) heat per unit of length for round pipe

- Presently, vacuum chamber of 4.55 K RHIC SC magnets is a round, stainless steel 316LN beam pipe.



- Resistive-wall heating in nominal 69 mm diameter pipe for highest Ecm beam (most demanding scenario) is greater than dynamic heat budget (~ 0.5 W/m):

	Species	E (GeV/u)	M	N (10 ⁹ ppb)	I _{ave} (A)	σ _z (m)	P' (W/m)*
RHIC	p↑	255	111	197	0.27	0.6	0.05
EIC	p↑	275	290	198	0.72	0.06	4.03 🤯

(*Only RW heating for on-axis beam; this slide assumes negligible e-cloud thanks to low SEY of a-C film. RRR=1.46 stainless steel)

Unacceptable resistive-wall impedance of the RHIC vacuum chamber for EIC beams

- If heat is not reduced or extracted, the superconducting magnets will **quench**.

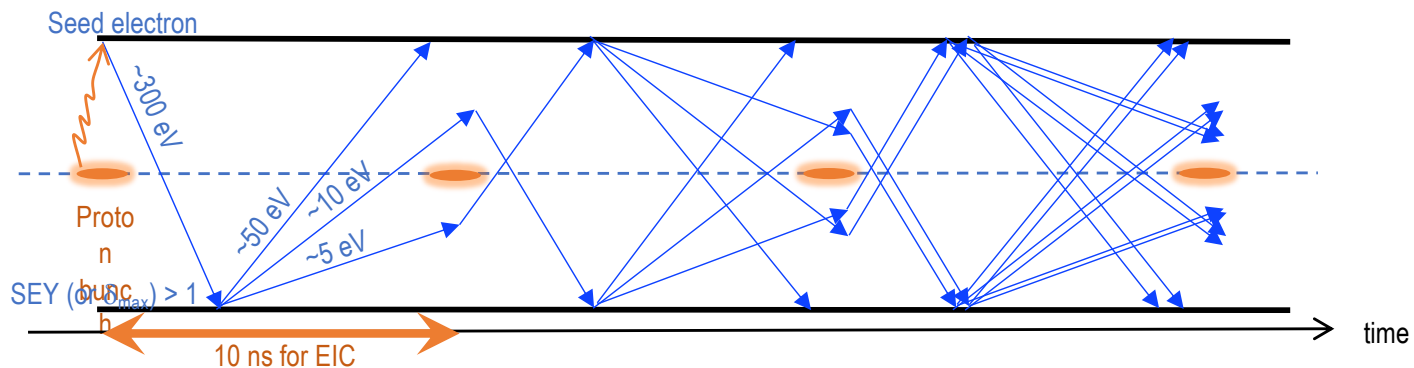
OR

- If **reducing bunch charge to avoid quench**, luminosity decrease is unacceptable:
 - for highest E_{cm} scenario: $L = 0.15 \rightarrow 0.05$ ($\times 10^{34} \text{ cm}^{-2}\text{s}^{-1}$)
 - for highest lumi scenario: $L = 1.0 \rightarrow 0.5$ ($\times 10^{34} \text{ cm}^{-2}\text{s}^{-1}$)

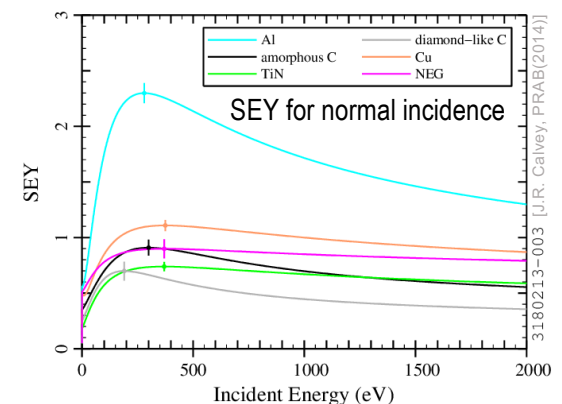
UPGRADE \Rightarrow use better electrical conductor (Cu at 10 K \rightarrow $P' \sim 0.35 \text{ W/m}$)

Unacceptable secondary electron yield (SEY) of the RHIC vacuum chamber for EIC beams

- **Electron cloud buildup** refers to a **cascade multiplication** of the electrons present in the vacuum chamber of a particle accelerator as result of the electrons acquiring energy from the passing beam and featuring the appropriate energy to extract electrons from the surface of the chamber.



- Electron clouds **deteriorate vacuum and beam quality, heat up the chamber and**, in some cases, lead to **beam loss**.
- The number of emitted secondary electrons per primary electron is the **Secondary Electron Yield (SEY)** and is **material dependent** (surface topography and electronic properties of material).



Unacceptable secondary electron yield (SEY) of the RHIC vacuum chamber for EIC beams

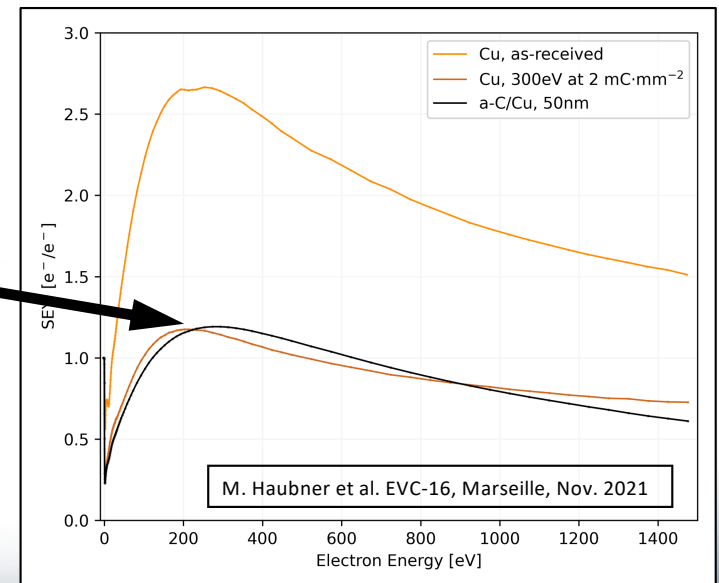
The high-intensity EIC beams, with short bunch spacing, lead to e-cloud buildup.

	RHIC	LHC	EIC HSR
Bunch charge ($\times 10^{11}$ ppb)	1.35	1.15	0.69
Bunch spacing (ns)	108	50 -- 25	10.15

SEY of scrubbed stainless steel is about 1.35.

To mitigate risks of electron cloud buildup:

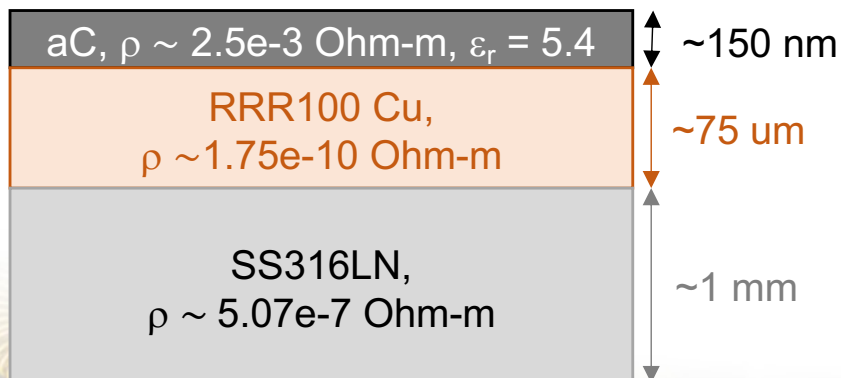
UPGRADE \Rightarrow use low SEY surface (a-C)



High Beam Intensity : HSR

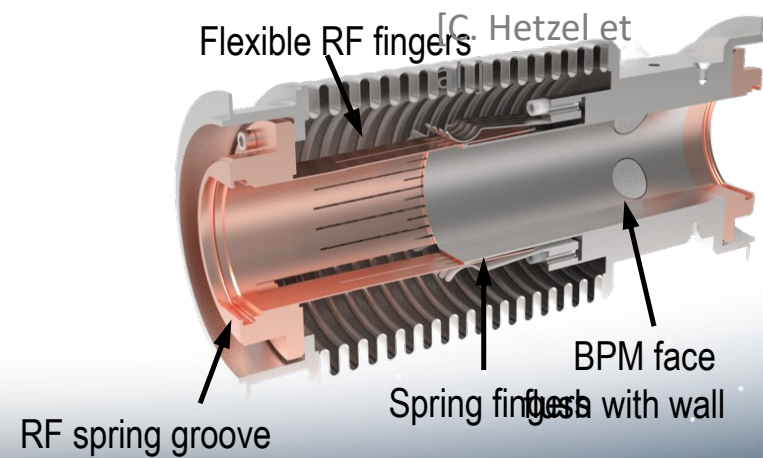


Copper-clad stainless steel with aC coating.
Gas-cooled channel on top.



HSR beam screen wall

- Beam current: 1 A; a factor three higher than used in the RHIC operation.
- Cryo-load on cold beam pipe:
 - Resistive heating
 - Electron cloud
 - Enhanced by larger radial orbit shift (up to 20 mm)
- Beam screens will be installed into existing beam pipe to stay below 0.5 W/m cryo-load limit.
- Also, new bellows and BPMs.

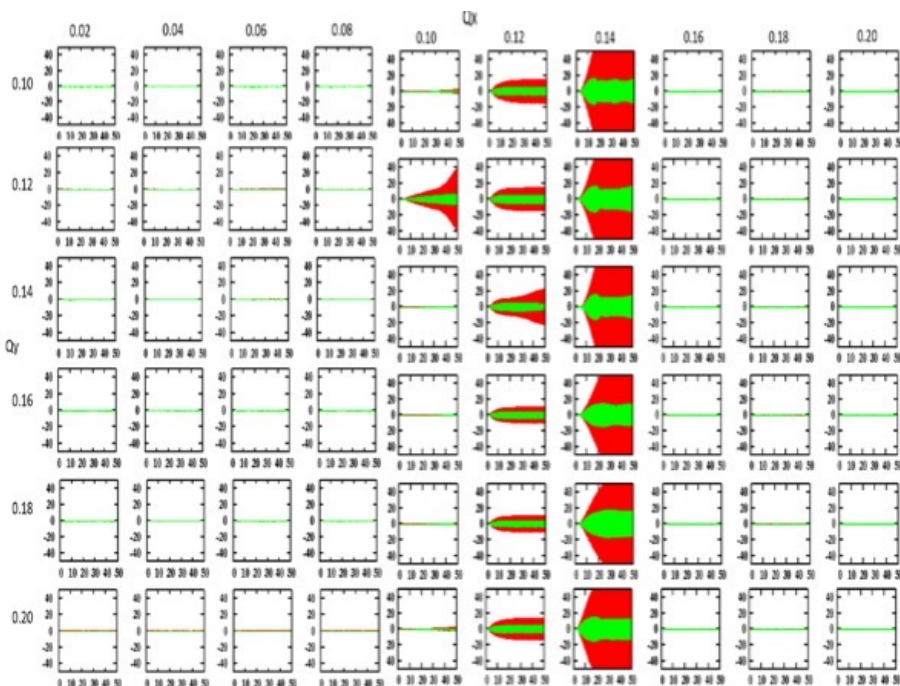


EIC Beam-Beam Studies

Study areas:

1. Limits in beam-beam parameters and beam flatness.
2. Selecting candidates for store working points in both storage rings.
3. Studies with the lattice and hardware errors. Defining tolerances.

Coherent Instability during ESR tune scan



Strong-Strong (BeamBeam3D and BBSS):

- verifying absence of coherent beam-beam instability with design parameters
- the tune scans for defining the working points.

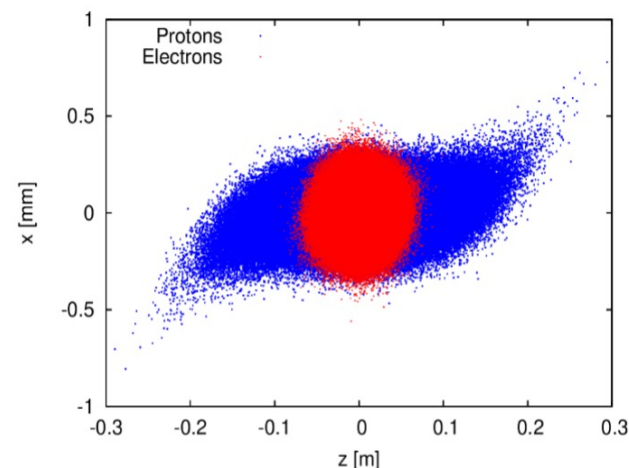
Emittance growth studies strongly affected by artificial emittance growth from numerical effects.

Weak- strong (SimTrack):

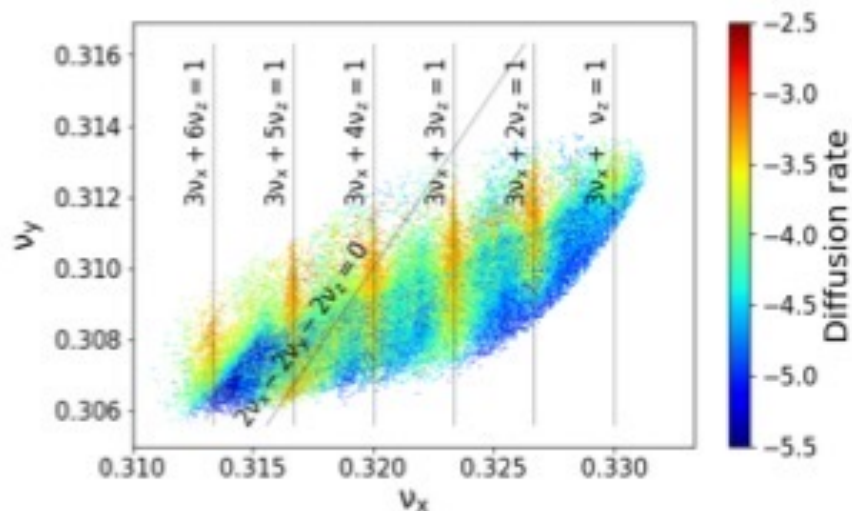
emittance growth, DA studies, tune scans

Beam-Beam with crab-crossing

- Synchro-betatron resonances are prominent feature of working point landscape.
($3\nu_x + 6\nu_z = 1$)
- Impact of RF waveform on the 6 cm long hadron bunches leads to crabbed offsets in the head and the tail.
- HSR includes second harmonic crab-cavity to mitigate the offsets.



Frequency Map Analysis for the HSR



Best working points (found:

(0.228, 0.21) for protons

(0.08, 0.14) for electrons (compatible with good polarization)

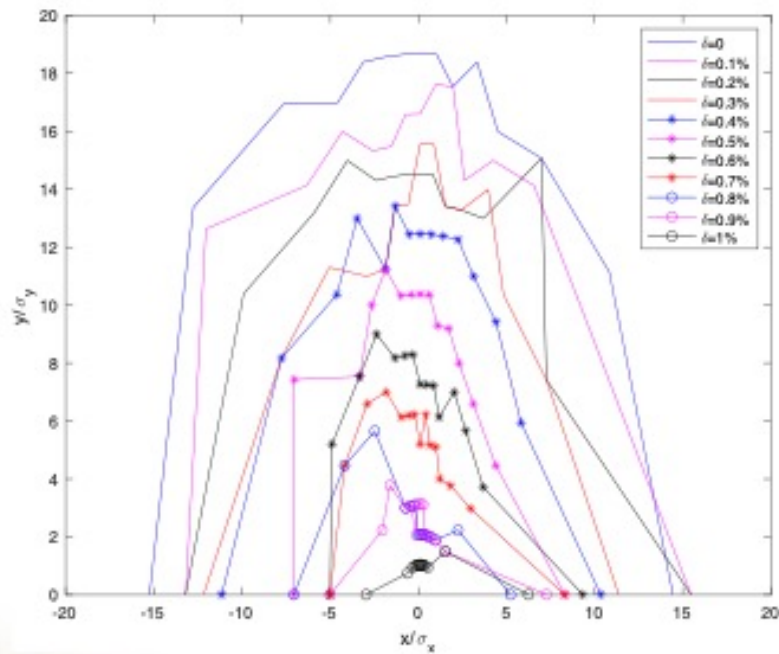
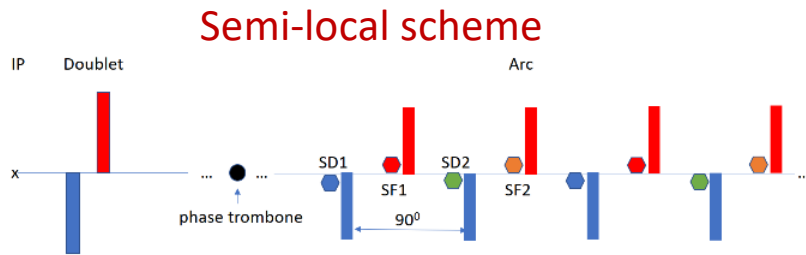
From emittance growth studies:

Min beam flatness $K = 0.09$

Max $\xi_p = 0.012$

D.Xu, Y.Hao, Y.Luo, and J.Qiang, Phys. Rev. Accel. and Beams, vol. 24, p. 041002, 2021

ESR Dynamics Aperture

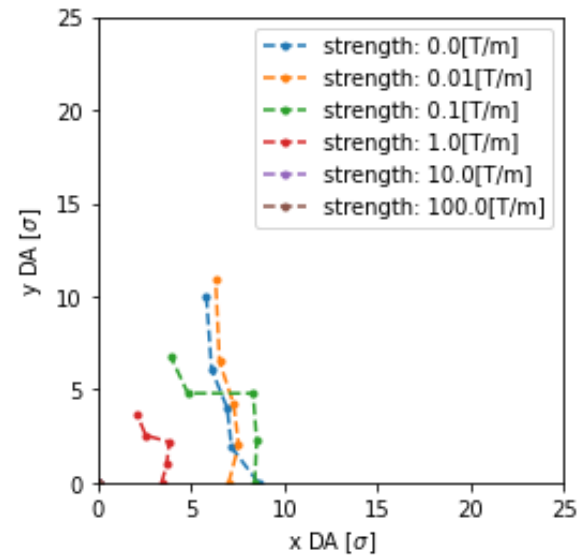


- ESR two lattice options: 60° for operation at lower energies (5-10 GeV) and 90° for 18 GeV operation
- Biggest challenge: achieving DA goal (10σ) at 18 GeV; with two low-beta IRs
- Not possible to apply local chromatic correction
- **Hybrid chromatic compensation scheme** has been proposed by SLAC experts:
 - Semi-local scheme to correct for IR quads induced chromaticity (4 sextupole sets + phase trombones)
 - Optimizing chromatic correction between IP6 and IP8 as periodic system
 - Additional sextupole sets for checking in control the second-order dispersion function and third order resonance terms

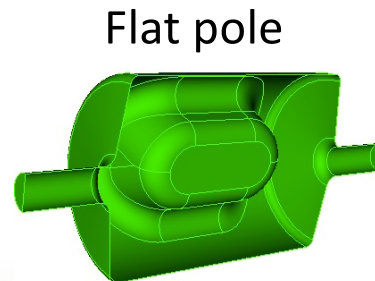
Crab-Cavity and HSR Dynamics Aperture

- Effect of crab-cavity field multipoles of the crab-cavity on DA
- Found that the sextupole field component of crab-cavity decreases dynamic aperture well below the goal 6σ .
- Re-optimization of the crab cavity design is underway to reduce multipoles components.

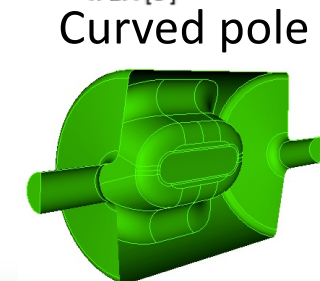
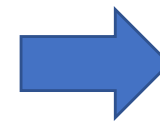
DA at different cc sextupole strength



Mitigation by adjusting crab-cavity walls making pole piece more curved



$b_3 = 1.4 \text{ T/m}$



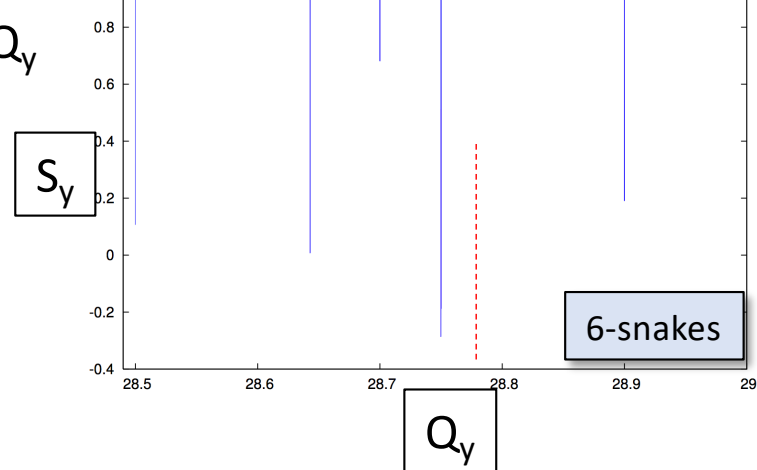
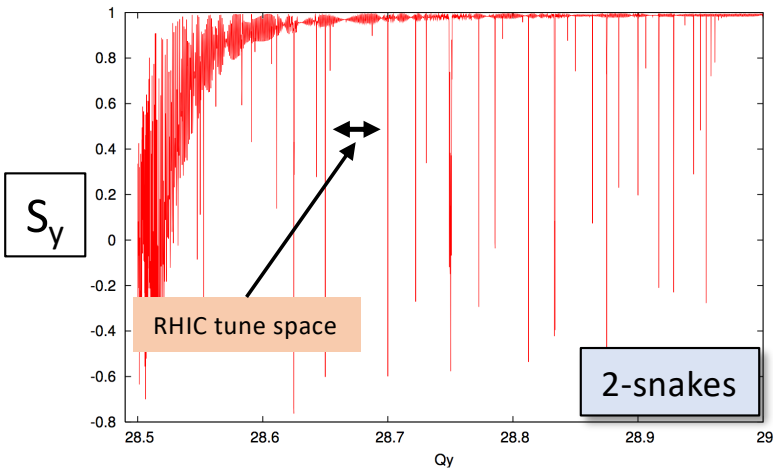
$b_3 = 0.003 \text{ T/m}$

Hadron Polarization

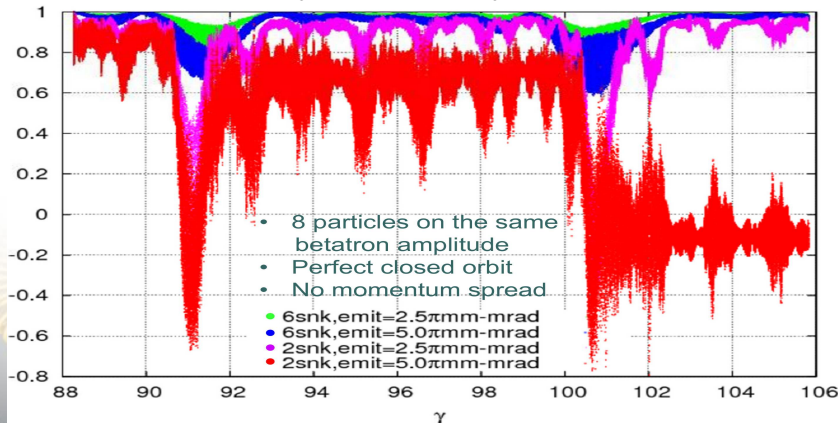
RHIC with 2 Snakes

Snake resonance spectrum

EIC Hadron Ring with 6 Snakes



Crossing strongest spin resonance with 2 and 6 Snakes
411- Q_y and 393+ Q_y

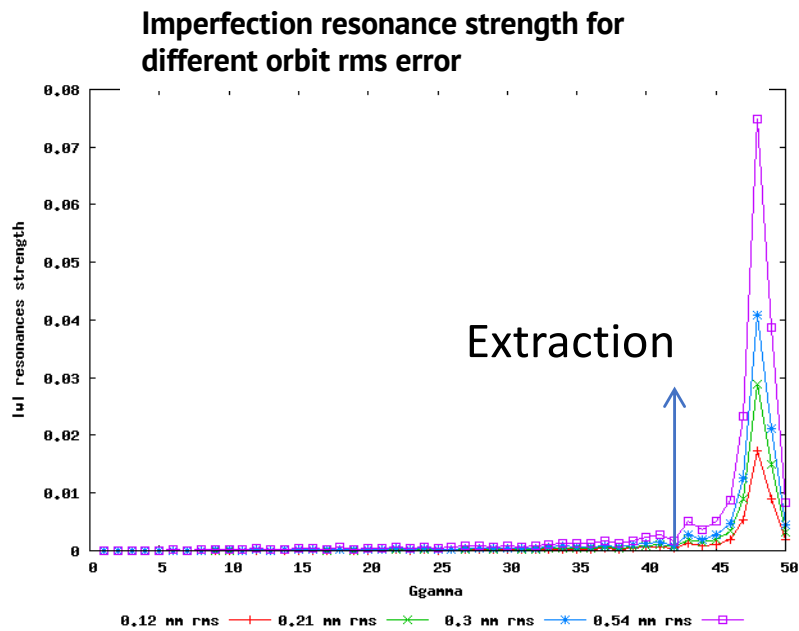


- **Main challenge:** preserving polarization of helions (3He^{+2} ions) and protons during acceleration process
- More Snakes help to preserve polarization.
- **Six Snakes configuration** preserve polarization well.

Zgoubi, F.Meot

Electron Polarization: Acceleration in RCS

- Polarized electrons of both spin orientation generated in the electron source and accelerated to a full collision energy.
- RCS Challenge: preserve electron polarization during 100 ms acceleration from 400 MeV to 18 GeV. Spin tune range: $0.907 < \gamma a < 41$.
- Solution: **highly periodical lattice with properly matched straight sections.**



Strong spin resonances are moved out of the acceleration range !

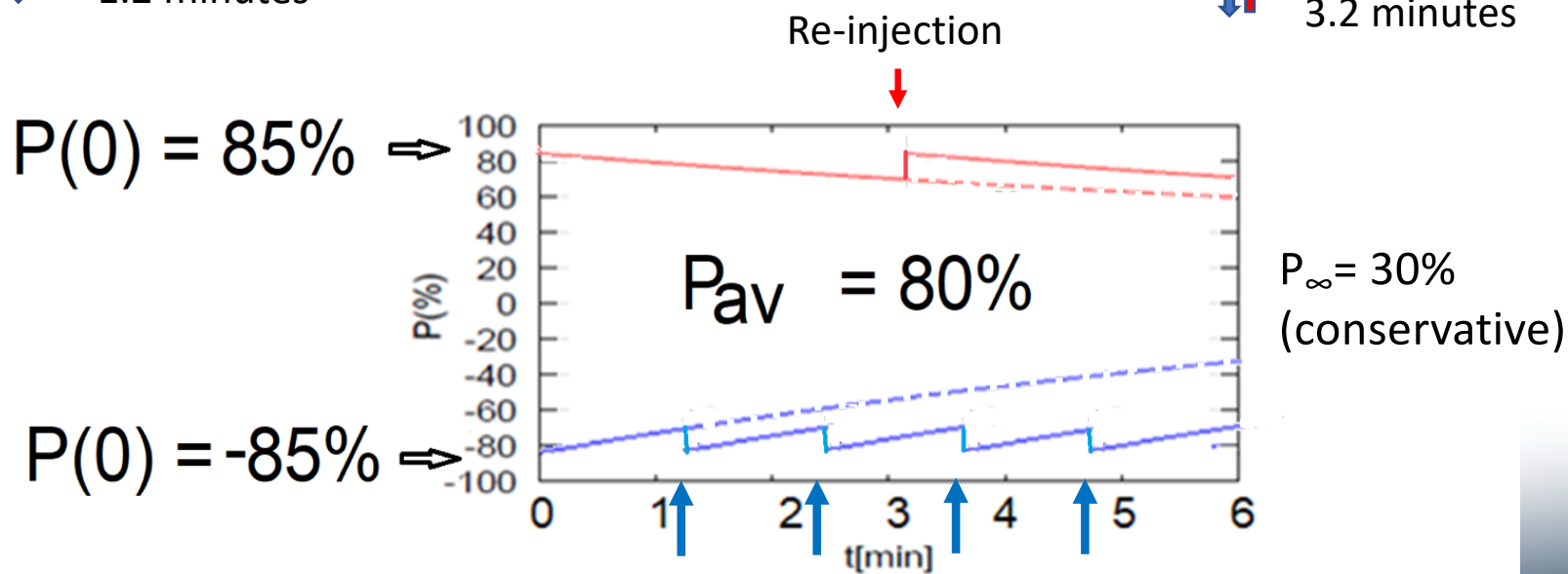
- Spin tracking confirmed:
No polarization loss from intrinsic resonances.
- Imperfection spin resonances:
vertical RMS orbit 0.5 mm to keep losses $< 5\%$.

High average polarization in electron storage ring of 80% by

- Frequent injection of bunches on energy with high initial polarization of 85%
- Initial polarization decays towards $P_\infty < \sim 50\%$
(equilibrium of self-polarization and stochastic excitation)
- At 18 GeV, every bunch is refreshed within minutes with RCS cycling rate of 2Hz
- Need both polarization directions present at the same time

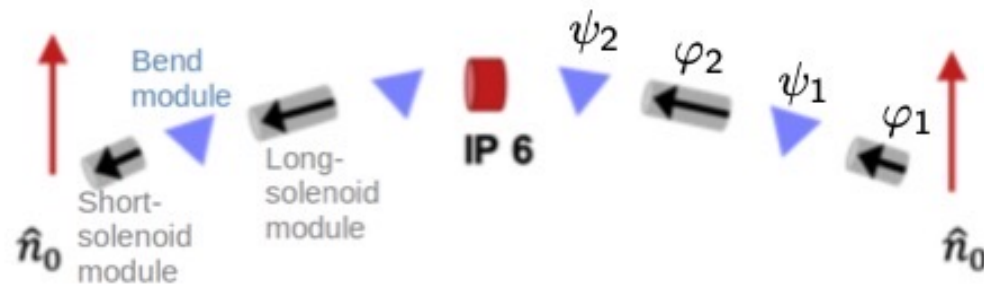
B P
 Refilled every
 1.2 minutes

B P
 Refilled every
 3.2 minutes



Preserving ESR polarization with spin rotator

- Stochastic character of synchrotron radiation introduces stochastic depolarization, which can significantly shorten depolarization time.
- Special spin matching conditions must be satisfied in the storage ring optics to minimize this harmful effect.



Spin rotators: combination of solenoids and bending magnets, producing longitudinal polarization in the IP in 5-18 GeV range.

Beam Polarization

Vadim Ptitsyn

EIC Project

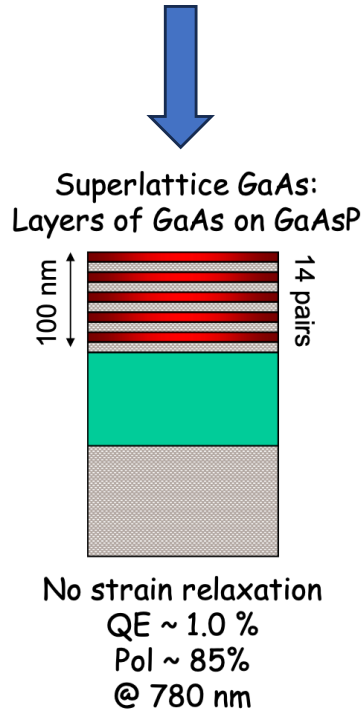
Brookhaven National Laboratory

USPAS 2025

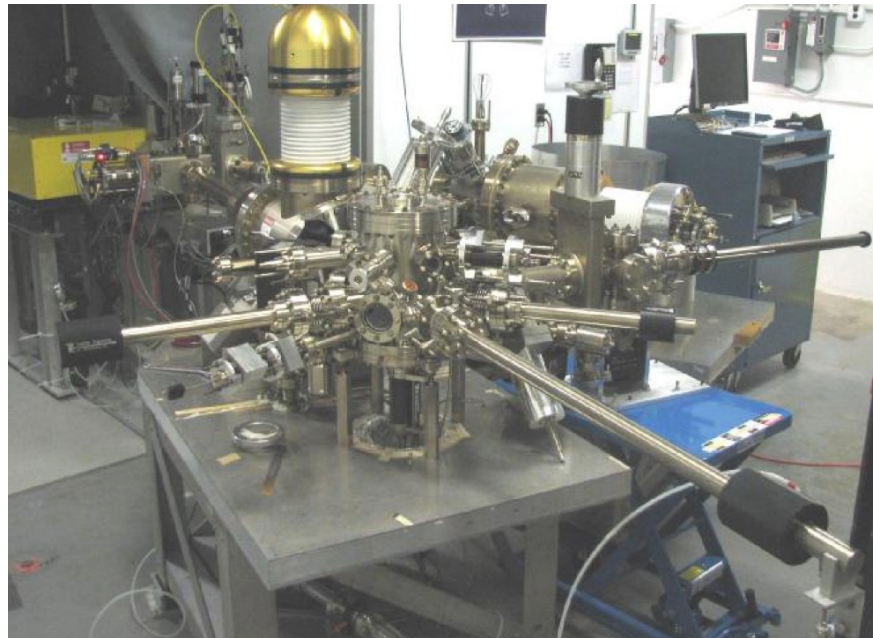
How to get polarized beams?

- One way is to produce the polarized beams from the source and then accelerate them to the high energy required for physics experiment.
 - The acceleration process can easily destroy beam polarization, since many spin resonance must be crossed on the way to high energy.
 - Several special techniques and hardware are used to preserve polarization during the acceleration.

Polarized Electron Source

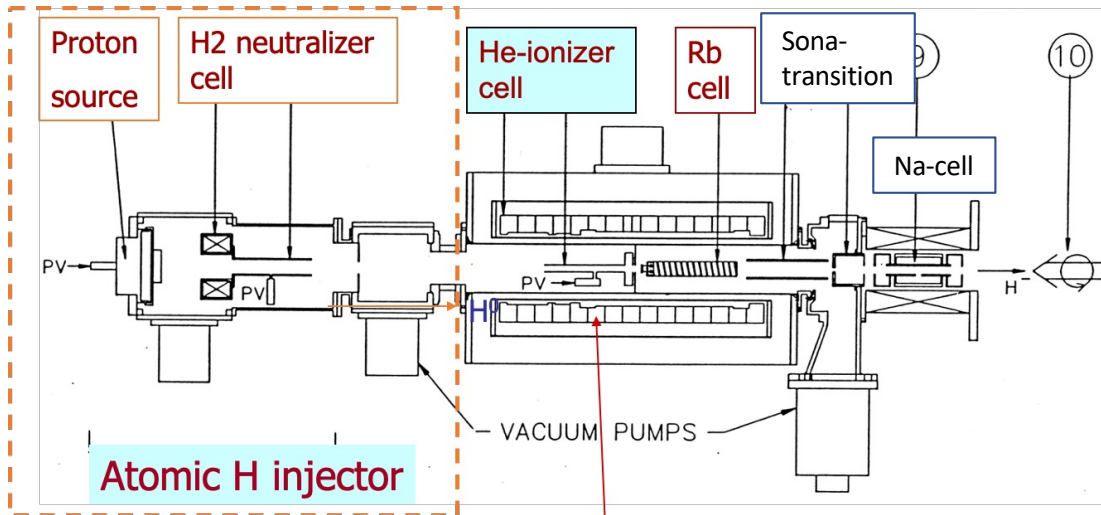


Polarized electrons are produced by photoemission from circular polarized laser light falling on very special cathode, based on interleaved layers of GaAs-based materials.



Polarized gun in
Jefferson Lab
CEBAF facility

Optically pumped polarized ion source (OPPIS)



He-ionizer cell serves as a proton source in the high magnetic field.

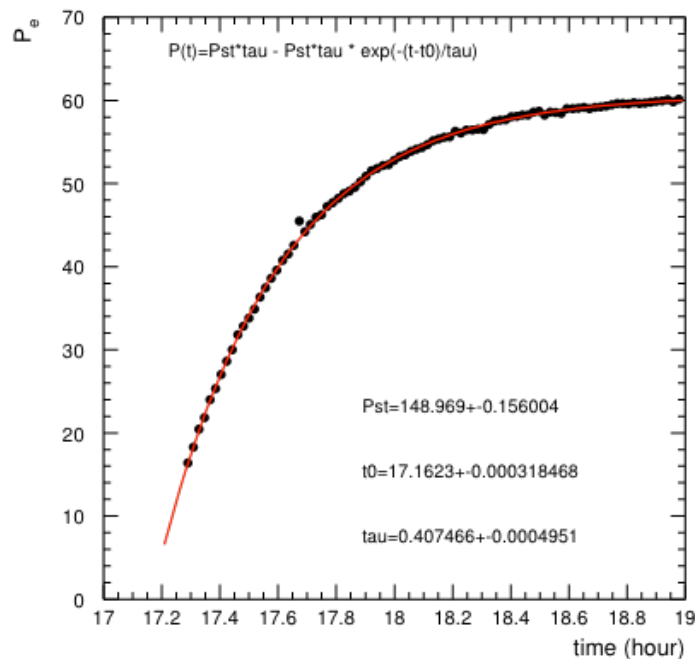
- Used for RHIC $p\uparrow+p\uparrow$ program from 2000
- Protons pickup polarized electrons in an optically pumped Rb vapor cell
- Electron polarization of H-atoms is transferred to protons in a magnetic field reversal region (Sona-transition)
- H⁻ ions are produced then by passing through Na-cell
- Polarized protons are obtained by charge exchange injection of H⁻ into the Booster
- Several upgrades and modifications over years increasing polarization and intensity



up to 84% polarization
reliably 0.5 - 1.0 mA (max 1.6 mA) (?)
up to $1 \cdot 10^{12}$ H⁻/pulse polarized H⁻ ions (?)

Electron Self-Polarization

Electron Polarization build-up in HERA



$E_e = 27 \text{ GeV}$

- Electrons takes advantage of synchrotron radiation, which drives Sokolov-Ternov self-polarization:
 - gradual spin build-up along direction opposite to guiding bending field.

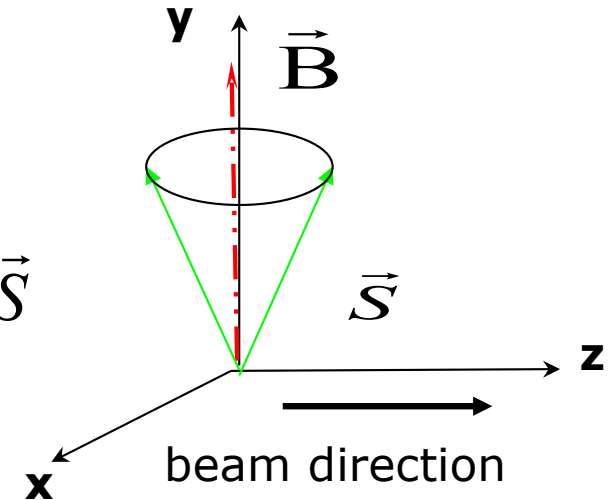
- $\tau_{ST}^{-1} \sim \frac{\gamma^5}{\rho^3}$

For EIC electron ring the polarization build-up time at 18 GeV is ~ 30 min.

Spin motion in a circular accelerator

- Thomas BMT equation

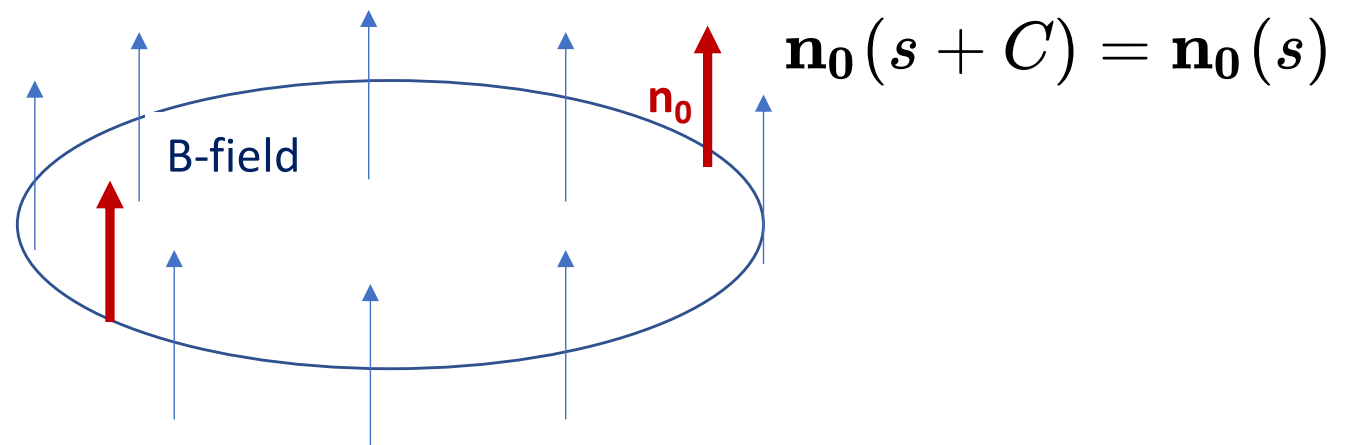
$$\frac{d\vec{S}}{dt} = \vec{\Omega} \times \vec{S} = -\frac{e}{\gamma m} [(1 + G\gamma)\vec{B}_{\perp} + (1 + G)\vec{B}_{\parallel}] \times \vec{S}$$



- In a perfect accelerator, spin vector precesses around its guiding field, i.e. vertical
- Spin tune Q_s : number of precessions in one orbital revolution. In general, $\nu_{sp} = G\gamma$
- G is the anomalous magnetic moment.
For protons, $G=1.793$. For electrons, $G=0.0012$.

Stable Spin in Ideal Circular Accelerator

- Let's consider circular accelerator with no spin rotators.
- Ideal accelerator: no misalignment and magnet errors
- Central beam orbit is formed by guiding vertical dipole field. It lies all in the horizontal plane.



In this case periodical spin solution \mathbf{n}_0 is vertical at any ring azimuth.

Spin tune and depolarizing resonances

Kicks on the spin vector from horizontal field leads the spin vector away from its stable direction, i.e. vertical.

- Depolarizing resonance condition:

- Number of spin rotations per turn = Number of spin kicks away from stable direction per turn
- Spin resonance strength ε = spin rotation from resonance per turn / 2π

- Imperfection resonance (magnet errors and misalignments):

$$\nu_{sp} = n$$

- Intrinsic resonance (Vertical focusing fields):

$$\nu_{sp} = Pn \pm \nu_y$$

P: Superperiodicity [AGS: 12]

ν_y : Betatron tune [AGS: 8.75]

- Weak resonances: some depolarization

- Strong resonances: partial or complete spin flip

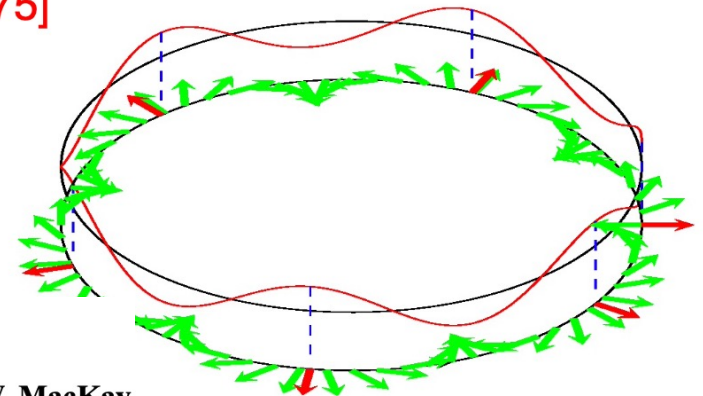


Illustration by W.W. MacKay

Crossing an isolated resonance

- Froissart-Stora formula: general form, directly applicable to the case of an imperfection resonance with strength $|\varepsilon|$.

$$P_f = P_0 \left(2e^{-\frac{\pi|\varepsilon|^2}{2\alpha}} - 1 \right)$$

$\alpha = \frac{dG\gamma}{d\theta}$ where $\theta = \omega_0 t$
 Resonance crossing rate

- Effective Froissart-Stora formula for a Gaussian distributed beam crossing an isolated intrinsic spin resonance

$$P_f = P_0 \frac{1 - \frac{\pi|\mathcal{E}_{rms}|}{\alpha}}{1 + \frac{\pi|\mathcal{E}_{rms}|}{\alpha}}$$

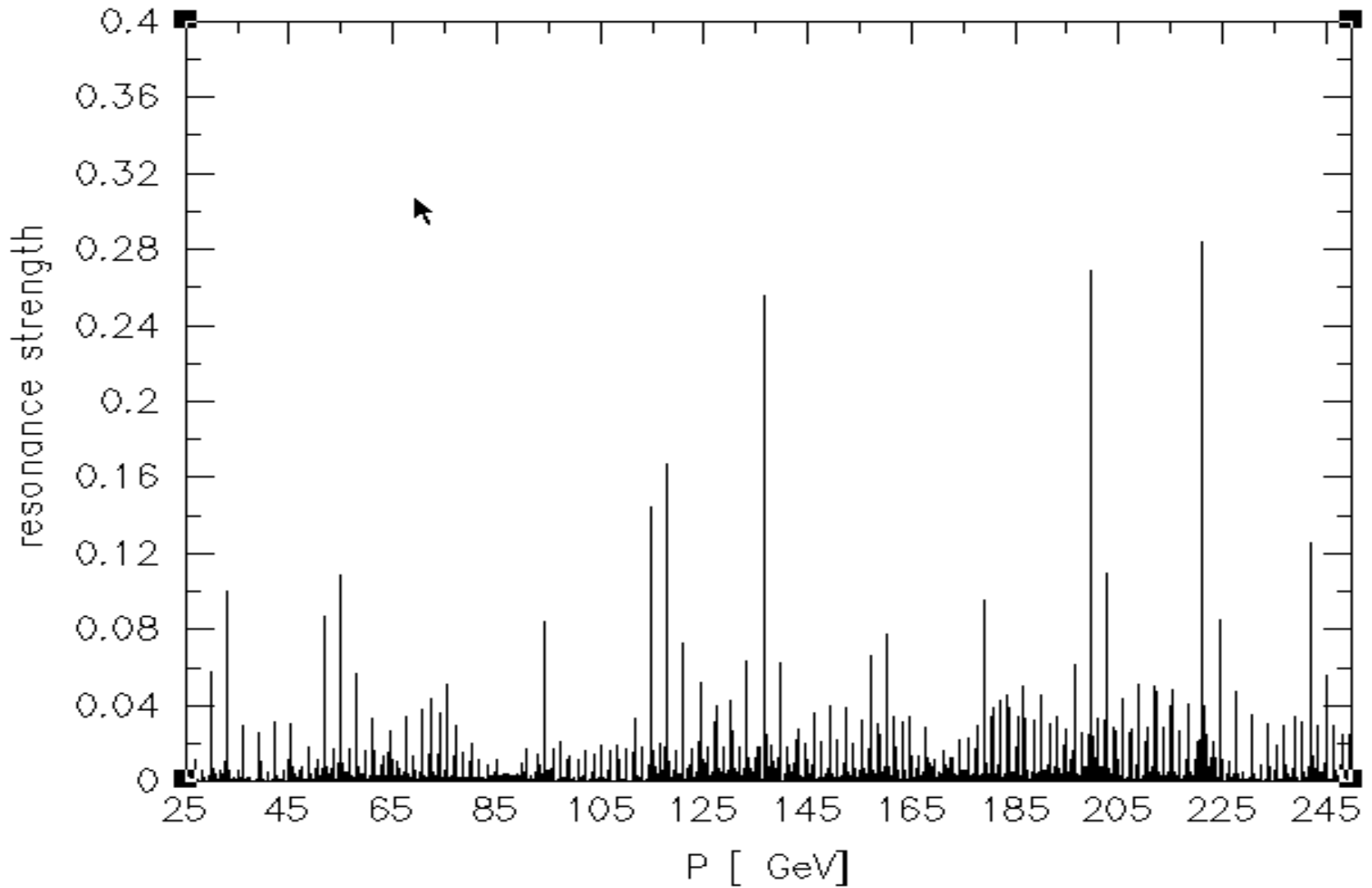
\mathcal{E}_{rms} : resonance strength of a particle at rms emittance

Two methods of resonance crossing

- Fast crossing: $\frac{|\varepsilon|^2}{\alpha} \ll 1$
preserves polarization
- Adiabatic or slow crossing: $\frac{|\varepsilon|^2}{\alpha} \ll 1$
flips polarization (from +1 to -1)
preserves absolute value of polarization

RHIC intrinsic spin resonance strength

Intrinsic spin resonance
 $Q_x=28.73$, $Q_y=29.72$, $\text{emit}=10$



Technologies for spin resonance crossing

Non-adiabatic ($\varepsilon^2/\alpha \ll 1$)

\leftrightarrow

Adiabatic ($\varepsilon^2/\alpha \gg 1$)

$P_f/P_i = 1$

$P_f/P_i = -1$

Imperfection Resonances:

Correction Dipoles (ε small) (RHIC Booster)

Enhanced orbit excursion (ε large)
(RHIC Booster)

Partial Snake (ε large) (AGS, IUCF)

Intrinsic Resonances:

Pulsed Quadrupoles (α large) (ZGS, AGS)

RF Dipole (ε large) (AGS past)

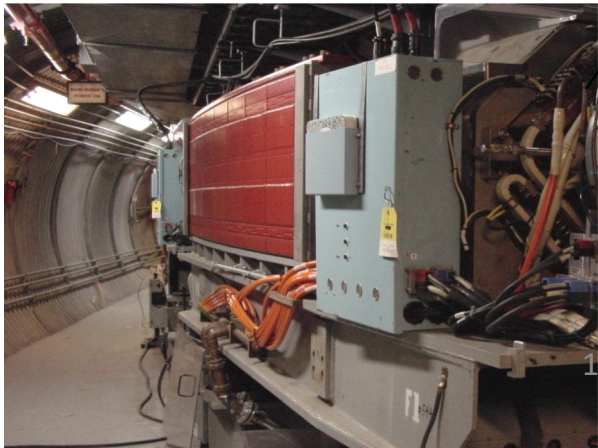
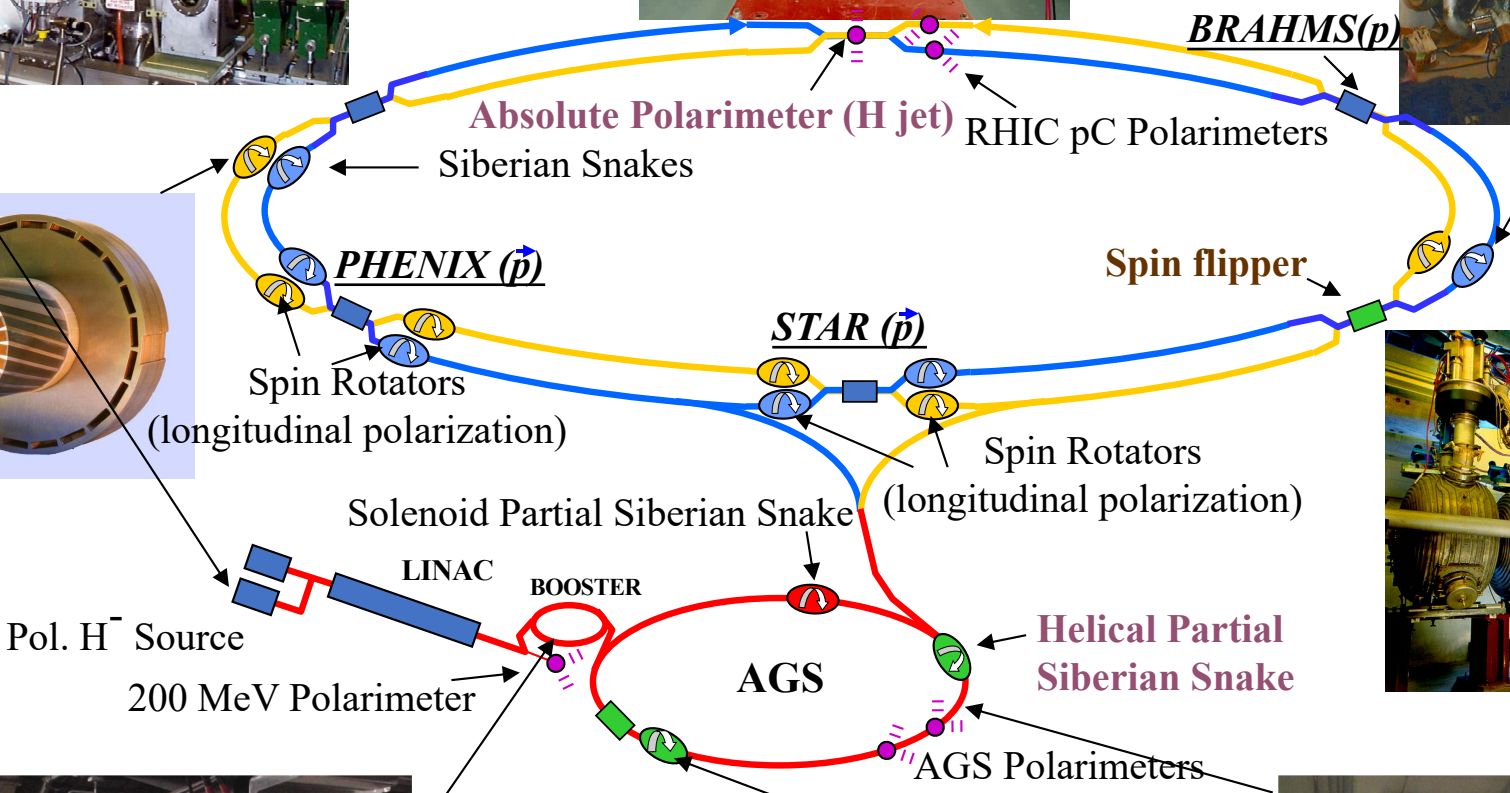
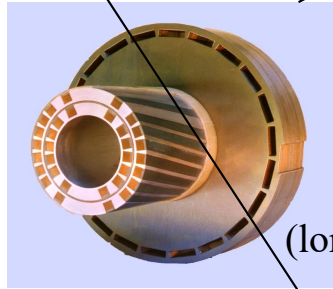
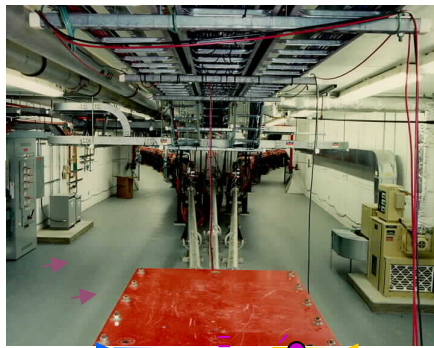
Lattice modifications (ε small)

Strong Partial Snake (ε large) (AGS present)

Ultimate tool:

Full Siberian Snakes in RHIC (2 per ring) prevent first-order spin resonance conditions. Weak depolarization still possible due to high-order spin resonances.

ed proto in complex a



Resonance-Free : 18 GeV e- RCS

- 85% polarized electrons from a polarized source and a 400 MeV s-band linac get injected into the fast cycling synchrotron in the RHIC tunnel
- Depolarization suppressed by lattice periodicity to $E > 18$ GeV, $[Q]=50$

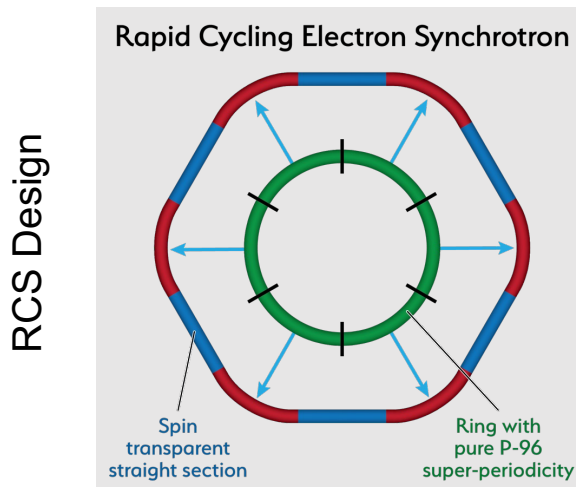
intrinsic spin
resonances
condition

$$G\gamma = nP \pm [Q_y]$$

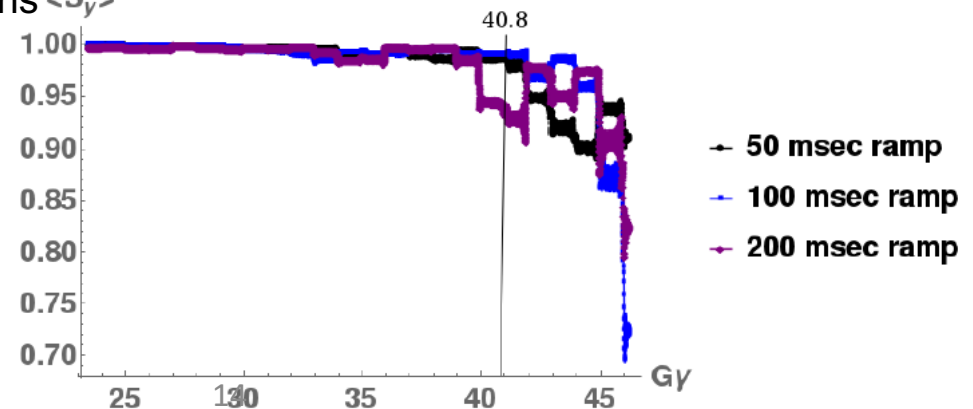
$G = \frac{g-2}{2} = 0.00115965$ is the anomalous gyromagnetic ratio of the electron

- Good orbit control $y_{cl.o.} < 0.05$ mm; good reproducibility suppresses depolarization by imperfection resonances
- ➔ No depolarizing resonances during acceleration 0.4-18 GeV
no loss of polarization on the entire ramp up to 18 GeV (100 ms ramp time, 2 Hz)

@V.Ranjbar



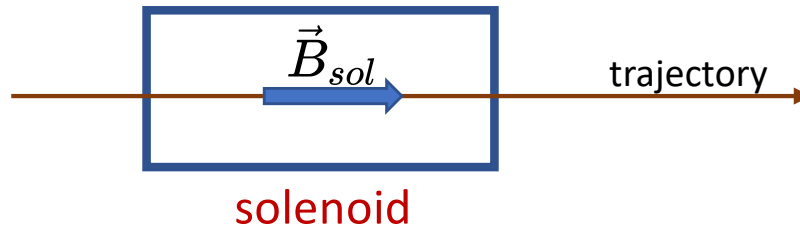
RCS Polarization Performance confirmed by extensive simulations $\langle S_y \rangle$



Spin rotation in different type of accelerator magnets

- Solenoid magnet
- Dipole magnet
- Helical Dipole magnet

Spin rotation: solenoidal field



- Particle on ideal orbit travels along the magnetic field. Particle trajectory is just straight line, since

$$\vec{v} \times \vec{B}_{sol} = 0$$

- Spin rotates around longitudinal direction (the field direction). Longitudinal spin direction is preserved.

- Spin rotation angle is:

$$\phi_{sp} = -(1 + G) \frac{e}{p} \int B_{sol} \cdot ds$$

- Solenoid spin transformation matrix:

$$M_{sol} = \cos(\phi_{sp}/2) - i\sigma_2 \sin(\phi_{sp}/2)$$

Spin rotation: solenoidal field (2)

- Required field integral for 180 degree rotation:

$$B_{sol} L = \frac{10.479}{1 + G} \cdot p(\text{GeV}/c)$$

Required field integral in solenoid is proportional to the particle momentum.

Examples:

for protons $G = 1.79$, thus to rotate spin by 180 degrees for 20 GeV beam

$$B_{sol} L = 75.1 \text{ Tm is needed}$$

for electrons $G = 1.3\text{E-}3$, thus to rotate spin by 180 degrees for 20 GeV beam

$$B_{sol} L = 200 \text{ Tm is needed}$$

Spin rotation: dipole magnet

- The magnetic field is orthogonal to the particle trajectory. The trajectory is curved.

$$\vec{v} \cdot \vec{B}_{dip} = 0$$

- Spin equation in a dipole magnet:

$$\frac{d\vec{S}}{ds} = -\frac{e(1 + G\gamma)}{p} \vec{B}_{dip} \times \vec{S}$$

Spin rotation: dipole magnet

- Resulting spin rotation angle in the laboratory frame:

$$\phi_{sp} = -(1 + G\gamma) \frac{e}{p} \int B_{dip} \cdot ds = -\left(\frac{1}{\gamma} + G\right) \frac{e}{m\beta c} \int B_{dip} \cdot ds$$

For relativistic beams ($\gamma \gg 1$) the spin rotation does not depend on beam energy

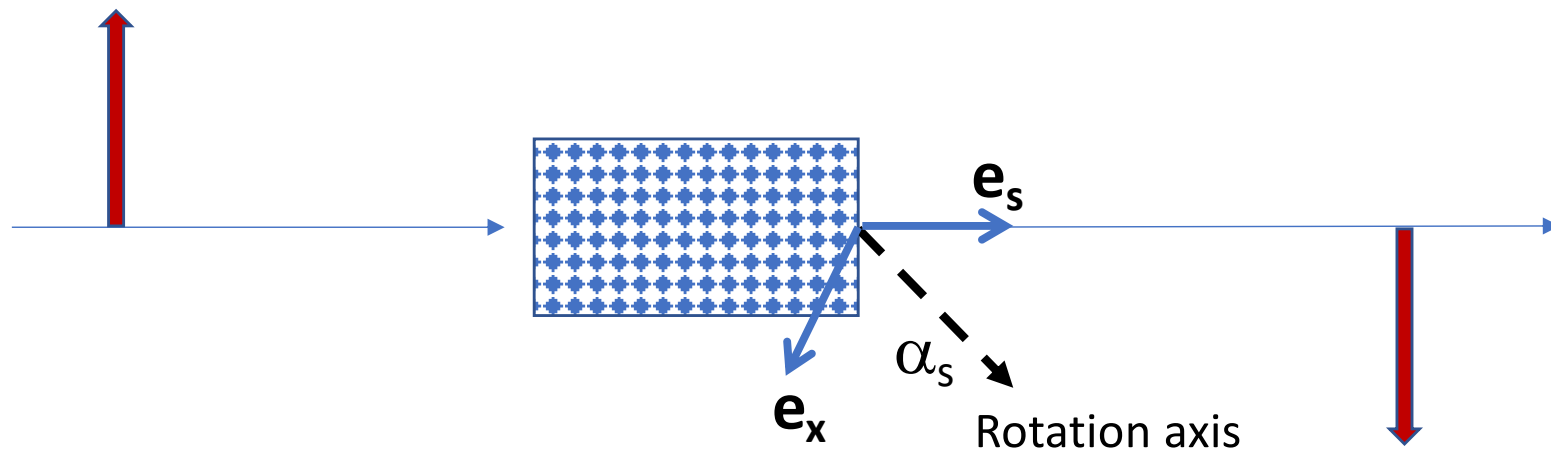
- But, in the accelerator frame, the rotation of particle velocity is subtracted, giving the rotation proportional to γ with respect to beam velocity:

$$\phi_{sp} = G\gamma \frac{e}{p} \int B_{dip} ds = G\gamma\theta$$

From here one can conclude for a ring with only vertical guiding field that one turn spin rotation is $2\pi G\gamma$, which defines the spin tune equal to $G\gamma$.

Siberian Snakes and their properties

Siberian Snake (Full Snake)

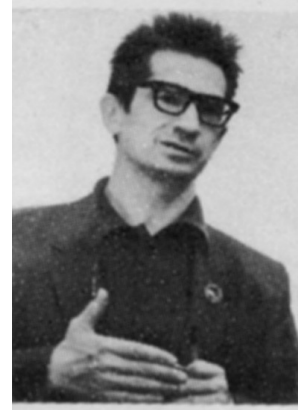


Siberian Snake (or Full Snake):

spin rotating device which rotates particle spin by 180 degree around a rotation axis, called **Snake axis** (which is usually in horizontal plane).

Snake axis angle α_s characterizes the orientation of the Snake axis in the horizontal plane.

Siberian Snake invention



Ya. Derbenev
(Novosibirsk)
“Siberian Snake”
concept

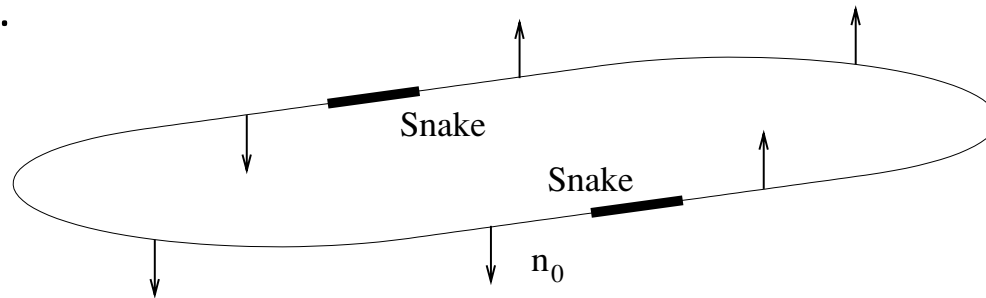
- Original concept was proposed in Budker Institute in Novosibirsk (Russia):
Ya.S. Derbenev and A.M.Kondratenko,
Soviet Physics Reports, 20, p 562 (1976).
- Major purpose: eliminate the depolarizing resonances.
Invention of the Siberian Snake opened a way for achieving highly polarized proton beams at the energies of tens of GeV and higher.

History of Snakes

- Idea: 1976
- Electron Partial Snake experiment at VEPP-2M (1977)
- Snakes studies for SSC (in 80s): 36000 resonances!
- IUCF cooler: Siberian Snake proof of principle studies (from 1989)
- Proton Partial Snake at AGS(1994)
- Electron Siberian Snakes in AmPS (1995) and SHR (MIT-Bates)
- Proton Siberian Snakes (and Spin Rotators) in RHIC 1999-now

Two Siberian Snakes Configuration Properties

Let's consider two Snakes placed on the opposite azimuths of the ring and having Snake Axis angles α_{s1} and α_{s2} .

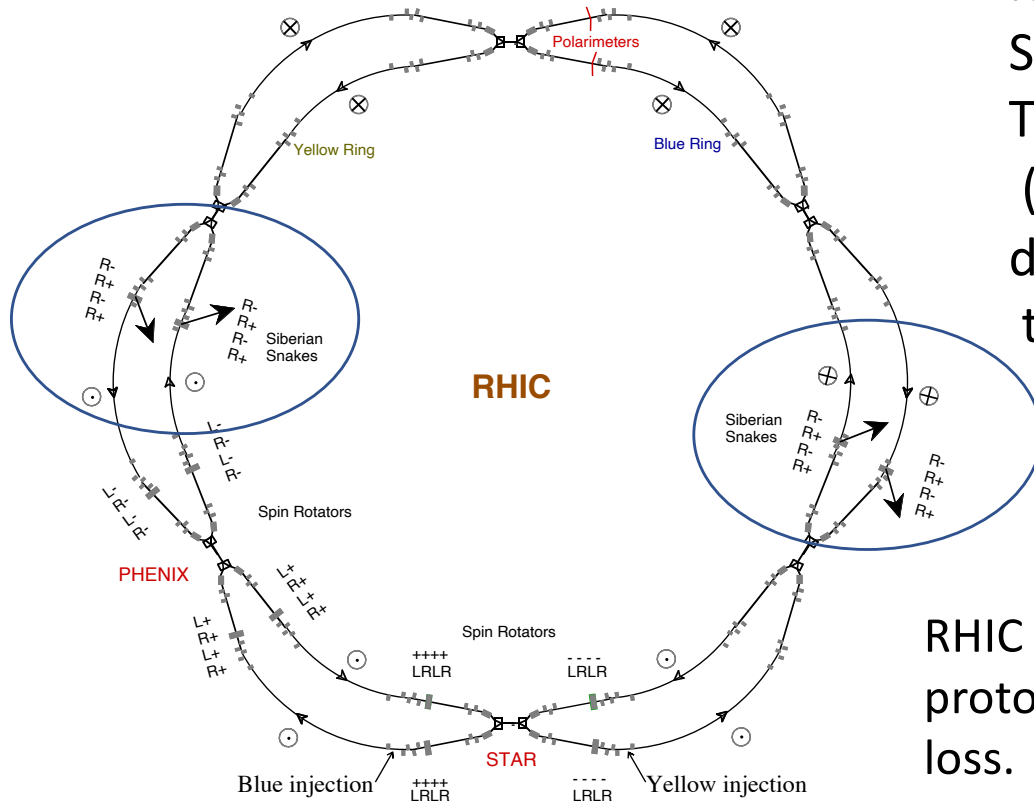


- a) Stable spin direction \mathbf{n}_0 is vertical in the ring arcs, pointing up in one half, and down on another.
- b) Spin tune is independent on energy and defined by the Snake axis orientations:

$$\nu_{sp} = \frac{2(\alpha_{s1} - \alpha_{s2})}{2\pi} = \frac{(\alpha_{s1} - \alpha_{s2})}{\pi}$$

Thus, for instance, to get the spin tune equal to 0.5, the Snake axes should be at 90 degree angle to each other.

Siberian Snakes in RHIC



RHIC employs the configuration with two Siberian Snakes in each ring. The Snake axes are at 45 and 135 degrees (symmetrical around longitudinal direction), thus giving the spin tune 0.5

RHIC Snakes allowed for acceleration of polarized protons up to 255 GeV with minimal polarization loss. Up 60% polarization in the store.

High order resonances (Snake resonances) are pronounced at higher energies and has to be avoided:

$$\nu_{sp} = N + m \cdot Q_y$$

Properties of Configuration with Even Number of Snakes

Spin tune then is:

$$\nu_{sp} = \frac{G\gamma}{2\pi} \underbrace{\sum_{i=1}^{2N} (-1)^{i-1} (\theta_i - \theta_{i-1})}_{\text{Main rule: place the Snakes in such locations that this term becomes 0.}} + \frac{1}{\pi} \sum_{i=1}^N (\alpha_{s,2i} - \alpha_{s,2i-1})$$

Main rule: place the Snakes in such locations that this term becomes 0.

The spin tune is independent on energy.

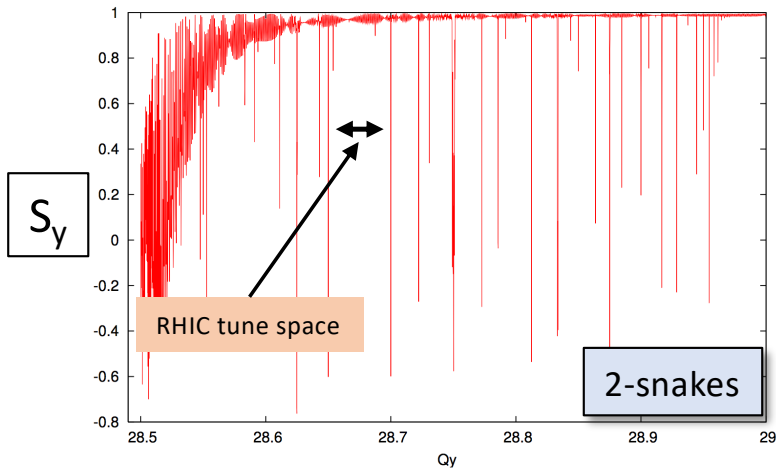
- If spin tune is independent on energy the spin resonance conditions are avoided during the acceleration process.
- By selecting proper orientations of Snake axes one can choose the value of the spin tune. Common approach to have it at 0.5.
- Stable spin direction \mathbf{n}_0 is vertical in arcs. Each Snake switches \mathbf{n}_0 from up to down, and vice versa.

High-order spin resonance with different number of Snakes

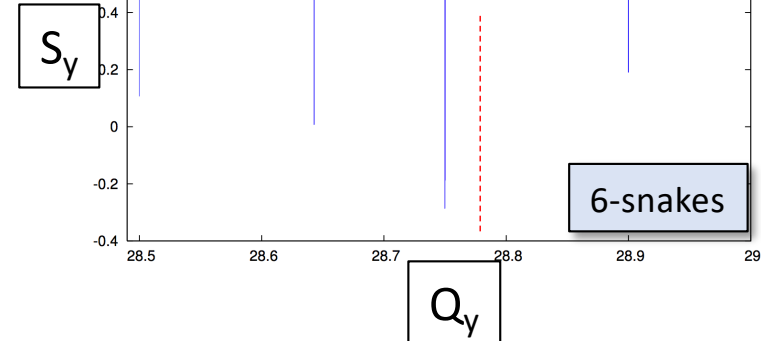
RHIC with 2 Snakes

Snake resonance spectrum

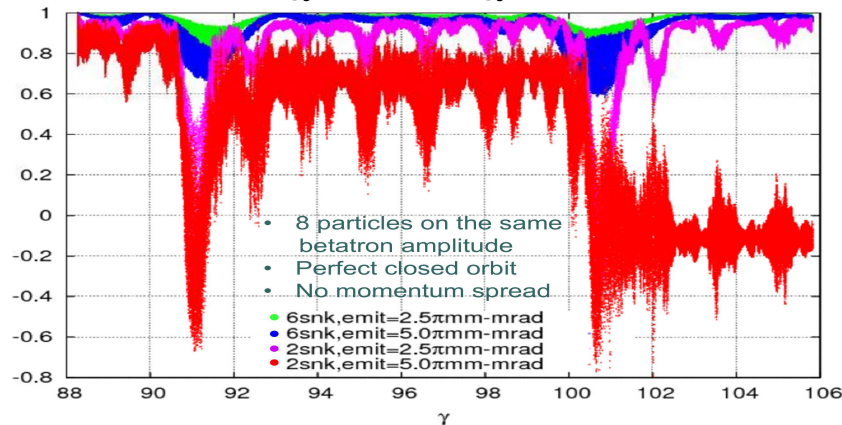
EIC Hadron Ring with 6 Snakes



$$\frac{1}{2} = m \pm nQ_y$$

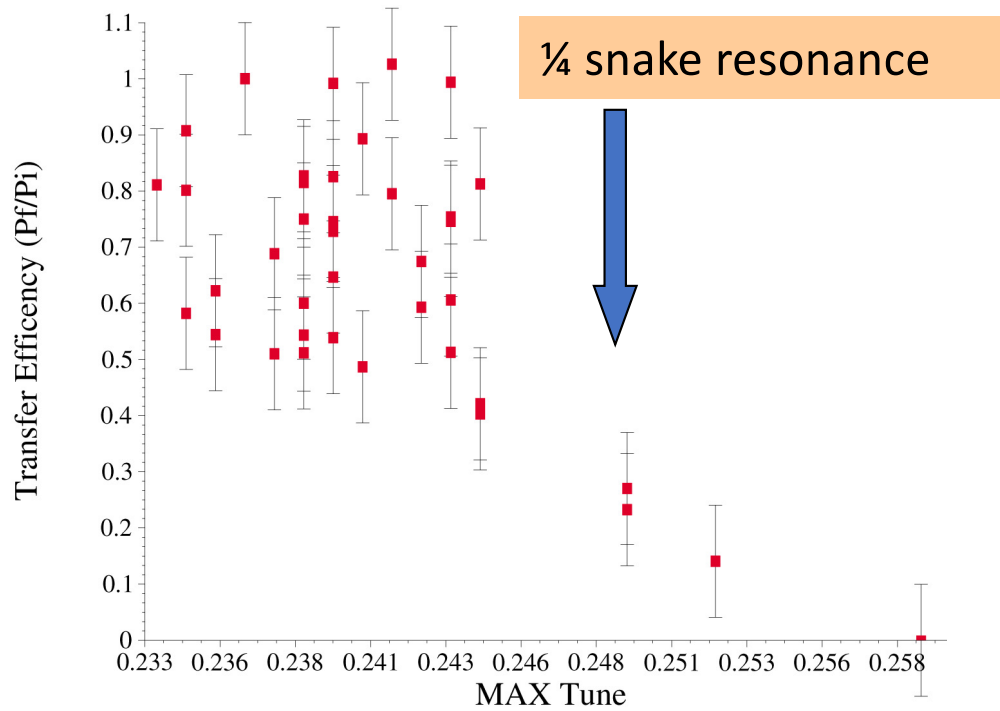


Crossing strongest spin resonance with 2 and 6 Snakes
 $411 - Q_y$ and $393 + Q_y$

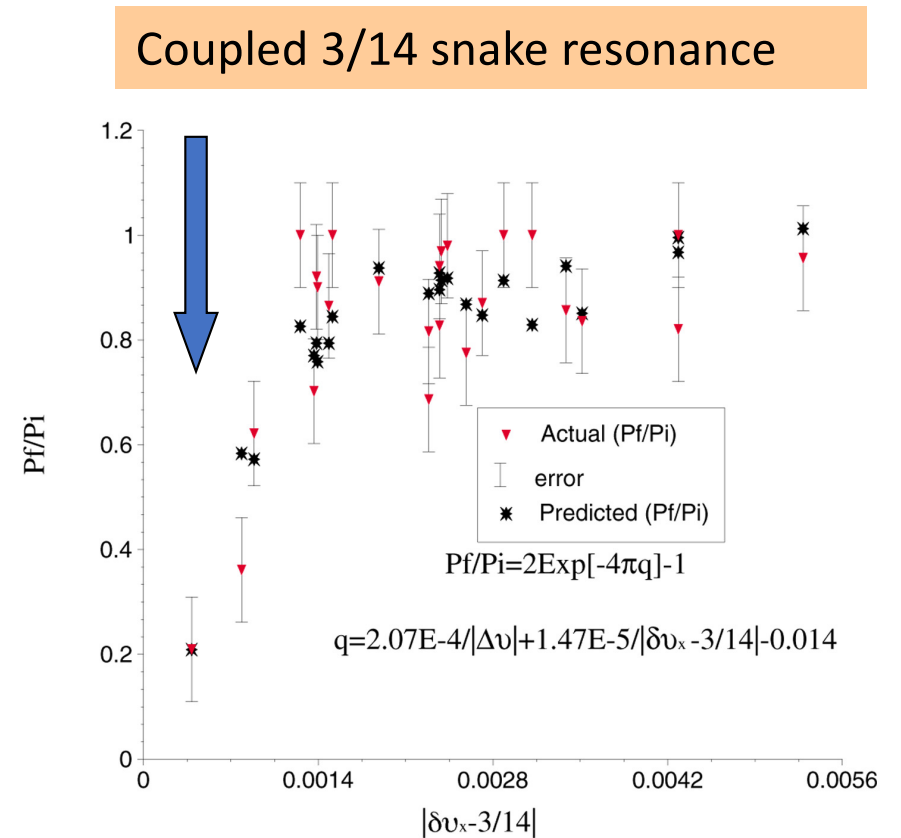


Zgoubi, F.Meot

Snake resonances observed in RHIC



@M.Bai

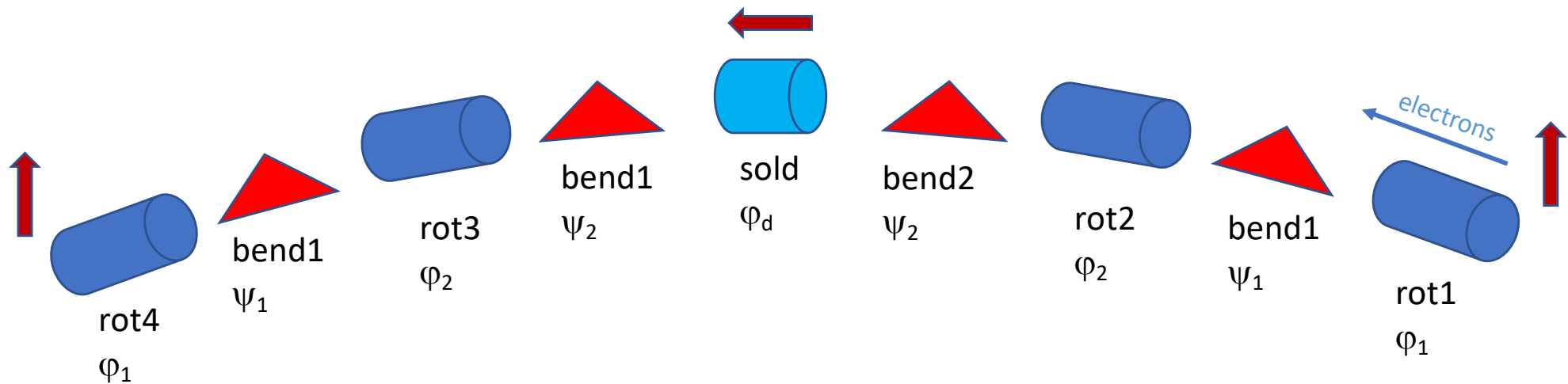


Spin Rotators in Accelerators

- Natural orientation of stable spin direction in accelerators is vertical. Particle physics experiments often require a specific polarization orientation (often, longitudinal) in experimental detectors.
- In a circular accelerator usually a pair of spin rotators is installed, where the second rotator restored the polarization orientation to vertical.
- Spin rotators also often used at low energies to convert the beam polarization produced by the particle source to a wanted orientation.

Solenoidal Rotator for EIC

- To operate in wide energy range the rotator scheme must use at least two solenoidal insertions
- General rotator scheme for EIC electrons (5-18 GeV):



Relations for longitudinal polarization:

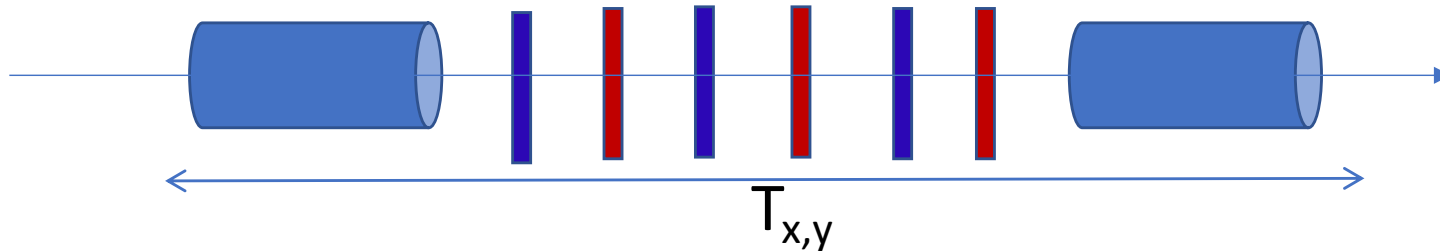
$$\tan \varphi_1 = \pm \frac{\cos \psi_2}{\sqrt{-\cos(\psi_1 + \psi_2) \cos(\psi_1 - \psi_2)}}$$

$$\cos \varphi_2 = \cot \psi_1 \cot \psi_2$$

Example of Solenoid insertion for spin rotator

Optics of the solenoid insertion in electron ring must realize two independent conditions:

- Betatron coupling has to be compensated by the use of normal and skew quadrupoles
- Specific spin matching conditions has to satisfied to minimize depolarization (Next week lecture!)



For a betatron spin-matched and fully decoupled solenoidal insertion the horizontal and vertical transport matrices must have following forms:

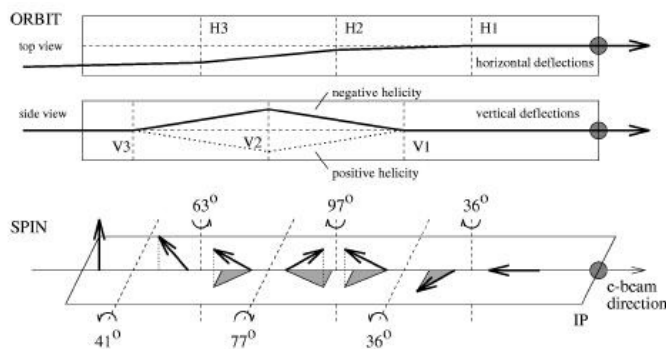
$$T_X = \begin{pmatrix} -\cos(\varphi) & -\frac{2}{K_s}\sin(\varphi) \\ \frac{K_s}{2}\sin(\varphi) & -\cos(\varphi) \end{pmatrix}; \quad T_Y = -T_X = \begin{pmatrix} \cos(\varphi) & \frac{2}{K_s}\sin(\varphi) \\ -\frac{K_s}{2}\sin(\varphi) & \cos(\varphi) \end{pmatrix}$$

$$K_s = \frac{B_s}{B\rho} \quad \varphi = (1+a)K_s L$$

HERA spin rotator

- HERA was the first e-p collider, operated with 27.5 GeV electrons and 820 (920) GeV protons.
- The spin rotators were implemented for electron beam to produce longitudinal polarization at the experimental detectors

HERA MiniRotator: Buon + Steffen



56 m ("short") → no quads.

27 – 39 GeV, both helicities, variable geometry

Sequence of horizontal and vertical bends:

(V1, H3, V2, H2, V3, H1).

Vertical orbit is restored:

$$V3 = -(V1+V2)$$

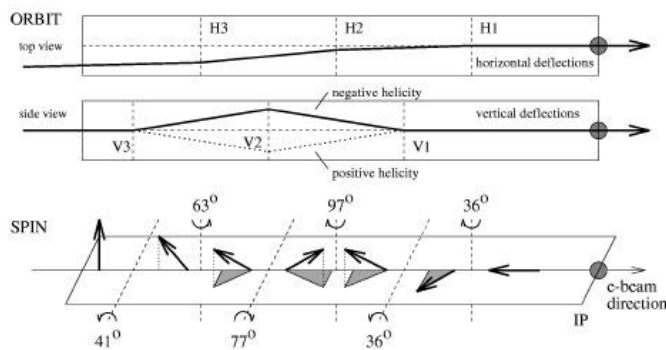
But horizontally there is a small net bending angle coming from the rotator.

Rotator insertion optics was designed to satisfy the spin matching conditions.

HERA spin rotator

- HERA was the first e-p collider, operated with 27.5 GeV electrons and 820 (920) GeV protons.
- The spin rotators were implemented for electron beam to produce longitudinal polarization at the experimental detectors

HERA MiniRotator: Buon + Steffen



56 m ("short") → no quads.

27 – 39 GeV, both helicities, variable geometry

Sequence of horizontal and vertical bends:

(V1, H3, V2, H2, V3, H1).

Vertical orbit is restored:

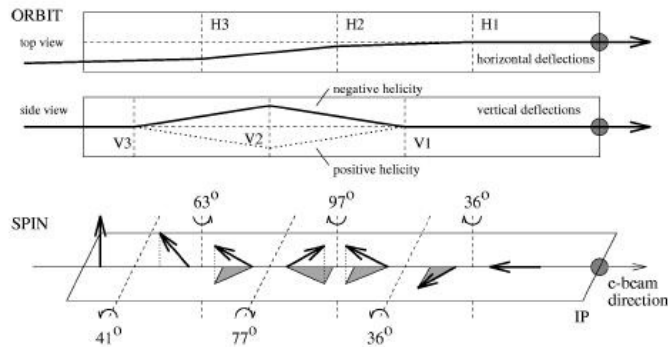
$$V3 = -(V1+V2)$$

But horizontally there is a small net bending angle coming from the rotator.

Rotator insertion optics was designed to satisfy the spin matching conditions.

HERA Rotators

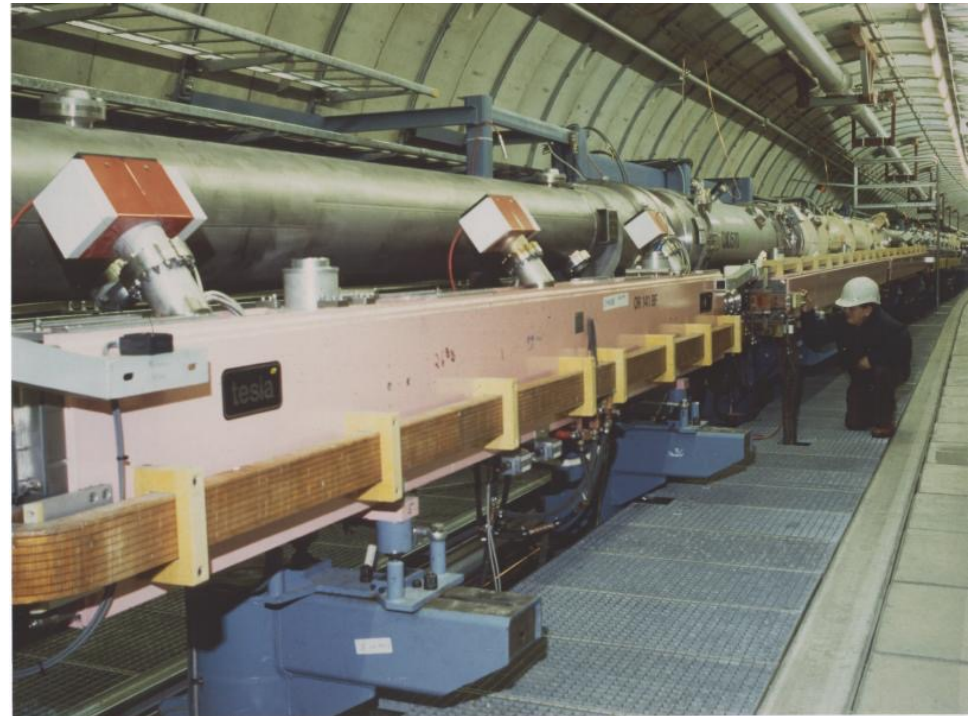
HERA MiniRotator: Buon + Steffen



56 m ("short") → no quads.

27 – 39 GeV, both helicities, variable geometry

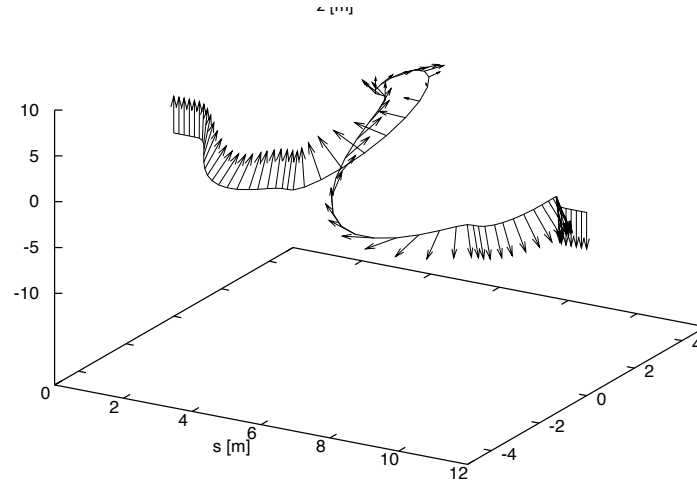
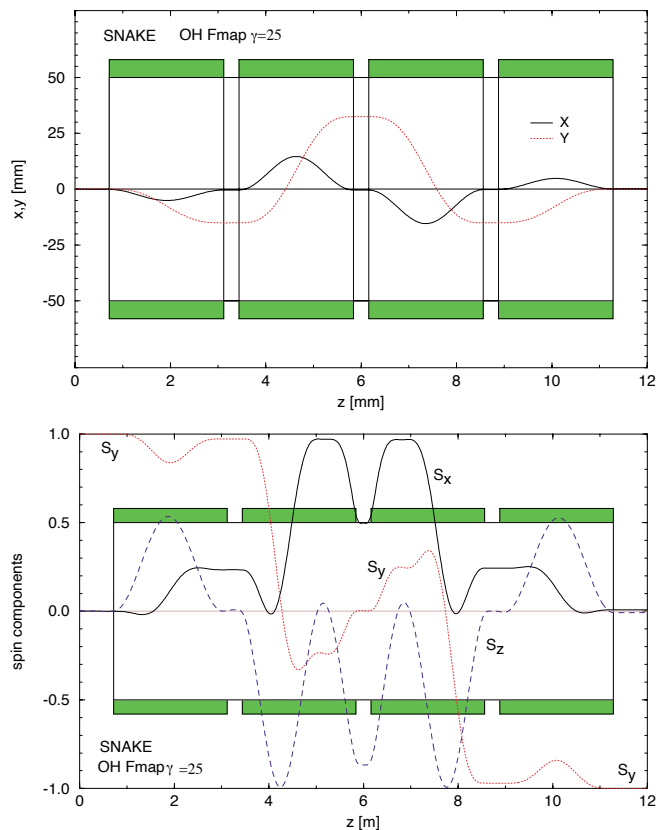
Implemented as normal conducting magnets



Inconvenient feature of this design:
Changing polarization direction at the experiments required vertical movement of the magnets

RHIC Helical Snake

Spin and orbit evolution through RHIC helical Snake



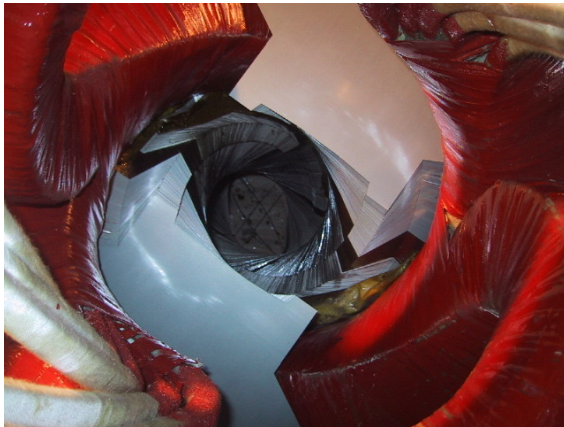
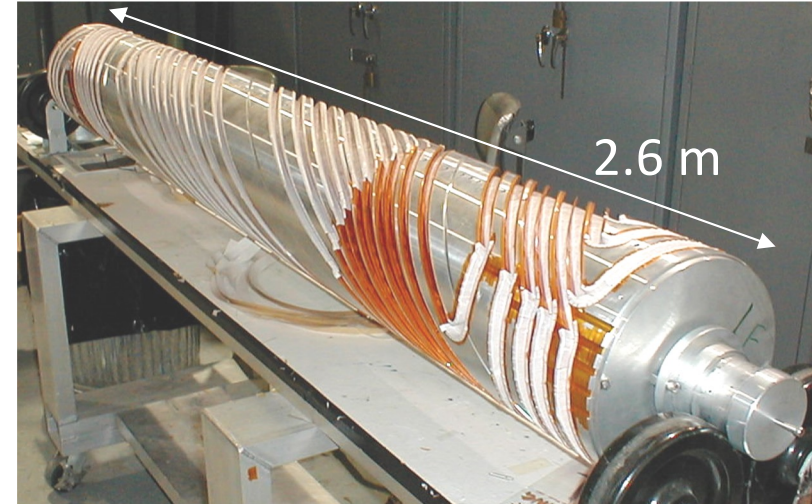
Orbit deviation drops inversely proportionally to beam energy.

The resulting orbit excursion is considerably less than in Steffen's snake!

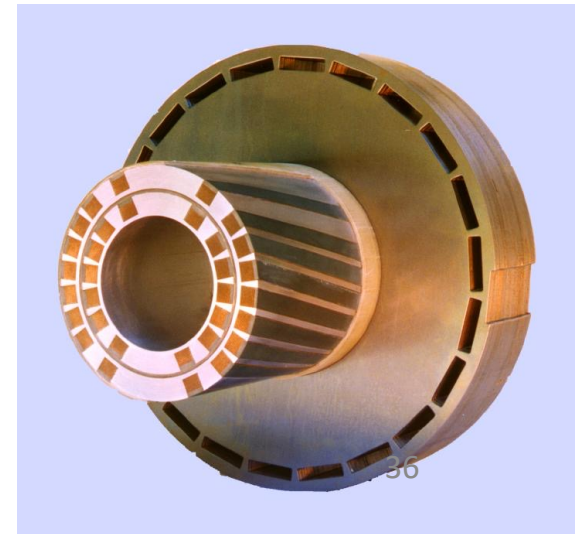
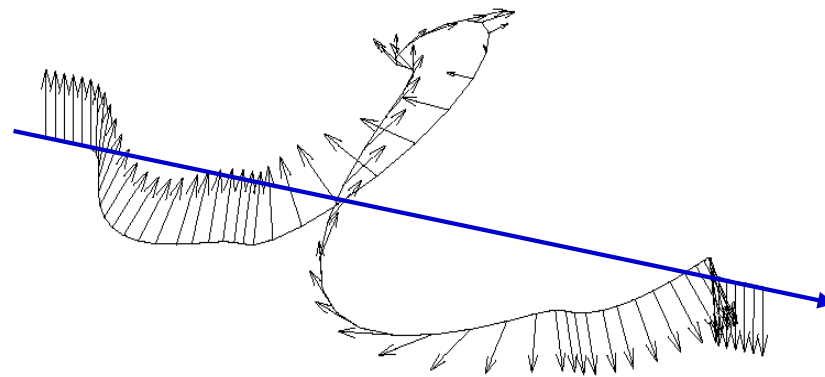
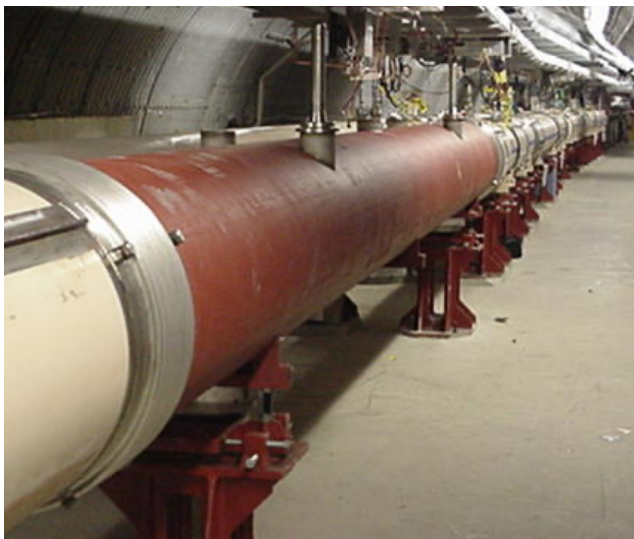
But helical magnets have intrinsically non-linear fields, thus the effect on particle dynamics should be carefully evaluated.

(Betatron tune shift, beta-function distortions)

Siberian Snakes



- AGS Siberian Snakes: variable twist helical dipoles, 1.5 T (RT) and 3 T (SC), 2.6 m long
- RHIC Siberian Snakes: 4 SC helical dipoles, 4 T, each 2.4 m long and full 360° twist



Dipole Magnet Snake vs Solenoidal Snake

- Unpleasant feature of the dipole magnet Snake, as compared with solenoidal snake/rotators, is that the beam orbit significantly distorted inside the Snake.
- Below 20 GeV energy the orbit excursion reaches tens of centimeters.
- But a solenoidal Snake would require very large field integral (hundreds T*m) at the energies above 20 GeV.
- Thus, use:
 - dipole field Snakes/rotators at the energies above 10 GeV
 - solenoidal Snakes/rotators below 20 GeV.

Some Key Points Re-Iterated

- Siberian Snake is an amazing device allowing polarization preservation while crossing numerous and numerous spin resonances during beam acceleration.
- Most efficient use of Snakes is in pairs (even number), with proper distribution of an accelerator ring. Proper selection of the snake axis angle ensures spin tune 0.5
- Even with Snakes: be careful about depolarization, there are higher order resonances, “Snake” resonances. Larger beam energies require larger number of the Snakes
- Spin rotator is very important device: most of experiments done on colliders want longitudinally polarized beam at collision points.
- Practical realization of Snakes and rotators depends on the energy of a particular accelerator.
Dipole, and helical dipole based Snakes are proper choice at higher energies (>20 GeV);
while solenoidal based snakes at lower energies (<20 GeV)

Thank you for your attention!

Additional Reading

In addition to materials listed in the course, for this particular topic (Snakes and Rotators) following materials are recommended:

1. Handbook of Accelerator Physics and Engineering, sections 2.6.3 (Spin Rotators and Siberian snakes) and 7.2.18 (Spin Manipulation).
2. “Siberian Snakes in high-energy accelerators”, S.R.Mane, Yu.M.Shatunov, K.Yokoya, Journal of Physics G: Nuclear and Particle Physics, 31 (2005) R151.
- 3.”Helical Spin Rotators and Snakes”, V.Ptitsyn and Yu.M.Shatunov, NIM A 398 (1997), p.126.
4. S.Y.Lee, NIM A 306 (1991), p.1.

Beam Cooling

Vadim Ptitsyn
EIC Project, BNL

USPAS 2025, January 27-January 31

Electron-Ion Collider



Introduction

- Presently, there are two major methods of the cooling the electron cooling and stochastic cooling.
- The stochastic cooling can be additionally separated on
 - the microwave stochastic cooling
 - the optical stochastic cooling (OSC)
 - the coherent electron cooling (CEC)

Requirements for Cooling in Collision Mode

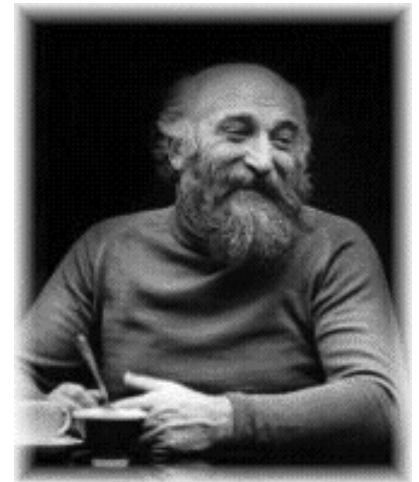
- Cooling time is typically set by IBS and beam-beam diffusion
 - ◆ For EIC collider for cooling one would want to have:
 - ◆ 30min colling time at injection energy, 25 GeV
 - ◆ and ~1h at the store at 275 GeV
- Cooling acceptances
 - ◆ Good beam lifetime in the presence of beam-beam effects requires cooling range to be $> 4 - 5 \sigma$
- Overcooling in the bunch center has to be avoided
 - ◆ Overcooling greatly amplifies beam-beam effects

Electron cooling

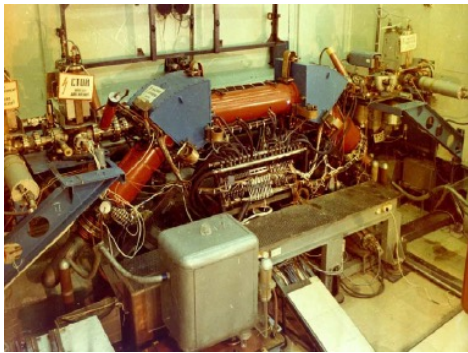
- Invented in 1966 by A. M. Budker
 - ◆ Electron beam is copropagating with an ion beam
 - ◆ Electron and ion beams have the same longitudinal velocity
 - ◆ In the beam frame – by interaction with electrons heavy particles come into equilibrium with electron gas
 - ◆ If temperatures of electrons and ions in Beam Frame are equal then in Lab Frame the angular spread relation is:

$$\theta_i = \theta_e \sqrt{\frac{m_e}{M_i}}$$

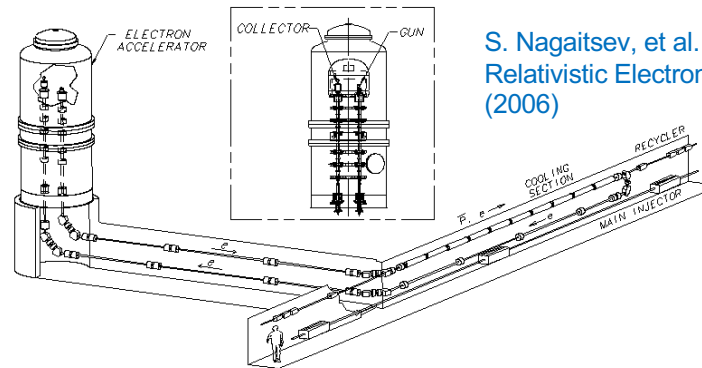
- Tested experimentally in BINP, Novosibirsk, in 1974-79 at NAP-M
 - ◆ 35 keV electron beam (65 MeV protons)



Electron Cooling Technique



Experimental demonstration of electron cooling at NAP-M (Novosibirsk, 1974).



S. Nagaitsev, et al. "Experimental Demonstration of Relativistic Electron Cooling", Phys. Rev. Lett. 96, 044801 (2006)

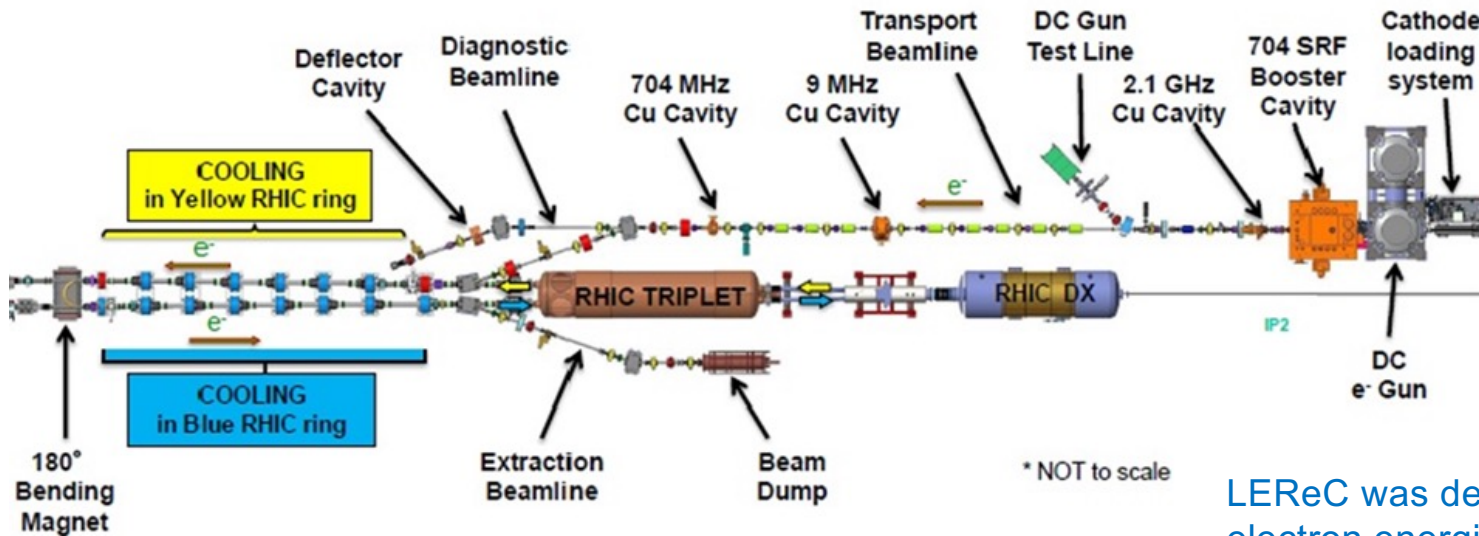
Electron Cooling is a well-established technique with **50 years** of experimental experience.

High Voltage DC coolers: (1974-): all DC electrostatic accelerators; all use magnetic field to confine electron beam (magnetized cooling). **FNAL cooler (2005-11):** Extension to relativistic energies (4MeV electrons), transport of electron beam without continuous magnetic field.

RF acceleration (High Energy approach): **BNL LReC electron cooler (2019-):** First RF-linac based electron cooler (concept directly extendable to higher energies). LReC does not use any magnetization of electrons. LReC was successfully used for RHIC operations in 2020-21 to cool ion bunches directly at collision energy.

A. V. Fedotov et al. "Experimental Demonstration of Hadron Beam Cooling Using Radio-Frequency Accelerated Electron Bunches", Phys. Rev. Lett. 124, 084801 (2020)

Operational Electron Cooler LEReC @ RHIC



LEReC was designed to operate at electron energies up to 2.6 MeV (using single-cell SRF accelerating cavity).

- LEReC is a fully-operational electron cooler which utilizes **RF-accelerated** electron bunches
- LEReC approach was chosen for the EIC LEC (12.5 MeV electron kinetic energy).

Cooling Force in non-magnetized Cooling

In the beam frame an ion travelling through the electron gas with velocity \mathbf{v} encounters a friction force:

$$\mathbf{F}(\mathbf{v}) = \frac{4\pi n_e e^4 L_c}{m_e} \int f(\mathbf{v}') \frac{\mathbf{v} - \mathbf{v}'}{|\mathbf{v} - \mathbf{v}'|^3} d\mathbf{v}'^3 = \frac{4\pi n_e e^4 L_c}{m_e} \nabla_{\mathbf{v}} \left(\int \frac{f(\mathbf{v}')}{|\mathbf{v} - \mathbf{v}'|} d\mathbf{v}'^3 \right)$$

$$\text{Coulomb logarithm } L_c = \ln \left(\frac{r_{\max}}{r_{\min}} \right), \quad r_{\min} \approx \frac{2e^2}{m_e v_{\text{eff}}^2}, \quad r_{\max} \approx \frac{v_{\text{eff}}}{\omega_p}, \quad v_{\text{eff}} = \max(|\mathbf{v}|, \bar{v}_e),$$

As in the case of the IBS we consider Gaussian electron velocity distribution (in BF) which is much colder longitudinally.

$$f(\mathbf{v}_{\perp}, v_{\parallel}) = \frac{1}{(2\pi)^{3/2} \sigma_{v_{\parallel}} \sigma_{v_{\perp}}^2} \exp \left(-\frac{v_{\parallel}^2}{2\sigma_{v_{\parallel}}^2} - \frac{\mathbf{v}_{\perp}^2}{2\sigma_{v_{\perp}}^2} \right), \quad v_{\parallel} \ll v_{\perp}$$

Using this distribution function, averaging of the friction force over the ion distribution and transforming into the laboratory frame leads to the cooling rates.

Cooling Rates for Highly Relativistic Electron Cooling

- For practical applications one can use following cooling rates:

$$\lambda_{\parallel} \approx \frac{4\sqrt{2\pi}n_e r_e r_p L_c}{\gamma^4 \beta^4 (\Theta_{\perp} + 1.083\Theta_{\parallel} / \gamma)^{3/2} \sqrt{\Theta_{\perp} \Theta_{\parallel}}} L_{cs} f_0, \quad \frac{\Theta_{\parallel}}{\gamma \Theta_{\perp}} \leq 2. \quad \Theta_{\parallel} = \sqrt{\theta_{\parallel e}^2 + \theta_{\parallel p}^2},$$

$$\lambda_{\perp} \approx \frac{\pi\sqrt{2\pi}n_e r_e r_p L_c}{\gamma^5 \beta^4 \Theta_{\perp}^2 (\Theta_{\perp} + \sqrt{2}\Theta_{\parallel} / \gamma)} L_{cs} f_0, \quad \Theta_{\perp} = \sqrt{\theta_{\perp e}^2 + \theta_{\perp p}^2},$$

1. For heavy ions the rates are multiplied by Z^2/A .

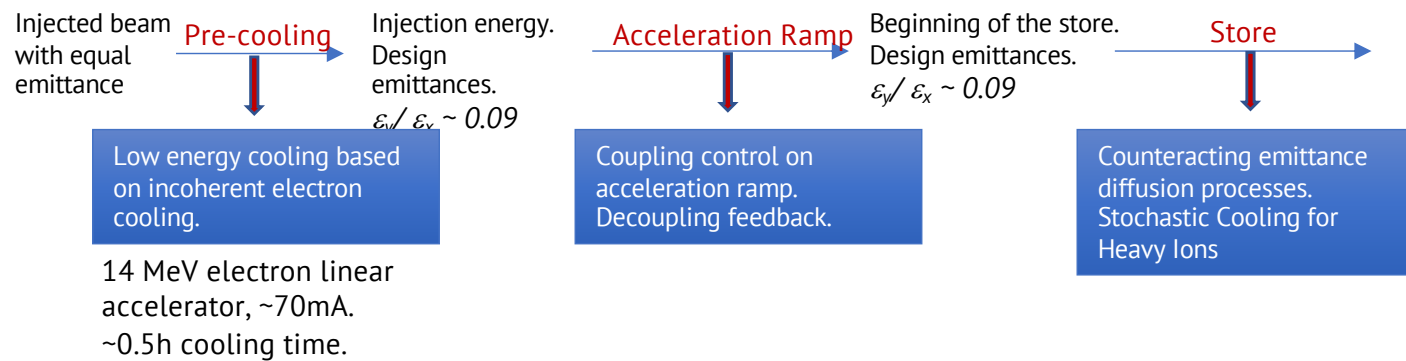
For instance, the rates for cooling Au ions are $79^2/197 \sim 32$ times stronger than for protons.

2. Cooling rates has very strong dependence on proton γ , making cooling at energies higher than 20 GeV significant challenge.

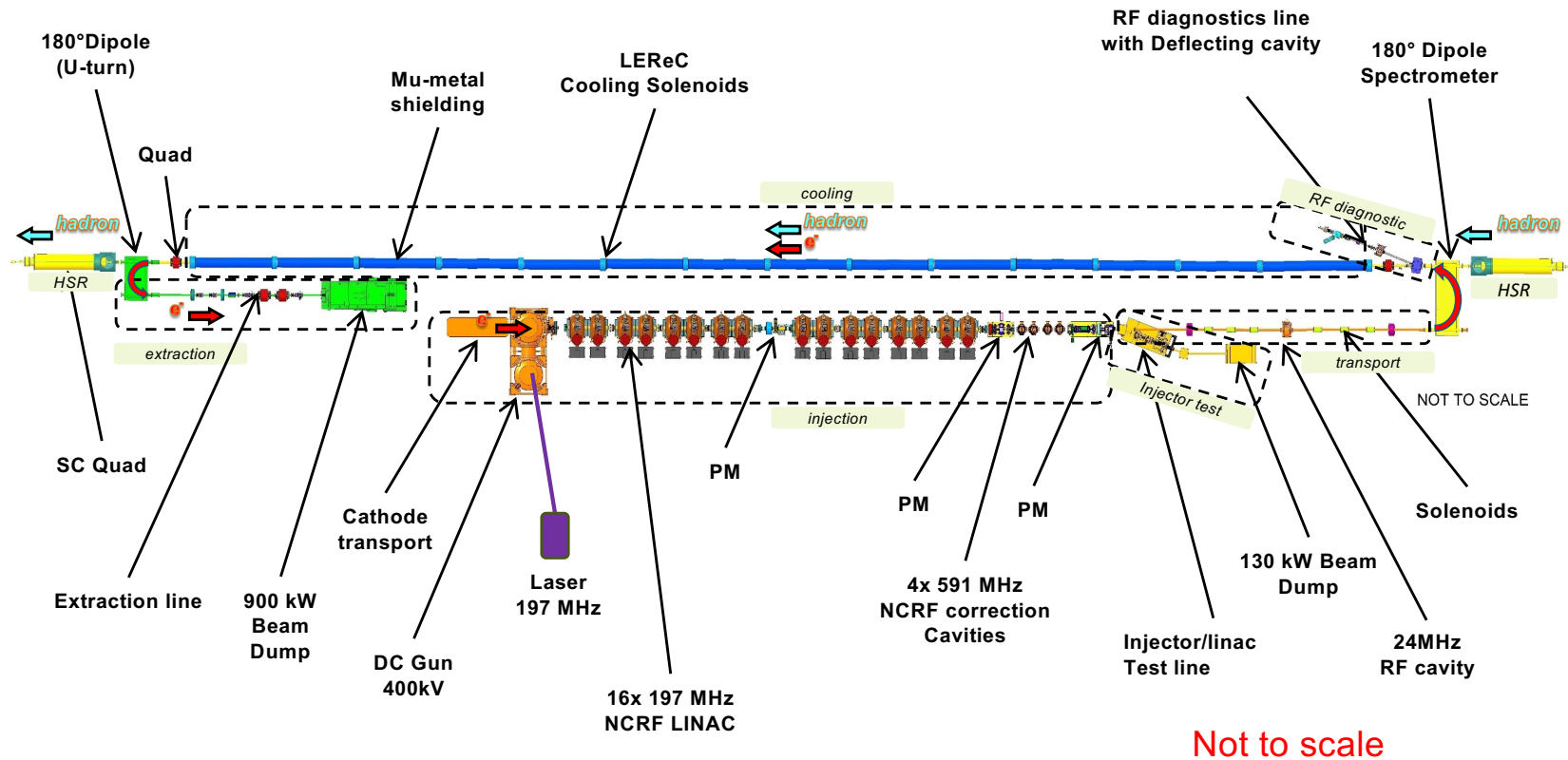


Electron cooling consideration for the EIC

HSR emittance formation



LEC Layout at IR2 (using NCRF Linac approach)



13 MeV Electron Linac

EIC Low Energy Cooler Parameters

	electrons	protons
gamma	25.4	25.4
RHIC RF frequency, MHz	197	24.6
Cooling section length, m	168	168
Cooling sections beta function, m	150	100-200
Hadrons D_y , D_y' , m, rad		<1, <0.02
Total charge per proton bunch, nC	3	45
Electrons kinetic energy, MeV	12.5	
Electron average current, mA	74	
Normalized emittance, rms, μm	<1.5	2
rms bunch length, cm	5	70
rms dp/p	<5e-4	6e-4
Angles in cooling section, urad	20-30	20

LEReC key parameters for reference

electrons
4-5
704 MHz (9 MHz)
20 m
30 m
3 nC
1.6-2 MeV
30 (60 mA in tests)
<2 μm
5 cm
<5e-4
<150 urad

Beam Structure in Cooling Section

Protons bunch structure:

$f_{\text{rep}}=24.6$ MHz
 $N_p=2.8e11$, $I_{\text{peak}}=3$ A (with 2nd harmonic)
Rms length=1m

Electrons bunch structure:

$f_{\text{RF}}=197$ MHz
Single bunch: $Q_e=1$ nC
Number of bunches in macro-bunch: 3
Rms length=0.04m

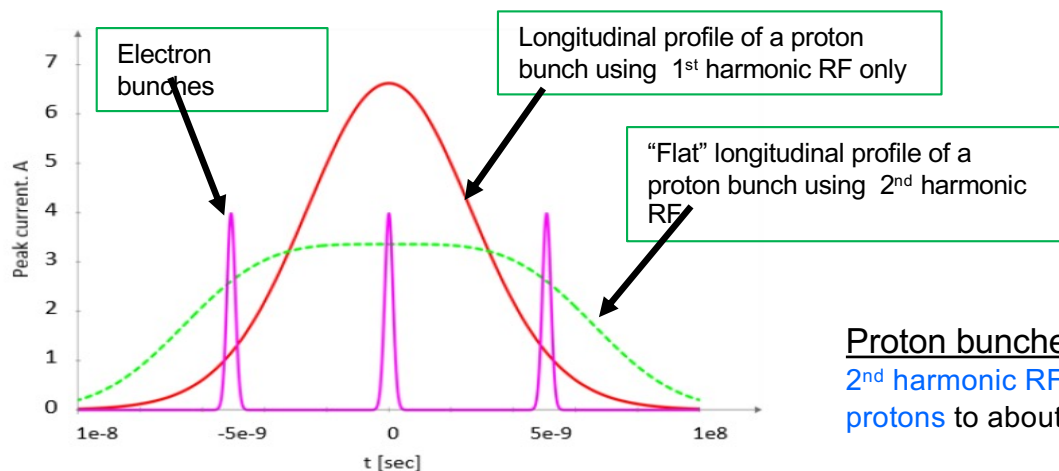


Figure 3: Three electron bunches (magenta) spaced by 5.1ns placed on a single proton bunch (red: single RF harmonic; green: double RF harmonic).

Proton bunches during cooling:

2nd harmonic RF alleviates space-charge effects reducing peak current of protons to about 3A so the space charge tune shifts are $\Delta Q_{\text{sc},x,y}=\mathbf{0.07, 0.13}$

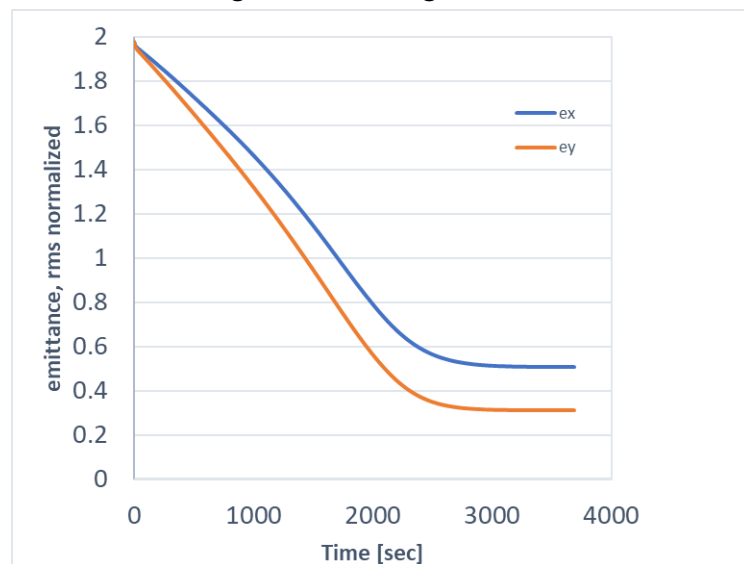
Use of double RF system and making flattened bunch profiles was recently demonstrated at proton injection energy in RHIC (**APEX May 8, 2024**).

Cooling Performance

Average current of electrons: $I_{av}=74\text{mA}$

Electrons rms angles in the cooling section: **25 urad**

Effective cooling section length: **168 meters**



Cooling simulations of protons at $\gamma=25$, with decoupled transverse motion (**IBS+Cooling only**, single harmonic RF).

Longitudinal emittance is kept constant during cooling process.

After cooling the **normalized rms emittances of protons** $ex, ey=0.5, 0.3 \mu\text{m}$ (horizontal emittance can be increased further as needed.)

- The design of cooling sections and optimization of electron beam dynamics are in progress to minimize various contributions to rms electron angles in the cooling sections.

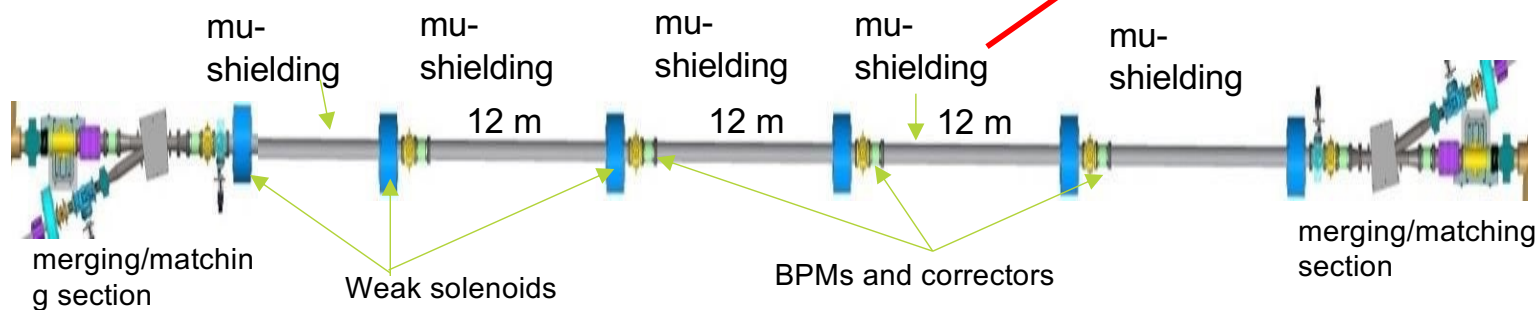
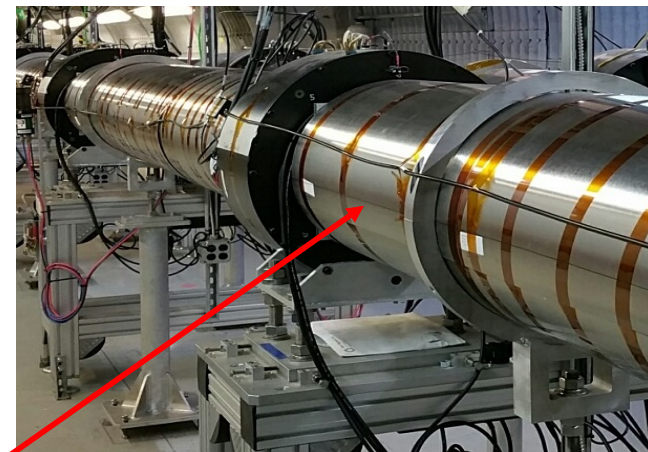
Major contributions to the rms electrons angles **budget** in cooling sections:

- Electron beam emittance: < 20 urad
- Electron beam space charge: < 10 urad
- Focusing from proton beam: < 10 urad
- Remnant magnetic fields (with shielding) < 7 urad

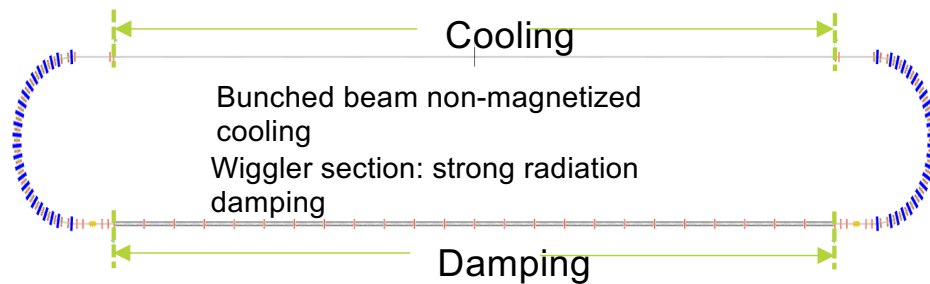
Total preliminary budget (added in quadrature): 25 urad

EIC LEC Cooling Sections

- Requirements on residual transverse magnetic field between correctors in the cooling region **is 1 $\mu\text{T}\cdot\text{m}$** , which is similar to LEReC requirements.
- Assuming 12 m long sections, **the transverse magnetic fields should be shielded to 1 mG level in each section.**
- Shielding of the residual magnetic field to such level can be achieved using concentric cylindrical layers of high-permeability alloy in the cooling sections, similar to LEReC.



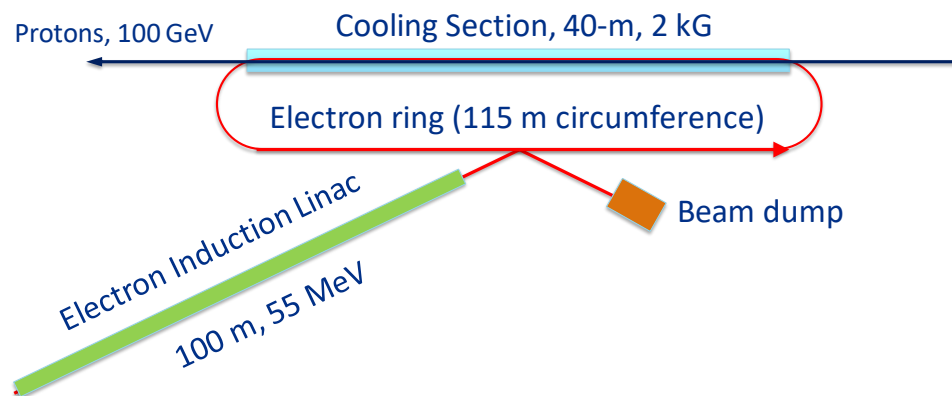
Options of High Energy Electron Cooling (at 275 GeV)



The electron ring with strong radiation damping using long wiggler section.
 $I \sim 1-2A$

Major challenges:

- dynamic aperture,
- collective effects



Induction linac accelerating very high current pulses (up to 100A) with $\sim 10K$ turns recirculations.

Major challenges:

- space charge in electron beam,
- beam stability (CSR impedances),
- emittance growth due to interaction
- with proton bunches

Stochastic Cooling

- First cooling method used in the accelerators
- Invented in 1969 by Simon van der Meer
- Nobel Prize 1984
- Naive transverse cooling model
 - 90 deg. between pickup and kicker
 - Signal travel time between pickup and kicker equal to the particle travel time



$$\delta\theta = -g\theta$$

Averaging over betatron oscillations yields

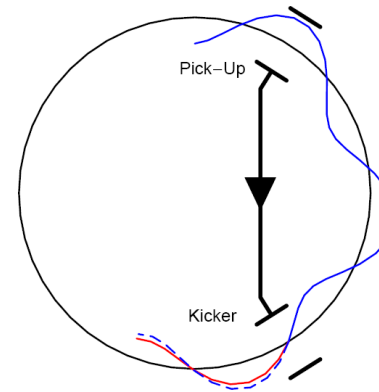
$$\overline{\delta\theta^2} = -\frac{1}{2} 2g\overline{\theta^2} \equiv -g\overline{\theta^2}$$

Adding noise of other particles yields

$$\overline{\delta\theta^2} = -g\overline{\theta^2} + N_{sample}g^2\overline{\theta^2} \equiv -(g - N_{sample}g^2)\overline{\theta^2}$$

That yields

$$\overline{\delta\theta^2} = -\frac{1}{2} g_{opt}\overline{\theta^2} \quad , \quad g_{opt} = \frac{1}{2N_{sample}} \quad , \quad N_{sample} \approx N \frac{f_0}{W}$$

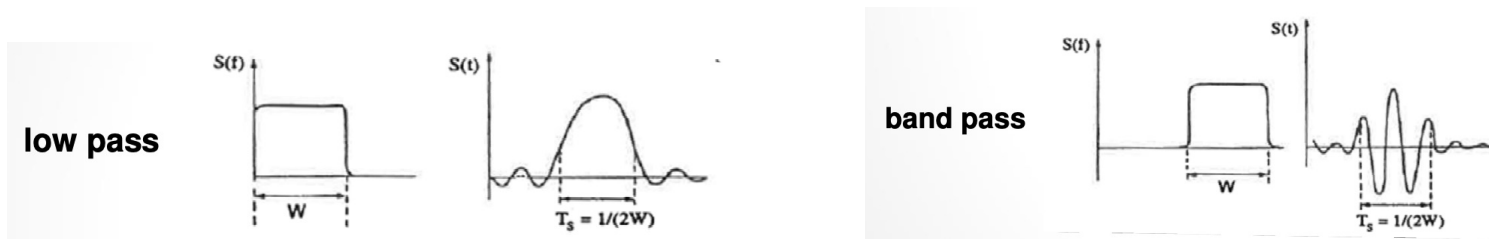


SC Bandwidth

- Nyquist theorem:

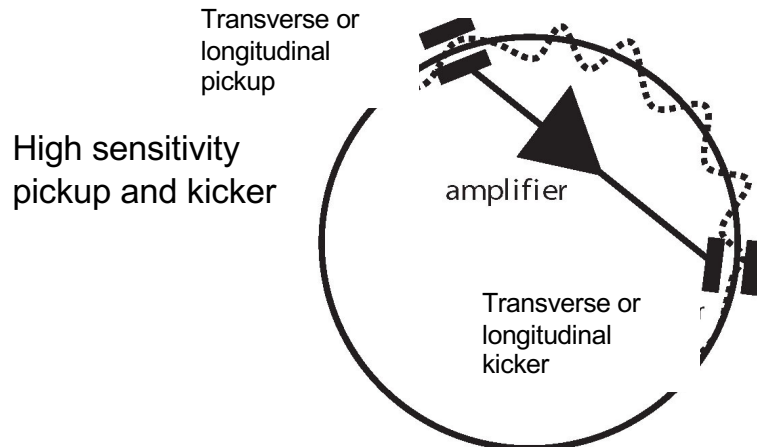
with frequency bandwidth $\Delta f = W$ the minimum time resolution is $\Delta t = 1/(2W)$

Also, it is important to use band pass bandwidth:



Microwave cooling efficiently works in 3-6 GHz bandwidth

Microwave stochastic cooling



$$\frac{1}{\tau} = \frac{W}{T_0 \lambda_N} [2g - g^2(M + U)] = K_{red} \frac{W}{T_0 \lambda_N}$$

Optimal values for gain and cooling time:

$$g = g_0 = 1/(M + U)$$

$$\tau = \tau_0 = \frac{N}{2W} (M + U)$$

U – electronic noise-to-signal ratio
M – mixing time (in turns)
W – signal bandwidth (use band pass)
 λ_N - Max linear density
 T_0 - revolution time

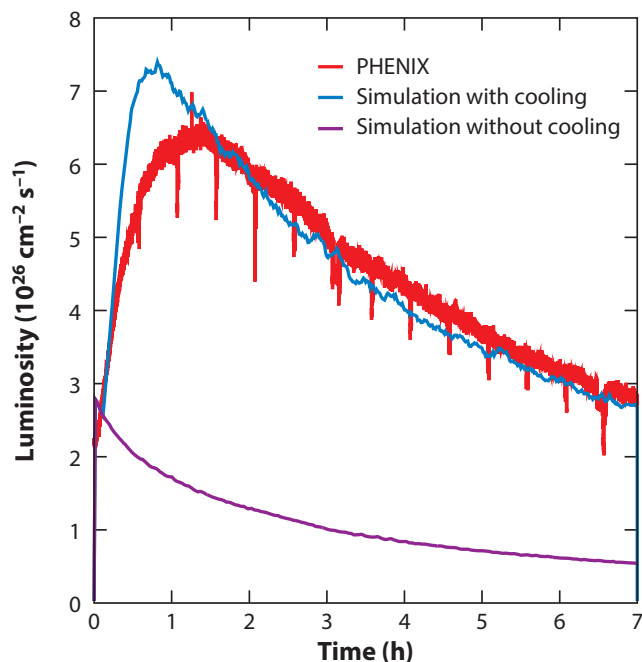
$$K_{red} < 1$$

Major properties:

- Energy independent
- Limited by linear density of hadrons
- Limited by the signal bandwidth, which is typically ~1-5 GHz
- Works best for large hot beams with moderate intensities.

Microwave stochastic cooling

- Major application for high energy accelerators:
 - Cooling coasting beams of antiprotons in CERN and Fermilab (8GeV).
 - Cooling of bunched heavy ion beams in RHIC. (For example, Au⁺⁷⁹ ions at 100 GeV/u)



In RHIC 3D stochastic cooling was realized:

- Longitudinal cooling prevents the ion losses out of the RF buckets– higher average luminosity.
- Transverse cooling shrinks emittances -> higher peak luminosity.
- The luminosity lifetime is defined by ion burn-off from collisions.

For protons the stochastic cooling in RHIC is not efficient, since the proton bunch intensity is ~100 time higher than for ions.

© M. Blaskiewicz and M.Brennan

RHIC SC equipment

longitudinal pickup



Transverse pickups, FO
Transverse kicker

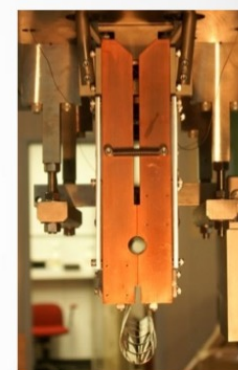
3 tanks with longitudinal (narrow band) kicker units

Fiber Optic Links, transverse

MicroWave Links, longitudinal

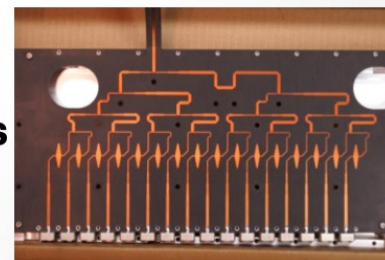
70 GHz carrier with 16 GHz local oscillator

Transverse pickups, FO
Transverse kicker



longitudinal kicker open for injection and ramping (left), closed during cooling (right)

horizontal and vertical pickups



Electron-Ion Collider

USPAS, January 27-31, 2025

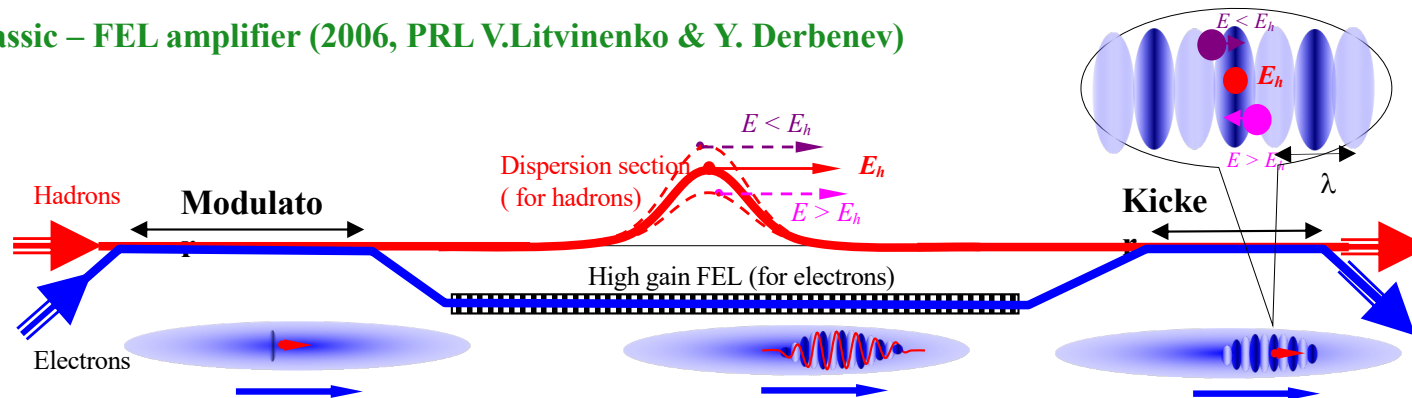
Vadim Ptitsyn

Stochastic cooling approach considerations for EIC

- Microwave stochastic cooling may be applied in the EIC to cool heavy ion beams with some system upgrade,
- Cooling EIC protons with microwave SC would take ~250h. Not realistic.
- In order to significantly reduce the cooling time (by 2-3 orders of magnitude), the bandwidth of stochastic cooling has to be increased by similar amount.
- Novel proposed techniques aim to achieve THz-scale bandwidth:
 - Optical stochastic cooling,
 - Coherent electron cooling
 - Microbunching cooling (CeC with microbunching amplification)

Coherent electron Cooling with FEL amplifier

Classic – FEL amplifier (2006, PRL V.Litvinenko & Y. Derbenev)



Electron energy density modulation caused by an ion

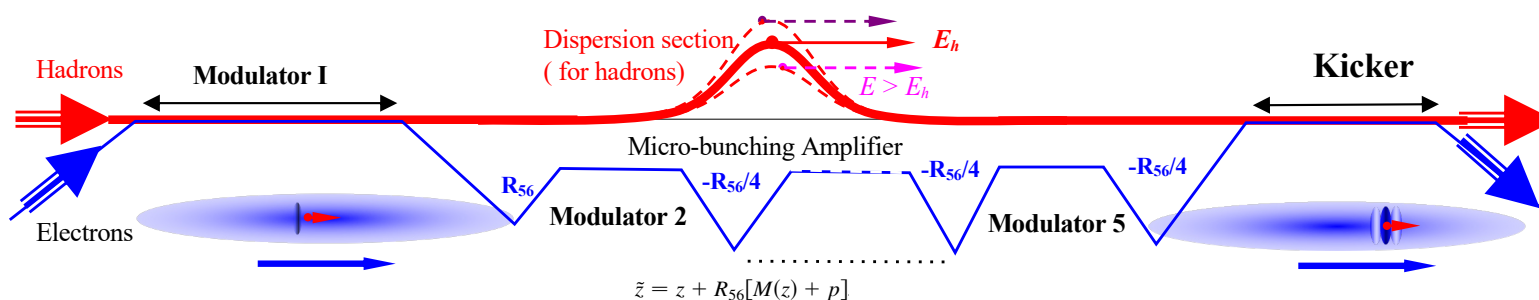
FEL instability amplifies the density modulation. Resulting modulation contains several periods.

Ion, delayed accordingly to its energy, encounter the electron density modulation in a phase proper for cooling

- An electron beam serves as both the pickup and kicker of the stochastic cooling scheme.
- A free-electron laser (FEL) is used as an amplifier of the electron signal.
- Bandwidth is lower than for other techniques ~ several 100 GHz

Micro-bunching Cooling

Micro-bunching: MB Amplifier, Single & Multi-stage, D. Ratner, PRL, 2013



Electron energy modulation caused by an ion:

$$M(z) = \frac{-2cqL_m}{\gamma a^2 I_A} \left[\frac{z}{|z|} - \frac{\gamma z}{\sqrt{a^2 + \gamma^2 z^2}} \right]$$

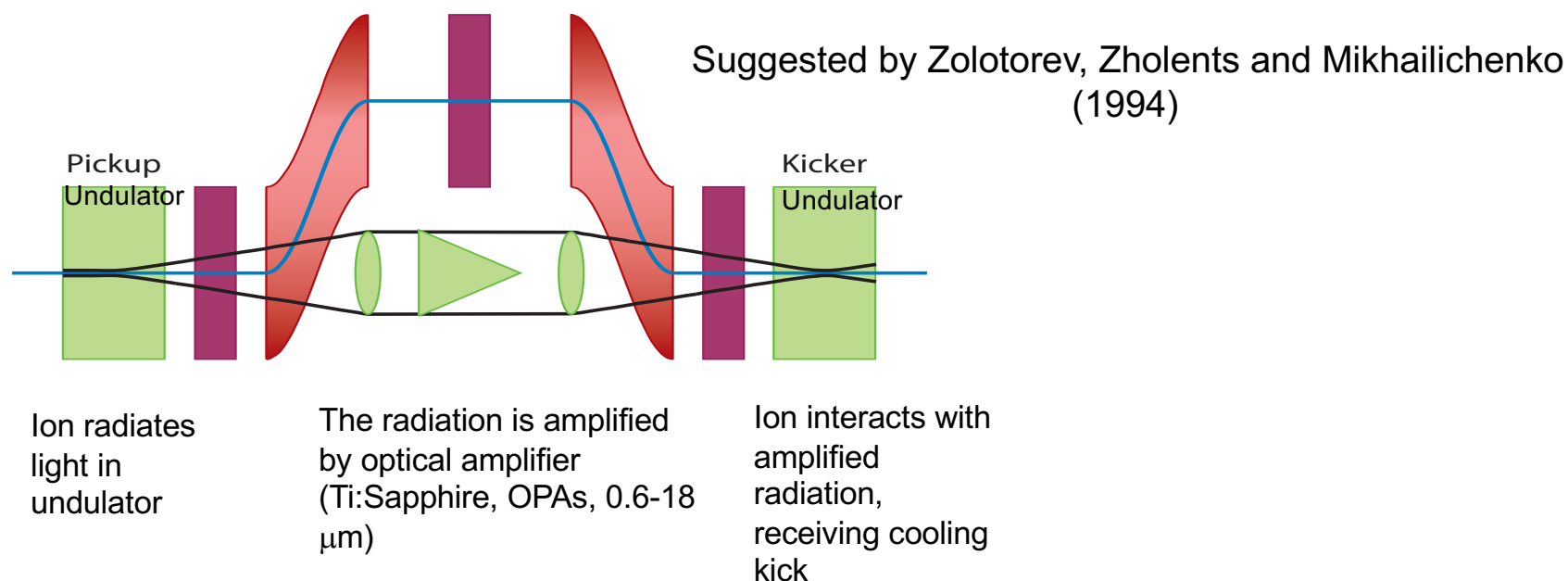
Micro-bunching instability in dispersive lattice insertion converts energy into density modulation, and amplifies it.

One ion \rightarrow one density modulation spike !

For EIC MBEC would give \sim an order improvement in the cooling rate compared with CeC-FEL method. Or, correspondingly reduced electron cooler current. Bandwidth > 1 THz

Still big challenges remain: noise in electron beam which produce heating effect, precise ion delay timing (< 1 μm), cooling diagnostic

Optical Stochastic Cooling



- The bandwidth of optical amplifiers can be above 10 THz
- Cooling efficiency is limited strongly by the power of existing optical amplifiers.
- Challenges for EIC applications:
 - Wide range of hadron energies demands high tuning range of undulator (factor 30 between 275 GeV and 50 GeV).
 - Light optics elements can produce some considerable delay ($\sim 10\text{cm}$) that has to be accommodated by the ion lattice.
 - State-of-the art optical amplifiers

Novel Techniques

- There have been significant advances for the novel cooling techniques aimed in cooling protons at high energies (above 100 GeV).
- Proof-of-principle experiments have been underway in IOTA(FNAL) for OSC and RHIC(BNL) for CeC.
- With respect to the EIC there is still ~10-15 years to resolve scientific and technical challenges. In this case one of the approaches can be implemented in the EIS as a future upgrade for increasing the average luminosity.

Electron cooling vs Stochastic Cooling

- The electron and stochastic cooling are based on completely different principles.
- The electron cooling is dissipative in its principle of operation. That enables direct reduction of the beam phase space.
- The stochastic cooling is a “Hamiltonian” process which formally does not violate the Liouville theorem and cooling happens due to the phase space mapping so that phase space volumes containing particles are moved to the beam center while the rest mostly moves out. That makes stochastic cooling rates strongly dependent on the beam particle density.
- Each method has its own domain where it achieves a superior efficiency.
 - The electron cooling is preferred at a smaller momentum spread, and its efficiency weakly depends on the particle density in the cooled beam.
 - While the stochastic cooling is preferred at a higher energy, but its efficiency reduces fast with increase of particle phase density.